22nd International Symposium on Ballistics

Vancouver BC, Canada

14-18 November 2005

Agenda

Tuesday, 15 November 2005

Invited Presentation: by From Columbia To Discovery: Understanding the Impact Threat to the Space Shuttle, by James D. Walker, Southwest Research Institute

General Oral Session #1

- Plasma Ignition of a 30mm Cannon, Richard A. Beyer, Andrew L. Brant, Joseph J. Colburn, US Army Research Laboratories
- Numerical Computations of Subsonic and Supersonic Flow Choking Phenomeana in Grid Finned Projectiles, Nicolas Parise, SNC Technologies, Inc; Alain Dupuis, Precision Weapons Section, Defense Research and Development Canada
- The Use of Electric Power in Active Armour Applications, Martin van de Voorde, R. Boeschoten, TNO Defence, Security and Safety
- Prevention of Sympathetic Detonation Between Reactive Armor Sandwiches, Andreas Holzwarth, Fraunhofer-Institut Fur Kurzzeitdynamik

Terminal Ballistics Oral Session #1

- Bullet Impact on Steel and Kevlar®/Steel Armor - Experimental Data and Hydrocode Modeling with Eulerian and Lagrangian Methods, Dale S. Preece, Vanessa S. Berg, and Loyd R. Payne, Sandia National Laboratories
- Progress on the NDE Characterization of Impact Damage in Armor Materials, Joseph M. Wells, JMW Associates
- The influence of sabot threads on the performance of KE penetrators, Nick Lynch and John Stubberfield, QinetiQ
- The Use of Electric Power in Active Armour Applications, Martin van de Voorde, R. Boeschoten, TNO Defence, Security and Safety
- Prevention of Sympathetic Detonation Between Reactive Armor Sandwiches, Andreas Holzwarth, Fraunhofer-Institut Fur Kurzzeitdynamik

Exterior Ballistics Oral Session #1

- Micro-Adaptive Flow Control Applied to a Spinning Projectile, Dr. Jubaraj Sahu, U.S. Army Research Laboratory
- Micro-Adaptive Flow Control and Nonlinear Aerodynamics (Combustion Gas Generators), Dr. Jubaraj Sahu and Ms. Karen Heavey, U.S. Army Research Laboratory
- Aerodynamic Characteristics of a Grid Finned Projectile from Free-Flight Tests at Supersonic Velocities, Alain Dupuis, DRDC - Valcartier; Claude Berner, French-German Research Institute
- Recent Computations and Validations of Projectile Unsteady Aerodynamics, Roxan Cayaz, Eric Carette, Giat Industires; Remy Thepot, Patrick Champigny, Office National D'Etudes et de Recherches Aerospatiales
- Research of Flight Characteristics of Rod-Type Projectile with Triangular Cross-section, Dr. Wenjun Yi, Prof. Xiaobing Zhang, and Prof. Jianping Qian, Ballistic Research Laboratory of China

Wednesday, 16 November 2005

Exterior Ballistics Oral Session #2

- Impact of Nose-Mounted Micro-Structures on the Aerodynamics of a Generic Missile, Dr. Daniel Corriveau, Defence R&D Canada (DRDC - Valcatier)
- Analyses of Gliding Control for an Extended-Range Projectile, Prof. Zhongyuan Wang, Prof. Houqian Xu, Dr. Jinguang Shi, Dr. Wenjun Yi, Prof. Shaosong Chen, Ballistic Research Laboratory of China
- Theoretical Design for a Guided Supersonic Projectile, Pierre Wey, Claude Berner, Eckhart Sommer, Volker Fleck, Henry Moulard, French-German Research Institute of Saint-Louis (ISL)

Interior Ballistics/Launch Dynamics Oral Session #1

- Ceramic Gun Barrel Technologies, Larry Burton, Jeff Swab, Rob Carter, Ryan Emerson, U.S. Army Research Laboratory, Weapons & Materials Research Directorate
- M865 TID Improvement Study, Kerry Henry, Army Research Development & Engineering Center; Jason W. Gaines, General Dynamics-OTS
- Two-Dimensional Modeling of Mortar Interal Ballistics, Clive R. Woodley, David Finbow, QinetiQ; Vladimir Titarev, Eleuterio Toro, Umeritek Limited
- The Mechanism Analysis of Interior Ballistics of Serial Chamber Gun, Dr. Sanjiu Ying, Charge Design Laboratory of China; Prof. Xiaobing Zhang, Prof.

Yaxiong Yuan, and Dr.Yan Wang, Ballistic Research Laboratory of China

Terminal Ballistics Oral Session #2

- Behind Armor Debris Computations with Finite Elements and Meshless Particles, Gordon R. Johnson and Robert A. Stryk, Network Computing Services, Inc.
- Experimental and Numerical Study of the Penetration of Tungsten Carbide Into Steel Targets During High Rates of Strain, Eva K. Friis, Nammo Raufoss AS; Oyvind Froyland and John F. Moxnes, FFI (Norwegian Defence Research Establishment)
- Mine Neutralisation with Small Calibre Projetile Impact, Mark Dijkstra, J.H. Meulman, TNO Defence Safety and Security

Vulnerability, Lethality and Wound Ballistics Oral Session

- The Application of Critical Perforation Analysis (CPA) to Military Personal Armour Research and Evaluation, Catherine H. Crawford and Philip Gotts, Defence Clothing Research and Project Support
- Fragment Patterns Behind Concrete Structures Caused by KE Projectiles, S. Lampert, Fene Jeanquartier, D. Hoffmann, and B. Lehmann, Armasuisse
- Mine Neutralisation with Small Calibre Projetile Impact, Mark Dijkstra, J.H. Meulman, TNO Defence Safety and Security

Thursday, 17 November 2005

Warhead Mechanisms Oral Session #1:

- Soft-Recovery of Explosively Formed Penetrators, David Lambert and Matthew Pope, Air Force Research Laboratory, Munitions Directorate; Stanley E. Jones and Jonathan Muse, Aerospace Engineering and Mechanics, University of Alabama
- The Gurney Velocity: A “Constant” Affected by Previously Unrecognized Factors, Joseph E. Backofen, BRIGS Co.
- The Influence of Post Detonation Burning Process on Blast Wave Parameters in Air, Meir Mayseless and I. Belsky, IDF, Armor Branch; E. Muzychuk, IMI, Central Laboratory

Interior Ballistics/Launch Dynamics Oral Session #2

- 3-D Finite-Element Gun Launch Simulation of a Surrogate Excalibur 155-mm Guided Artillery Projectile - Modeling Capabilities and its Implications, M.R. Chowdhury and A. Frydman, US Army Research Laboratory; J. Cordes, L. Reinhardt and D. Carlucci, US Army ARDEC, Analysis and Evaluation Division
- Caseless Ammunition and Advances in the Characterization of High Ignition Temperature Propellant (HITP), Paul Shipley, AAI Corporation; Erin K. Hardmeyer, US Army ARDEC; and Ben Ashcroft, Alliant Technical Systems
- Ballistic Launch to Space, Ed Schmidt and Mark Bundy, Army Research Laboratory
- A Novel Launcher for Cavitating Weapons, Chris Weiland and Pavlos Vlachos, Mechanical Engineering Department, Virginia Polytechnic Institute and State University; and Jon Yagla, Engagement Systems Department, Naval Surface Warfare Center

Warhead Mechanisms Oral Session #2

- The Role of Rayleigh Taylor Instability in Shaped Charge Jets Formation and Stability, Dr. Simcha Miller, Mr. Gershon Kliminz, Rafael Ballistic Center,
- Simulation of Cylinder Expansion Tests Using an Eulerian Multiple-Material Approach, Laura Donahue, R.C. Ripley, Martec, Ltd
- Application of Powder Tantalum Material for Explosively Formed Penetrator (EFP) Warhead, Richard Fong, Mike Hespos, William Ng, and Steven Tang, US Army ARDEC
- Oilwell Perforators: Theoretical Considerations, Brenden Grove, Schlumberger Reservoir Completions Center
- The Study on Lethality Simulation Method for Fragmentation Warhead, Yang Yunbin, Qu Ming, and Qian Lixin, Institute of Structual Mechanics, China Academy of Engineering Physics

Friday, 18 November 2005

Terminal Ballistics Oral Session #3:

- Performance Evaluation of Multi-Threat Body Armour Systems, B. Anctil and M. Keown, Biokinetics and Associates Ltd.; G. Pageau, M. Bolduc, and D. Bourget, Defence R&D Candada - Valcartier
- The Residual Damage in CFRP Composite After Ballistic Impacts (Experiments & Simulations), Koen Herlaar, TNO Defence, Security and Safety
- The Effect of Boundary Conditions on the Ballistic Performance of Textile Fabrics, Colin R. Cork, University of Manchester, School of Materials

General Oral Session #2

- Wind Tunnel Verification of the Performance of a Smart Material Canard Actuator, Paul Weinacht, William F. Drysdale, Travis Bogetti, and Rod Don, US Army Research Laboratory; James T. Arters, Jack R. Vinson, Aaron R. Hickman, University of Delaware; Lamar Auman, US Army Aviation and Missile RD&E Center; Oded Rabinovitch, Technion Israel Institute of Technology
- The Fragmentation of Metal Cylinders Using Thermobaric Explosives, William Andrews, Royal Military College of Canada; Michael Dunning, Defence R&D Canada – Suffield; and Kevin Jaansalu, Montana Tech (University of Montana)
- A Novel Test Methodology to Assess the Performance of Ballistic Helmets, B. Anctil and M. Keown, Biokinetics and Associates Ltd.; G. Pageau and D. Bourget, Defence R&D Candada - Valcartier
- Ballistic Analysis of Bulgarian Electroslag Remelted Dual Hard Steel Armor Plate, William Gooch, Matthew Burkins, and David Mackenzie, US Army Research Laboratory Weapons and Materials Research Directorate; Stefan Vodenicharov, Institute of Metal Science, Bulgarian Academy of Sciences

NATIONAL DEFENSE INDUSTRIAL ASSOCIATION

STRENGTH THROUGH INDUSTRY & TECHNOLOGY

22ND INTERNATIONAL SYMPOSIUM ON BALLISTICS

November 14-18, 2005

Vancouver
BC, Canada
Event #6210

International Ballistics Committee

International Symposium on Ballistics 2005

International Symposium on Ballistics 2005 is jointly organized and supported by the National Defense Industrial Association, USA in conjunction with the International Ballistics Committee

Symposium Co-Chairman: William Flis
Symposium Co-Chairman: Brian Scott

PREVIOUS INTERNATIONAL SYMPOSIA ON BALLISTICS

1st	Orlando, Florida, USA	1974
2nd	Daytona, Florida, USA	1976
3rd	Karlsruhe, Germany	1977
4th	Monterey, California, USA	1978
5th	Toulouse, France	1980
6th	Orlando, Florida, USA	1981
7th	The Hague, The Netherlands	1983
8th	Orlando, Florida, USA	1984
9th	Shrivenham, UK	1986
10th	San Diego, California, USA	1987
11th	Brussels, Belgium	1989
12th	San Antonio, Texas, USA	1990
13th	Stockholm, Sweden	1992
14th	Quebec City, Canada	1993
15th	Jerusalem, Israel	1995
16th	San Francisco, California, USA	1996
17th	Midrand, South Africa	1998
18th	San Antonio, Texas, USA	1999
19th	Interlaken, Switzerland	2001
20th	Orlando, Florida, USA	2002
21st	Adelaide, South Australia	2004
22nd	Vancouver, BC Canada	2005

SYMPOSIUM SCOPE AND OBJECTIVES

The objective of the 22nd International Symposium on Ballistics is to focus on potential technical advances and break-throughs in the 21st century in the general areas of:

- Interior Ballistics
- Launch Dynamics
- Exterior Ballistics
- Projectile and Warhead Design
- Terminal Ballistics
- Vulnerability
- Modeling and Simulation
- Wound Ballistics

Over 200 papers will be presented by authors from 26 countries.

SYMPOSIUM PROGRAM

Monday, November 14, 2005

2:00 pm - 5:00 pm	Registration
5:00 pm - 6:30 pm	Reception in Exhibit Area

Tuesday, November 15, 2005

7:00 am	Continental Breakfast and Registration
7:00 am - 6:00 pm	Exhibits Open
8:00 am	Opening Remarks ***C. Samuel Campagna***, National Defense Industrial Association
8:10 am	Welcome and Opening Remarks **William Flis,** DE Technologies, Inc. & **Brian Scott,** US Army Research Laboratory
8:20 am	**Keynote Address** ***Dr***. ***Robert Walker*****,** Director-General, Research and Development Programs (DGRDP), Defense Research and Development Canada
9:05 am	**Invited Presentation** From Columbia to Discovery: Understanding the Impact Threat to the Space Shuttle ***James D. Walker*****,** Southwest Research Institute
9:50 am	Morning Break

General Oral Session #1
Chairpersons: *B. Janzon and J. Carleone*

10:20 am	Plasma Ignition of a 30mm Cannon ***Richard A. Beyer, Andrew L. Brant, Joseph J. Colburn,*** US Army Research Laboratories
10:40 am	Numerical Computations of Subsonic and Supersonic Flow Choking Phenomena in Grid Finned Projectiles ***Nicolas* Parisé,** SNC Technologies, Inc.; ***Alain Dupuis***, Precision Weapons Section, Defense Research and Development Canada
11:00 am	Multiple Explosively Formed Penetrator (MEFP) Warhead Technologies for Mine and Improvised Explosive Device (IED) Neutralization **Richard Fong, William Ng, Steve Tang, LaMar Thompson**, U.S. Army Armament Research, Development and Engineering Center
11:20 am	The Use of Electric Power in Active Armour Applications ***Martin van de Voorde***, ***R. Boeschoten***, TNO Defence, Security and Safety
11:40 am	Prevention of Sympathetic Detonation between Reactive Armor Sandwiches **Andreas Holzwarth**, Fraunhofer-Institut für Kurzzeitdynamik
12:00 pm	Lunch

1:30 pm - 3:10 pm	**Exterior Ballistics Poster Session** **Chairpersons: Z. Wang and P.A. Karsten**

Terminal Ballistics Oral Session #1
Chairpersons: E. Lindén and C. Anderson

1:30 pm	Bullet Impact on Steel and Kevlar®/Steel Armor – Experimental Data and Hydrocode Modeling with Eulerian and Lagrangian Methods* ***Dale S. Preece, Vanessa S. Berg, Mathew A. Risenmay,*** Sandia National Laboratories
1:50 pm	Progress on the NDE Characterization of Impact Damage in Armor Materials ***Joseph M. Wells,*** JMW Associates
2:10 pm	Design, Analysis, and Testing of an Unconfined Ceramic Target to Induce Dwell ***Timothy J. Holmquist***, Network Computing Services, Inc.; ***C. Anderson, Jr***., Southwest Research Institute; ***Thilo Behner***, Ernst-Mach-Institut
2:30 pm	The Influence of Sabot Threads on the Performance of KE Penetrators against multiple plate targets ***Nick J. Lynch***, ***J. Stubberfield***, QinetiQ
2:50 pm	Visualization of Wave Propagation and Impact Damage in a Polycrystalline Transparent Ceramic - AlON ***Elmar Strassburger***, Fraunhofer Institut für Kurzzeitdynamik; ***Parimal Patel, James W. McCauley,*** US Army Research Laboratory; ***Douglas W. Templeton,*** US Army TARDEC
3:10 pm	Afternoon Break
3:40 pm - 5:20 pm	**Terminal Ballistics Poster Session #1** **Chairpersons: A. Diederen**

Exterior Ballistics Oral Session
Chairpersons: W. Reinecke and A. Dupuis

3:40 pm	Advanced Time-Accurate CFD/RBD Simulations of Projectiles in Free Flight **Jubaraj Sahu**, US Army Research Laboratory
4:00 pm	Aerodynamic Characterstics of a Grid Finned Projectile from Free-Flight Tests at Supersonic Velocities ***Alain Dupuis*****,** DRDC - Valcartier; ***Claude Berner***, French-German Research Institute
4:20 pm	Recent Computations and Validations of Projectile Unsteady Aerodynamics ***Roxan Cayaz***, ***Eric Carette***, Giat Industries; ***Rémy Thépot, Patrick Champigny***, Office National d'Études et de Recherches Aérospatiales
4:40 pm	The Derivation of Spin Stabilised Projectile Yaw Rates and Ballistic Model Coefficients Using Conventional CW Doppler Radar Systems ***John Tate***, FLEET
5:00 pm	Research of Flight Characteristics of Rod-Type Projectile with Triangular Cross-Section ***Wenjun Yi***, ***Xiaobing Zhang, Jianping Qian***, Ballistic Research Laboratory of China, Nanjing University of Science & Technology
5:20 pm	Adjourn for the Day

Wednesday, November 16, 2005

7:00 am — Continental Breakfast and Registration

7:00 am - 5:00 pm — Exhibits Open

8:00 am — Administrative Remarks

8:10 am - 9:50 am — **Terminal Ballistics Poster Session #2**
Chairpersons: J. Riegel and E. Hirsch

Exterior Ballistics Oral Session #2
Chairpersons: P. Nel and E. Schmidt

8:10 am — Impact of Nose-Mounted Micro-Structures on the Aerodynamics of a Generic Missile
Daniel Corriveau, Defence R&D Canada (DRDC - Valcatier)

8:30 am — Ballistic Simulations and Wind Tunnel Testing of 120 mm Mortar Bomb Tail Fin Geometries – In Search for Extra Range
Jukka Tiainen, Ari Makkonen, Patria Weapon Systems Oy; ***Mikko Korhonen, Timo Sailaranta***, TKK/Laboratory of Aerodynamics

8:50 am — Bringing Solid Fuel Ramjet Projectiles Closer to Application – An Overview of the TNO/RWMS Technology Demonstration Programme
Ronald G. Veraar, TNO Defence, Security and Safety Research Group Rocket Technology; ***Guido Giusti***, Rheinmetall Waffe Munition Schweiz AG

9:10 am — Analysis of Gliding Control for an Extended-Range Projectile
Zhongyuan Wang, ***Houqian Xu, Jinguang Shi, Wenjun Yi, Shaosong Chen***, Ballistic Research Laboratory of China, Nanjing University of Science & Technology

9:30 am — Theoretical Design for a Guided Supersonic Projectile
Pierre Wey, ***Claude Berner, Eckhart Sommer, Volker Fleck, Henry Moulard***, French-German Research Institute of Saint-Louis (ISL)

9:50 am — Morning Break

10:20 am - 12:00 pm — **Warhead Mechanisms Poster Session**
Chairpersons: R. Fong and F. Mostert

Interior Ballistics/Launch Dynamics Oral Session #1
Chairpersons: C. Candland and C. Woodley

10:20 am — Ceramic Gun Barrel Technology
Lawrence W. Burton, Jeffrey J. Swab, Ryan Emerson, Robert Carter, US Army Research Laboratory, Weapons & Materials Research Directorate

10:40 am — M865E3 Cold Target Impact Dispersion Study
Kerry Henry, Army Research Development & Engineering Center; ***Jason W. Gaines***, General Dynamics-OTS

11:00 am — An Alternative Technique to Evaluate and Characterize Pressure Waves in Large Calibre Guns
Victor Schabort, Denel Land Systems Western Cape

11:20 am — Two-Dimensional Modelling of Mortar Internal Ballistics
Clive R. Woodley, David Finbow, QinetiQ; ***Vladimir Titarev, Eleuterio Toro***, Numeritek Limited

11:40 am	The Mechanism Analysis of Interior Ballistics of Serial Chamber Gun ***Sanjiu Ying***, Charge Design Laboratory of China, Nanjing University of Science & Technology; ***Xiaobing Zhang, Qaxiong Yuan, Yan Wang***, Ballistic Research Laboratory of China, Nanjing University of Science & Technology
12:00 pm	Lunch

Terminal Ballistics Oral Session #2
Chairpersons: M. Mayseless and T. Holmquist

1:30 pm	Behind Armor Debris Computations with Finite Elements and Meshless Particles ***Gordon R. Johnson*****, Robert A. Stryk,** Network Computing Services, Inc.
1:50 pm	Expirmental and Numerical Study of the Penetration of Tungsten Carbide into Steel Targets During High Rates of Strain ***Eva K. Friis,*** Nammo Raufoss AS, ***Oyvind Froyland, John F. Moxnes,*** FFI (Norwegian Defence Researdh Establishment
2:10 pm	Fragmentation Behavior of Tungsten Alloy Cubes on Normal Aluminum Plate Targets ***Karl Weber*****,** Fraunhofer-Institut für Kurzzeitdynamik, Ernst-Mach Institut
2:30 pm	The Failure Kinetics of High Density DEDF Glass Against Rod Impact at Velocities From 0.4 to 2.5 km/s ***Thilo Behner***, ***V. Hohler, M. Moll***, Fraunhofer Institut für Kurzzeitdynamik (Ernst-Mach Institut); ***Ch. E. Anderson Jr.***, Southwest Research Institute; ***D. L. Orphal***, International Research Associates, Inc.; ***D. W. Templeton***, US Army RDECOM-TACOM
2:50 pm	Mine Neutralisation with Small Calibre Projectile Impact ***Mark Dijkstra, J.H. Meulman,*** TNO Defence, Safety and Security
3:10 pm	Afternoon Break

Vulnerability, Lethality and Wound Ballistics Oral Session
Chairpersons: R. Vaziri, A. Persson

3:40 pm	The Application of Critical Perforation Analysis (CPA) to Military Personal Armour Research and Evaluation ***Catherine H. Crawford, Philip Gotts***, Defence Clothing Research and Project Support
4:00 pm	An Efficient Mechanistic Approach to Modelling the Ballistic Response of Multi-Layer Fabrics ***Ali Shahkarami, Reza Vaziri, Anounsh Poursartip,*** Composites Group, Departments of Civil Engineering and Materials Engineering The University of British Columbia; ***Navin Tajani***, DuPont Advanced Fibers Systems
4:20 pm	Pencilling – A Novel Behind Armour Blunt Trauma Injury ***Eluned A. Lewis,*** Defence Clothing Research and Project Support; ***Ian Horsfall, Celia Watson***, Engineering Systems Department, Royal Military College of Science, Cranfield University
4:40 pm	Scaling the Dynamic Response of Armored Vehicle’s Floor Subjected to a Large Buried Charge ***Avidov Neuberger***, MOD, Tank Program Management; ***S. Peles***, IMI, Central Laboratory Division; ***D. Rittel***, Technion, Israel Institute of Technology, Faculty of Mechanical Engineering

5:00 pm — Fragment Patterns Behind Concrete Structures Caused by KE Projectiles
René Jeanquartier, D. Hoffmann, S. Lampert, B. Lehmann, Armasuisse

5:20 pm — Adjourn for the Day

<u>Thursday, November 17, 2005</u>

7:00 am — Continental Breakfast and Registration

8:00 am - 11:00 am — Exhibits Open

8:00 am — Adminstrative Remarks

8:10 am - 9:50 am — **Interior Ballistics/Launch Dynamics Poster Session**
Chairpersons: C. Woodley and C. Candlant

Warhead Mechanisms Oral Session #1
Chairpersons: M. Murphy and P.Y. Chanteret

8:10 am — Soft-Recovery of Explosively Formed Penetrators
David E. Lambert, ***Matthew Pope***, Air Force Research Laboratory, Munitions Directorate; ***Stanley Jones, Jonathan Muse***, University of Alabama, Aerospace Engineering and Mechanics

8:30 am — The Gurney Velocity: A "Constant" Affected by Previously Unrecognized Factors
Joseph E. Backofen, BRIGS Co.

8:50 am — Influence of Post Detonation Burning Process on Blast Wave Parameters in Air
Meir Mayseless, E. Muzychuk, IDF, Mil.; ***M. Mayseless, I. Belsky, IMI,*** Central Laboratory

9:10 am — Steerable Fragment Masses
Manfred Held, TDW/EADS

9:30 am — Penetration Performances of Tungsten-Copper Shaped Charge Liner
Seong Lee, Eun Pyo Kim, Youngmoo Kim, Sung Ho Lee, Moon-Hee Hong, Joon-Woong Noh, Agency for Defense Development

9:50 am — Morning Break

10:20 am - 12:00 pm — **Vulnerability/Lethality/Wound Ballistics Poster Session**
Chairpersons: *W. Gooch*

Interior Ballistics/Launch Dynamics Oral Session #2
Chairpersons: ***B. Burns and R. Cayzac***

10:20 am — 3-D Finite-Element Gun Launch Simulation of a Surrogate Excalibur 155-mm Guided Artillery Projectile - Modeling Capabilities and its Implications
M.R. Chowdhury, A. Frydman, US Army Research Laboratory; ***J. Cordes, L. Reinhardt, D. Carlucci***, US Army ARDEC, Analysis and Evaluation Division

10:40 am — Method of Calculating Initial Firing Data of Artillery Laser Terminal-Guidance Weapon System
Feipeng Zeng, ***Liren Liu***, Faculty of Artillery Command, Nanjing Artillery Academy

11:00 am Caseless Ammunition & Advances in the Characterization of High Ignition Temperature Propellant
Patricia M. O'Reilly, Erin Hardmeyer, Chad Sensenig, US Army ARDEC; ***Ben Ashcroft***, Alliant Techsystems; ***Dave Cleveland***, The Johns Hopkins University, 0Applied Physics Laboratory; ***Bo Engel, Paul Shipley***, AAI Corporation

11:20 am Ballistic Launch to Space
Edward Schmidt, M. Bundy, US Army Research Laboratory

11:40 am A Novel Launcher for Cavitating Weapons
Chris J. Weiland, Pavlos P Vlachos, Dept of Mechanical Engineering Virginia Tech; Jon J Yagla, Mechanical Engineer Engagement Systems Department Naval Surface Warfare Center

12:00 pm Lunch

Warhead Mechanisms Oral Session #2
Chairpersons: R. Brown and M. Held

1:30 pm The Role of Rayleigh Taylor Instability in Shaped Charge Jets Formation and Stability
Simcha Miller, Gershon Kliminz, Rafael Ballistic Center

1:50 pm Simulation of Cylinder Expansion Tests Using an Eulerian Multiple-Material Approach
Laura K. Donahue, ***R.C. Ripley***, Martec, Ltd.

2:10 pm Application of Powder Tantalum Material for Explosively Formed Penetrator Warhead
Richard Fong, ***William Ng, Steven Tang, Michael Hespos***, US Army Armament Research, Development and Engineering Center

2:30 pm Oilwell Perforators: Theoretical Considerations
Brenden M. Grove, Schlumberger Reservoir Completions Center

2:50 pm Planar Cutting Jets from Shaped Charges
Geoffery EB Tan, ***T.K. Lam, Y.K. Tham***, DSO National Laboratories

3:10 pm The Study on Lethality Simulation Method for Fragment Warhead
Yang Yunbin, Qu Ming, Qian Lixin, Institute of Structural Mechanics, China Academy of Engineering Physics

3:30 pm Adjourn for the Day

4:00 pm - 5:30 pm Reception

Friday, November 18, 2005

7:00 am Continental Breakfast and Registration

8:00 am Adminstrative Remarks

Terminal Ballistics Oral Session #3
Chairpersons: I. Cullis and D. Nandlall

8:10 am Performance Evaluation of Multi threat Body Armour Systems
B. Anctil, M. Keown, Biokinetics and Associates Ltd.; **G. Pageau, M. Bolduc D. Bourget**, Defence R&D Canada – Valcartier

8:30 am	Finite Element Simulations and Experiments to Determine the Residual Damage of a CFRP Composite Material After Ballistic Impacts ***Koen Herlaar, M. Van der Jagt-Deutekom,*** TNO Defence, Security and Safety
8:50 am	The Effect of Boundary Conditions on the Ballistic Performance of Textile Fabrics ***Colin R. Cork***, University of Manchester, School of Materials
9:10 am	Terminal Ballistic Effects of Low Density Materials Used as Confinement Plates for Explosive Reactive Armours ***Hanspeter Kaufmann,*** RUAG Land Systems; ***André Koch***, Armasuisse
9:30 am	Quantification of the Effect of Using the Johnson-Cook Damage Model in Numerical Simulations of Penetration and Perforation ***Charles E. Anderson Jr., T. R. Sharron***, Southwest Research Institute; ***Timothy J. Holmquist***, Network Computing Services, Inc.
9:50 am	Morning Break

General Oral Session #2
Chairpersons: V. Sanchez-Galvez and P. Cuniff

10:20 am	Comparisons of Internal Ballistics Simulations of the AGARD Gun ***Clive R. Woodley***, QinetiQ; ***Alain Carriere, Patrice Franco, Dieter Hensel, Julien Nussbaum***, Institut Franco-Allemand de Recherches de Saint-Louis (ISL); ***Tatjana Gröge***, Ernst-Mach-Institut (EMI); ***Stefan Kelzenberg***, Fraunhofer-Institut für Chemische Technologie (ICT), ***Baptiste Longuet***, DGA/DCE/ETBSr3
10:40 am	Wind Tunnel Verification of the Performance of a Smart Material Canard Actuator ***Paul Weinacht***, ***William F. Drysdale, Travis Bogetti, Rod Don***, US Army Research Laboratory; ***James T. Arters, Jack R. Vinson, Aaron R. Hickman***, University of Delaware; ***Lamar Auman***, US Army Aviation and Missile RD&E Center; ***Oded Rabinovitch***, Technion Israel Institute of Technology
11:00 am	Fragmentation of Metal Cylinders Using Thermobaric Explosives ***M.R. Dunning***, Defence Research and Development - Suffield, ***W.S. Andrews,*** Department of Chemistry and Chemical Engineering, Royal Military College of Canada; ***K.M. Jaansalu***, Department of Metallurgical and Materials Engineering, The University of Montana
11:20 am	A Novel Test Methodology to Assess the Performance Ballistic Helmets ***B. Anctil, M. Keown,*** Biokinetics and Associates Ltd.; ***D. Bourget, G. Pageau,*** Defence R&D
11:40 am	Ballistic Analysis of Bulgarian Electroslag Remelted Dual Hard Steel Armor Plate ***William Gooch, Matthew Burkins and David Mackenzie***, US Army Research Laboratory, Weapons and Materials Research Directorate; Stefan Vodenicharov, Institute of Metal Science, Bulgarian Academy of Sciences
12:00 pm	Presentation of Awards The Rosalind and Pei Chi Chou Award for Young Authors The Neil Griffiths Memorial Award The Louis and Edith Zernow Award
12:15 pm	Invitation to the 23rd International Symposium on Ballistics, Tarragona, Spain, 2007
12:25 pm	Closing **William Flis,** DE Technologies, Inc. & **Brian Scott,** US Army Research Laboratory

POSTER SESSIONS START HERE

Exterior Ballistics Poster Session
1:30 pm - 3:10 pm Tuesday, November 15

1913 Fractional Calculus for Design of Aerodynamic Missile's Autopilot and Digital Realization
Bangchu Zhang, ***Chenming Li, Zipeng Han, Zou Yun, Fuming Xu***, Ballistic Research Laboratory of China, Nanjing University of Science & Technology

1915 The Simulation of Rocket Trajectory in Simulink
Xin Changfan, Nanjing University of Science & Technology

1924 Establishing a Pitch Damping Test Capability at CSIR Defencetek
Fabrizio Dionisio, CSIR, Defencetek

1944 The Investigation About Using Different Guidance Laws on Improving Impact Point Deviation of a Rocket
Handong Zhao, ***Fang Wang, Qingshang Liu***, Key Laboratory of Instrumentation and Dynamic Measurement, North University of China

1951 Numerical Integration Method Based on 4th Largrange Polynomial of Strap-Down INS System
Guoguang Chen, ***Xiaoli Tian, Changfan Xin, Yaqi Bao***, North University of China

1952 Research on Real Time Trajectory Measure Device of Range
Changfan Xin, Guoguang Chen, Xiaoli Tian, North University of China

1953 Research on Attitude Control Strategy of Glide Range Extend Rocket
Xiaoli Tian, Guoguang Chen, Changfan Xin, North University of China

1954 Optimal Algorithm of Glide Range Extend Rocket's Trajectory
Guoguang Chen, Xiaoli Tian, Changfan Xin, North University of China

1978 Practical Propulsion by Directed Energetic Processes
Joseph P. Backofen, BRIGS Co.

2014 Investigating the Method of Obtaining Ammunition Roll Attitude by Detecting the Geomagnetic Vector
Hongsong Cao, ***Guoguang Chen***, Department of Mechatronics Engineering, North University of China

2065 External Ballistic Trajectory Computations for Direct/Indirect Fire Weapon Systems
David J. Norton, General Dynamics Canada

2087 The Influence of Laser Rangefinder Parameters on the Hit Probability in Direct Tank Fire
Vladimir Cech, OPROX, Inc., ***Jiri Jevicky***, Department of Mathematics, University of Defense

2123 Flight Dynamics Modeling and Experiment for Composite Concepts. Application to Ribbon Aerodynamic Stabilization
Christopher Grignon, S.Heddadj, Giat Industries

2128 Onboard Measurements with Magnetic Sensors: Determination of the Attitude and the trajectory Position
V. Fleck, E. Sommer, S. Changey, French-German Research Institute (ISL); ***D. Beauvois***, Ecole Superirure d'Electrecite (Supelec)

2133 Aerodynamic Characteristics of a Long Range Spinning Artillery Shell Obtained from 3D Magnetic Sensors
V. Fleck, E. Sommer, C. Berner, French-German Research Institute (ISL); ***A. Dupuis***, DRDC

2143 Experimental Testing and Numerical Simulation of Separation Disturbances for Two-Stage Kinetic Energy Missiles
Nicolas Parisé, SNC Technologies, Inc.; ***Richard Lestage, Francoise Lesage***, Precision Weapons Section, Defense Research and Development Canada Valcartier

2147 Numerical Study on the Base Drag Characteristics of a Base Bleed Projectile with a Central Propulsive Jet
Chang-Kee Kim, Agency for Defense Development; ***J.Y. Choi***, Pusan National University, Department Aerospace Engineering

2169 Solid Fuel Ramjet (SFRJ) Propulsion for Artillery Projectile Applications – Dynamic Testing Progress
Anton Stockenström, Dynax

3010 Pitch and Bending During In-Flight Extension
W. G. Reinecke, Institute for Advanced Technology; ***M. G. Miller,*** Physical Sciences, Inc.

4004 Improvements in Aerodynamic Design for KE Less-Lethal Projectiles
Jamie H. Cuadros, Arts & Engineering

Terminal Ballistics Poster Session #1
3:40 pm - 5:20 pm Tuesday, November 15

1001 Numerical Simulations of Silicon Carbide Tiles Impacted by Tungsten Carbide Spheres
Constantine G. Fountzoulas, Jerry C. LaSalvia, Bryan A. Cheeseman, Weapons and Materials Research Directorate; ***Michael J. Normandia***, Ceradyne, Inc.

1007 Shock Mitigation for Blast Protection Using Hertzian Tapered Chains
Robert Doney, US Army Research Laboratory; ***Surajit Sen***, Department of Physics, State University of New York at Buffalo

1011 A Predictive Model for the Dwell/Penetration Transition Phenomenon
Jerry C. LaSalvia, US Army Research Laboratory

1012 Effect of Ceramic Thickness on the Dwell/Penetration Transition Phenomenon
Jerry C. LaSalvia, US Army Research Laboratory

1014 The Development of Hybridized Thermoplastic-Based Structural Materials with Applications to Ballistic Helmets
Shawn Walsh, ***Brian R. Scott, David M. Spagnuolo***, AMSRD-ARL-WM-MB

1015 Time Resolved Observation of the Deformation and Surface Strain of a Textile Fabric Subject to Ballistic Impact
Brian Scott, ***Peter Dehmer***, US Army Research Laboratory; ***Timothy Schmidt***, Trilion Quality Systems

1016 Analytic Design Trends of Fabric Armor
Brian Scott, ***Chian-Fong Yen***, US Army Research Laboratory

1018 High-Speed Photographic Study of Wave and Fracture Propagation in Fused Silica
Elmar Strassburger, Fraunhofer-Institut für Kurzzeitdynamik, Ernst-Mach-Institut (EMI); ***Parimal Patel, James W. McCauley,*** US Army Research Laboratory; ***Douglas W. Templeton***, US Army TARDEC

1022 Low Velocity Ballistic Properties of Shear Thickening Fluid (STF)–Fabric Composites
M. J. Decker, R. G. Egres, N. J. Wagner, University of Delaware, Dept. of Chemical Engineering and Center for Composite Materials; E. D. Wetzel, U.S. Army Research Laboratory

1023 An Approximate Solution of the Long-Rod Penetration Equations
William Walters, ***Cyril Williams,*** ARL, Terminal Effects Division

1901 Tubular Projectile Interaction with Stationary and Moving Oblique Plates
Olof Andersson, Swedish Defence Research Agency (FOI), Weapons and Protection Division

1911 A Study on the Moving Features of Double-Layer Explosive Reactive Armor with Definite Angle by Numerical Simulation and Experiments
Zhengxiang Huang, ***Xianfeng Zhang, Gang Li,*** School of Mechanical Engineering, Nanjing University of Science & Technology

1927 Mechanics of Structural Design of EPW Warhead
X.W. Chen, Institute of Structural Mechanics, China Academy of Engineering Physics

1928 Armour Qualification Utilizing Maximum Likelihood Ballistic Limit Calculation
Moshe Ravid, ***Shlomo Galperin***; Rimat Advanced Technologies, Ltd.

1934 Perforation of Concrete Targets by an Eroding Tungsten-Alloy Rod
Stephan Lampert, Rene Jeanquartier, Armasuisse

1955 Ballistic Properties of Single-Melt Titanium-6Aluminum-4Vanadium Alloy Plate
Brij J. Roopchand, US Army Tank-Automotive and Armament Command, Armament Research, Development, & Engineering Center

1987 Preliminary Investigations of Potential Light Weight Metallic Armour Applications
Martin van de Voorde, A.M. Dierderen, K. Herlaar, TNO Defence, Safety and Security

2001 Oblique Warhead Penetration and Perforation of Multi-Layered Metallic Targets
Yongxiang Dong, ***Feng Shunshan, Wang Fang***, State Key Laboratory of Explosion Science & Technology, Beijing Institute of Technology

2019 Influence of Projectile Material on Yawed Long Rod Projectiles Penetrating Oblique Plates
Ewa Lidén, Swedish Defence Research Agency (FOI), Weapons and Protection Division

2035 Advanced Aliphatic Polyurthane Resins for High Durability and Superior Ballistic Performance Laminated Glass
Francisco Folgar, INTER Materials, LLC

2037 Impact and Penetration of B4C Ceramic, Aluminum, and Berlyllium by Depleted Uranium Rods at 2.0 KM/S
Scott A. Mullin, ***James D. Walker, Carl E. Weiss***, Southwest Research Institute; ***Paul O. Leslie***, Los Alamos National Laboratories

2122 A Comparison of Some Analytical and Empirical Models for Kinetic Energy Penetration of Semi-Infinite and Finite Thickness Steel Targets
Nick J. Lynch, ***J T Mills***, QinetiQ

2181 Computed Tomography of High-Speed Events
Karsten Michael, Philip Helberg, Fraunfoher Institute for High Speed Dynamics, Ernst-Mach-Institut

2186 Characterization of Behind-Armor Debris Particles from Tungsten Penetrators
Brad A. Pedersen, ***S. Bless***, Institute for Advanced Technology

Terminal Ballistics Poster Session #2
8:10 am - 9:50 am Wednesday, November 16

2050 On the Critical Thickness of Ceramic to Shatter WC-Co Bullet Cores
Paul J. Hazell, Engineering Systems Department, Cranfield University, Royal Military College of Science; ***C. J. Roberson***, Advanced Defence Materials Limited

2060 The Effect of Spaced Armour on the Penetration of Shaped Charge Warheads
James D. Shattock, Cranfield University

2072 Modeling Impact and Penetration Using a Deterministic and Probabilistic Design Tool
David S. Riha, ***Jason B. Pleming, Ben H. Tucker, Scott A. Mullin, James D. Walker, Carl E. Weiss***, Southwest Research Institute; ***Edward A. Rodriguez, Paul O. Leslie***, Los Alamos National Laboratories

2106 On the Ballistic Efficiency of the Three Layered Metallic Targets
Stanislav Rolc, Military Technical Institute of Protection; ***Jaroslav Buchar***, Mendel University; ***Giovanni Cozzani***, OTO MELARA S.p.A ***Vojtech Hruby***, University of Defence

2107 Effect of the Temperature on the Ballistic Efficiency of Plates Made From Cast Iron
Stanislav Rolc, Military Technical Institute of Protection; ***Jaroslav Buchar***, Mendel University

2113 Displacement Device to Measure the Acceleration of the Bulge of RHA Plates Under Anti-Tank Mine Blast
Manfred Held, TDW/EADS; ***Peter Heeger***, WTD; ***Josef Kiermeir***, CONDAT

2116 Defeating Mechanisms of Explosive Reactive Armour Sandwiches
Manfred Held, TDW/LFK/EADS

2121 Comparisons of Unitary and Jacketed Rod Penetration into Semi-Infinite and Oblique Plate Targets at System Equivalent Velocities
John Stubberfield, N J Lynch, QinetiQ; ***I Wallis***, QinetiQ Farnborough

2126 Finite Element Simulations and Experiments of Ballistic Impacts on High Performance PE Composite Material
Koen Herlaar, M. Van der Jagt-Deutekom, TNO Defense, Security and Safety

2129 The Use of Foam Structures in Armoured Vehicle Protection Against Landmines
David A. Cendón, ***Vincente Sanchez-Galvez, Francisci Galvez, Alejandro Enfedaque***, Departamento de Ciencia de Materiales, E.T.S.I. Caminos, Canales y Puertos, Universidad Politecnica de Madrid, Spain

2136 The Numerical Simulation of the Impact of an Aluminum Cylinder into a Steel Cone
Izak M. Snyman, Defencetek Landwards Programme, CSIR

2139 Characterization of Al 6061-T6 using Split Hopkinson Bar Tests and Numerical Simulations
Amal Bouamoul, ***Manon Bolduc***, DRDC - Valcartier

2145 Finite Element Modeling of Light Armoured Vehicles (LAV) Welds Heat Affected Zones Sublected to an Anti-Vehicular (AV) Blast Landmine Loading: A Summary of the Numerical Model and Experiment
Patrice Gaudreault, Defence Research & Development Canada; ***Amal Bouamoul, Robert Durocher, Benoit St-Jean***, DRDC Valcartier

2151 Designer Projectiles by Density Variation: Towards the Nano-Projectile
John P. Curtis, QinetiQ

2160 Numerical Simulation for the Front Section Effect of Missile Warhead on the Target Perforation
Ho Soo Kim, ***Ki-Sun Yeom, Seong Shik Kim***, Agency for Defense Development (ADD); Larry Sotsky, US Army ARDEC

2180 The Penetration Process of Projectiles into Long Bars in the Axial Direction
Dan Yaziv, G. Gans, Y. Reifen, RAFAEL

2199 The Electromagnetic Launch Trends Utilization for Shaped Charge Jets Penetration Depth Decrease
S.V. Demidkov, Effective Soft Ltd.

3003 Simulation of the Perforation of Low Mass Long L/D Rods Against Finite RHA Plates
P. Church, ***I. Cullis, A Bowden, D Gibson***, QinetiQ, Ltd.

3011 Deflection and Fracture of Tungston Rods by Yawed Impact
S. Bless, R. Russell, Instutite for Advanced Technology; ***K. Tarcza***, US Army ARDEC; ***E. Taleff***, Department of Mechanical Engineering, The University of Texas at Austin; ***M. Huerta***, The University of Texas at El Paso

3012 Anomalies in the Strength of Alumina under Dynamic Compression
T. Beno, S. Bless, S.Nichols, Instituite for Advanced Technology

3014 On the 3D Visualization of Ballistic Damage in TI-6AL-4V Applique Armour with X-Ray Computed Tomography
J.M. Wells, JMW Associates; ***W.H. Green, N.L. Rupert***, US Army Research Laboratory, Weapons & Materials Research Division; J***ohn M. Winter, Jr.***, ORISE Contractor at WMRD; ***S.J. Cimpoeru***, DSTO Melbourne

4012 Analytical Models for Foam, Ice and Ablator Impacts into Space Shuttle Thermal Tiles
James D. Walker, Sidney Chocron, Walt Gray, Southwest Research Institute

4013 CTH Simulations of Foam and Ice Impacts into the Space Shuttle Thermal Protection System Tiles
Sidney Chocron, Walt Gray, James D. Walker, Southwest Research Institute

4016 Damage Created in Composite Sheet by Explosives – Effects of Fibre Type, Explosive Mass and Attenuating Material
M. R. Edwards, R. Unwin, Centre for Materials Science and Engineering, Cranfield University

Warhead Mechanisms Poster Session
10:20 am - 12:00 pm, November 16

1914 Experimental Investigation of Equivalent Blast Characteristics for Aluminiferous Explosive in Shallow Underwater
Wenbin Gu, ***Jianqing Liu, Qingli Su, Weiping Zhou***, Ballistic Research Laboratory of China, Nanjing University of Science & Technology

1935 Break-up of Copper Shaped – Charge Jets: A Combined Experimental/Numerical/Analytical Approach
Jacques Petit, Centre d'Etudes de Gramat; ***V. JeanClaude, C. Fressemgeas***, Laboratoire de Physique et Mecanique des Materiaux, Universite de Metz/CNRS

1949 A Theoretical Analysis for Initial Fragment Velocity and Peak Overpressure of a Blast Fragmentation Device
Jin Jianming, Institute of Structural Mechanics, China Academy of Engineering Physics

1963 Scaling the Dynamic Response of Armored Vehicle's Floor Subjected to a Large Buried Charges
Avidov Neuberger, IMOD, MANTAK, Tank Program Management; ***S. Peles***, IMI Central Laboratory Division; ***D. Rittel***, Technion, Israel Institute of Technology, Faculty of Mechanical Engineering

1984 High-Speed Flash X-Ray Computed Tomo-Cinematography
Philip Helberg, ***Karsten Michael***, Fraunhofer Institute for High-Speed Dynamics, Ernst-Mach-Institut

2002 The Influence of Parameters Other Than Liner Velocity on Shaped Charge Jet Coherence
Frederik Mostert, CSIR Defencetek; ***C. J. Terblanche***, Denel Land Systems - Western Cape; ***M. F. Maritz***, Department of Applied Mathematics, University of Stellenbosch

2053 Comparison of Vulnerability and Performances of Insensitive Munitions (IM) and Non IM Directed Energy Warheads
Frederic Peugeot, MSIAC, NATO HQ

2059 Trumpet Shaped Liners' Influence on Slug Properties
Eitan Hirsch, Consultor***; Meir Mayseless***, IMI Central Laboratory

2077 A Study on the Structure of Small Caliber EFP
Chen Zhigang, Zhao Taiyong, Hou Xiucheng, Dong Surong, The Research Institute of Explosive Demolition & Defence Technology, North University of China; ***You Zheng***, Department of Precision Instruments and Mechanics, Tsinghua University

2078 A Framework for the Analyses and Visualization of X-Ray Computed Tomography Image Data using a Compute Cluster
Jeffrey R. Wheeler, US Army Research Laboratory; ***William H. Green***, US Army Research Laboratory, Weapons & Materials Research Division; ***Michael Schuresko***, Baskin School of Engineering, University of California; Michael Patrick ***Lowery***, Computational Mathematics Department, University of California

2137 An Artillery Shell for Anti-Bunker Applications (155 ABS)
Rémi Boulanger, Giat Industries; ***Anders Vangen Jordet, Dagfinn Hoff***, NAMMO Raufoss

2141 Development of a TMRP-6 Surrogate Mine
Yves Baillargeon, ***A. Sirois and G. McIntosh***; DRDC Valcartier

2148 Use of Foamed TNT Mixtures as a Dispersion Charge of Submunitions
Jun Sik Hwang, S.-K. Kwon, C.-K. Kim, S.-W. Kwon, S.-S. Kim, S.-H. Moon, Explosive Trains and Gun Propellant Team, Agency for Defense Development

2152 Wall Breaching Tandem Warhead
Andreas Helte, Torgny Carlsson, Håkan Hansson, Svante Karlsson, Jonas Lundgren, Lars Westerling, Håkan Örnhed, Swedish Defence Research Agency, FOI, Weapons and Protection Division

2156 An Analytical Penetration Model for Jets with Varying Mass Density Profiles
Milton F. Maritz, Stellenbosch University; ***Klaus D. Werneyer***, TTP Products; ***Frederik J. Mostert***, Defencetek

2168 Peripheral Initiation Technology Development
Arthur S. Daniels, ***Ernest L. Baker, William J. Poulos, Vladimir M. Gold, B. Fuchs***, US Army ARDEC

2175 Shaped-Charge Jet Stability Calculations: The Role of Initial and Boundary Conditions
James S. Stolken, ***S. Christian Simonson, Mukul Kumar***, Lawrence Livermore National Laboratory

3007 Enhanced Focused Fragmentation Warhead Study
Richard Fong, ***William Ng, Peter Rottinger, Steve Tang***, US Army Armaments Research, Development and Engineering Center

4015 Microstructure and Properties of the Explosively Formed Petals in Aluminium Alloys
M. R. Edwards, J. M. Cassar, Centre for Materials Science and Engineering, Cranfield University

Interior Ballistics/Launch Dynamics Poster Session
8:10 am - 9:50 am November 17

1017 In-Bore Mechanics Analysis of the M855 Projectile
Joseph T. South, James F. Newill, US Army Research Laboratory

1020 Dynamic Strain Measured in a 105-mm Composite Gun Barrel - A Fiction or Reality
Jerome T. Tzeng, US Army Research Laboratory

1916 A Vector Way for Calculating Propellant's Combustion Performance
Wei Zhifang, Department of Mechanical and Electronic Engineering, North University of China

1931 Interior Ballistics Code Applied to ETC Concept: Computations and Validations
Gilles Legeret, ***Dominique Boisson***, Giat Industries

2004 The FHIBS Internal Ballistics Code
Clive R. Woodley, Steve Billett, QinetiQ; ***Caroline Lowe***, Department of Applied Mathematics and Theoretical Physics, Centre for Mathematical Studies, University of Cambridge; ***William Speares***, The Cylinders; ***Eleuterio Toro*** Laboratory of Applied Mathematics, Faculty of Engineering, University of Trento

2005 Modelling the Ignition of 40mm Gun Charges
Clive R. Woodley, QinetiQ

2020 Thermo-Mechanical Erosion Study of the 120mm Chromium Coated Gun Barrel: Computation and Validation of the Heat Exchange Boundary Condition
Dominique Boisson, ***Gilles Légeret, Roxan Cayzac***, Giat Industries

2031 MOBIDIC-NG: A 1D/2D CFD Code Suitable for Interior Ballistics and Vulnerability Modelling
Baptiste Longuet, Pascal Millet, Eric Taiana, ETBS; ***Patrick Della, Pieta Christiane Reynaud***, SNPE Matériaux Energétiques CRB; ***Patrice Franco, Alain Carrère***, Institut Franco-Allemand de Recherches de Saint-Louis (ISL); ***Gilles Légeret***, ***Dominique Boisson***, Giat Industries; ***Alexandre Papy***, ERM ABAL 30

2070 Barrell Life Results of the 5.56 mm XC77A1 Cartridge
Etienne Munger, SNC Technologies, Inc.

2117 Further Investigation of the Effect Known as Electrothermal Pyrolysis
Steve R. Fuller, M.J. Taylor, QinetiQ

2150 Determination of Force and Temperature Impact on Missile's Fuel Charge in Process of Ignition
Dmitriy Orlov, GDT Software Group

2161 Unsteady Intermediate Ballistics: 2D and 3D CFD Modelling, Application to Sabot Separation
Roxan Cayzac, ***Eric Carette***, Giat Industries, Division Munitions; ***Thierry Alziary de Roquefort***, Université de Poitiers, Laboratoire d'Études Aérodynamiques; ***Philippe Bidorini, Emmanuel Bret, Pascal Delusier, Serge Secco***, DGA/ETBS, Direction de l'Expertise Technique

2166 Large Caliber Firing with Electro Thermal-Chemical Ignition (ETI)
Jonathan D. Shin, ***John J. O'Reilly, David T. Keyser***, US Army Research, Development and Engineering Center - TACOM; ***Jahn Dyvik***, United Defense L.P.

3006 Rail Gun Test Projectile for Improved Developmental Testing of Precision Munition Electronics
T. Myers, D. Carlucci, J.A. Cordes, US Army ARDEC, Analysis and Evaluation Division, Fuze and Precision Munitions Technology Directorate

4010 Improved Mortar Barrel Thermal Model
M. Pocock, C. Guyott, Frazer-Nash Consultancy Ltd; ***P. Locking***, BAE Systems, Land Systems

Vulnerability/Lethality/Wound Ballistics Poster Session
10:20 am - 12:00 pm November 17

1855 On Incorporating XCT into Predictive Ballistic Impact Damage Modeling
Joseph M. Wells, JMW Associates

1878 New Soft-Target Failure Criteria for System-Analytical Considerations
Markus J. Estermann, RUAG Defence, Warhead Division; ***Beat P. Kneubuhl,*** Aramasuisse

1941 Protecting Vehicles from Landmine Blasts
Sheri L. Hlady, Denis Bergeron, Defence R&D Canada – Suffield; ***Rene Gonzalez***, US Army, PM Light Tactical Vehicles

1957 Office of Naval Research Limb Protection Program
Graham K. Hubler, NRL

1980 Survivability and Lethality Assessment Software Based on Virtual Mode Technology
Lu Yonggang, Qian Lixin, Yang Yubin, Liu Tong, Institute of Structural Mechanics, CAEP

1981 "TBM-Xpert" - A New Endgame Code: Features and Validation
Werner Arnold, EADS-TDW Gesellschaft für verteidigungstechnische; ***E. Rottenkolber***, NUMERICS GmbH

1989 The Use of Ballistic Knowledge in Ammunition Safety Cases
Martin van de Voorde, TNO Defence, Safety and Security

2011 A Note on the Roecker-Ricchiazzi Model of Penetrator Trajectory Instability
William J. Flis, DE Technologies, Inc.

2022 Numerical Calculation and Simulation of Missile Jet-Airplane Interaction
Feipeng Zeng, Faculty of Artillery Command, Nanjing Artillery Academy

2111 Need for Enhanced Protection Against Blast Threats for Soldiers Exposed to Roadside Improvised Explosive Devices (IEDs)
François-Xavier Jetté, Jean-Philippe Dionne, Aris Makris, Med-Eng Systems, Inc.; ***Karl Masters***, PEO Soldier; ***Christine Perritt,*** PM Soldier Equipment

2119 WitnessMan: *The* Software Tool to Design, Analyse and Assess a Witness Pack with Respect to Military and Medical Effects on an (Un)protected (Dis)mounted Soldier.
Theo L.A. Verhagen, R. Kemper, H. Huisjes, S.G. Knijnenburg, A. Pronk, M.H. van Klink, TNO Defence, Security and Safety

2154 Injury Risks Resulting from Deminer Position
François-Xavier Jetté, Jean-Philippe Dionne, Ismail El Maach, Aris Makris, Matt Ceh, Med-Eng Systems, Inc.; ***Denis Bergeron***, Defence R&D Canada Suffield

2163 RPG Mitigation for Military Vehicles
Karl Pfister, Dipl. Ing (FH) Armatec Survivability Corporation

2164 Protection Against Closely-Spaced Impacts by Small Arms Bullets
Michael J. Iremonger, Cranfield University, Royal Military College of Science; ***Abdullah Alsalmi***

3013 Vulnerability Evaluations of 30mm Airburst Ammunition
Quoc Bao Diep, ***Eimund Smedstad***, Nammo Raufoss AS; ***Nick Rogers***, System Design Evaluation (SDE)

3018 Challenges and a Solution in Determining Land Mine or IED Neutralization Effectiveness
Robert Colbert, Mark Majerus, William Clark, DE Technologies, Inc.

4011 Numerical and Experimental Analysis of the Detonation of Sand-Buried Mines
N. Heider, A. Klomfass, Fraunhofer-Institut für Kurzzeitdynamik, Ernst-Mach-Institut

The symposium registration fees are:

	Regular	Late/Onsite after 10/28/05
	$950 (US)	$1045 (US)
IBC Committee Appreciation Dinner	$75 (US)	
Guest at Both Receptions	$75 (US)	
Guest at One Reception	$50 (US)	

The symposium registration fee includes attendance at all sessions, bound symposium proceedings with CD, continental breakfasts, coffee breaks, lunches, receptions, and administrative costs. The registration fee will also include a compact disc (CD) which contains a cumulative database of titles, authors and abstracts of all of the 22 Ballistics Symposia.

To register online for this conference visit: http://register.ndia.org/interview/register.ndia?~Brochure~6210. You can also visit the NDIA website at www.ndia.org and select "Schedule of Events". Then select 2005 November and scroll down to the 22nd International Symposium on Ballistics. Once there, select the blue "Register" link in the lower left hand corner of your screen. Review your information and then select "submit" one time only and then select "confirm". On-line registration will close at 5:00 pm EST on October 28, 2005. You must register on-site after this date.

-or-

You may fax the completed registration form contained in this brochure to (703) 522-1885.

-or-

You may mail the completed registration form contained in this brochure to: Event # 6210, National Defense Industrial Association, 2111 Wilson Boulevard, Suite 400, Arlington, VA 22201-3061.

Payment must be made at the time of registration. Registrations will not be taken over the phone.

Cancellations and Refund Policy

Registrants who cannot attend the 22nd International Symposium on Ballistics must provide written notification via email to bbommelje@ndia.org or fax to (703) 522-1885 on or before September 16, 2005 to avoid a cancellation fee.

Cancellations received between September 16, 2005 and October 28, 2005 will receive a refund minus a $75 cancellation fee. No refunds will be given to cancellations recieved after October 28, 2005 however, **SUBSTITUTIONS ARE WELCOME IN LIEU OF CANCELLATIONS.**

You must have a government picture identification (drivers license, passport, military ID, etc.) to receive a symposium badge. Badges must be worn at all times during the symposium.

Special Needs

NDIA supports the Americans with Disabilities Act of 1990. Attendees with special needs should call (703) 522-1820 prior to October 3, 2005.

Hotel Accommodations

A limited block of rooms have been reserved at the Fairmont Waterfront Hotel. The industry room rate is $219 Canadian (approximately $180 US). The government symposium room rate is approximately $114 Canadian ($94 US). Please call (604) 691-1991 to make reservations.

In order to ensure the discounted NDIA rate, please make reservations early and ask for the NDIA room block. Rooms will not be held after Tuesday, October 11, 2005 and may sell out before than. Rates are also subject to increase after this date.

**The government room rate applies only to active duty military and civilian government employees. It is not available to government contractors, retired military or retired civilian government employees. ID cards and/or travel orders will be required at check-in to verify rate eligibility.*

GENERAL INFORMATION

Symposium Attire
Appropriate dress for this symposium is business for civilians (coat and tie) and class A uniform for military.

Inquiries
For more information regarding the symposium contact Britt Bommelje, Meeting Planner at (703) 247-2587 or bbommelje@ndia.org.

Promotional Partnerships
Increase your company or organization exposure at this premier event by becoming a Promotional Partner. A Promotional Partnership ($5,000) will add your company name to the back cover of the on-site brochure as well as main platform recognition throughout the conference, signage at all events including the opening reception and a 350-word organization description in the conference agenda. For more information, please contact Sam Campagna at 703-247-2544 or scampagna@ndia.org.

www.defensejobs.com
The Defense Industry's leading employment website; find a job, post a job listing, post a resume, and search resumes. For more information please contact info@defensejobs.com or (703) 247-9461. Please visit www.defensejobs.com

IBC Committee Appreciation Dinner
The IBC Committee Appreciation Dinner will be held on Friday, November 18, 2005 in Vancouver. This dinner is open to IBC Committee members and their guests only. If you and your guest would like to attend, please make a note of it on the registration form. There is a $75 charge per person to attend.

"The Department of Defense finds this event meets the minimum regulatory standards for attendance by DoD employees. This finding does not constitute a blanket approval or endorsement for attendance. Individual DoD component commands or organizations are responsible for approving attendance of its DoD employees based on mission requirements and DoD regulations."

EXHIBITOR CONTRACT

NDIA NATIONAL DEFENSE INDUSTRIAL ASSOCIATION
STRENGTH THROUGH INDUSTRY & TECHNOLOGY

22nd International Symposium on Ballistics

Vancouver Convention Center ~ Vancouver, BC, CANADA

November 14-18, 2005

Event # 6210

Organization Information

Organization Name (as it should appear on booth sign -- limited to 40 characters and spaces)			
Point of Contact (for fees and exhibitor service kit)	Title		
Street Address	City	State	Zip Code
Telephone	Fax	E-mail	

Reserve your booth and register your exhibit staff at http://exhibits.ndia.org

Exhibit Space Information:

Corporate Members and bona-fide government organizations:

Please reserve ________ 10' x 10' booth(s) at $2,650 each

Non-Corporate Members:

Please reserve ________ 10' x 10' booth(s) at $3,250 each

Remember:

Add an additional $250 for corner booth space

Add an additional $500 for island space

PAYMENT POLICY:

Total booth cost is due with this application to guarantee space. Booths will be assigned on a first-paid, first-served basis. Purchase orders are not acceptable as payment unless paid in advance of show dates. This contract is your invoice. All payments are due by September 30, 2005.

CANCELLATION POLICY:

Fees will be refunded, less a service charge of 50% of total booth fee, if written notice of cancellation is received by September 30, 2005. No refunds will be given for cancellations received after September 30, 2005.

Booth Choices: (List booth number(s) in order of preference)

1st _______________ 2nd _______________ 3rd _______________

Payment Computation:

$______Booth Fee **x** _______ sq. ft **+** $_________ Corner Fee **=** $_________ **Total**

☐Check (payable to NDIA, Event #6210-3140)

☐ VISA ☐ Diners Club ☐ MasterCard ☐American Express

Credit Card Number	
Expiration Date	Authorized Signature

The undersigned agrees to abide by the rules and regulations set forth by NDIA on show web site and the Exhibitor Service Kit.

AUTHORIZED SIGNATURE ____________________ DATE ____________

Contact: Tina Lynn Mercardo - NDIA, 2111 Wilson Blvd., Suite 400, Arlington, VA 22201
TEL: (703)247-2582~ FAX: (703)522-1885 ~ E-MAIL:tmercardo@ndia.org

22nd International Symposium on Ballistics

Vancouver Convention Center
Vancouver, BC, CANADA
November 14-18, 2005

The objective of the 22nd International Symposium on Ballistics is to focus on potential technical advances and breakthroughs in the 21st century in the general area of: interior ballistics, launch dynamics, exterior ballistics, projectile and warhead design, vulnerability, wound ballistics, and armored and personal protection. The symposium is an opportunity for ballistic scientists, engineers and others to report, share and discuss current research and advances in ballistics and visions of the future.

NDIA invites you to take advantage of this tremendous opportunity to demonstrate your organization's products and services to this specialized community by exhibiting at this year's event.

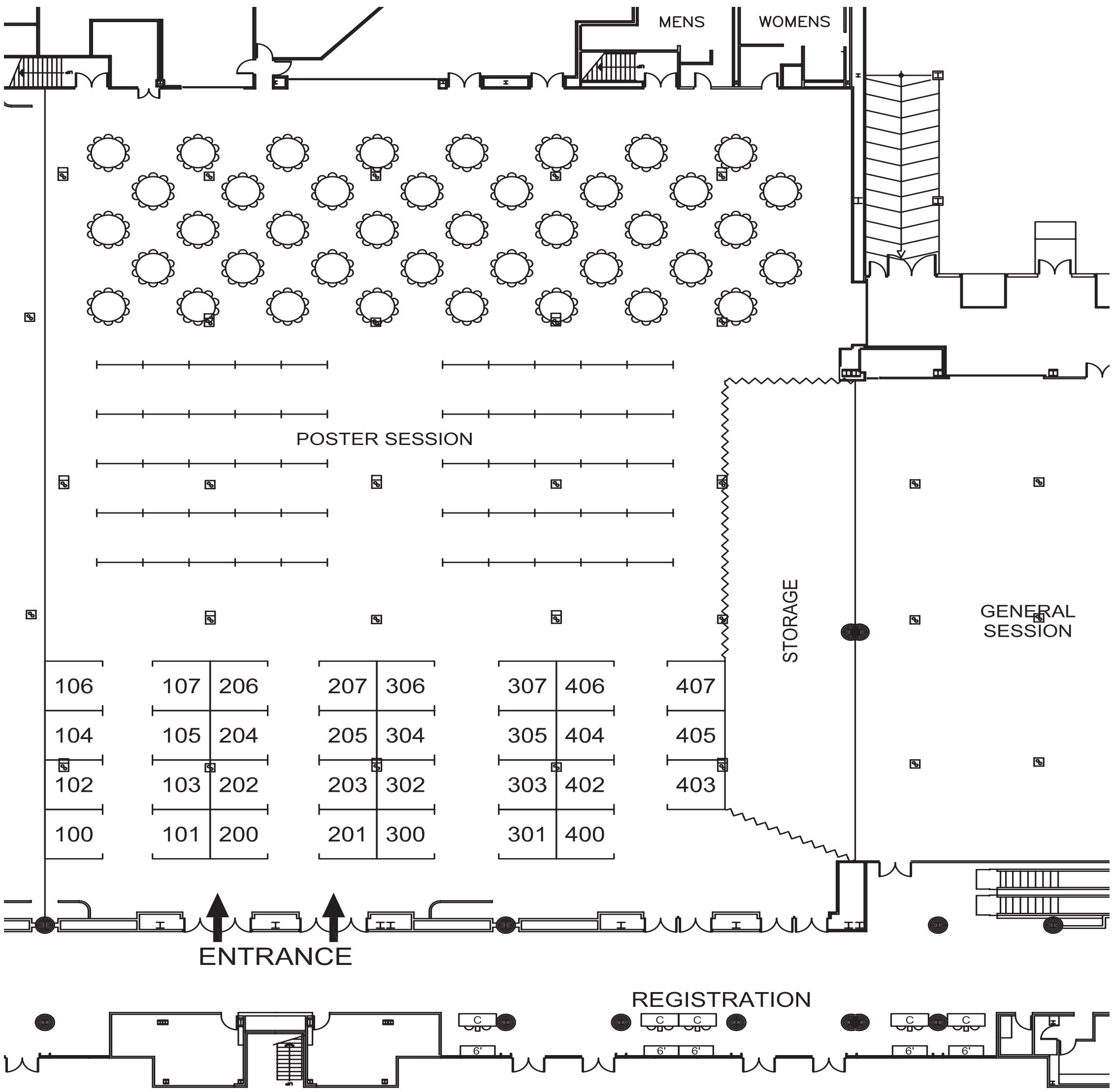

Exhibit Rate:

•$2,650 per 10' x 10' booth space for NDIA corporate members/Government organizations
•$3,250 for non-members and Industry
•Add $250 for corner booths
•Add $500 for island booths

Tentative Exhibit Schedule*:

Monday, November 14: 4:00pm - 7:30pm
Tuesday, November 15: 7:00am - 6:00pm
Wednesday, November 16: 7:00am - 5:00 pm
Thursday, November 17: 8:00am - 11:00am
Friday, November 18: 8:00am - 11:00am

**Show days only. Does not include move-in and move-out. For complete exhibit schedule go to http:exhibits.ndia.org.*

Reserve your booth on-line and in real time. Go to http://exhibits.ndia.org

Questions? Contact Tina Lynn Mercardo at TMercardo@ndia.org or 703-247-2582

22nd International Symposium on Ballistics
Vancouver Convention Center
November 14-18, 2005 • Event #6210

National Defense Industrial Association
2111 Wilson Boulevard, Suite 400
Arlington, VA 22201-3061
(703) 522-1820 • (703) 522-1885 fax
www.ndia.org

3 Ways to sign up:
1. Online with a credit card at www.ndia.org
2. By fax with a credit card — Fax: 703-522-1885
3. By mail with a check or credit card

Address change needed

NDIA Master ID/Membership # ______________________ Social Security # ______________________
(if known—hint: on mailing label above your name) *(last 4 digits – optional)*

Prefix ______________________
(e.g. RADM, COL, Mr., Ms., Dr., etc.)

Name First ______________________ MI ______ Last ______________________

Military Affiliation ______________________ Nickname ______________________
(e.g. USMC, USA (Ret.) etc.) *(for Meeting Badges)*

Title ______________________

Organization ______________________

Street Address ______________________

Address *(Suite, PO Box, Mail Stop, Building, etc.)* ______________________

City ______________ State ________ Zip ________ Country ______________

Phone ______________ ext. ________ Fax ______________

E-Mail ______________________

Signature* ______________________ Date ________

Preferred way to receive information

Conference information address above Alternate *(print address below)* E-mail

Subscriptions address above Alternate *(print address below)*

Alternate Street Address ______________________

Alternate Address *(Suite, PO Box, Mail Stop, Building, etc.)* ______________________

City ______________ State ________ Zip ________ Country ______________

** By your signature above you consent to receive communications sent by or on behalf of NDIA, its Chapters, Divisions and affiliates (NTSA, AFEI, PSA, NCWG, WID) via regular mail, e-mail, telephone, or fax. NDIA, its Chapters, Divisions and affiliates do not sell data to vendors or other companies.*

By completing the following, you help us understand who is attending our meetings.

Primary Occupational Classification. *Check ONE.*
- A. Defense Business/Industry
- B. R&D/Laboratories
- C. Army
- D. Navy
- E. Air Force
- F. Marine Corps
- G. Coast Guard
- H. DOD/MOD Civilian
- I. Gov't Civilian (Non-DOD/MOD)
- J. Trade/Professional Assn.
- K. Educator/Academia
- L. Professional Services
- M. Non-Defense Business
- N. Other ______________

Current Job/Title/Position.
Check ONE.
- A. Senior Executive
- B. Executive
- C. Manager
- D. Engineer/Scientist
- E. Professor/Instructor/Librarian
- F. Ambassador/Attaché
- G. Legislator/Legislative Aide
- H. General/Admiral
- I. Colonel/Navy Captain
- J. Lieutenant Colonel/Commander/Major/Lieutenant Commander
- K. Captain/Lieutenant/Ensign
- L. Enlisted Military
- O. Other ______________

Year of birth ______________
(Optional)

Registration Fees

	Regular	Late *after 10/28/05*
All Attendees	$950	$1045
IBC Committee Appreciation Dinner	$75	
Number of people attending the dinner		________
Guest at Both Receptions	$75	________
Guest at One Reception	$50	________

No refunds for cancellations received after 10/28/05. **Substitutions are welcome in lieu of cancellation.**

Questions? Contact Meeting Planner, Britt Bommelje
(703) 247-2587 email: bbommelje@ndia.org

Mail to: NDIA, Event #6210
2111 Wilson Boulevard, Suite 400
Arlington, VA 22201

Fax to: (703) 522-1885

Payment Options

- Check *(payable to NDIA)*
- Cash
- Government PO/Training Form # ______________
- VISA
- MasterCard
- American Express
- Diners Club

If paying by credit card, you may return by fax to (703) 522-1885.

Credit Card Number

Exp. date __ __ / __ __

______________________ ______________
Signature Date

NDIA
NATIONAL DEFENSE INDUSTRIAL ASSOCIATION
STRENGTH THROUGH INDUSTRY & TECHNOLOGY
2111 Wilson Blvd.
Suite 400
Arlington, VA 22201

Plasma Ignition of a 30-mm Cannon

Richard A. Beyer
Andrew L. Brant
Joseph J. Colburn

US Army Research Laboratory
Aberdeen Proving Ground, Maryland

22nd International Symposium on Ballistics
14-18 November, 2005
Vancouver, BC

Goal of This Study

- Apply the knowledge learned in our earlier **Plasma-Propellant Interaction** research to the Ignition of a 30-mm cannon
- Start to Develop "Design Rules" for plasma ignition

Ultimately: Make plasma ignition in large-caliber guns more efficient

Hardware

- Power Supply
  - Standard PFN 600 mF, 3 kv, 3 kj
  - Short (300 ms) or Long (900 ms) Pulse
- Propellants
  - JA2, M30, Graphite-Free JA2
- Standard Ignition for 30-mm cannon
  - M52 primer w/1.5 grams Benite in bayonet

Small-Scale Experiments

Plasma into bayonet igniter tube

Schematic of Test “Igniter”

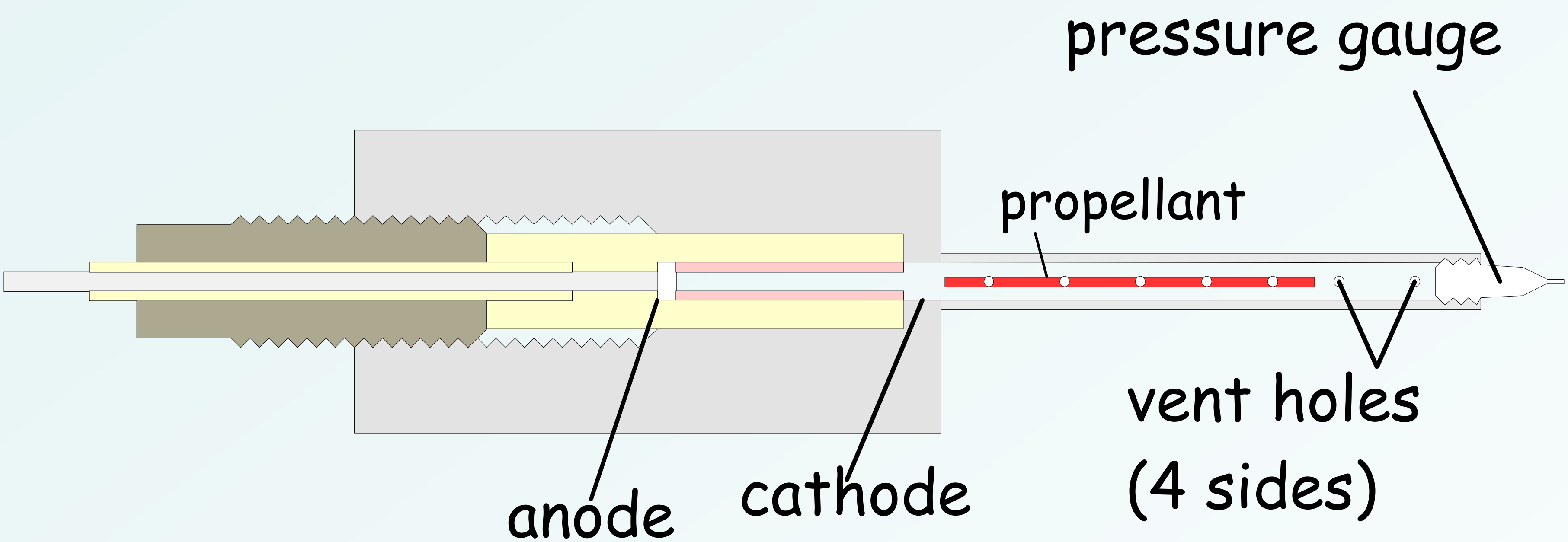

Designed to look like an igniter we can put into 30-mm cannon.
32 total 1/16-inch vent holes (8 per side)

Response with 1.5 grams Standard JA2 in tube

Parameter = discharge energy

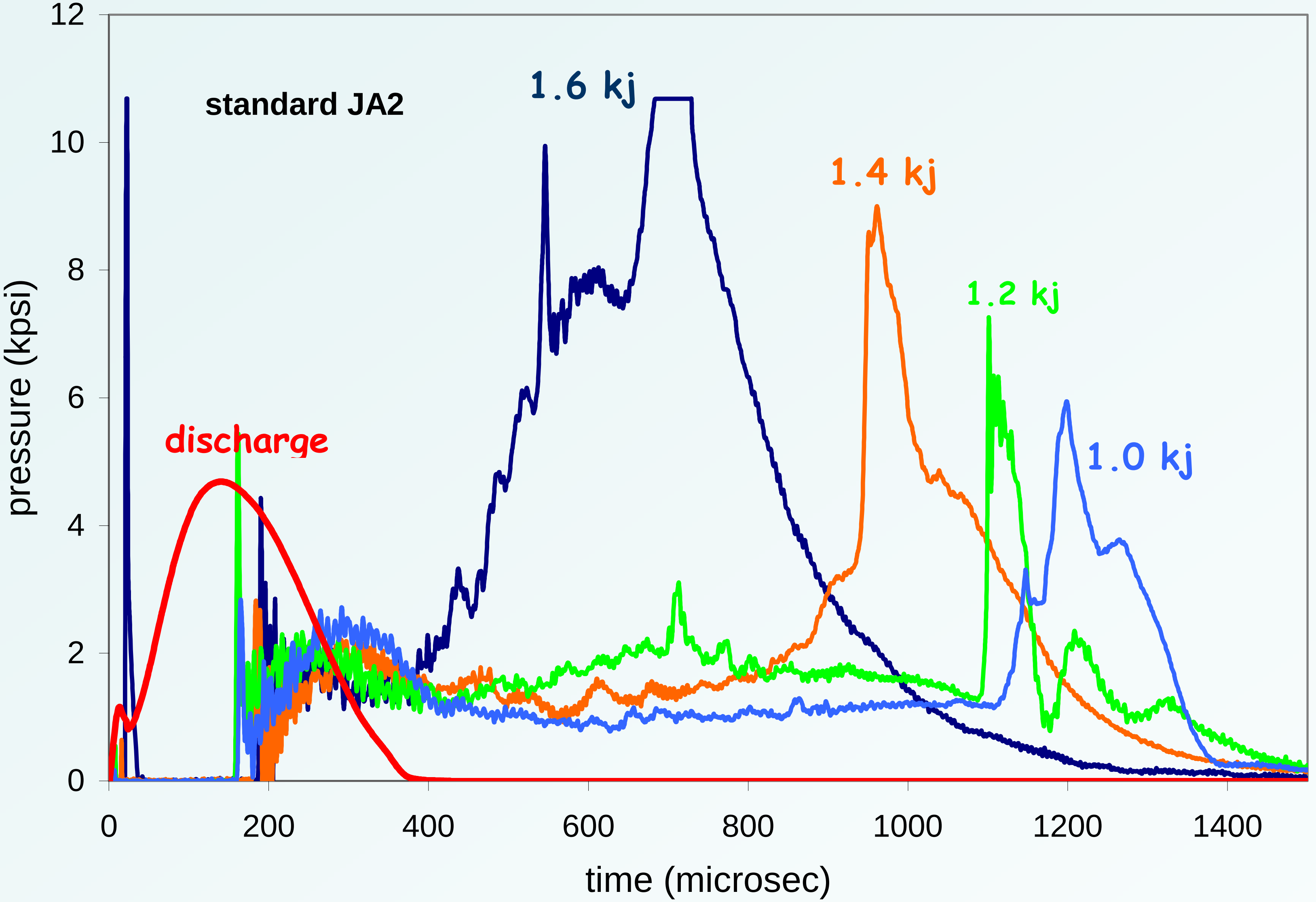

(1.5 g JA2 ≈ 8.5 kj chemical energy)

Response with 1.5 grams Graphite-Free JA2 in tube

Parameter = discharge energy

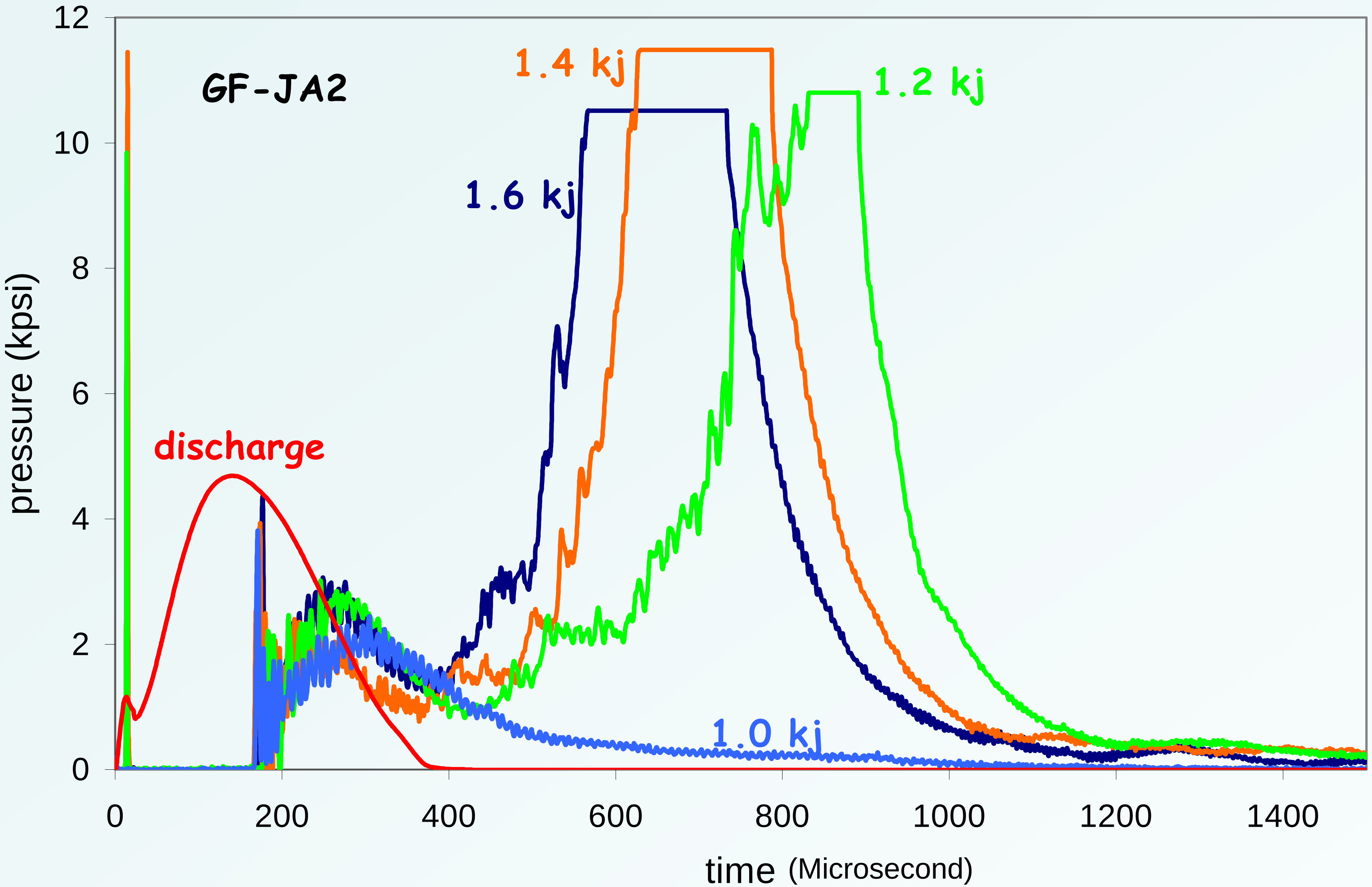

(1.5 g JA2 ≈ 8.5 kj chemical energy)

30-mm Cannon

30-mm Stub-Case Cartridge for Plasma Injection

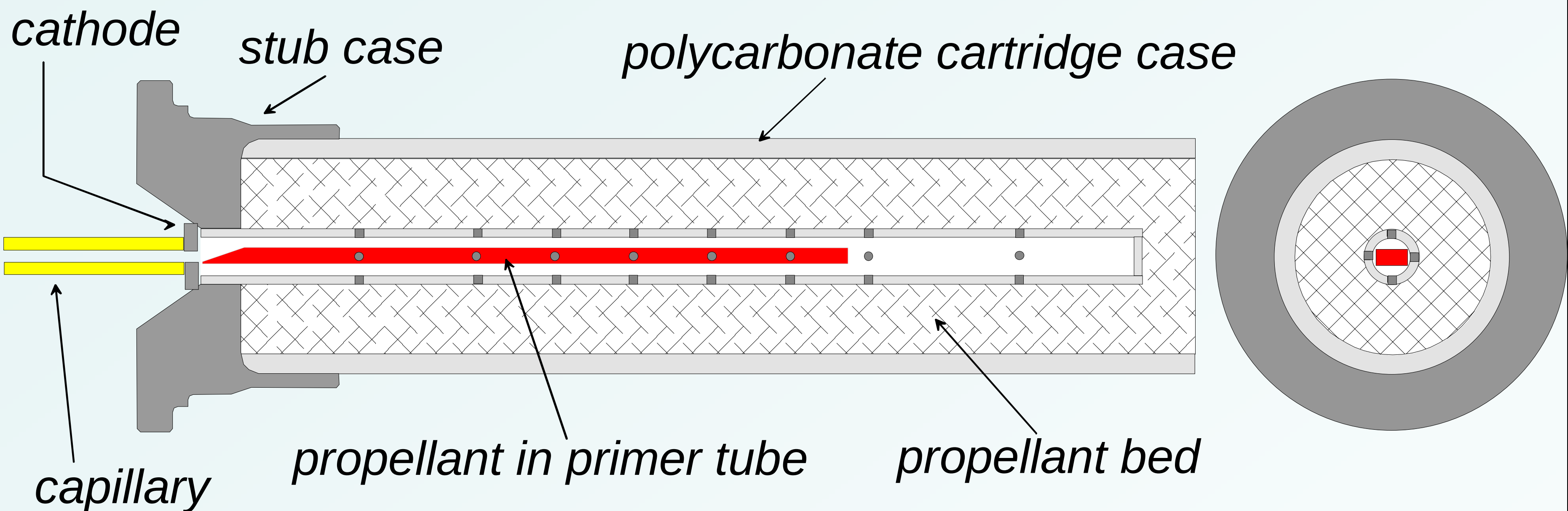

Plasma Discharge Energy: 2.1 to 2.3 kj
Propellant in primer tube: 1.6 to 1.9 grams (8.1 to 9.6 kj chem energy)
Chamber volume: 135 cc
Projectile mass: 550 g
Shot-Start Pressure: very low
Conventional ignition baseline: M52 primer and 1.5 grams Benite in bayonet

M30 Propellant Charge

(GF-JA2 in plasma igniter tube)

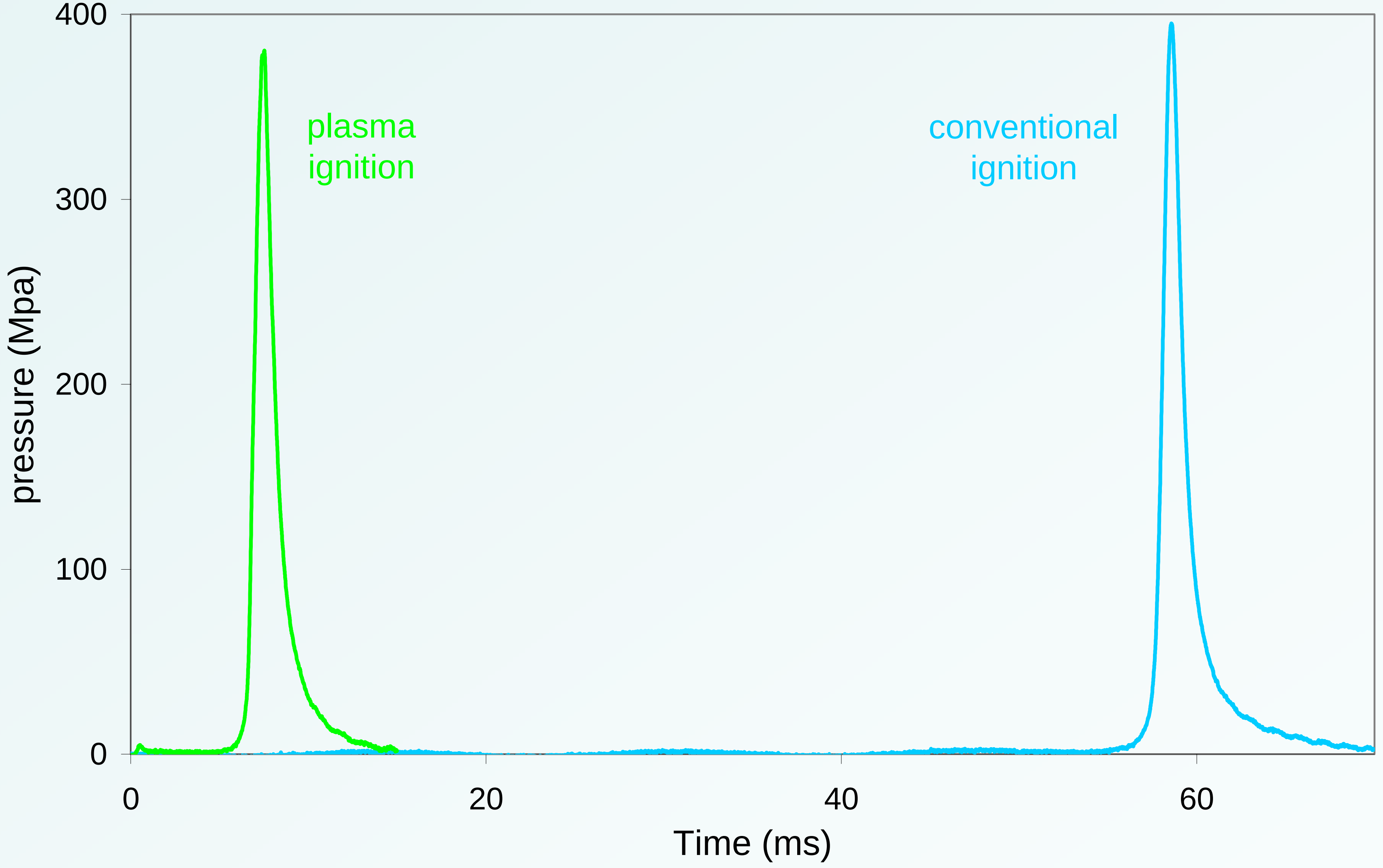

JA2 Propellant Charge

Plasma: GF-JA2 in igniter tube

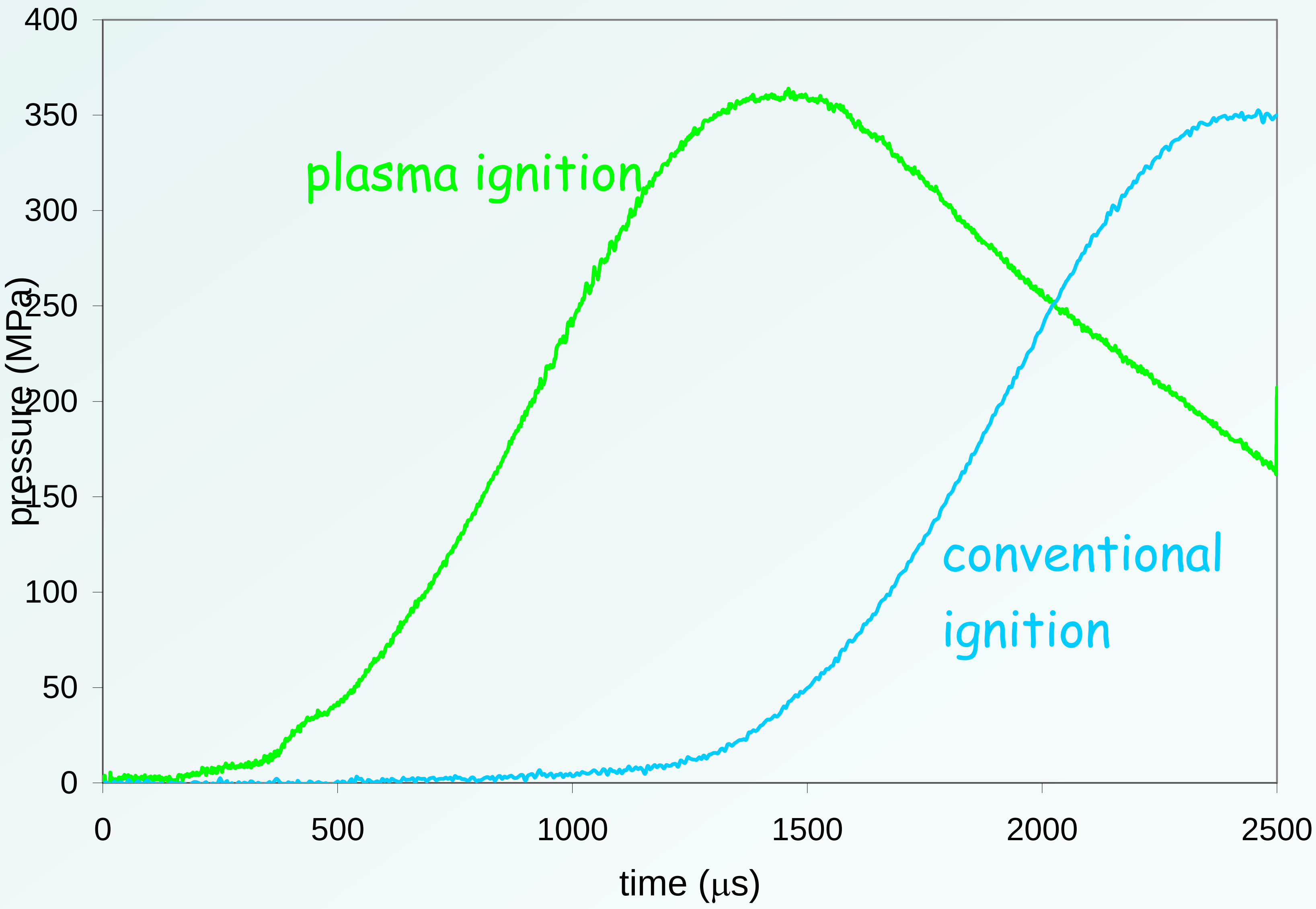

JA2 Propellant Charge

GF-JA2 vs. Standard JA2 <u>in igniter tube</u>

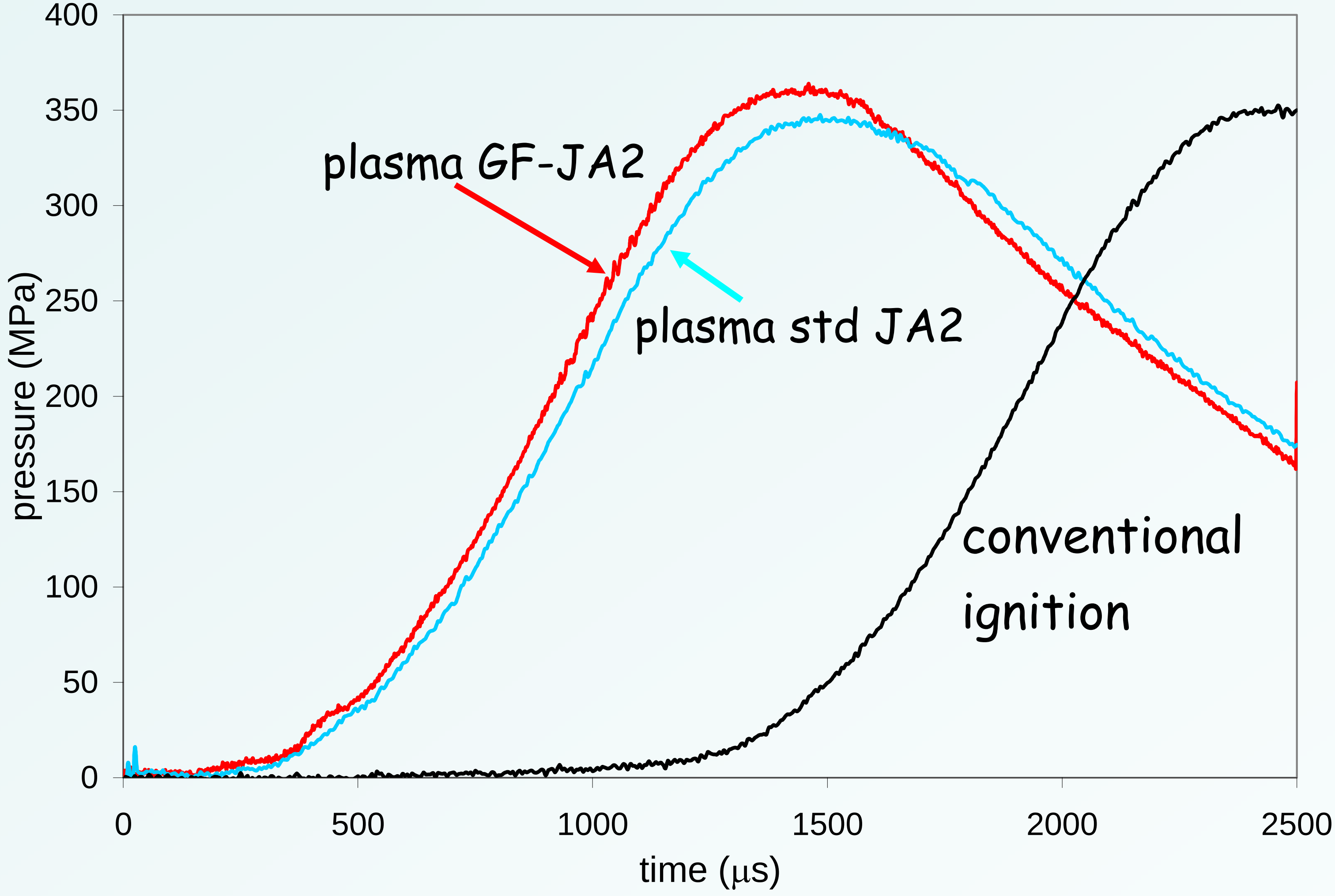

JA2 Propellant Charge

Soda straw vs. empty igniter tube

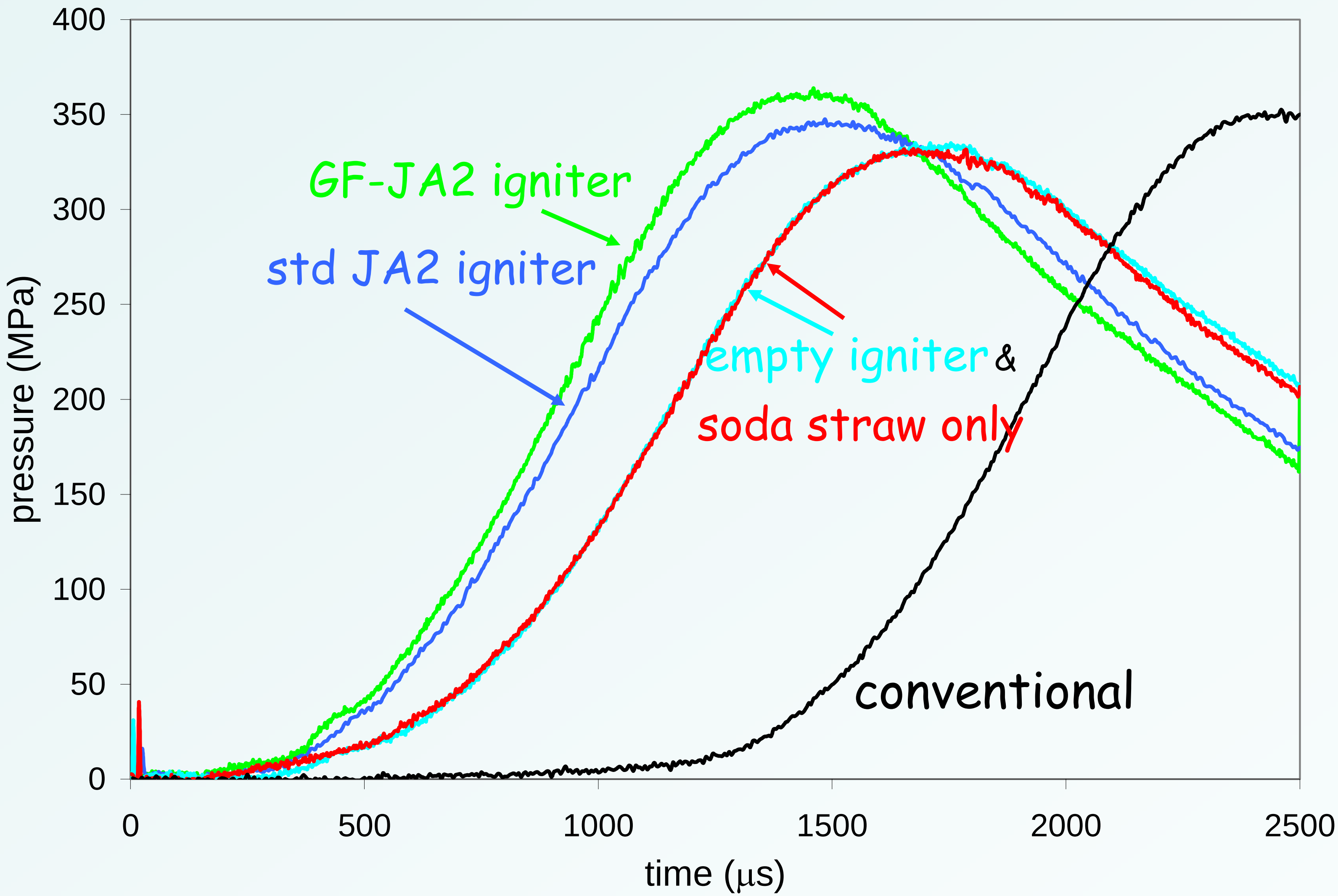

JA2 Propellant Charge

Soda straw w/ GF-JA2 “box”

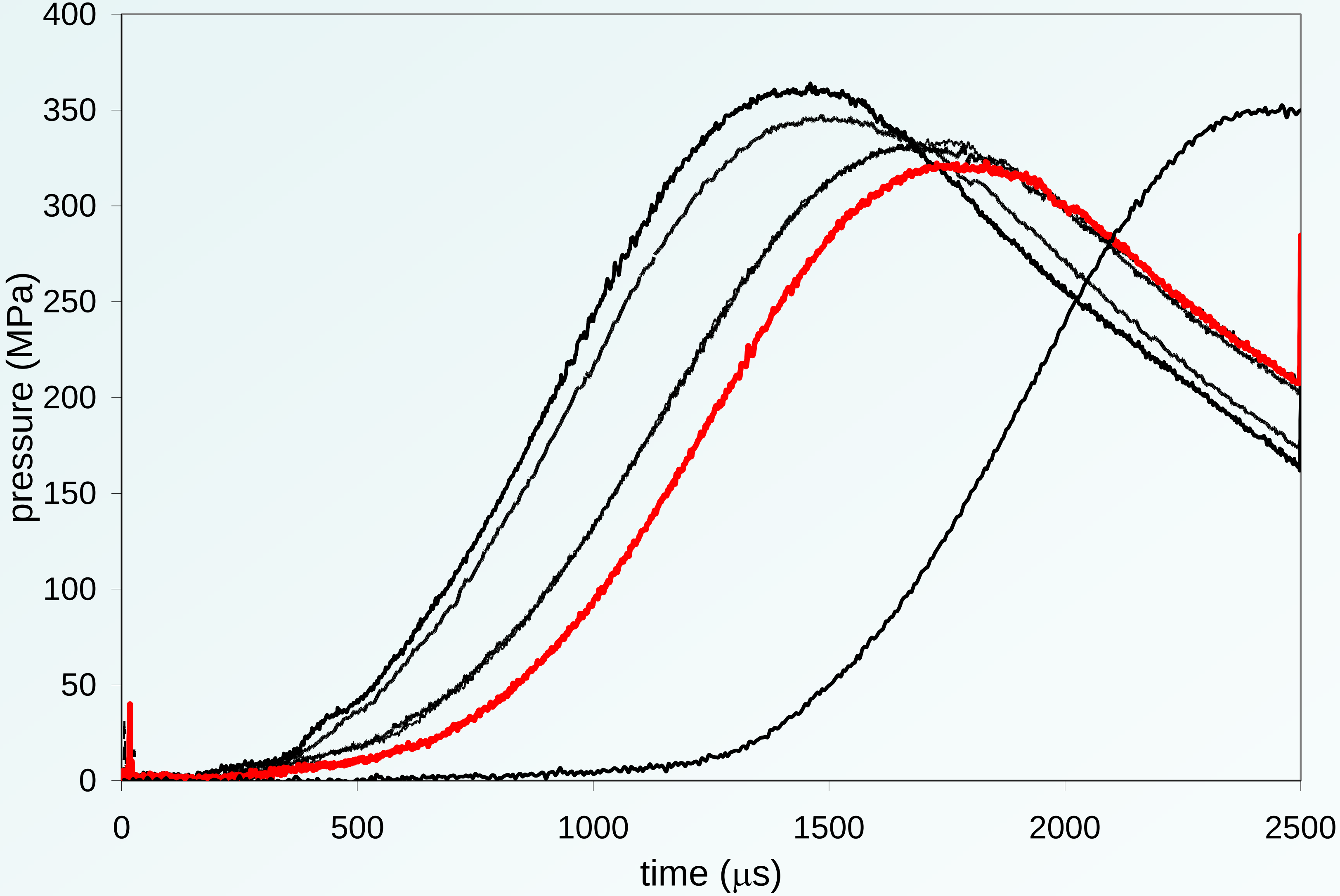

JA2 Propellant Charge

Long plasma pulse

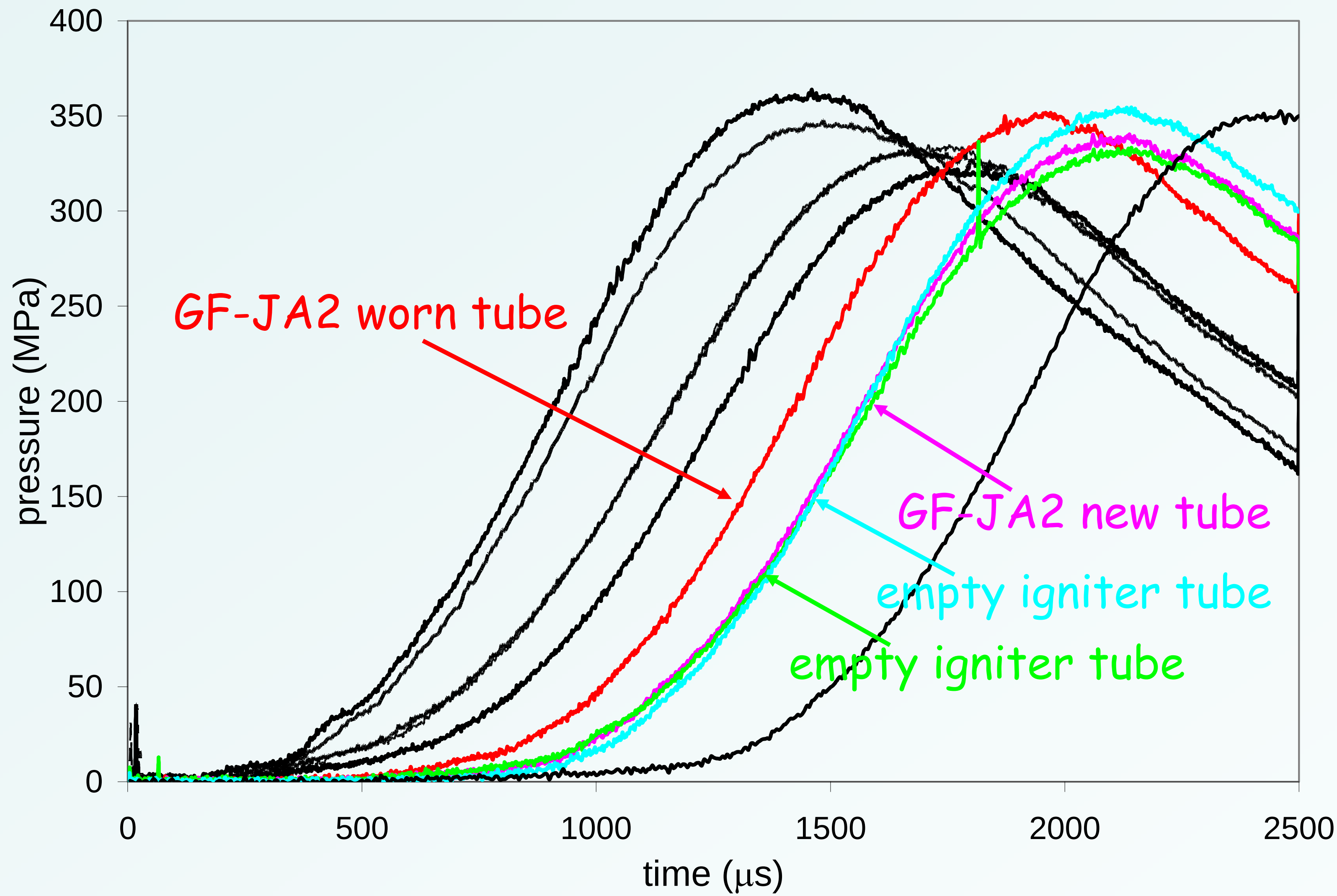

Early Time Behavior

with short-pulse plasma ignition

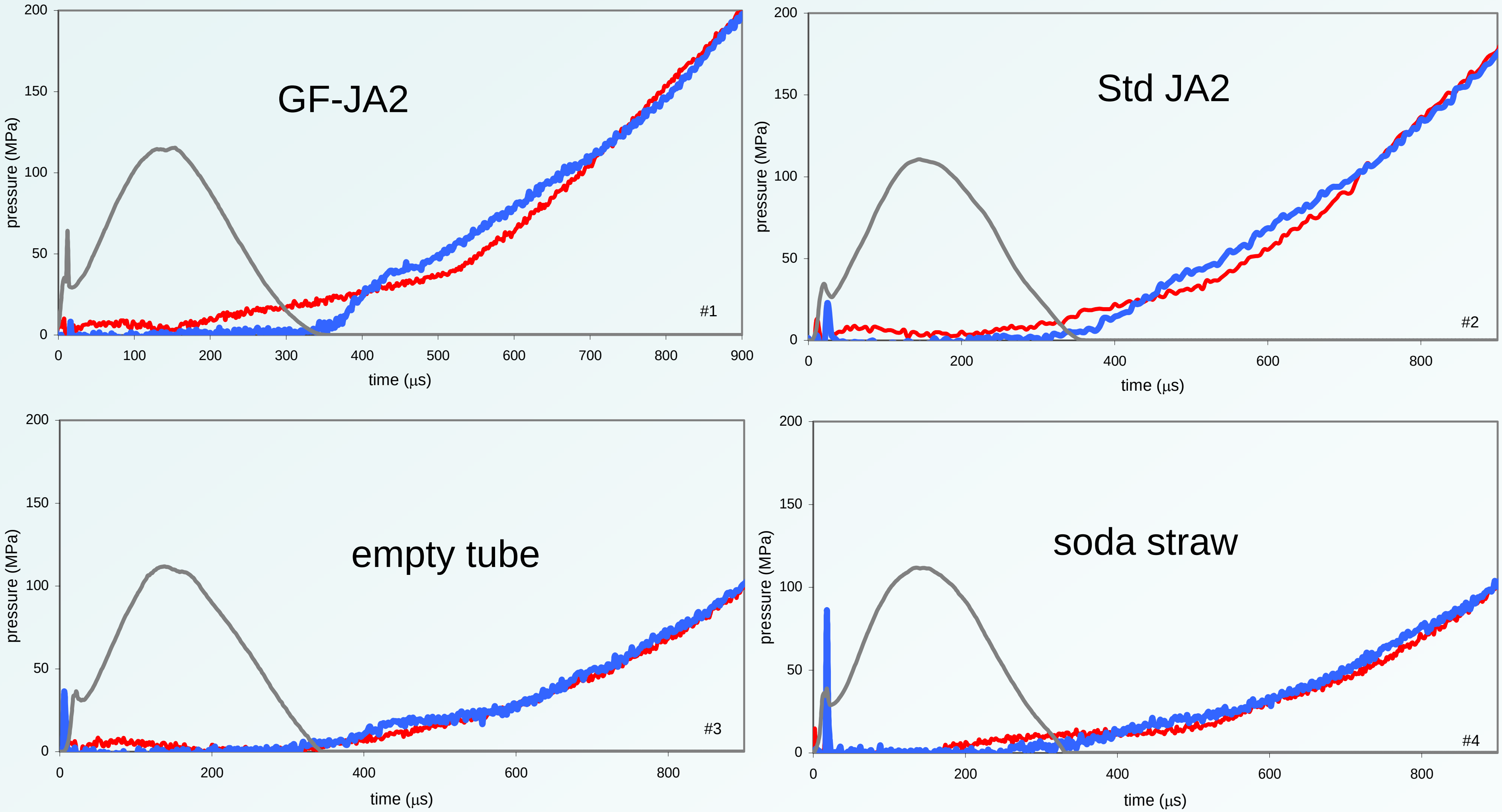

KEY: **red line: breech** **blue line: projectile** **gray line: discharge**

Early Time Behavior

with long-pulse plasma ignition

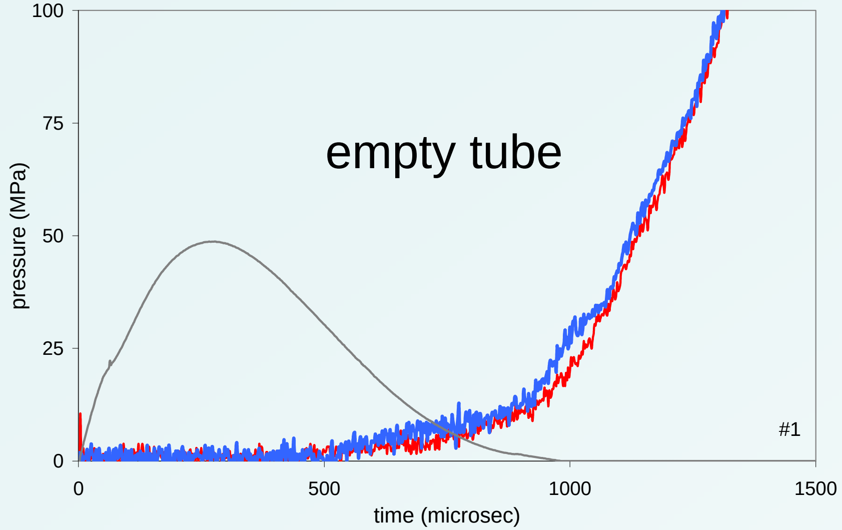

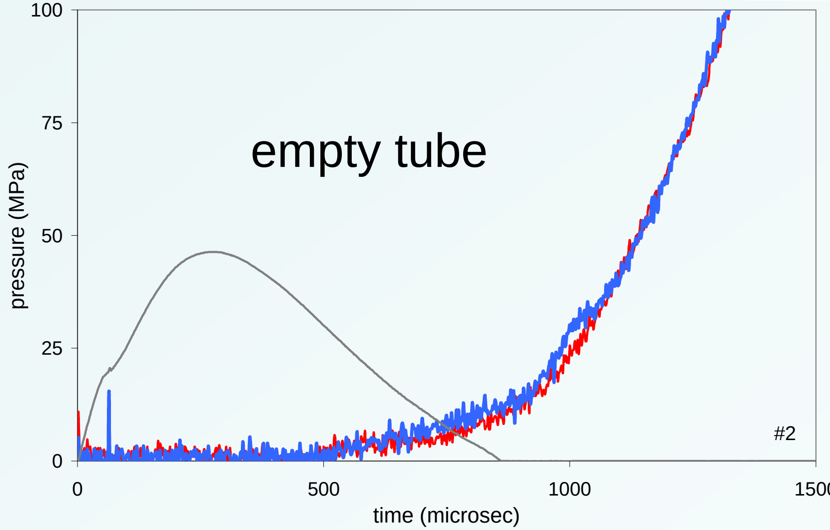

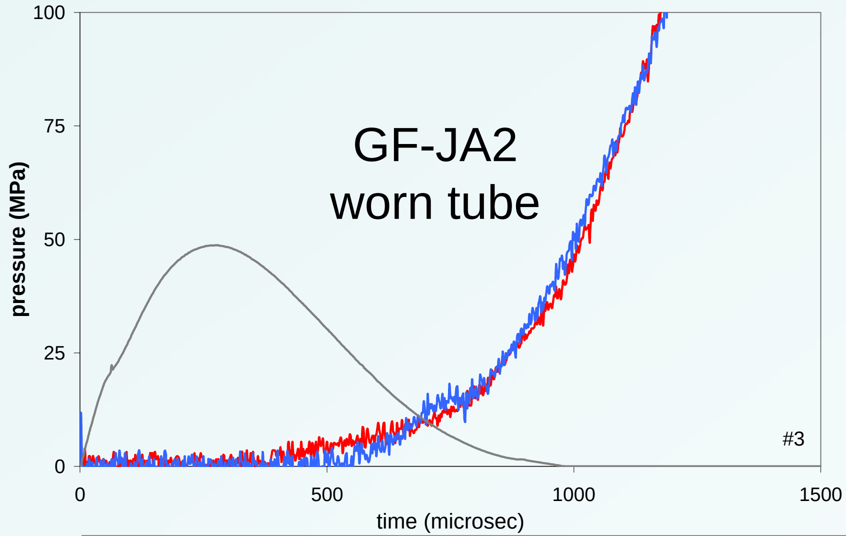

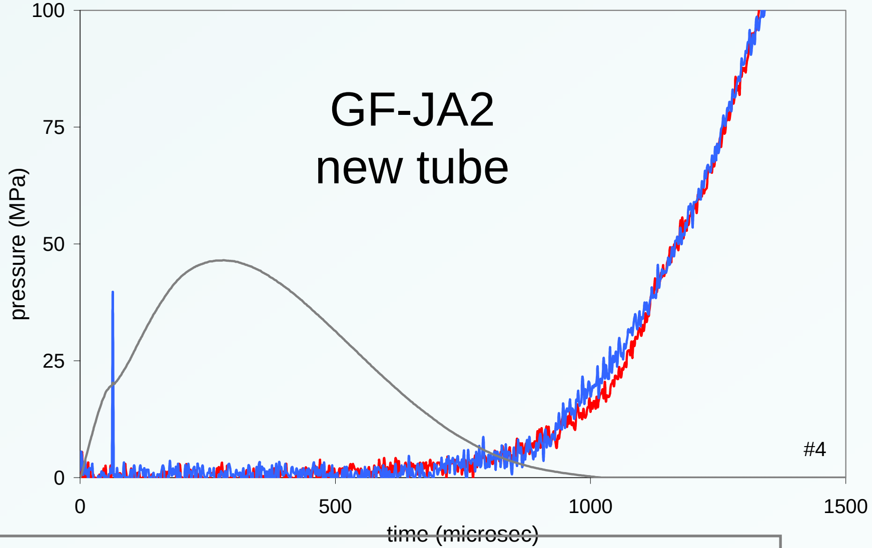

KEY: **red line: breech** **blue line: projectile** **gray line: discharge**

Summary

- Graphite Free JA2 provides higher/faster pressurization inside igniter tube
  - But … The differences not as dramatic in gun firings
- Plasma ignition more prompt than conventional ignition
  - At low (2 kj) plasma energy
  - With M30 “boosted” with JA2 igniter
- Relative quickness of ignition follows our intuition regarding strength of plasma-propellant interactions
  - GF faster than STD JA2
  - Filled igniter tube faster than empty
  - Short pulse faster than long pulse
- Is faster better?
  - Short pulse: Fast and more PPI
  - Long pulse: Only slightly slower; smoother in our cannon

- **Key to Plasma Ignition: Rapid Pressurization of Charge**

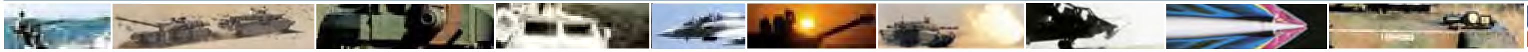

Recent Computations and Validations

of

Projectile Unsteady Aerodynamics

R.Cayzac, E.Carette, R.Thépot and P.Champigny

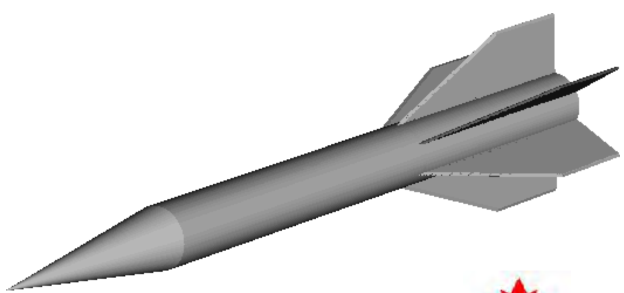

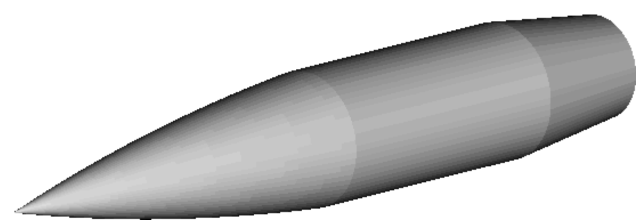

- **OBJECTIVES**
- **THEORETICAL AND NUMERICAL APPROACHES**
- **WIND TUNNEL TESTS**
- **VALIDATION RESULTS**
  - > **YAWING AND SPINNING PROJECTILES**
  - > **KINETIC PROJECTILES**
- **CONCLUSIONS**

Main Aerodynamic Coefficients Concerned

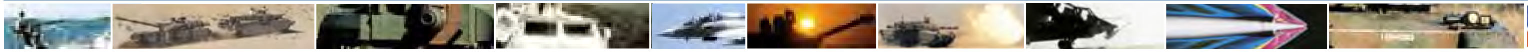

- **FORCE COEFFICIENTS**
  - > **$CA = CA(\alpha=0) + \Delta CA\ (M, \alpha, \beta)$**
  - > **$CN = CN\alpha(M)\alpha + CNq(M).qD/V + \Delta CN\ (M, \alpha, \phi)$**
  - > **$CY = Cyp\alpha(M).p.\alpha.D/V + \Delta CY\ (M, \alpha, \phi)$**

- **MOMENT COEFFICIENTS**
  - > **$Cm = Cm\alpha(M).\alpha + \Delta Cm\ (M, \alpha, \phi) + Cmq(M).qD/V$**
  - > **$Cn = Cnp\alpha(M).p.\alpha.D/V + \Delta Cn\ (M, \alpha, \phi) + Cnr(M).rD/V$**
  - > **$Cl = Clo(M) + \Delta Cl\ (M, \alpha, \phi) + Clp(M).pD/V$**

- **DYNAMIC COEFFICIENTS→ DAMPINGS, MAGNUS AND PSEUDO-MAGNUS EFFECT**

Computational Fluid Dynamics

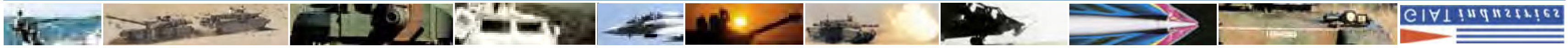

- **Theoretical and Numerical Approaches (FLU3M and elsA)**
  - **3D Navier-Stokes equations, RANS and URANS**
  - **Baldwin-Lomax, Spalart-Allmaras, k-ω,.., turbulence models**
  - **Finite volume method**
  - **Cell-centered discretization in an absolute frame**
  - **Fully implicit Gear scheme (1st and 2nd order)**
  - **(Pulliam under-iteration technique (URANS), grid movement)**

- **Grid : multiblocks structured with hexahedral cells**
  - **Wall cell $\approx$ 1 μm**
  - **30 to 50 cells in the boundary layer**
  - **Stretching factor < 1.2**
  - **$Y^+ \approx 1$ (a posteriori criterion)**
  - **Up to 5,000,000 cells**

- **Computational Performances**
  - **$\approx$ 1 μs/cell/iteration NEC SX-6**
  - **$\approx$ 45 μs/cell/iteration SGI Octane RISC 12000**
  - **$\approx$ 20 μs/cell/iteration Cluster of Xeon (2.2 GHz)**

Main Aerodynamic Coefficients Concerned and CFD Generalities

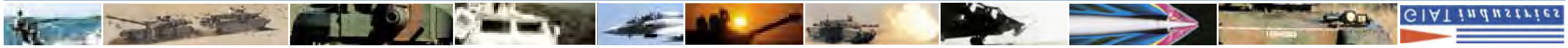

- Cell-centered discretization of RANS equations expressed in an absolute framework R, grid partition in blocks of rigid hexahedral cell

	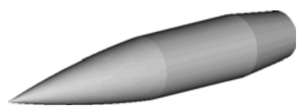	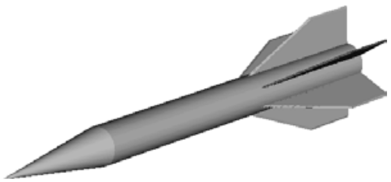
• Magnus • Clp • Cmq	• “Steady algorithm” • “Steady algo.” • “Pseudo unsteady”	• “Unsteady algorithm” • “Unsteady algo.” • “Pseudo unsteady”
• Grid	• Not moving	• Spinning at Ω for unsteady algo

Validation: Wind Tunnel Tests

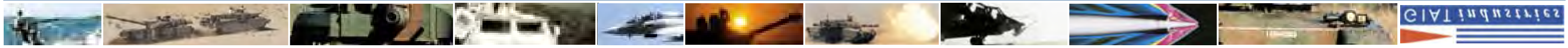

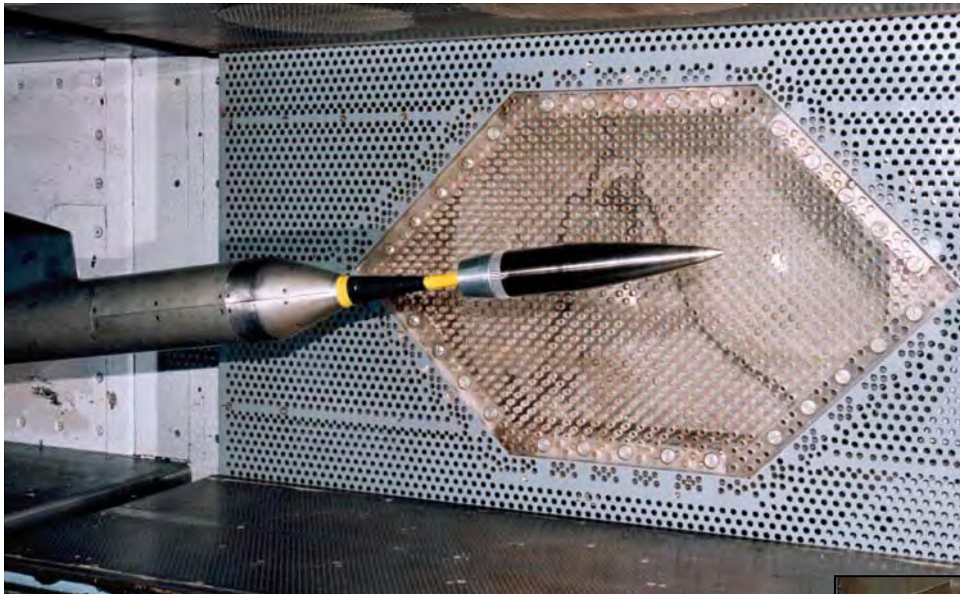

ONERA: S3MA

- **Static coefficients**
  - > CA, CN, Cy, Cl, Cm, Cn
- **Dynamic coefficients**
  - > Cy (Cypα), Cn (Cnpα)
  - > CNq+CNα, Cmq+Cmα
  - > Clp

- **Mach number**
- **Reynolds number**
- **Roll rate p** (P*=p.D/v_∞)
- **Pitch rate q**
- **Damping frequency**
- **Angle of attack**
- **Roll position ϕ**

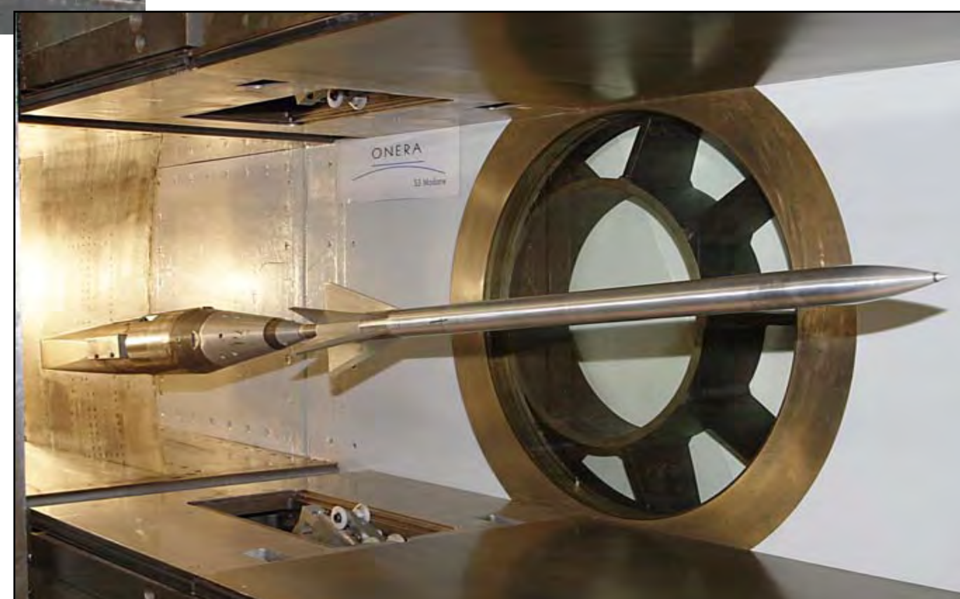

Example of Yawing and Spinning Projectile Grid

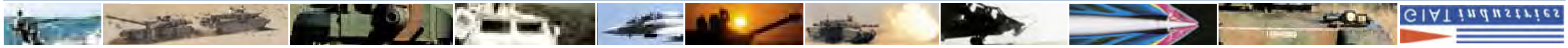

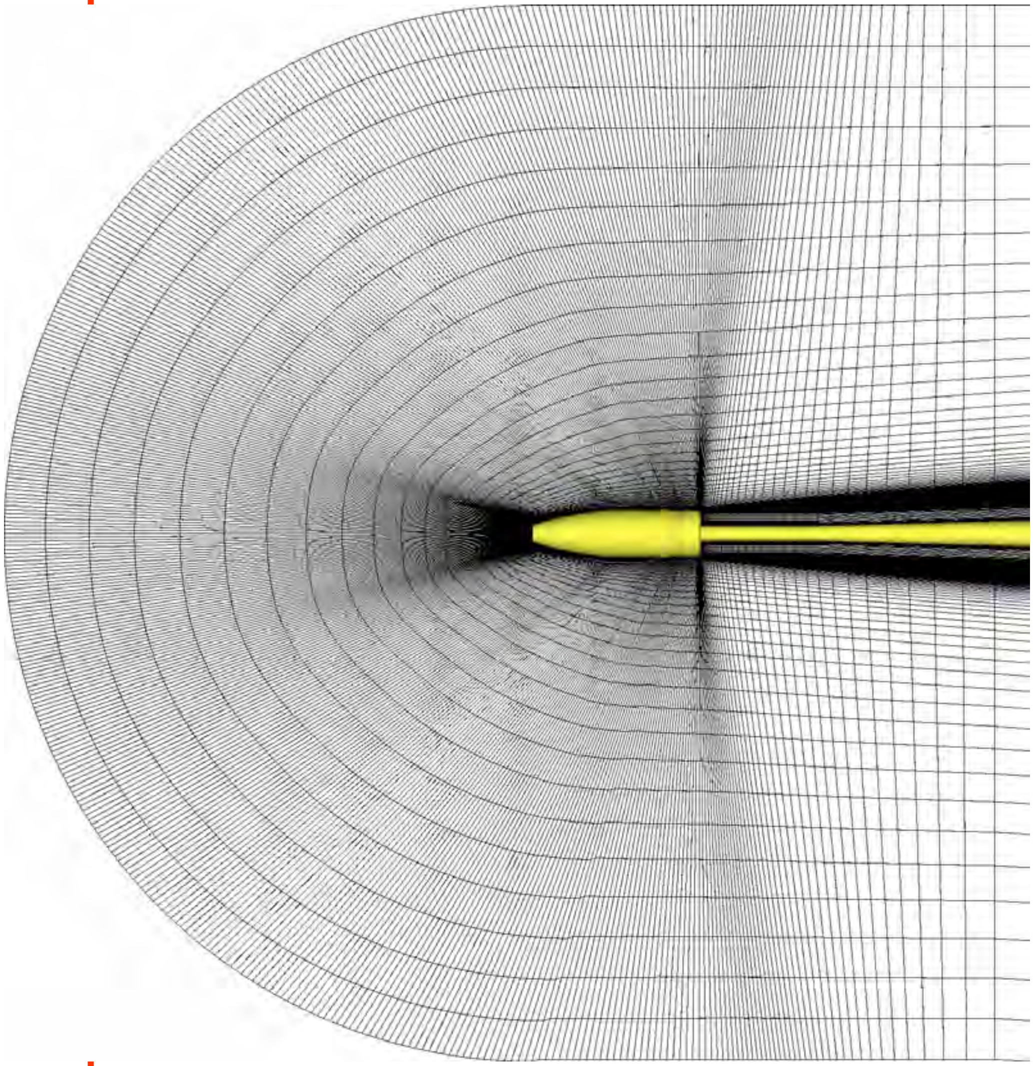

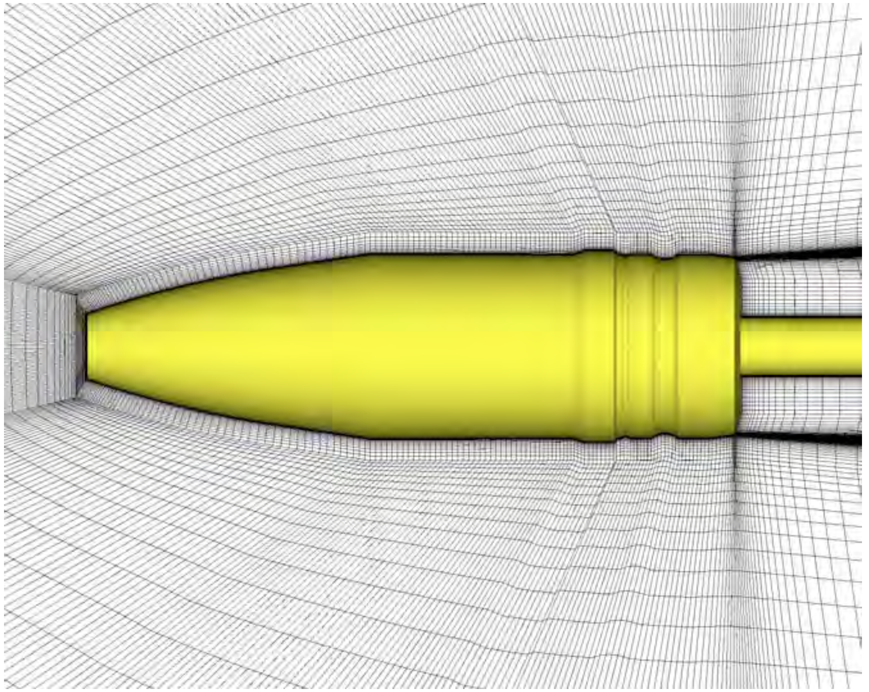

2,074,896 cells

$Y^+ \approx 1$

40 cells in the boundary layer

Example of Kinetic Projectile Grid

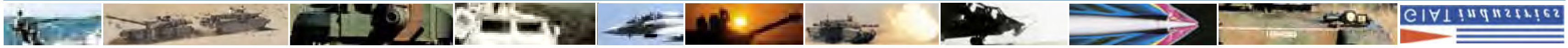

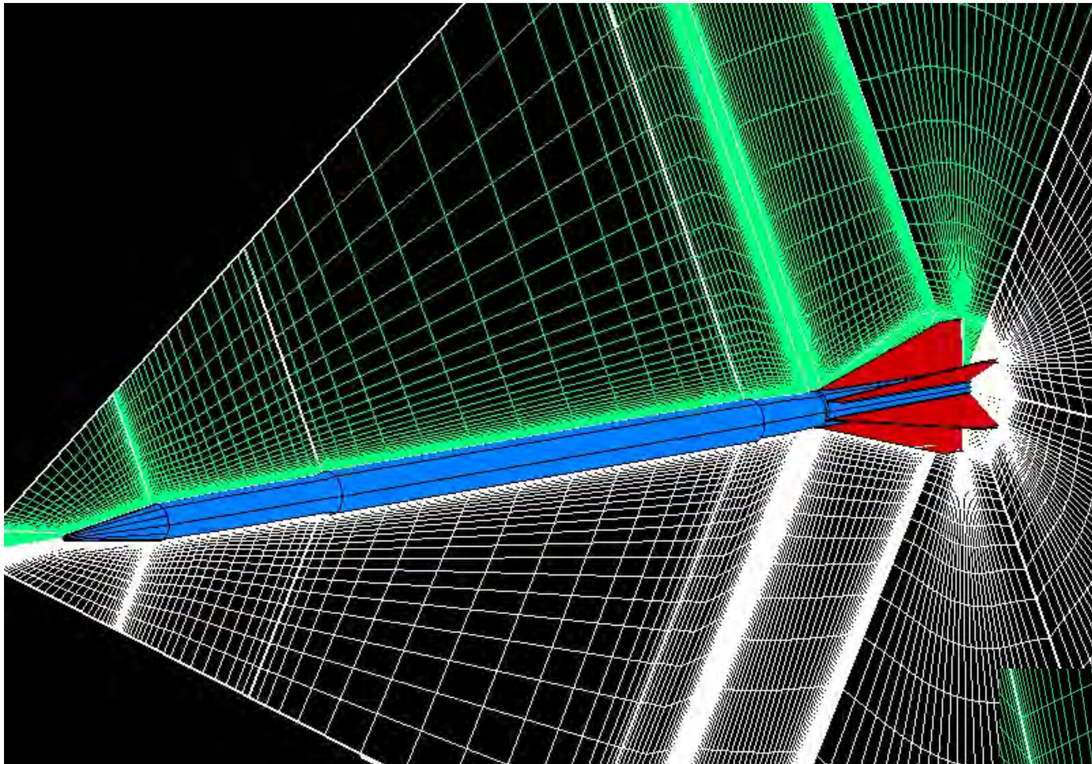

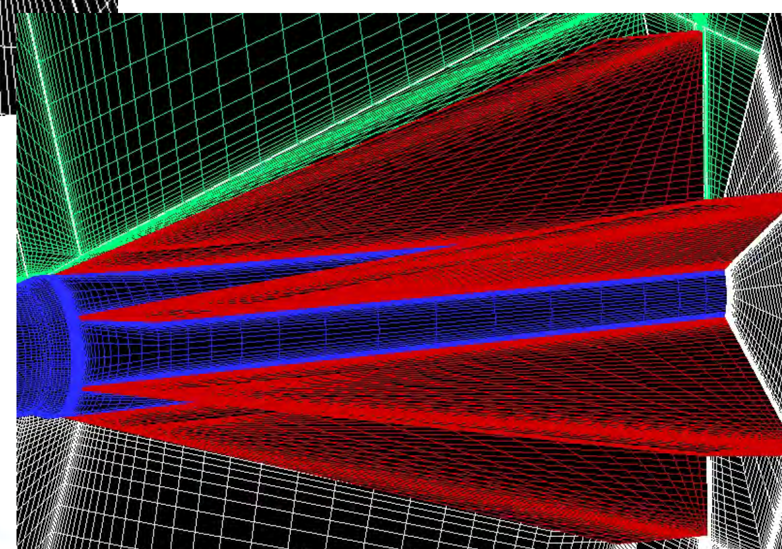

90 Blocks
≈2,700,000 cells
$Y^+ \approx 1$
40 cells in the boundary layer

Example of Y⁺ A Posteriori Verification Criterion

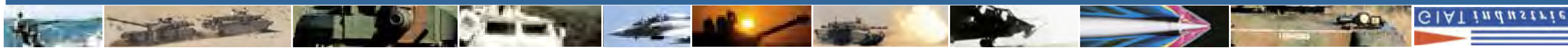

- **y^+ distribution**

  (Mach = 0.90, α = 3°, Pi = 1.20E+05 Pa, Ti = 300.0 K)

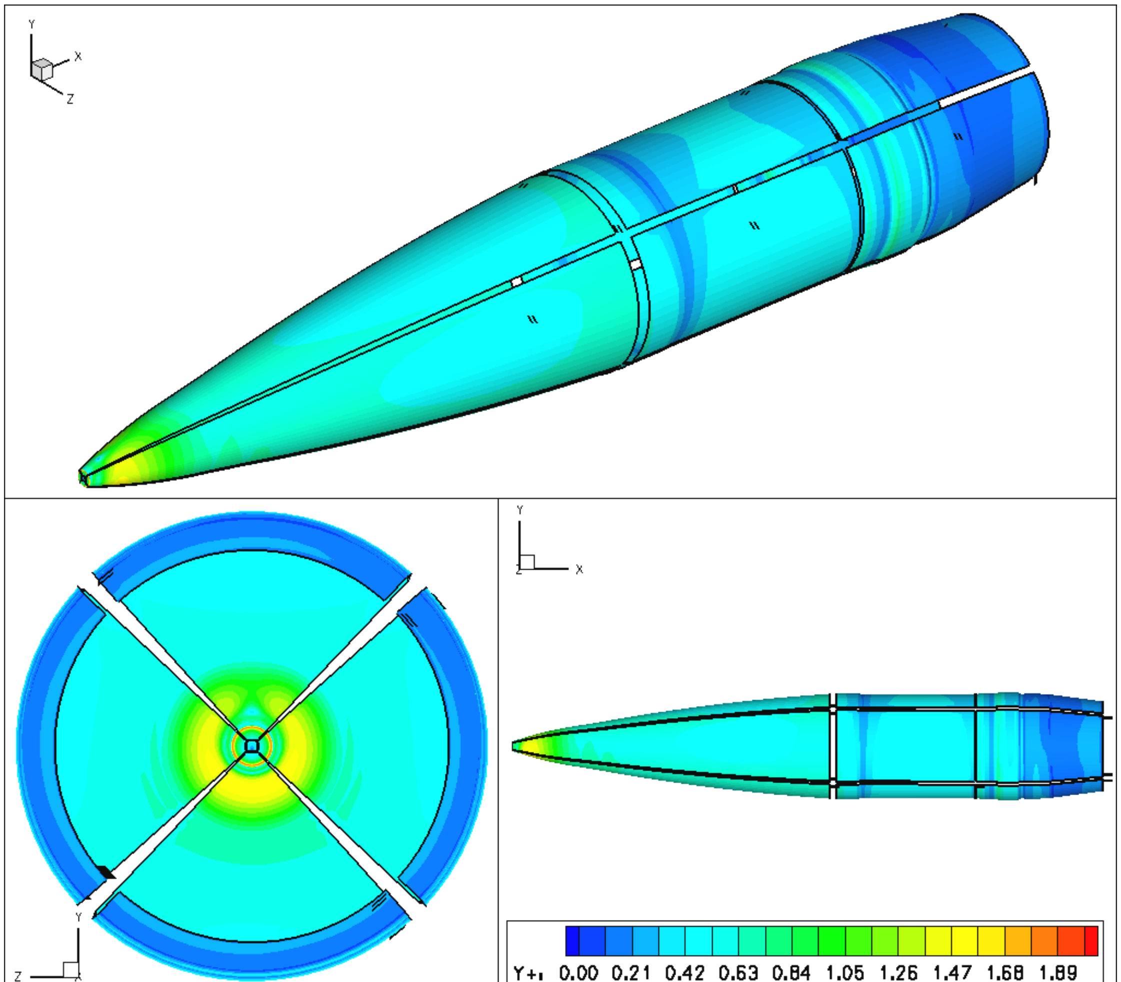

ONERA

Yawing and Spinning Projectiles: Magnus Validation Results

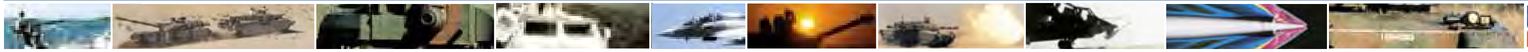

- [1]"Navier-Stokes Computations and Validations of a Yawed Spinning Projectile", 18th International Symposium on Ballistics, 15-19 November, San Antonio, Texas, USA, 1999.
- [2]"Recent Developments on Aeroballistics of Yawing and Spinning Projectiles: Part I, Wind Tunnel Tests ", 20th International Symposium on Ballistics, 7-11 October, Orlando, USA, 2002.
- [3]"Recent Developments on Aeroballistics of Yawing and Spinning Projectiles: Part II, Free Flight Tests ", 20th International Symposium on Ballistics, 7-11 October, Orlando, USA, 2002.
- [4]"Recent Developments on Aeroballistics of Yawing and Spinning Projectiles: Part III, Validation Results", 20th International Symposium on Ballistics, 7-11 October, Orlando, USA, 2002.
- [5]"Analysis of Static and Dynamic Stability of Spinning Projectiles", 21st International Symposium on Ballistics, Adelaide, Autralia, 19-23 April , 2004.

- **Agreement between computations and experiments is satisfactory at moderate angles of attack on the Magnus dynamic coefficients**
- **Strong difficulties at high incidence (up to 10°) and in the transonic regime**
- **RANS → MILES, DES, etc., simulations (ARL, De Spirito, etc.)**

Example of Validation Results: Cmq, Pseudo-URANS

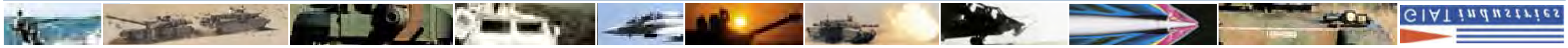

Supersonic Conditions: Wind Tunnel C4/ FLU3M Baldwin-Lomax
(M_∞= 2.89, α = 0° (1° for static), Pi = 3.224 bar, Ti = 299 K, $\theta \pm$ 1°, f = 9 to 13 Hz)

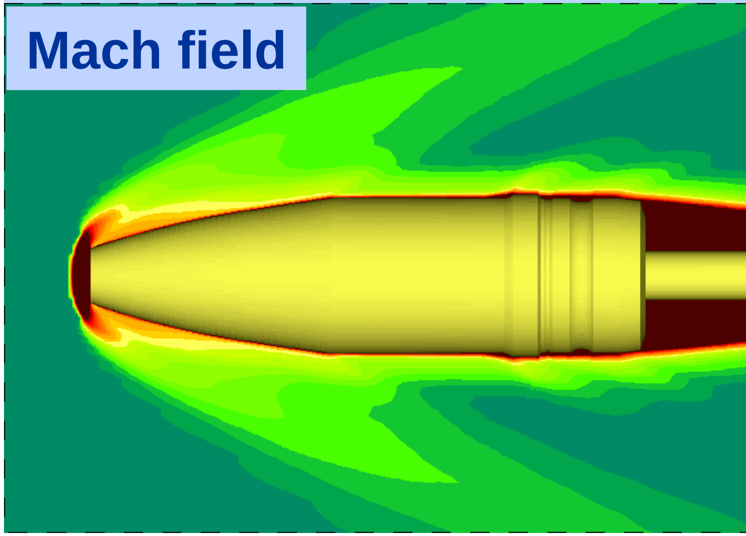

FLU3M	TEST	CFD	Error(%)
$C_{N\alpha}$	2,52	2,36	6,3
$C_{m\alpha}$	-3,55	-3,38	4,8
X_F/D	1,41	1,43	-1,4
C_{mq}	-5,1	-5,4	-5,8

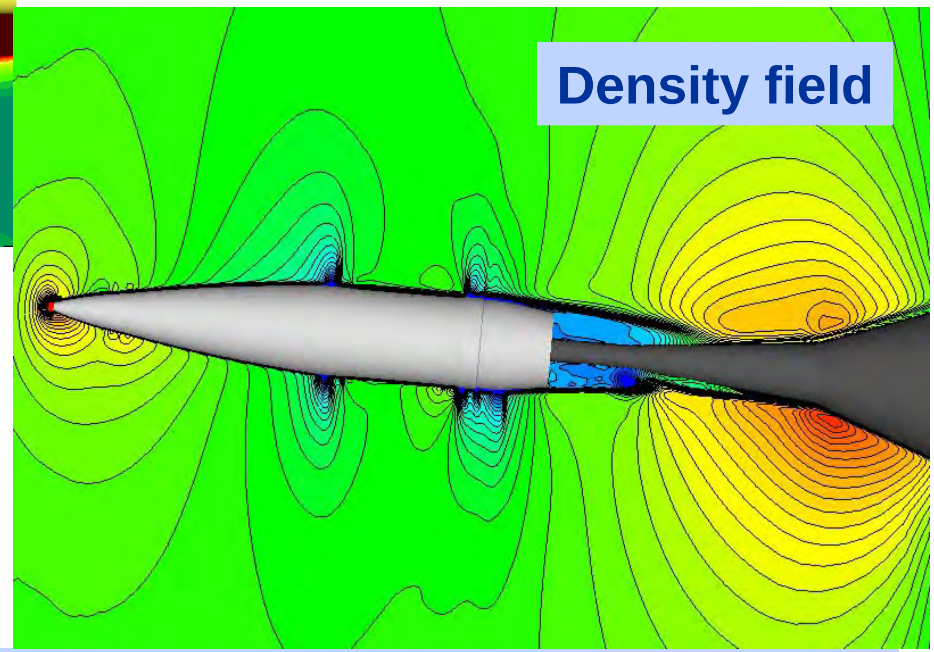

Elsa	CFD	TEST	Error(%)
C_{mq}	-6,3	-7,1	11%

Transonic Conditions: Wind Tunnel S3Ma/ elsA k-ω
(M_∞= 0.9, α = 3°, Pi = 1.2 bar, Ti = 300 K, $\theta \pm$ 1°, f = 6 à 10 Hz)

Example of Validation Results: Magnus of Kinetic Projectiles

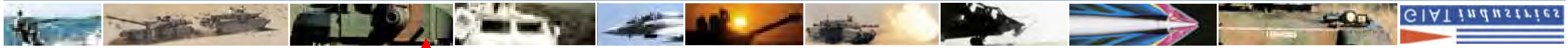

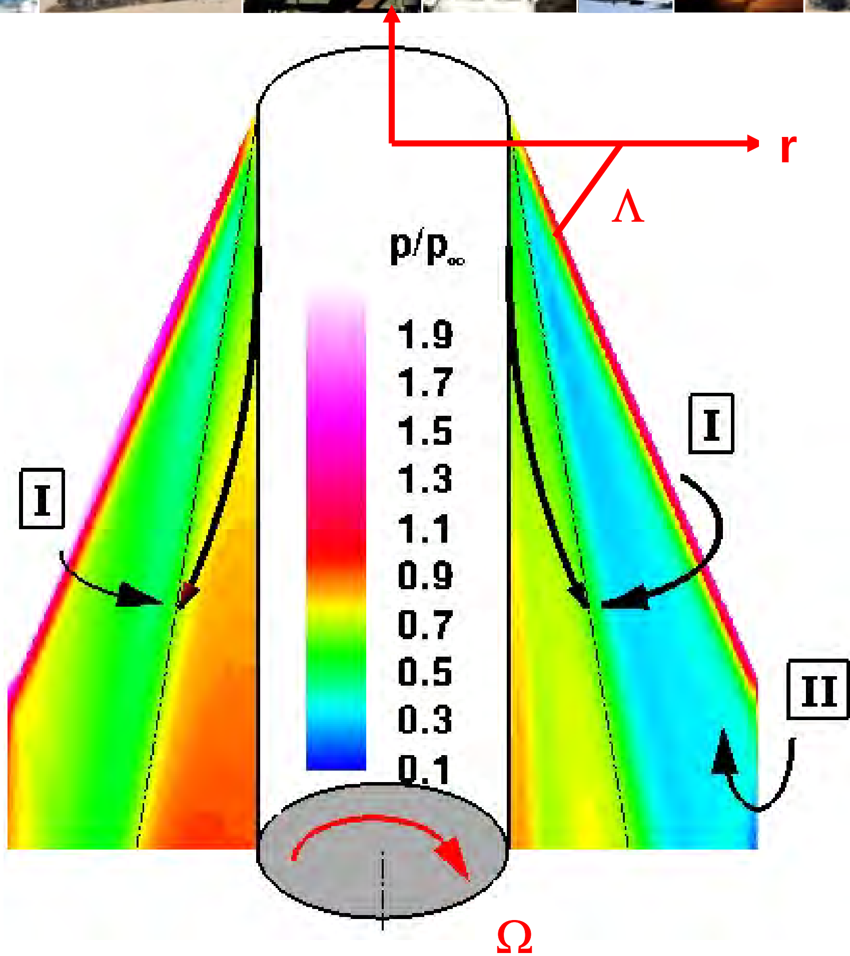

- **Magnus effect origin on fins**
  - **Interaction with asymmetric fuselage wake**
  - **Modifications of the local incidences induced by spin (apex shock & tip vortex)**
- **Flow description**
  - **I Apex shocks**
  - **II Tip vortex**

- → $\alpha_{local} = f(\alpha, \delta, r, \Omega)$ $\alpha_{local} = \alpha \pm \delta \pm r.\,\Omega/V_\infty$
- → $\alpha_N = \tan^{-1}(\tan \alpha_{local} / \cos \Lambda)$
- → $Mach_N = Mach_\infty \sqrt{(1 - \cos^2 \alpha_{local} \,.\, \sin^2 \Lambda)}$

- **URANS, Baldwin-Lomax, Mach 4.3, $p^* = 0.041$, Pi = 7.7 Bar, Ti = 295 K, α = 4.22°, L/D = 12.5.**

Example of Validation Results: Magnus of Kinetic Projectile

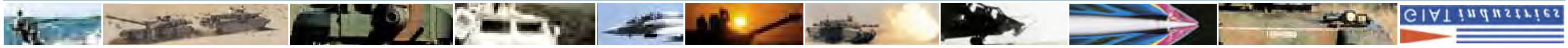

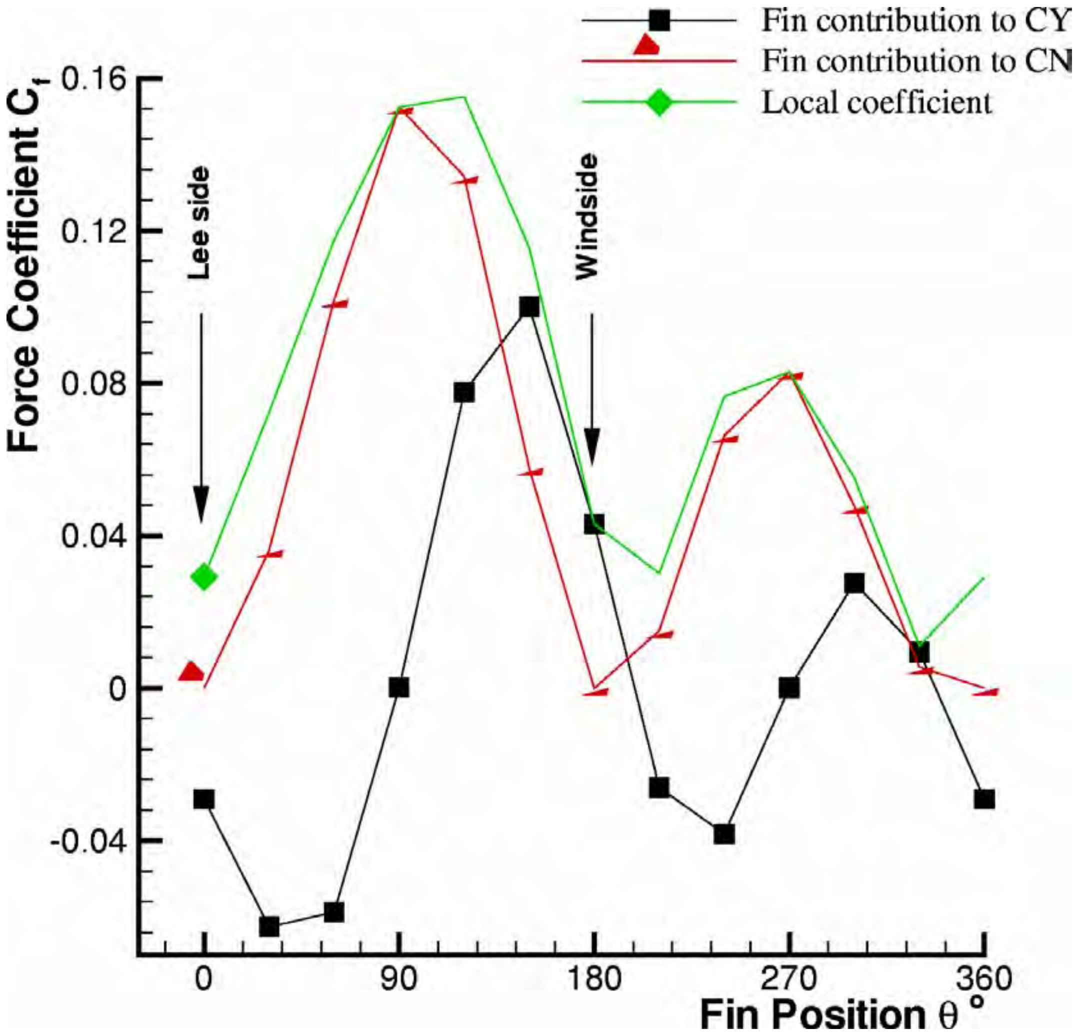

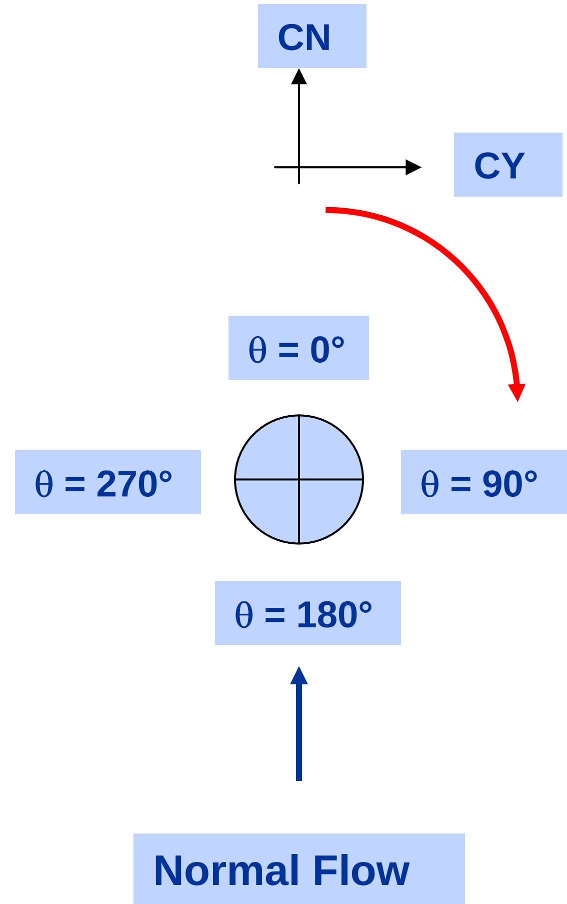

Fin azimuthal position influence (variations of the local incidence) on force coefficients
URANS, Baldwin-Lomax, Mach 4.3, p^*= 0.041, Pi = 7.7 Bar, Ti = 295 K, α = 4.22°, L/D = 12.5.

Example of Validation Results: Magnus of Kinetic Projectile

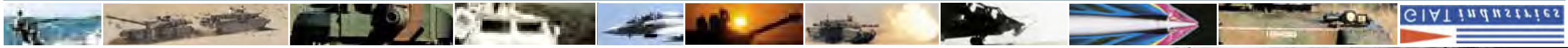

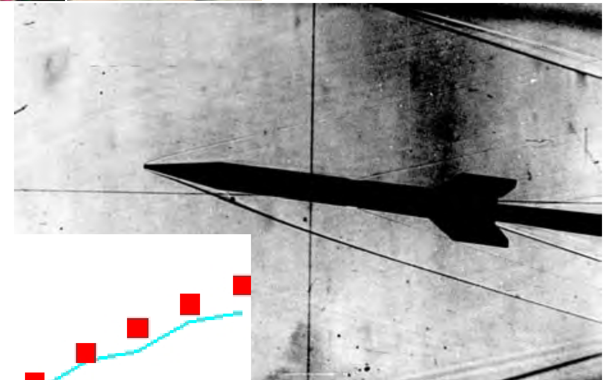

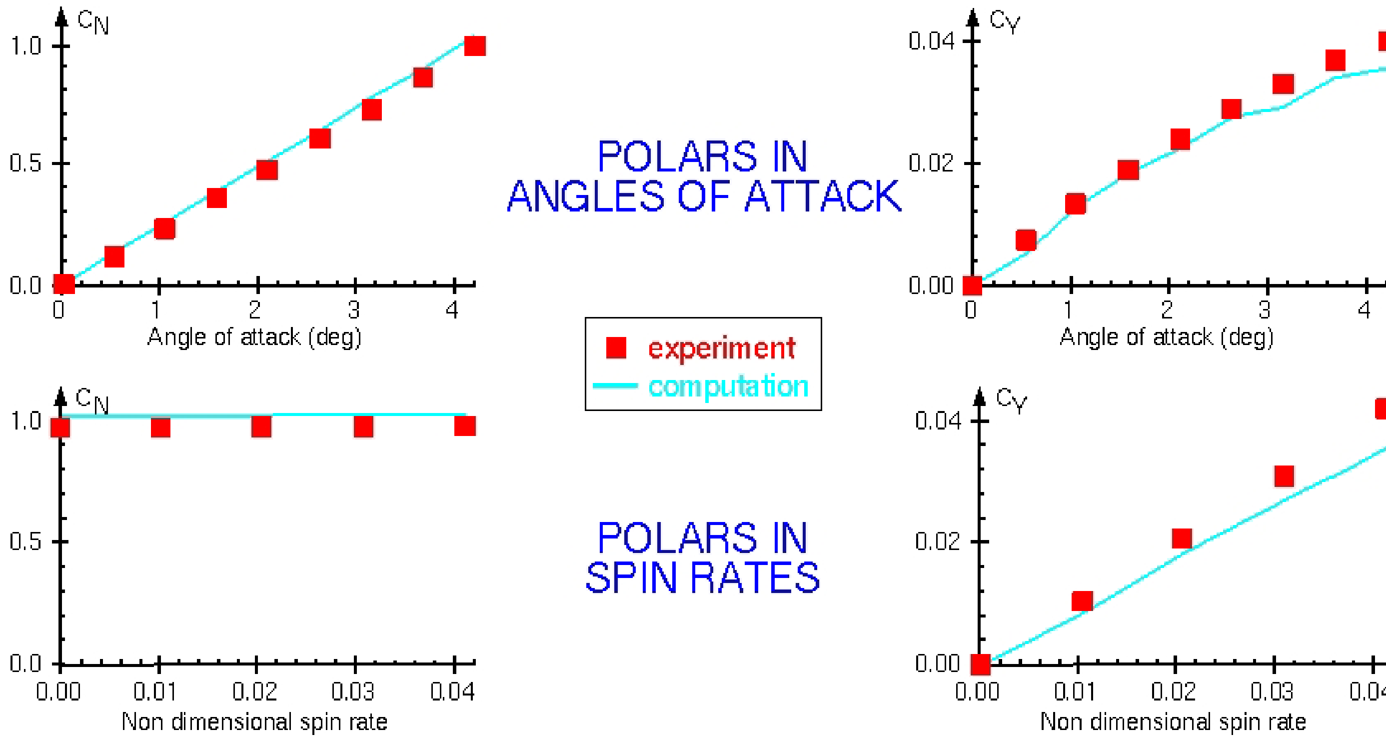

- **URANS FLU3M Baldwin-Lomax**
  - > **Mach 4.3, p*= 0 → <u>0.041</u>, Pi = 7.7 Bar, Ti = 295 K, α = 0°→ <u>4.22</u>°, L/D = 12.5.**

Example of Validation Results: Normal force and Magnus Coefficients of Kinetic Projectile

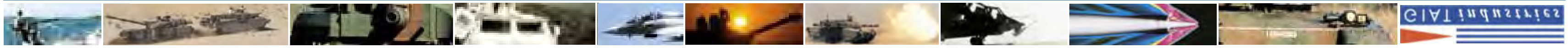

- Global normal force is independent of the rotation
- Mach 4.3, p*= 0.041 (100 rounds/s), Pi = 7.7 Bar, Ti = 295 K, α = 4.22°, L/D = 12.5.

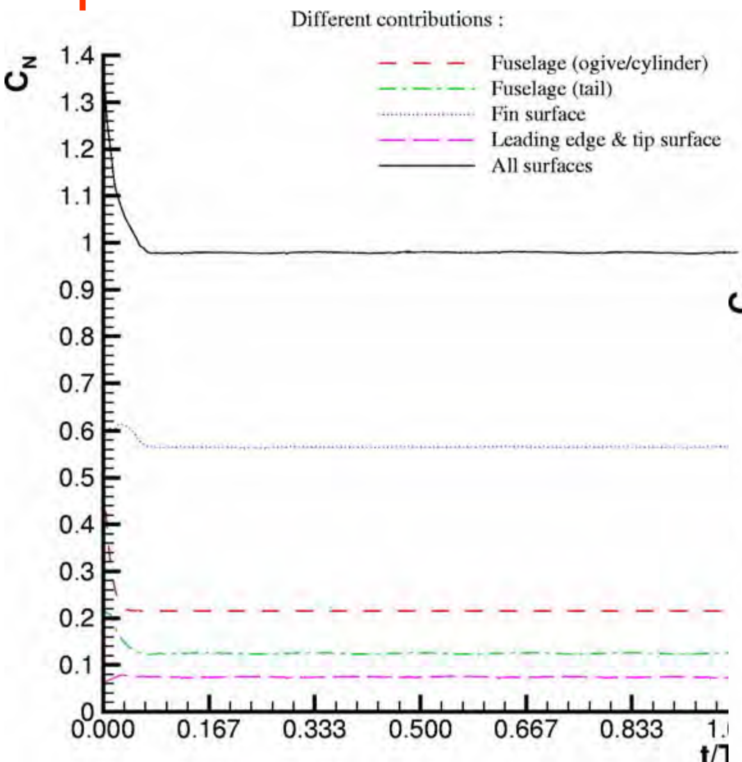

Numerical convergence
- 7200 iterations/round
- 6 under-iterations/iteration

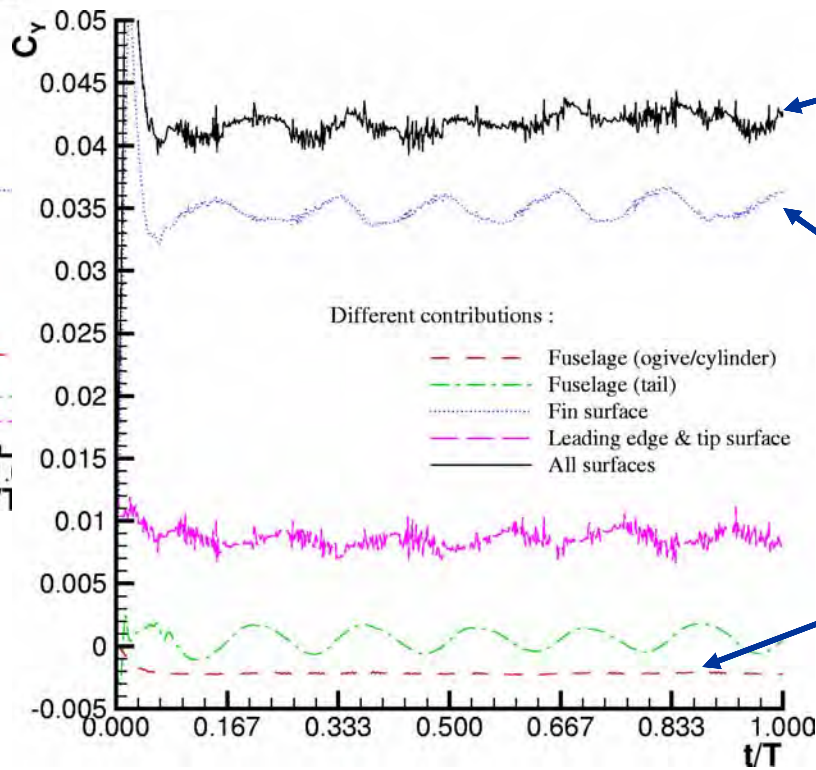

- Global Magnus force

- Fin surface contribution

- Inverse contribution of the fuselage

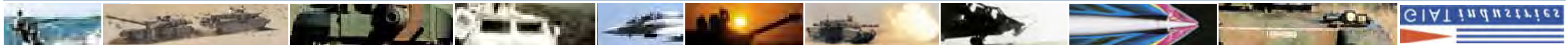


Wind Tunnel S3Ma
Model's scale: 1.6, L/D = 30
V16
TD

Example of Validation Results: Cmq, Clp and Magnus of Kinetic Projectiles

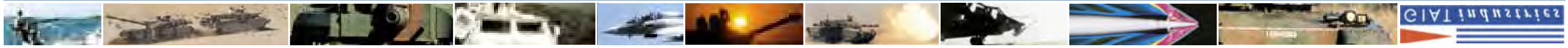

CFD (URANS FLU3M+Balwin-Lomax and Elsa+k-ω) / Wind Tunnel S3Ma (L/D = 30)

Cmq: M_∞= 4.5, α = 0°→ 5°, Pi = 6 bar, Ti = 299 K, θ ± 1.5°, f = 2.2 → 4.2 Hz (FLU3M)
Clp: M_∞= 4.5, α = 0°→ 5°, Pi = 6 bar, Ti = 299 K, p = 1.5 → 55 Rd/s (elsA)
Magnus: M_∞= 4.5, α = -1°→ 5.5°, 3°, Pi = 6 bar, Ti = 356 K, p = 10→ 90 Rd/s (65) (FLU3M)

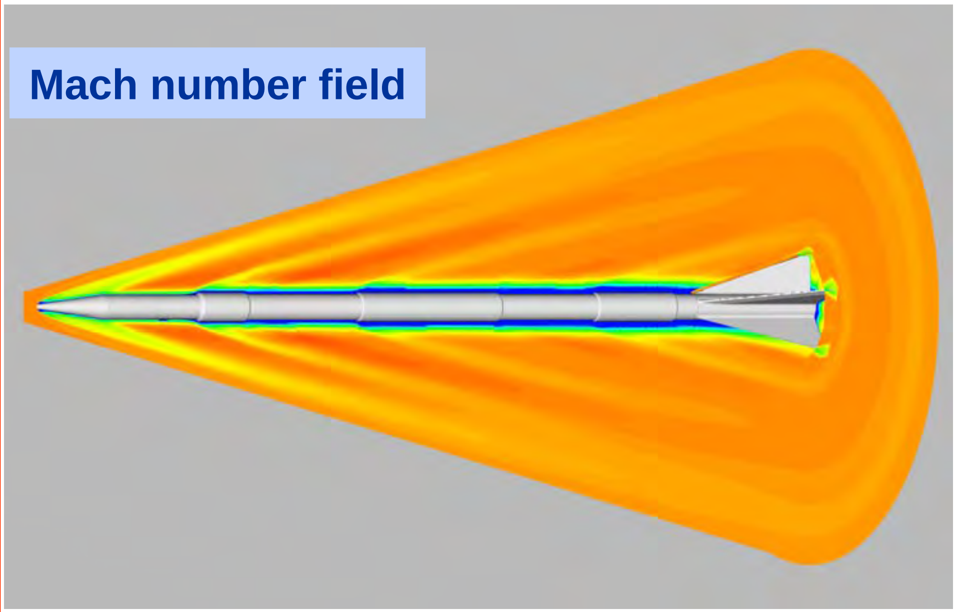

	TESTS	CFD	Errors (%)
Clp	–15	-15.35	**2.3**
Cmq	-2800	-2619	**6.5**
Cy	0.045	0.0474	**-5.3**
Cn	-1.071	-1.112	**-4**

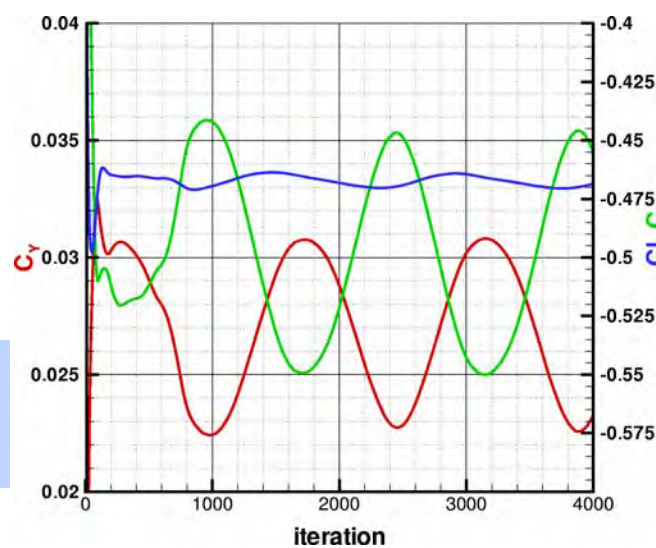

- **Periodic behaviour of the Magnus and roll moment coefficients during unsteady computation**
- **Mach 4.4, p^*= 0.02, Pi = 6 Bar, Ti = 360 K, α = 2°, L/D = 30.**

CONCLUSIONS

- **Extensive wind tunnel database for validation, need free flight results**

- **Progress in CFD allows us to predict projectile unsteady aerodynamics. With respect to spinning and kinetic projectiles, a demonstration of the capability of the numerical approach was carried out**

- **Satisfactory agreement between computations and experiments on the pitch and roll dampings and on the Magnus effect**

Example of Validation Results: Clp of Spinning Projectile

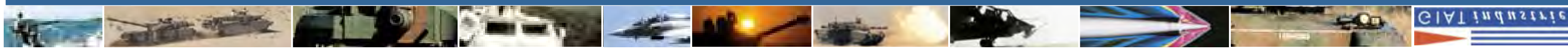

- $Cl_p = (Cl_{(p)})/(p.L_{réf}/V_\infty)$

CFD (RANS, Baldwin-Lomax), p* ≈ 0.2, α = 0°)

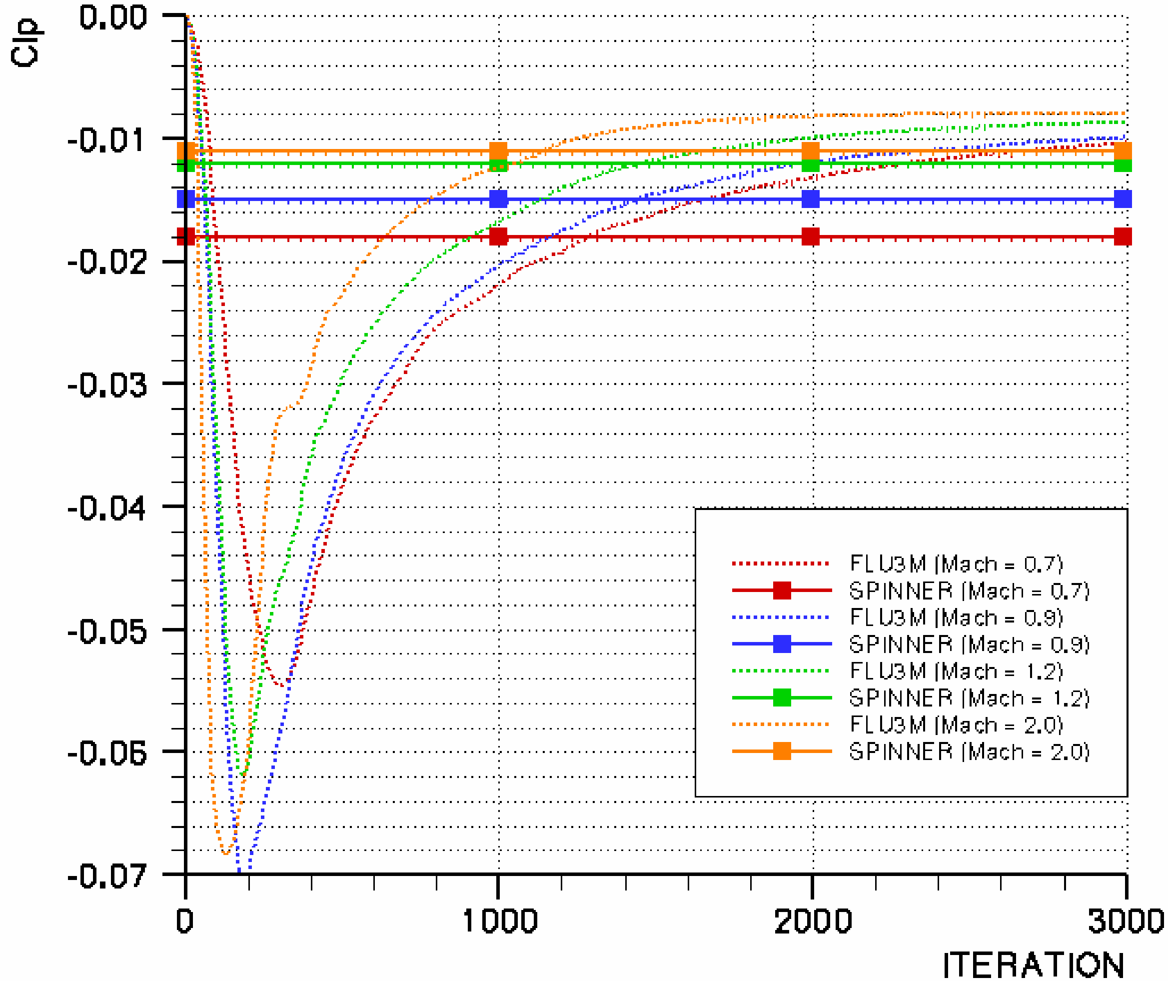

Mach Number	Clp	
	FLU3M	SPINNER
0.70	-0.010	-0.018
0.90	-0.010	-0.015
1.20	-0.009	-0.012
2.00	-0.008	-0.011

CFD Prediction of the Pitch Damping Coefficient: Pseudo-URANS

- $Cm_q = (Cm_{(q)} - Cm_{(q=0)})/(q.L_{réf}/V_{\infty})$

  (Mach = 0.90, α = 3°, Pi = 1.20 Bar, Ti = 300 K)

> q = 0 rad/s

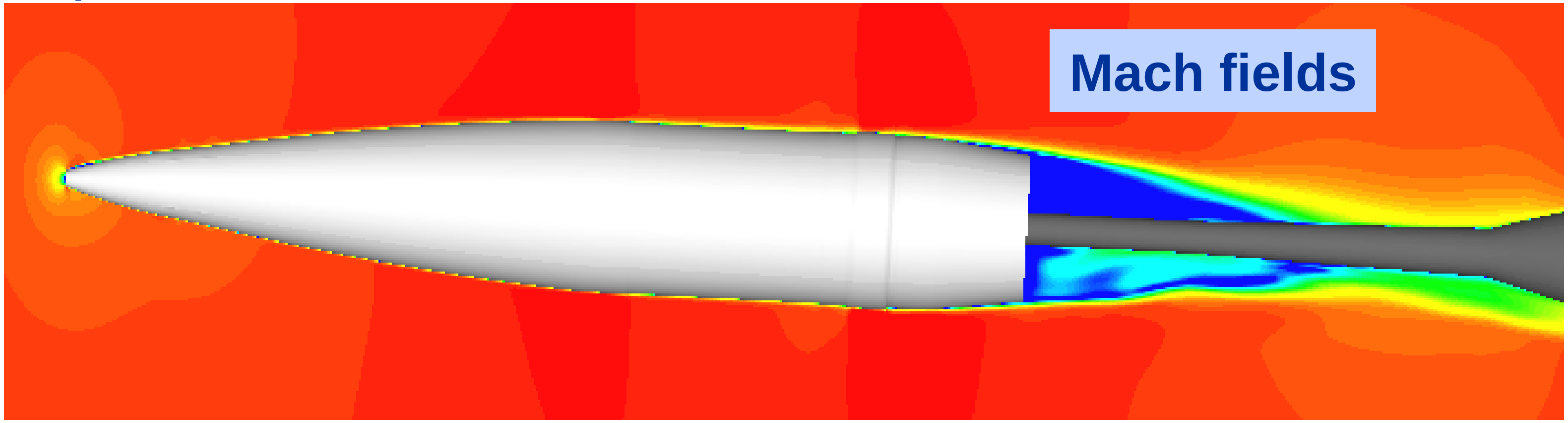

> q = 10 rad/s

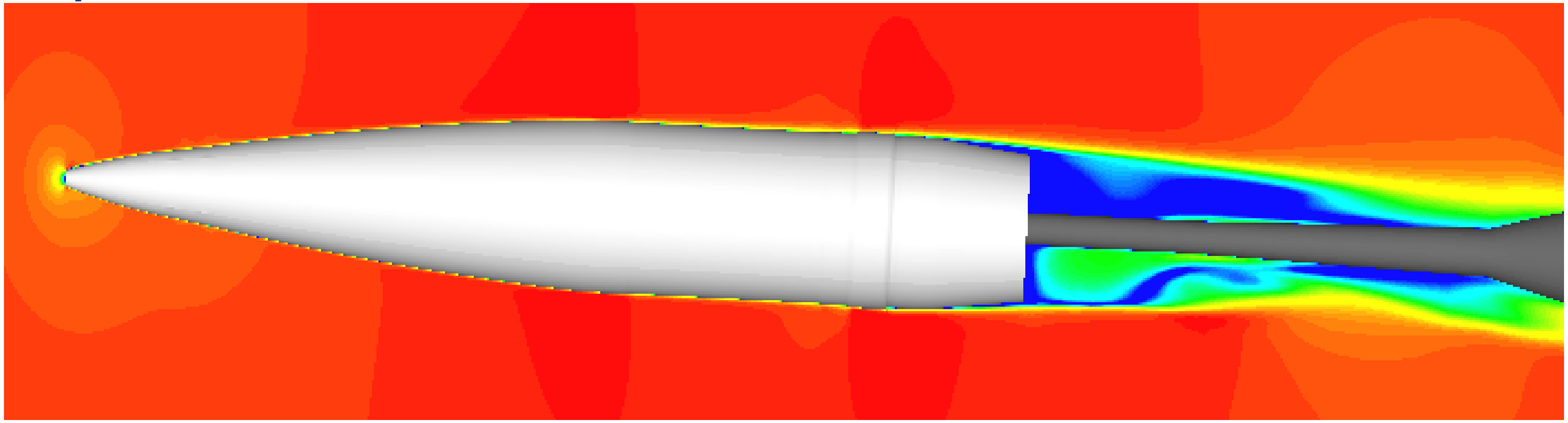

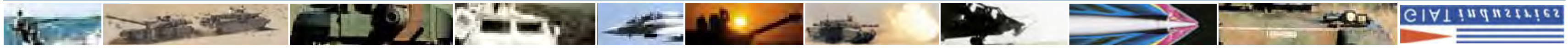

CLASSIFICATION OF LEESIDE FLOWFIELDS FOR THICK DELTA WINGS WITH SHARP LEADING EDGES

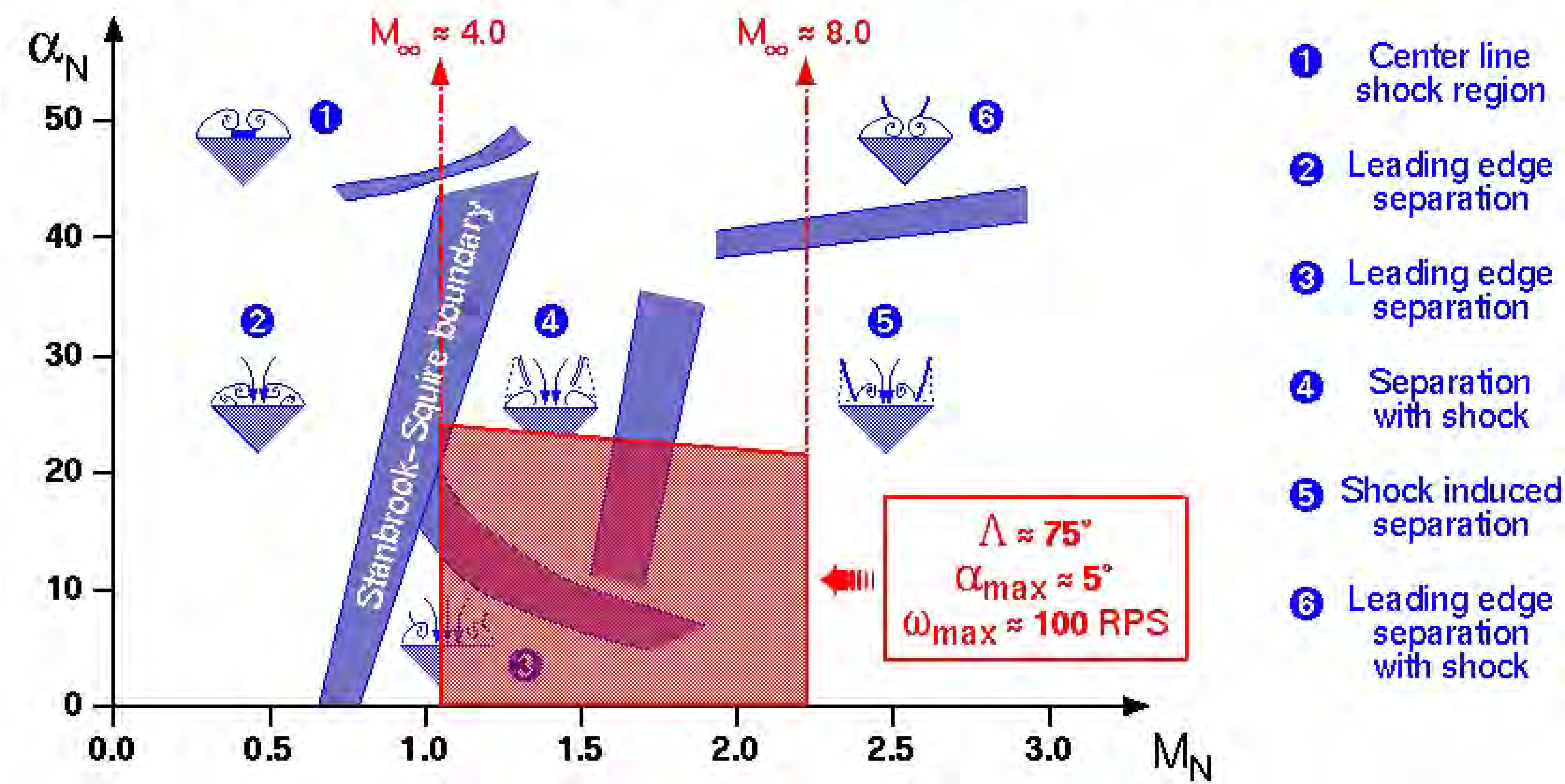

Λ= 70°, Mach 4.3, p^*= 0.041, Pi = 7.7 Bar, Ti = 295 K, α = 4.22°→ M_N = 1.52 et α_N = 0.27

Boundary Conditions

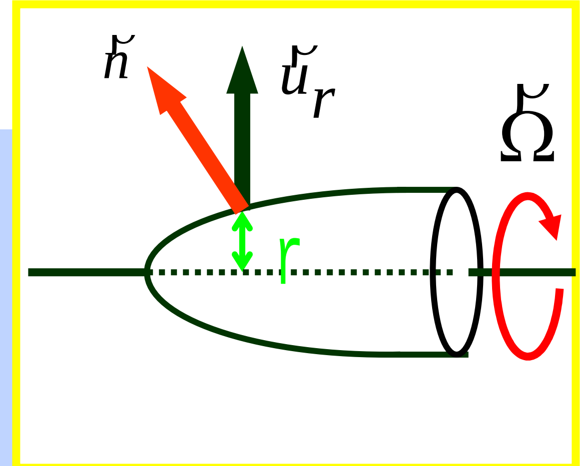

- **Fuselage state**
  - > no slip condition $\vec{V}_w = r\vec{\Omega}$
  - > adiabatic wall $\left.\dfrac{\partial T}{\partial n}\right|_w = 0$
  - > normal pressure gradient $\left.\dfrac{\partial P}{\partial n}\right|_w = \rho r \Omega^2 . \left(\vec{u}_r . \vec{n}\right)$
- **Fin state**
  - > slip or no slip conditions $\vec{V}_w . \vec{n} = 0$ $\vec{V}_w = r\vec{\Omega}$
- **Outer boundary condition is obtained from the Theory of Characteristics**

Aerodynamic Characteristics of a Grid Finned Projectile from Free-Flight Tests at Supersonic Velocities

A. Dupuis
DRDC-Valcartier
Canada

C. Berner
ISL
France

OUTLINE

- **Background**
- **Model Configuration**
- **Experimental Tests**
- **Results**
  - **Grid finned**
  - **Planar (Air Force Finner)**
- **Conclusions**

BACKGROUND

- Grid fins are being studied
  by several organizations

- Favorable lift characteristics at high α
- Low hinge moments
- Good storability

- High drag (can be minimized through web tailoring)

- Prior research include wind tunnel tests and recently CFD
  - Results presented at last 3 ISBs

OBJECTIVES

- **Obtain Aero. Coeffs. & Stability Derivatives**
- **From Free-flight Tests**
  - **DRDC Aeroballistic Range**
- **Establish Data base to compare WT andCFD results**

CONFIGURATION

1 set of fins canted at 2.0° to produce roll

1 set of fins canted at 0.5° to produce trim forces & moments

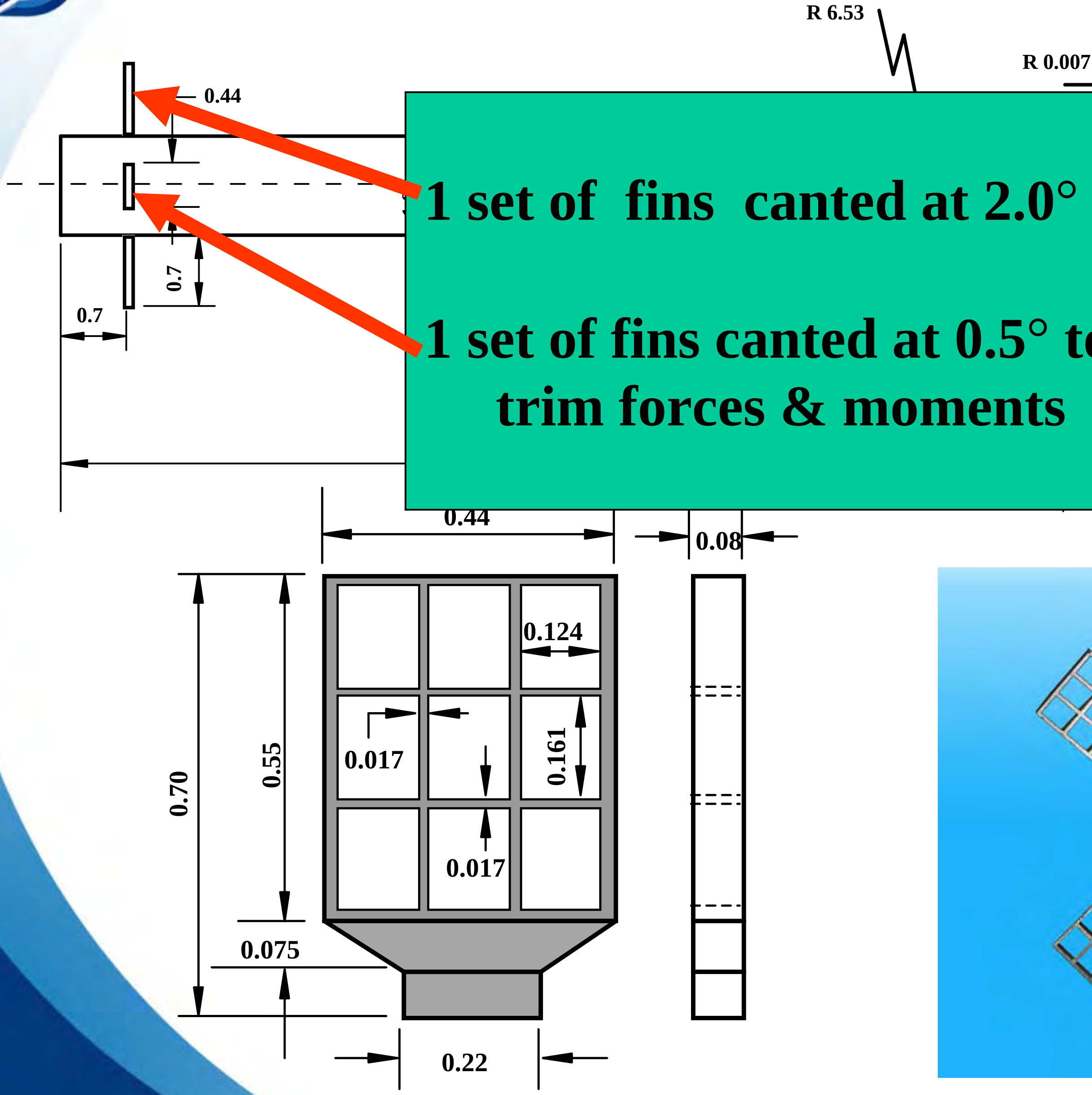

PHYSICAL PROPERTIES

(A/B model)

d (mm)	m (g)	I_x (g-cm^2)	I_y (g-cm^2)	l (mm)	CG from nose (X_{CG} /l)
30.0	881.2	954.55	64517.07	300.0	0.405

DRDC AEROBALLISTIC RANGE

- Length: 250 m
- Model size: 5.56 mm to 155 mm
- Speeds: up to Mach 7.0
- Temperature et humidity
  controlled

DRDC AEROBALLISTIC RANGE

- Instrumented length: 220 m
- Section: 6 m x 6 m
- 54 Stations: Indirect orthogonal shadowgraphs
- 4 Schlieren stations
- at least 4 firings/day

DRDC AEROBALLISTIC RANGE

ARFDAS - Aeroballistic Range Facility Data Analysis

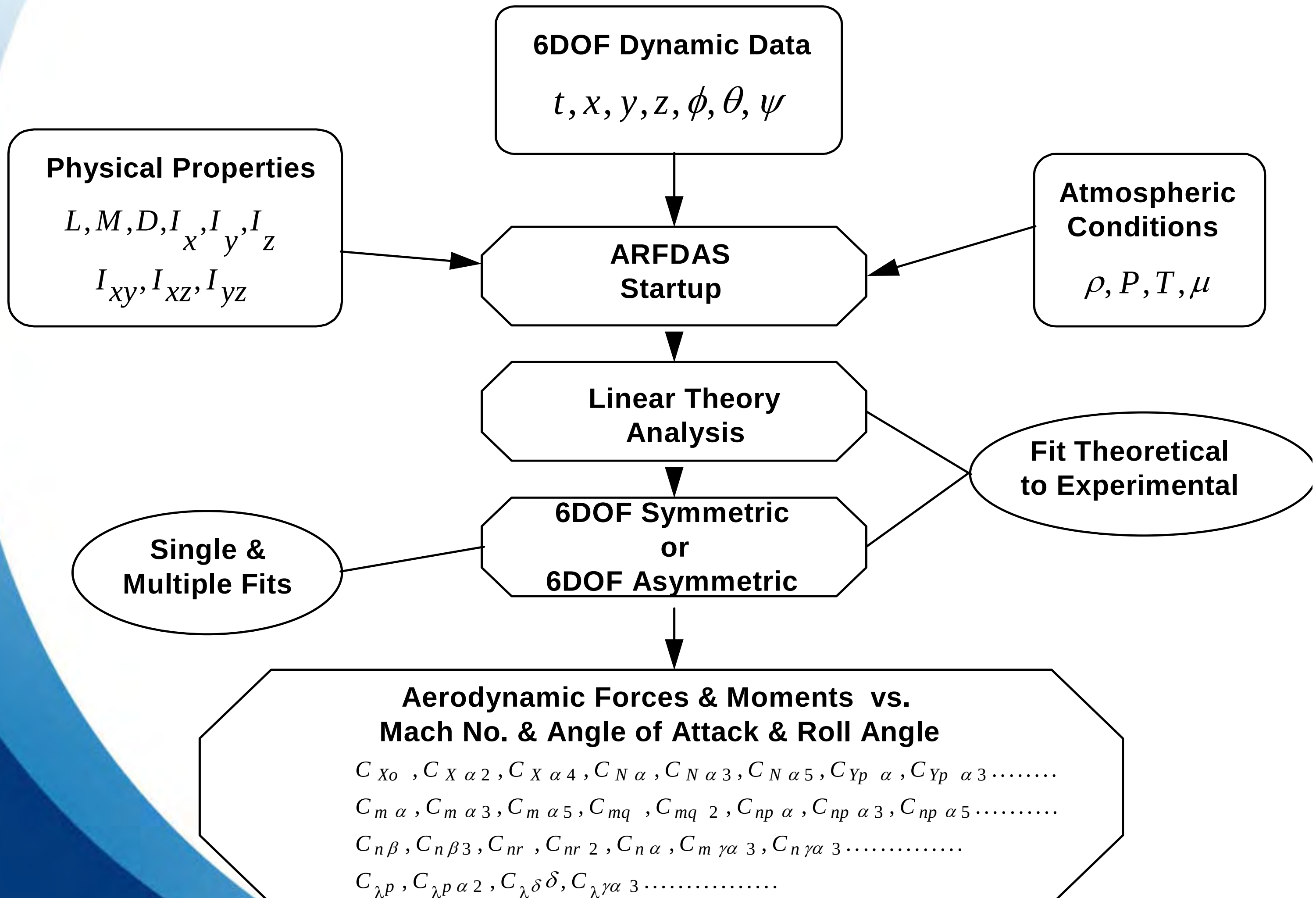

A/B TESTS

- 11 projectiles fired
  - Mach 1.4 to 3.5
- 110 mm Smooth Bore Gun
- First Max Yaws ranged from 2.4° to 10.5°
- Down range spin rate 20.0 °/m

A/B TESTS

V_{MUZ} = 1215 m/s

A/B TESTS

M = 2.12

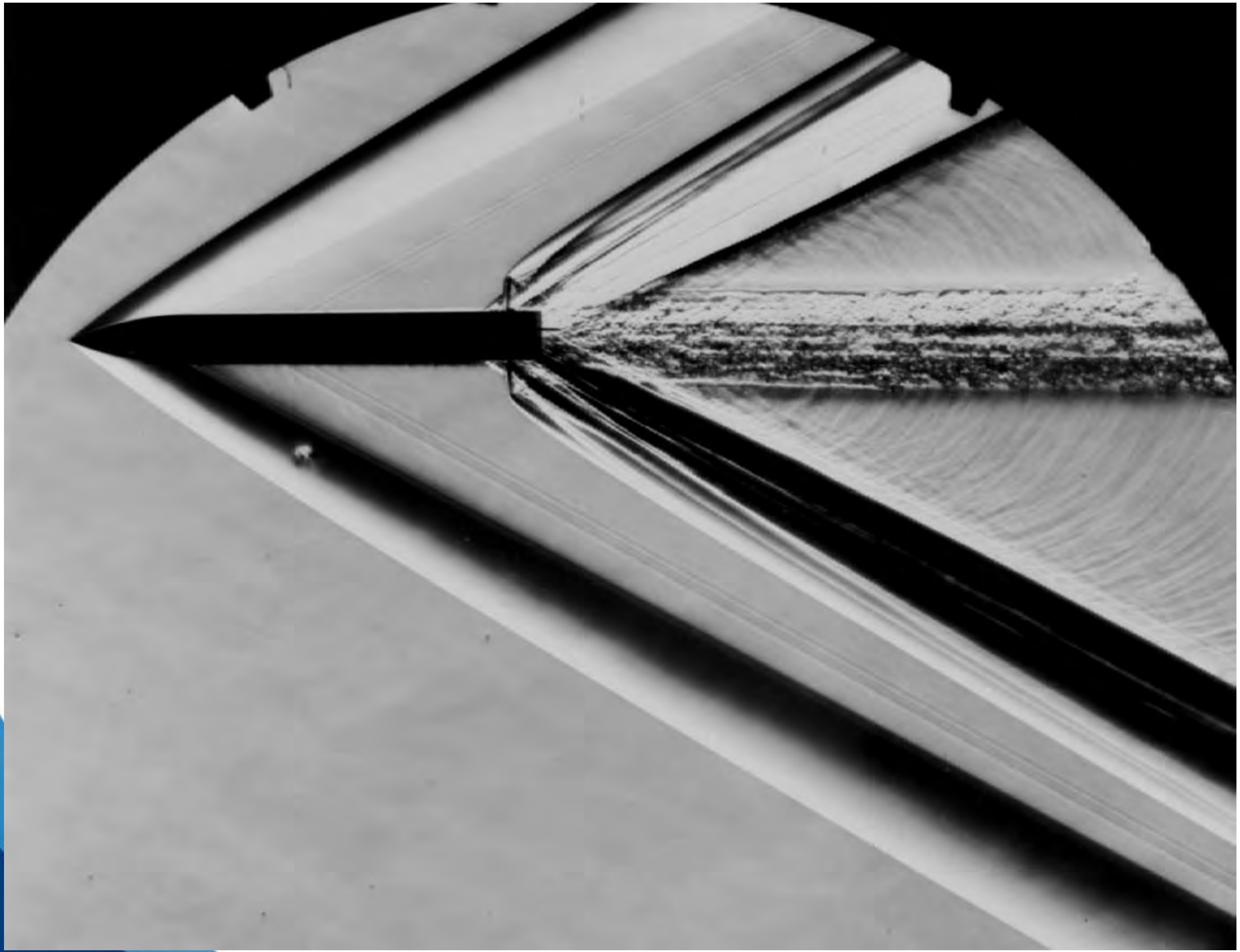

Shot K01

A/B TESTS

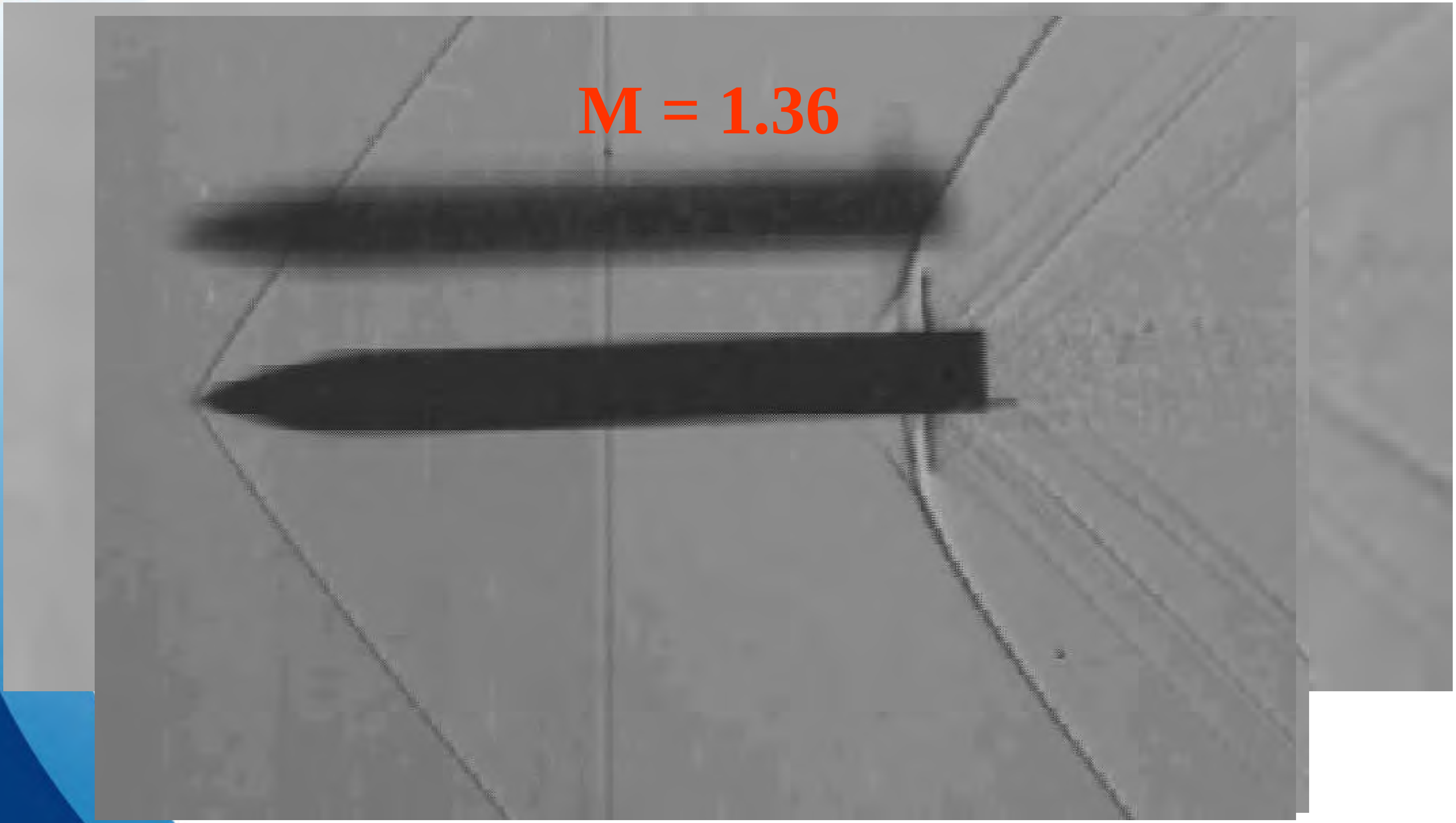

RESULTS

- Grid Finned Results

- Compare with Air Force Finner
  - Tested in DRDC and Eglin Air Force Base Free-Flight Ranges

AIR FORCE FINNER

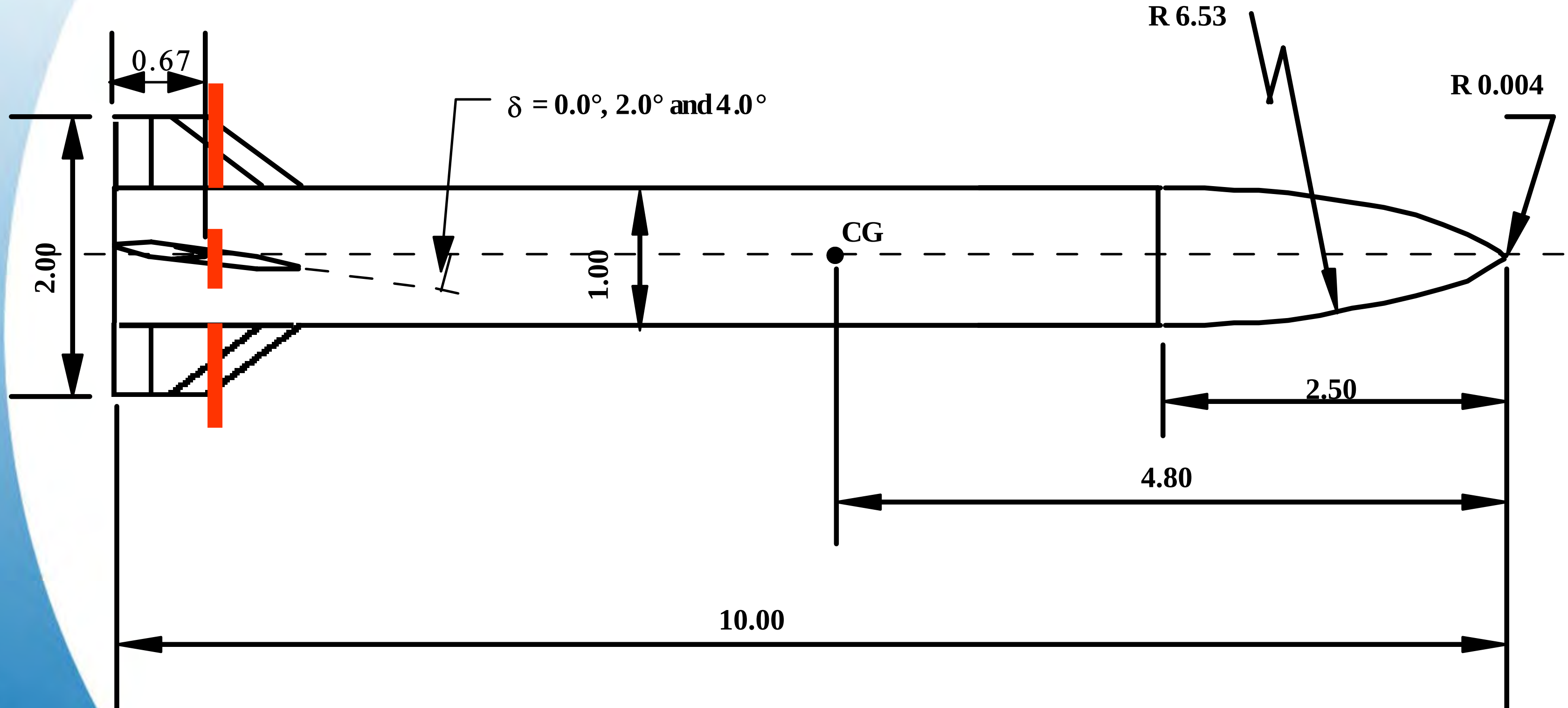

(All moments transferred to 4.05 cal from nose)

AXIAL FORCE

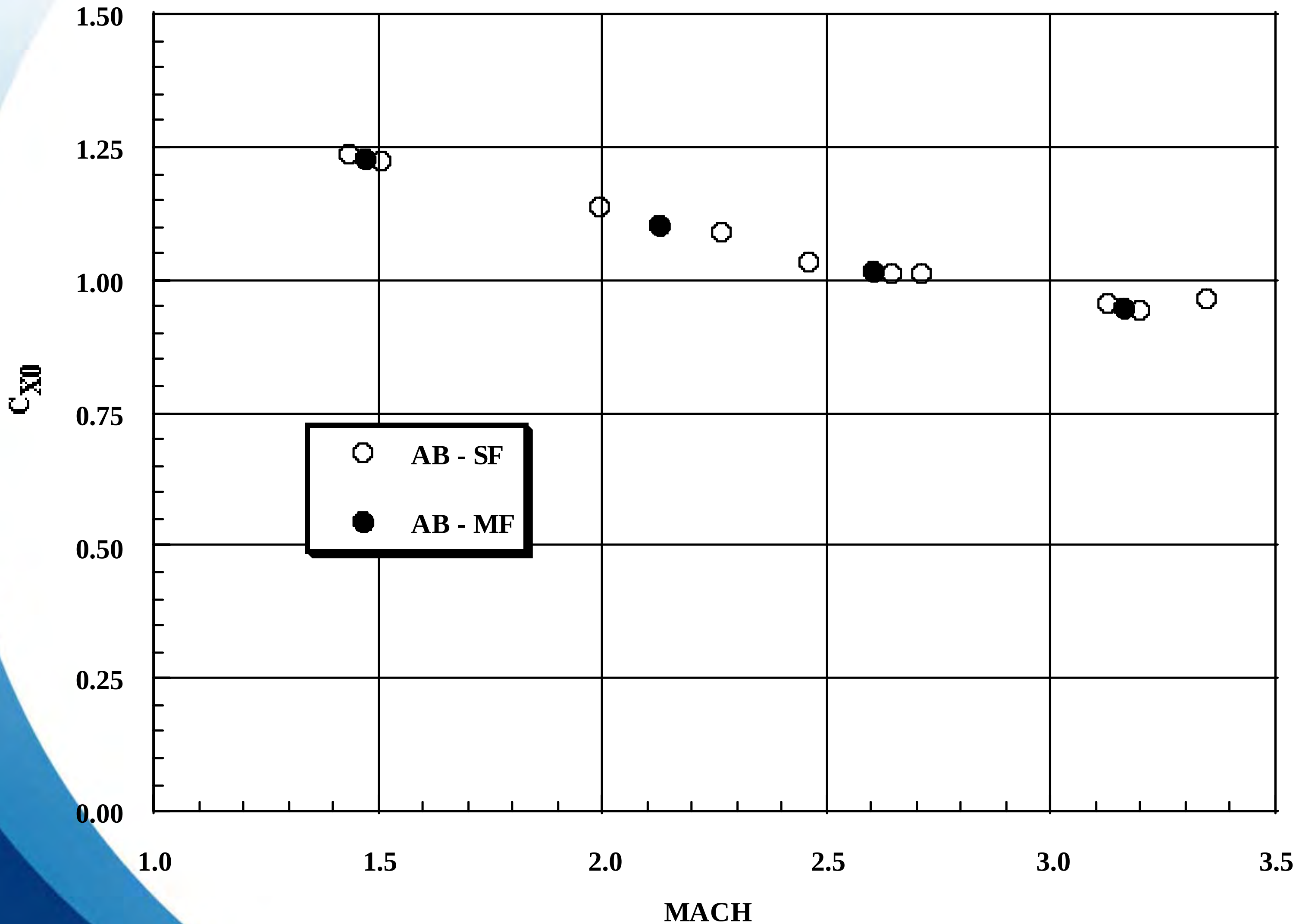

AXIAL FORCE

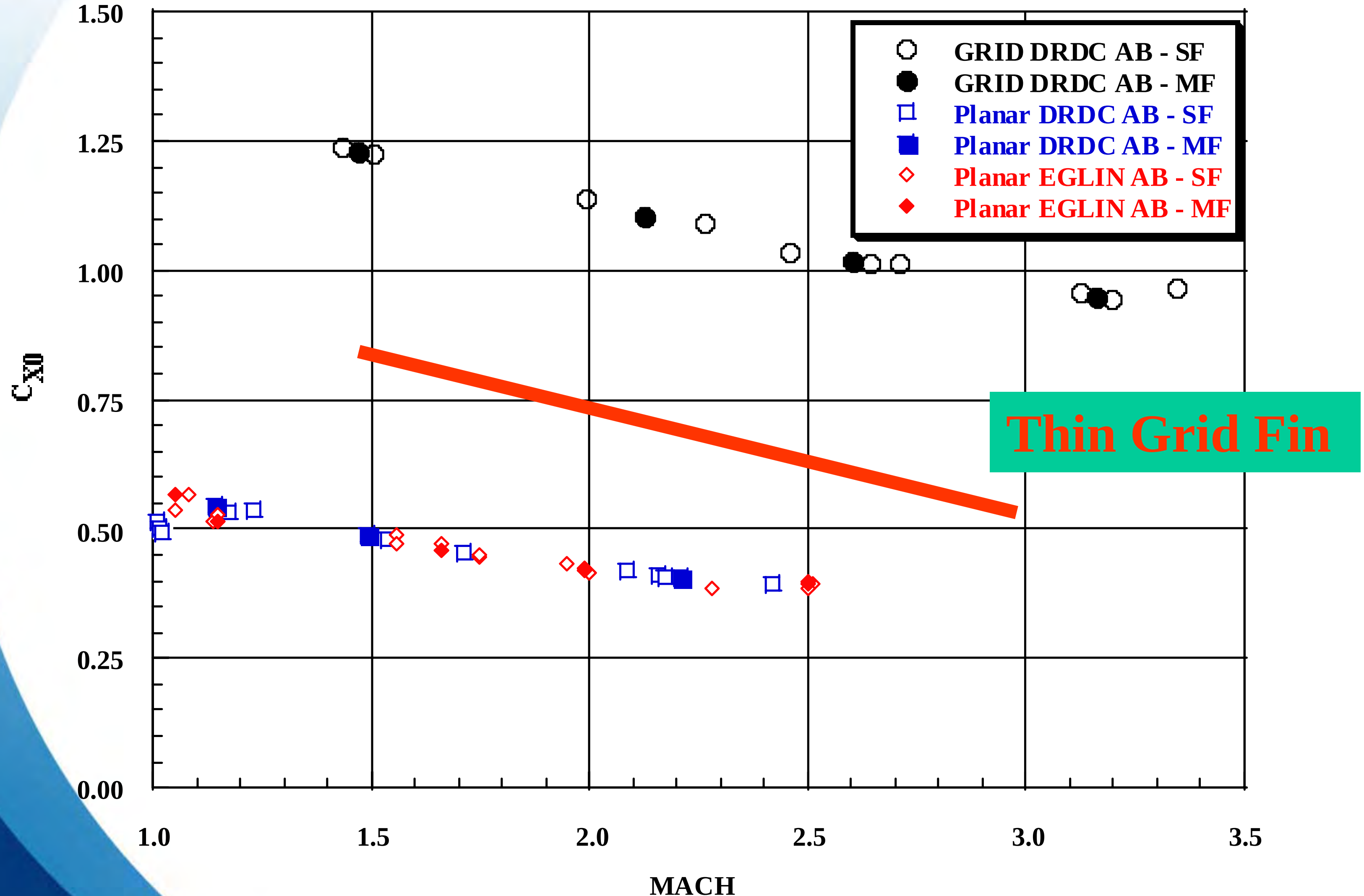

1.50
1.25
1.00
0.75
0.50
0.25
0.00
C_{X0}
1.0
1.5
2.0
2.5
3.0
3.5
MACH
GRID DRDC AB - SF
GRID DRDC AB - MF
Planar DRDC AB - SF
Planar DRDC AB - MF
Planar EGLIN AB - SF
Planar EGLIN AB - MF
Thin Grid Fin

NORMAL FORCE SLOPE

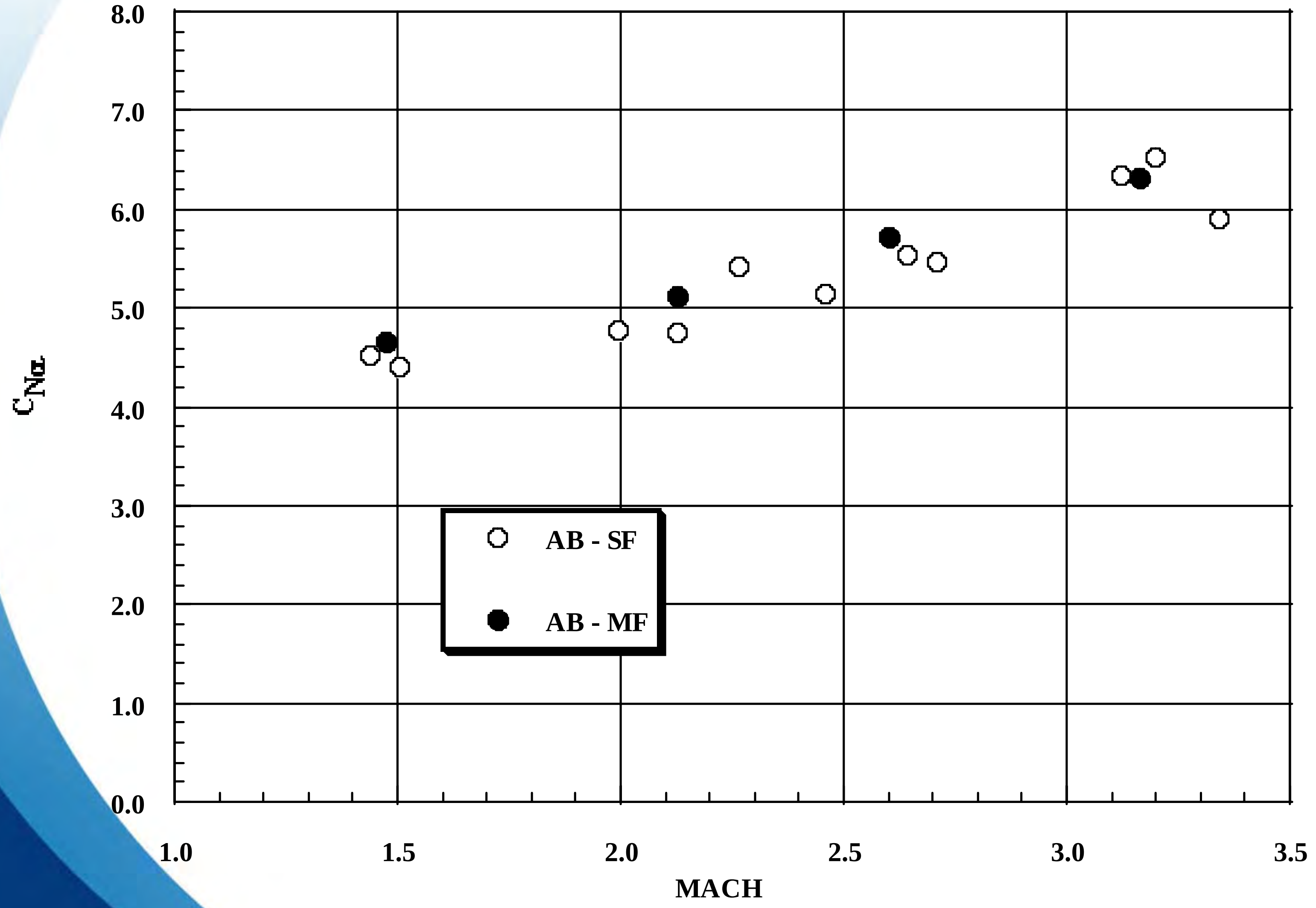

NORMAL FORCE SLOPE

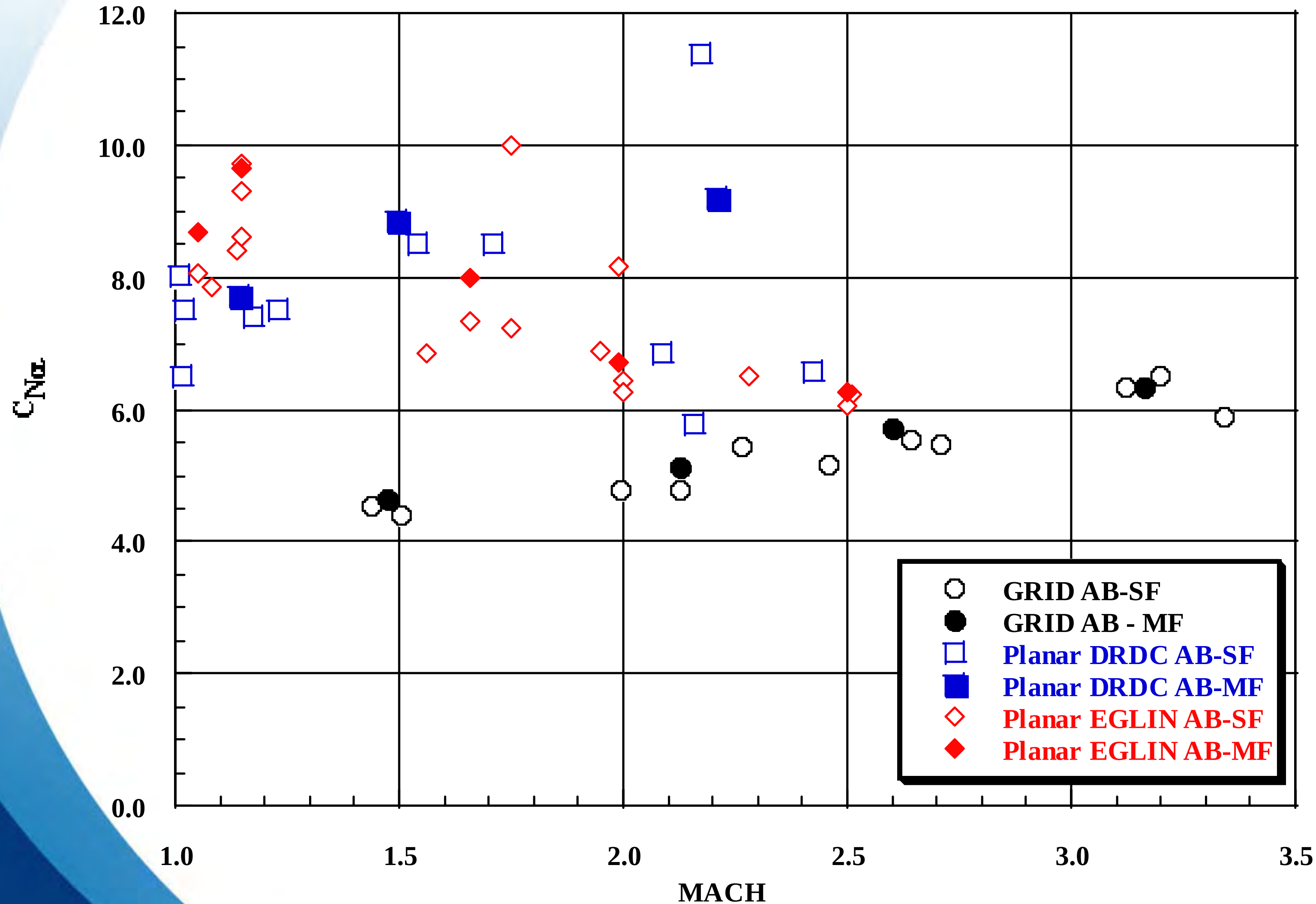

STATIC PITCH MOMENT COEFFICIENT SLOPE

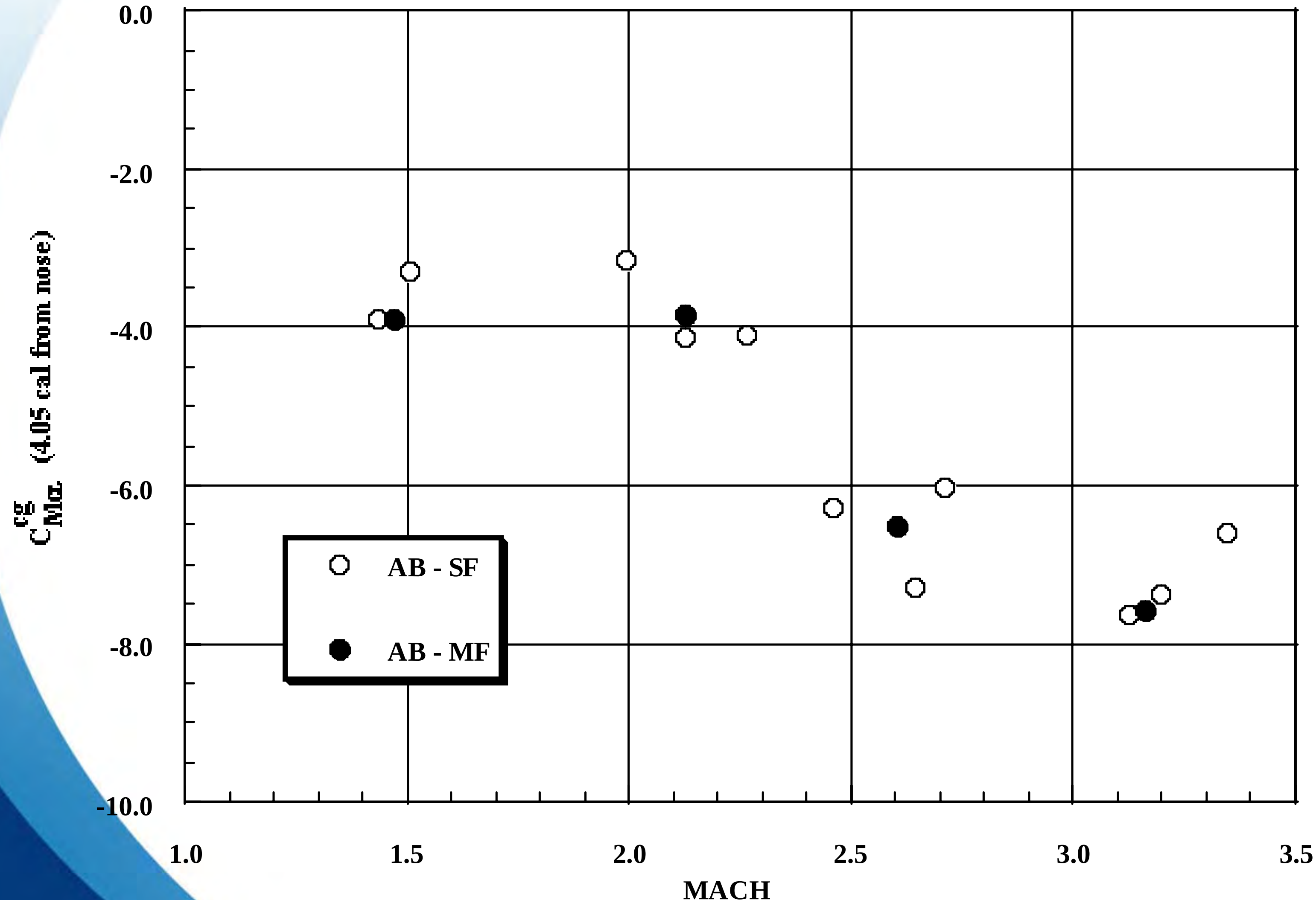

STATIC PITCH MOMENT COEFFICIENT SLOPE

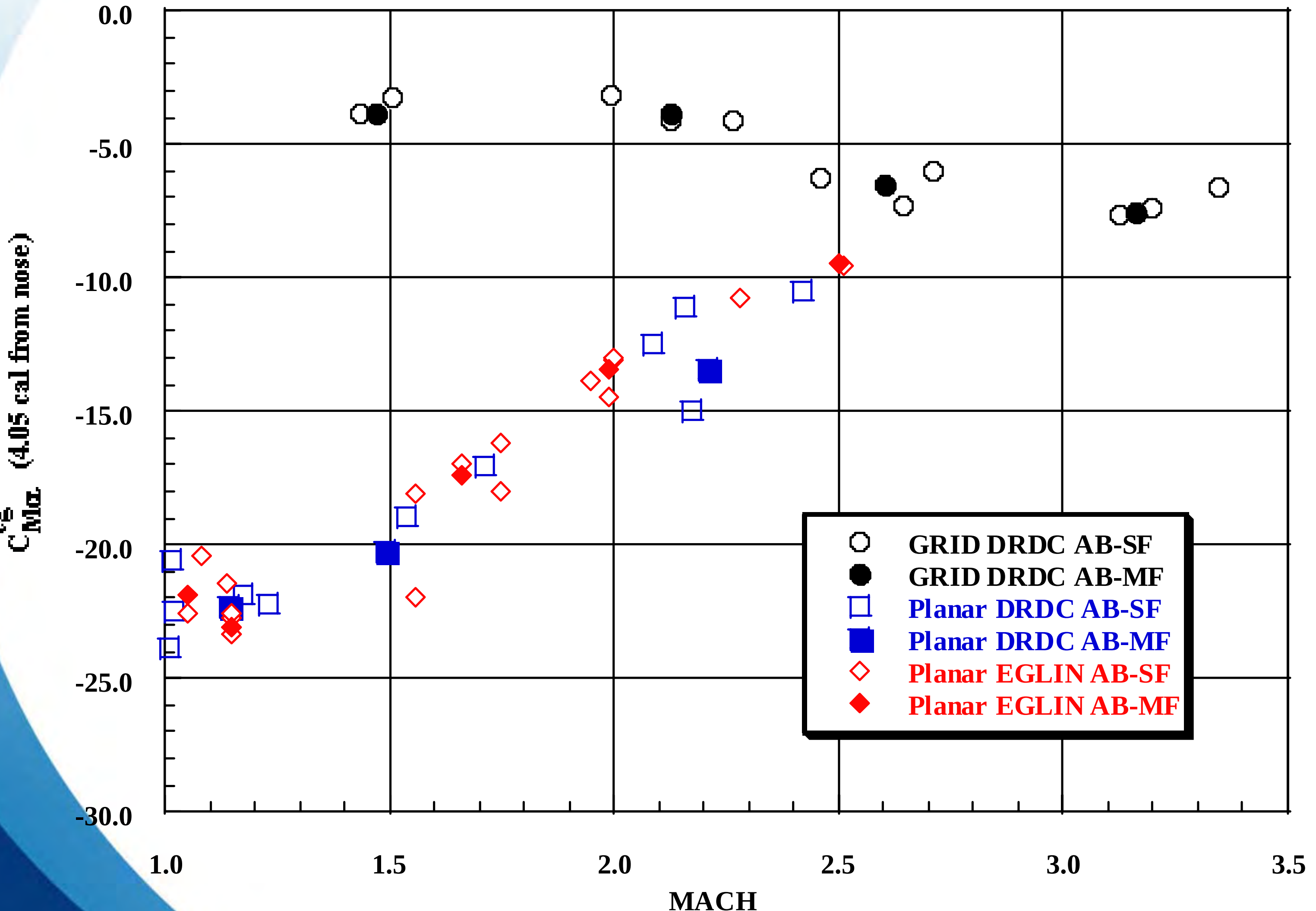

CENTER OF PRESSURE

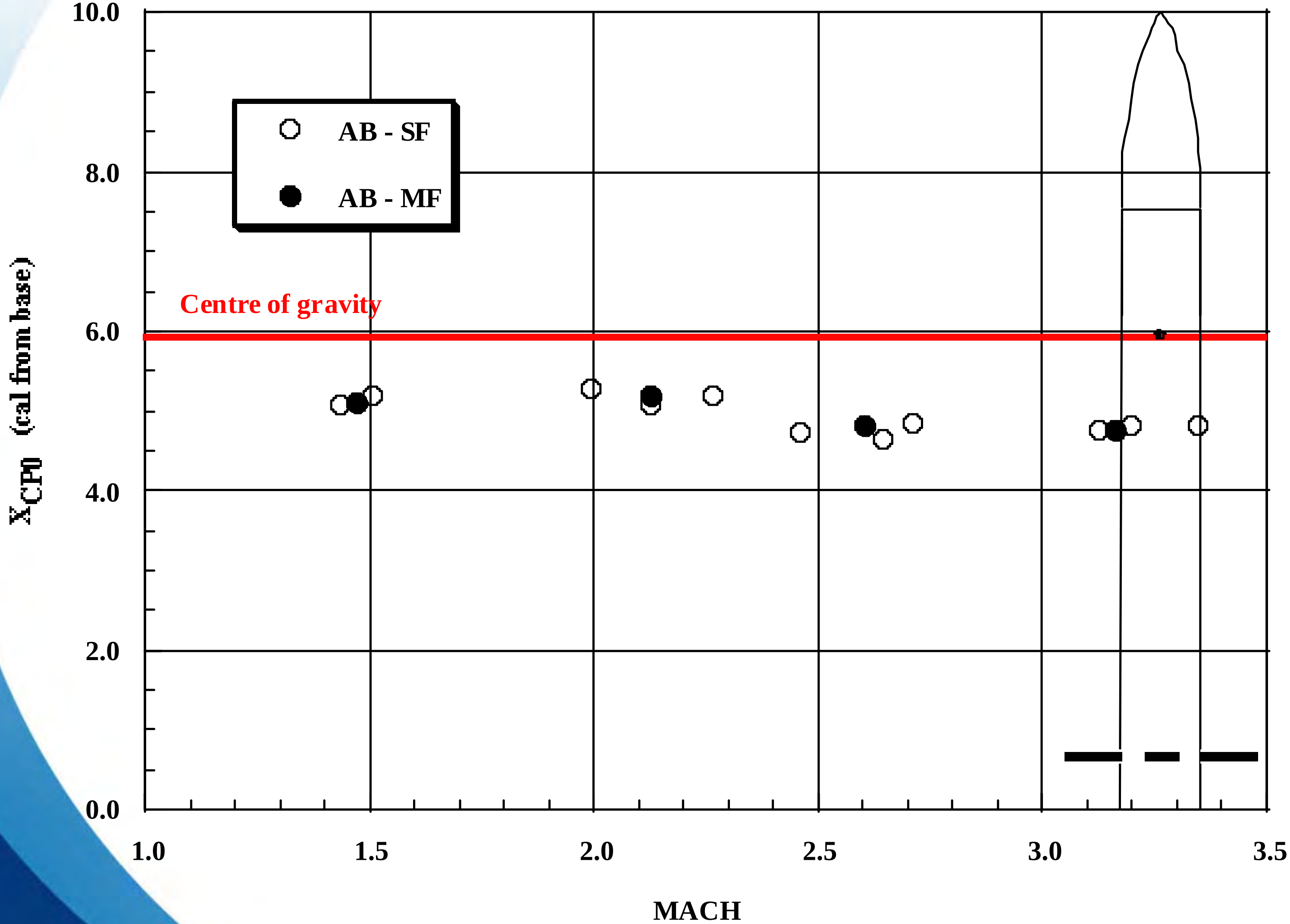

CENTER OF PRESSURE

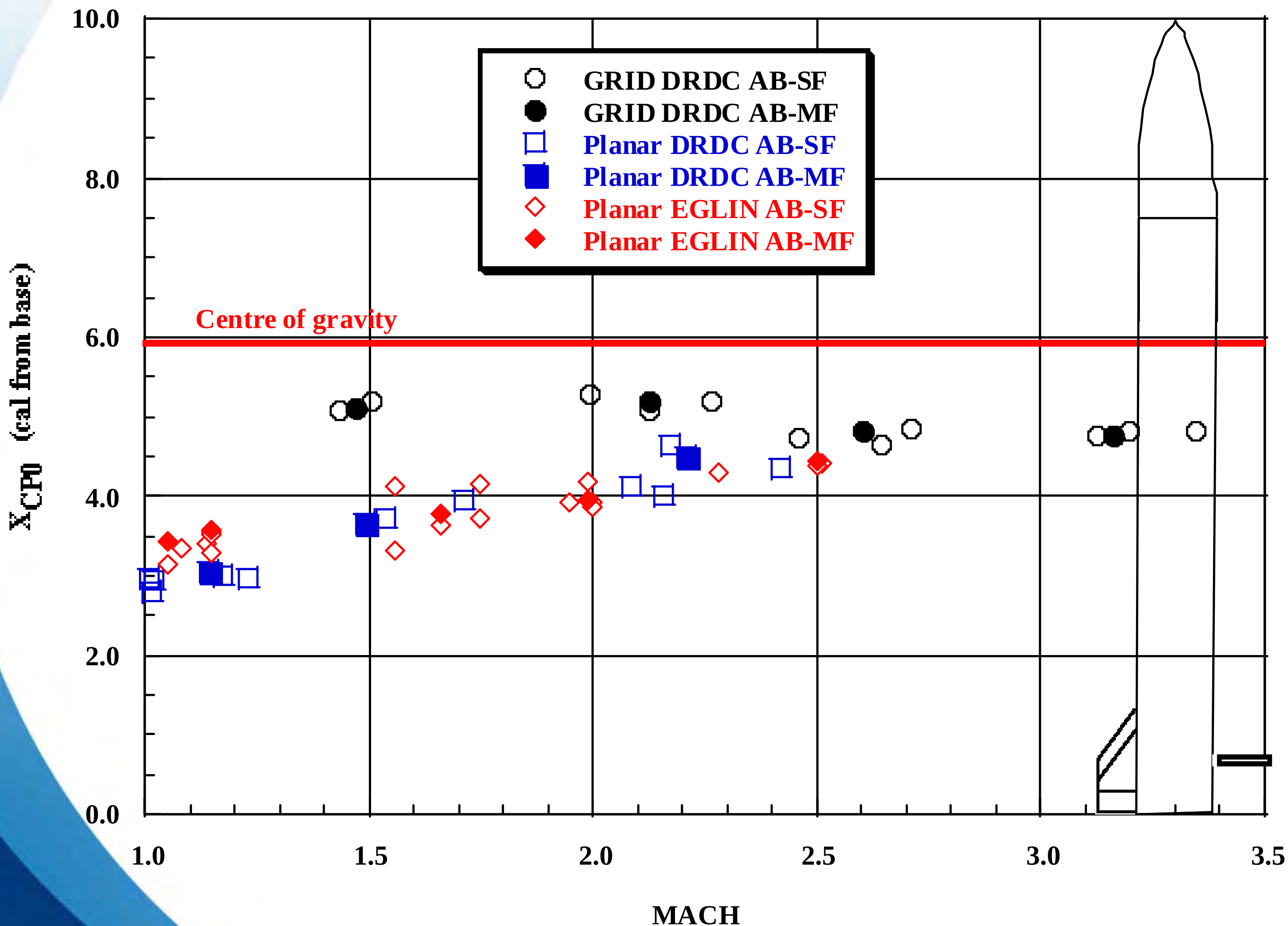

PITCH DAMPING MOMENT

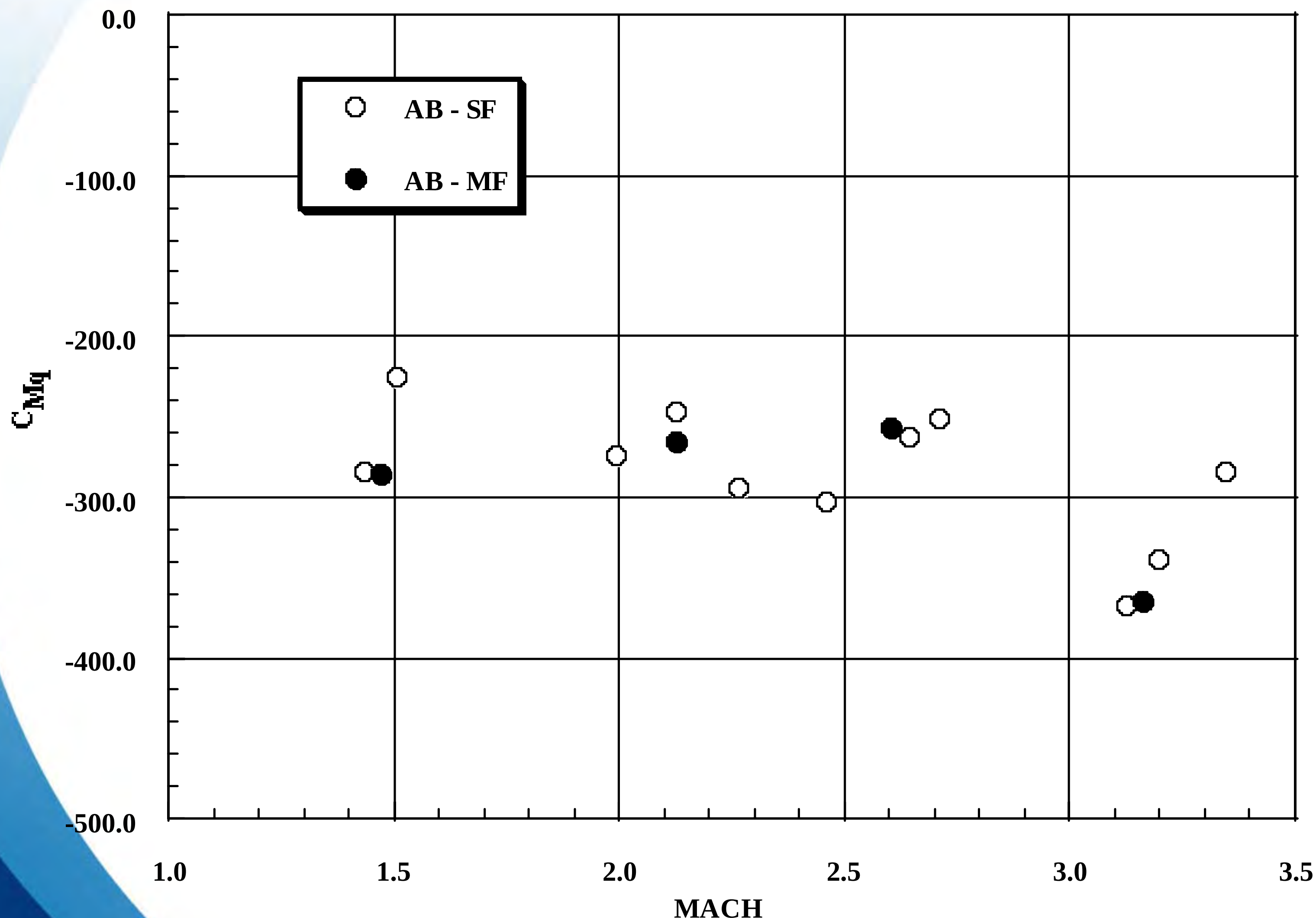

PITCH DAMPING MOMENT

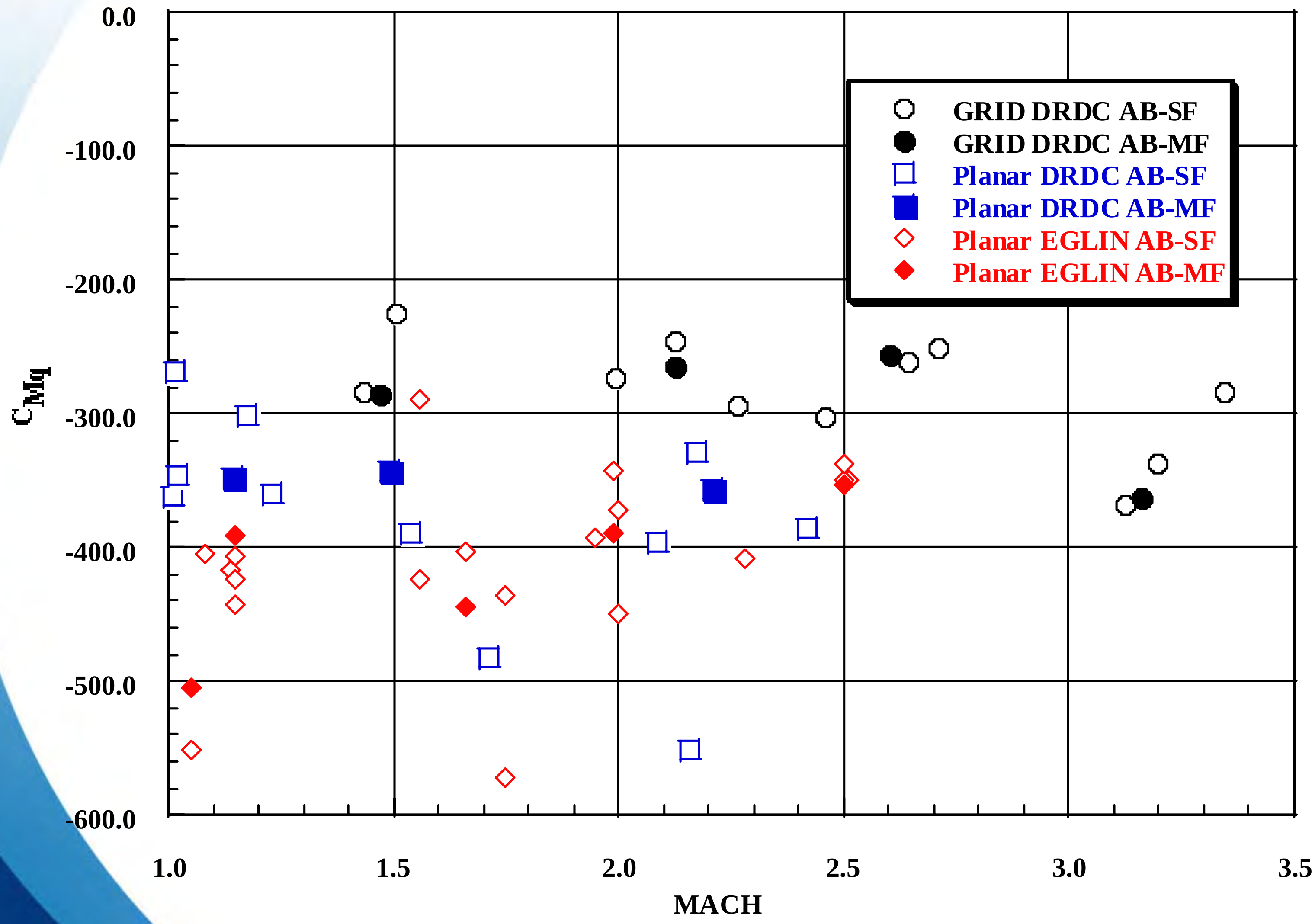

ROLL DAMPING MOMENT

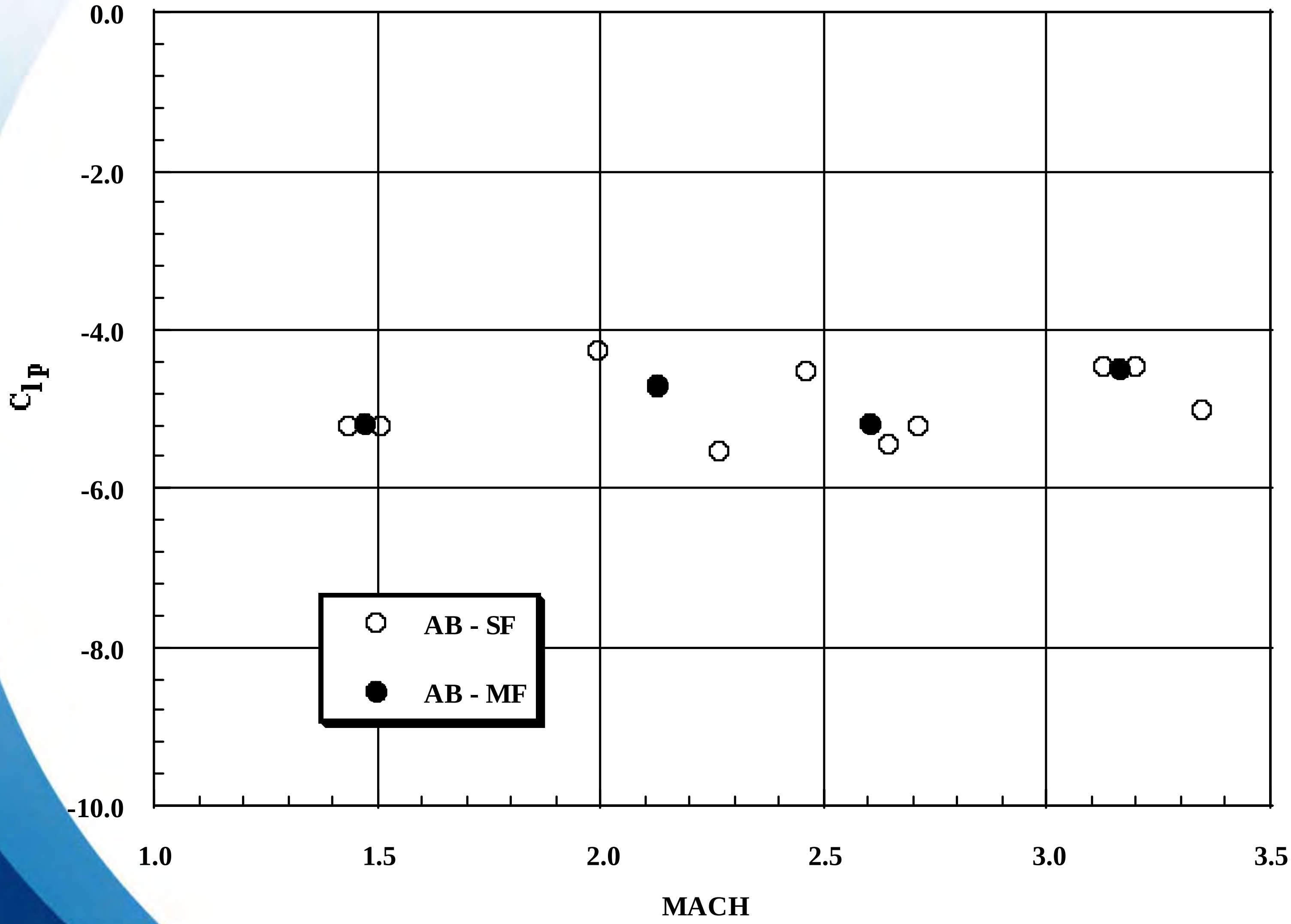

ROLL DAMPING MOMENT

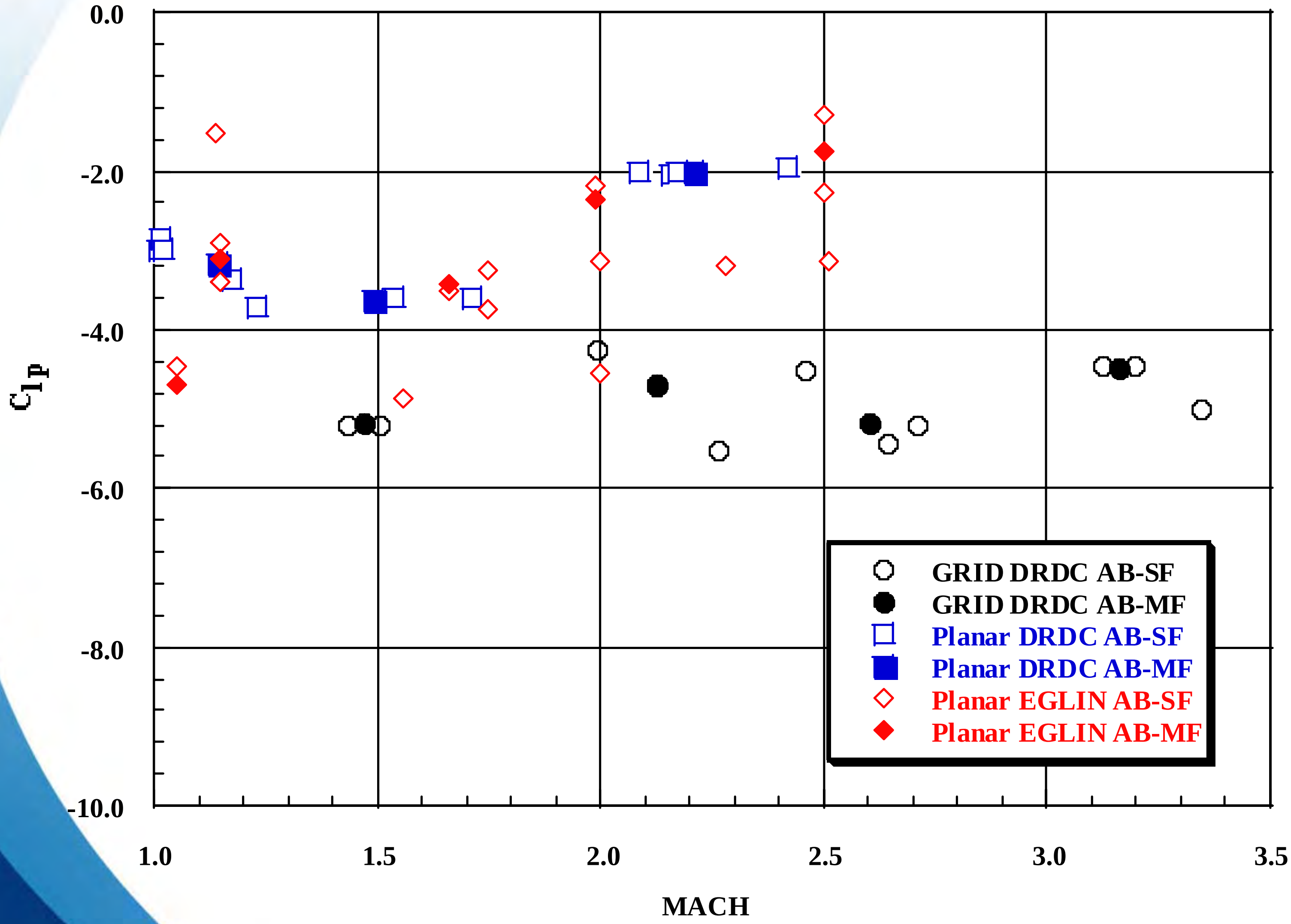

ROLL PRODUCING MOMENT

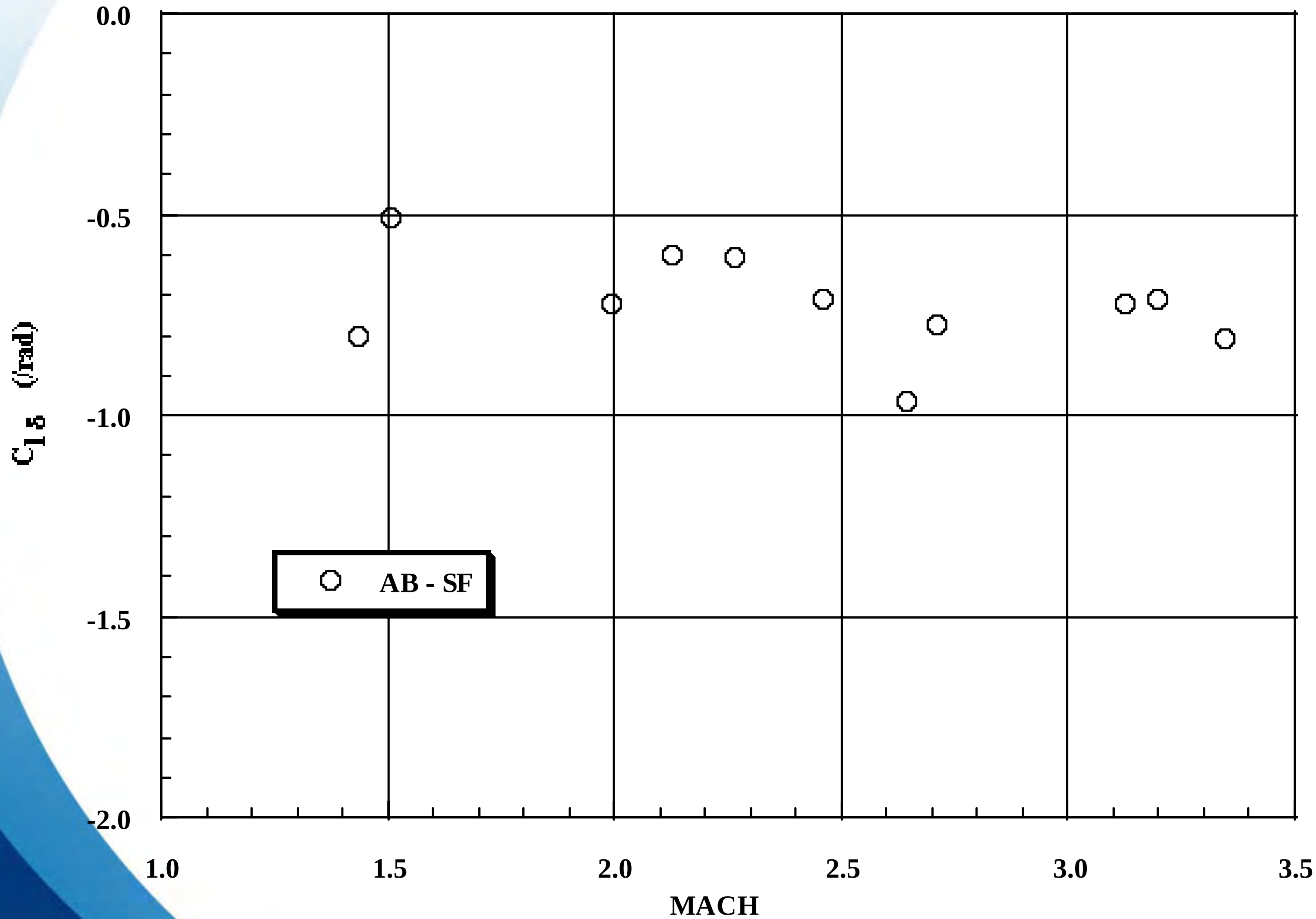

ROLL PRODUCING MOMENT

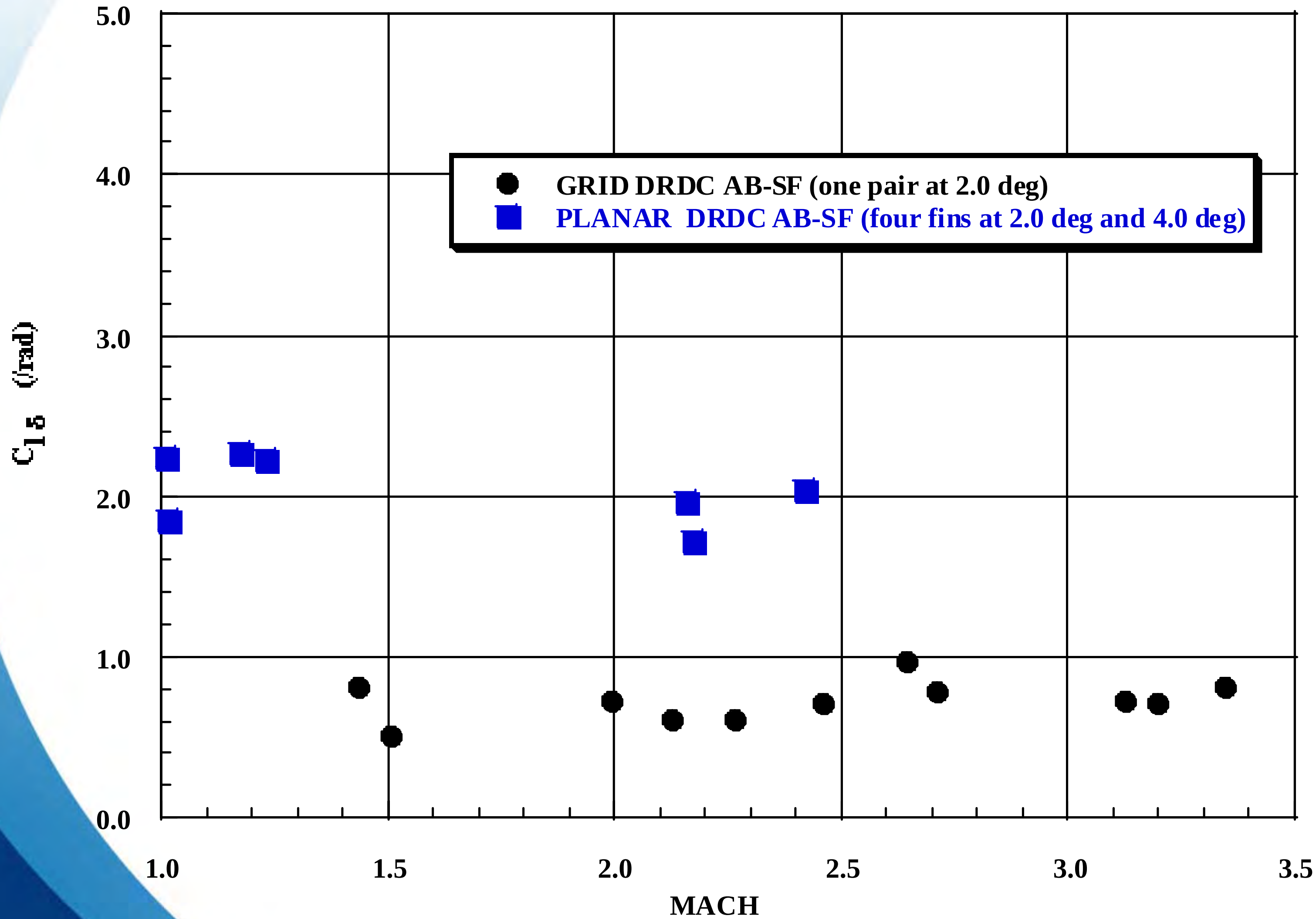

CONCLUSIONS

- 11 Projectiles Fired Mach 1.4 to 3.5
- All Main Aerodynamics well Determined
  - First Time for Reliable C_{Mq} & C_{lp}
  - Some nonlinear ones also
- Comparison with Planer Fin Model

AMC

22nd International Symposium on Ballistics
November 14-18, 2005 Vancouver Convention Center
Vancouver, BC

Multiple Explosively Formed Penetrator (MEFP) Warhead Technologies for Mine and Improvised Explosive Device (IED) Neutralization

*Richard Fong
William Ng
Steve Tang
LaMar Thompson

rfong@pica.army.mil
(973) 724-2516
U.S. Army RDECOM-ARDEC
Picatinny, NJ 07806

AMC

OUTLINE

- Overview
    - Current Neutralization Techniques
    - Program Objective
- Technical Approach
    - MEFP Warhead Technology
        - Mine Neutralization
        - IED Neutralization
- Summary

Overview

Current IED/Bomb/Mine Neutralization Techniques & Devices

AMC

RE-70/MK40

No Universal Mine/IED Neutralizer Exists to Effectively Defeat Threats in All Environments

M112 Demo Blocks

M82A1 Sniper Rifle

M221 Clipped Demo Charge

PAN – Percussion Actuated Neutralizer

EOD Robots

AMC

PROGRAM OBJECTIVE

Concealed In Dirt/Sand

Miniaturized

Concealed In Concrete

To understand the critical MEFP parameters required to cause various reactions (detonation, deflagration, damage) against mines and Improvised Explosive Devices (IEDs).

Concealed In Cloth/Sheathing

Concealed In Plaster

External Components

Typical Threats

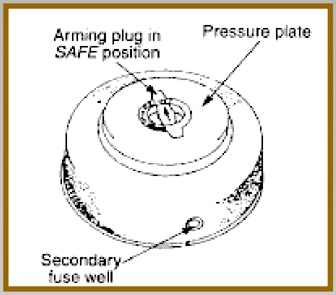

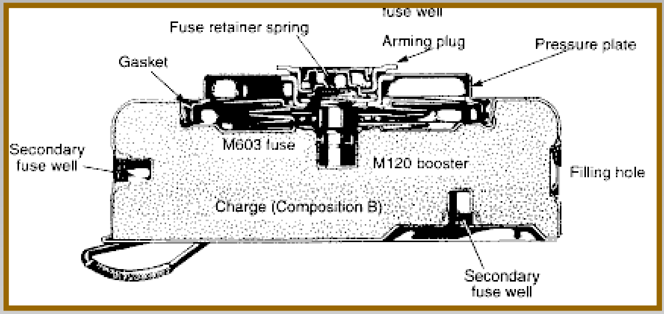

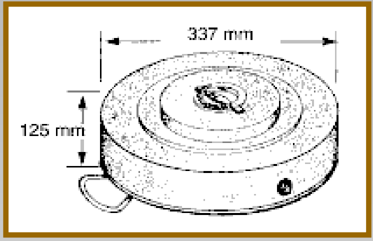

82mm Mortar

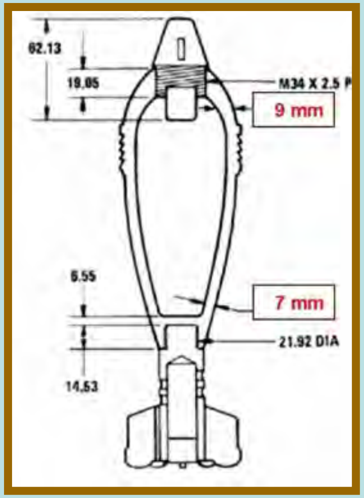

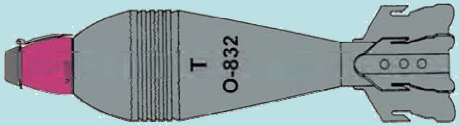

120mm Mortar

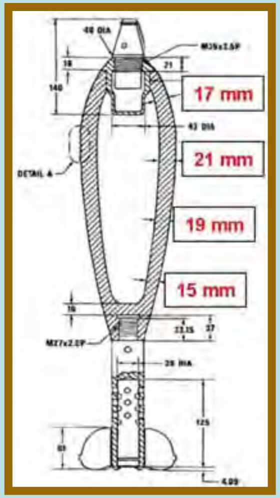

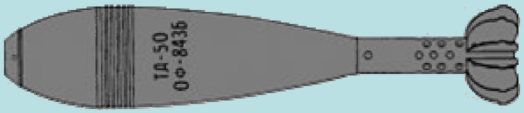

152mm Projectile

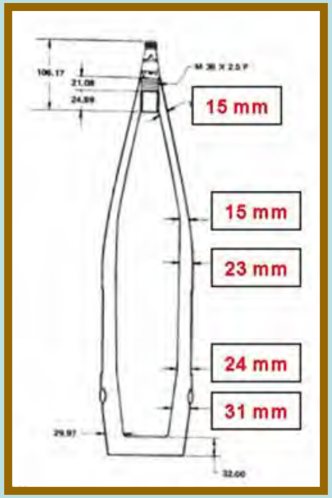

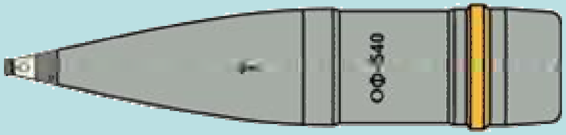

AMC

TECHNICAL APPROACH

WHY MEFP?

- Standoff Capability
- Increase Hit Probability
- Design Flexibility
- Lightweight and Compact
- Versatile Deployment

MEFP Warhead Pattern

AMC

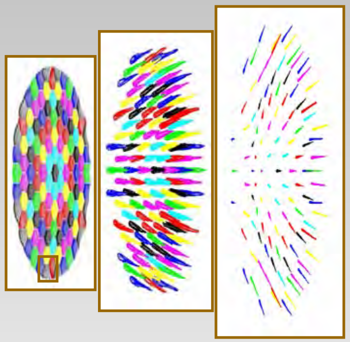

Simulation

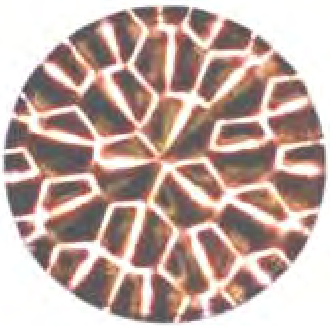

Hardware

DEMONSTRATED CONTROLLED FRAGMENTATION PATTERNS

"Happy Face" Simulation

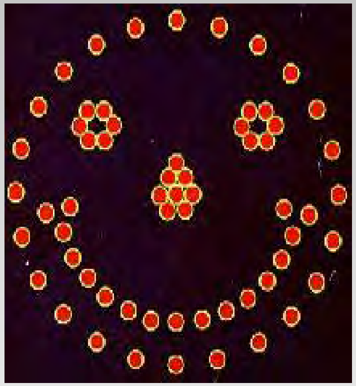

"Mine-Killer" Simulation

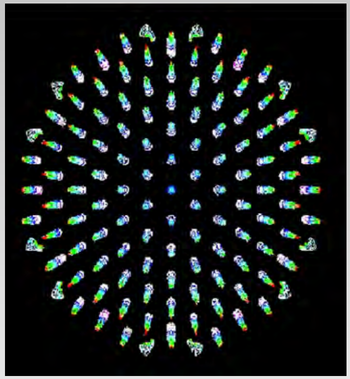

"Letter - A" Simulation

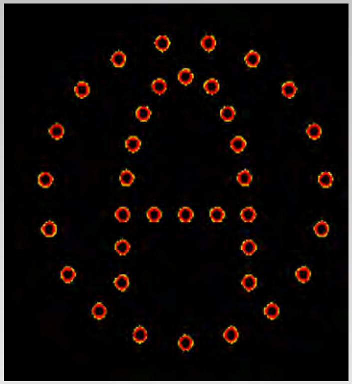

"Happy Face" Target

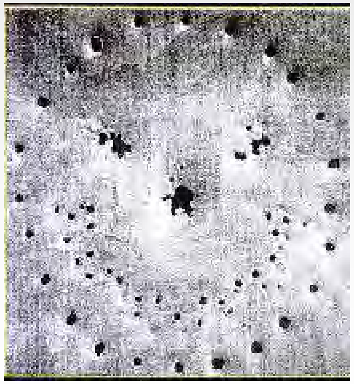

"Mine-Killer" Target

"Letter - A" Target w/ Highlights

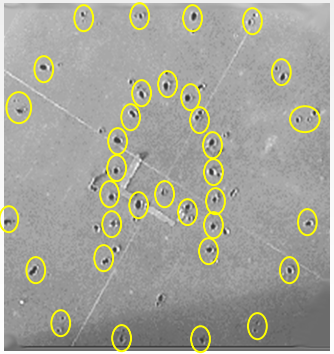

Mine Neutralization

AMC

- Design Approach
  - Preliminary Warhead Evaluation
  - MEFP Optimization Study
    - Mass
    - Velocity
    - Shape
  - Prototype Design & Test

Preliminary Warhead
7 MEFP Configuration

AMC

MEFP WARHEAD

- Effective Range: 1 ~ 150 Meters
- Spheroids to Long Rods (L/D 1-3)
- On-Target Pattern Control
- Multiple EFP's from a Single Warhead
- Proven Against Many Different Light Targets

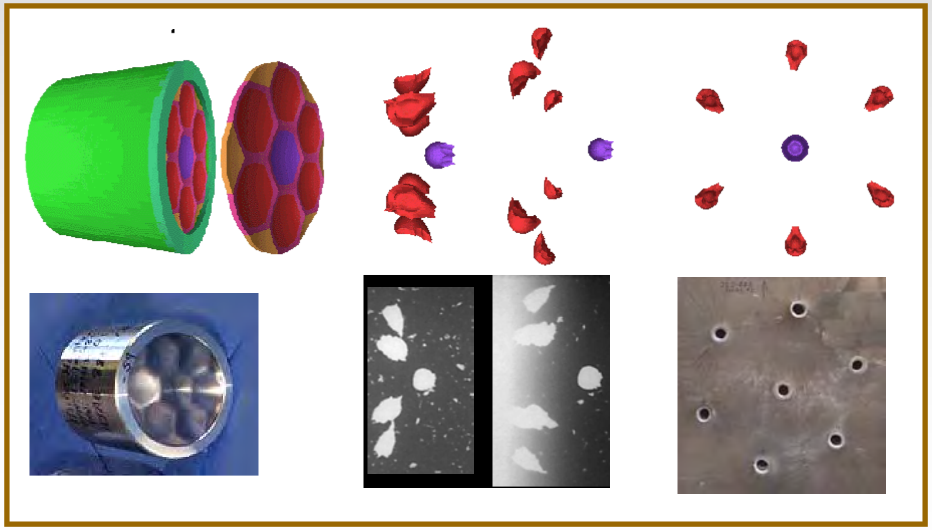

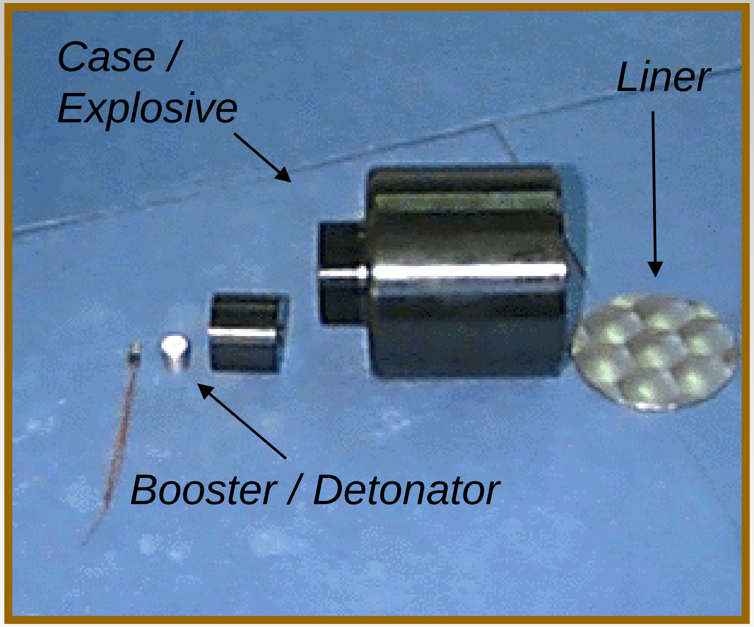

AMC

MEFP Optimization

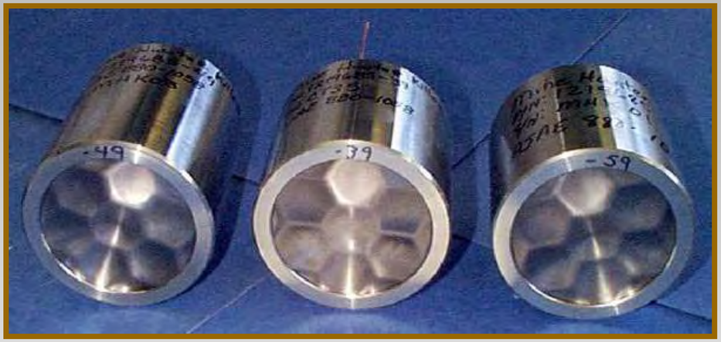

Warhead with different L/D
MEFP liner design

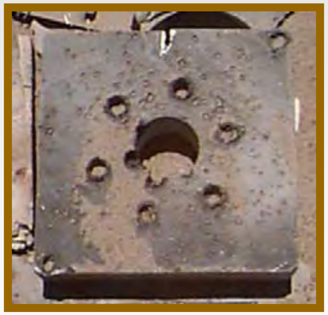

Stripper Plate

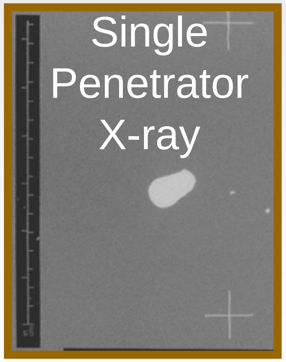

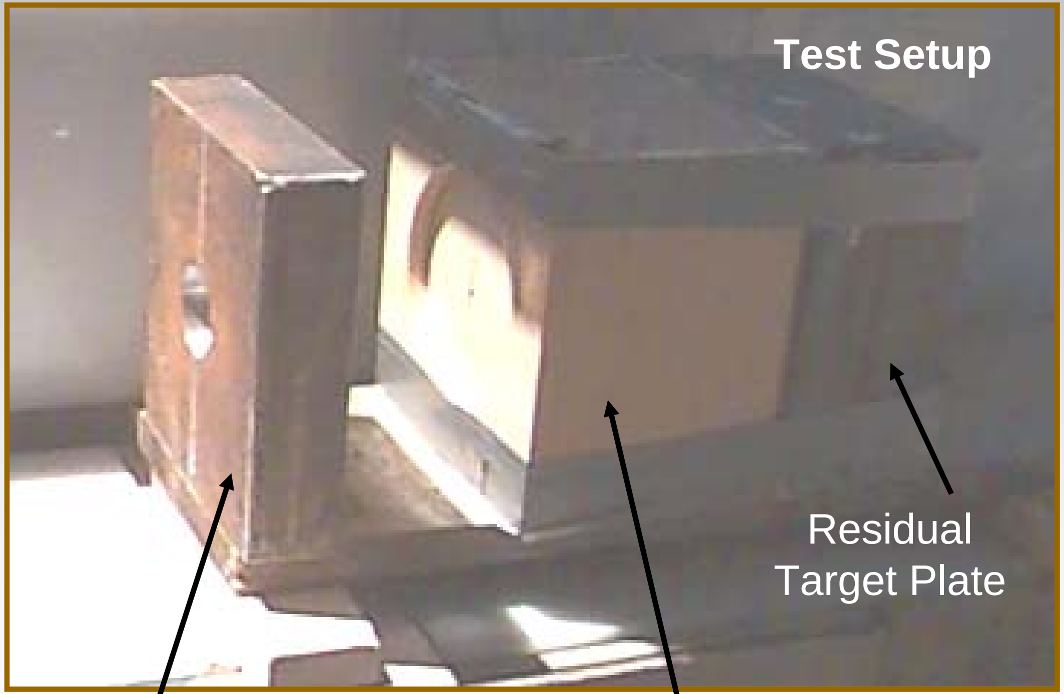

Stripper Plate

Sand Box (Overburden)

MEFP Optimization Test Results

“5 Warhead Designs Tested”

AMC

Flash Radiograph of EFP	Recovered MEFPs	Length/Diameter (L/D)	Remark
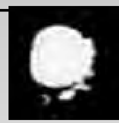		1.00	**No Residual Pen.**
		2.00	**No Residual Pen.**
		2.85	**No Residual Pen.**
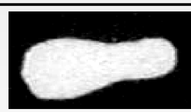		3.00	**No Residual Pen.**
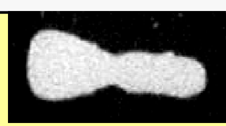		3.85	**Perforated Sandbox With 1/4” Residual Penetration in Armor**

AMC

Prototype Design
"MEFP Warhead"

- 61 Multiple EFPs From A Single Warhead
- On-Target Pattern Control ~ Uniformly Spaced

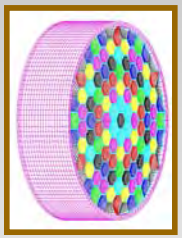

0 μsec

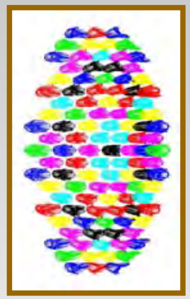

50 μsec

100 μsec

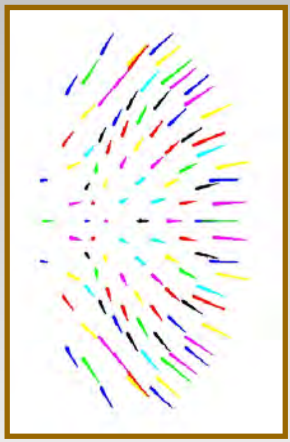

1000 μsec

Hardware

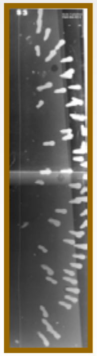

Flash X-ray

Target Plate

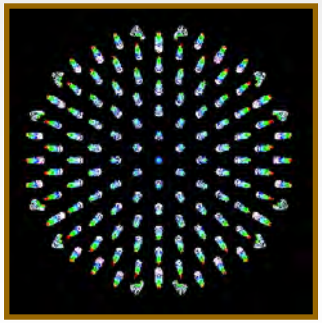

Simulated Target Pattern

Prototype Warhead Test Results

“Residual Penetration Through Sand Overburden”

AMC

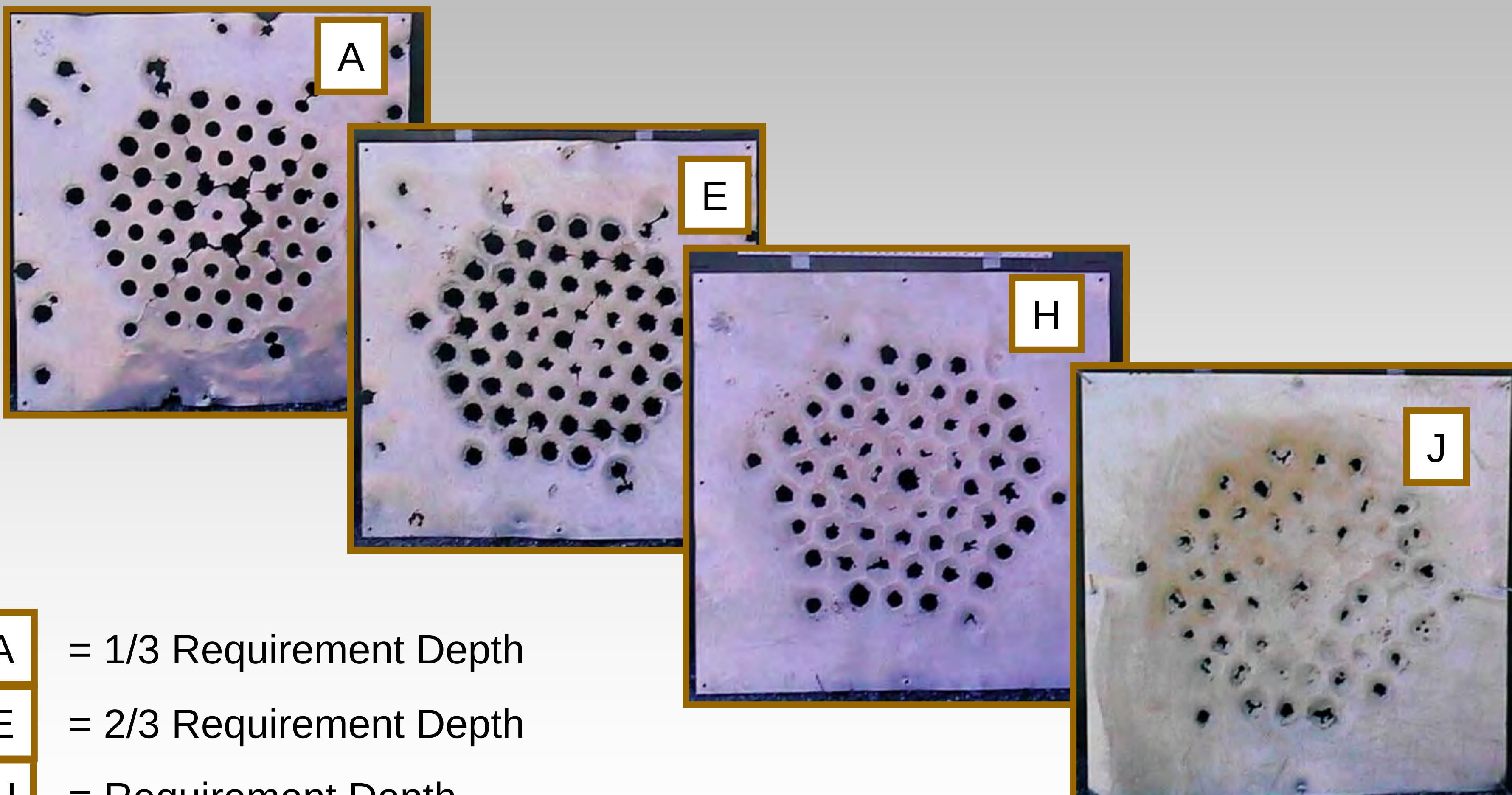

A = 1/3 Requirement Depth

E = 2/3 Requirement Depth

H = Requirement Depth

J = 1 1/3 Requirement Depth

Prototype Warhead

“Test Setup”

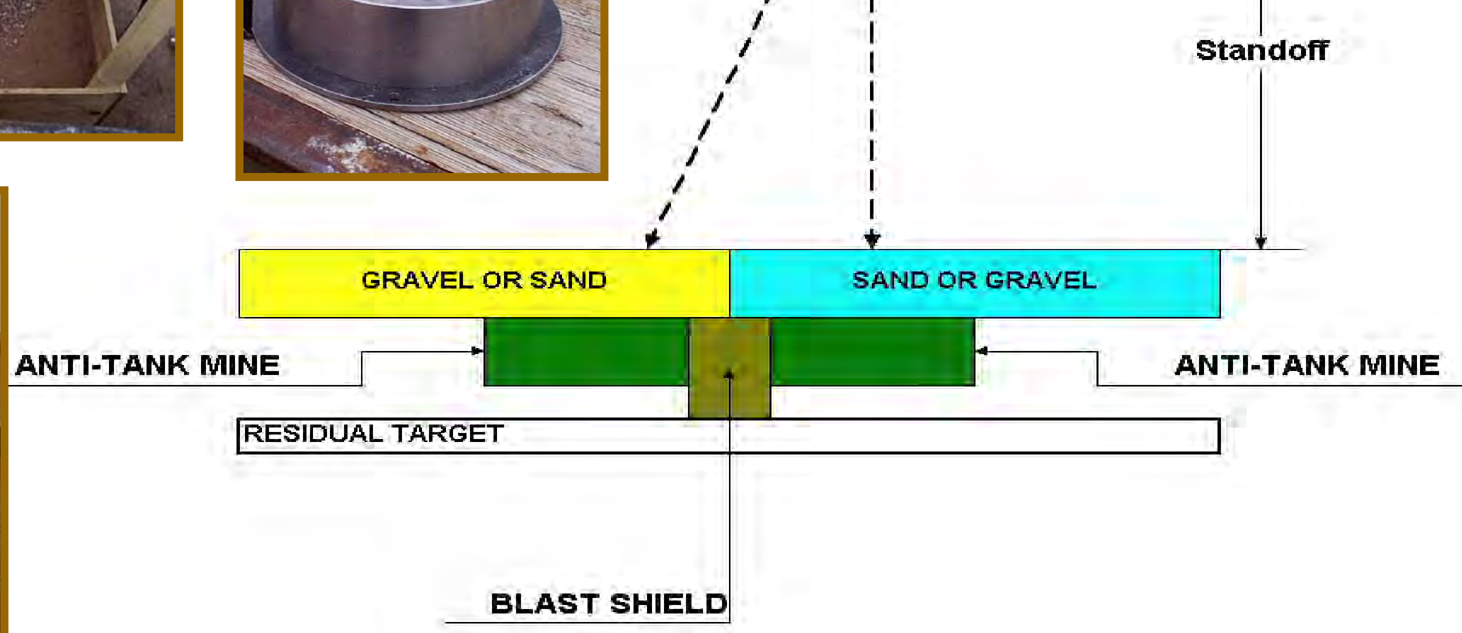

AMC

Prototype Warhead Test Results

System Demonstrator Requirement → G

Depth	Sand Overburden	Gravel Overburden
A	*	*
B	*	Detonation
C	Detonation	*
D	*	*
E	*	*
F	*	*
G	Detonation	Detonation
H	Deflagrate	*
I	*	Deflagrate
J	No Reaction	*
K	Deflagrate	Deflagrate
L	No Reaction	Deflagrate
M	No Reaction	No Reaction
N	*	No Reaction

***Not tested**

AMC

IED Neutralization

- MEFP Parametric Study
  - L/D Study
  - Four Prototype Warhead Designs Evaluated

AMC

Parametric Study Test Matrix

		Overburden (Sand)		Threat								
				81mm 			120mm 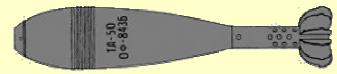			155mm 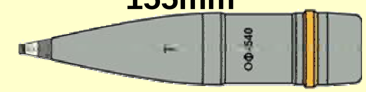		
L/D	KE (kJ)	A	D	0”	A	D	0”	A	D	0”	A	D
1	29.6									x	x	
	34.0	x	x	x	x		x	x		x		
	34.9				x			x		x		x
	48.5					x			x	x	x	x
1.5	34.0	x	x	x			x			x		
3	26.0	x								x	x	x
	34.0	x	x		x		x			x		
3+	34.1			x	x		x	x		x	x	

** Shaded Boxes correspond to the L/D Study

AMC

120 mm Surrogate Simulations

"Penetration Analysis"

Parameters Used To Evaluate L/D

"Constant Kinetic Energy of 34 kJ"

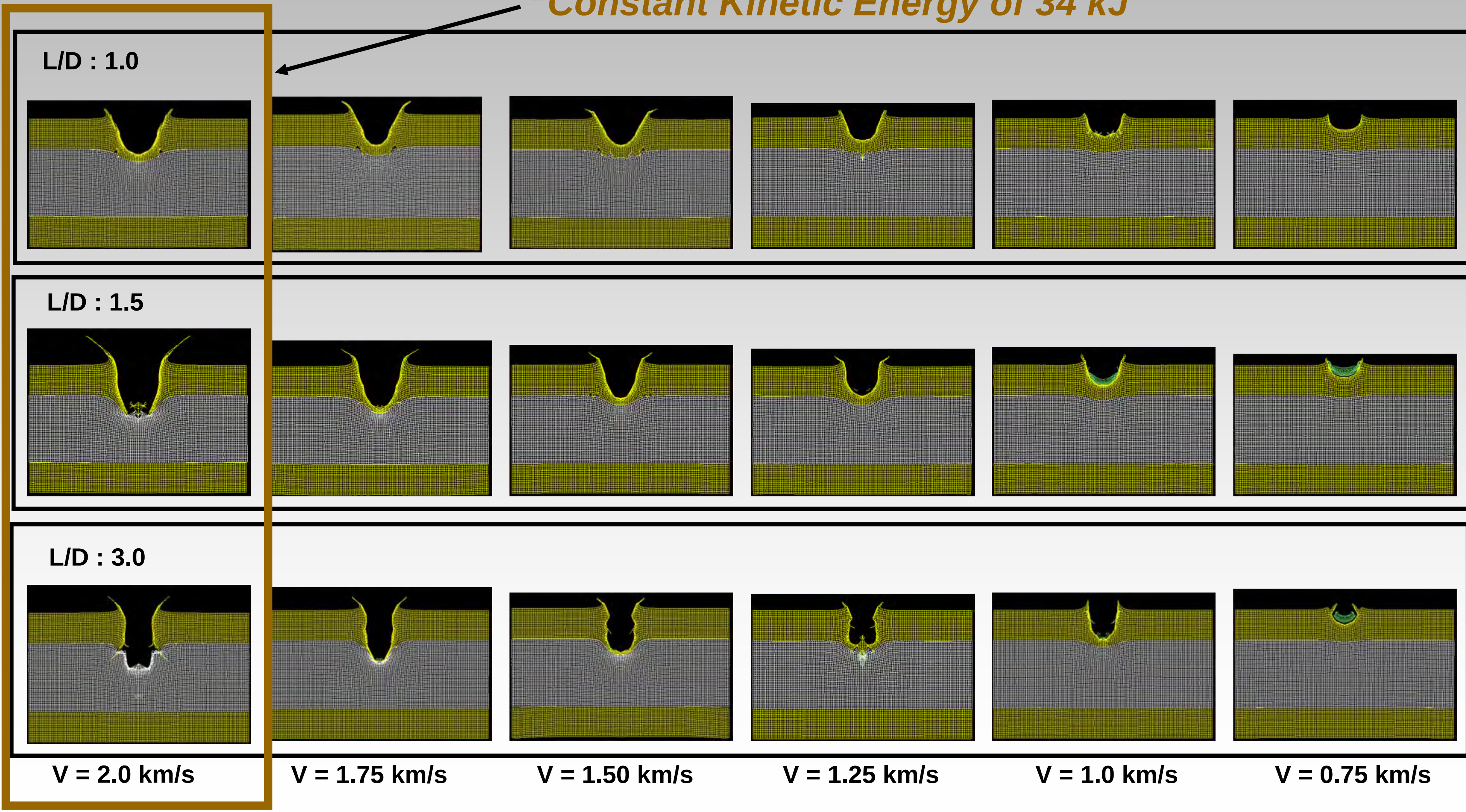

Penetrator L/D Study

L/D Study Warhead

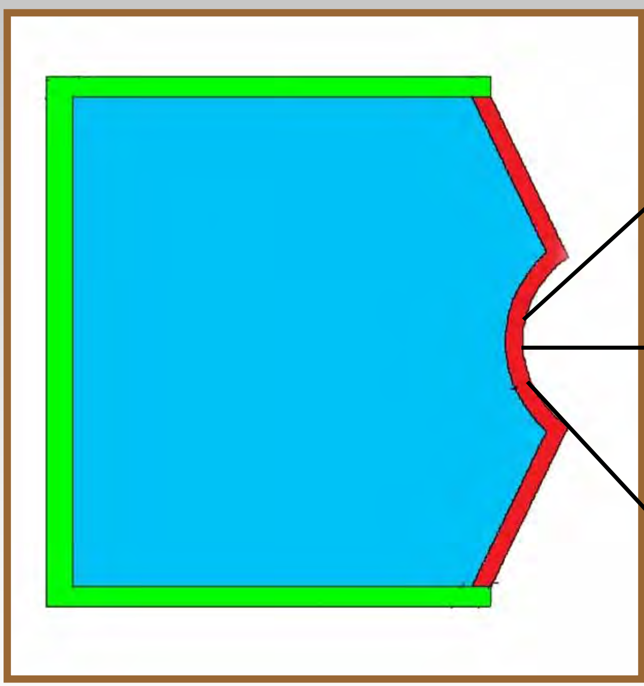

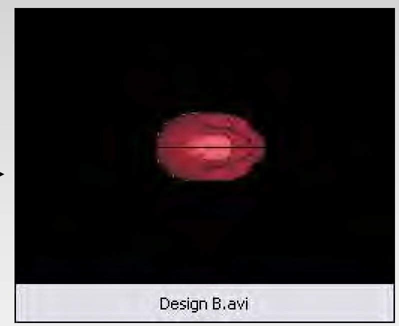

L/D = 1

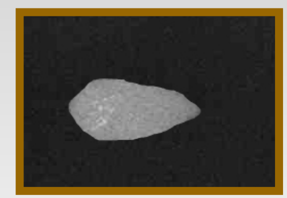

L/D = 1.5

L/D = 3.0

Overburden Test Setup

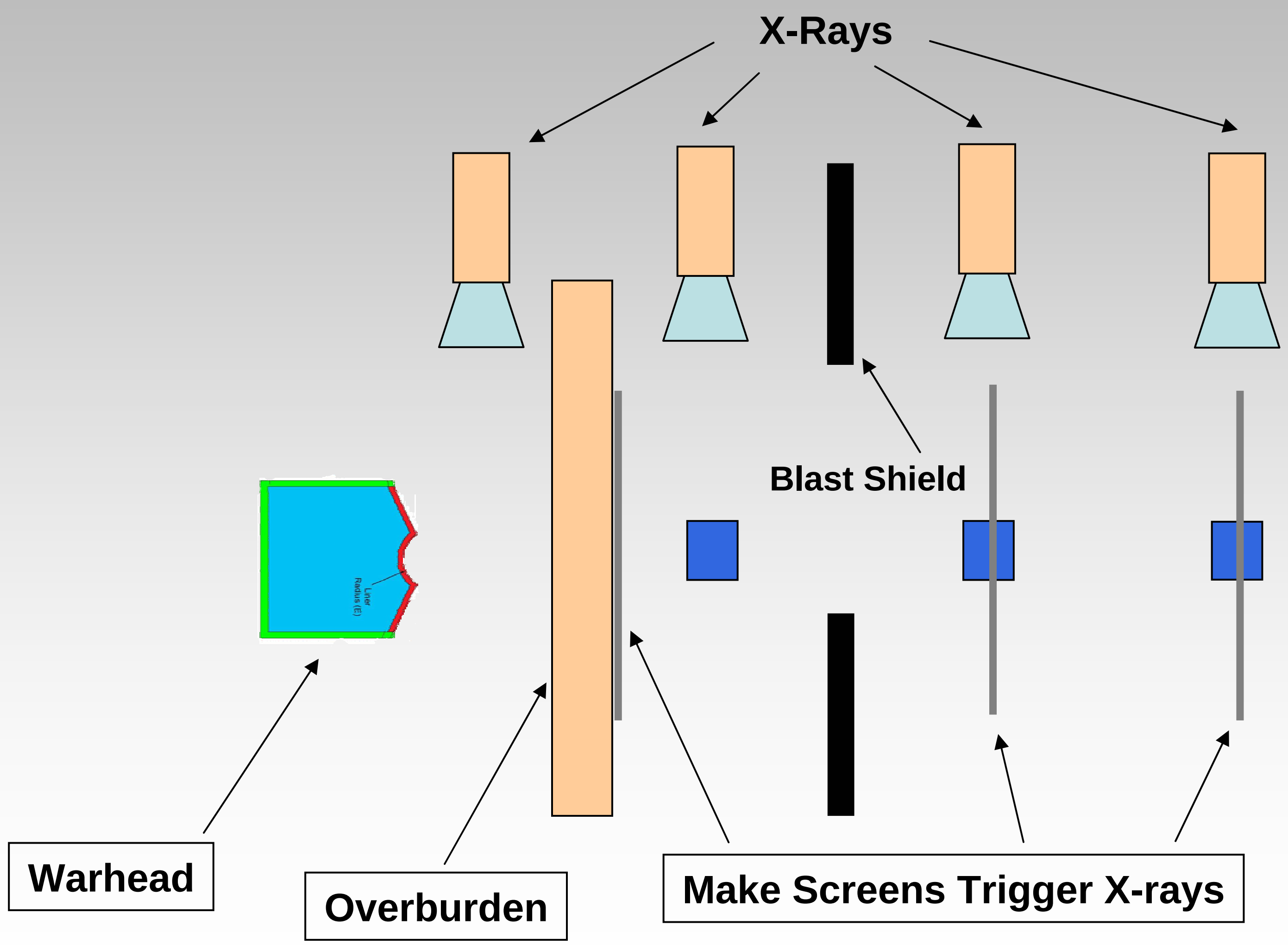

Overburden Test Results For Residual K.E.

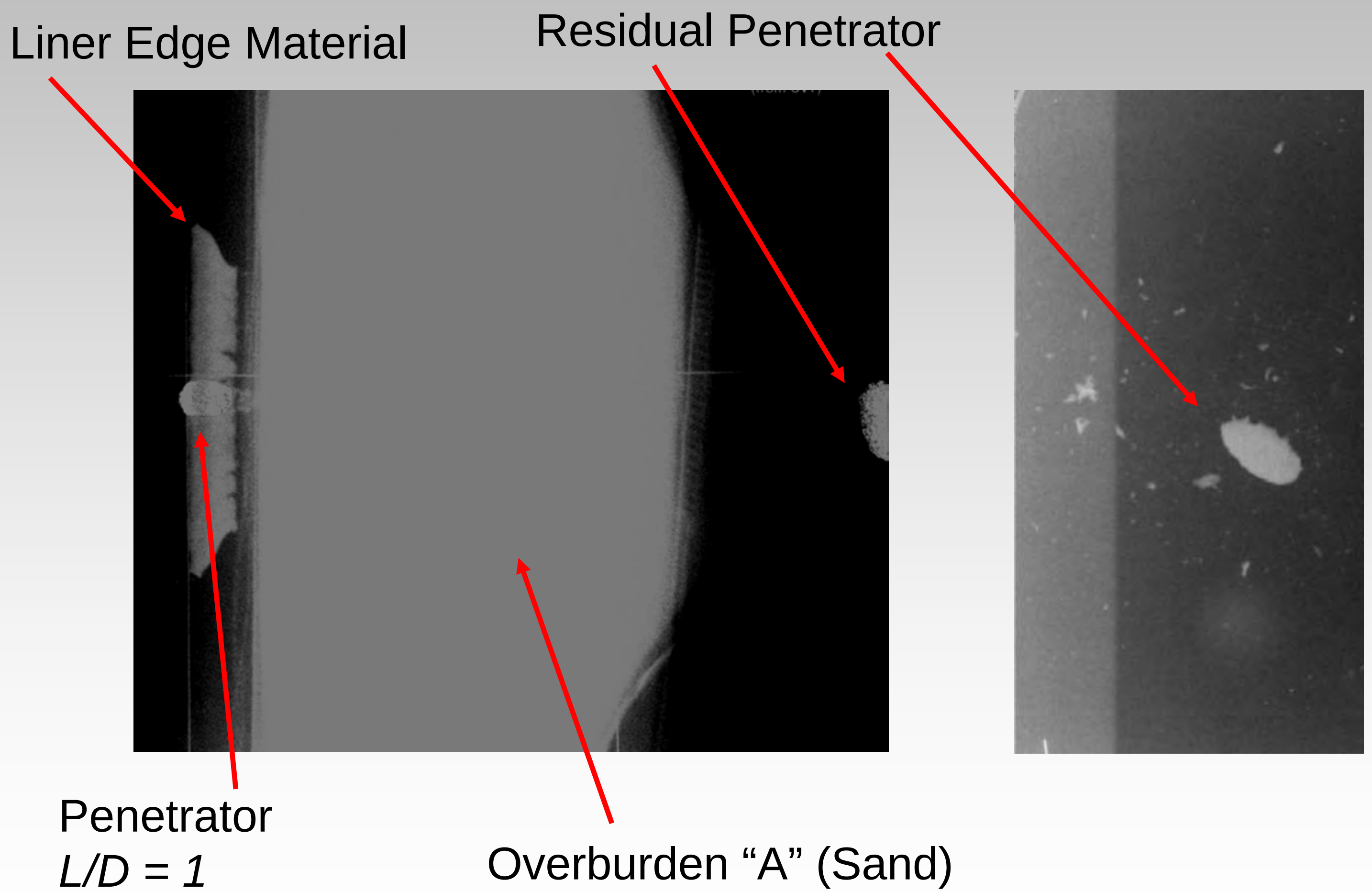

AMC

Overburden Test Results For Residual K.E.

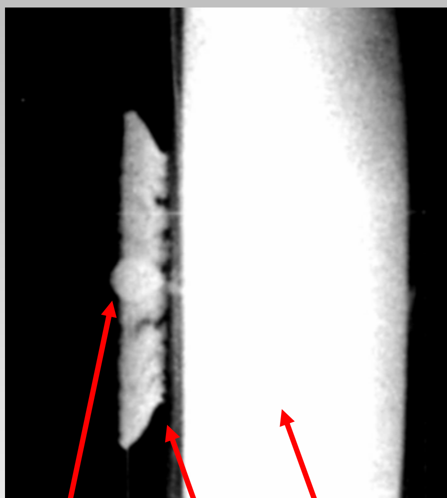

Penetrator
L/D = 1

Overburden
“D” (Sand)

Edge Material

29”

46”

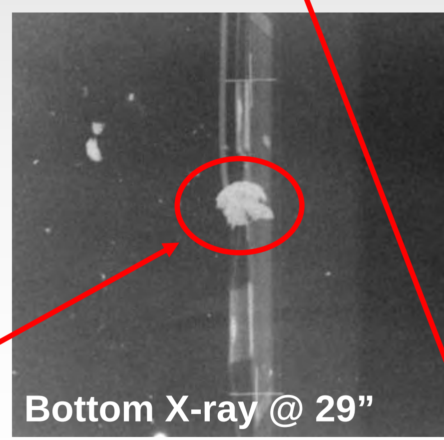

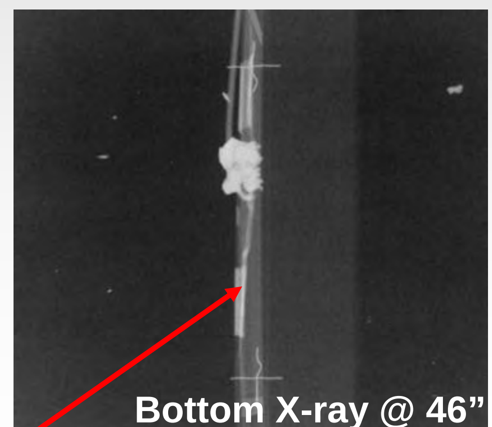

Residual Penetrator

Make Screens that triggered X-Rays

Overburden Test Results For Residual K.E.

AMC

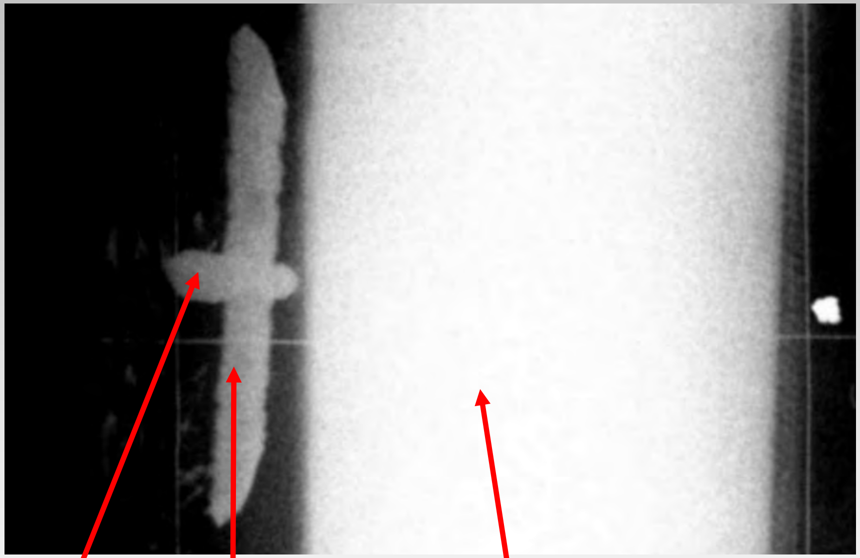

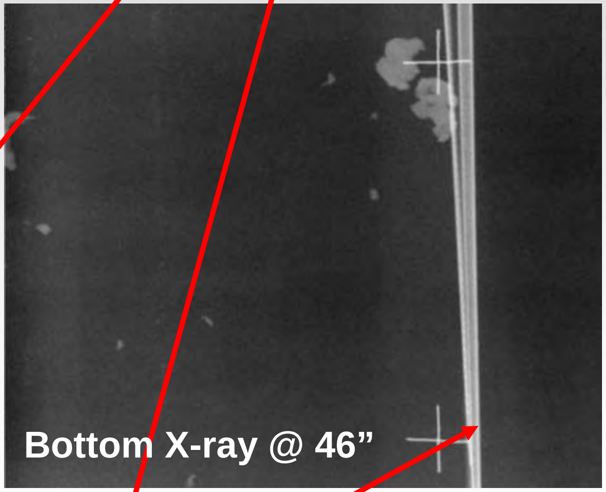

Penetrator
L/D = 3

Overburden "A" (Sand)

Edge Material

Residual Penetrator

Make Screens that triggered X-Rays

AMC

Warhead Test Summary

“ Effects of L/D”

		Over-burden (sand)		Threat								
				81mm			120mm			155mm		
	Warhead Design	A	D	0”	A	D	0”	A	D	0”	A	D
KE 34. KJ	L/D = 1	x	x	x	x		x	x		x		
	L/D = 1.5	x	x	x			x			x		
	L/D = 3	x	x		x		x			x		

No Effect | Damage | Deflagrate | Detonate

AMC

Prototype Warheads Evaluated

Single (1) Penetrator Warhead

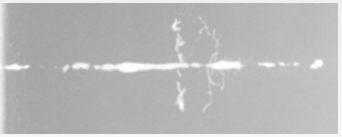

Seven (7) Penetrator Warhead

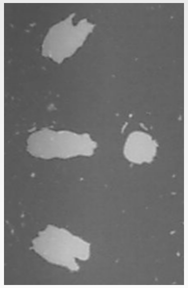

Nineteen (19) Penetrator Warhead

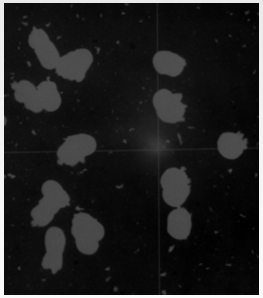

Sixty-One (61) Penetrator Warhead

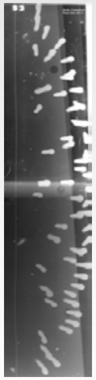

Typical Test Setup

CTH Simulations

Simulation vs. Test Data

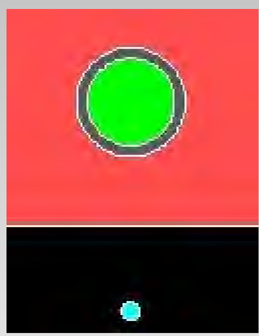

81mm

Residual Threat
“Detonation”

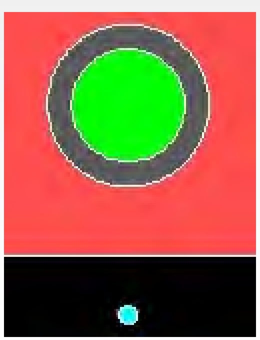

120mm

Residual Threat
“Deflagration”

AMC

DETONATION

Penetrator K.E. = 48.5 KJ
Overburden = A

155mm Round
Behind Overburden

Residual 155mm

Penetrator K.E. = 48.5 KJ
No Overburden

155mm Round
with Base Plate

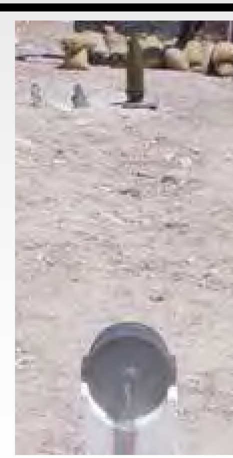

Frontal View

Residual of Base Plate

AMC

DEFLAGRATION

K.E. = 34.1 KJ
No Overburden

120 mm Round Setup

120 mm Round

Residual 120mm

K.E. = 34.1 KJ
Overburden = A

81mm Round
Frontal View Setup

Deflagrated Round

Residual 81mm

DAMAGE

AMC

Penetrator K.E. = 29.6 KJ
No Overburden

155 mm Round Setup

Damaged Round

Penetrator K.E. = 48.5 KJ
“D” Overburden

81 mm Round Setup

Damaged Round

NO EFFECT

AMC

Penetrator K.E. = 26 KJ
Overburden = A

Overburden Test Fixture

155mm Post-Test

Penetrator K.E. = 29.6 KJ
Overburden = A

155mm Post-Test

AMC

Prototype Warhead Test Summary

		Overburden (Sand)		Threat								
				81mm			120mm			155mm		
Penetrator L/D	KE (kJ)	A	D	0”	A	D	0”	A	D	0”	A	D
1	29.6									x	x	
	34.9				x			x		x		x
	48.5					x			x	x	x	x
3	26.0	x								x	x	x
3+	34.1			x	x		x	x		x	x	

No Effect | Damage | Deflagrate | Detonate

MEFP Warhead Test Summary

Kinetic Energy Vs Target Reaction

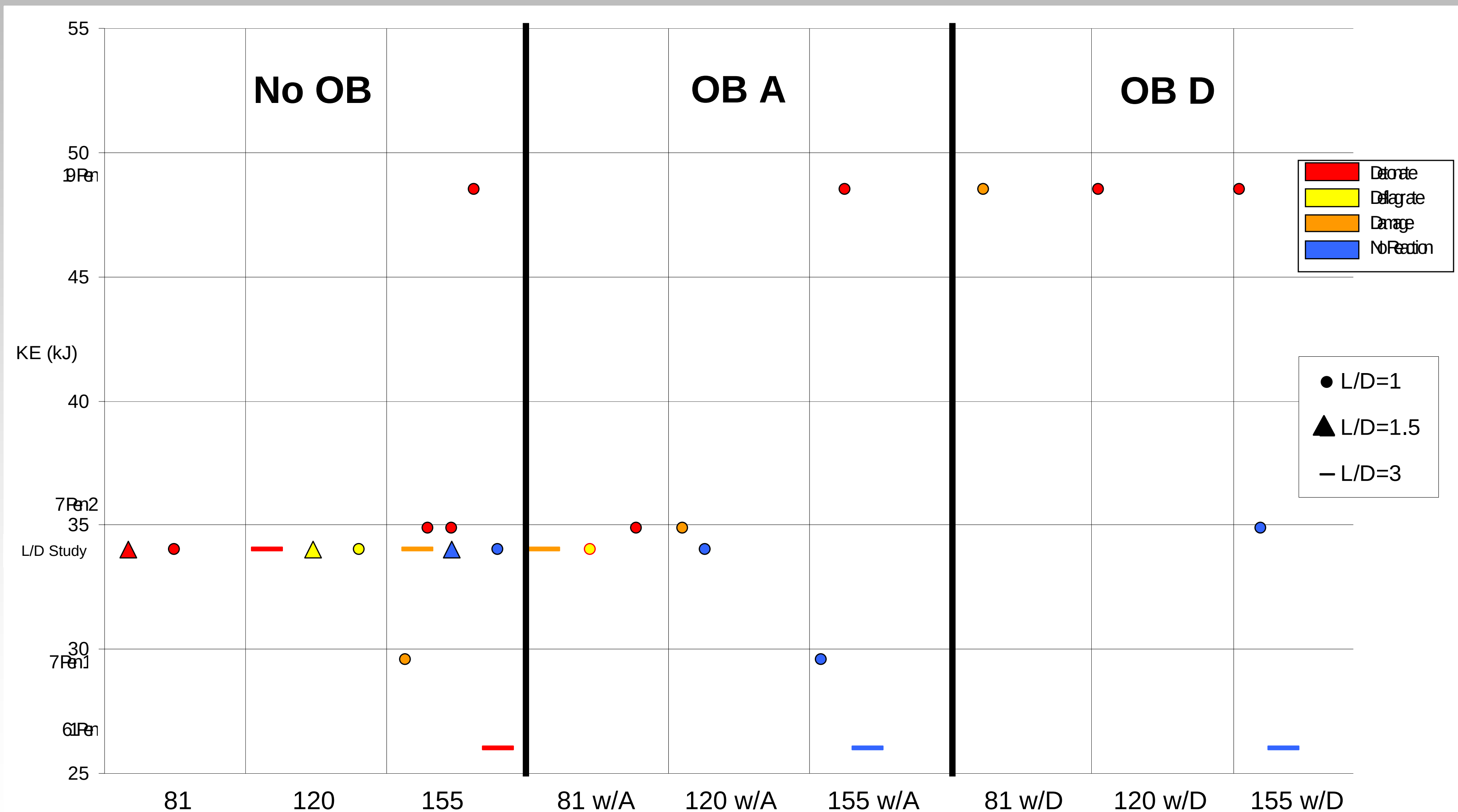

AMC

Summary

- Established MEFP warhead design parameters required to cause various reactions against mines and IEDs.
  - MEFP mass & velocity
  - MEFP L/D
- Demonstrated prototype warheads that can be used to neutralize mine and IEDs.
- Results from this study supports two Army S&T programs
  - Mine Neutralization Program
  - Extended Area Protection System (EAPS) Program

Prevention of Sympathetic Detonation between Reactive Armor Sandwiches

A. Holzwarth

22nd International Symposium on Ballistics
Vancouver BC, November 14-18, 2005

EMI
Fraunhofer Institut
Kurzzeitdynamik
Ernst-Mach-Institut

ontents

Introduction and objectives

Experiments

- Test set-ups
- Materials
- Tests with foams
- Tests with layers
- Flash x-ray photographs
- Experimental results

Summary and conclusions

Fraunhofer Institut Kurzzeitdynamik Ernst-Mach-Institut
A. Holzwarth

unctioning of Reactive Armor Sandwiches

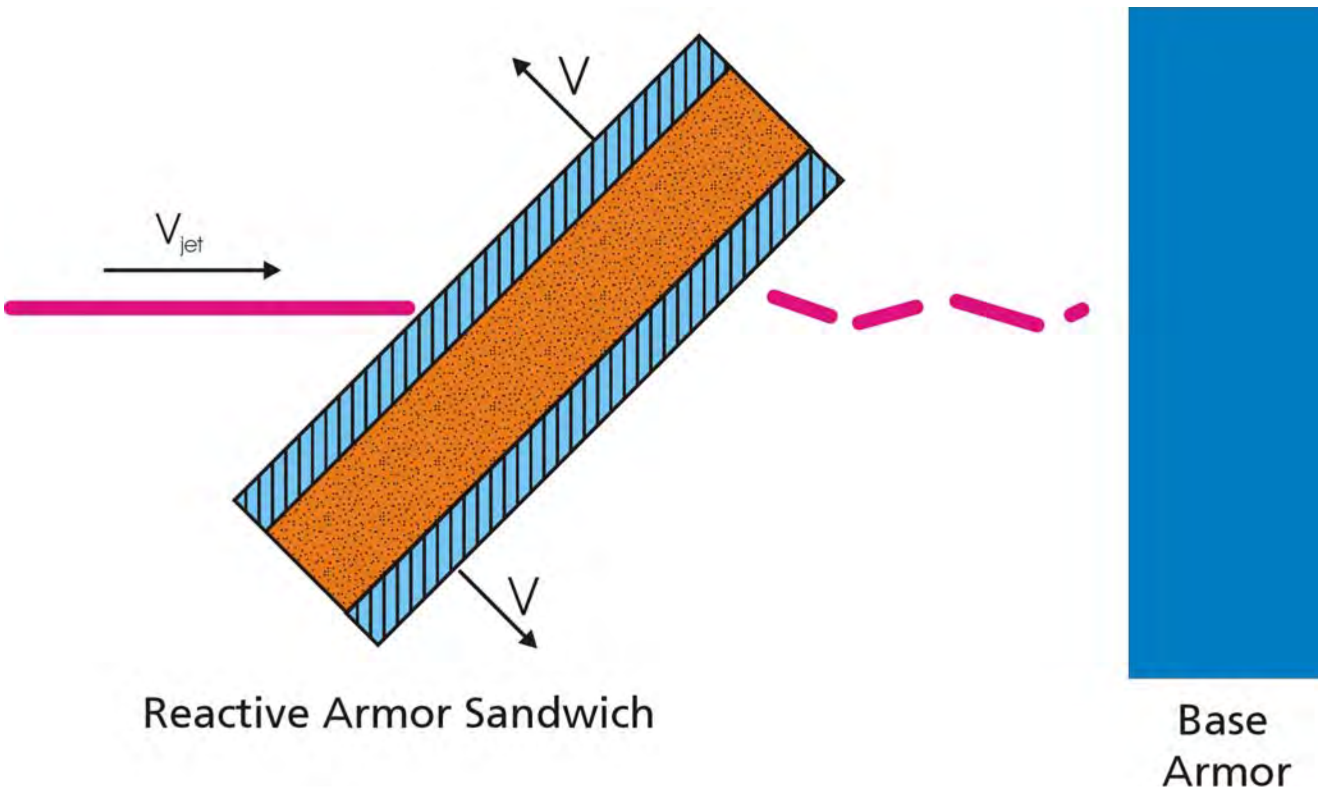

Fraunhofer Institut
Kurzzeitdynamik
Ernst-Mach-Institut

A. Holzwarth

Sympathetic Detonation between Reactive Armor Sandwiches

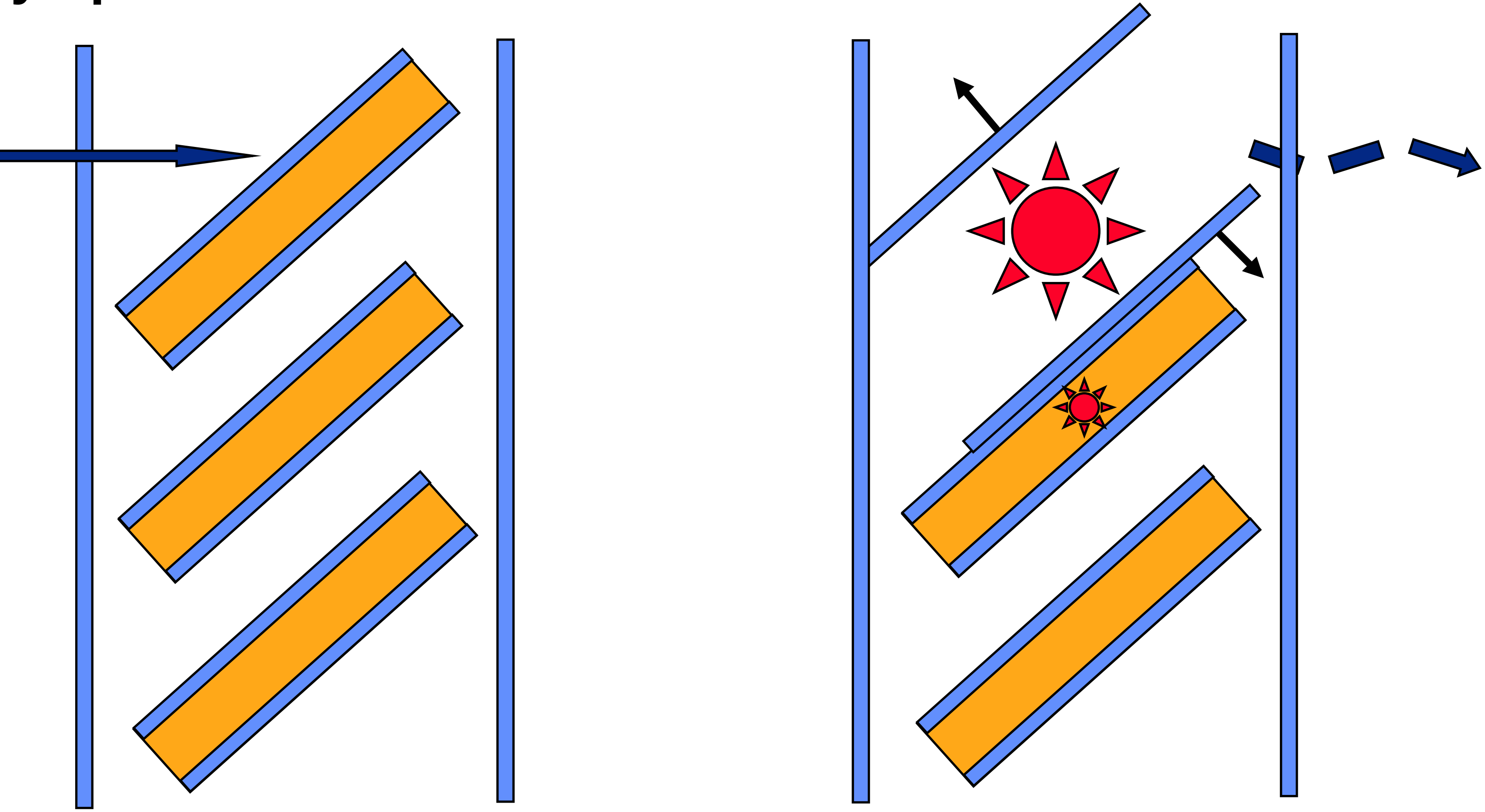

Fraunhofer Institut Kurzzeitdynamik Ernst-Mach-Institut

A. Holzwarth

evention of Sympathetic Detonation between Reactive Armor ndwiches

1. 2.

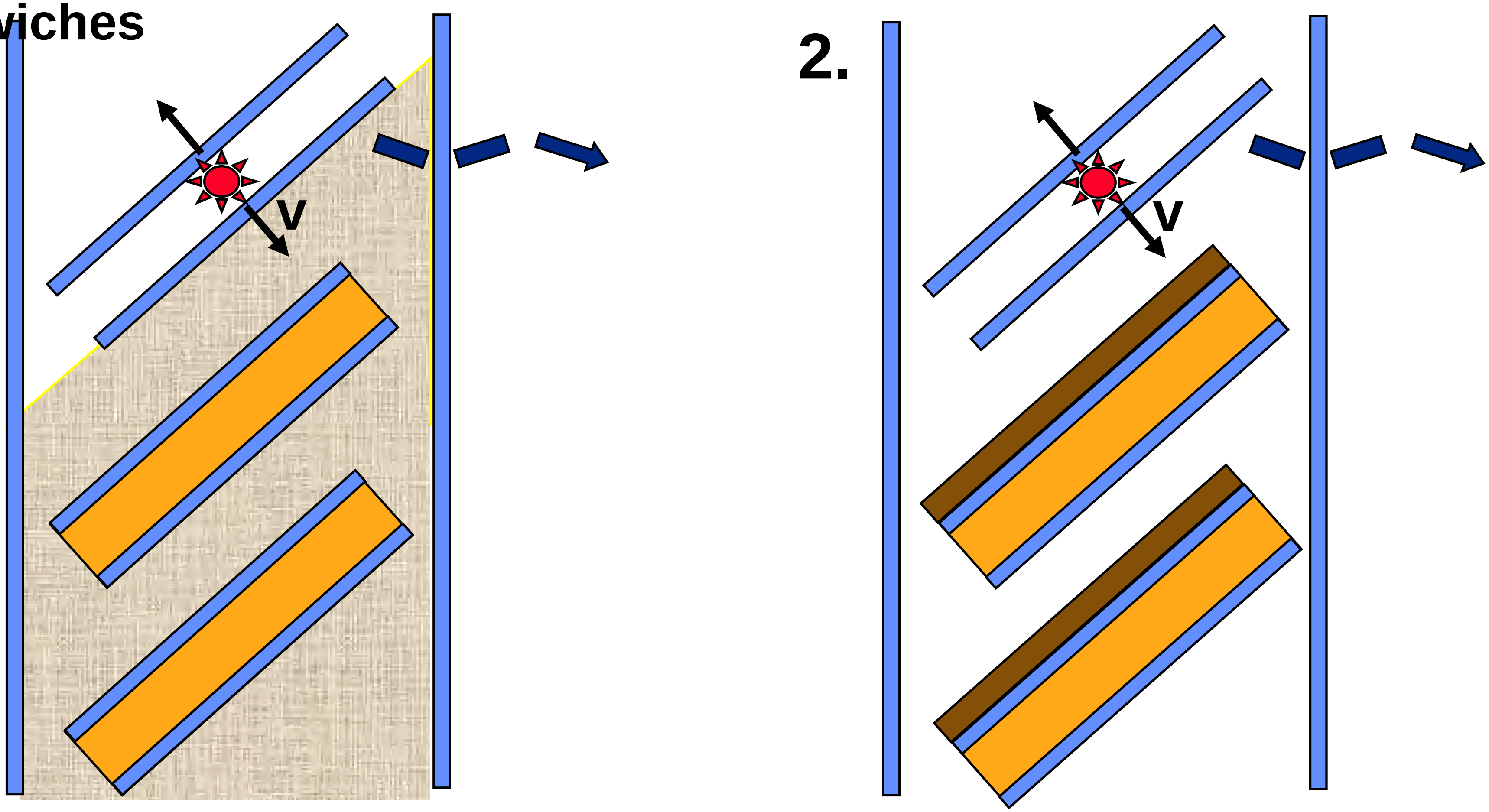

EMI
Fraunhofer Institut Kurzzeitdynamik Ernst-Mach-Institut

A. Holzwarth

ubjects of Investigations

Appropriate materials

- Absorption of kinetic energy
- Damping of shock waves

Useful and necessary densities

Arrangement of materials

Fraunhofer Institut Kurzzeitdynamik Ernst-Mach-Institut
A. Holzwarth

est Set – ups: Tests of Foams and Layers

am between 2 ERA-SWs

Layer on Acceptor-SW

Foam-Layer on Acceptor-SW

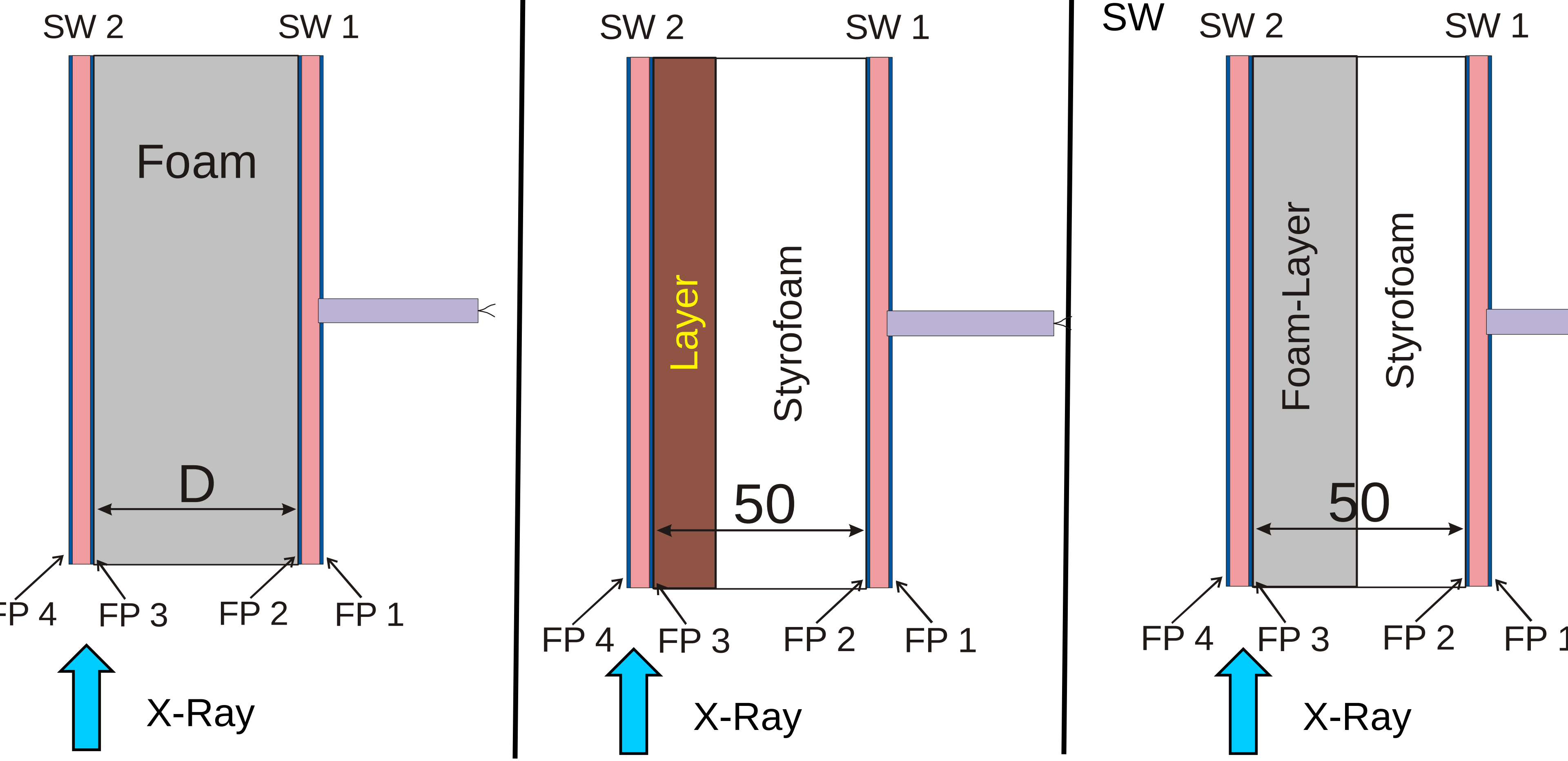

Fraunhofer Institut Kurzzeitdynamik Ernst-Mach-Institut

A. Holzwarth

xperiments 1:   Foams between 2 ERA-Sandwiches

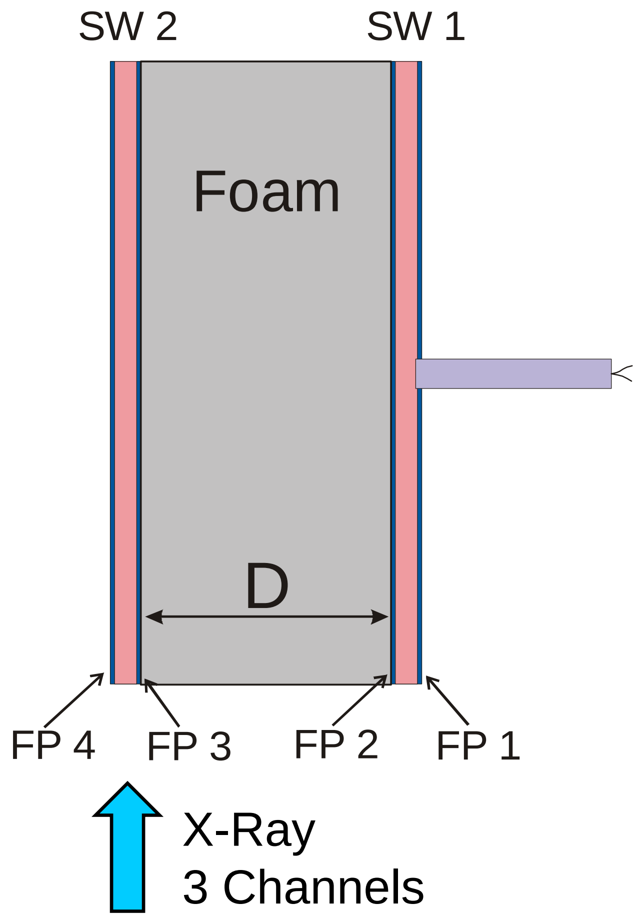

Test set-up data

Sandwiches:	<2 / 4 / 2>, 160 x 40 mm^2
Flyer plates:	Mild steel, 2 mm dick
Explosive:	Seismoplast (PETN + binder) 4 mm thick; 42,5 g
Distance D:	D = 50 mm – 80 mm Standard value: D = 50 mm

Fraunhofer Institut Kurzzeitdynamik Ernst-Mach-Institut

A. Holzwarth

ested Foams

ρ < 400 kg/m^3

PS 28, ρ=28 kg/m^3
PS 50, ρ=50 kg/m^3

PP 50, ρ=50 kg/m^3
PP 300, ρ=255 kg/m^3

U - Foam, ρ=330 kg/m^3

uminum-Honeycomb, ρ=152 kg/m^3

hite Foam, ρ=137 kg/m^3

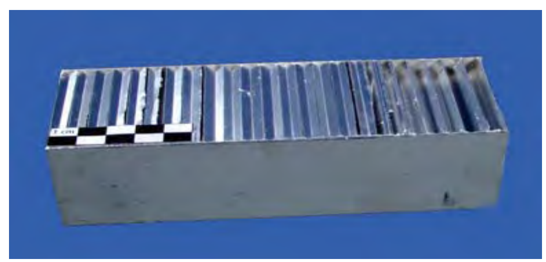

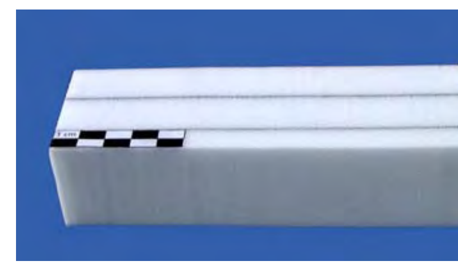

EMI
Fraunhofer Institut
Kurzzeitdynamik
Ernst-Mach-Institut

A. Holzwarth

bservations with flash x-ray

elocity of flyer plate FP 4:

- o Strength of reaction in SW 2
    - Detonation / Partial Detonation
      Deflagration / No Reaction

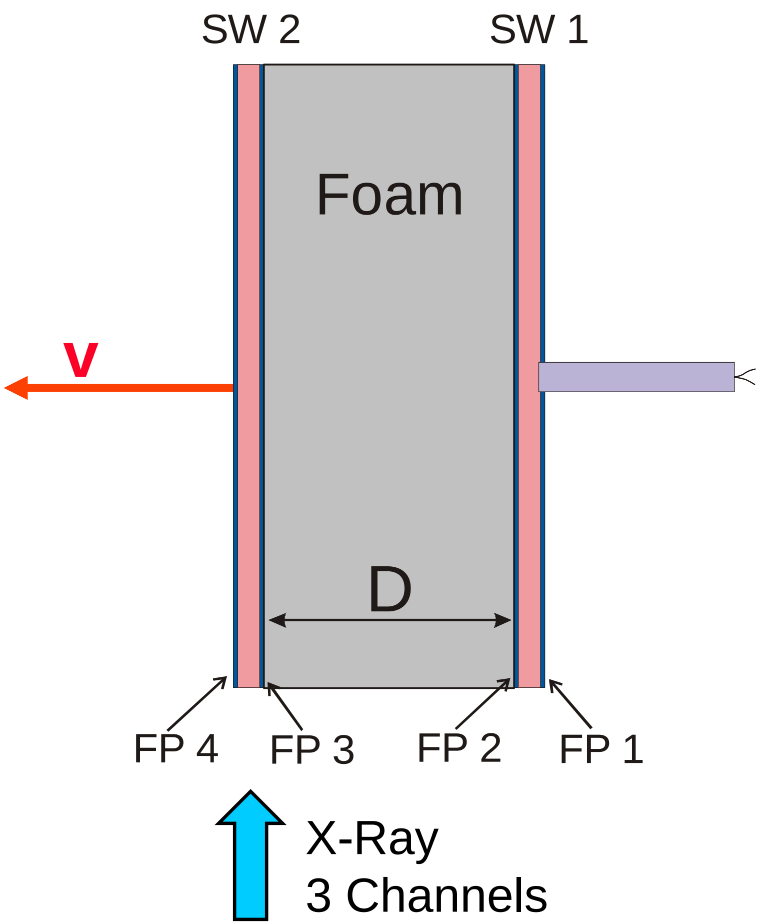

Fraunhofer Institut Kurzzeitdynamik Ernst-Mach-Institut
A. Holzwarth

reliminary Tests: No Material between Reactive Sandwiches

SW 2 reactive - detonation | **SW 2 inert – no reaction**

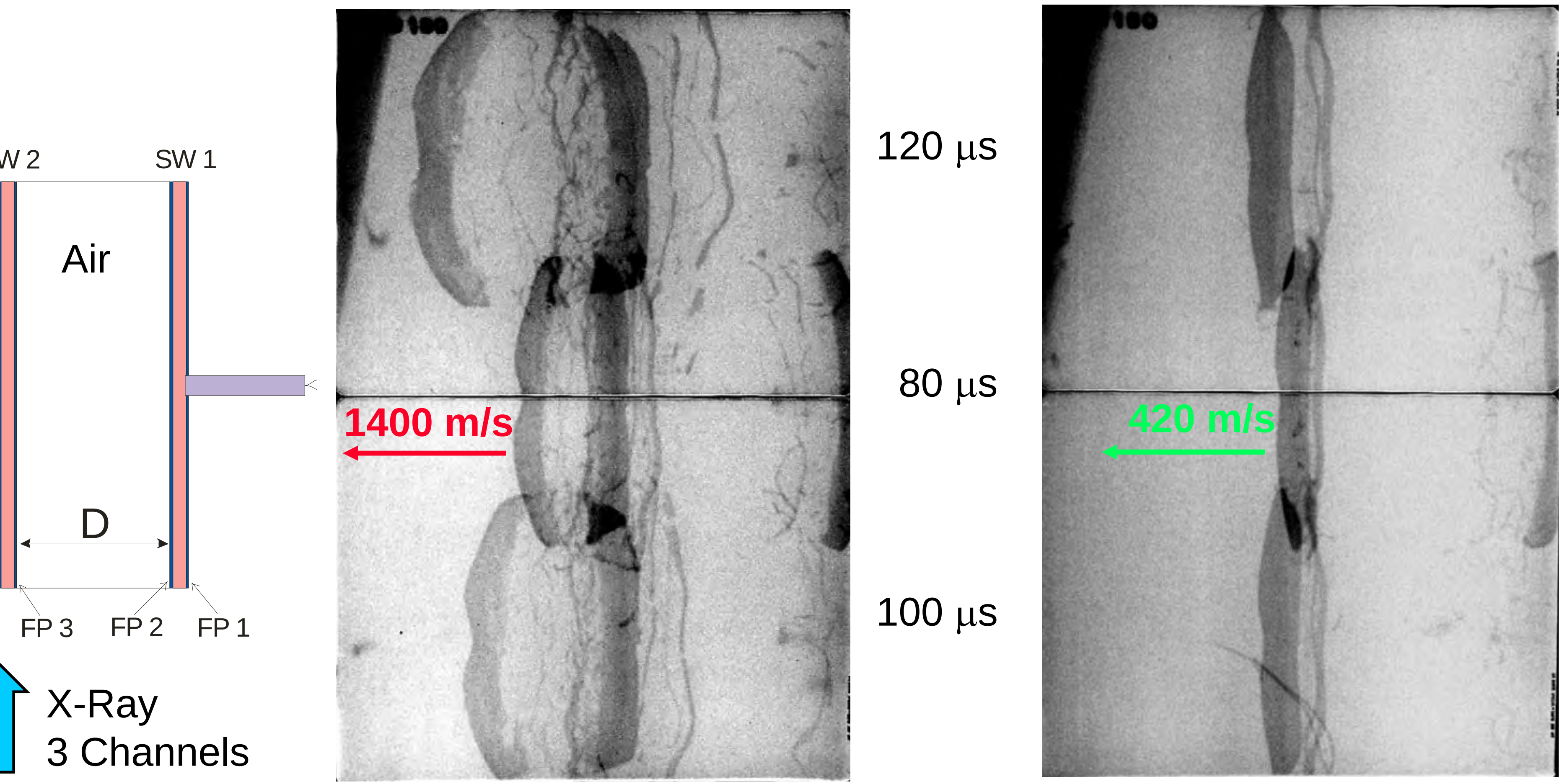

Flash X-Ray Photographs: Foams

EPS 28 – D=50 mm

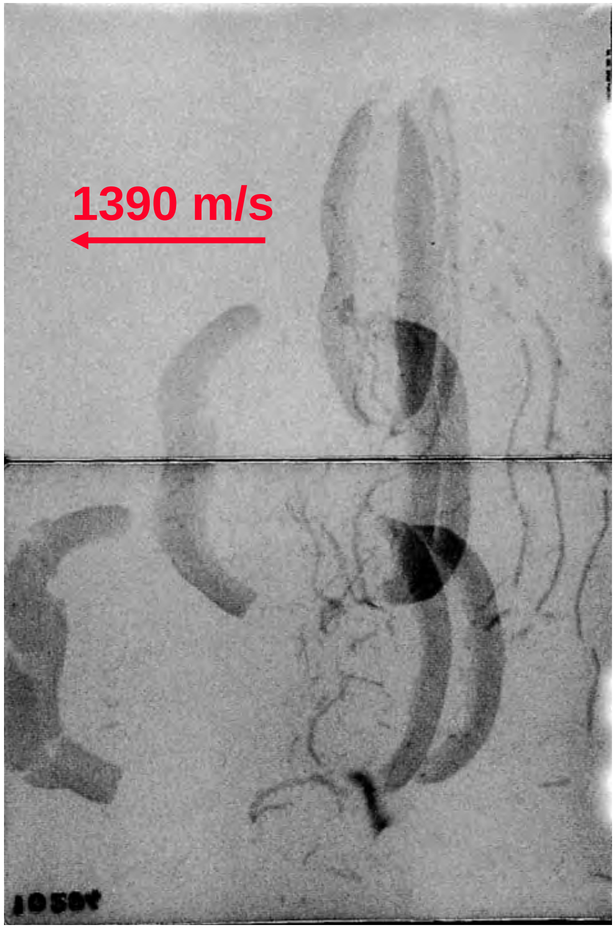

80 µs

140 µs

200 µs

EPS 50 – D=50 mm

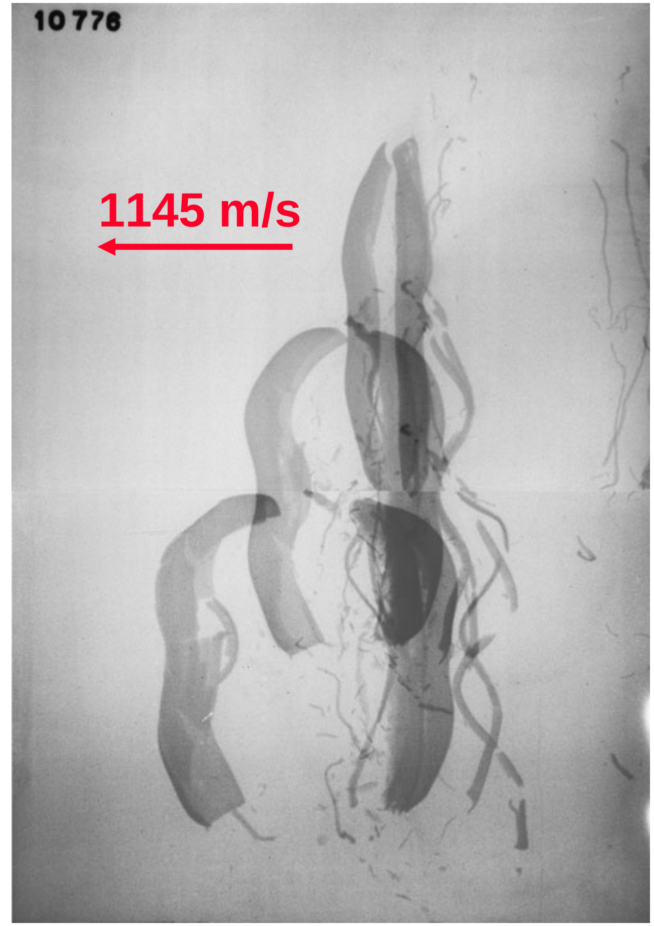

80 µs

120 µs

160 µs

Fraunhofer Institut Kurzzeitdynamik Ernst-Mach-Institut

A. Holzwarth

Flash X-Ray Photographs: Foams

EPP 50 – D=50 mm

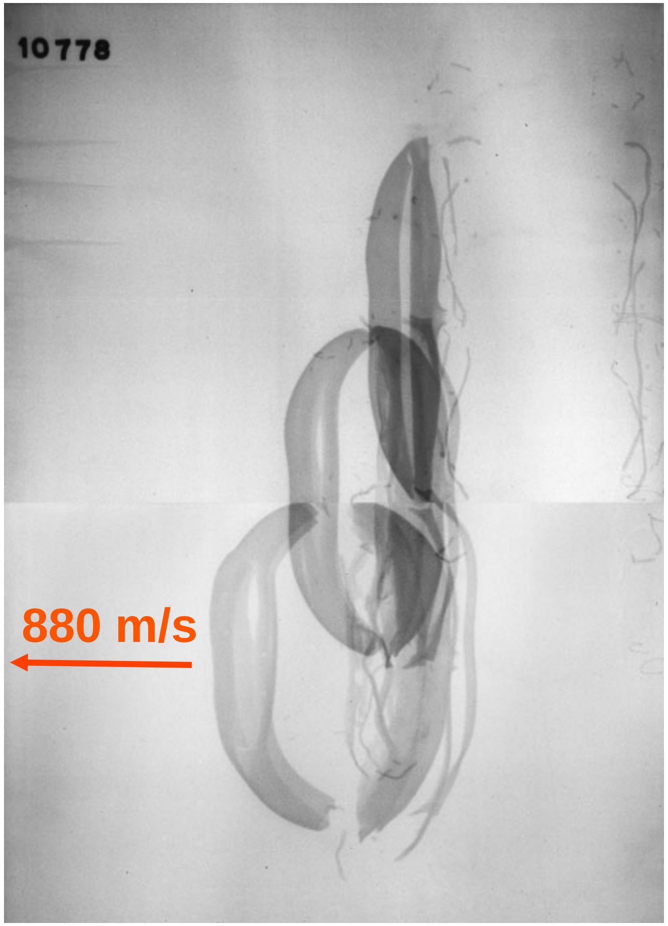

80 µs

120 µs

160 µs

White Foam – D=50 mm

80 µs

140 µs

200 µs

EPP 300 – D=50 mm

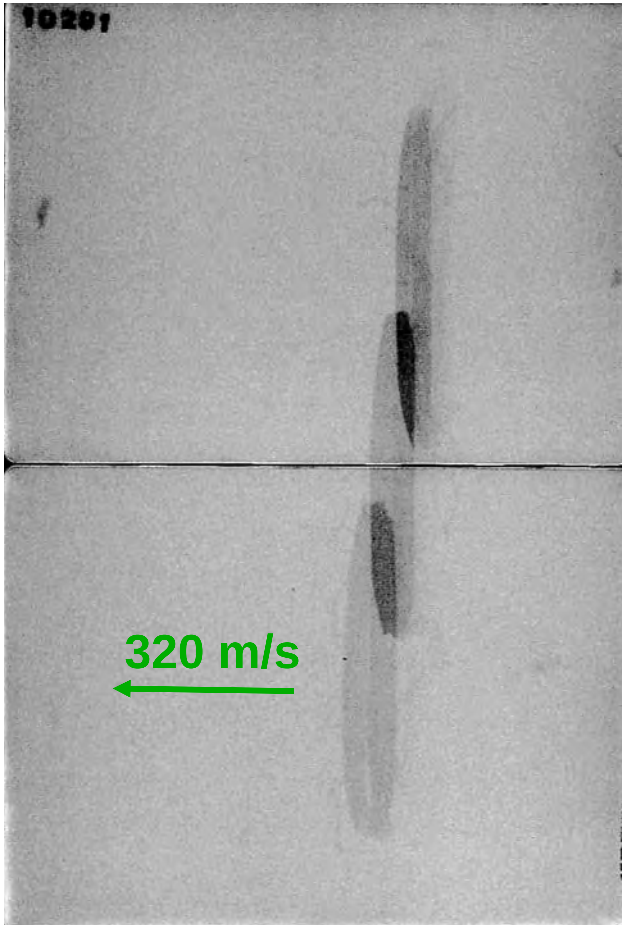

80 µs
120 µs
160 µs

PU-Foam – D=50 mm

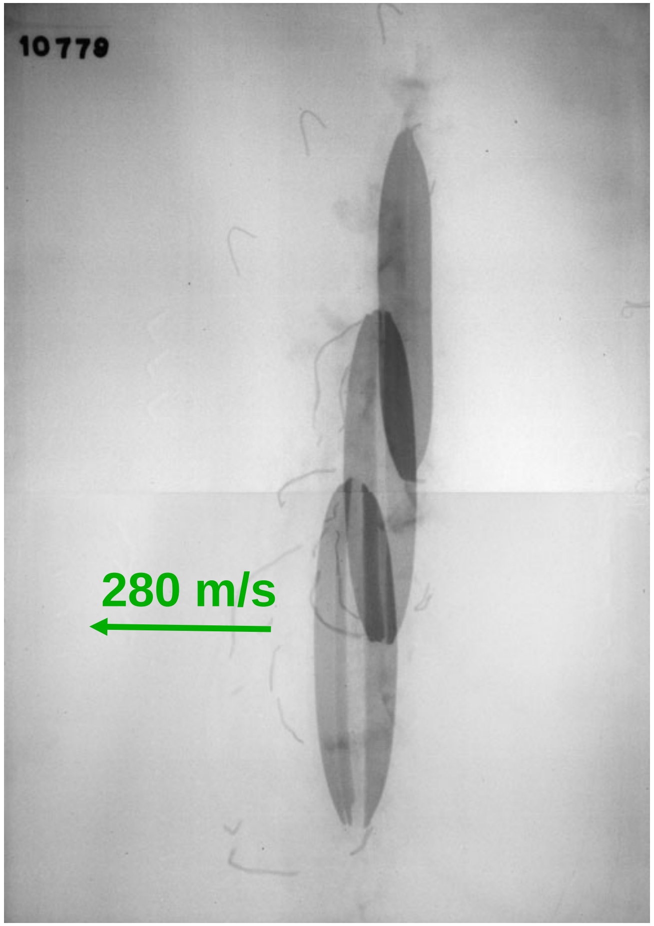

100 µs
160 µs
220 µs

(FP 4) versus Areal Density m_F of Foam Fillings

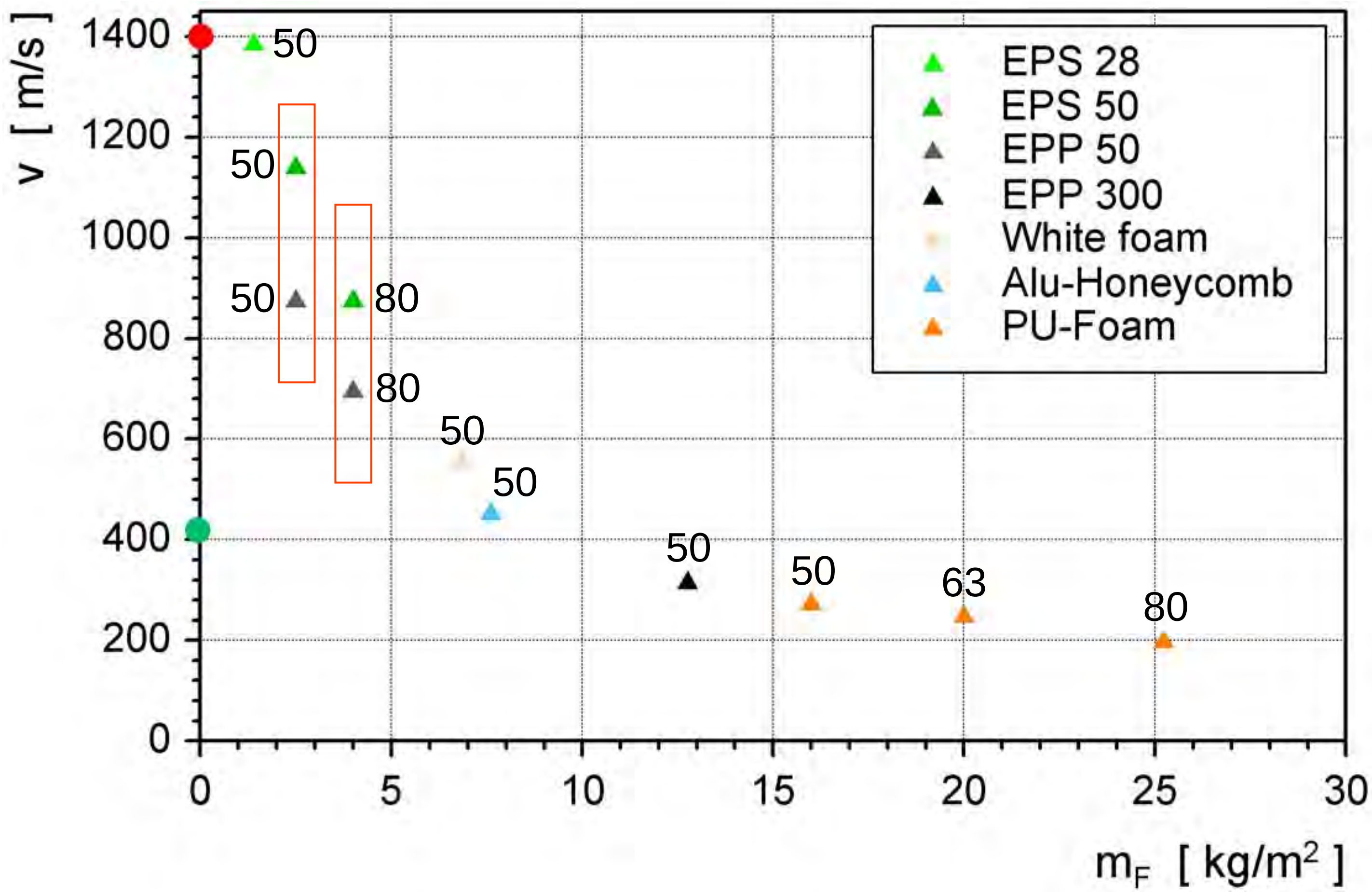

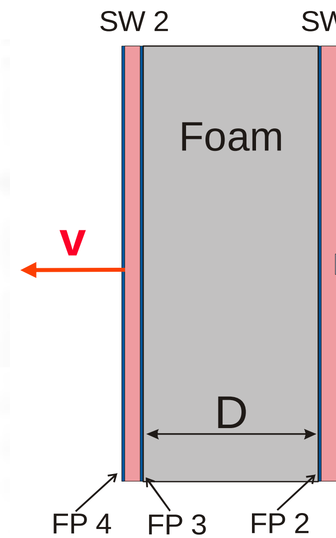

Fraunhofer Institut Kurzzeitdynamik Ernst-Mach-Institut

A. Holzwarth

xperiments 2:   Layers on Acceptor-Sandwich

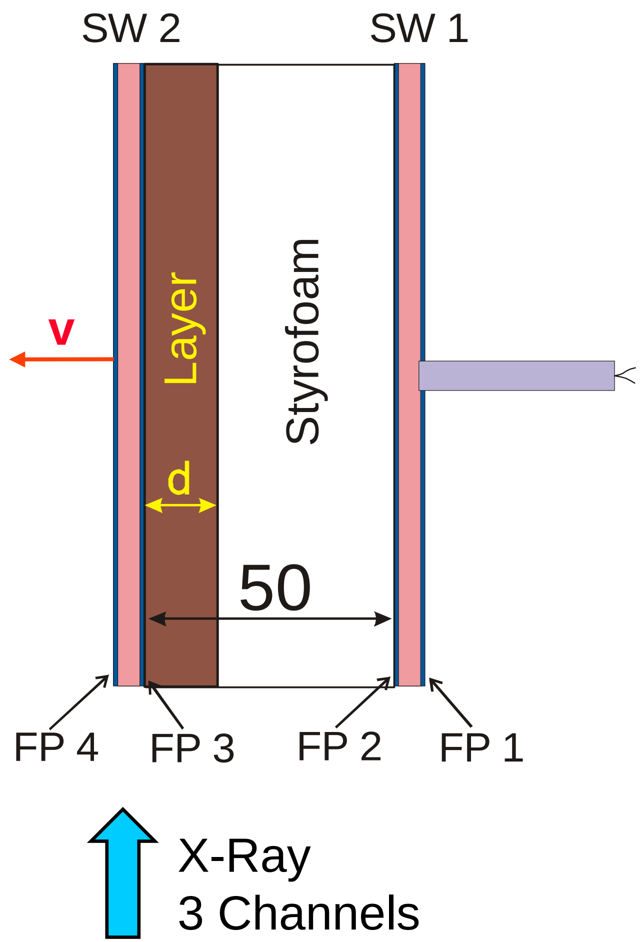

Distance between SWs: **D = 50 mm**

Thickness of layer: **d = variable**

ested Layers $\rho \geq 1100\ kg/m^3$

bber (Perbunan), ρ=1450 kg/m^3

lyurethane **(PU),** ρ=1260 kg/m^3

ganic–plastic material **(OGK),** ρ=1100 kg/m^3

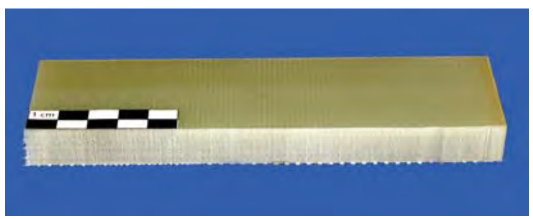

RP, ρ= 1950 kg/m^3

vlar, ρ= 1200 kg/m^3

EMI
Fraunhofer Institut Kurzzeitdynamik Ernst-Mach-Institut

A. Holzwarth

Flash X-Ray Photographs: Layers

Rubber

d=5,6 mm

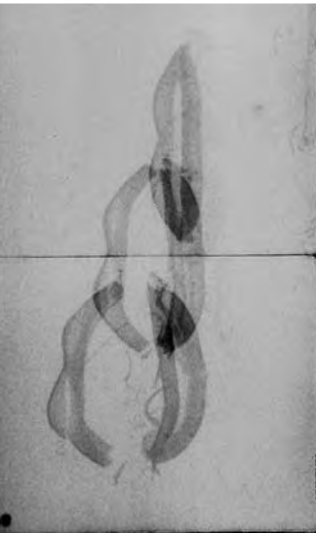

V_{FP4}: **800 m/s**

Flash times:

80, 140, 190 µs

PU

d=10 mm

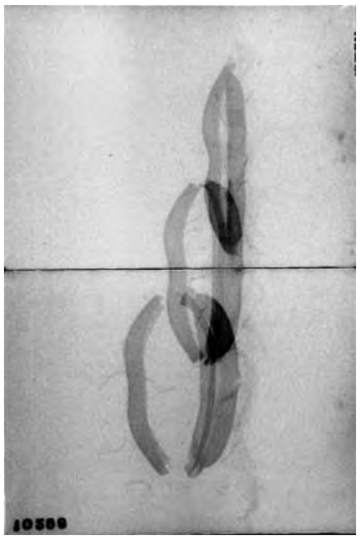

V_{FP4}: **585 m/s**

Flash times:

80, 140, 200 µs

OGK

d=14 mm

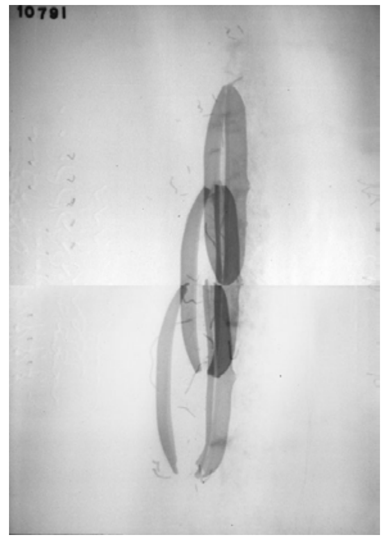

V_{FP4}: **490 m/s**

Flash times:

120, 160, 200 µs

PU

d=20 mm

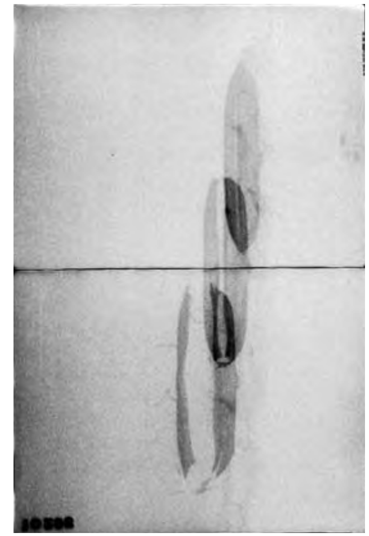

V_{FP4}: **350 m/s**

Flash times:

80, 140, 200 µs

OGK

d=22 mm

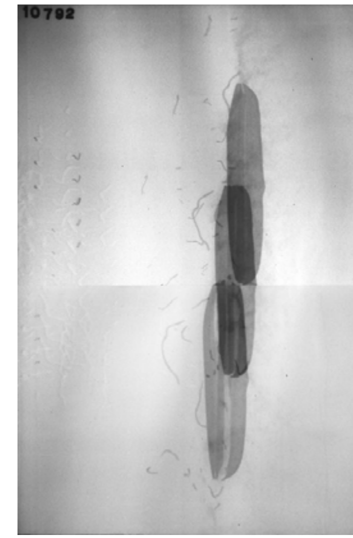

V_{FP4}: **265 m/s**

Flash times:

140, 180, 220 µs

Fraunhofer Institut Kurzzeitdynamik Ernst-Mach-Institut

A. Holzwarth

(FP 4) versus Areal Density m_F of Layers

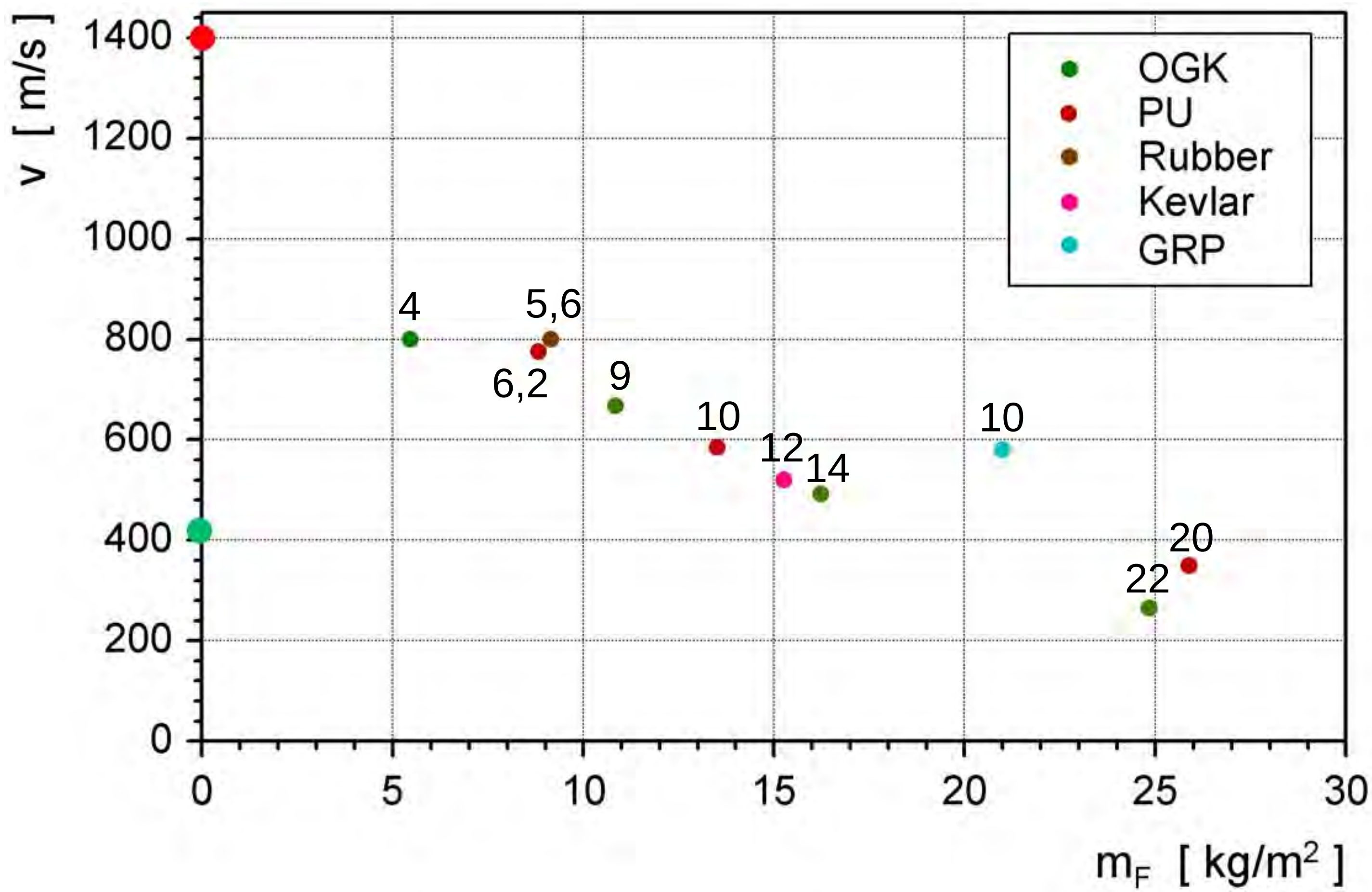

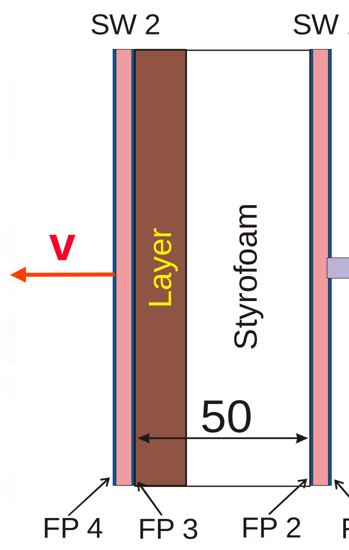

Fraunhofer Institut Kurzzeitdynamik Ernst-Mach-Institut

A. Holzwarth

omparison: v (FP 4) versus Areal Density m_F of Layers and oams

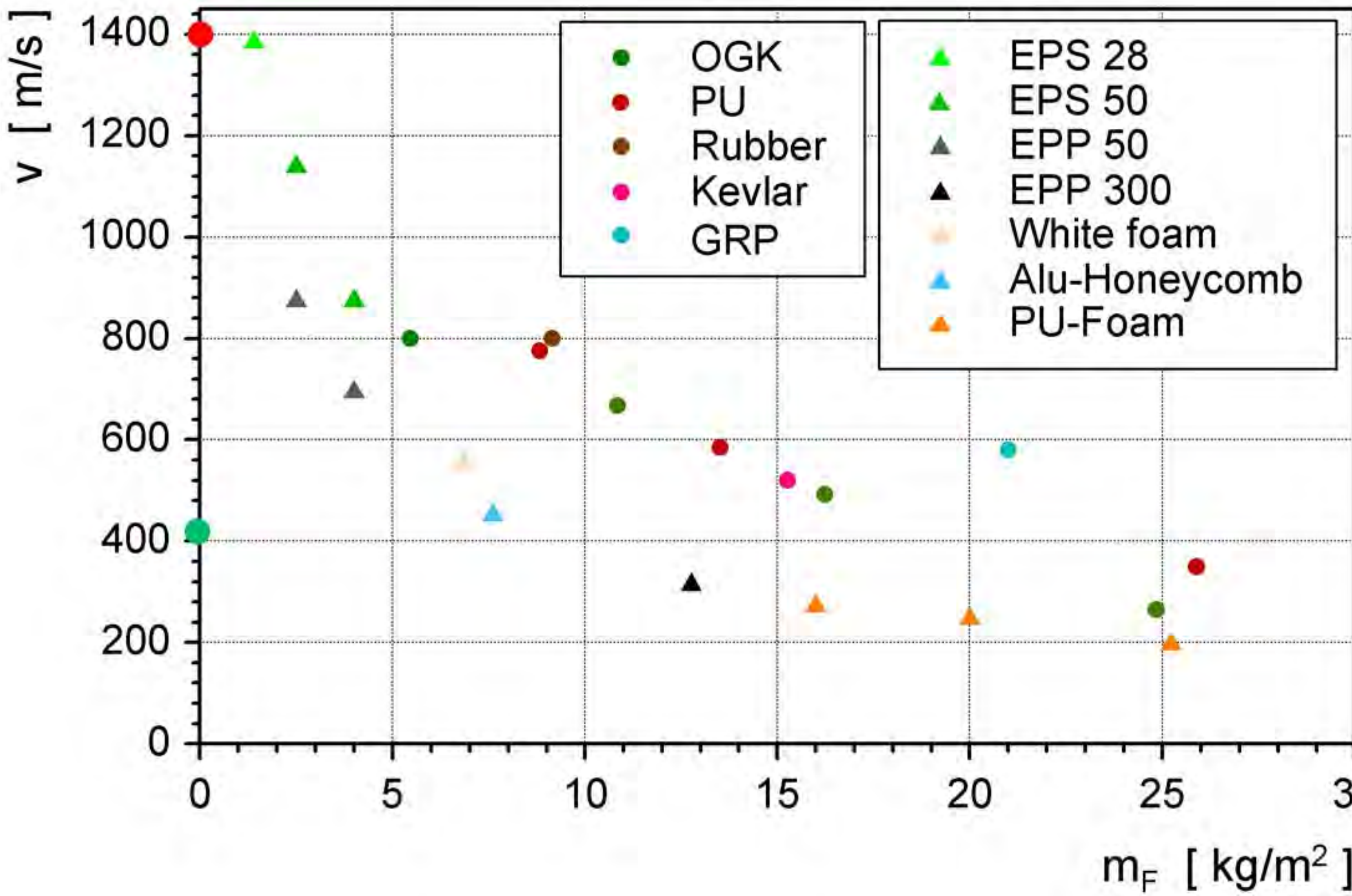

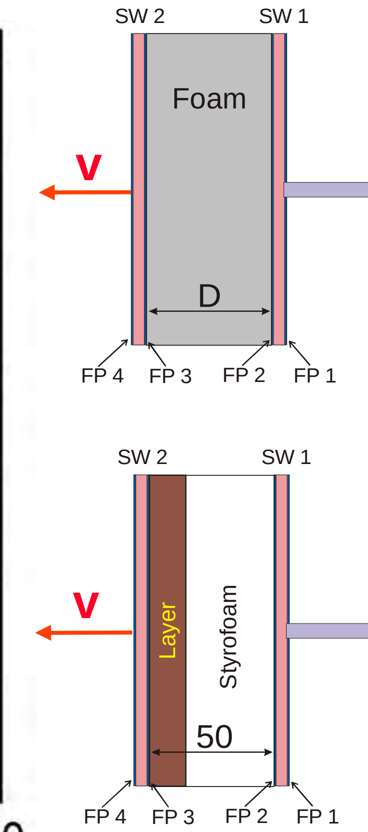

Fraunhofer Institut Kurzzeitdynamik Ernst-Mach-Institut

A. Holzwarth

xperiments 3: Foams as Layers on the Acceptor Sandwiche

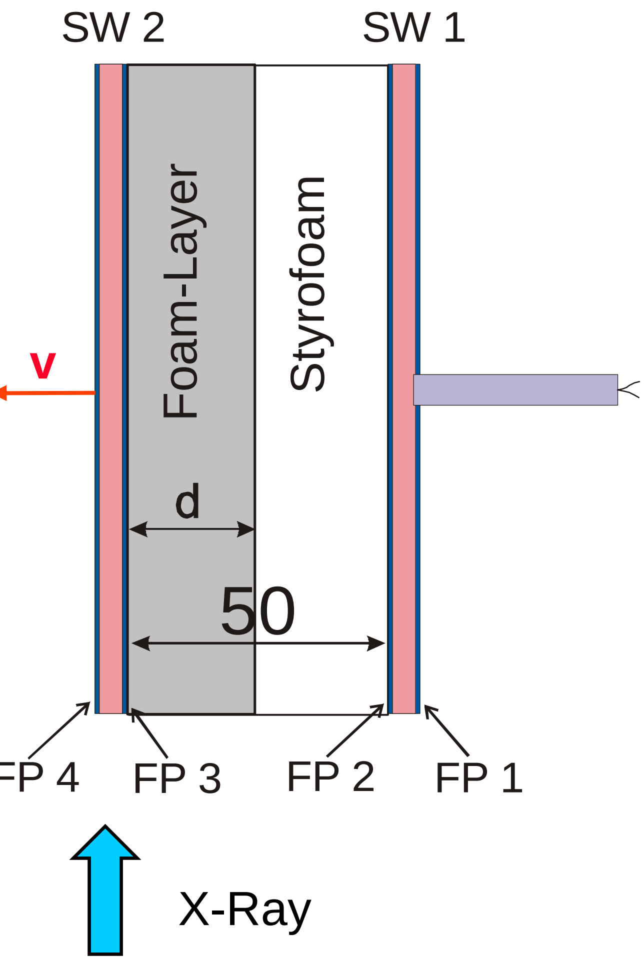

Tested foams: PU-foam, EPP 03

Distance between SWs: **D = 50 mm**

Thickness of layer: **d = 5 mm – 30 mm**

verview: Foams, Layers, Foam-Layers

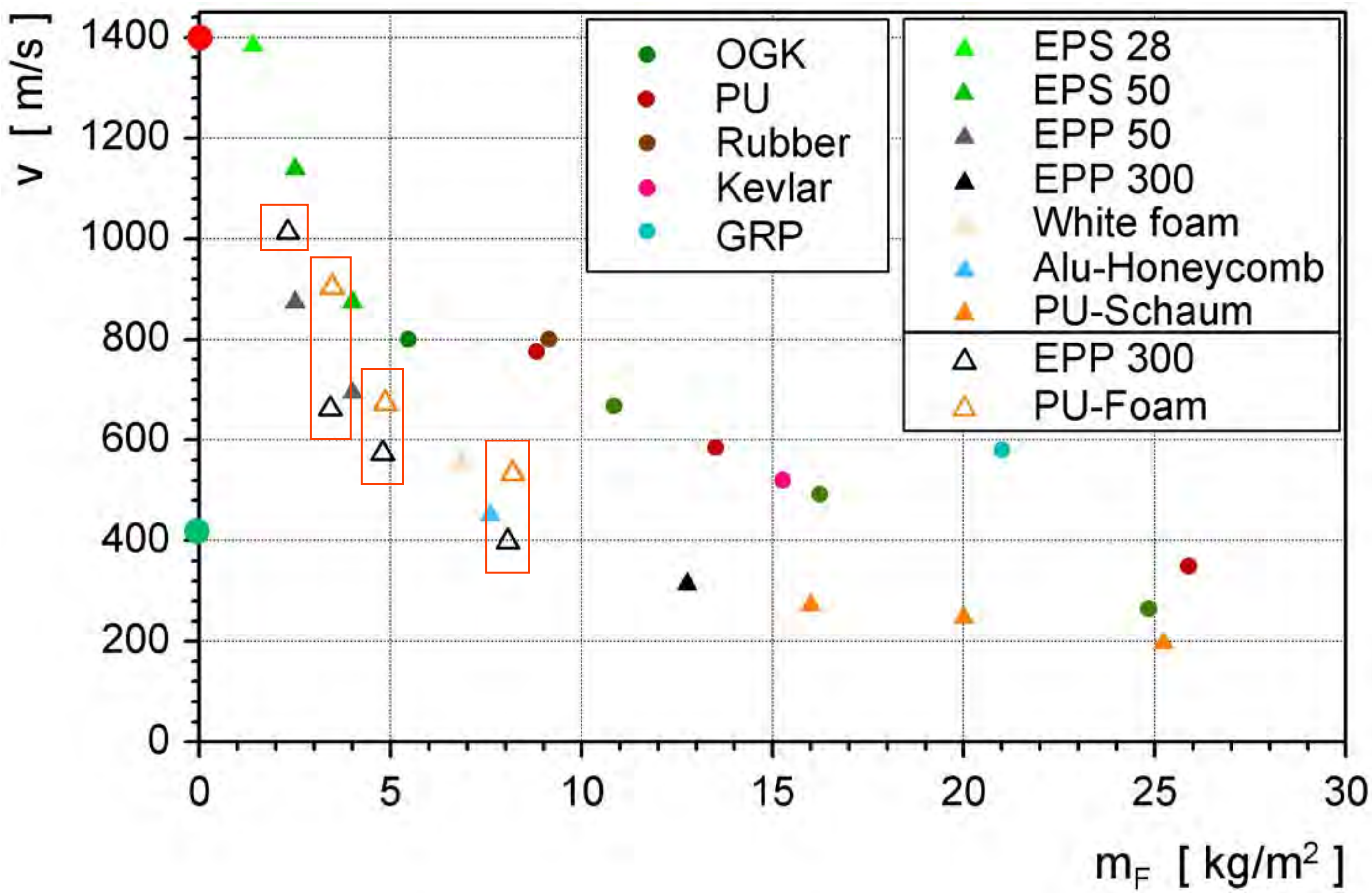

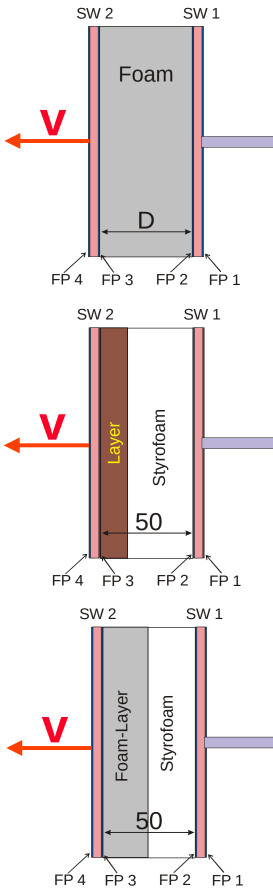

Fraunhofer Institut Kurzzeitdynamik Ernst-Mach-Institut

A. Holzwarth

ummary

The experiments didn't exhibit a clear distinction between detonation and no reaction.

Porous foams (ρ < 400 kg/m^2) are more effective than layers (ρ > 1100 kg/m^2) without porosity, regardless of the way they are placed between reactive sandwiches.

The areal densities necessary for a certain prevention of sympathetic detonation were :

- In case of foams: Areal density $\geq$ 8 – 10 kg/m^2
- In case of layers: Areal density $\geq$ 20 – 25 kg/m^2

For the prevention of sympathetic detonation not only the density of a material is important b
also other material properties, e.g. porosity.

End of Presentation

uture Work

More accurate investigation of the material properties important for the avoidance of sympathetic detonation

Decrease of protection power of reactive armor caused by damping materials

nvestigations with larger reactive armor systems

EMI
Fraunhofer Institut
Kurzzeitdynamik
Ernst-Mach-Institut

A. Holzwarth

ontact Information

r. Andreas Holzwarth

aunhofer-Institut für Kurzzeitdynamik

nst-Mach-Institut (EMI)

oteilung Experimentelle Ballistik

m Klingelberg 1

)588 Efringen-Kirchen

hone: +49 (0) 7628/9050-78

ax: +49 (0) 7628/9050-77

ndreas.Holzwarth@emi.fraunhofer.de

QinetiQ

The influence of sabot threads on the performance of KE penetrators

Nick Lynch, John Stubberfield: QinetiQ Ltd, Fort Halstead, UK

22nd ISB, Vancouver, November 2005

Introduction

- The majority of fin stabilised, kinetic energy (KE) projectiles use threads along the interface with the sabot to launch the penetrator from the gun
- The threads are generally undesirable at impact on a target since the thread root forms a stress concentration
- If the number of threads could be reduced, would this improve penetration performance ?
- Are threads needed in hydrocode simulations of impact events and a possible cause of discrepancies between experiment and simulation ?

Scope of the work

- Forward ballistic tests (40mm calibre)
  - Four designs of L/D 15 penetrator
  - Two types of multi-plate target
  - 1600 m/s
- Reverse ballistic tests (40mm calibre)
  - Two designs of L/D 30 penetrator
  - Oblique plate target fired at pitched attitude penetrators
  - 1650 m/s

QinetiQ

Projectiles

- Plain finish and full thread

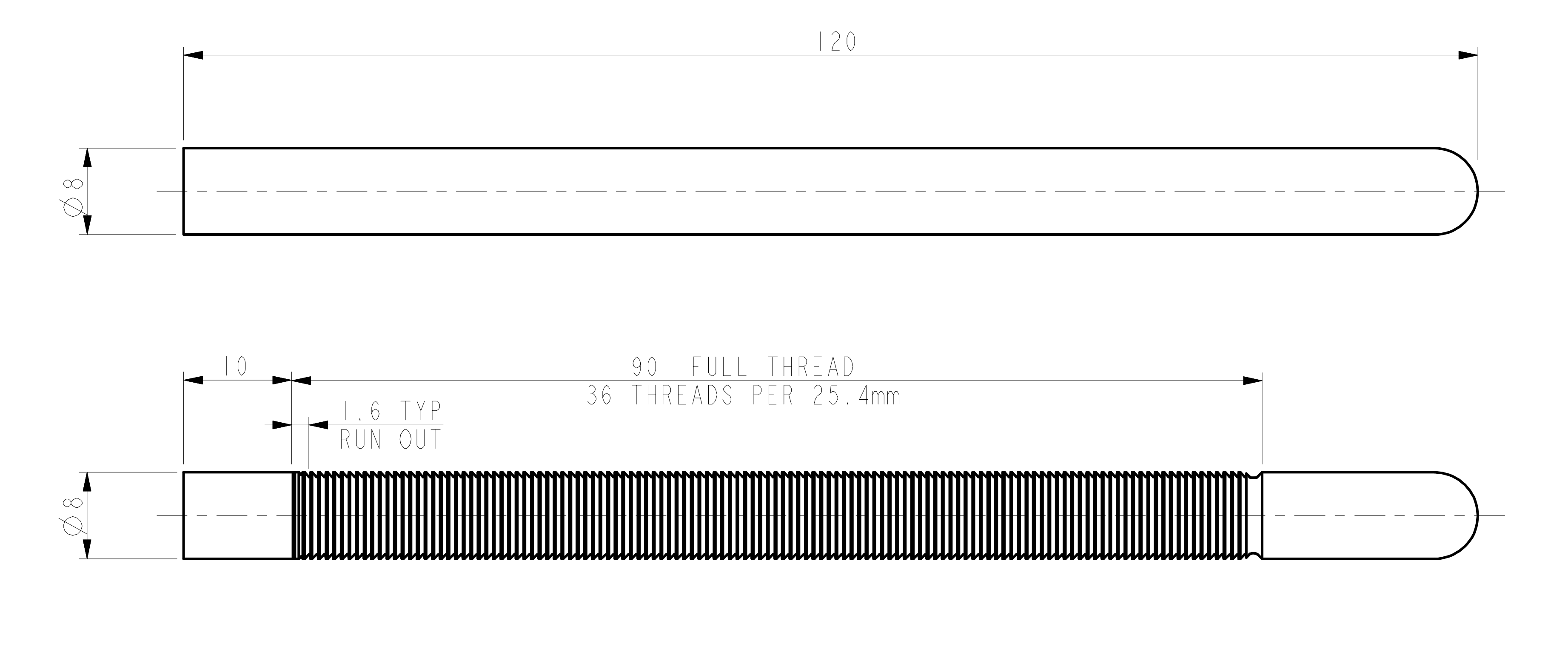

QinetiQ

Projectiles

- Half thread and double thread

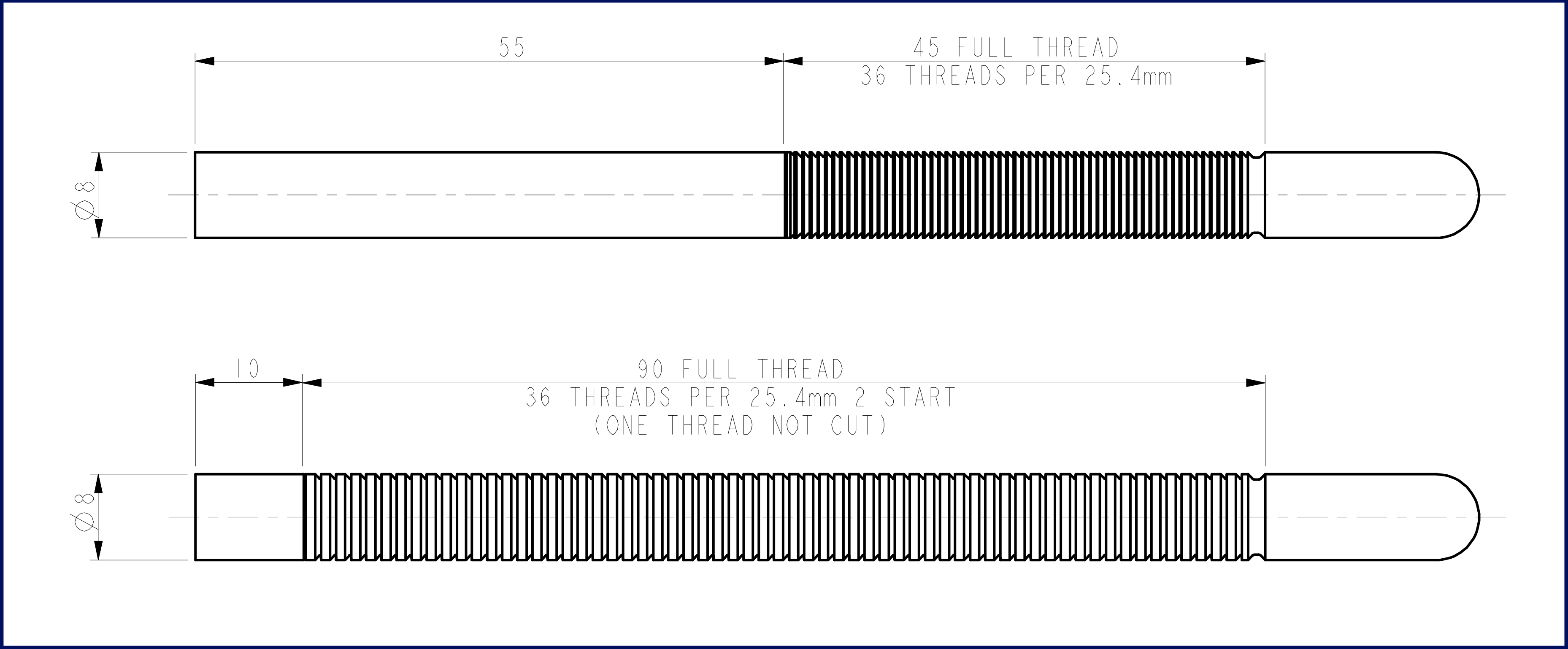

Target designs

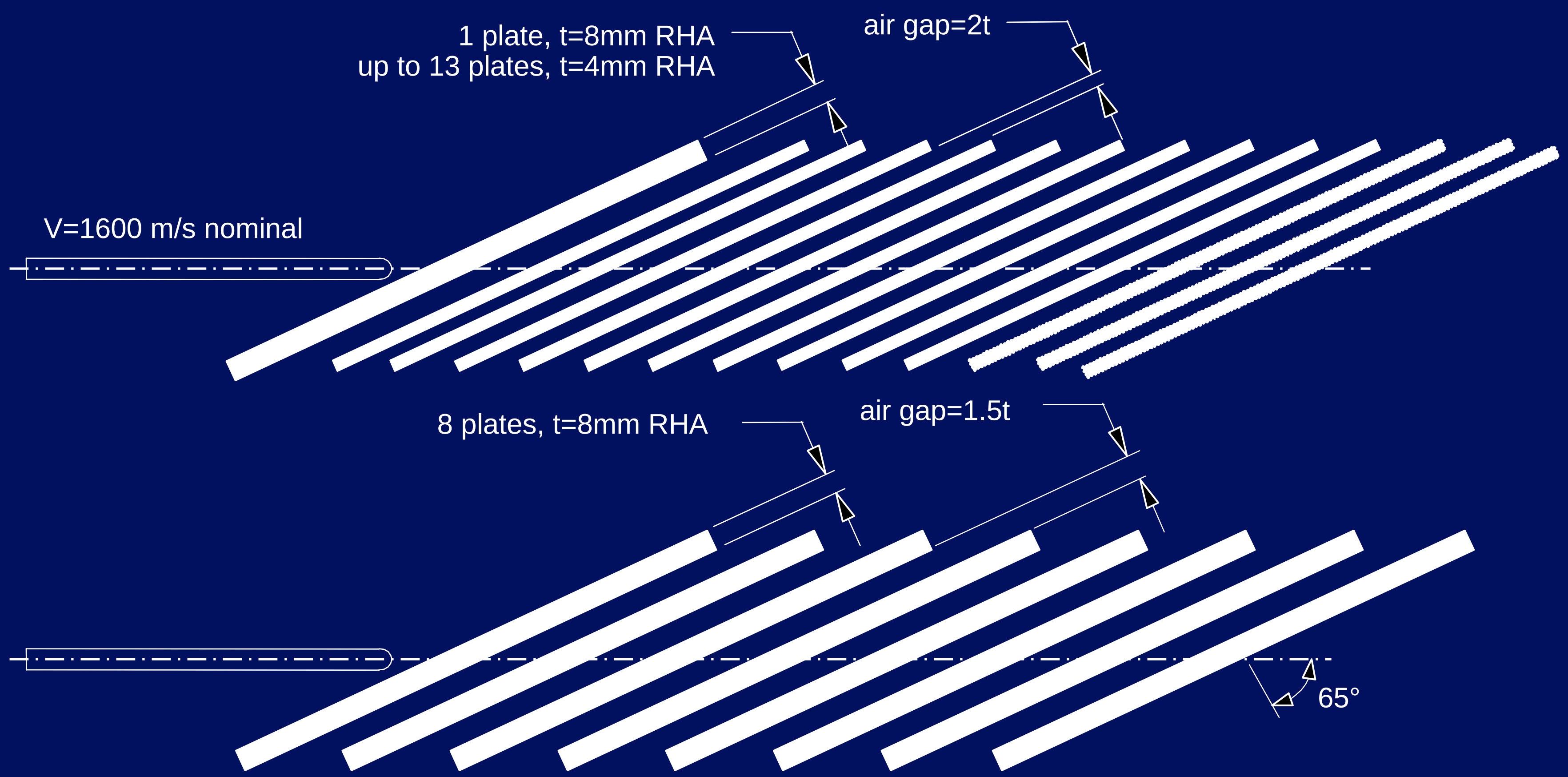

QinetiQ

Results against Target 1

- 3 rod types tested
- Assessment of results made difficult by variation in impact pitch angle
- The results can be ranked by pitch
- Allowing for this, no apparent difference in penetration

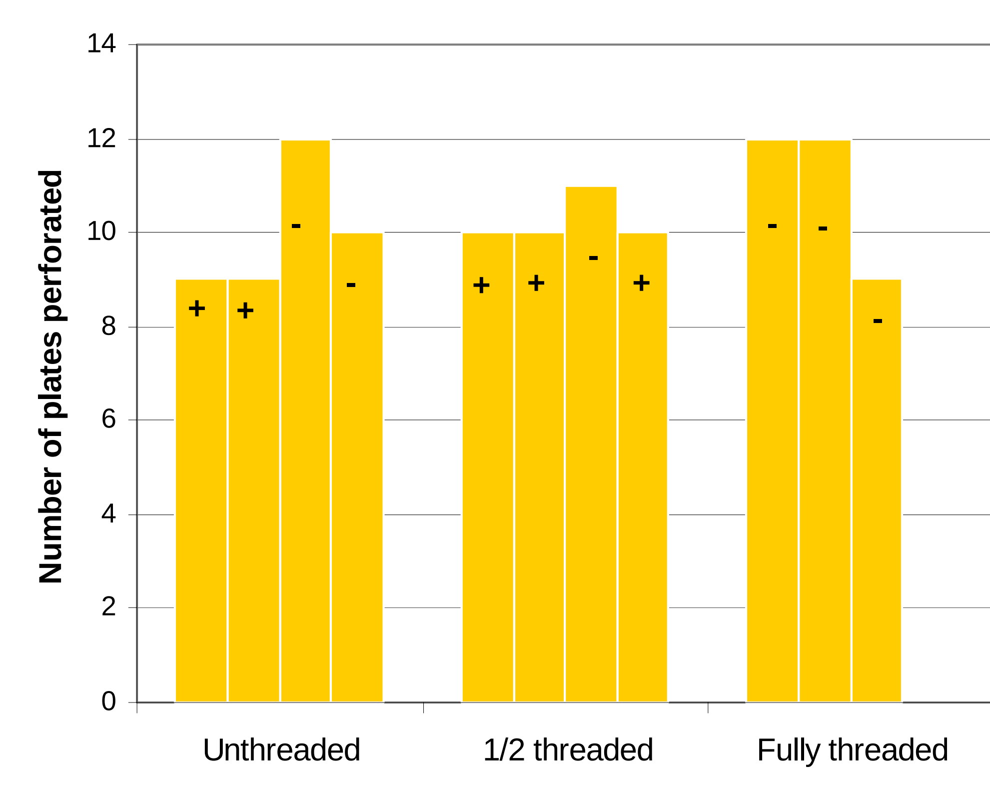

QinetiQ

Penetration into Target 2

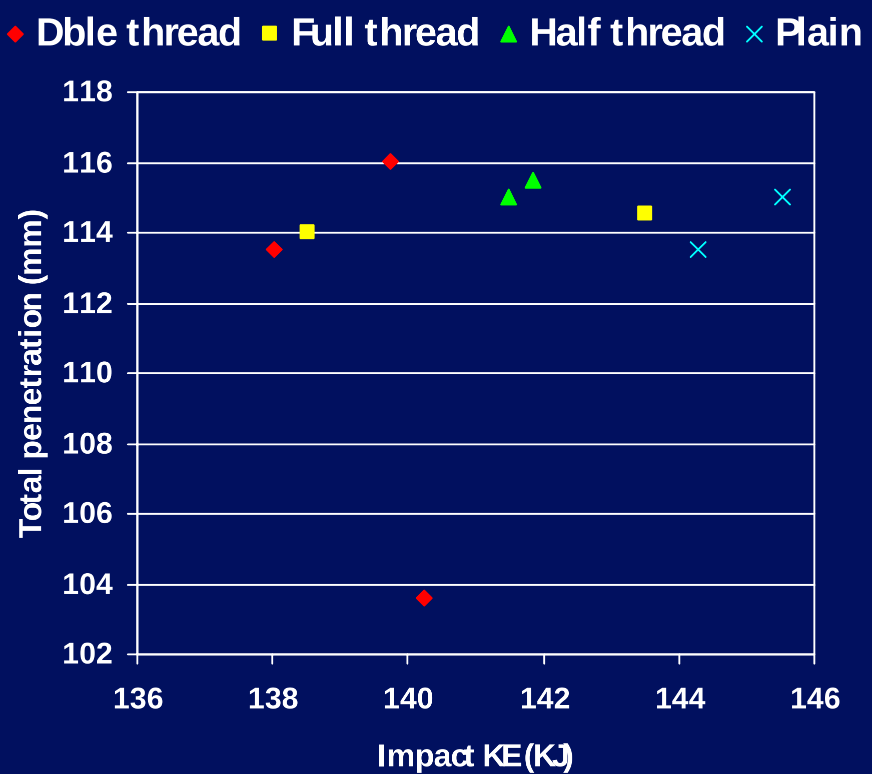

- Impact pitch less than 0.5°
- All except one result perforated 6 plates
- Need to compare line of sight penetration

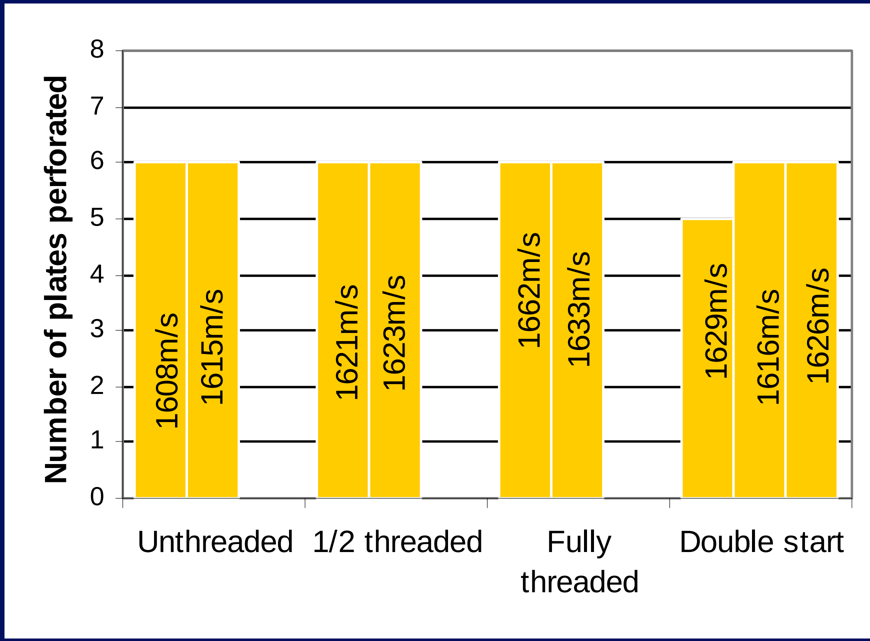

- Unthreaded rods with highest energy went no deeper than other designs
- 1615 m/s unthreaded rod has 5% greater KE than full thread design at 1633 m/s

QinetiQ

Average crater widths

- Crater width reduces due to projectile deceleration
- Crater width for un-threaded rods increased from plate 1 to plate 2 – widest craters in most of the plates
- Full thread rod tends to have a narrower crater

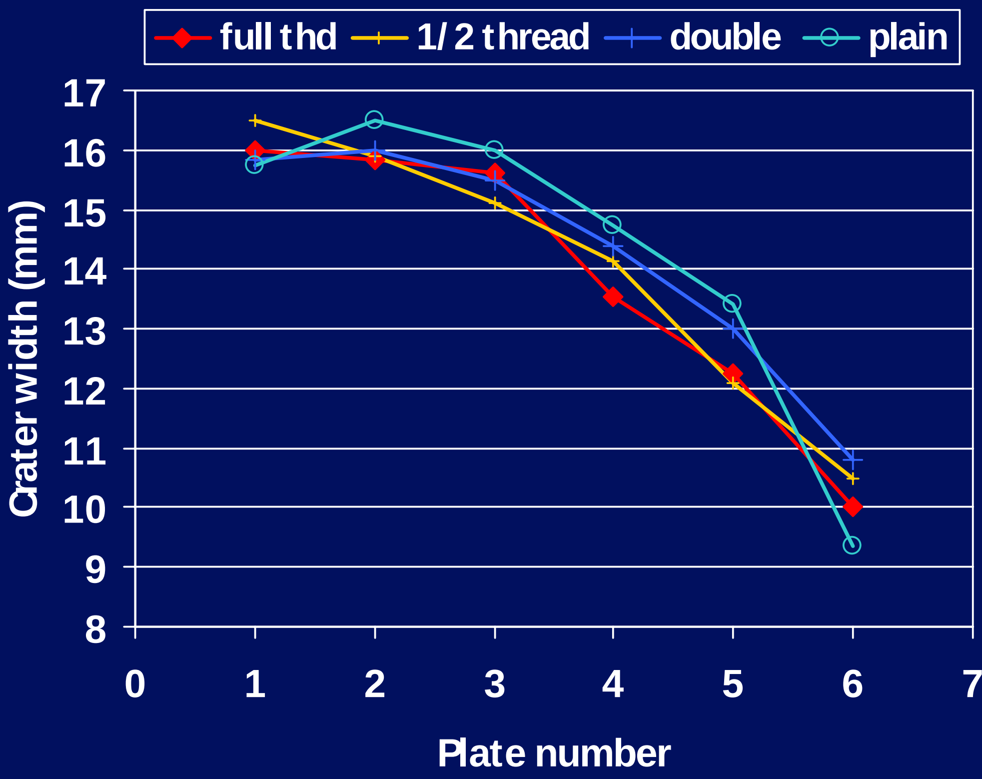

QinetiQ

How much change in penetration could be expected ?

- If the threaded rods lost one pitch per plate due to shear at break-out, what effect would this have on penetration ?
- This was assessed using an analytical penetration model, deleting part of the rod at plate exit
  - Nil deleted (plain rod)
  - 0.7mm deleted (standard thread)
  - 1.4mm deleted (double pitch)
- What effect could be expected just from the difference in effective rod diameter ?

QinetiQ

Penetration vs. time for rod loss options

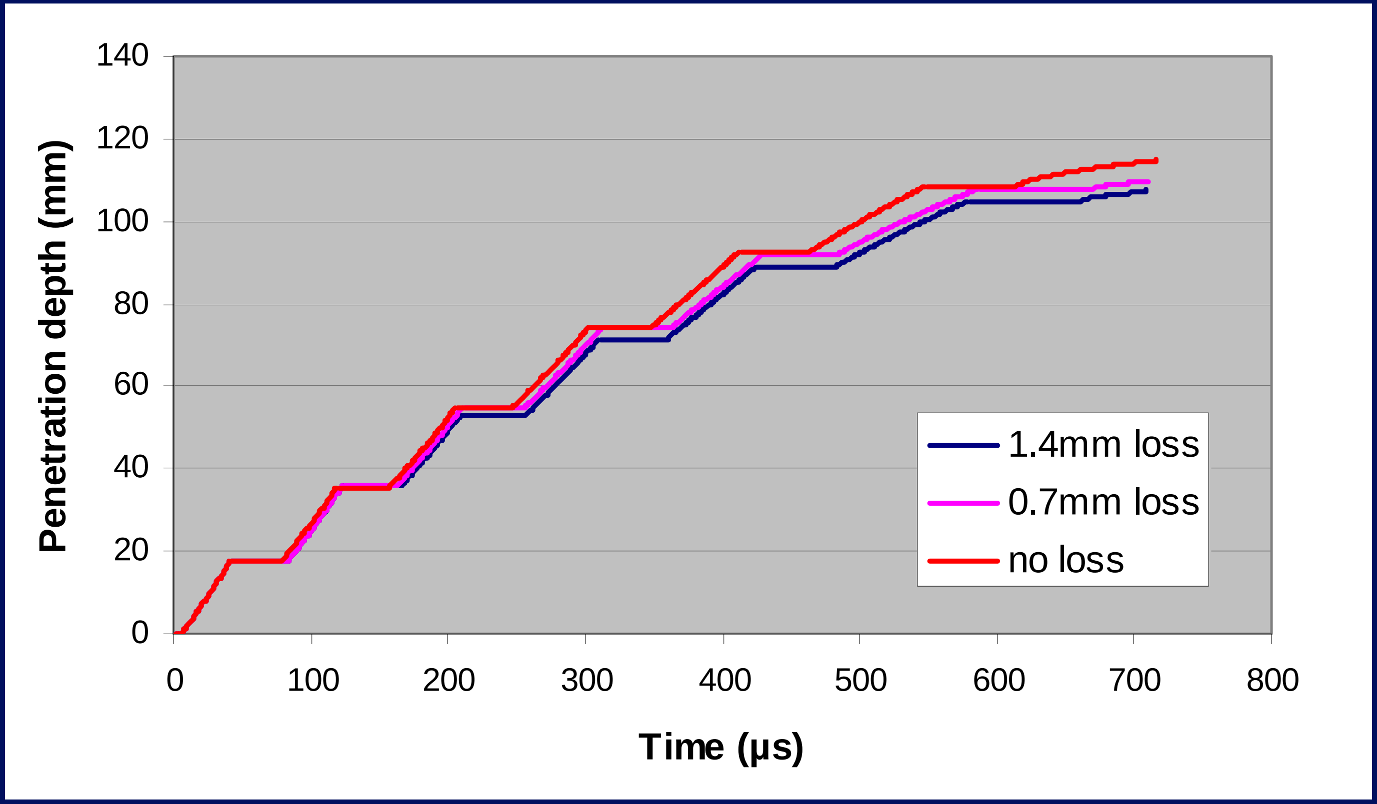

Predicted effect of rod loss

Rod type	Impact Velocity (m/s)	Rod diameter (mm)	Rod loss per plate (mm)	Total penetration (mm)
Unthreaded	1625	8	Nil	114
½ thread	1625	8		112 (interpolated)
Full thread	1625	8	0.7	110
Double thread	1625	8	1.4	106
Full thread	1625	7.70	Nil	112.85
Double thread	1625	7.77	Nil	112.8

- 1.2 mm change in penetration predicted due to effective diameter
- 8 mm change in penetration predicted due to pitch loss
- 8 mm difference would be observed. No evidence that this is occurring

QinetiQ

Comparison of X-rays - Target 2

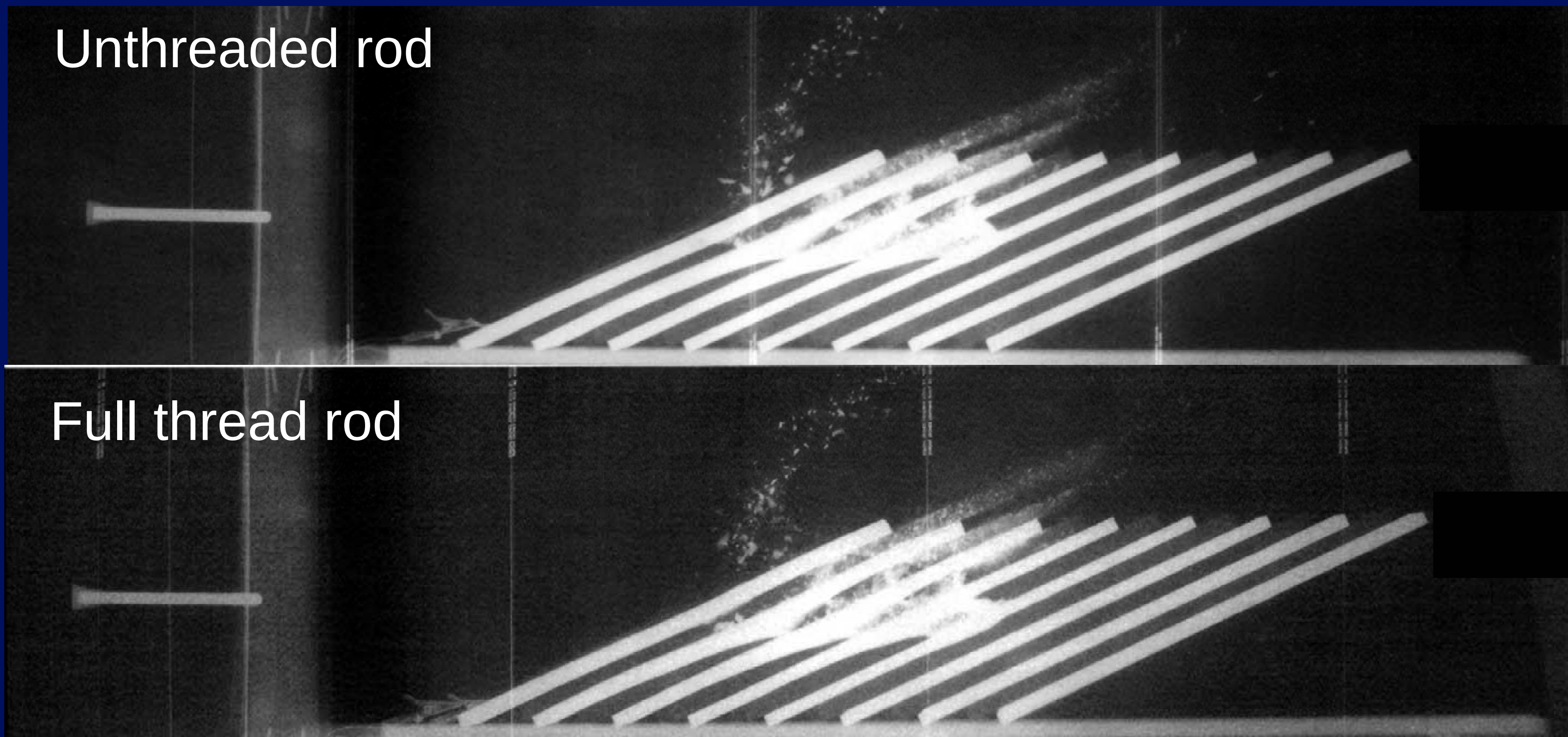

Reverse ballistic experiments

RHA target fired
at 1650 m/s

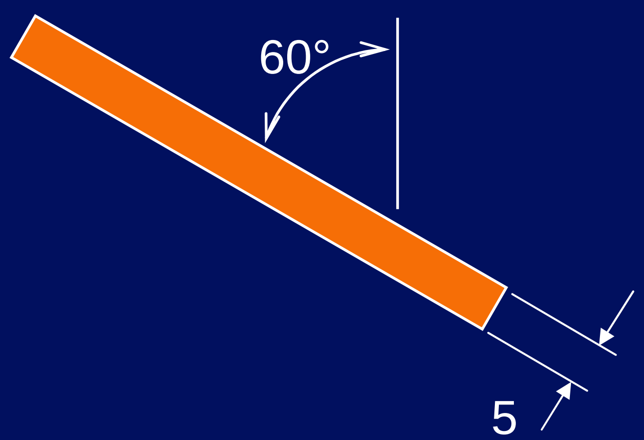

93% Tungsten alloy
projectiles

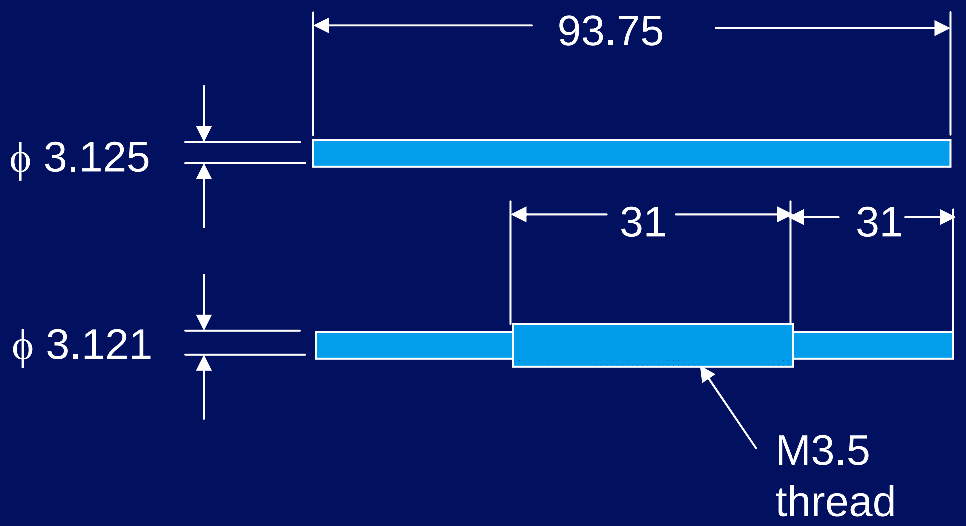

Projectiles pitched at 4°

Dimensions in
millimetres

Comparison of L/D 30 threaded vs. unthreaded

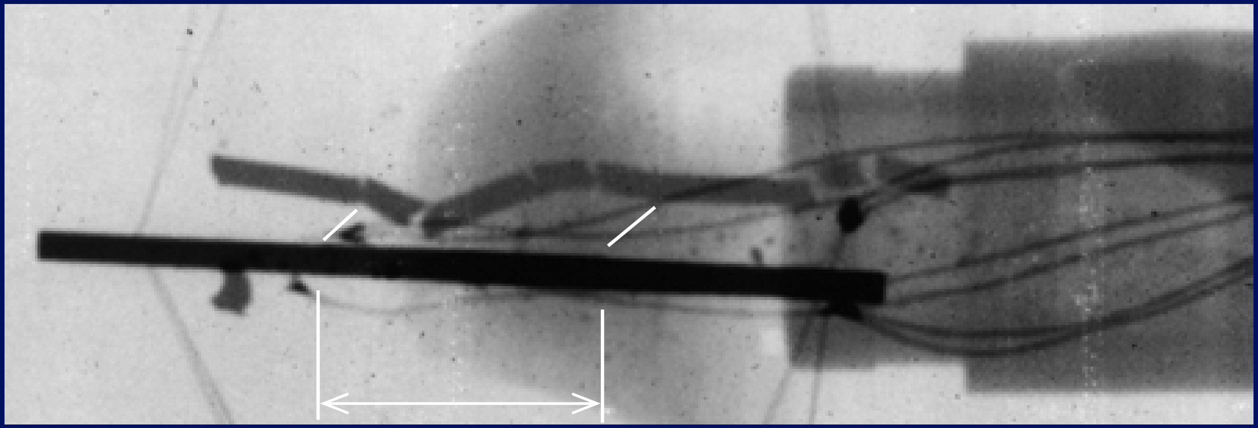

Threaded rod

Threaded region

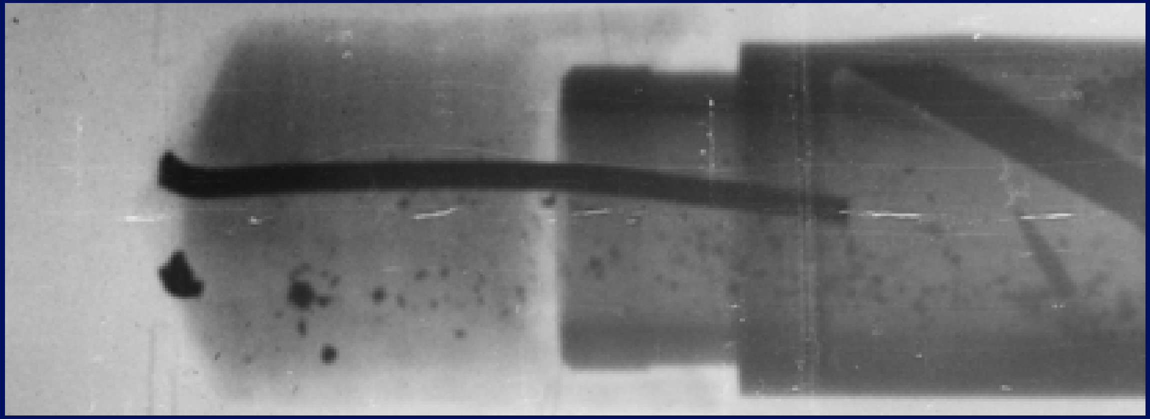

Unthreaded rod

Conclusions

- Four variants of L/D 15 threaded penetrator showed no significant difference in penetration depths against two multiple plate targets
- In contrast there was a marked difference in the fracture behaviour of L/D 30 pitched attitude rods with and without threads
- Conclude that representing threaded rods with plain surfaces in simulations is valid for multiple plate targets but not for more disruptive targets

QinetiQ

QinetiQ

DEFENCE R&D DÉFENSE

SNC TEC

Numerical Computations of Subsonic and Supersonic Flow Choking Phenomena in Grid Finned Projectiles

Nicolas Parisé, for SNC Technologies Inc.

Alain Dupuis, DRDC-Valcartier

22nd International Symposium on Ballistics,

Vancouver, BC, Canada

Defence Research and Development Canada

Recherche et développement pour la défense Canada

Canada

Presentation Outline

- Introduction
- Model Configuration
- Numerical Modeling
- Results
- Analysis of Choking Phenomena
- Conclusion

Introduction

- Grid-fin configurations offer interesting alternative to classical fin designs :
  - Low Hinge Moment,Easy storage, Good performance at high AoA.
  - Drawback : Higher drag penalty
- Experimental studies conducted at DRDC (in collaboration with ISL) demonstrated an aerodynamic choking phenomena on two configurations :
  - Thick fin model : flow is choked over a large range of Mach numbers
  - Thin fin model : flow choking occurs at specific Mach numbers
- Choking effect has not been reproduced by CFD or wind tunnel tests.

Introduction

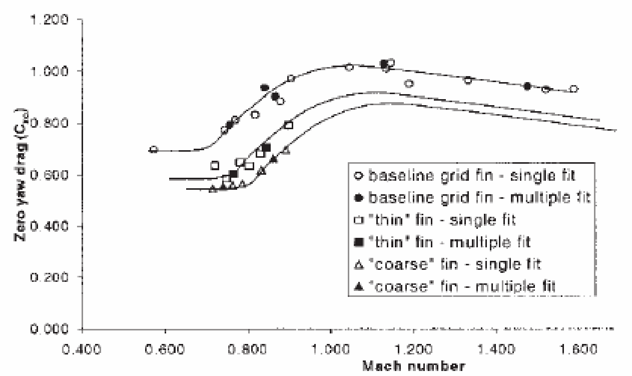

Figure 2. Zero yaw drag coefficient.

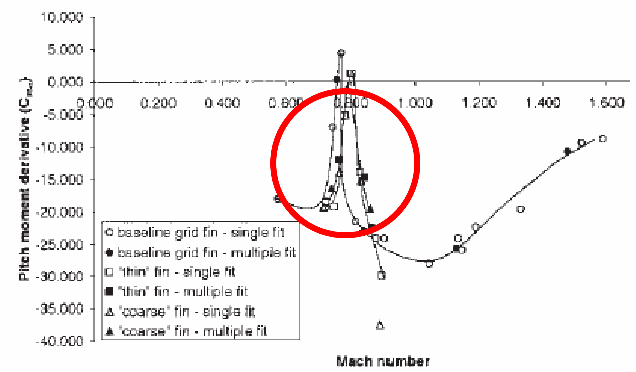

Figure 3. Pitch moment coefficient.

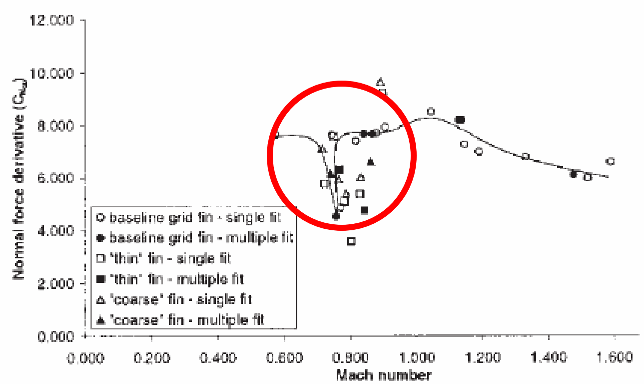

Figure 4. Normal force coefficient.

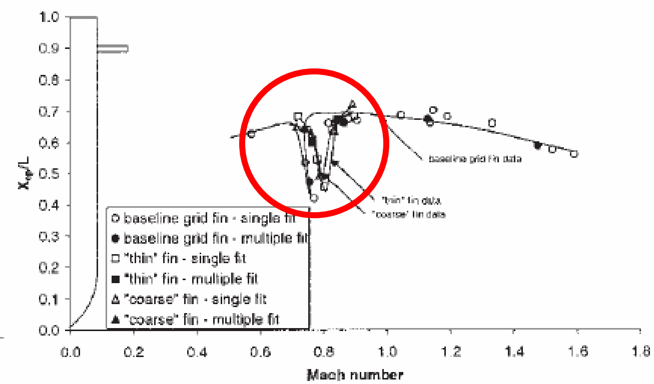

Figure 5. Center of pressure location.

⇒ Choking phenomena measured in aeroballistic range (Eglin AFB)

Model Configuration (Thin fins)

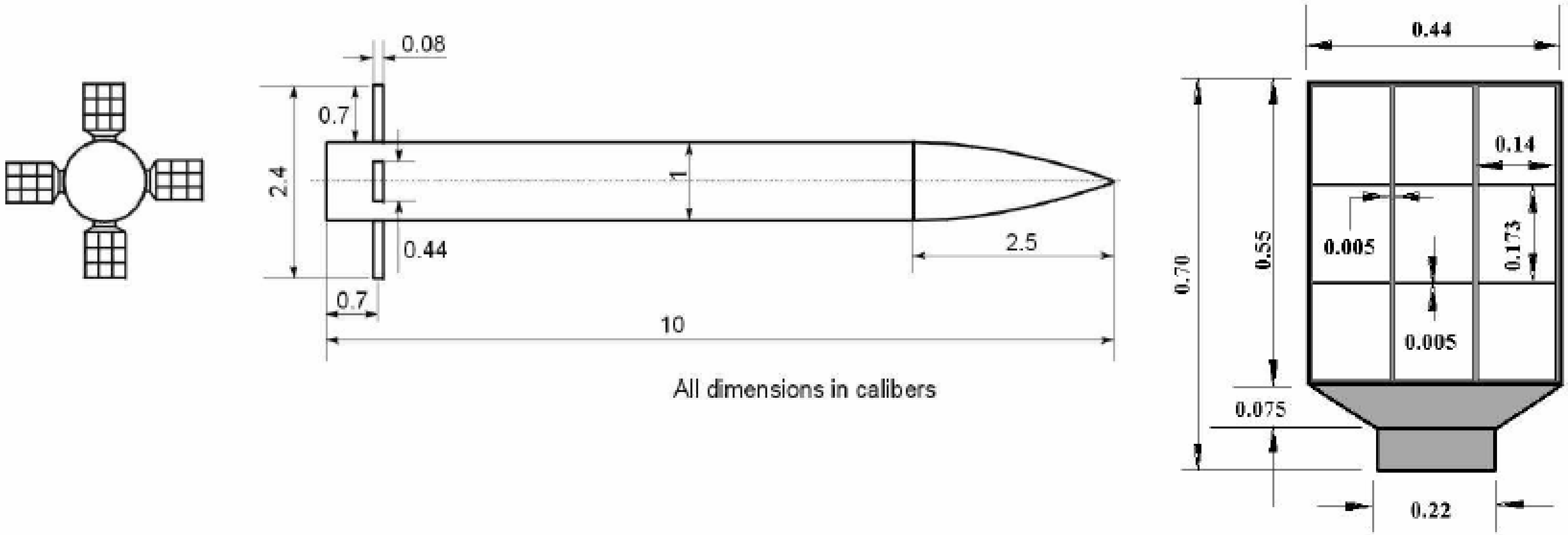

- Air Force Finner body, with four grid fins
- 9 grid cells per fin.
- No cant angle for fins
- 1 caliber = 20mm

Numerical Modeling

- CFD work done with ANSYS CFX 5.7
  - Navier-Stokes equations
  - 2nd order advection scheme
  - k-epsilon turbulence model was used
- Hexahedral mesh built with ANSYS ICEM CFD Hexa
  - 1.6 million elements for supersonic flow domain
  - 2.1 million elements for subsonic flow domain (with base flow)

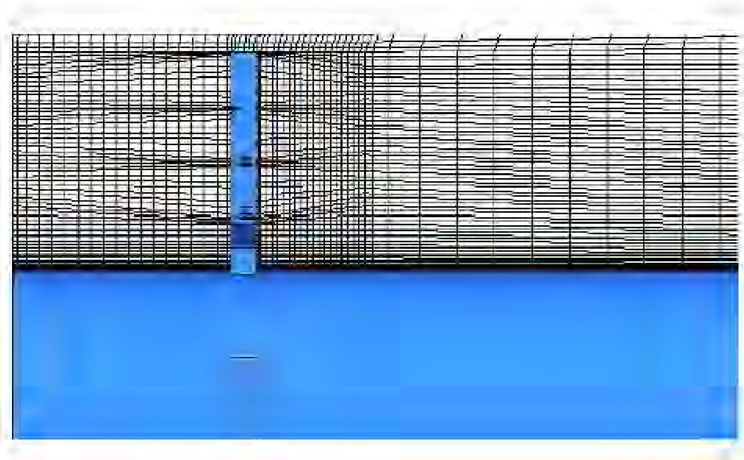

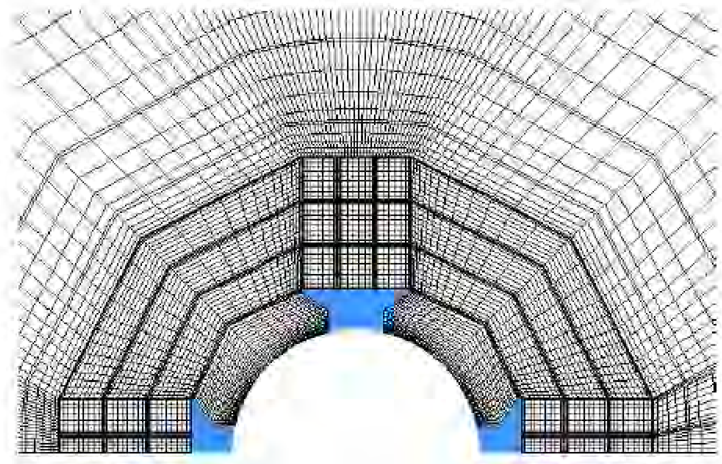

Numerical Modeling

- CFD computations performed at following conditions :
  - Baseline Mach no. 0.6, 0.8, 1.5, 2.0, 2.5, 3.0
  - Subsonic runs conducted at small increments between Mach 0.7 and 0.85 for flow choking simulations
  - Supersonic runs conducted at small increments between Mach 1.8 and 2.5 to explain sudden change in aerodynamic coefficients.
  - All runs made a 2° angle of attack
  - Cx, Cn, Cm and Xcp aerodynamic coefficients computed

Results – Normal Force Coefficient

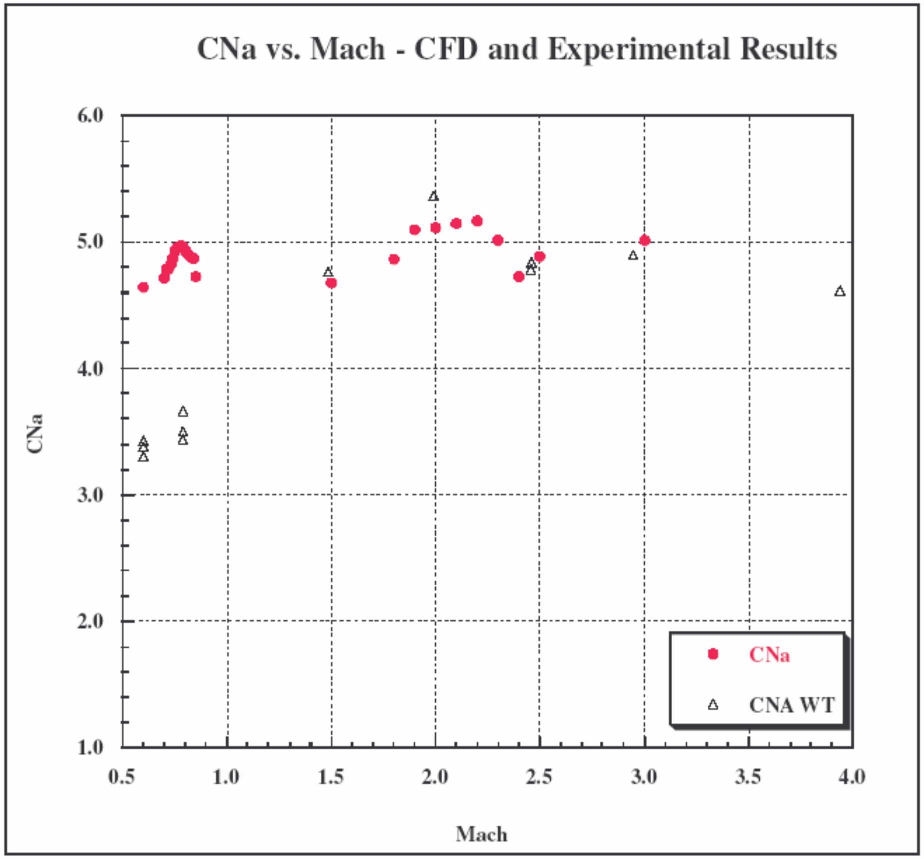

- Peak in CNa at M=0.78. Wind Tunnel results do not reproduce this peak.
- Theoretical Choking Mach for fin cells is M=0.744.
- Subsonic choking captured in CFD results.
- Discontinuous variation of CNa between Mach 1.8 and 2.4.
- Good agreement between CFD and Wind Tunnel results.

Results – Pitch Moment Coefficient

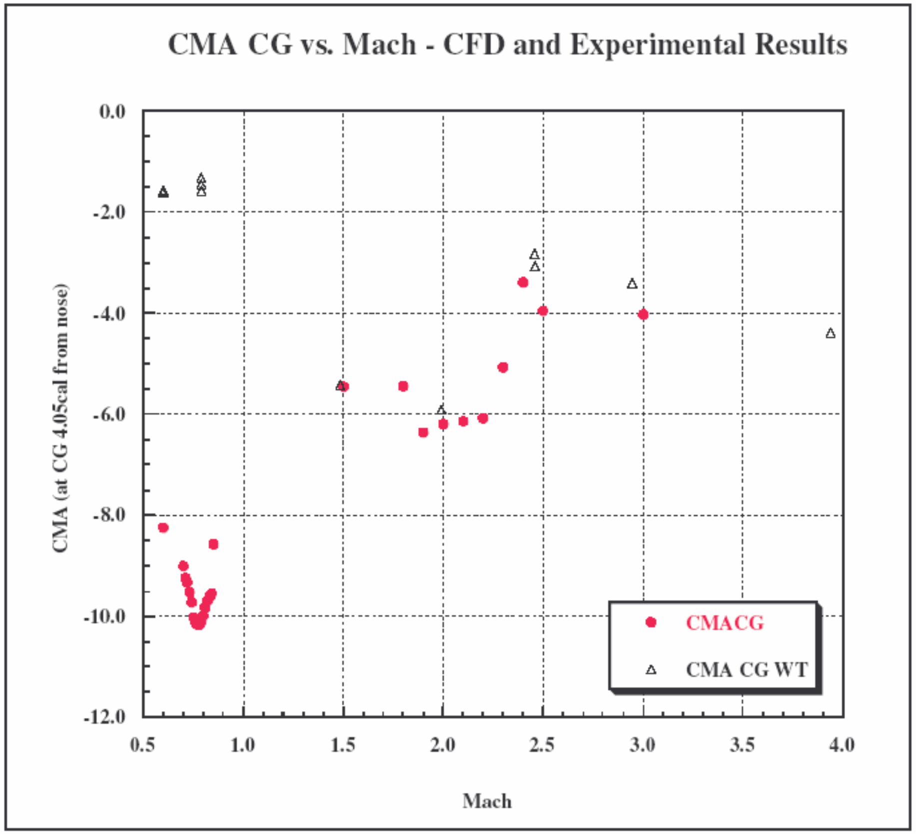

- Similar peak at M=0.78. Wind Tunnel results do not reproduce this peak.
- Effect of subsonic choking on CMa is to increase stability.
- Again, discontinuous variation of CMa between Mach 1.8 and 2.4.
- Good agreement between CFD and Wind Tunnel results.

Results – Axial Force Coefficient

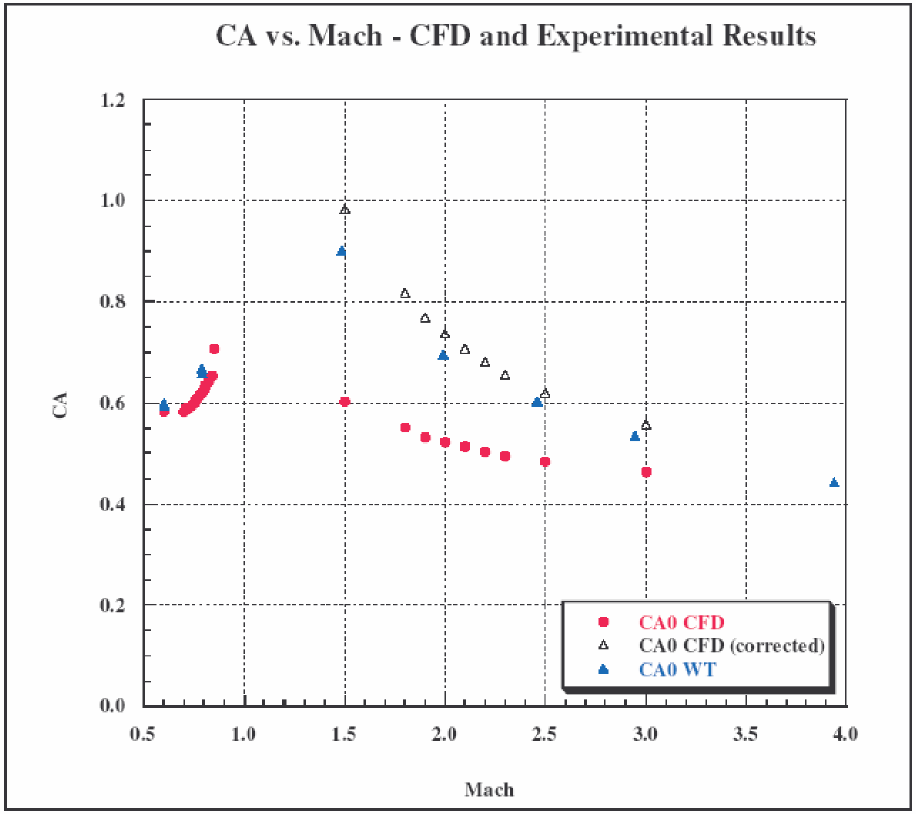

- Good agreement between CFD and Wind Tunnel results.
- CFD results in supersonic regime had to be corrected for base drag.

SNC TEC

Results - Center of Pressure

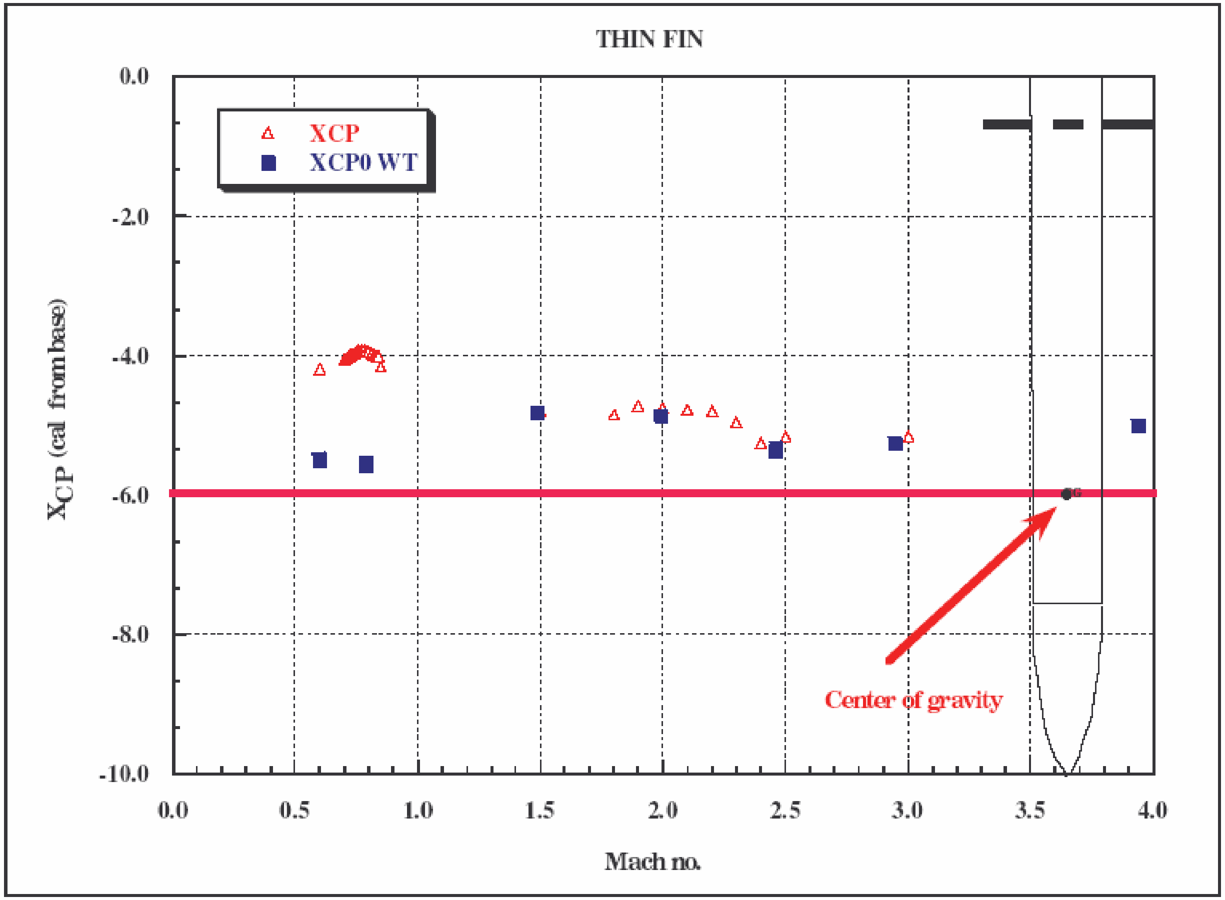

Analysis – Subsonic choking

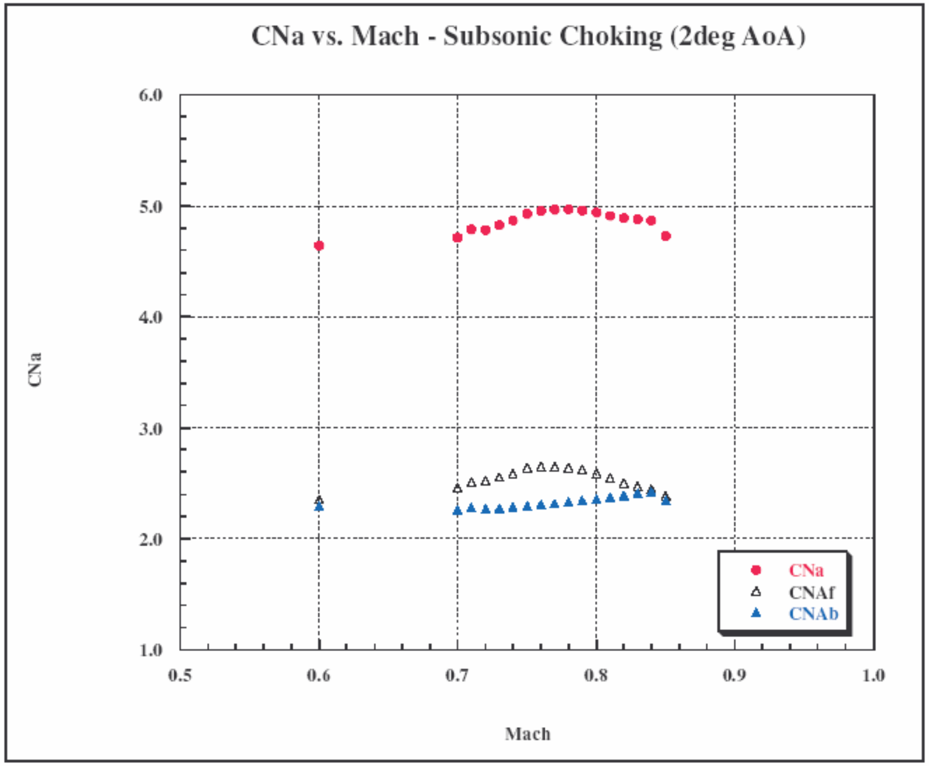

- CNa contribution breakdown : peak effects come from fins.
- Peak value at Mach 0.78 due to choking effects.
- Confirmed by apparition of Mach waves inside fin cells.

Analysis – Subsonic choking

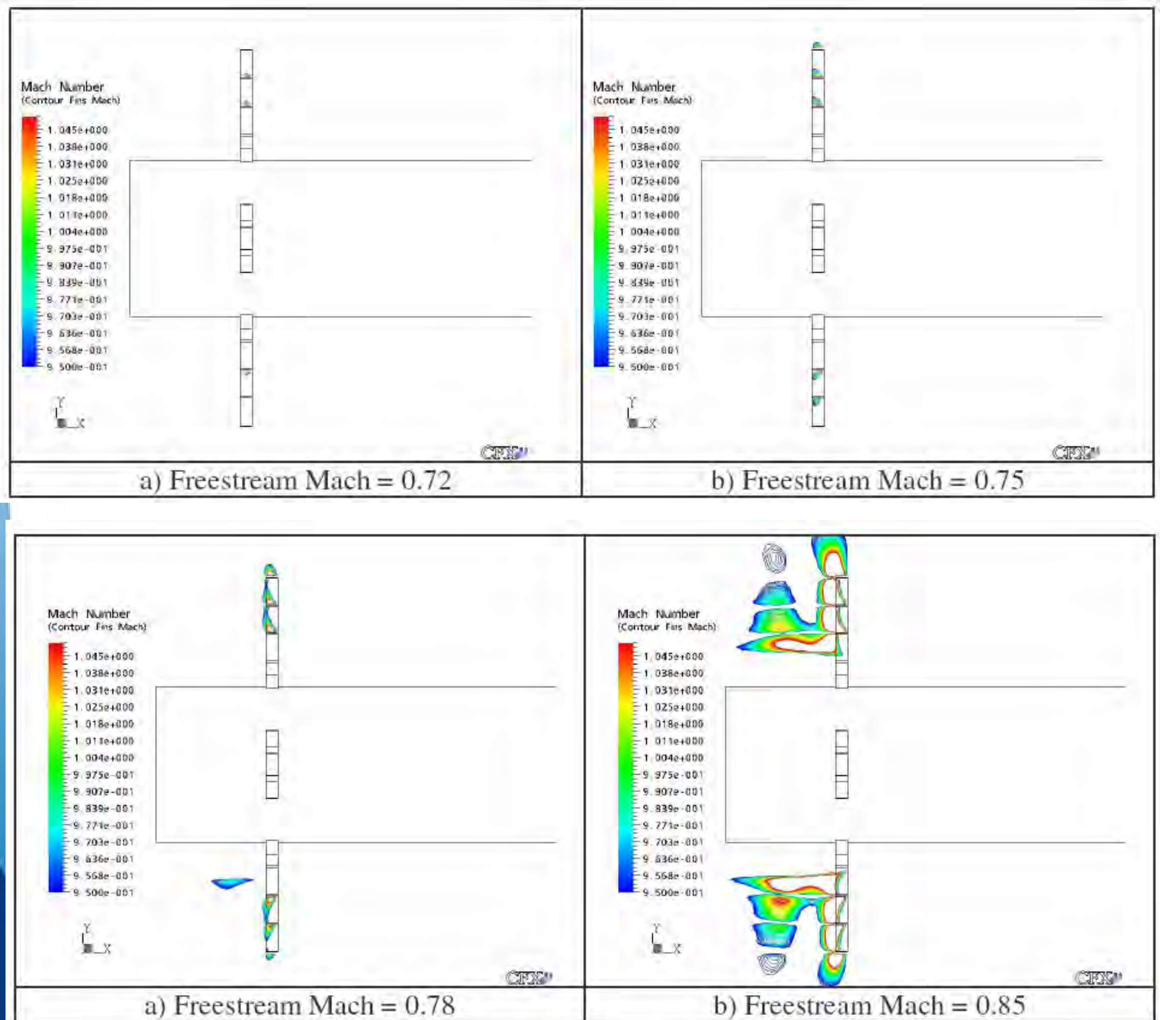

a) Freestream Mach = 0.72 b) Freestream Mach = 0.75

a) Freestream Mach = 0.78 b) Freestream Mach = 0.85

- Contour plots of sonic regions between Mach 0.95 and 1.05.
- As Mach number moves from 0.72 to 0.78, normal shockwaves appear in cells.
- Completely choked state reached at Mach 0.78.
- Good correlation between theoretical choking Mach number and CFD results.

Theoretical Grid Fin Flow Field Model

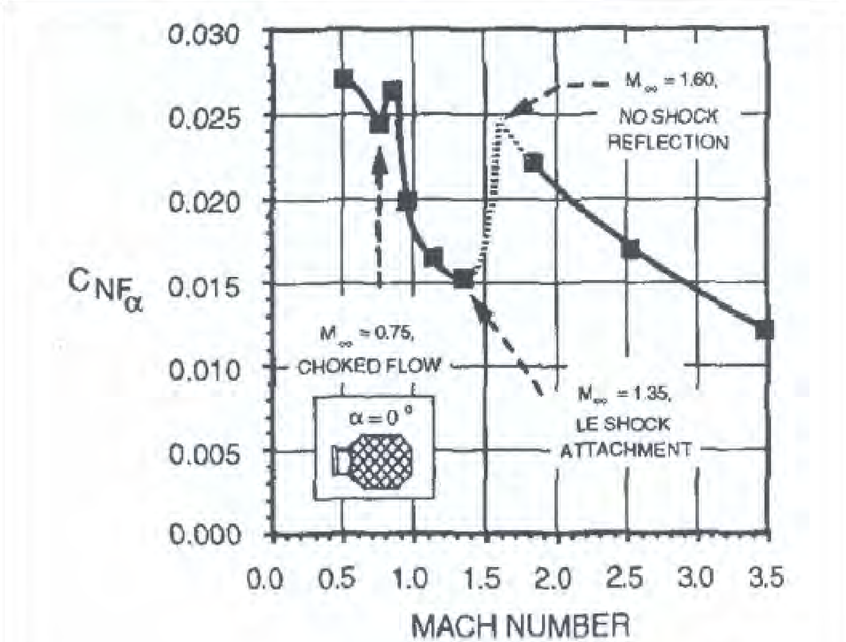

C_{NF_α} Versus Mach Number.

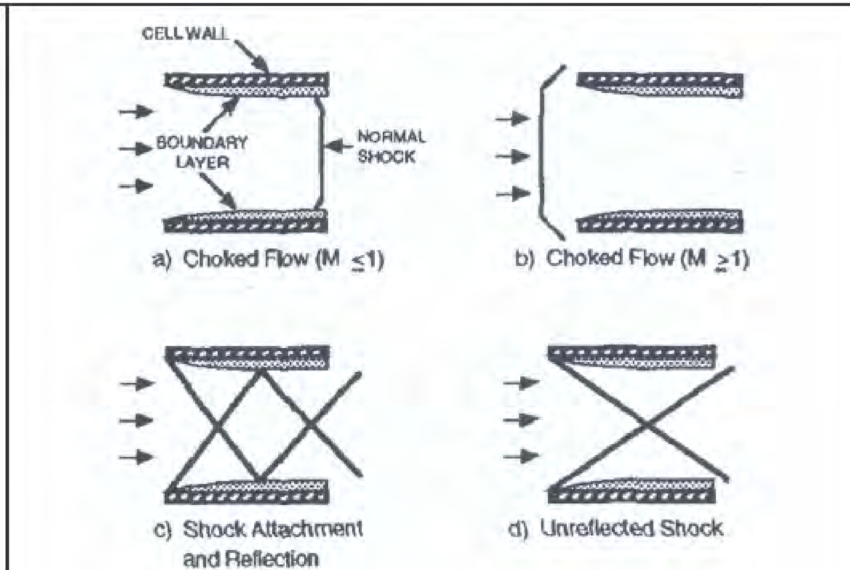

Grid Fin Flow Field.

Ref. Washington et al.

Analysis – Supersonic choking

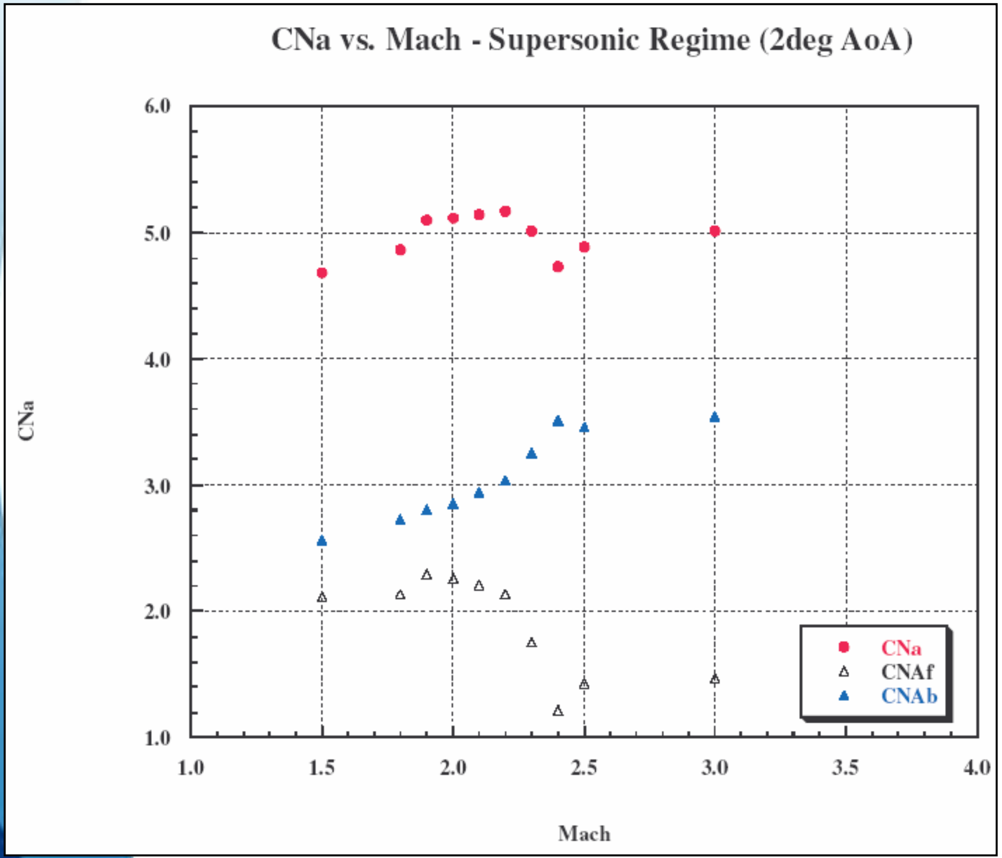

- CNa contribution breakdown : peak effects come from fins.
- Discontinuous behavior between Mach 1.8 and 2.4.
- Change in fin shock-wave configuration explains unusual variation in coefficients.

Analysis – Supersonic choking

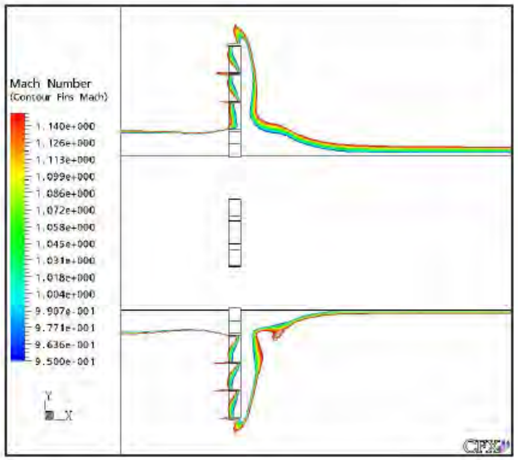

M = 1.50

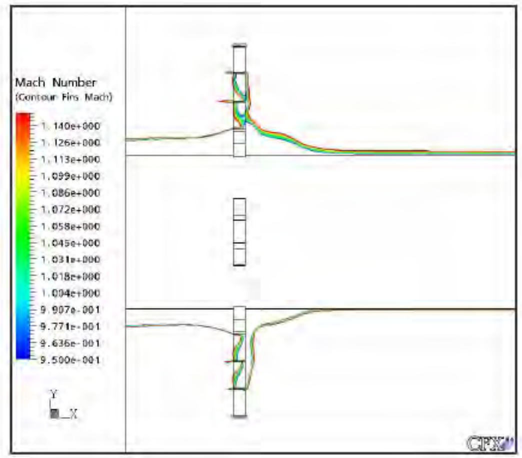

M = 1.80

Contour plots of sonic regions between Mach 0.95 and 1.05

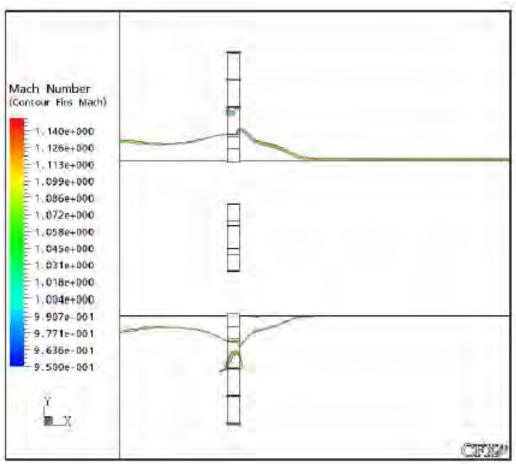

M = 2.30

- Flow completely choked at Mach 1.5, with transition to complete “unreflected” state at Mach 2.3.

- Irregular behavior between Mach 1.8 and 2.40 due to flow topology change from fully choked (shock outside of grid cells) to “non-reflecting” states.

Conclusion

- A detailed CFD analysis of flow inside grid fins gave insight on non-conventional behavior of the main aerodynamic coefficients.
- Flow choking effects successfully predicted in subsonic and supersonic flow regimes.
- Subsonic choking occurred at a specific Mach number. Important offset between wind tunnel and CFD results in subsonic regime.
- Supersonic flow transitions from fully choked to non-reflecting states over a large range of Mach numbers.

Conclusion

- Theoretical flow choking model by Washington (1993) demonstrated by CFD calculations.
- Experimental work Eglin AFB revealed loss of stability at subsonic choking conditions. With the present configuration, effect is opposite : gain in stability.
- CFD proved to be an essential tool in the study of this complex flowfield.

DEFENCE R&D DÉFENSE

Questions ?

References

REFERENCES

(1) Dupuis, A.D., and Berner. C., "Aerodynamic Aspects of a Grid Finned Projectile at Subsonic and Supersonic Velocities", 19th International Symposium on Ballistics Interlaken, Switzerland, May 7-11, 2001.

(2) Dupuis, A.D., and Berner. C., "Aerodynamic Aspects of Fin Geometries on a Lattice Finned Projectile", 20th International Symposium on Ballistics, Orlando, FL, USA, September 23-27, 2002.

(3) Bernier, A., and Dupuis, A.D., "Numerical Computations of Subsonic and Supersonic Flow for a Grid Finned Projectile", 21st International Symposium on Ballistics, Adelaide, Australia, April 19-23, 2004.

(4) Washington, W.D., and Miller, M.S., "Grid Fins – A New Concept for Missile Stability and Control", AIAA Paper 93-0035, 31st Aerospace Sciences Meeting & Exhibit, Reno, NV, January 11-14, 1993.

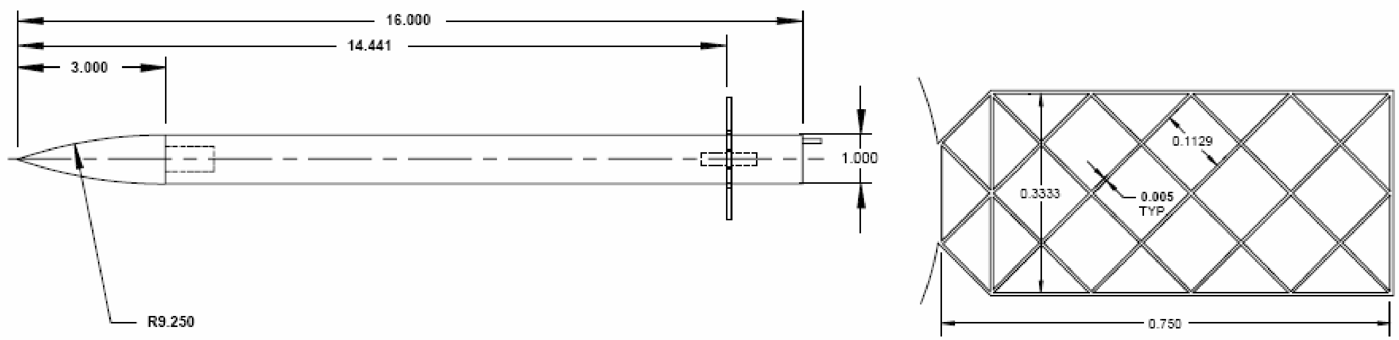

Figure 1 Generic tail control missile (GTCM) with grid fins

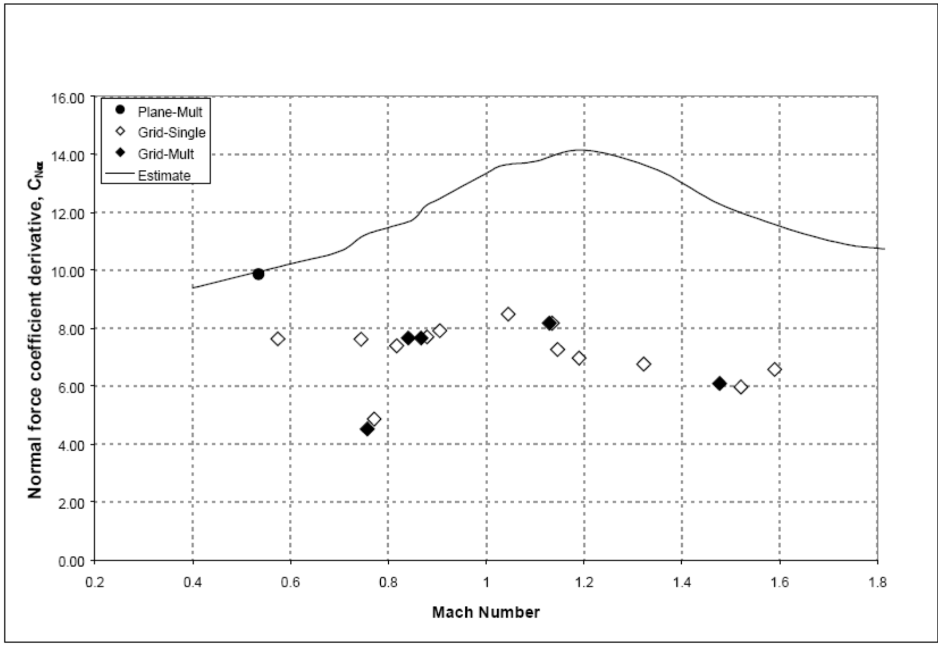

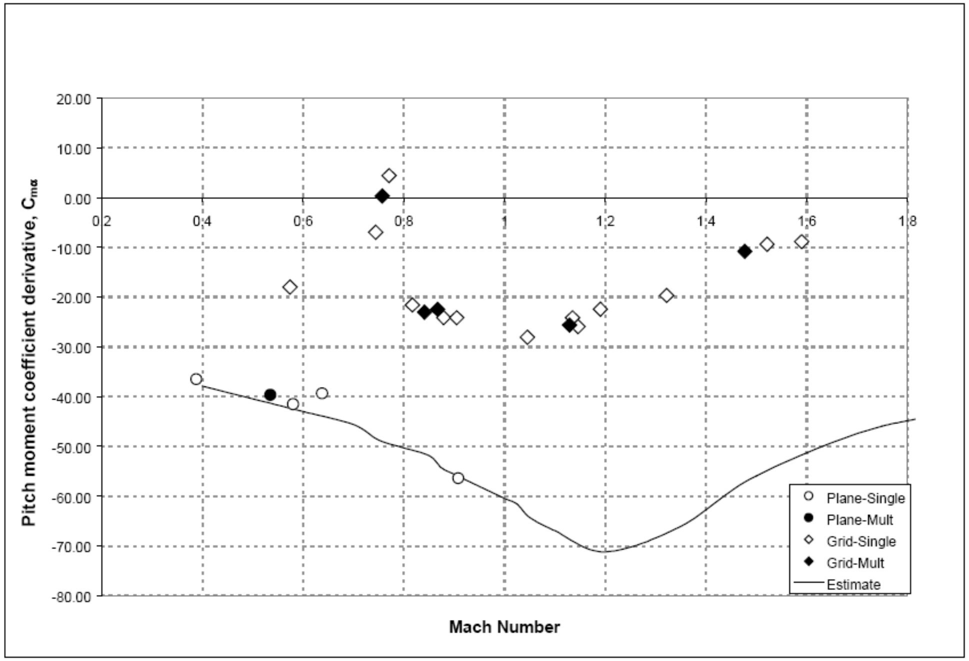

Bullet Impact on Steel and Kevlar®/Steel Armor - Experimental Data and Hydrocode Modeling with Eulerian and Lagrangian Methods

Dale S. Preece
Vanessa S. Berg
Loyd R. Payne

Explosives Applications Department, 5122
Sandia National Laboratories

Outline

- Introduction
- AUTODYN Simulations
  - Lead/Copper Bullet Impact on Mild Steel
  - “ “ “ “ “ Kevlar®/Steel armor
- Ballistics Lab Experiments
  - Lead/Copper Bullet Impact on Mild Steel
  - “ “ “ “ “ Kevlar®/Steel armor
- Comments on Results
- Conclusions

Introduction

- Projectile: Lead/Copper Partitioned (A-Frame) Hunting Bullet
- .338 Winchester Magnum
- Chronographed Muzzle Velocities
  - 842.16 m/s (2763 ft/s) Mild Steel Impacts
  - 854.35 m/s (2803 ft/s) Armor Impacts
  - 16 tests: mean = 847.98 m/s (2782 ft/s)
    std dev = ±7.44 m/s (24.4 ft/s) = ±0.877 %
- Witness Plate: Mild Steel
- Armor: Kevlar® and Kevlar®/Steel

Bullet Penetration of Mild Steel

Geometry and Material Definition

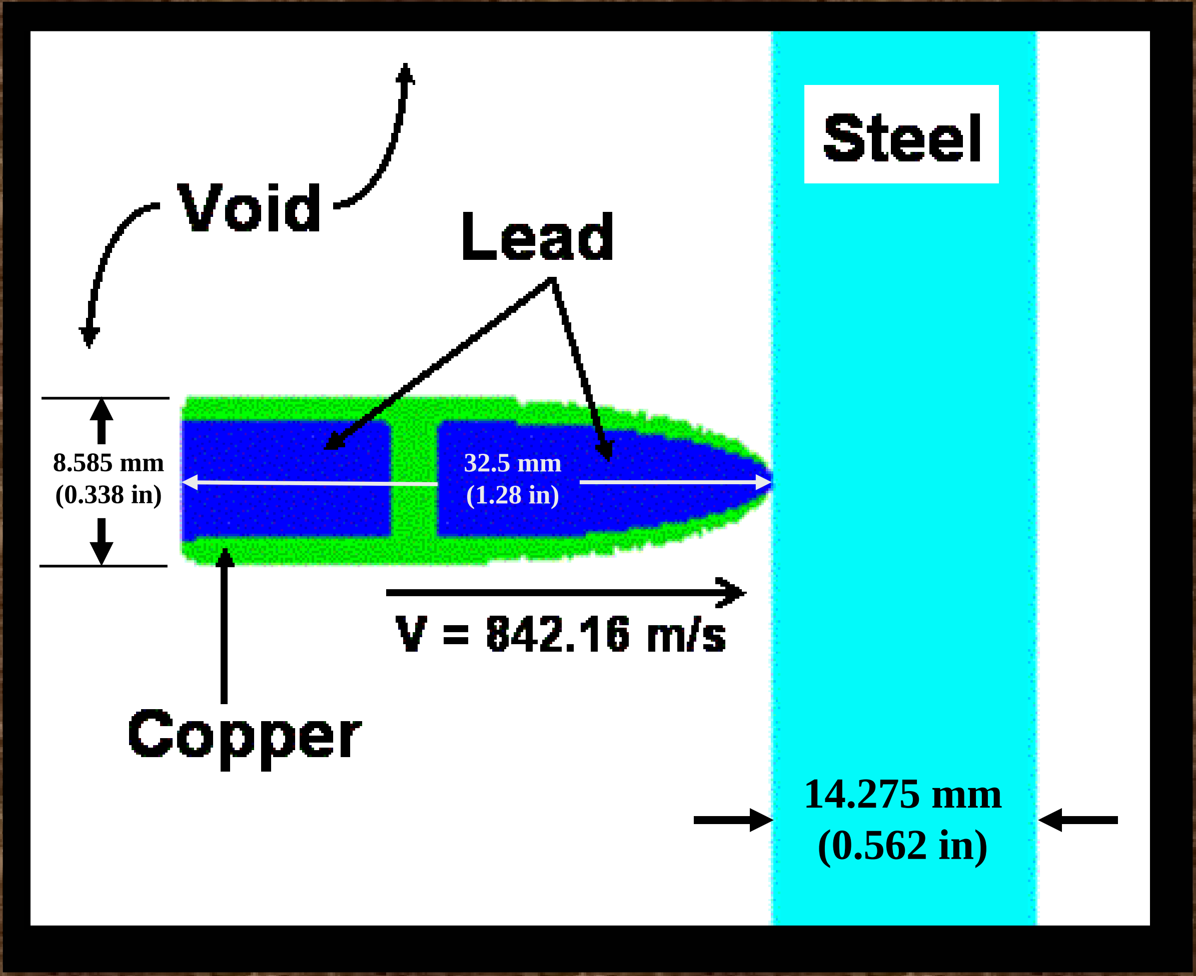

Material Properties for Impact Simulations

Lead

Equation of State	Shock
Reference Density (g/cm^3)	11.35
Gruneisen Coefficient	2.77
Parameter C_1 (m/s)	2.051E03
Parameter S_1	1.46
Strength Model	Von Mises
Shear Modulus (KPa)	5.6E6
Yield Strength (KPa)	5.0E3

Copper

Equation of State	Shock
Reference Density (g/cm^3)	8.93
Gruneisen Coefficient	1.99
Parameter C_1 (m/s)	3.94E03
Parameter S_1	1.489
Strength Model	Von Mises
Shear Modulus (KPa)	4.5E7
Yield Strength (KPa)	7.0E4

Steel

Equation of State	Shock
Strength Model	Johnson-Cook
Reference Density (g/cm^3)	7.896
Gruneisen Coefficient	2.17
Parameter C_1 (m/s)	4.569E03
Parameter S_1	1.49
Reference Temperature (K)	300
Shear Modulus (kPa)	8.18E07
Yield Stress (kPa)	5.17106E05
Hardening Constant (kPa)	2.75E05
Hardening Exponent	0.36
Strain Rate Constant	0.022
Thermal Softening Exponent	1.0
Melting Temperature (K)	1.811E03

Lead/Copper Bullet Penetration of Mild Steel

Color Represents Pressure

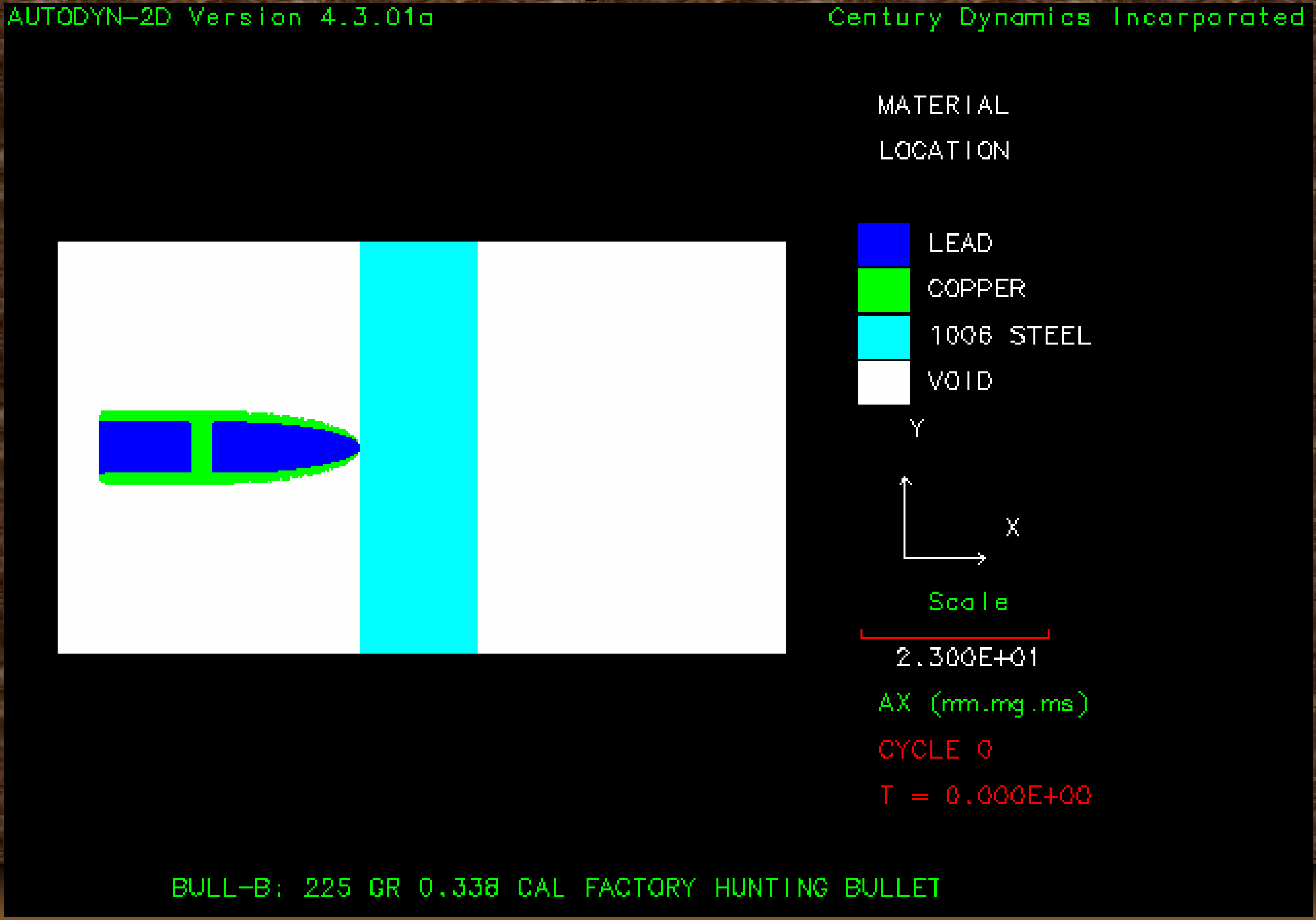

Lead/Copper Bullet Penetration of Mild Steel

Color Represents Absolute Velocity

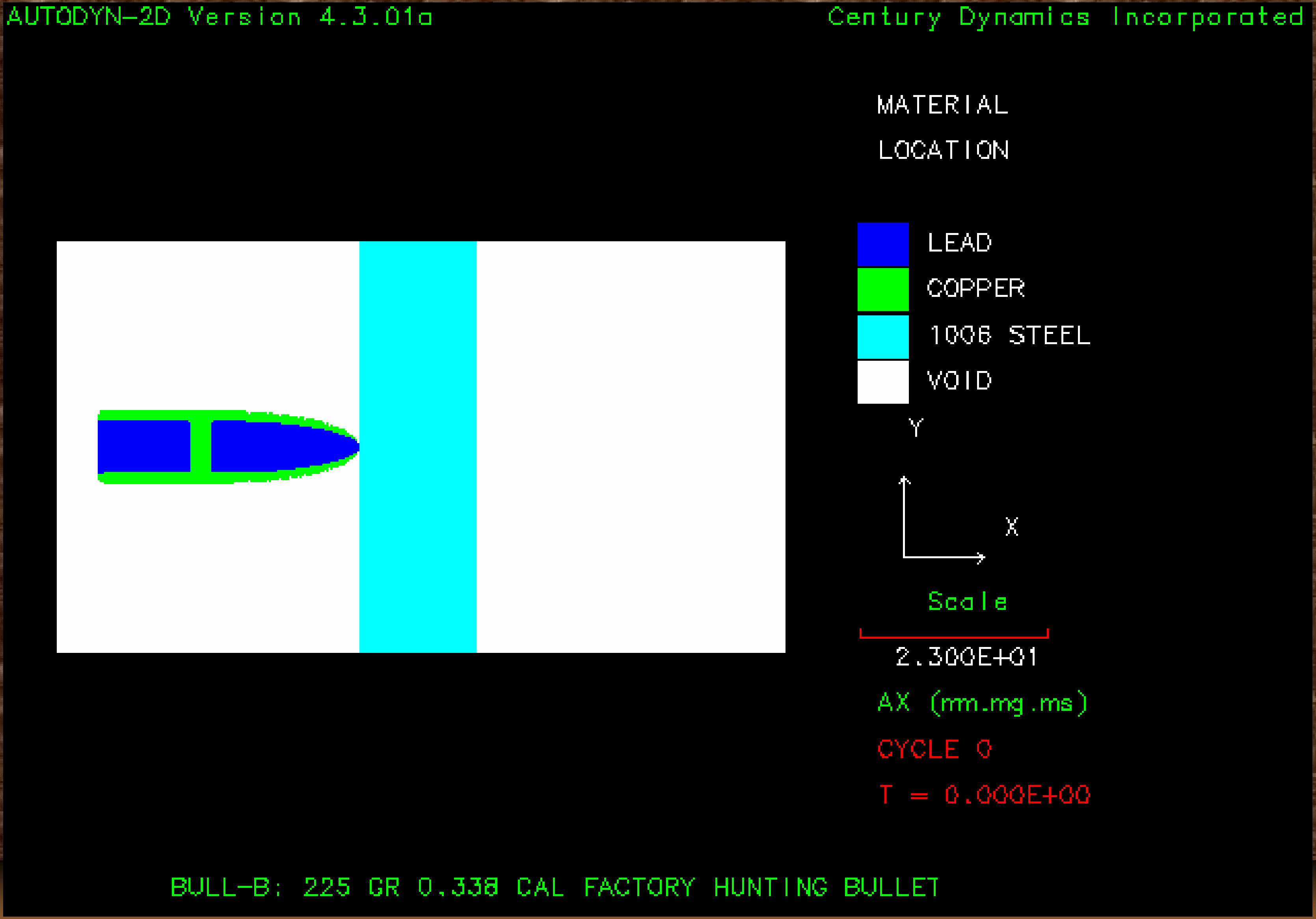

Lead/Copper Bullet Penetration of Mild Steel

Color Represents Absolute Velocity

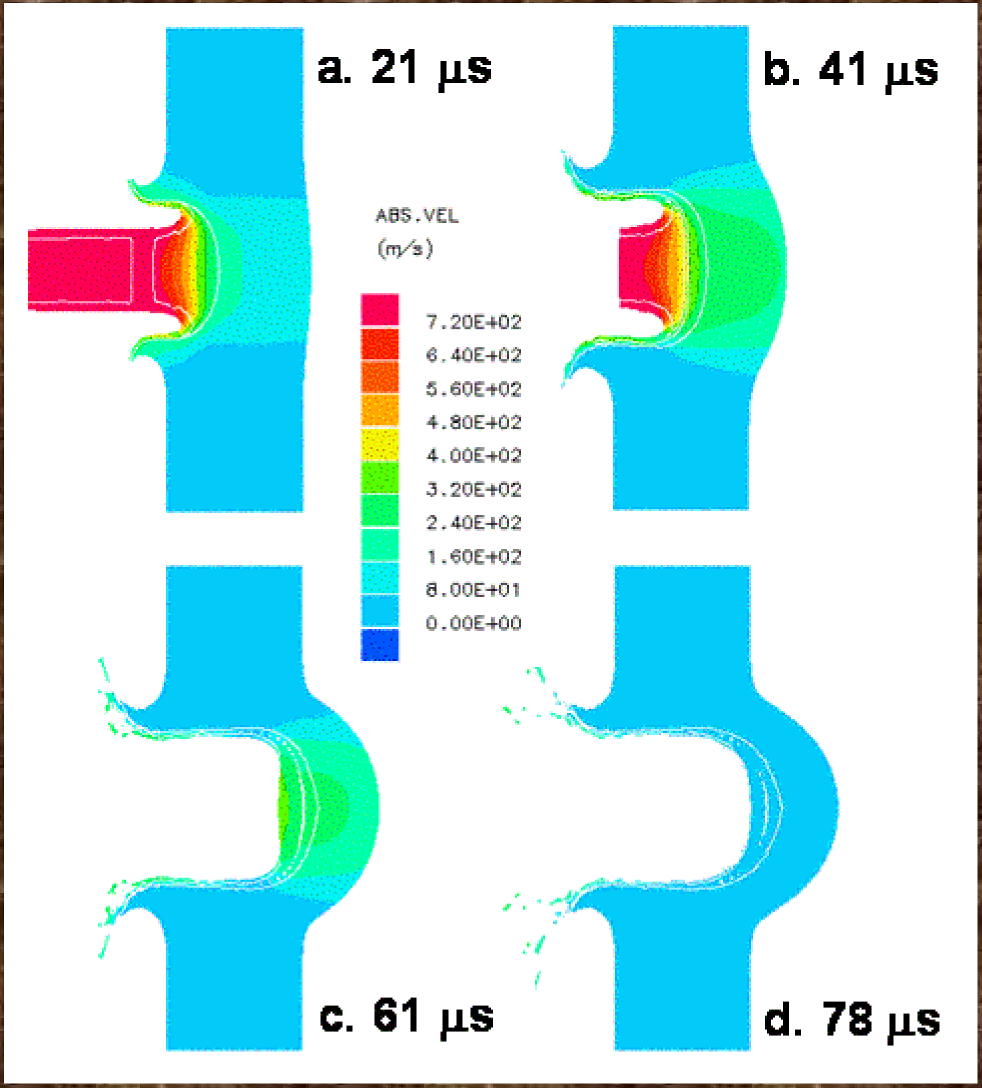

Lambert Equation for Projectile Penetration (Ballistic Limit)

$$V_l = \left(\frac{l}{d}\right)^{0.15}(4000)\sqrt{\left(\frac{d^3}{m}\right)\left(\left(\frac{t}{d}\right)Sec^{0.75}\theta + e^{-\left(\frac{t}{d}Sec^{0.75}\theta\right)} - 1\right)}\left[\frac{m}{s}\right]$$

Where:

l	=	Projectile length	= 3.25 cm
d	=	Projectile diameter	= 0.8585 cm
m	=	Projectile mass	= 14.578(g)
t	=	Target thickness	= 1.427 cm
θ	=	Impact Angle	= 0.0 deg

$$V_l = 939.12\frac{m}{s}$$

Compared to 848 m/s => almost penetrates

Ref: ***Introduction to Terminal Ballistics*** **– Course Notes, Donald R. Carlucci, 2004**

Ballistic Limit

Typical Experimental Results

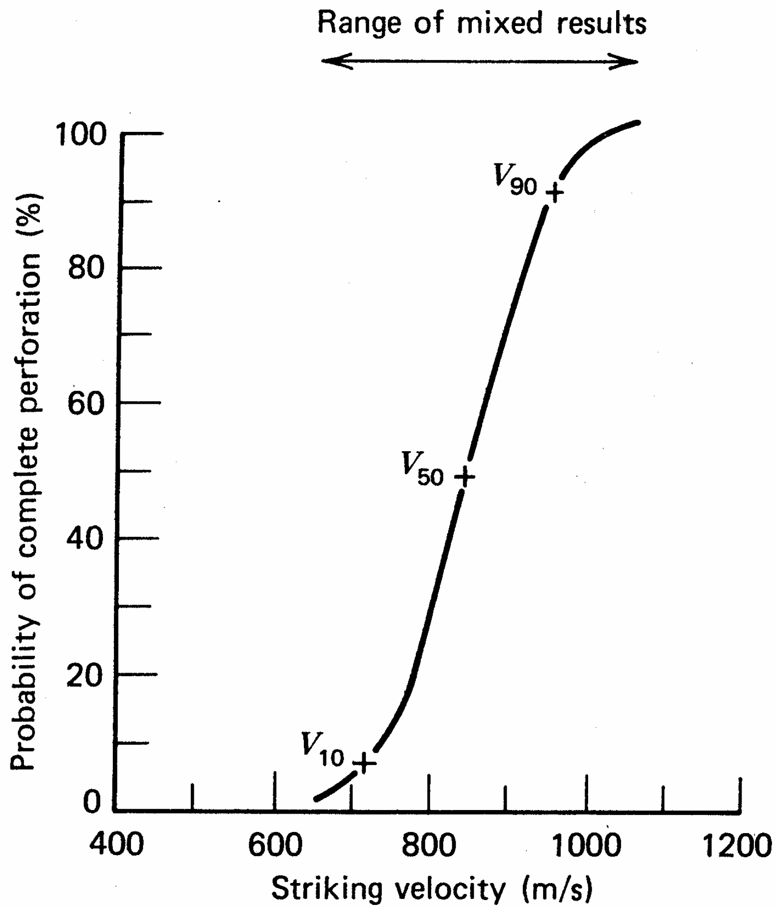

Ref: *Impact Dynamics*, Zukas et al

$$V_l = V_{50}$$

Material Properties for Impact Simulations (Cont)

Kevlar®

Equation of State	Puff
Reference Density (g/cm^3)	1.29
Parameter A_1 (kPa)	8.21E06
Parameter A_2 (kPa)	7.036E07
Parameter A_3 (kPa)	0.0
Gruneisen Coefficient	0.35
Expansion Coefficient	0.25
Sublimation Energy (J/Kg)	8.23E06
Parameter T_1 (kPa)	0.0
Parameter T_2 (kPa)	0.0
Reference Temp (K)	0.0
Specific Heat (C.V.) (J/kgK)	0.0
Strength Model	Von Mises
Shear Modulus	3.0E7
Yield Strength	3.0E5
Tensile Strength	-2.6E5

Lead/Copper Bullet Penetration of Kevlar and Mild Steel

Geometry and Material Definition

Eulerian Simulation

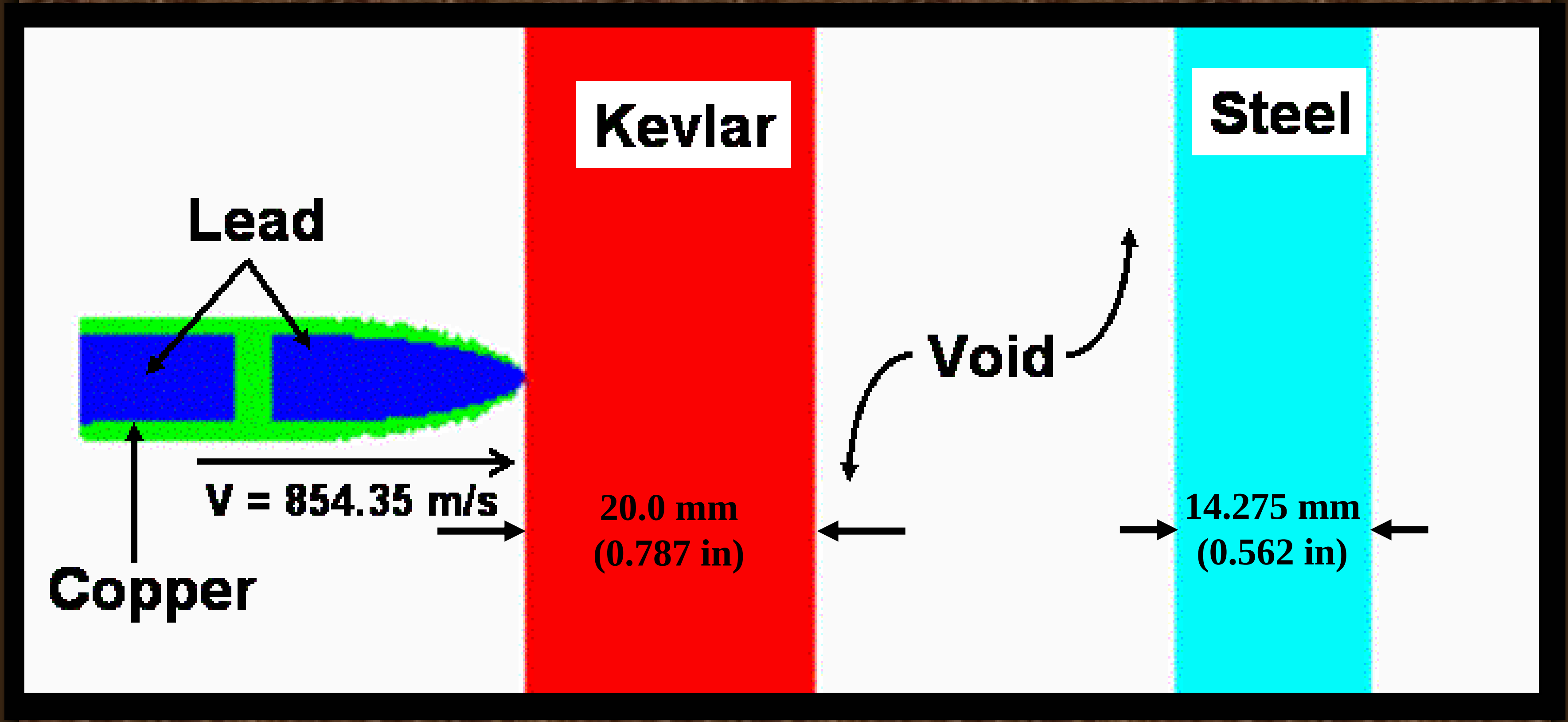

Lead/Copper Bullet Penetration of Kevlar® and Mild Steel

Color Represents Absolute Velocity

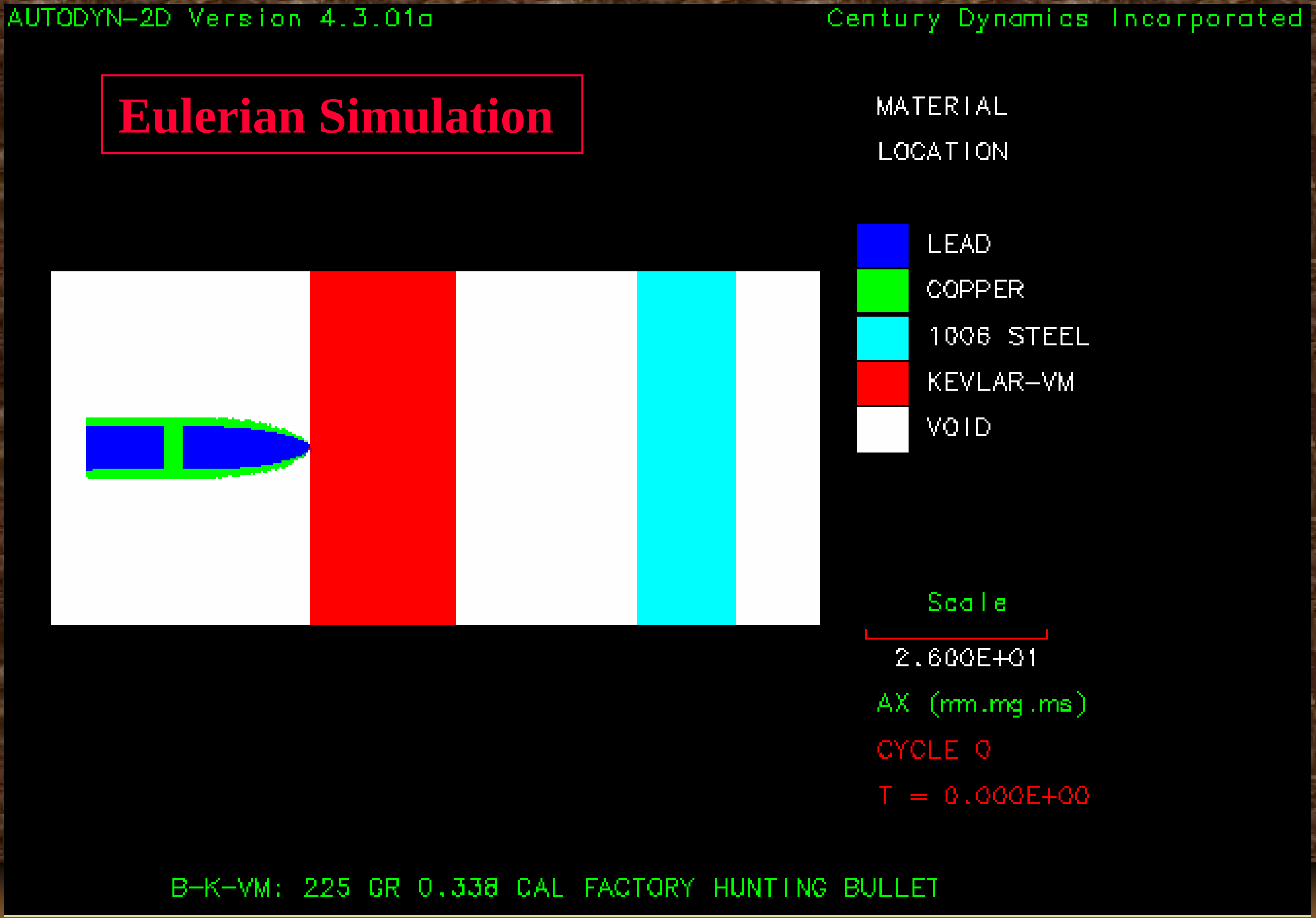

Lead/Copper Bullet Penetration of Kevlar® and Mild Steel

Color Represents Absolute Velocity

Eulerian Simulation

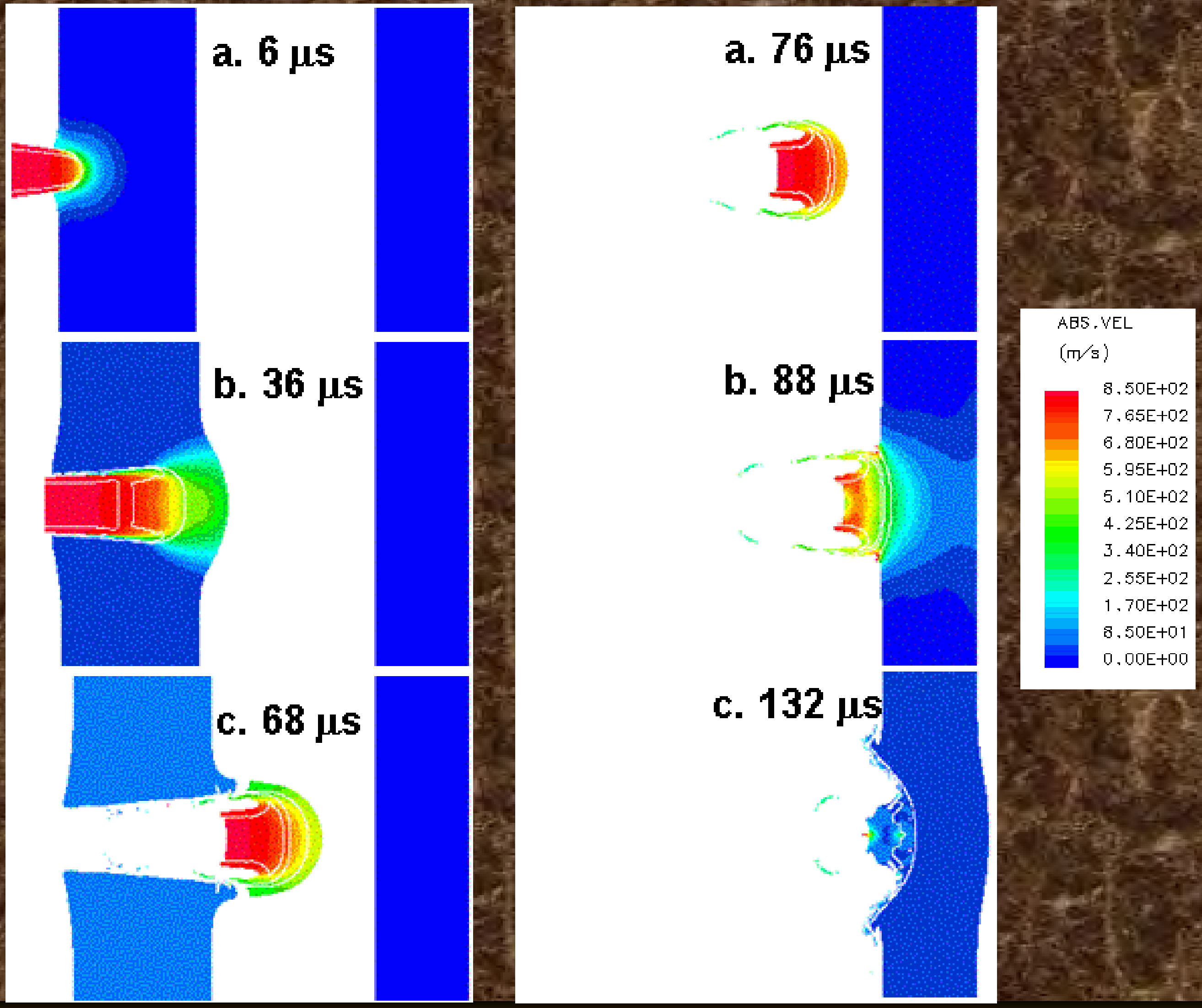

Lead/Copper Bullet Penetration of Kevlar® and Mild Steel

Color Represents Failure Mode

Lagrangian Bullet Transversely Isotropic Model

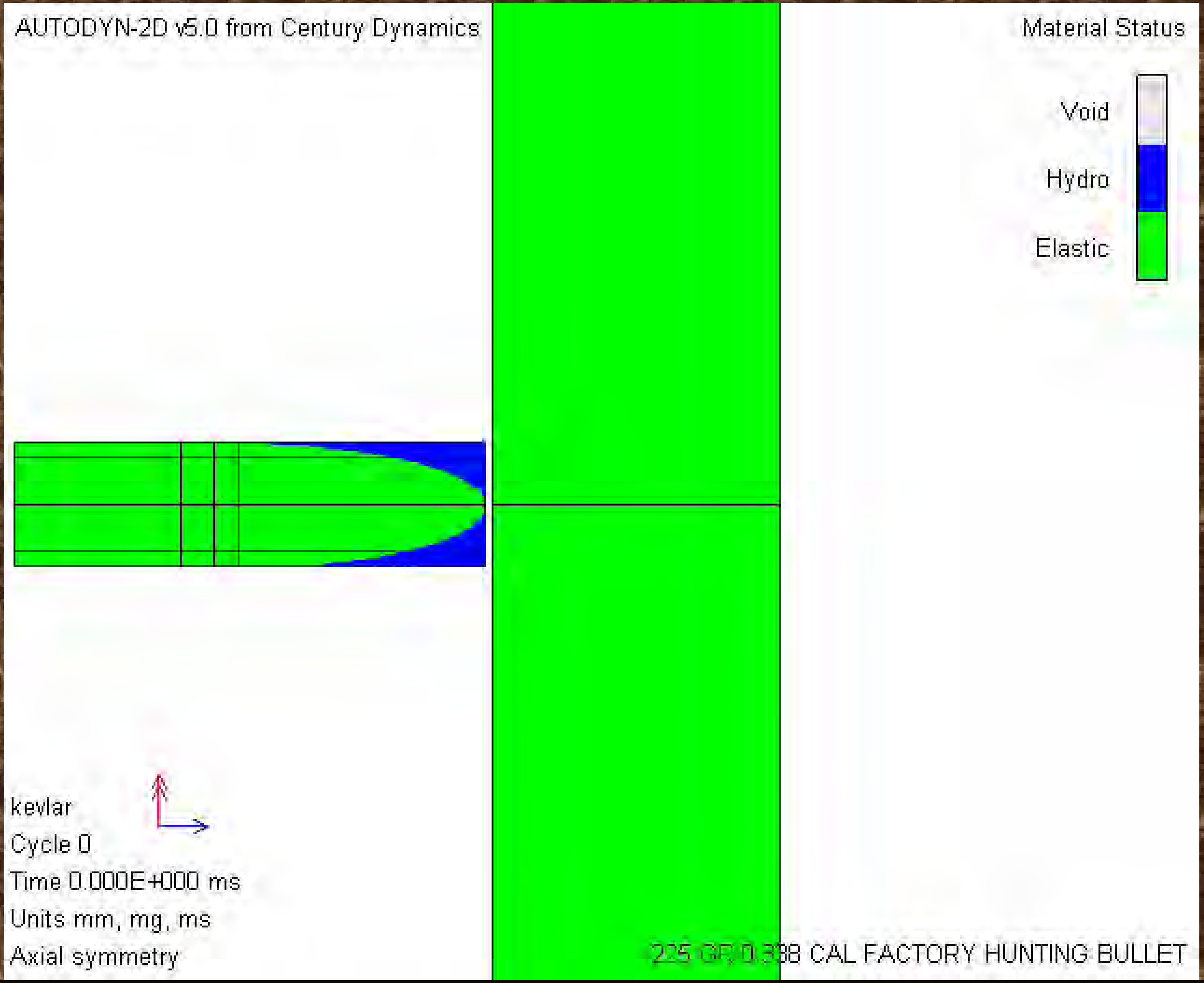

Lead/Copper Bullet Penetration of Kevlar® and Mild Steel

Color Represents Absolute Velocity

Lagrangian Bullet Transversely Isotropic Model

AUTODYN-2D v5.0 from Century Dynamics

Kevlar Model

225 Grain 0.338 Cal Hunting Bullet
Kevlar Board

Sandia National Laboratories
Explosives Applications Department, Org 15322

Reasonable Bullet Erosion

Lead/Copper Bullet Penetration of Kevlar® and Mild Steel

Color Represents Absolute Velocity

Lagrangian Bullet and Transversely Isotropic Kevlar Model

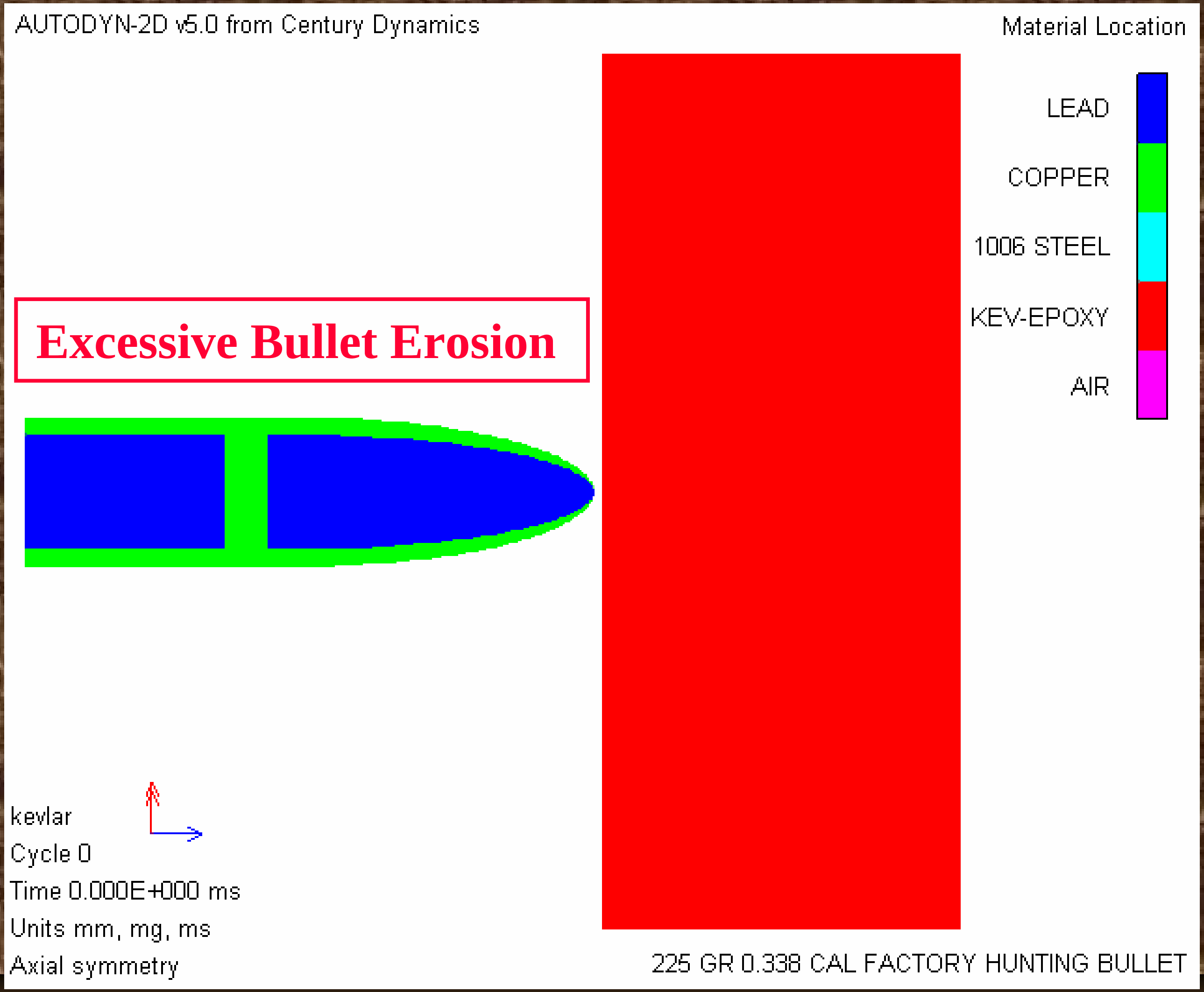

Ballistics Lab Results

Lead/Copper Bullet Impact on Steel

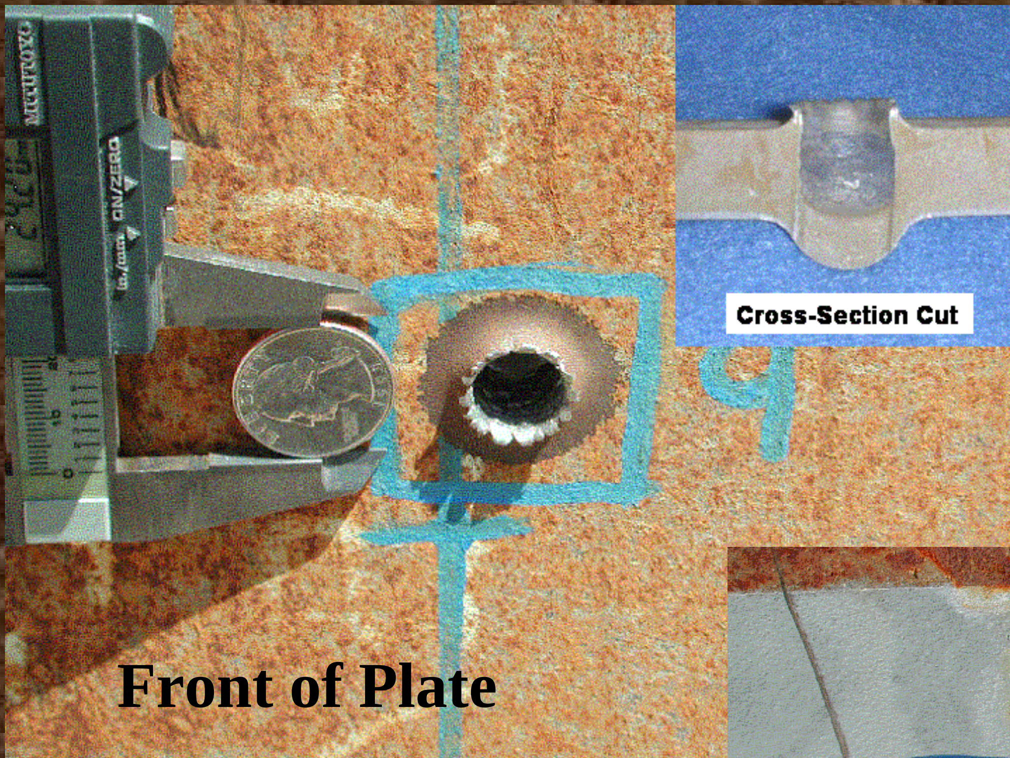

Comparison of Computer Predicted and Experimental Impact Crater – Steel Only

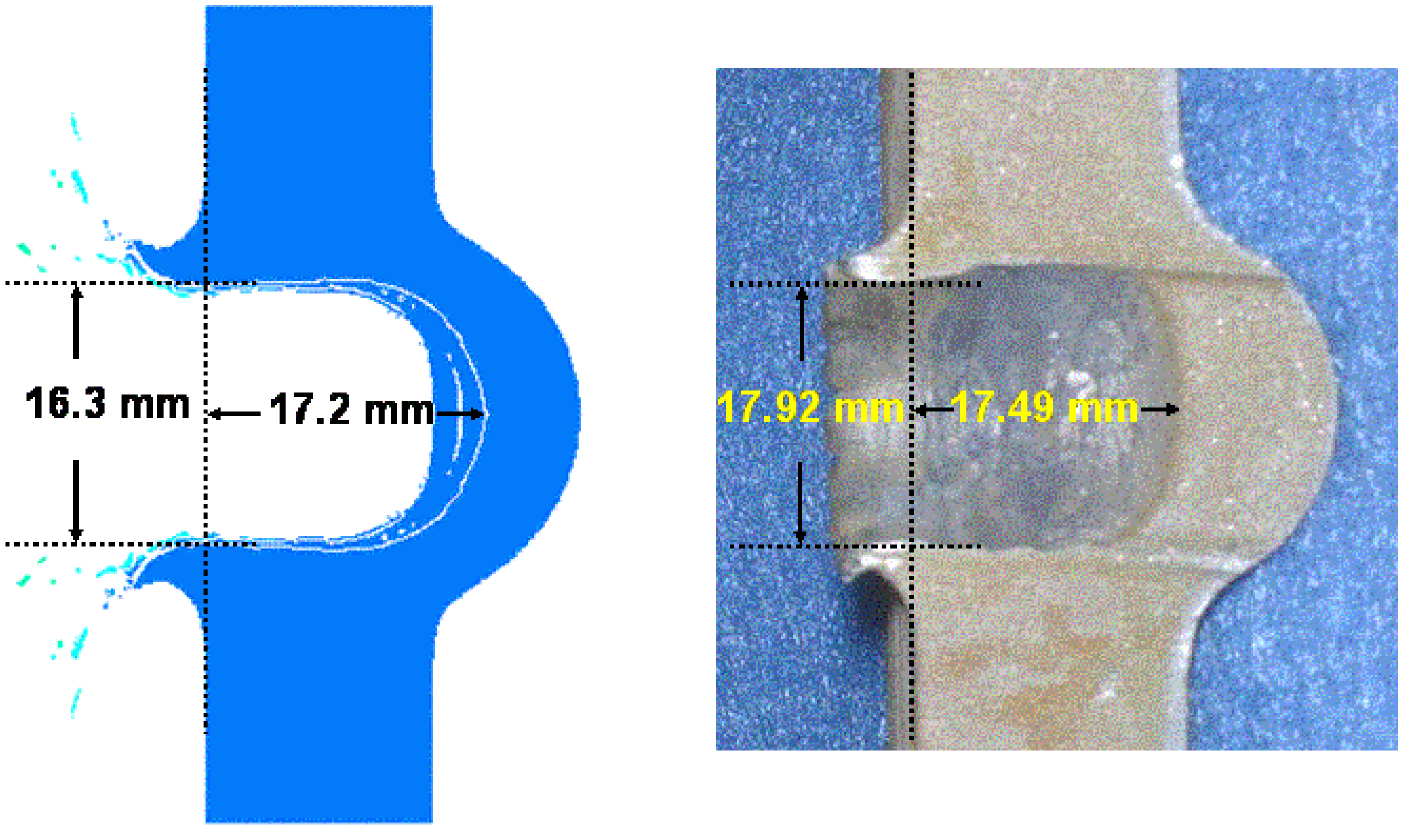

a. AUTODYN Simulation

b. Shot 9 Cross-Section

Lead/Copper Bullet Impact on Kevlar® and Steel

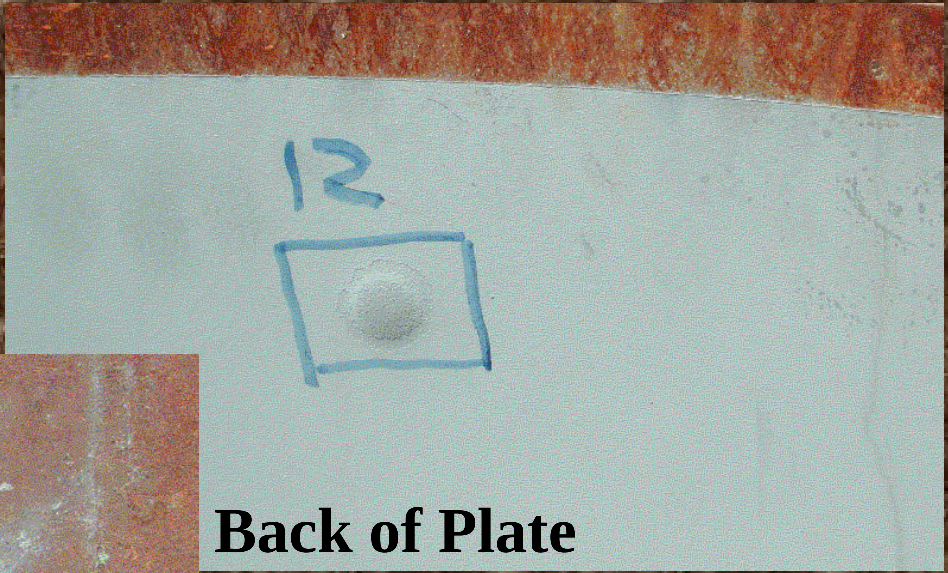

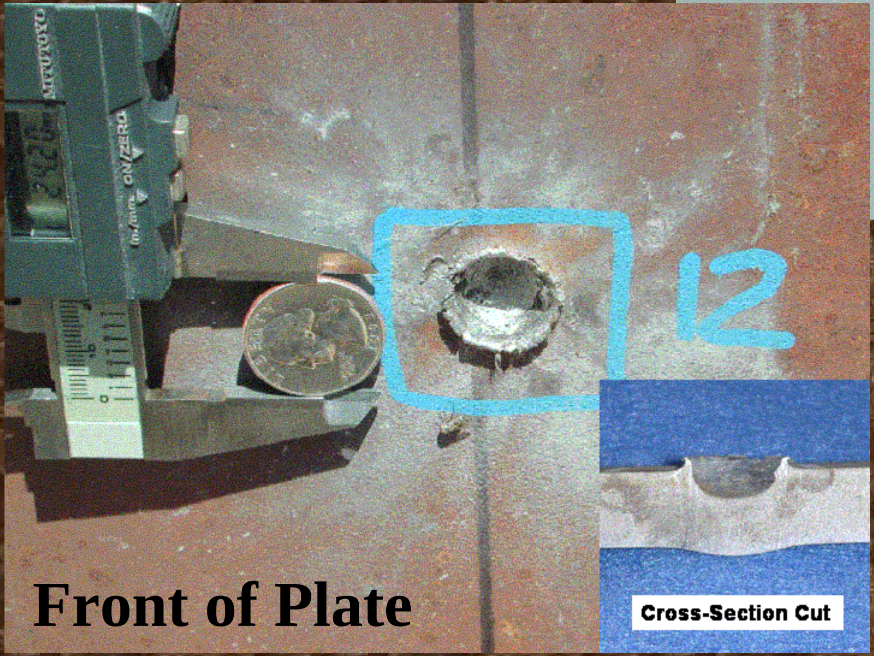

Comparison of Computer Predicted and Experimental Impact Crater – Kevlar® /Steel

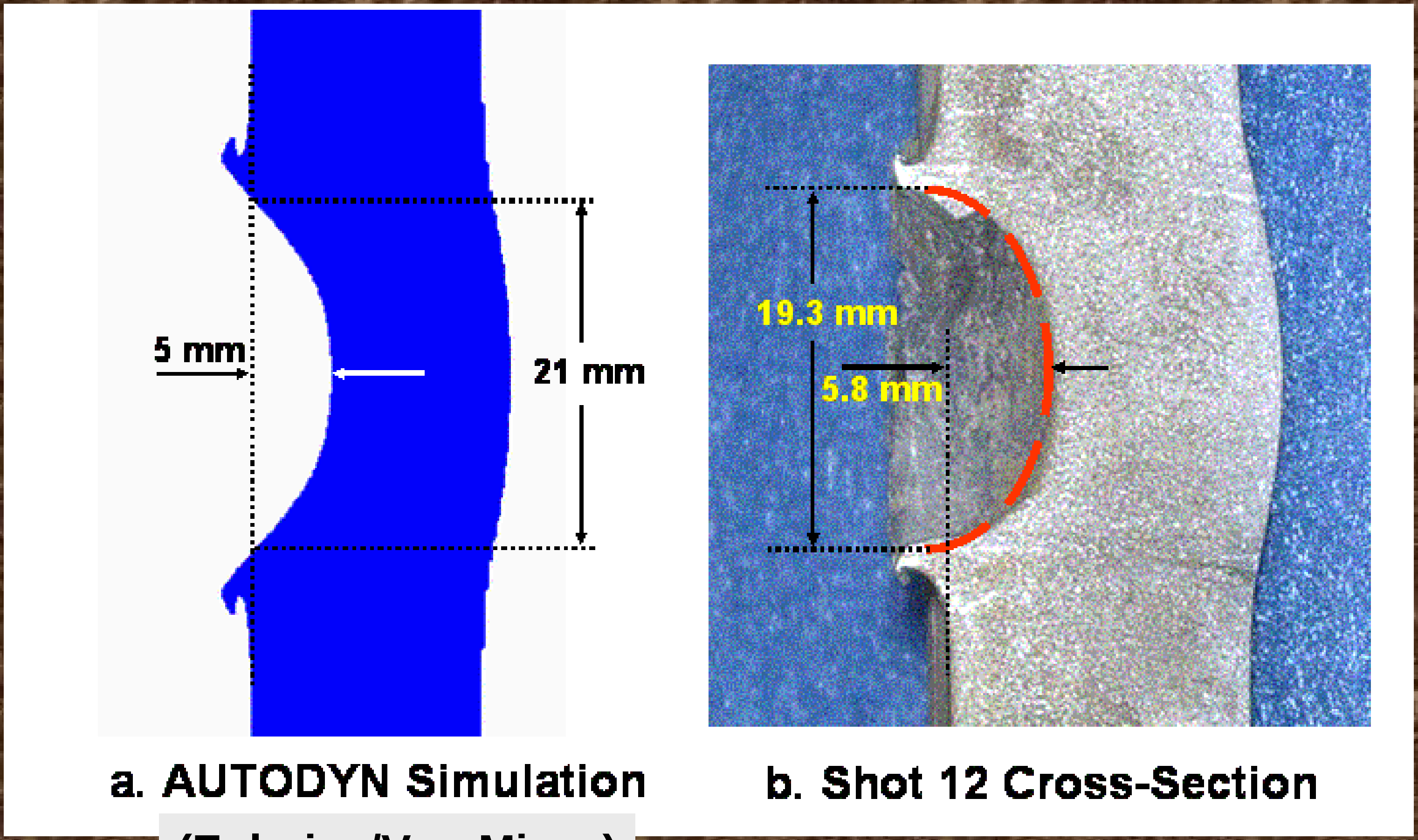

(Eulerian/Von Mises)

Impact on Kevlar® Panel

Fragment Splatter
– Ricochet Back From Steel

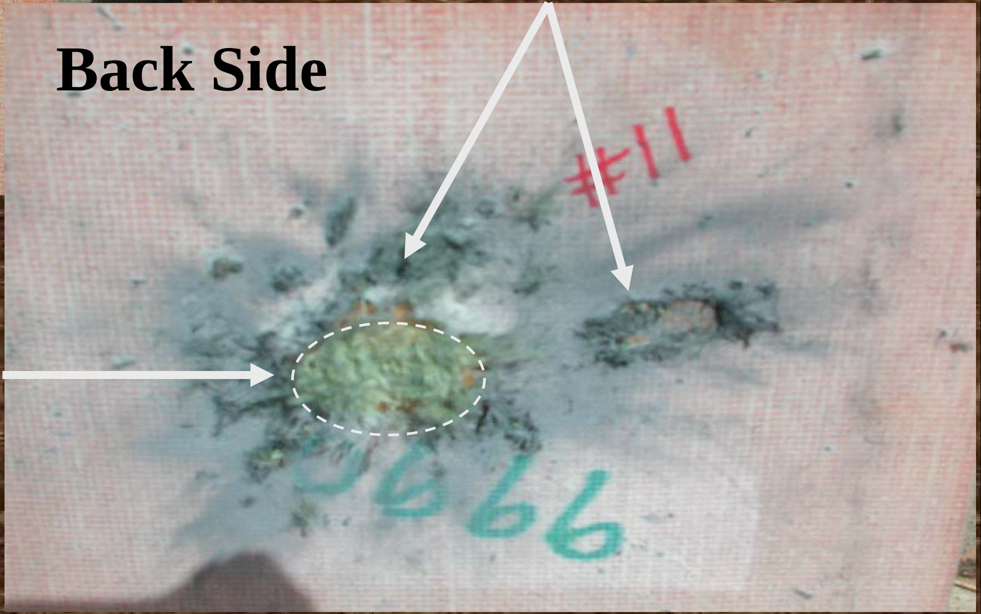

Process Zone – Substantial Size

Lead/Copper Bullet Penetration of Kevlar® and Mild Steel

Eulerian Bullet - Lagrangian Transversely Isotropic Kevlar

Increased Kevlar Erosion – Leaves Too Much Bullet

Lead/Copper Bullet Penetration of Kevlar® and Mild Steel

Eulerian Bullet - Lagrangian Transversely Isotropic Kevlar

Reasonable Kevlar Erosion – Exiting Bullet About Right

Lead/Copper Bullet Penetration of Kevlar® and Mild Steel

Eulerian Bullet - Lagrangian Transversely Isotropic Kevlar

Course Mesh, High Kevlar Erosion – Exiting Bullet About Right

Conclusions

- Hydrocode and ballistics lab results match well for lead/copper A-Frame bullets impacting on mild steel.
- A reasonable match between hydrocode predictions and ballistics lab results is obtained for Kevlar® armor using a Von Mises strength model. This "engineering" model was used to complete the armor design.
- A Von Mises strength model misses some of the essential physics of bullet penetration into a transversely isotropic material like Kevlar®.
- Use of a Lagrangian transversely isotropic material model yields more consistent results for the Kevlar. However, modeling the lead/copper bullet is more appropriate in the Eulerian Frame of Reference.
- Simulations using an Eulerian Bullet and Lagrangian Kevlar have been attempted with reasonable success.
  - The results are dependent on the Kevlar erosion rate selected

$$\text{Fun} = \frac{\text{Novelty}}{\text{Work}}$$

Acknowledgments

- Dave Paul - Ballistics experiments at the 6750 gun site.
- Leslie Kramer - Experimental digital Photograph acquisition & processing.
- Russ Payne - Experimental data compilation and reduction. Euler/Lagrange
- Erin Shrouf - Data recording.

Aerodynamics Branch

MICRO-ADAPTIVE FLOW CONTROL APPLIED TO A SPINNING PROJECTILE

Dr. Jubaraj Sahu

U.S. Army Research Laboratory

ATK Briefing

APG, MD, 6 October 2005

SCORPION

Self-CORrecting Projectile for Infantry OperatioN

GOAL: Demonstrate a Guided Spinning Projectile Using MAFC Technology

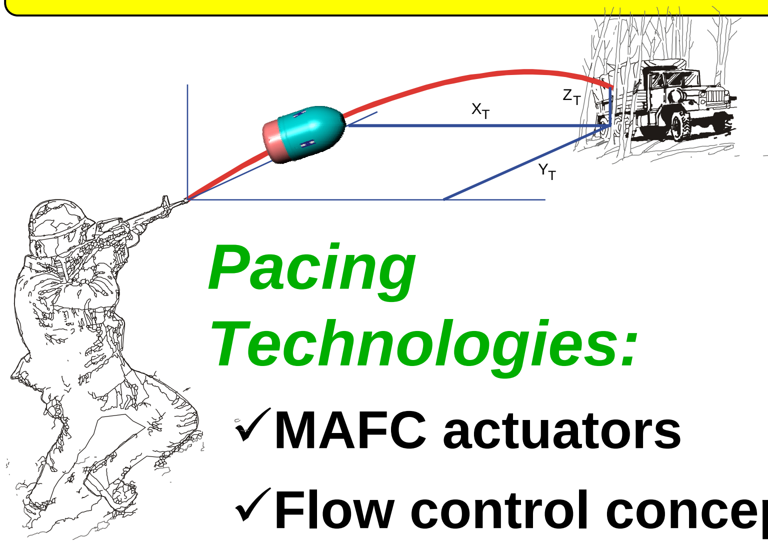

Pacing Technologies:

- ✓**MAFC actuators**
- ✓**Flow control concept for spinning projectiles**
- ✓**Flight control algorithm**
- ✓**Initialization and INS for spinning projectile**
- ✓**Compact, g-hardened electronics and packaging**
- ✓**Design tools: integrated computational fluid dynamics (CFD) and flight dynamics**

Objectives:

1. **Demonstrate microadaptive flow control (MAFC) authority and guidance algorithm for a medium-caliber munition at subsonic speeds.**
2. **Provide a suite of validated advanced design tools.**
3. **Establish technology transitioning pathways for tactical systems.**

Micro-jet CFD Flow Visualization

U_∞ = 37 m/s, α = 0°, Ujet = 31 m/s, f= 1000 Hz, no spin

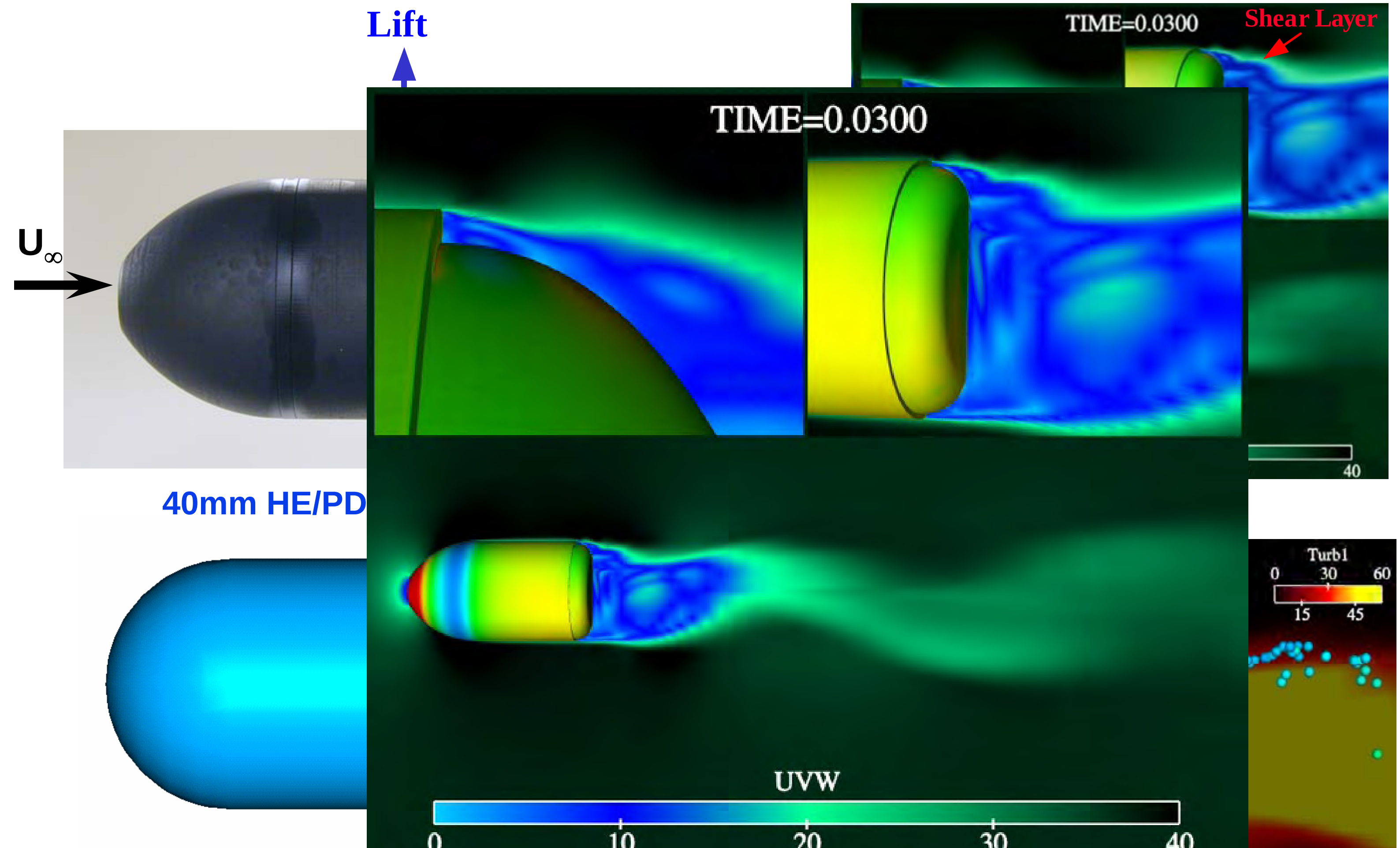

Asymmetric Flow Separation

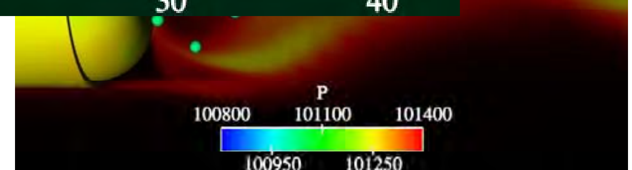

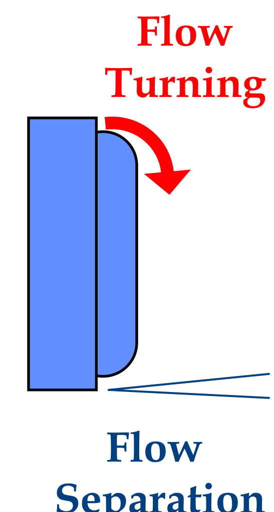

- Investigate “placement”of jets for
  - lift control to improve accuracy
  - side force for divert authority

Particle Traces Visualization

U = 82 m/s, α = 0°, Ujet = 31 m/s, f = 1000 Hz, Spin = 67 Hz

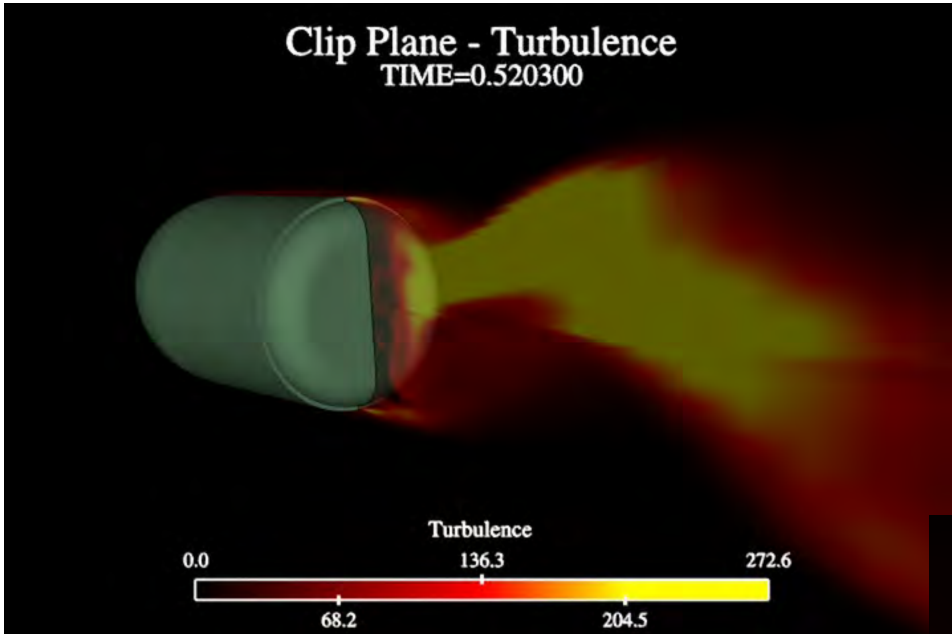

For Two Spin Cycles

1st cycle: Red

2nd cycle: Blue

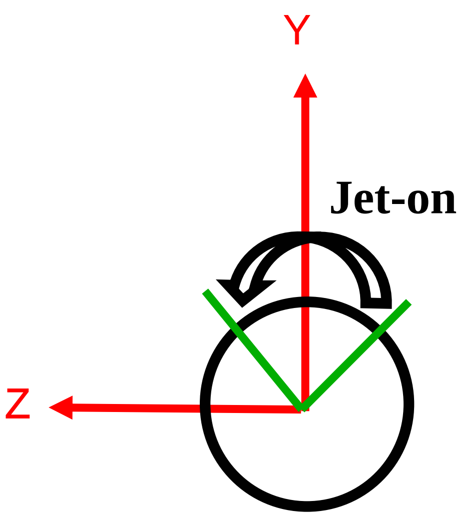

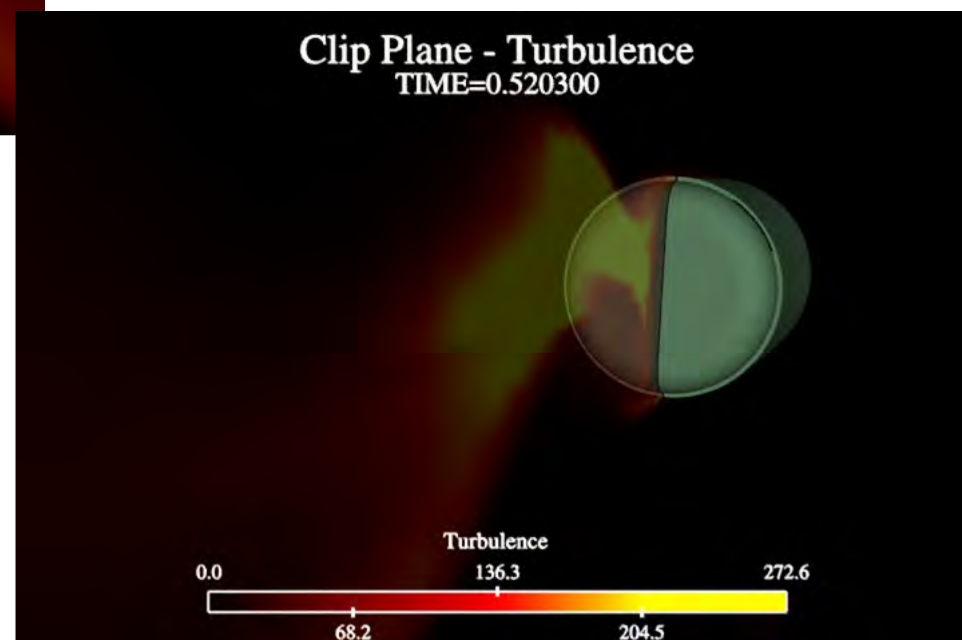

SCORPION Open-Loop Test
Flight Test Results Compared With Simulated Impacts

Experimental Muzzle Velocity Distribution Used for Simulation

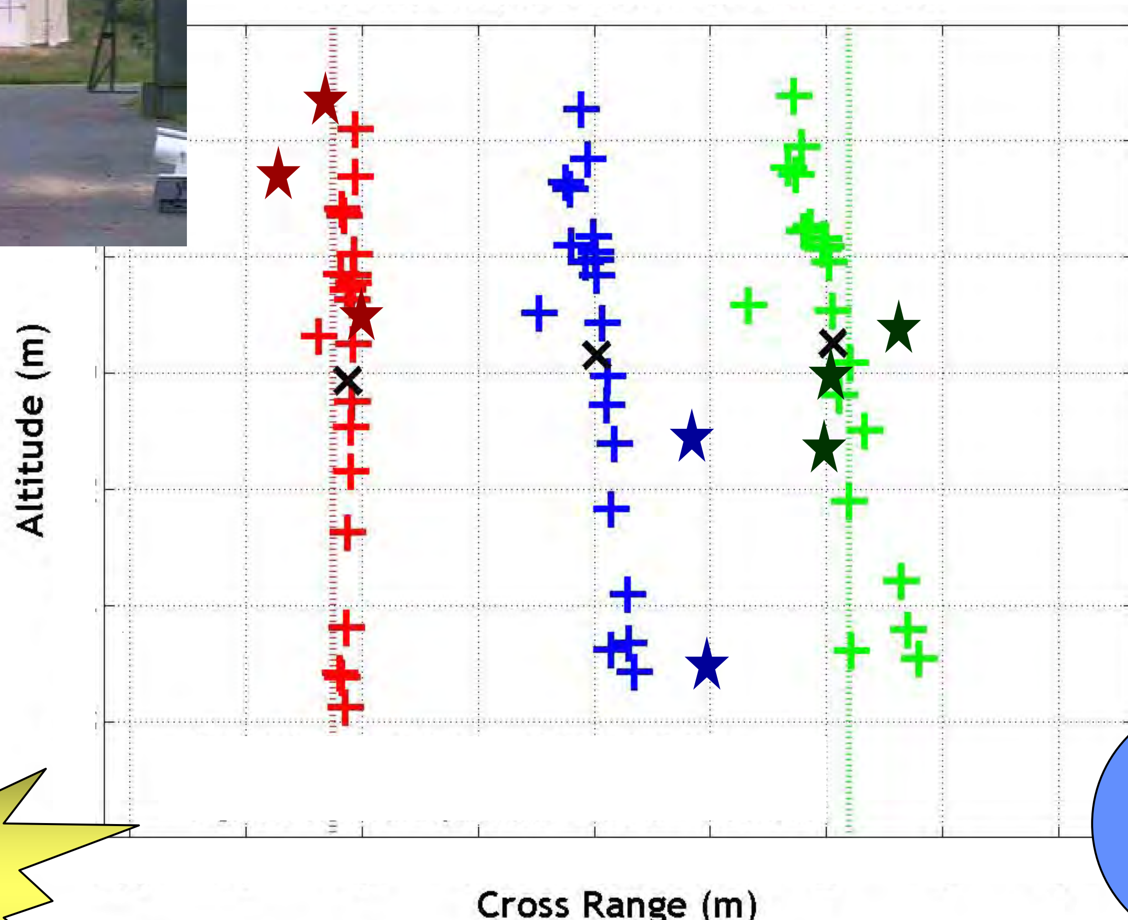

ONLY a few jet cycles are available

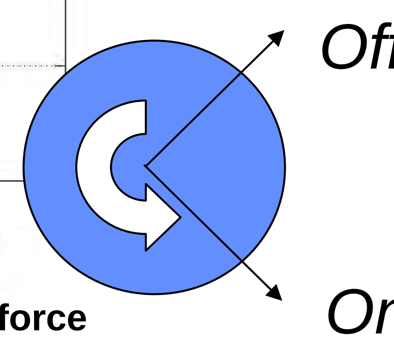

Activate for 1/4 revolution (about 4 jet cycles) such that force generated will be horizontal (left or right, as selected).

Flight Data Confirms Control Force

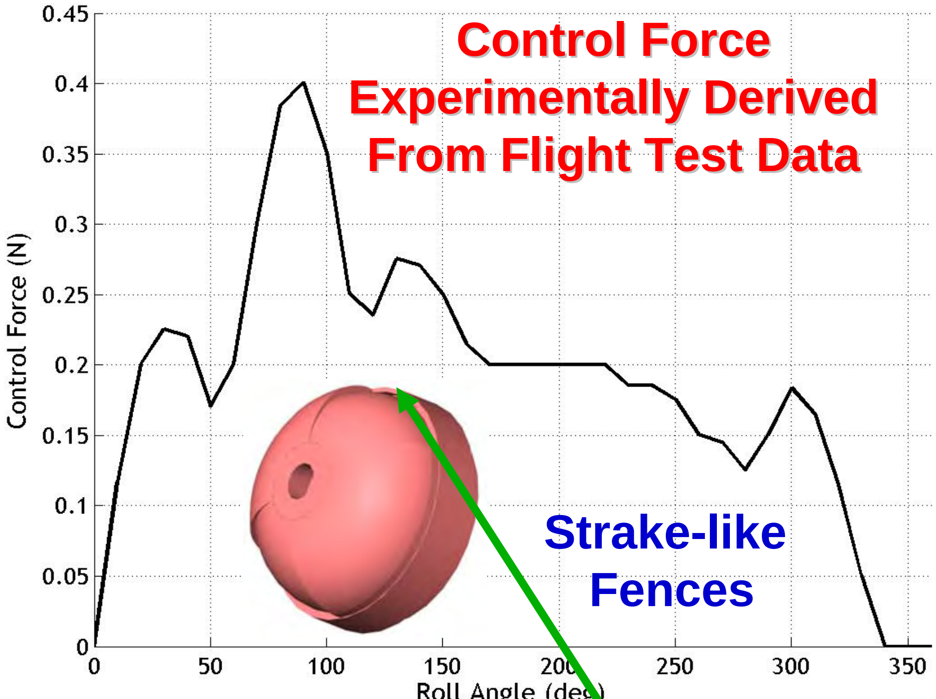

ARL Unsteady CFD
(Spinning)

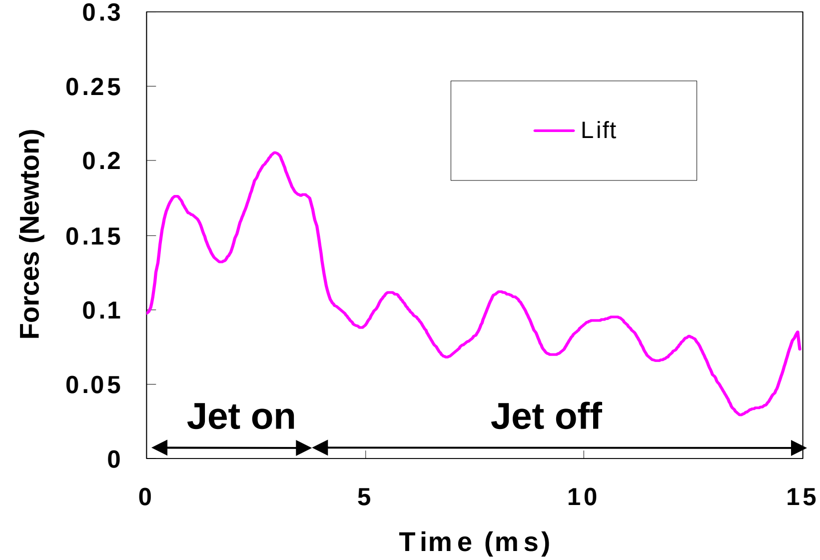

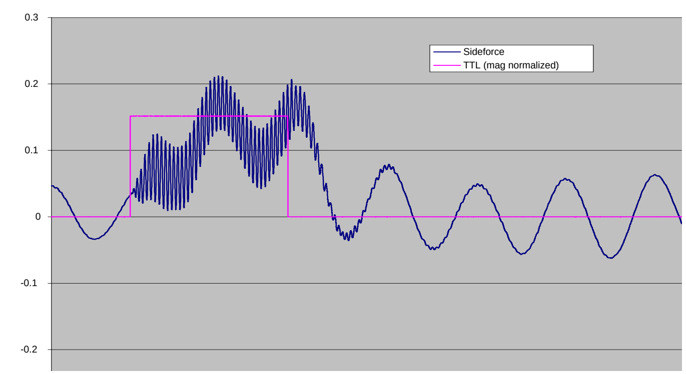

GTRI Wind Tunnel Experiments
(Non-spinning)

UNSTEADY AERODYNAMICS/FLIGHT DYNAMICS

DOD HPCMP Grand Challenge Project

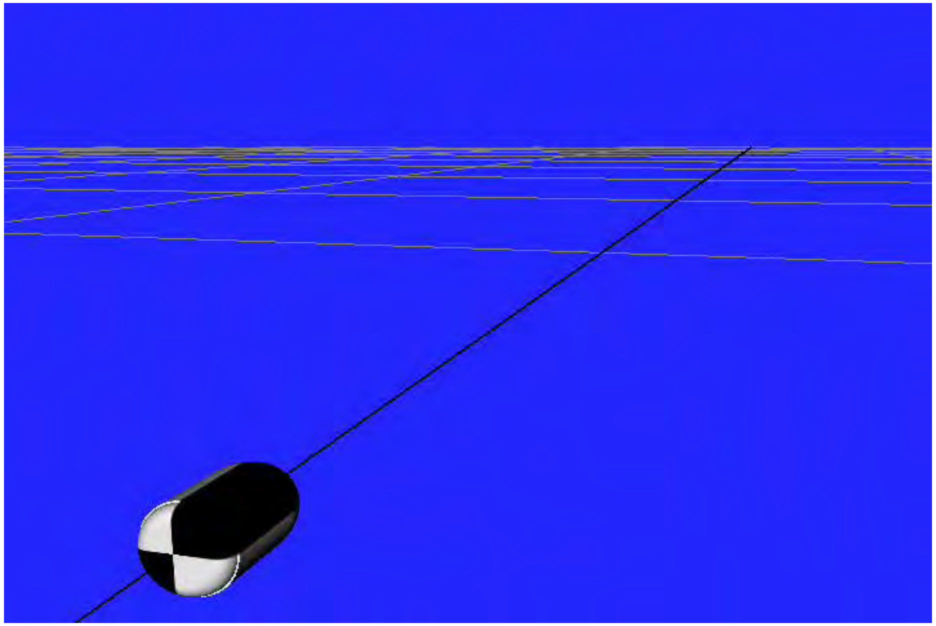

GOAL: Virtual Fly-Out of Projectiles

Coupled CFD/Rigid Body Dynamics (RBD) Simulations of in-flight spinning and finned projectiles

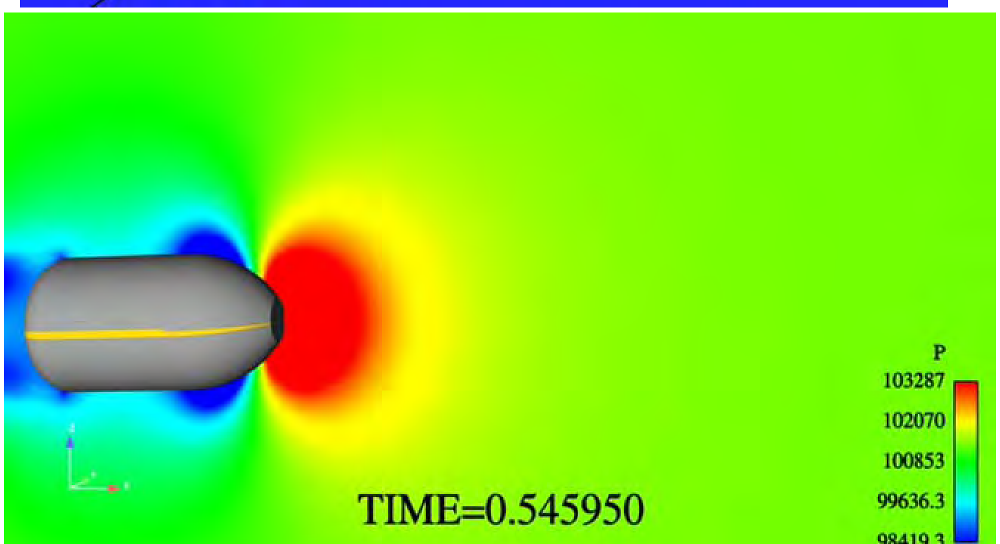

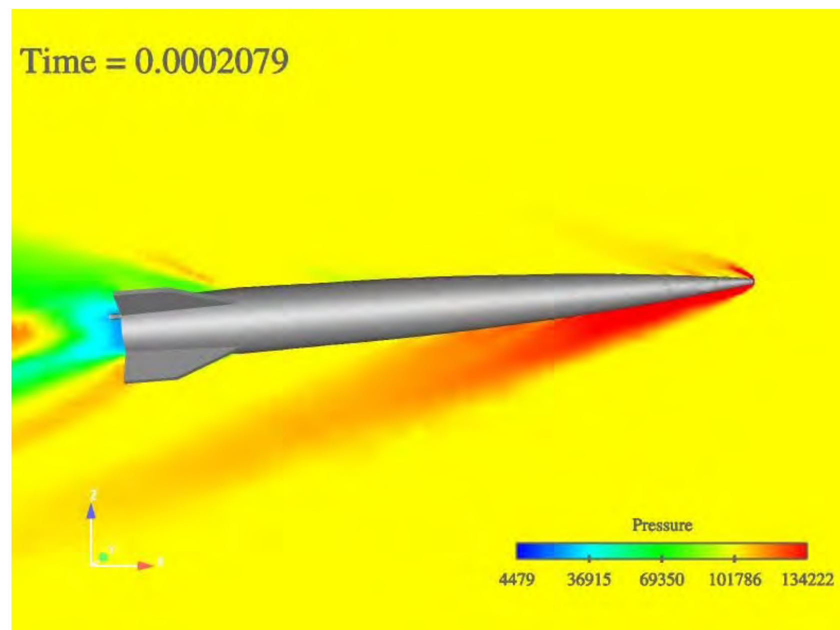

Guided Medium Caliber Munitions

- Demonstrated Micro-Adaptive Flow Control for divert of subsonic guided 40 mm grenade
- Demonstrated Multi-disciplinary physics modeling – flew munition through the computer using High Performance Computing
- First divert ever of a spin stabilized munition system at 60 hertz spin rate
- Developed a miniature, G hard, on board flight control system
- Demonstrated initialization at muzzle exit – Velocity - Orientation
- Demonstrated open loop divert
- Demonstrated closed loop guidance to the target on major error source - Velocity
- Cut on target dispersion due to muzzle velocity variation to one third of the system value

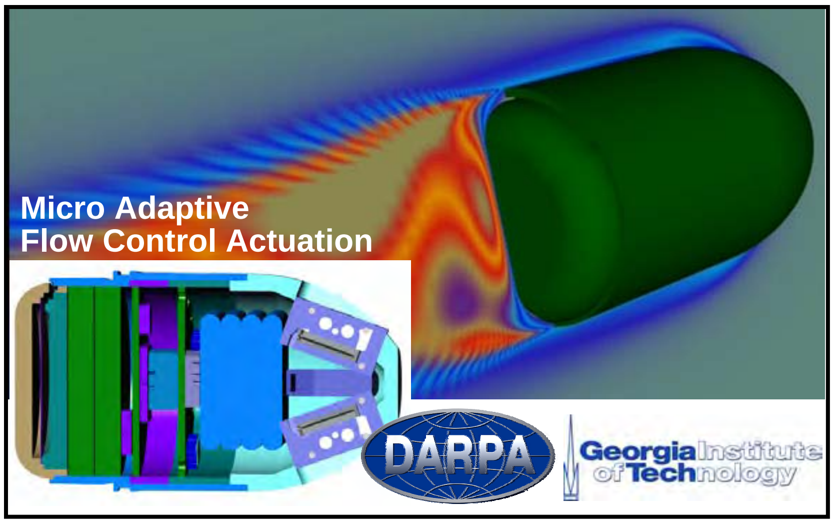

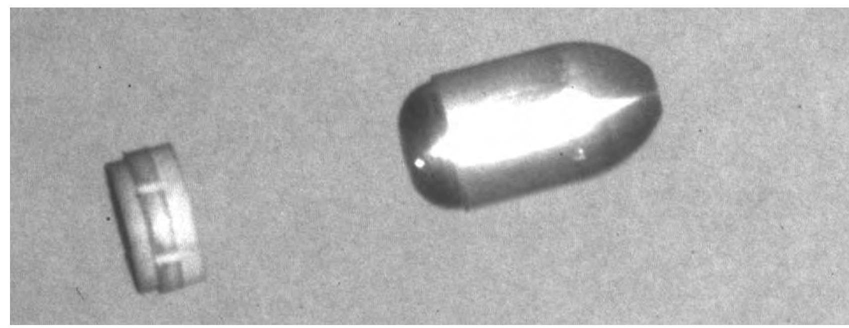

Experimentally Demonstrated Novel Aerodynamic Control Methodology Capable of Diverting Medium Caliber Munitions

Technologies developed in this research were critical in the design of flight control systems required for subsequent flight tests that demonstrated the ability of MAFC to divert the trajectory of a spinning projectile in flight

SCORPION CFD VIDEO

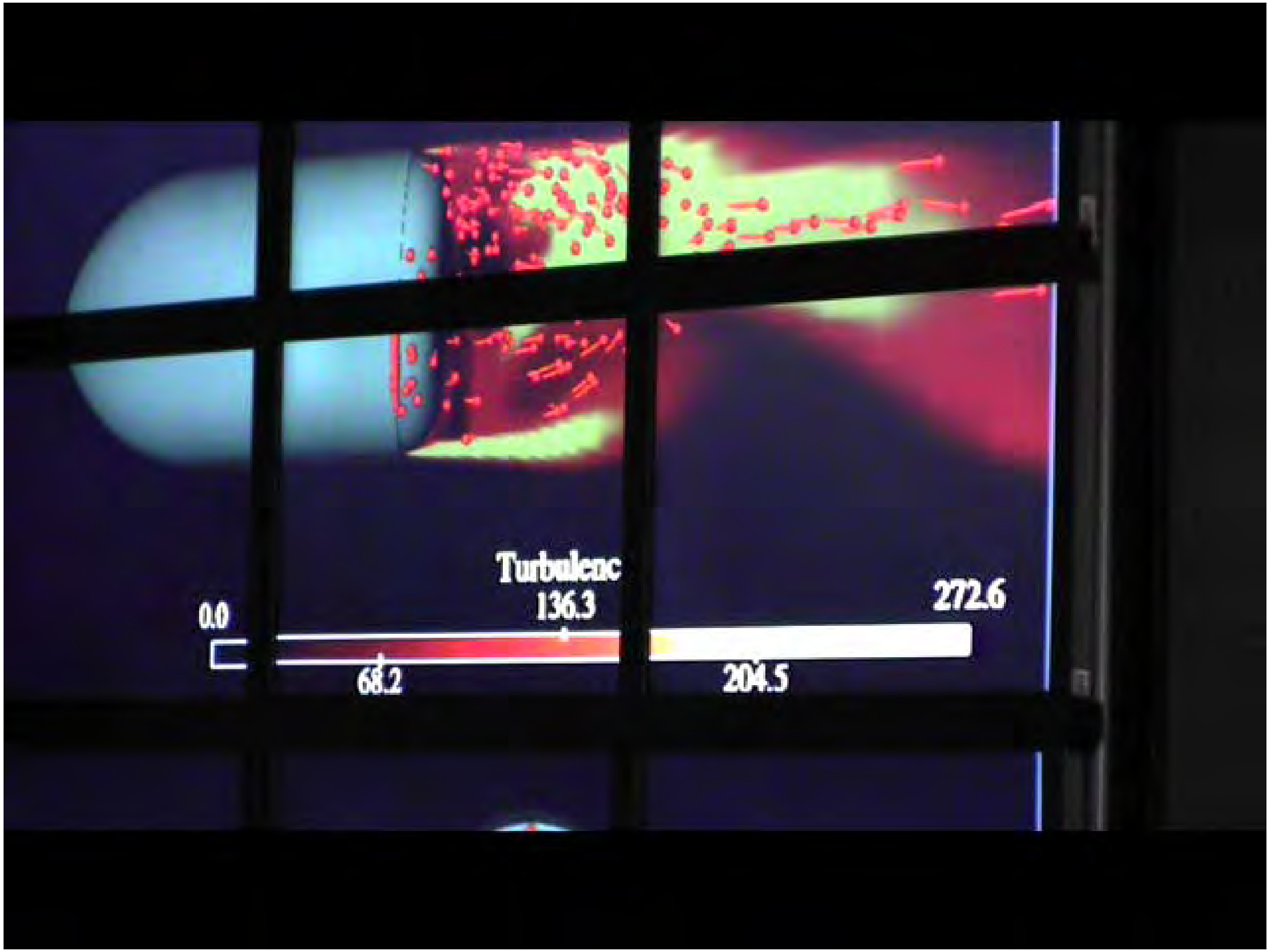

Aerodynamics Branch

MICRO-ADAPTIVE FLOW CONTROL AND NON-LINEAR AERODYNAMICS

(COMBUSTION GAS GENERATORS)

Dr. Jubaraj Sahu

Ms. Karen Heavey

U.S. Army Research Laboratory

GTRI, Atlanta, GA, 23 Sept 2005

Weapons & Materials Research Directorate

Aerodynamics with Flow Control

GAS COMBUSTOR JETS

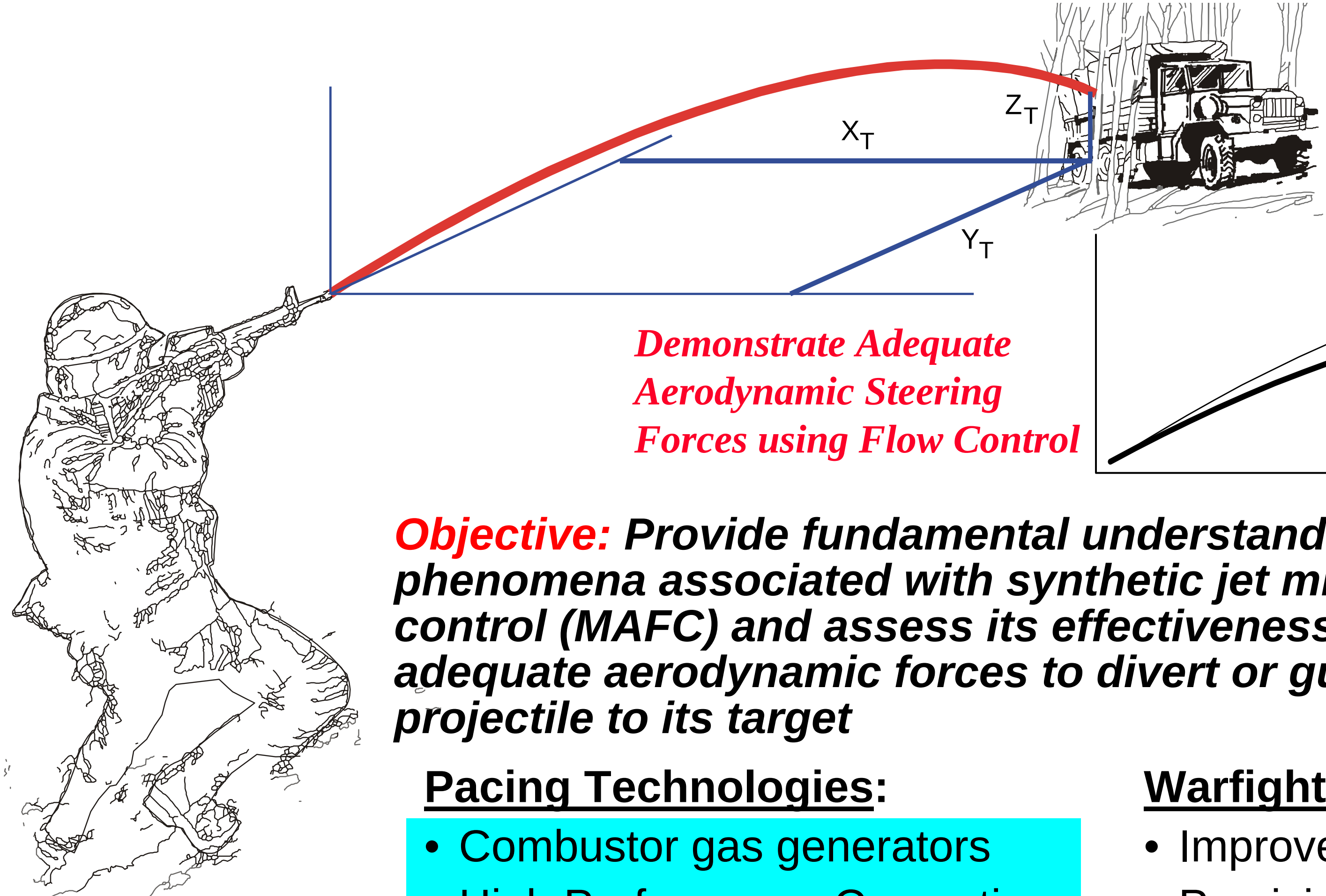

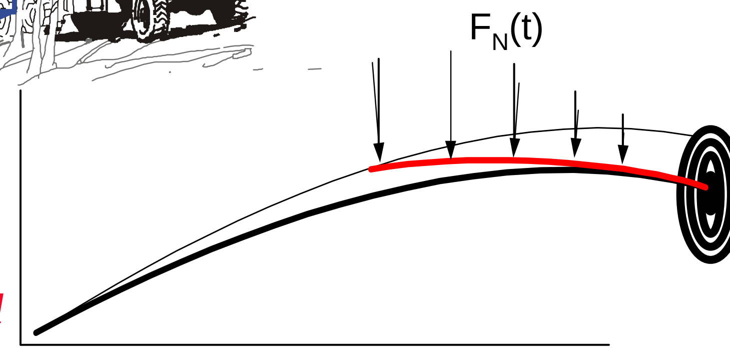

Demonstrate Adequate Aerodynamic Steering Forces using Flow Control

***Objective:* Provide fundamental understanding of the flow phenomena associated with synthetic jet micro-adaptive flow control (MAFC) and assess its effectiveness to provide adequate aerodynamic forces to divert or guide a small caliber projectile to its target**

Pacing Technologies:

- Combustor gas generators
- High Performance Computing
- Advanced Visualization
- Unsteady Aerodynamics

Warfighter Payoffs:

- Improved lift control
- Precision-guided munitions
- Increase lethality

High Fidelity Computational Tool for Improved Performance of Army Munitions

COMBUSTOR JET CFD

- 3-D Navier-Stokes computational technique
- Steady jet CFD
- Unsteady (time-accurate) jet CFD
- Fast convergence to steady state
- Fast computation of unsteady flows
- Dual time-stepping
- Special jet boundary conditions for unsteady CFD
- Validation of both non-spinning and spinning cases

SURFACE PRESSURE CONTOURS

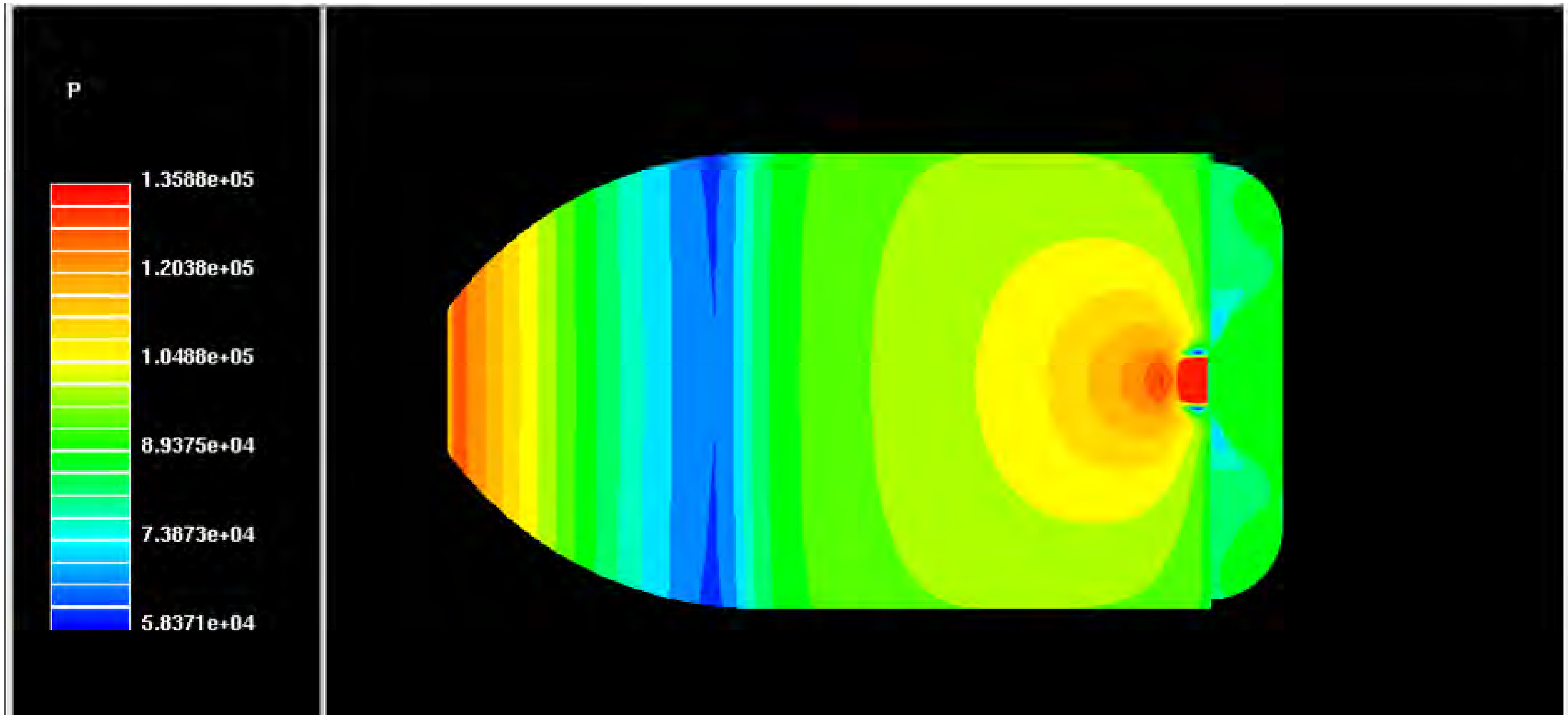

PRESSURE CONTOURS

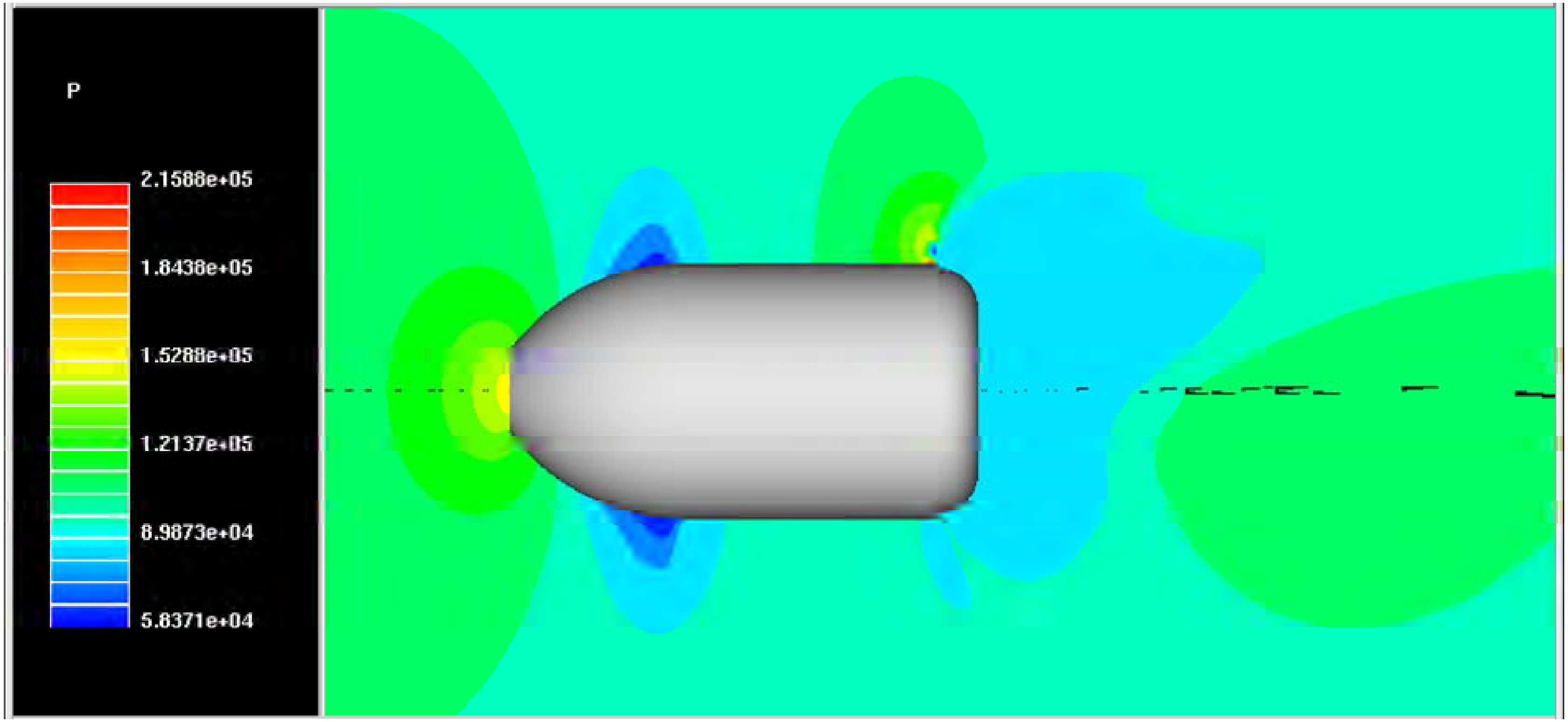

TEMPERATURE CONTOURS

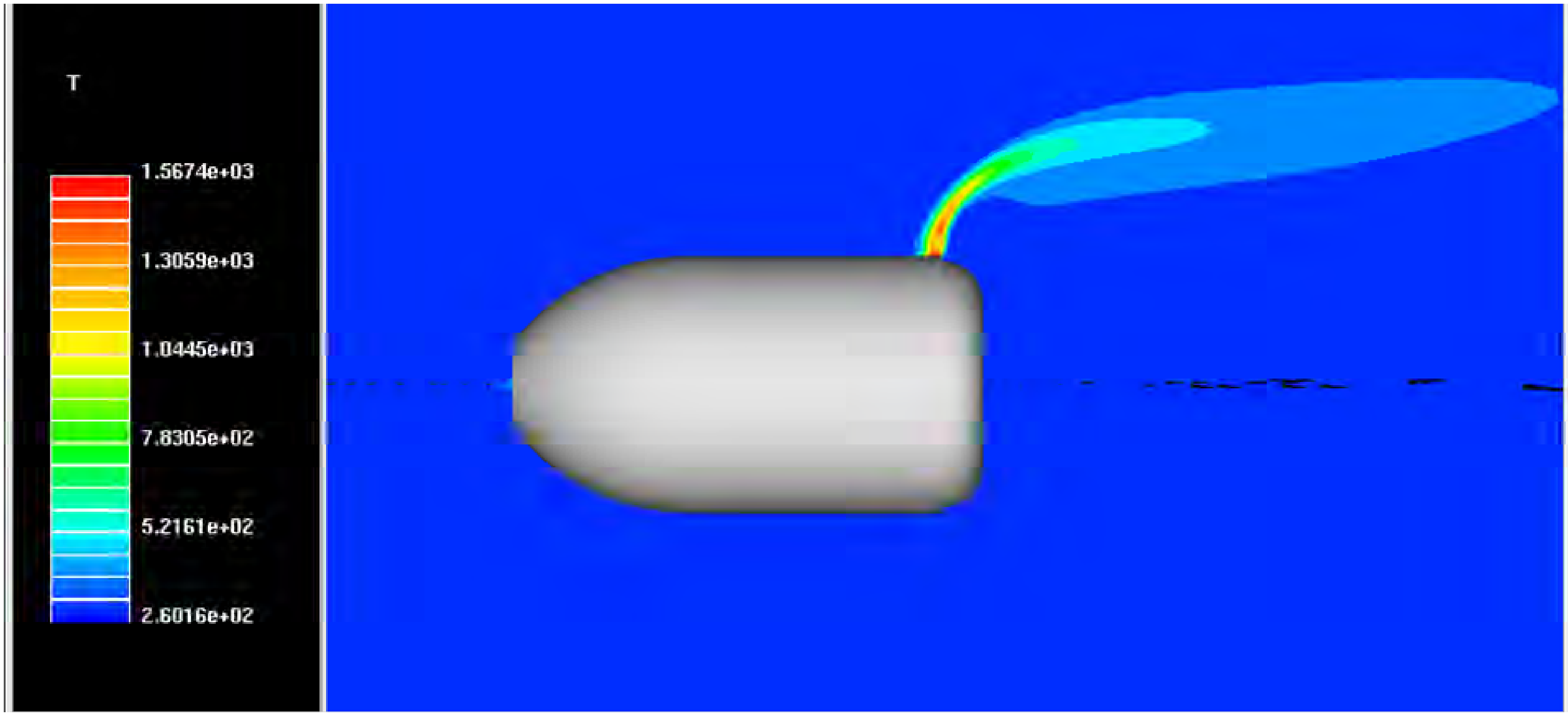

U-Velocity Contours

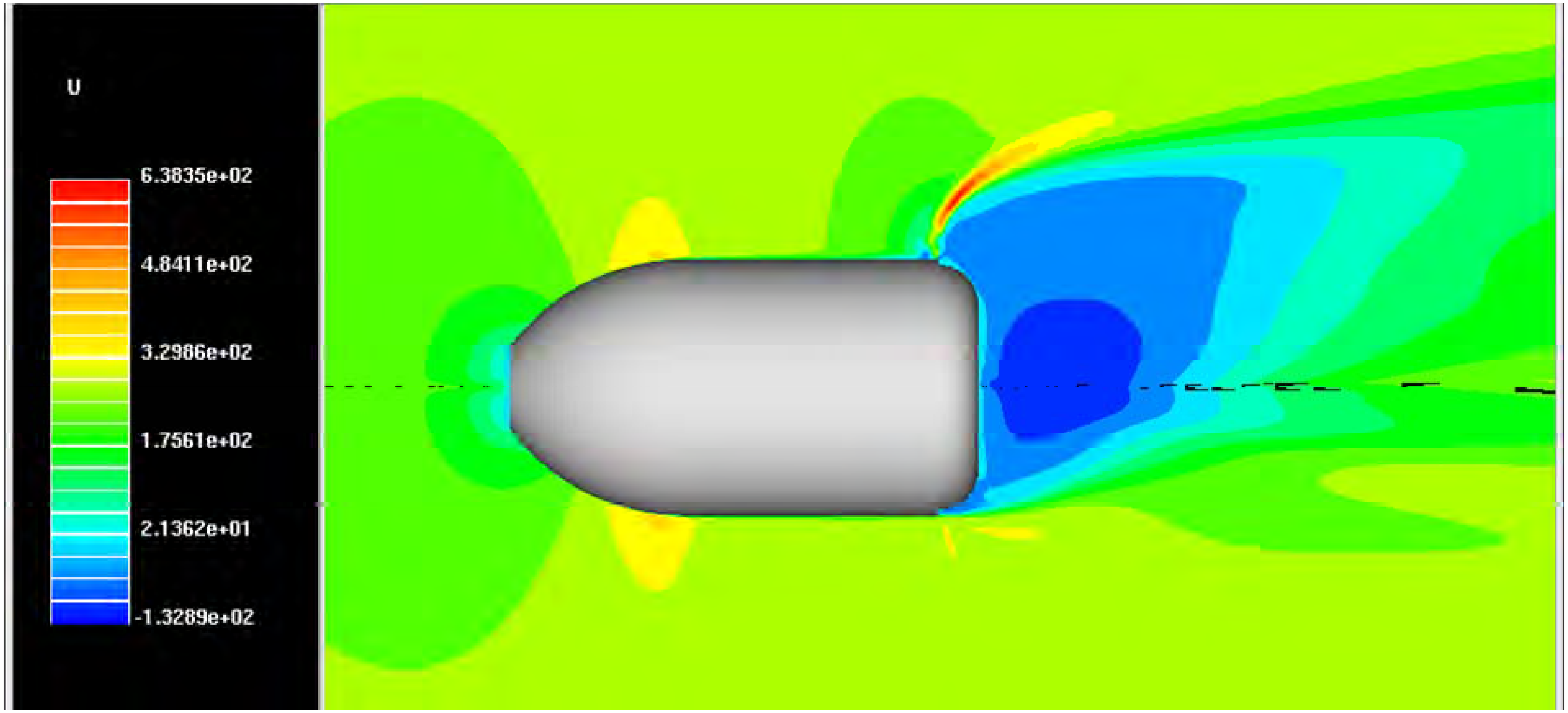

STEADY JET CFD

M = 0.8, α = 0°, P_0 = 5 atm, T_0 = 2000 K

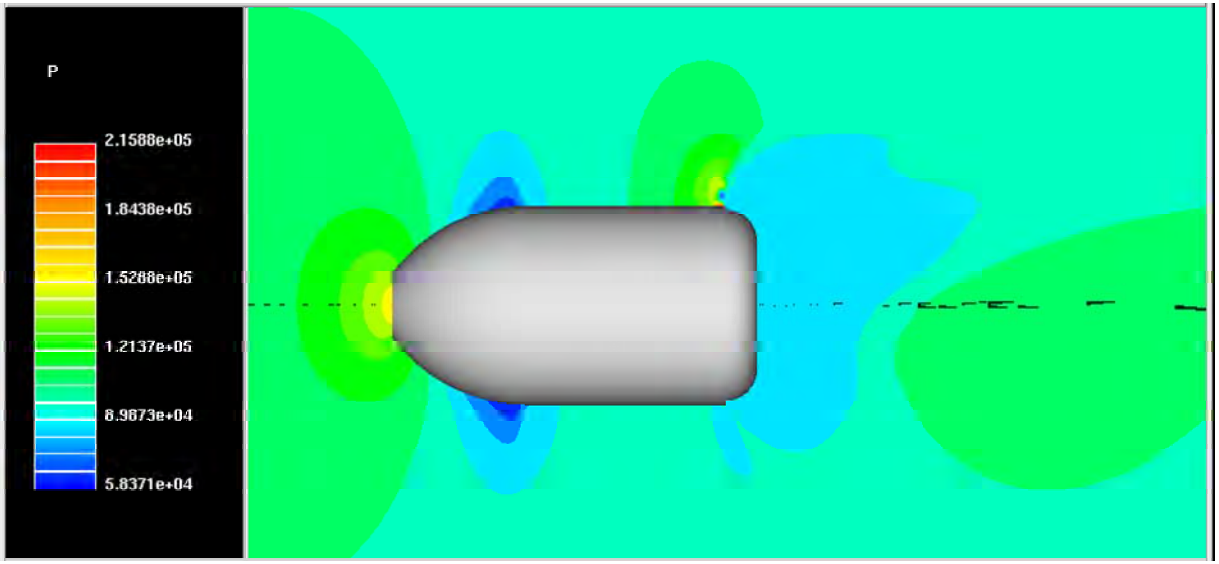

Pressure Contours

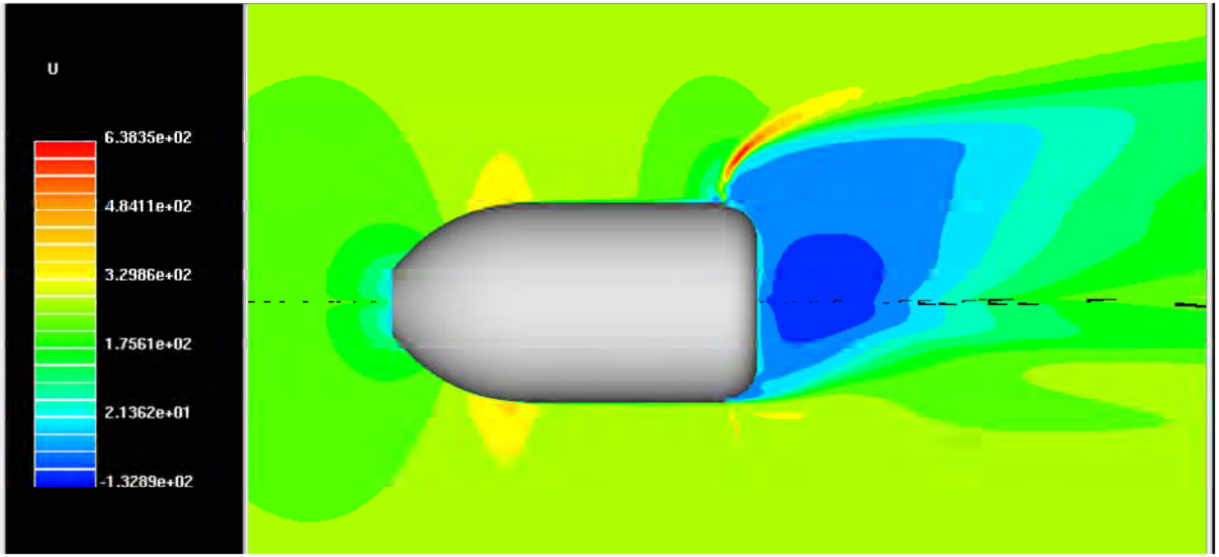

Velocity Contours

STEADY JET CFD

M = 0.8, α = 0°, P_0 = 5 atm, T_0 = 2000 K

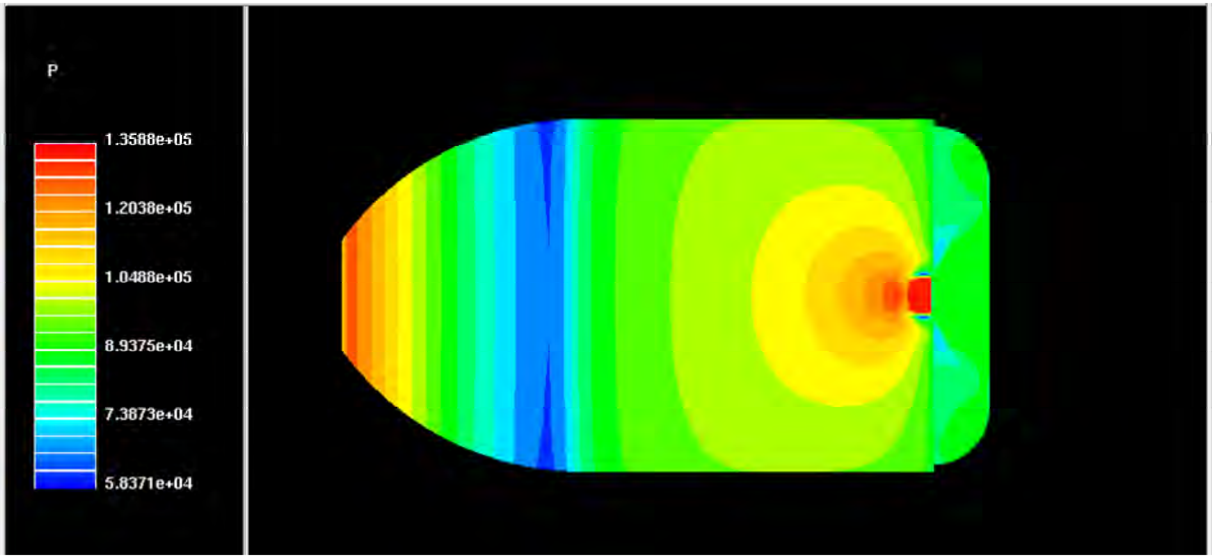

Surface Pressure Contours

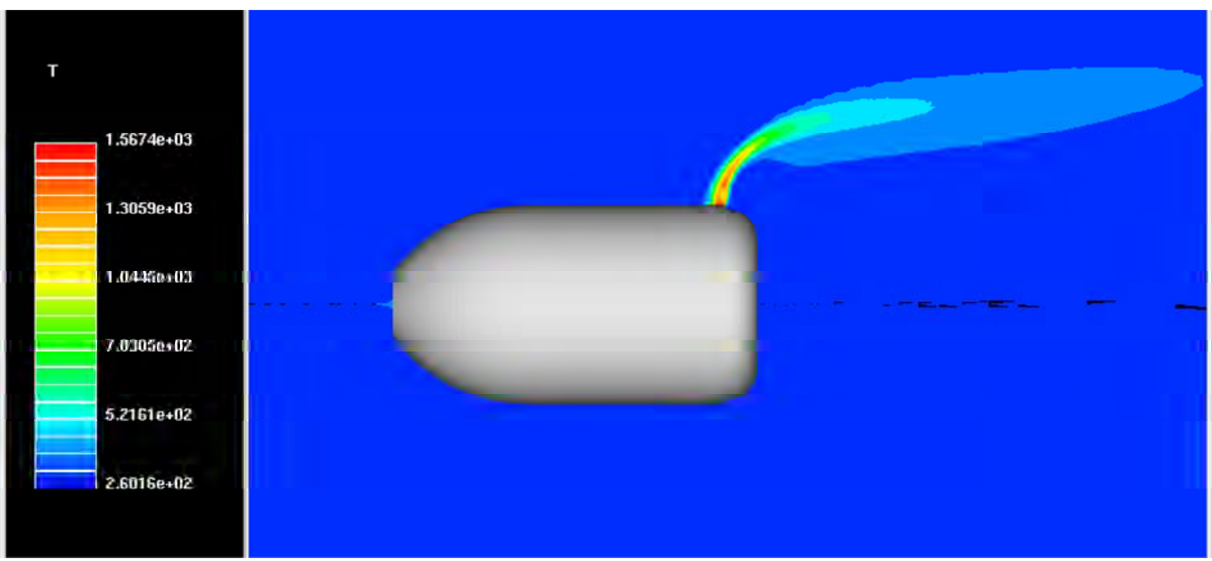

Temperature Contours

STEADY JET CFD

M = 0.8, α = 0°, P_0 = 5 atm, T_0 = 2000 K

Body jet-on, Fy = -9.1 N
Body jet-off, Fy = 0.0
Jet Force, F_{jet} = -3.8 N

Amplification Factor = $(F_{jet} + F_{ji}) / F_{jet}$

or, AF = (-3.8 + (-9.1 – 0.0)) / (-3.8) = 3.3

COMBUSTION JET CFD

Jet Size = 0.6 mm axial,
0.3 mm circumferential
Jet location = 31 mm ahead of the step

STEADY JET CFD

$M = 0.8$, $\alpha = 0°$, $P_0 = 5$ atm, $T_0 = 2000$ K

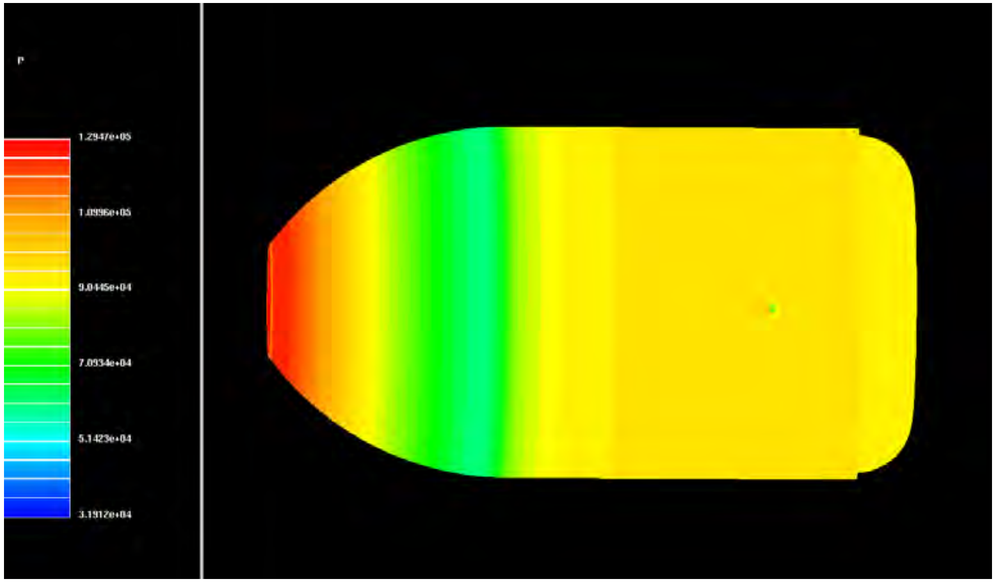

Pressure Contours

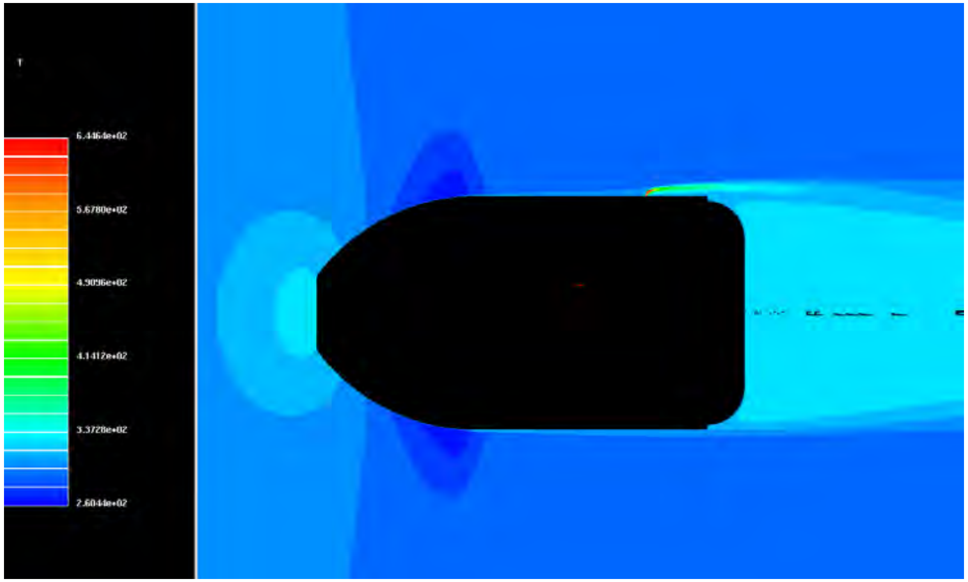

Temperature Contours

STEADY JET CFD

M = 0.8, α = 0°, P_0 = 20 atm, T_0 = 4000 K

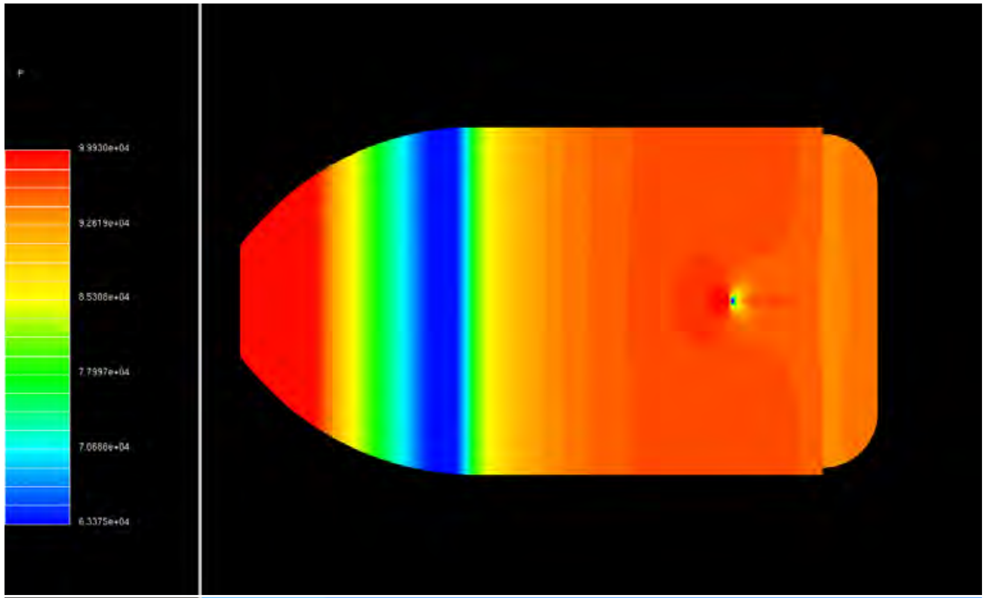

Pressure Contours

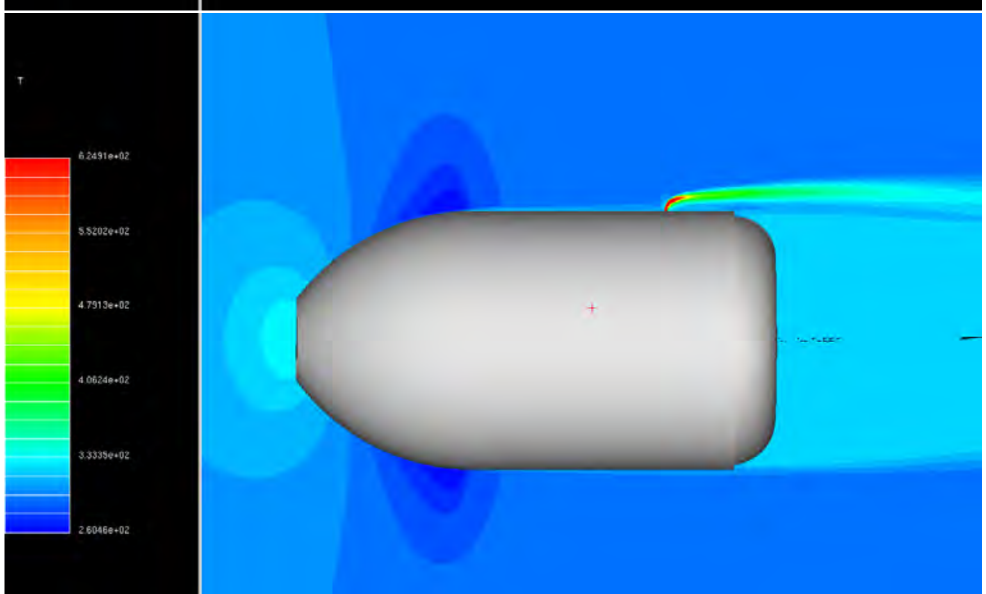

Temperature Contours

COMBUSTION JET CFD
80mm

STEADY JET CFD

$U = 30$ m/s, $\alpha = 0°$, $P_0 = 5$ atm, $T_0 = 2000$ K

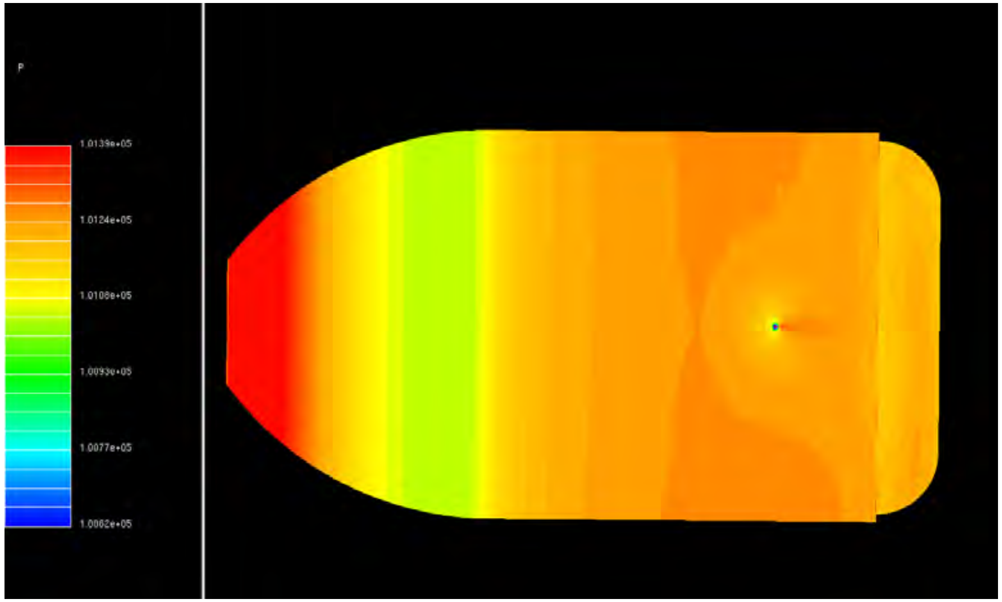

Pressure Contours

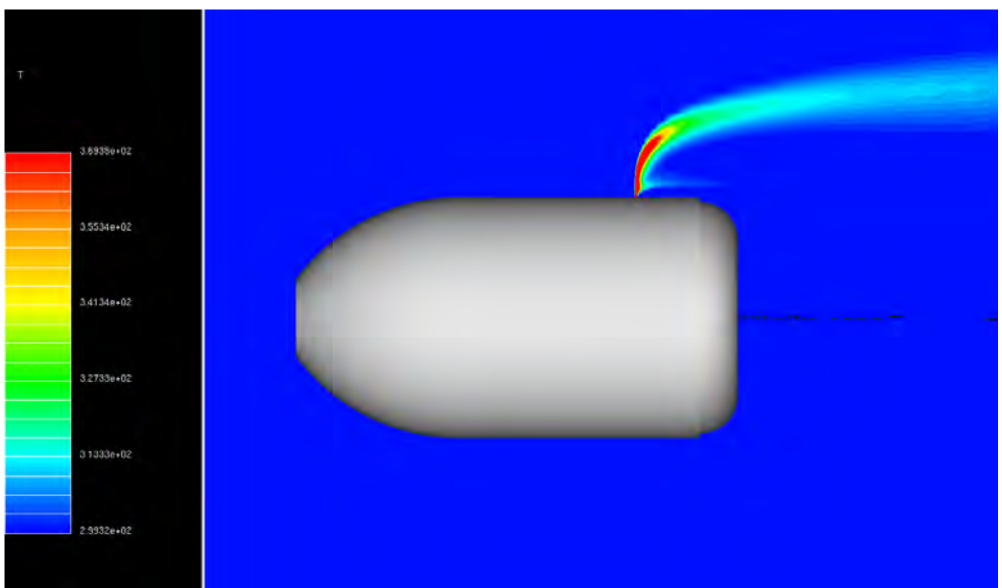

Temperature Contours

STEADY JET CFD

U = 30 m/s, α = 0°, P_0 = 5 atm, T_0 = 2000 K

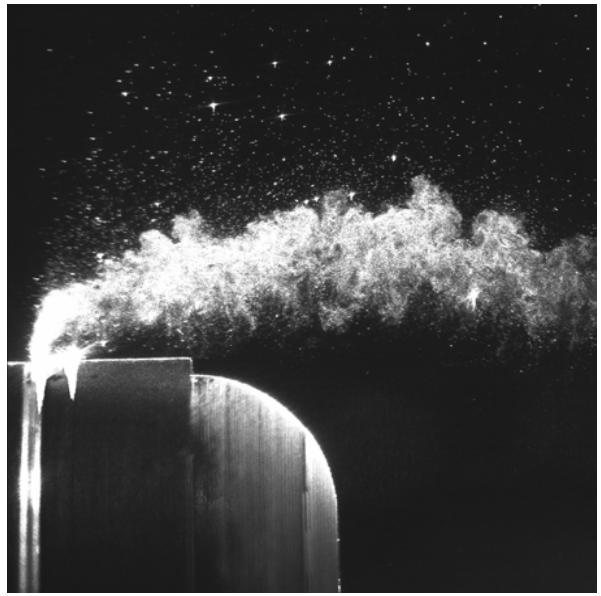

Experiment

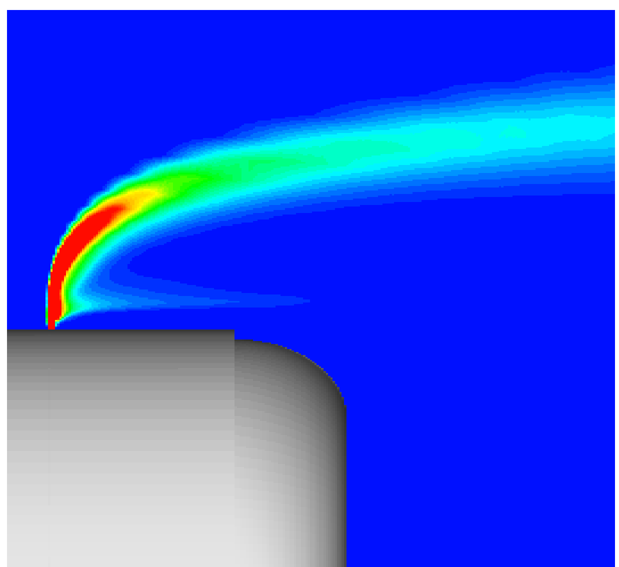

CFD

STEADY JET CFD

$U = 30$ m/s, $\alpha = 0°$, $P_0 = 5$ atm, $T_0 = 2000$ K

Body jet-on, Fy = 0.06 N
Body jet-off, Fy = 0.0
Jet Force, $F_{jet} = -0.08$N

Amplification Factor = $(F_{jet} + F_{ji}) / F_{jet}$

or, AF = (-0.08 + (0.06 – 0.0)) / (-0.08) = 0.25

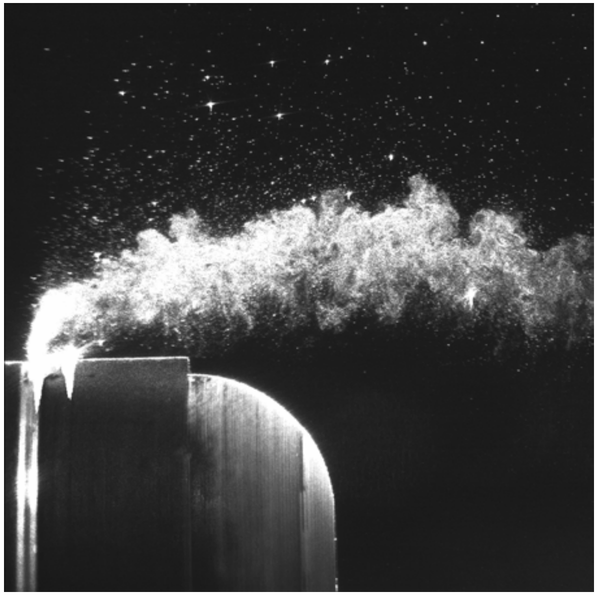

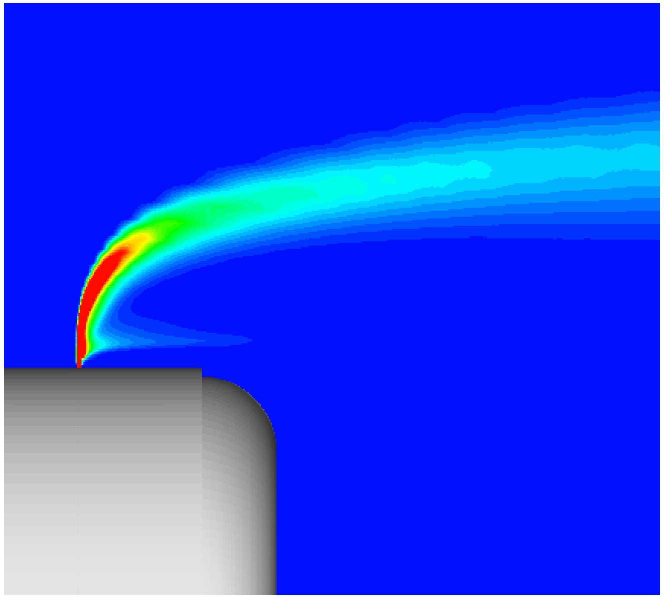

The use of electric power in active armour applications

IBS 2005

TNO | Knowledge for business

Martin.Vandevoorde@tno.nl
Ricolt.Boeschoten@tno.nl
Jos.Vanderburgt@tno.nl

Presentation Overview

- **Vehicle survivability**

- Countermeasure with pulsed power supply and directional control
- Sensor development

DAS

- Conclusion

martin.vandevoorde@tno.nl

Survivability Onion

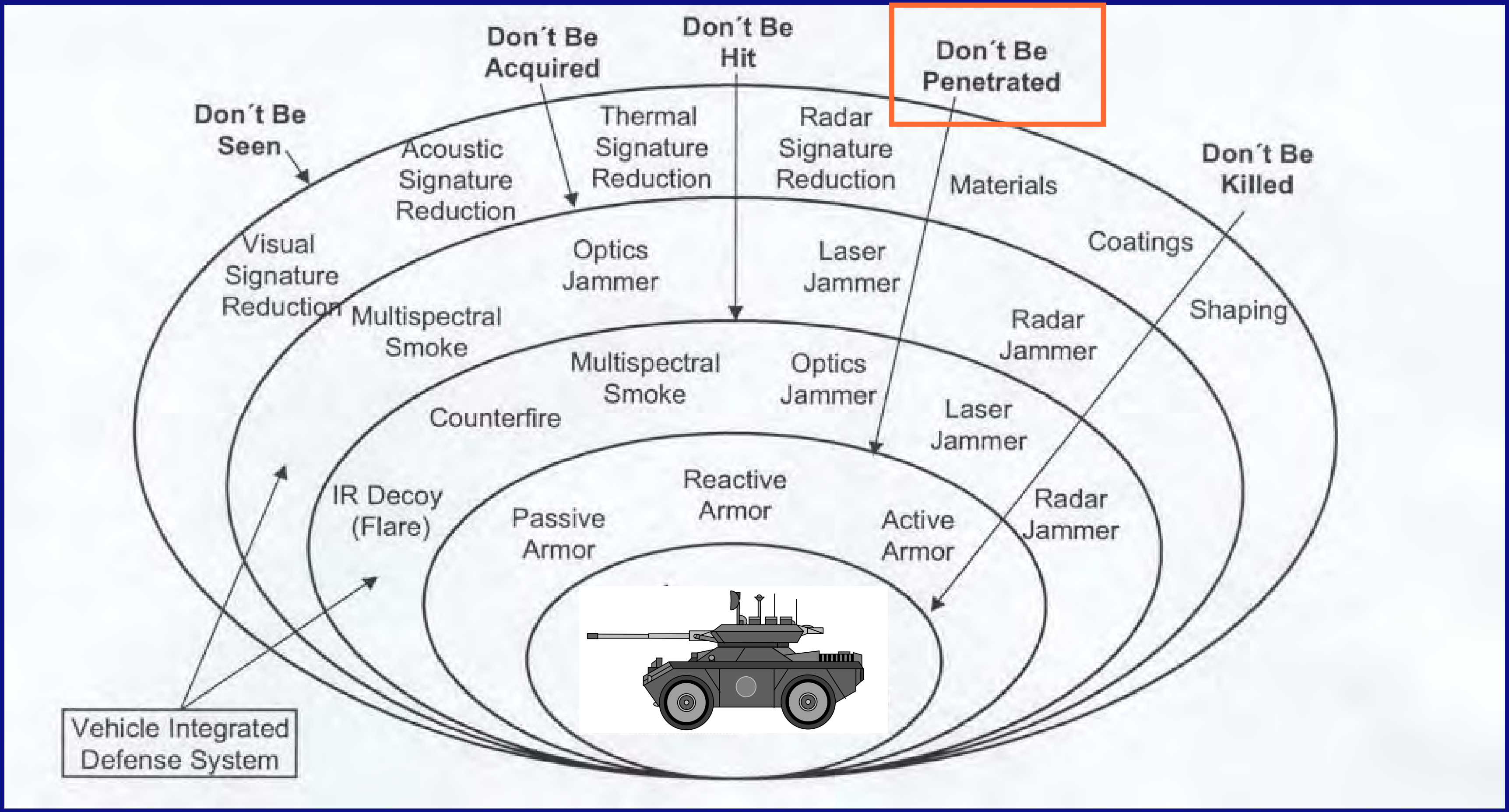

Presentation Overview

- Vehicle survivability
- **Countermeasure with pulsed power supply and directional control**
- Sensor development
- Conclusion

DAS

Advantages of EM launched plates

- On/Off switching capability
- No energetic material on the outside of the vehicle
- Directional launching
- Multi-hit capability
- Possibly effective against CE (shaped charge) and KE

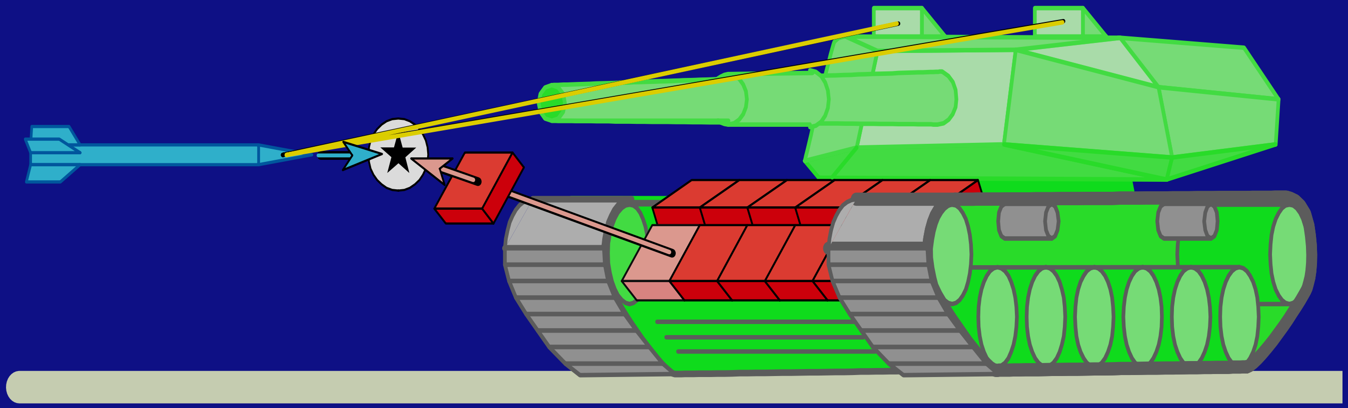

EM launched plate vs Shaped charge (1-D)

EM launched plate (3-D)

EM launched plate (2-D)

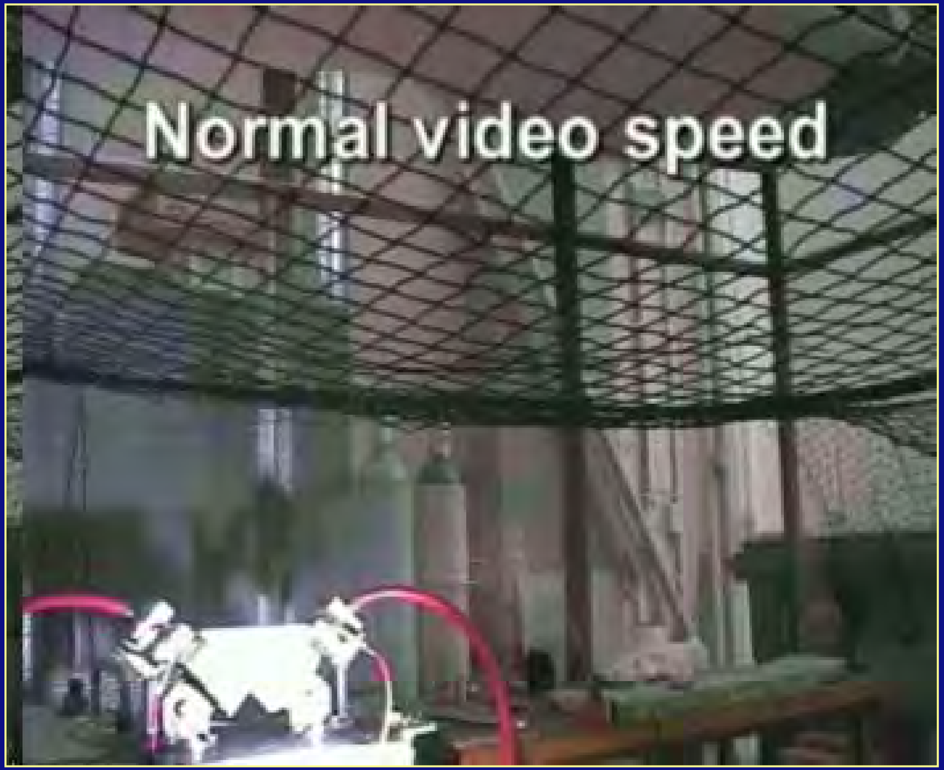

Plate velocity: 150-200 m/s
Plate mass: 0.5 kg

EM launched plates vs KE: static experiments

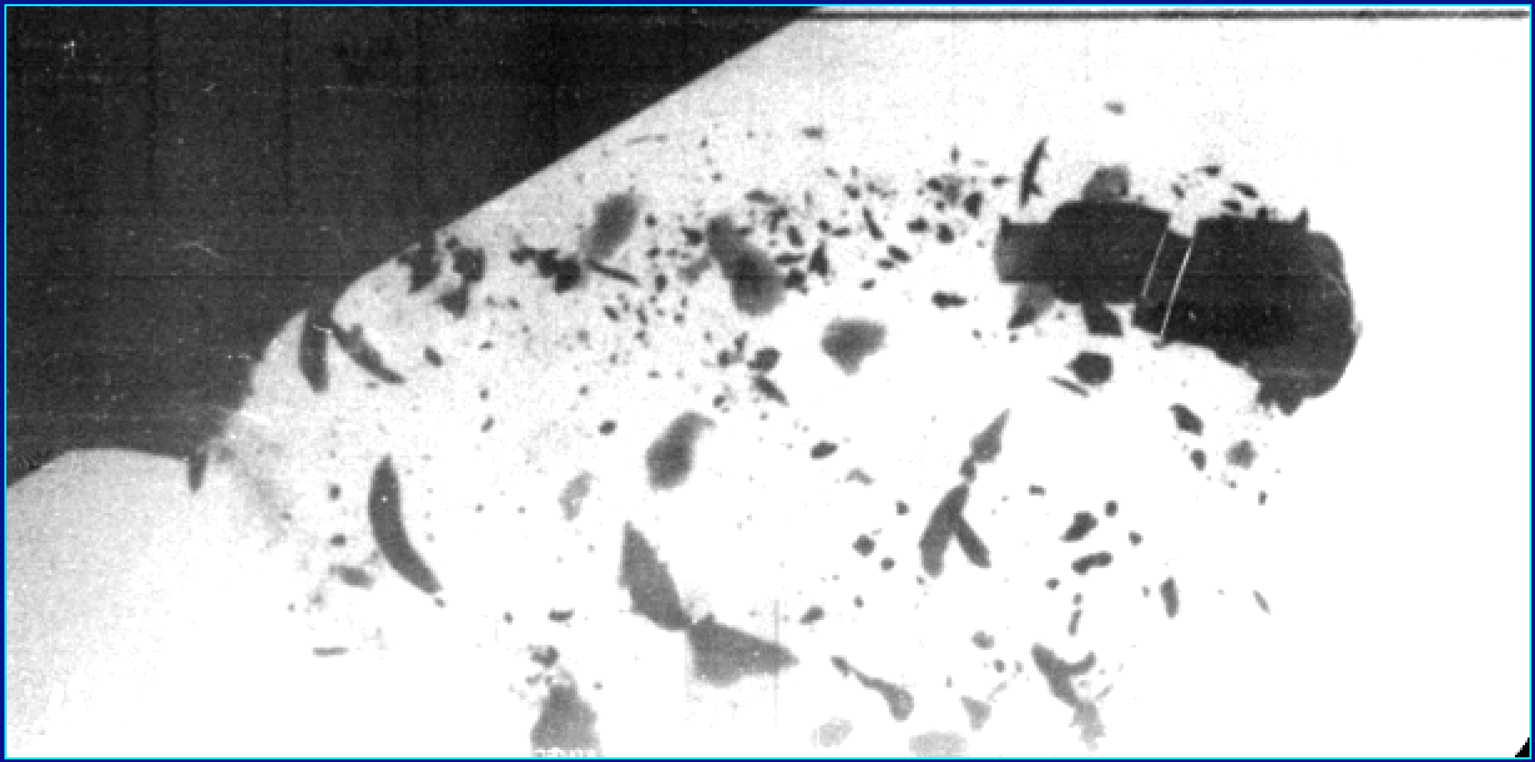

Effectiveness against 30*173 mm APFSDS

EM launched plates vs KE: numerical simulations

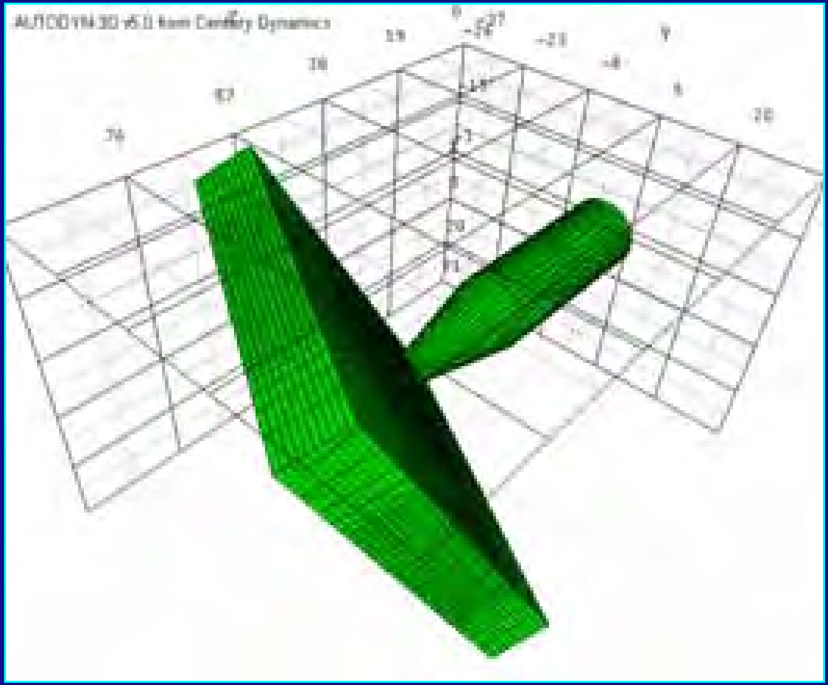

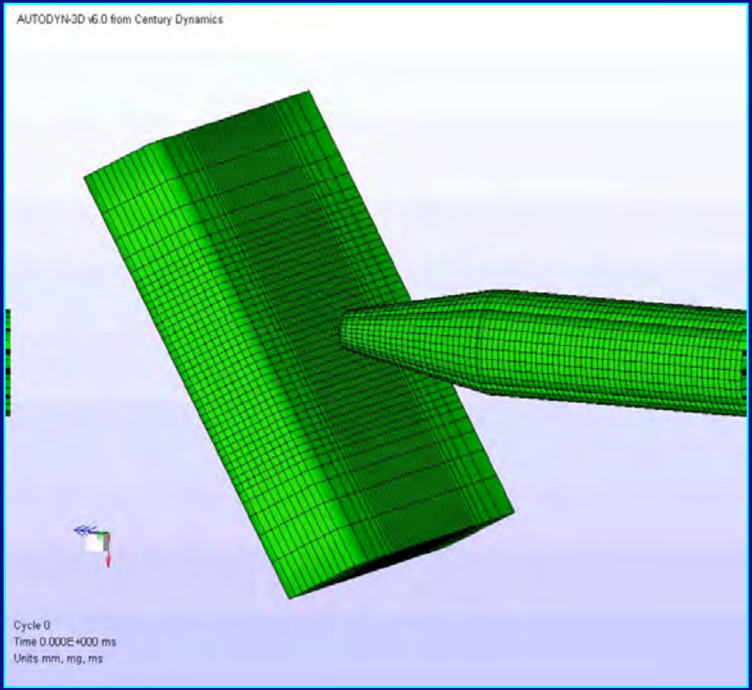

martin.vandevoorde@tno.nl

EM launched plates vs KE: dynamic experiments

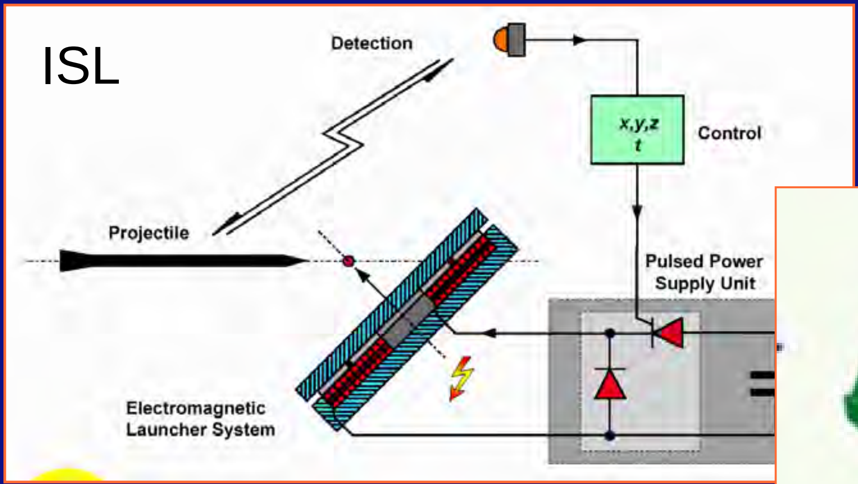

Launched plates

Plate velocity: 50 m/s
Plate mass: 3.0 kg

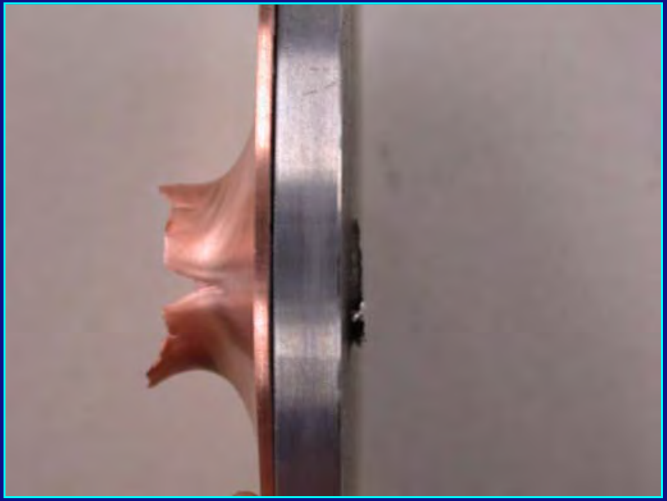

X-ray and camera images

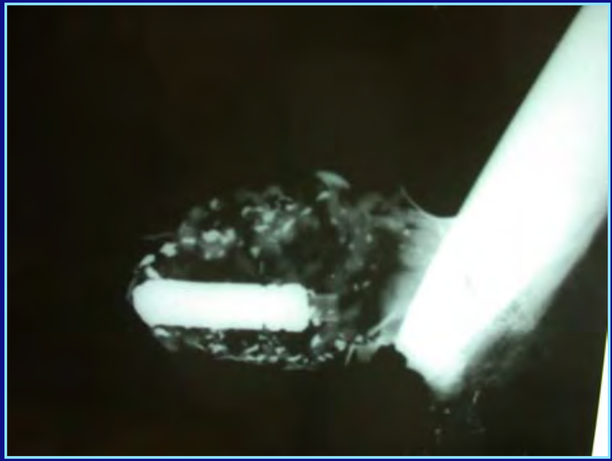

Reduction of DOP:
> 60%

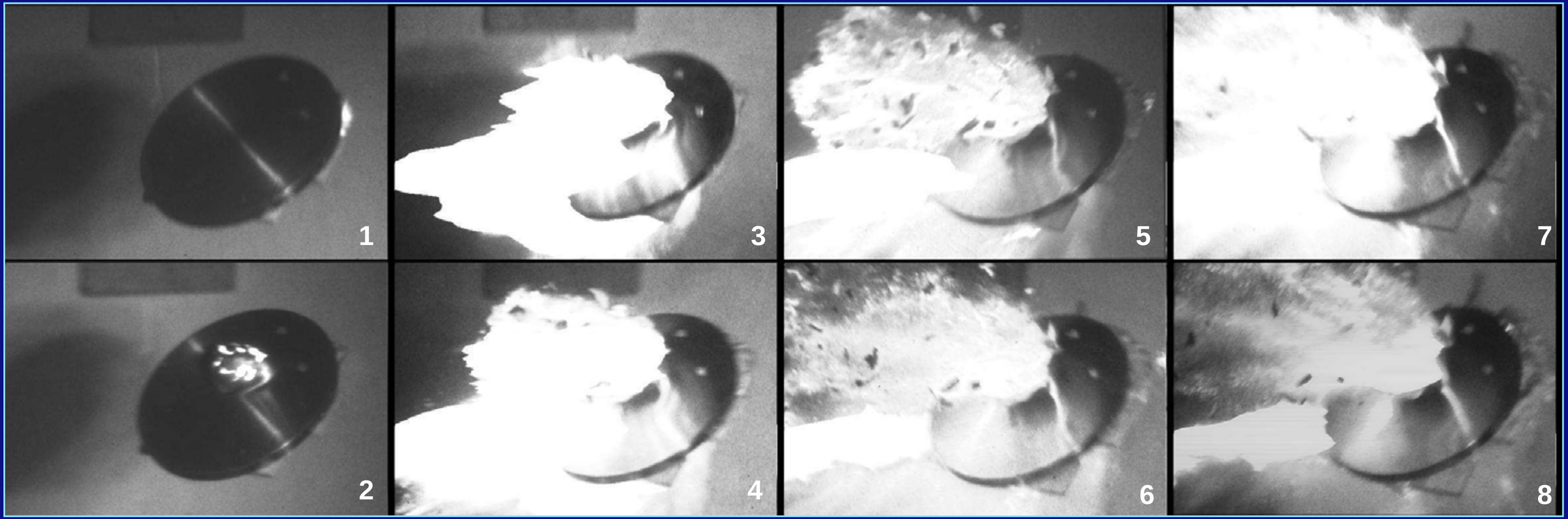

Presentation Overview

- Vehicle survivability
- Countermeasure with pulsed power supply and directional control
- Sensor development
- **Conclusion**

DAS

Conclusion

- Countermeasure steering
  - 3-D possible

- Countermeasure effectiveness
  - Initiates premature detonation of shaped charge
  - Break up or erosion of KE: Decreasing DOP

- Promising sensor design
  - Accuracy of 3D positioning and timing is a real challenge

Presentation Overview

- Vehicle survivability
- Countermeasure with pulsed power supply and directional control
- **Sensor development**
  - Sensor design
  - RPG-7 signatures from TNO experiments
- Conclusion

DAS

RPG-7 firing in Czech Republic

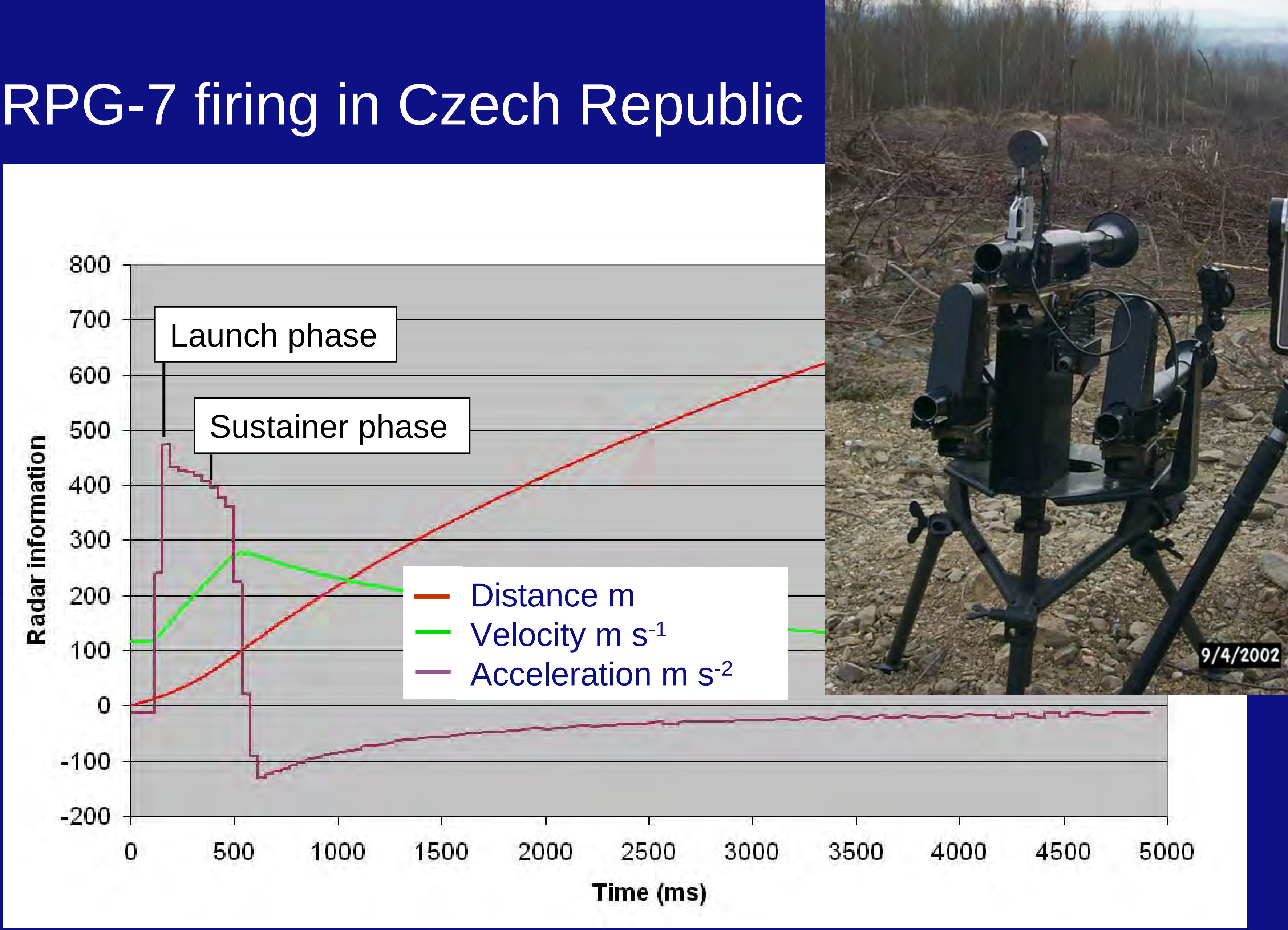

Experimental set-up

Gun

Capacitor bank

Coil

Steel plate; m=3kg

From *Columbia* to *Discovery*: Understanding the Impact Threat to the Space Shuttle (Abridged)

James D. Walker

Southwest Research Institute

San Antonio, Texas 78228

The work described in this talk was paid for by the American taxpayer through NASA and the Columbia Accident Investigation Board.

Lots of People

Photograph during *Columbia* investigation

Lots of people worked on the *Columbia* accident investigation and return to flight.

Some who directly helped with the impact-related material in this talk:

Donald J. Grosch (SwRI)
Sidney Chocron (SwRI)
Walt Gray (SwRI)
Justin Kerr (NASA/JSC)
Freeman Bertrand (Jacobs/Sverdrup)
Paul Parker (Boeing)
Mike Dunham (Boeing)

Southwest Research Institute

The *Columbia* Accident

STS-107

- 113th flight of the Space Shuttle Program
- 28th flight of *Columbia*
- *Columbia* was the first Shuttle to fly (April, 1981)
- Launched January 16, 2003
- Disintegrated on re-entry, February 1, 2003
- Crewed by
  - Rick Husband
  - William C. McCool
  - Michael P. Anderson
  - David M. Brown
  - Kalpana Chawla
  - Laurel Clark
  - Ilan Ramon

CAIB Report, Volume I

- Volume 1 of the Columbia Accident Investigation Report was published August 26, 2003
- It can be found at the CAIB web site: www.caib.us
- The conclusions were that there were two causes of the loss of the *Columbia*:
  - A physical cause
  - An organizational cause
- SwRI was involved in identifying the physical cause, discussed in Chapter 3 of the Volume I with more details in Volume II and a NASA report.

Columbia Accident Investigation Board Report, Volume II, Appendix D.12 (Oct. 2003)

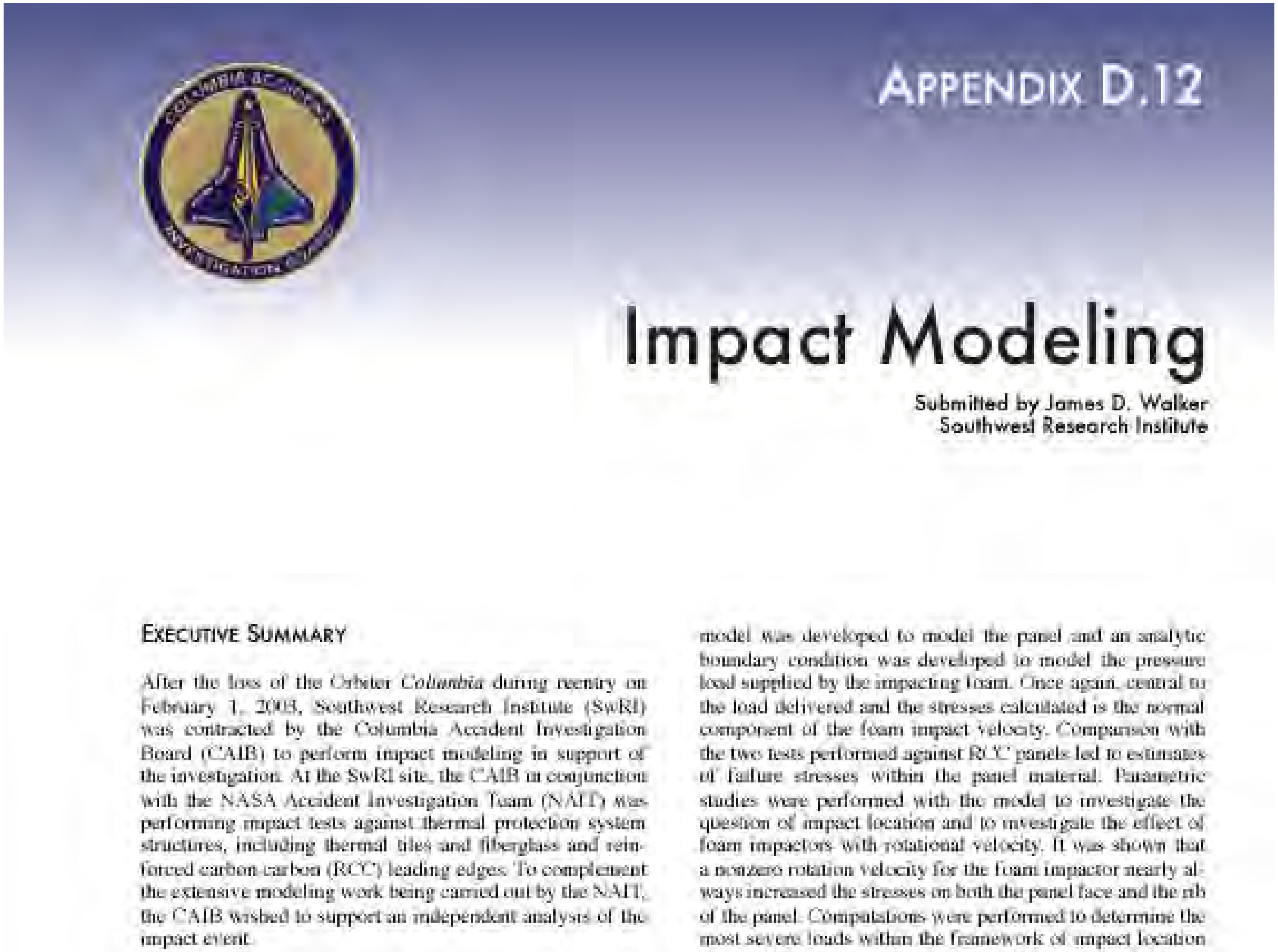

APPENDIX D.12

Impact Modeling

Submitted by James D. Walker
Southwest Research Institute

EXECUTIVE SUMMARY

After the loss of the Orbiter *Columbia* during reentry on February 1, 2003, Southwest Research Institute (SwRI) was contracted by the Columbia Accident Investigation Board (CAIB) to perform impact modeling in support of the investigation. At the SwRI site, the CAIB in conjunction with the NASA Accident Investigation Team (NAIT) was performing impact tests against thermal protection system structures, including thermal tiles and fiberglass and reinforced carbon-carbon (RCC) leading edges. To complement the extensive modeling work being carried out by the NAIT, the CAIB wished to support an independent analysis of the impact event.

model was developed to model the panel and an analytic boundary condition was developed to model the pressure load supplied by the impacting foam. Once again, central to the load delivered and the stresses calculated is the normal component of the foam impact velocity. Comparison with the two tests performed against RCC panels led to estimates of failure stresses within the panel material. Parametric studies were performed with the model to investigate the question of impact location and to investigate the effect of foam impactors with rotational velocity. It was shown that a nonzero rotation velocity for the foam impactor nearly always increased the stresses on both the panel face and the rib of the panel. Computations were performed to determine the most severe loads within the framework of impact location

Bipod Ramp Foam Insulation

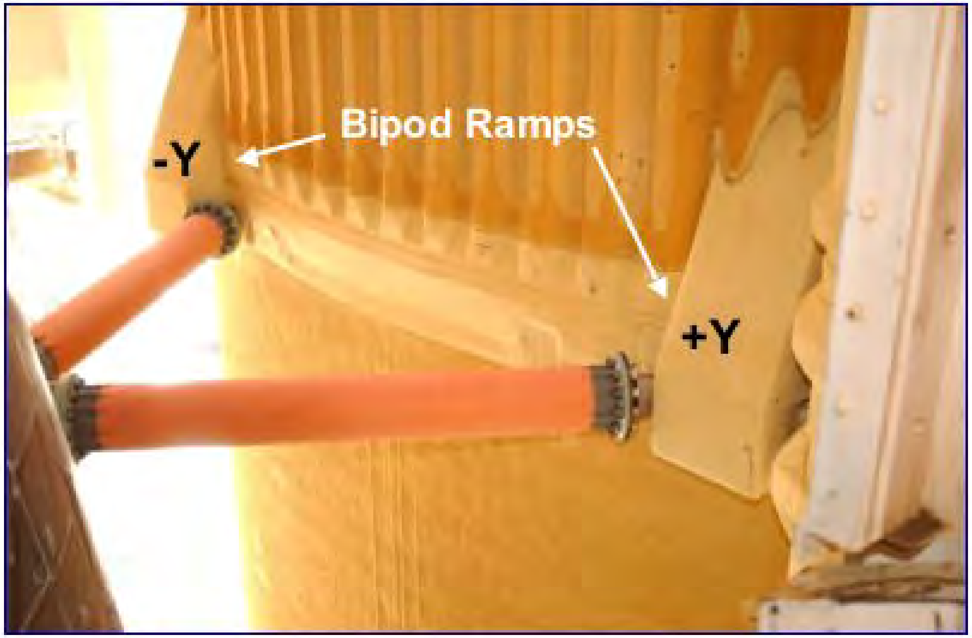

Foam Impact on STS-107

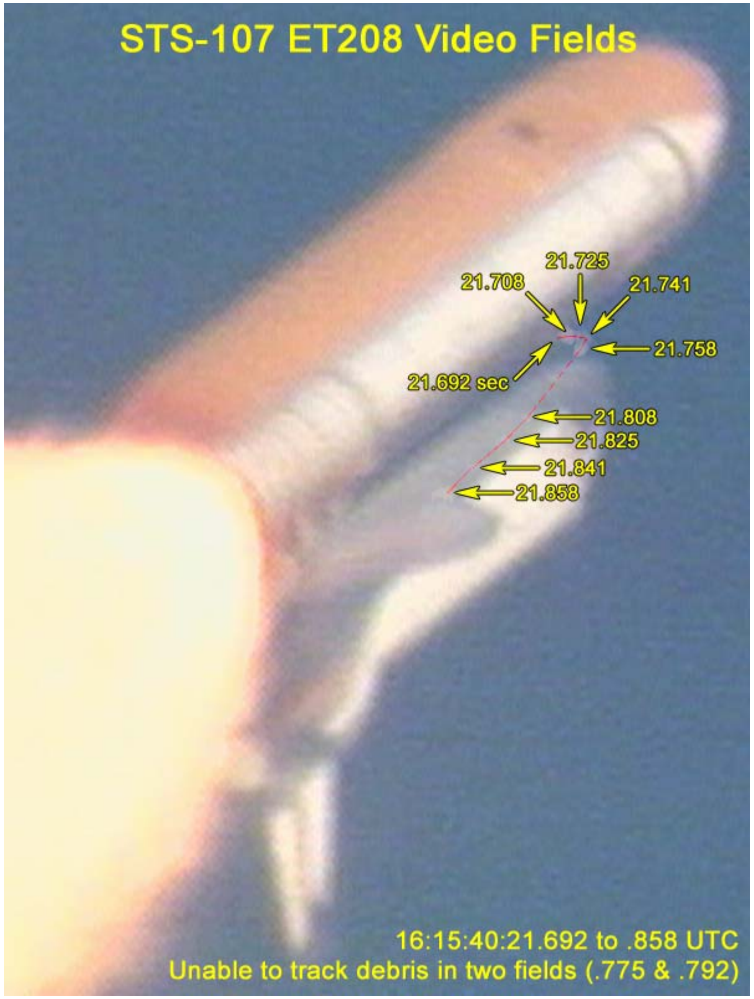

- 81.7 seconds into flight, the bipod ramp foam insulation broke away.
- The shuttle was at 66,000 ft.
- The shuttle velocity was mach 2.46 (1580 mph).
- The foam traversed the 58 feet between the bipod connection and the left wing in 0.16 seconds.
- The refined estimate of the impact velocity was 775 ft/s (528 mph).
- Estimated foam mass: 1.67 pounds.
- Estimated size: 21” × 11.5” × 5.5”

Possible Impact Locations

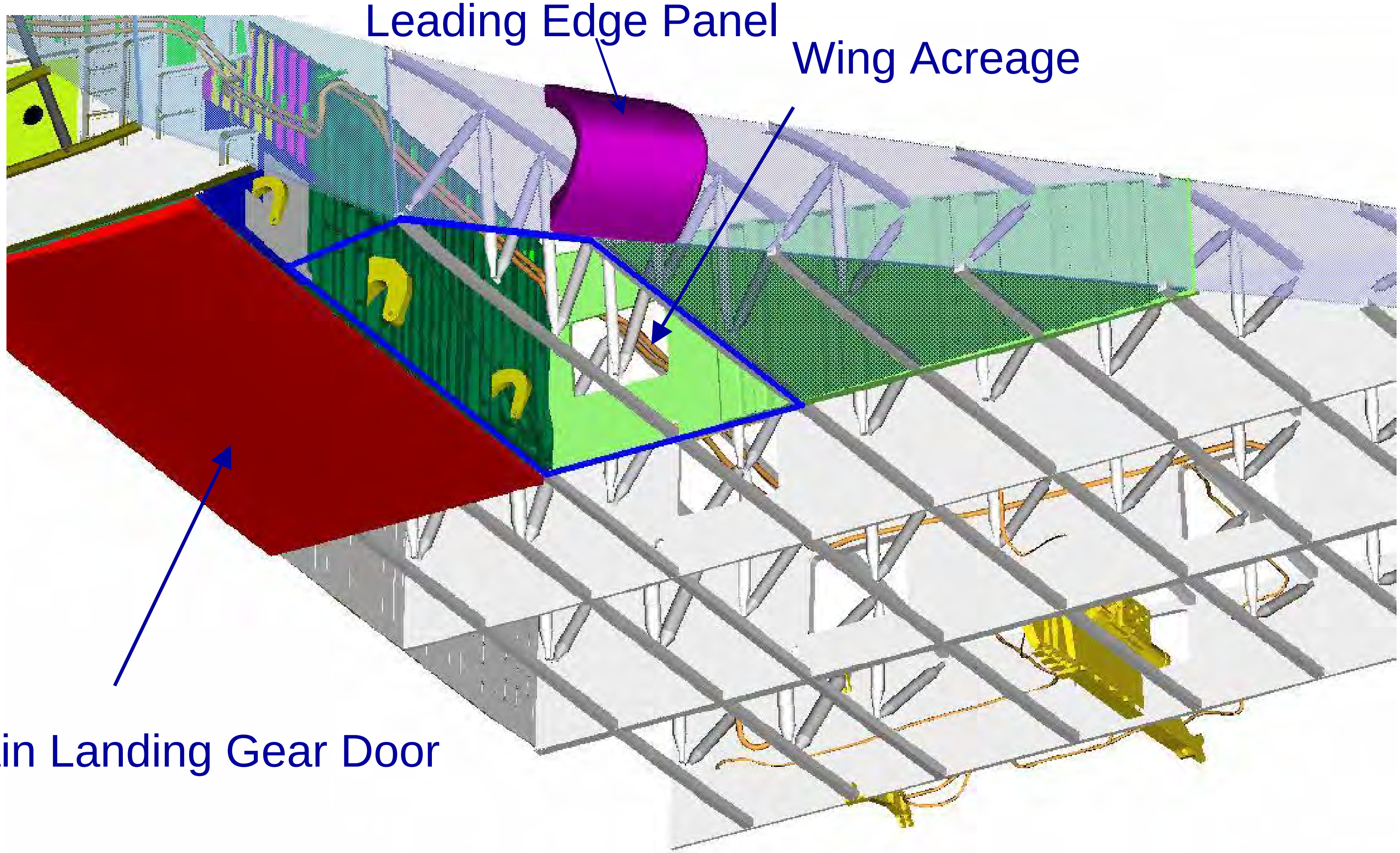

Shifting Focus

Modular Auxiliary Data System Recorder

- Early telemetry showed first anomalies in left main landing gear bay.
- Upon recovery of the Modular Auxiliary Data System recorder on March 19, 2003, analysis of the data led attention to the leading edge.

Main Landing Gear Door

Main Landing Gear Door from *Enterprise*

SwRI Large Compressed Gas Gun

- 500 gallon tank, 275 psi working pressure, 10-inch diameter by 35-foot long barrel.
- Typically used to launch large, irregularly-shaped projectiles.
- Helium or Nitrogen is used as the driver gas.

Launching Foam

Main Landing Gear Door Tests

- Performed 5 impact tests on the left Main Landing Gear Door.
- These impacts demonstrated that at the speed (775 ft/s) and angles of impact on the tiles (up to 13°) the foam barely damages the tiles.

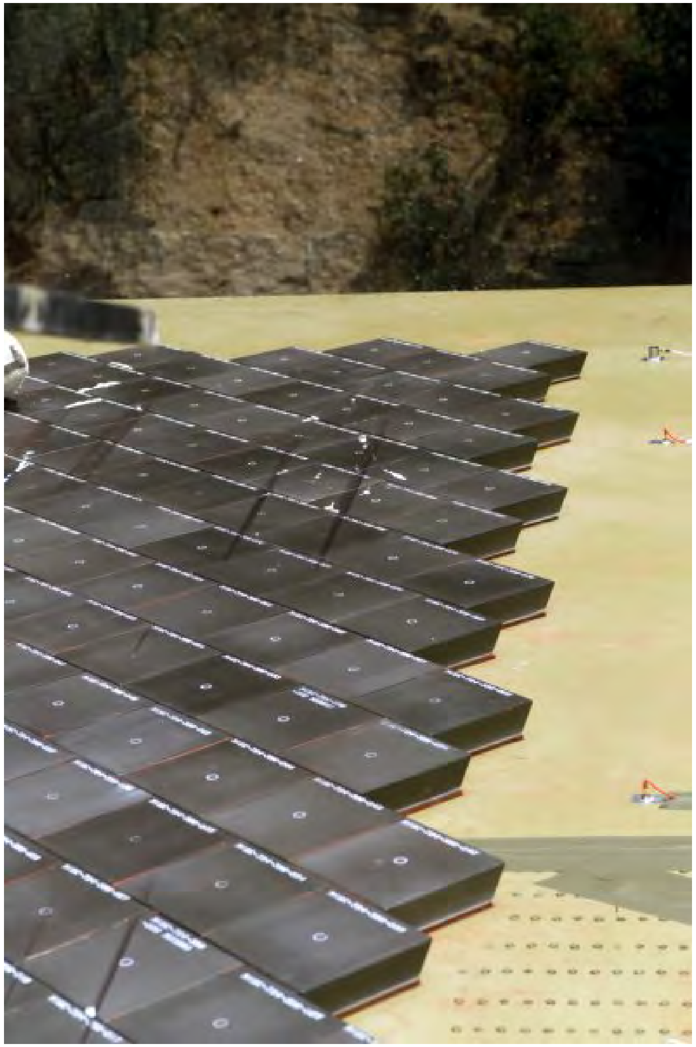

Tile and Foam Modeling

Foam Insulation Compression Tests

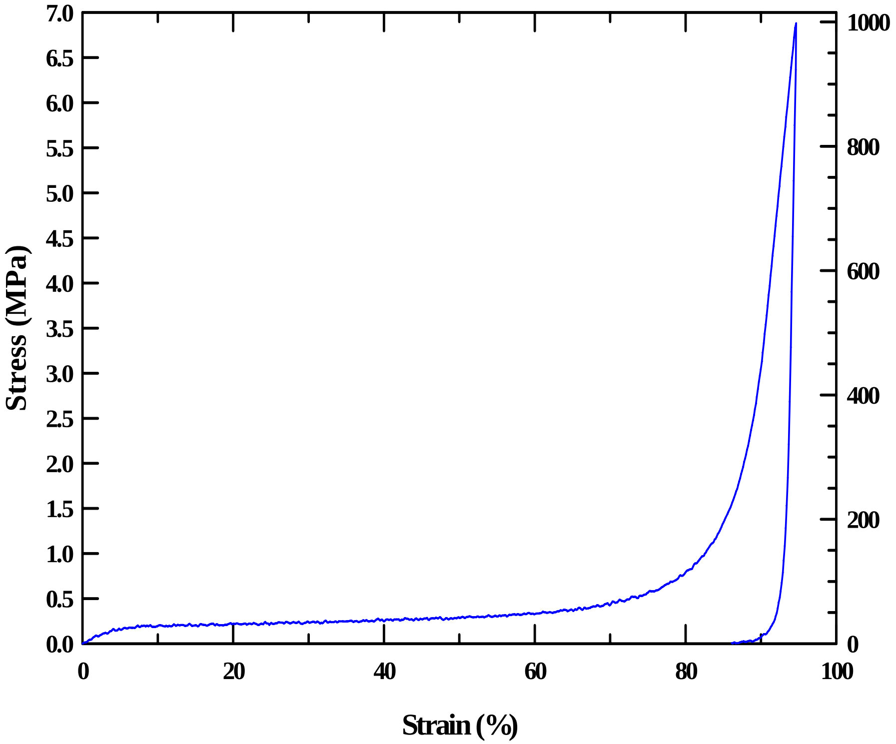

Stress-strain curve for sample 1

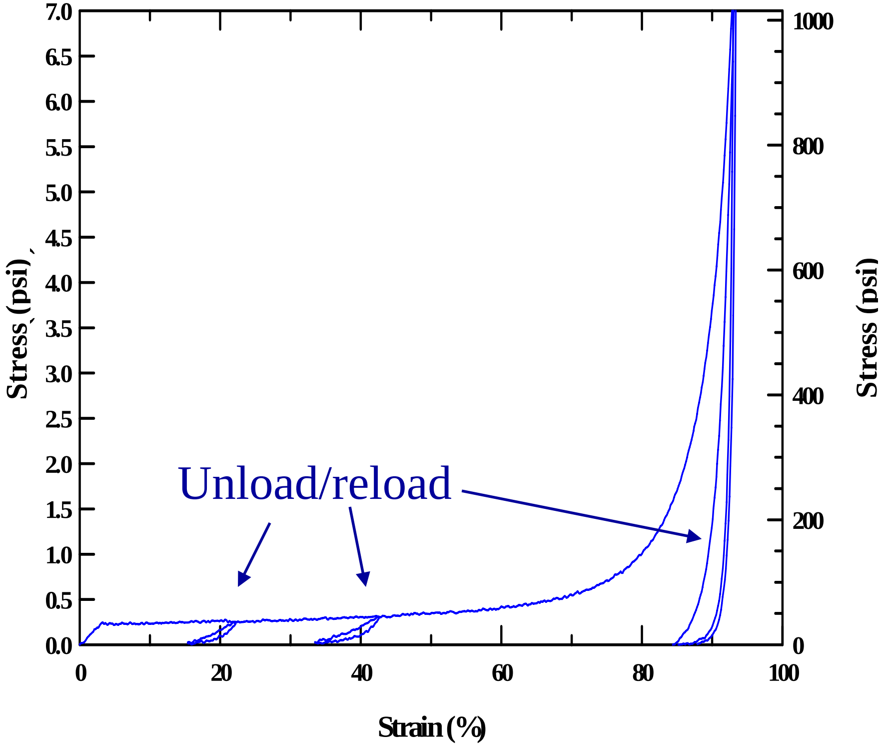

Stress-strain curve for sample 2

Transverse compression tests on roughly 2” cube tile samples taken from tile MISC-794-400-120

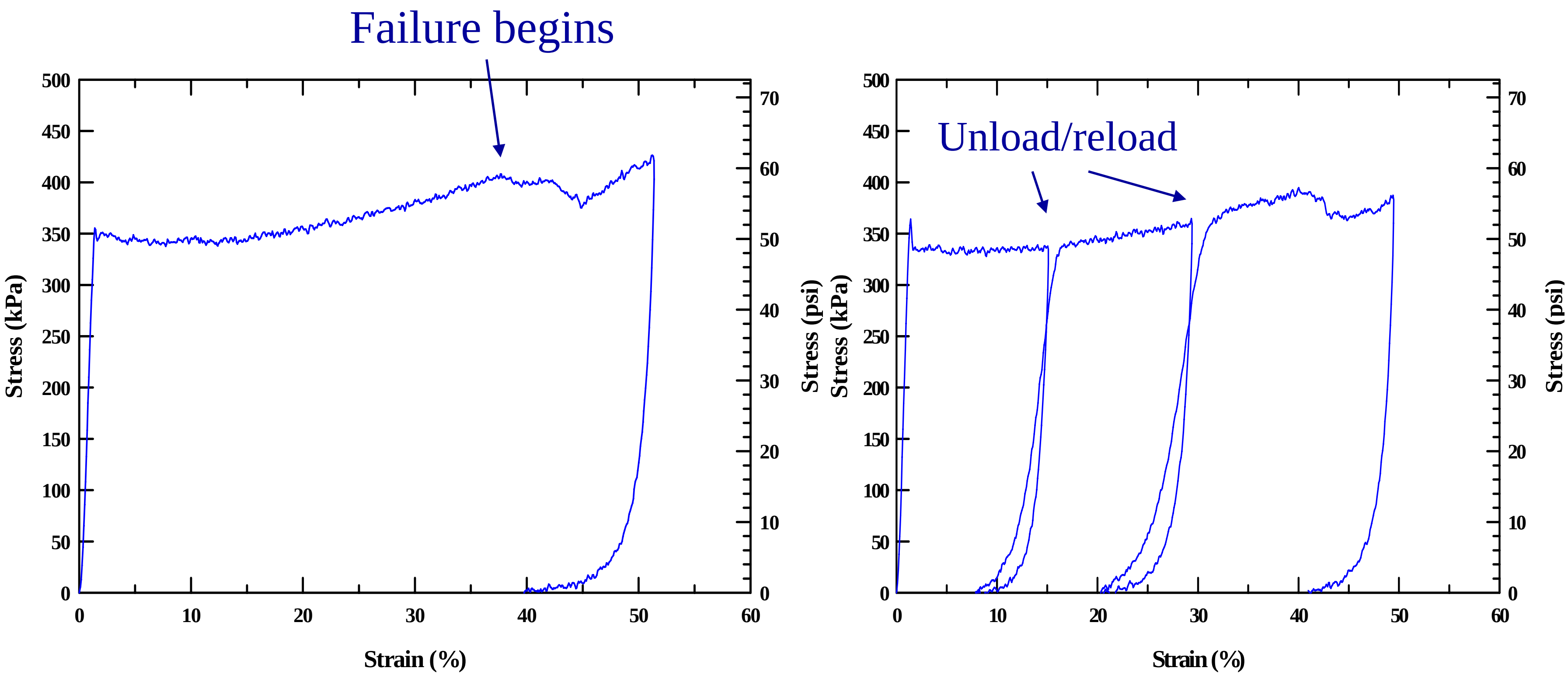

Crushing begins at 345 kPa (50 psi)

New EOS Model for Foam Insulation

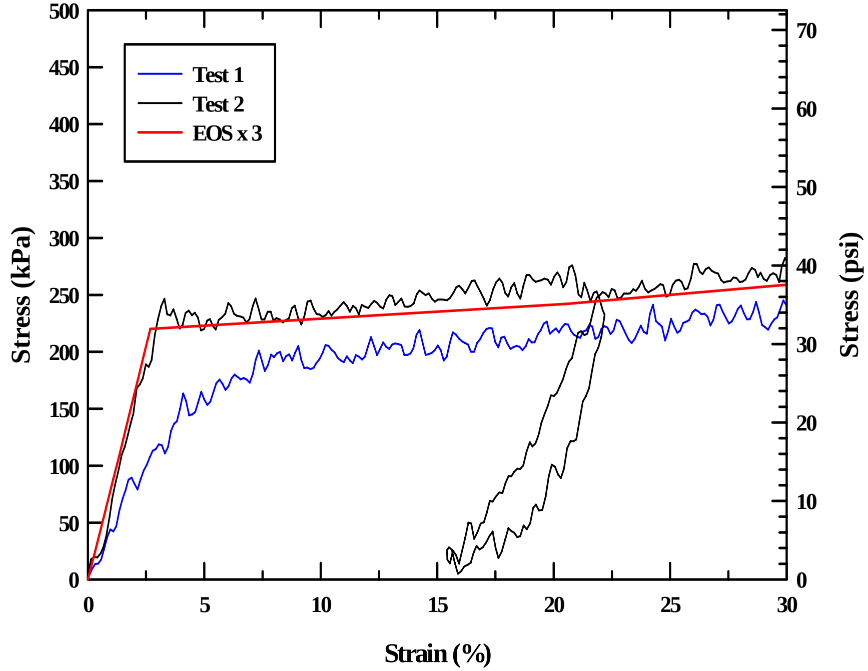

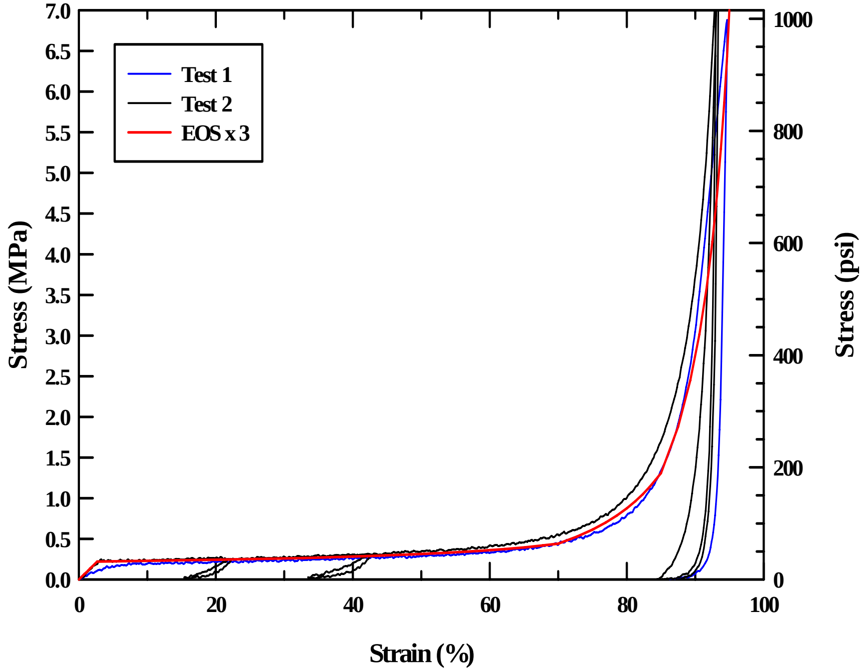

Enlargement of low strain region, blue and black are data, red is model

Full stress-strain curve, blue and black are data, red is model

Foam density is 0.03844 gm/cm^3 (2.4 lb/ft^3), initial crushup stress is 220 kPa (32 psi)

New EOS Model for Thermal Tile

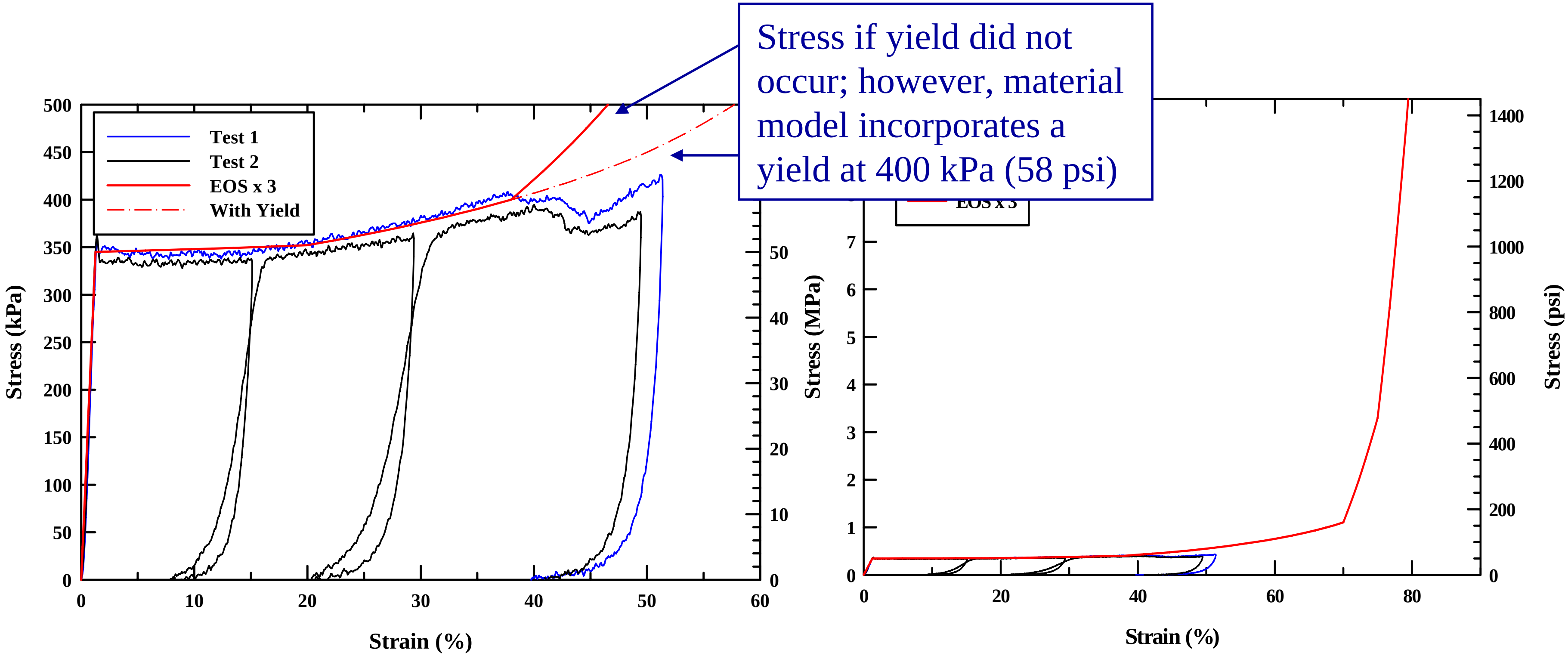

Enlargement of low strain region, blue and black are data, red is model

Full stress-strain curve, blue and black are data, red is model

Tile density is 0.18 gm/cm^3 (11.2 lb/ft^3), initial crushup stress is 345 kPa (50 psi)

Computations

Computations

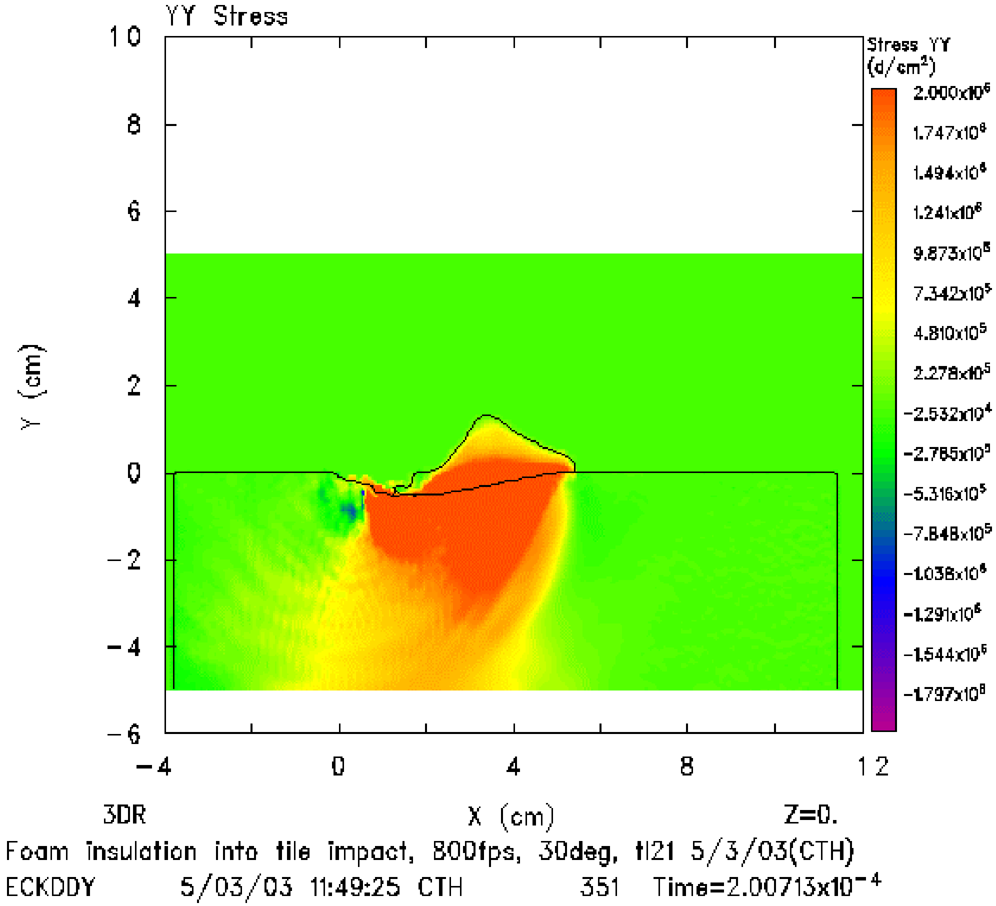

- Most computations were performed in 2D plane strain – however, there was excellent agreement between 2D plane strain and 3D.
- The normal stress was examined along the surface of the tile gages ("tracers") spaced 0.5 cm apart.
- The gage readings show the normal stress in the *y* direction at the respective location.
- Computations performed in CTH with new material models.

How Damage/No Damage was Decided

No Damage for 700 ft/s Impact at 15° Impact Angle

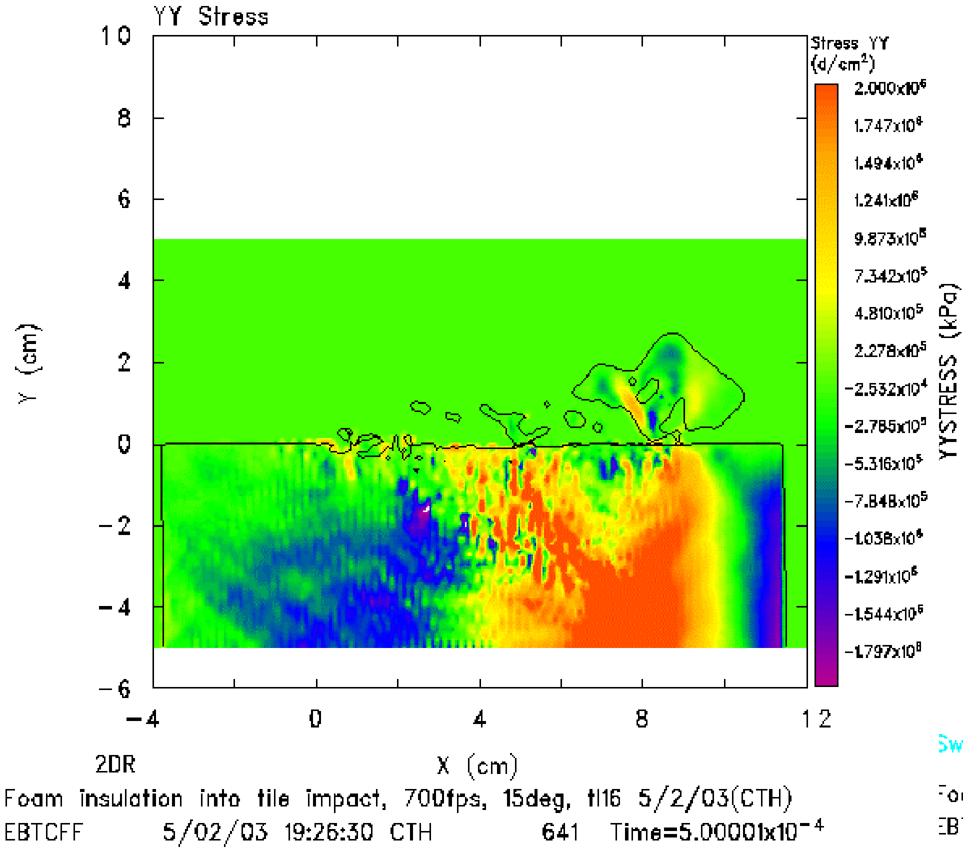

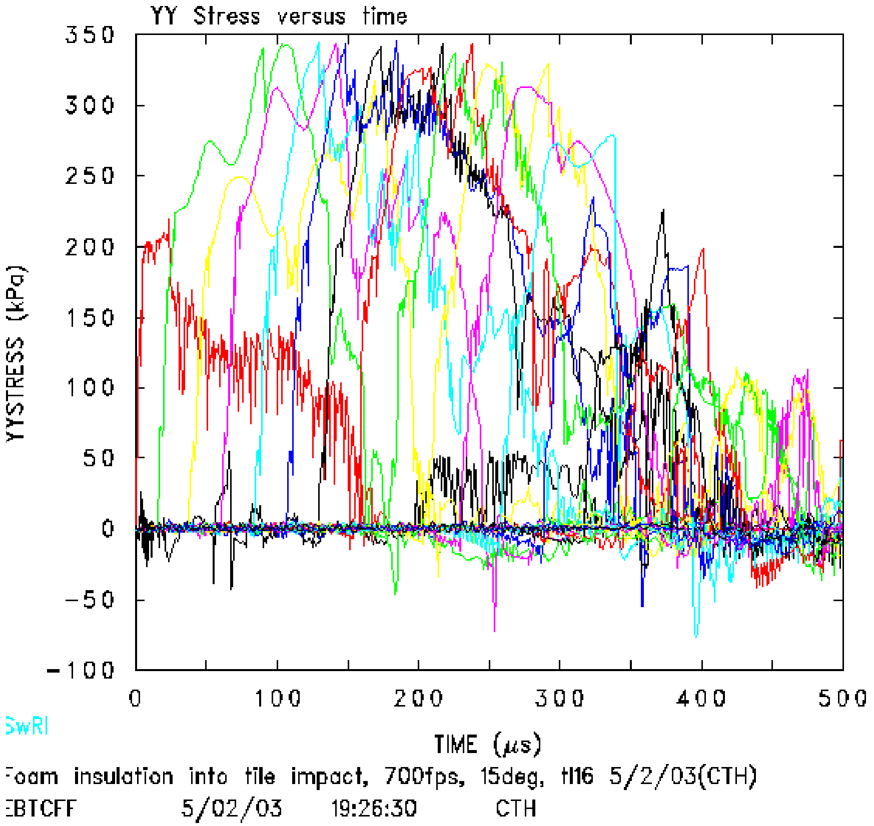

Tile surface mostly flat after impact; normal stresses are below 345 kPa (50 psi) tile crushup level

Crater for 700 ft/s Impact at 23° Impact Angle

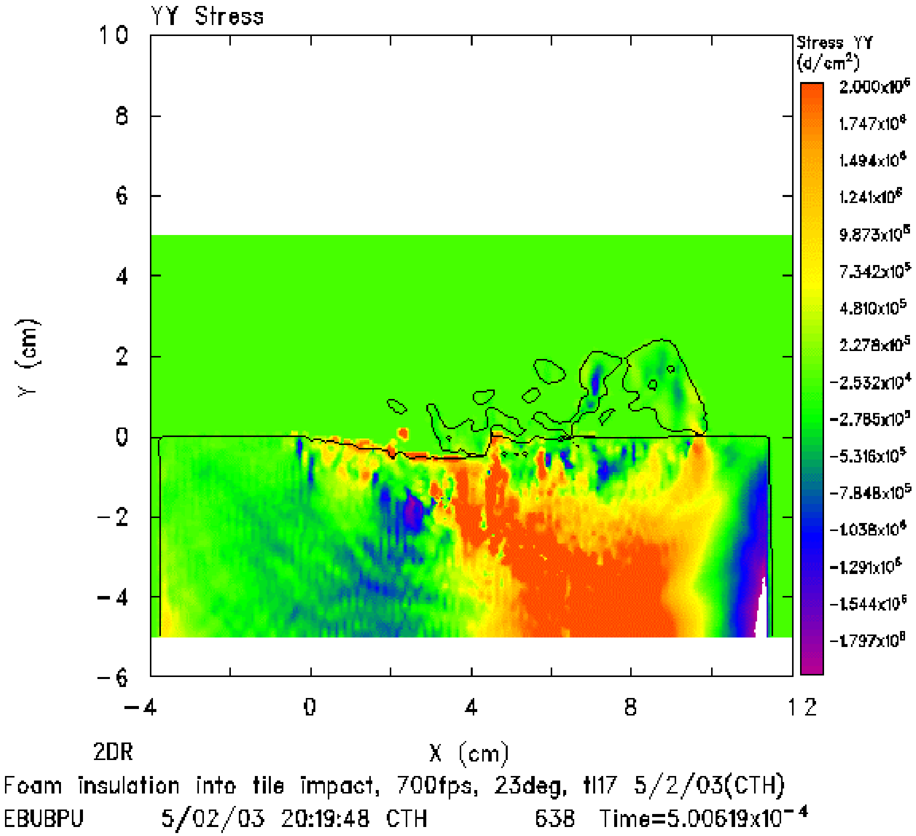

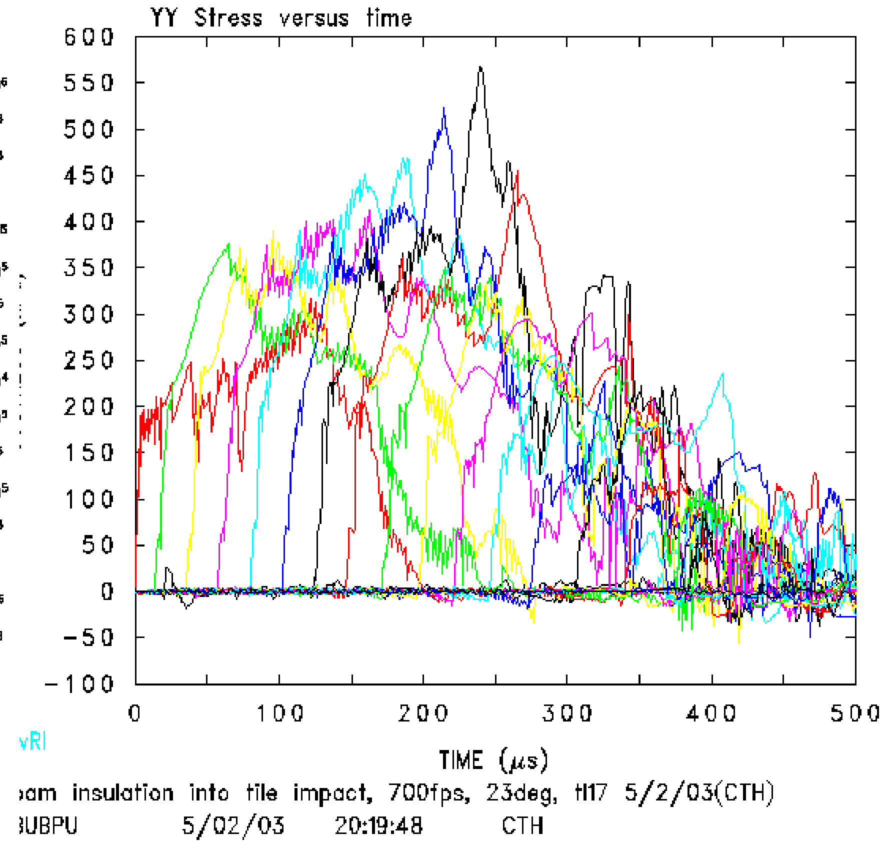

Crater (indention) seen in target; normal stresses are above 345 kPa (50 psi) tile crushup and 400 kPa (58 psi) tile yield/failure

Results on Damage/No Damage Transition Region

Damage/No Damage Transition

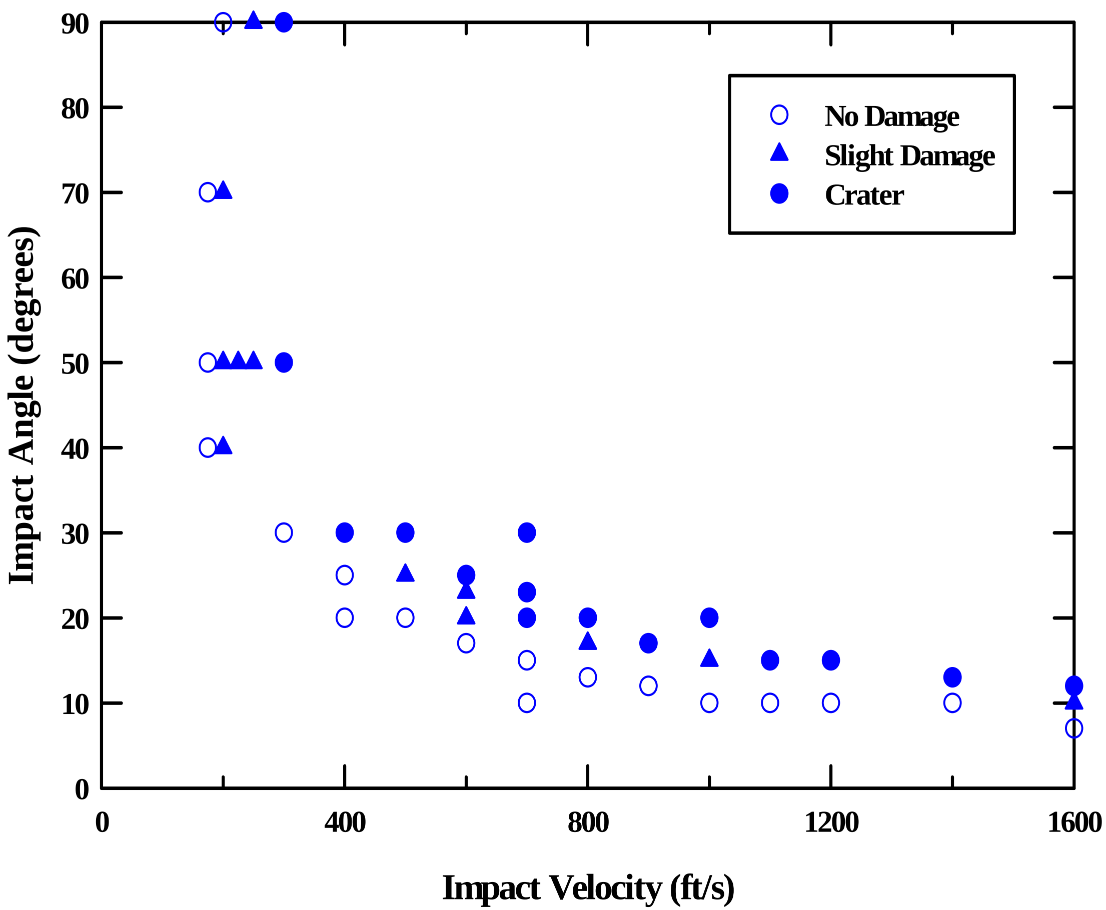

- Many CTH computations were performed using new EOS with 1” cubes of foam insulation impacting a tile.
- These computations allowed a determination of where the transition from no damage to damage occurred, in terms if impact velocity and impact angle.
- Figure shows results of computations.

Theory

- It is possible to determine the impact velocity at 90 degrees (flyer plate) at which the thermal tile just begins to crush. The velocity is given by

$$V_{crush} = u_{et} + u_{ef} + \frac{\sigma_{crush-t} - \sigma_{crush-f}}{\rho_{ef}(c_{1f} + u_{ef})}$$

where σ is stress, c is sound speed, subscript t refers to tile, f to foam, e to elastic, and

$$u_e = \sigma_{crush} / \rho_0 c_0, \qquad \rho_e = \rho_0 /(1 - u_e / c_e)$$

- When computed, V_{crush} = 68.2 m/s (224 ft/s). This value was confirmed by 1D CTH computations.

Theory

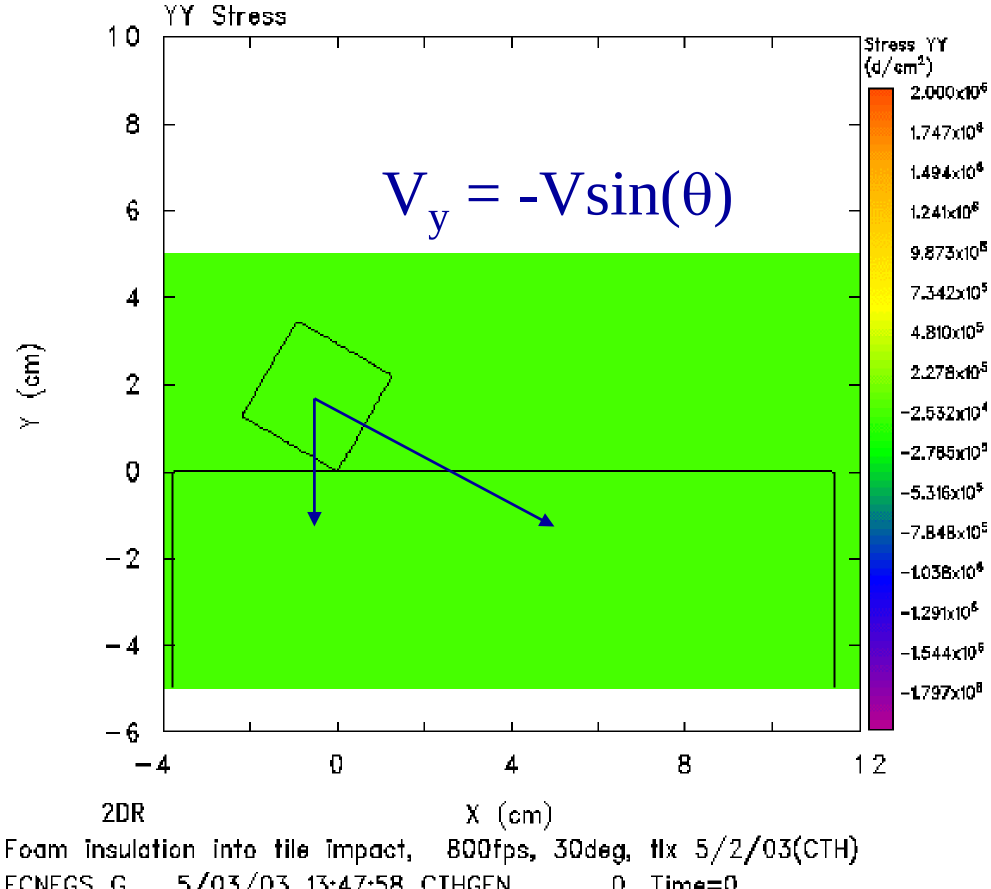

- When foam impacts the tile at an angle, the horizontal and downward components of the velocity interact nearly separately if the interface remains relatively flat.
- Thus, crushing of the thermal tile would be expected when

$$V = \frac{V_{crush}}{\sin(\theta)}$$

Damage/No Damage Transition

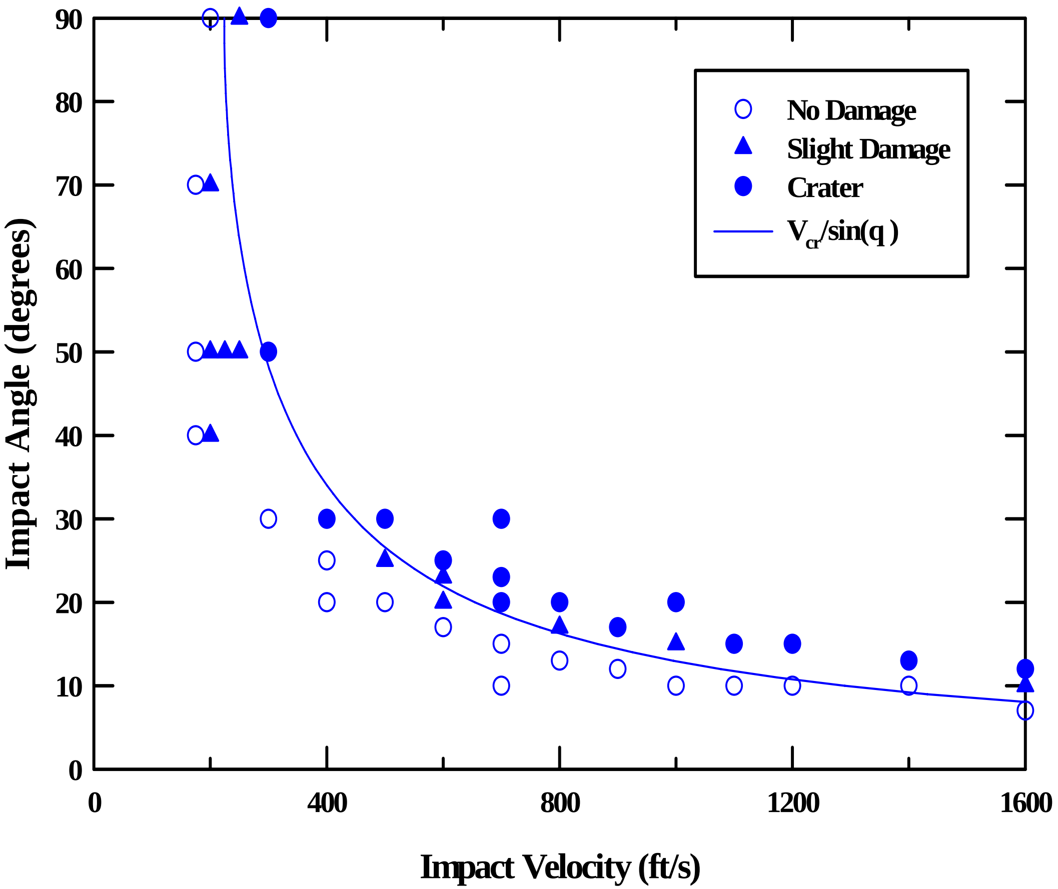

- When the computed V_{crush} = 68.2 m/s (224 ft/s) is used, good agreement is obtained with the computational results.

Damage/No Damage Transition

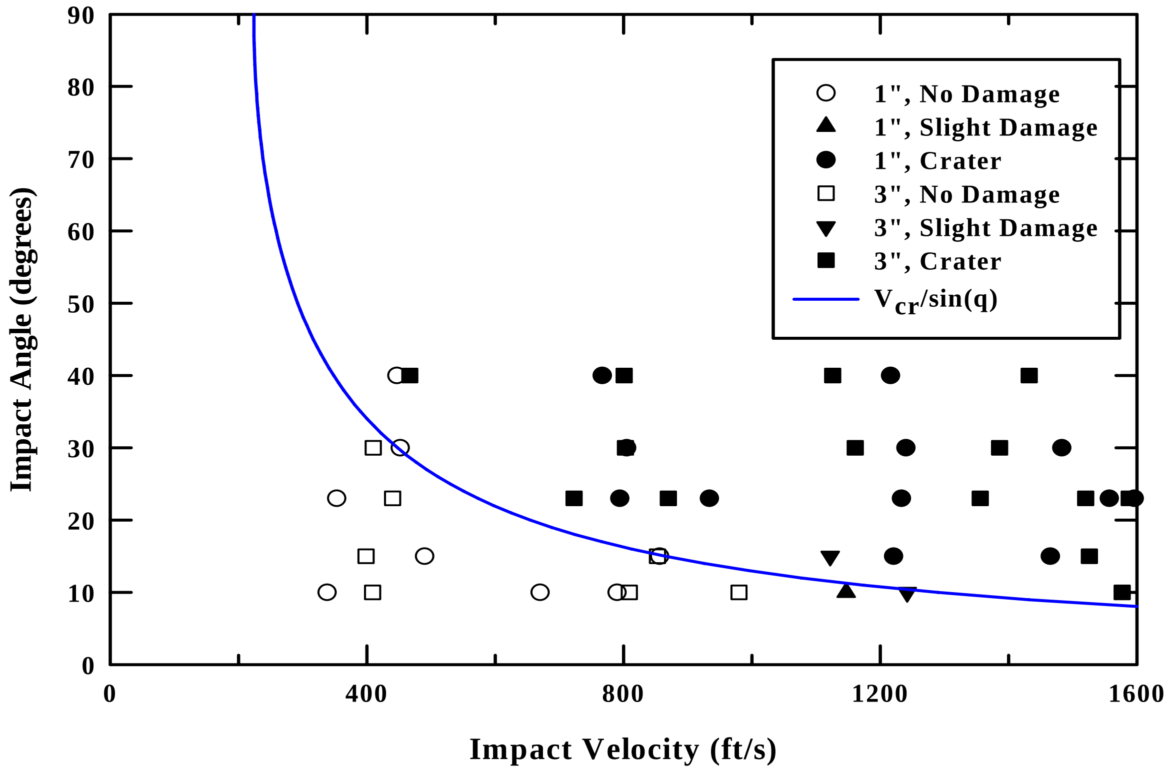

1999 foam impact data with 1” square cross section

Damage/No Damage Transition

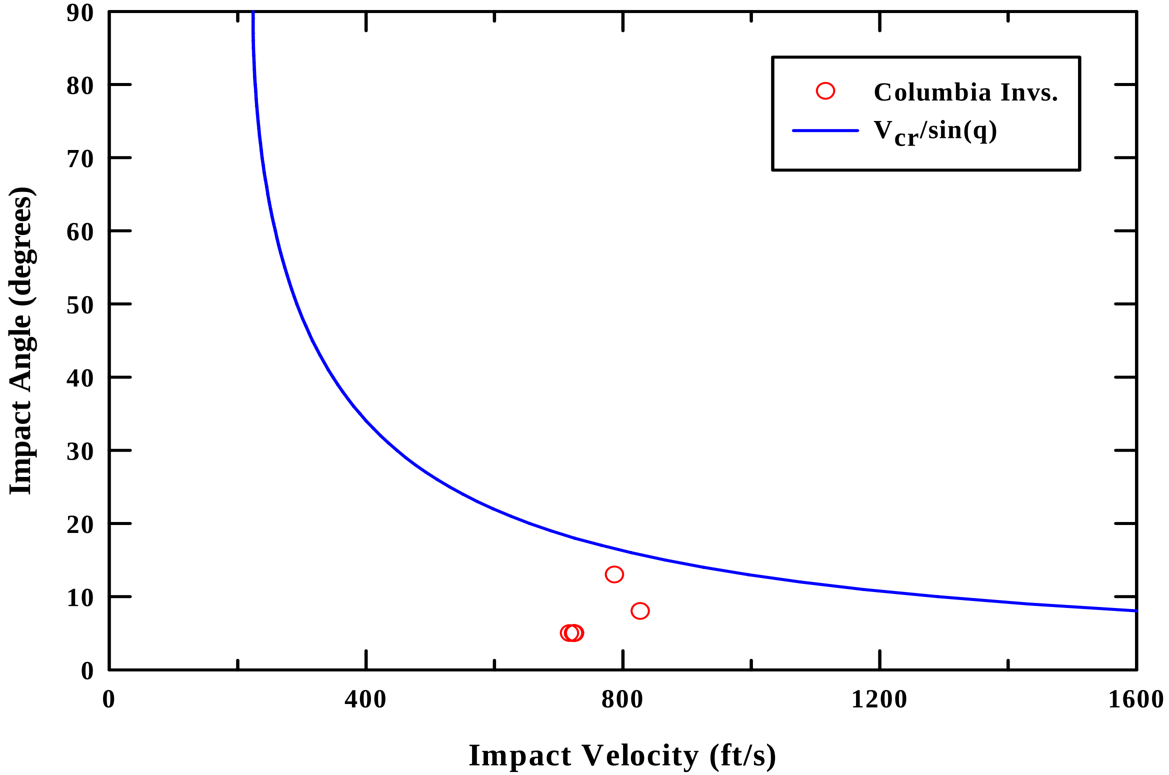

Five impact tests during Columbia investigation (minimal damage)

Damage/No Damage Transition

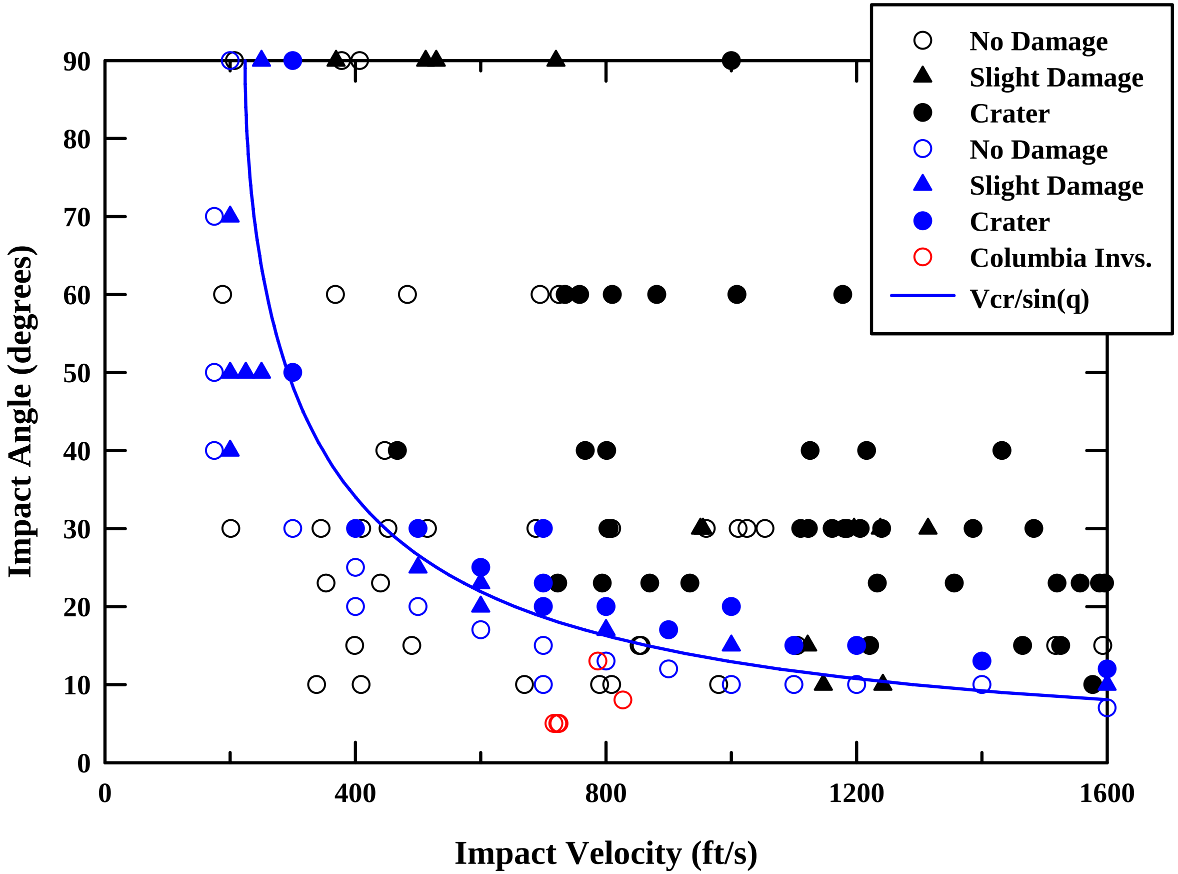

- All the foam data is plotted from Rand's 1979 report, SwRI's 1999 report and the Columbia investigation; there is good agreement with the theoretical curve.

RCC Panels 6 and 8 Tests

Final Estimates of Foam Path

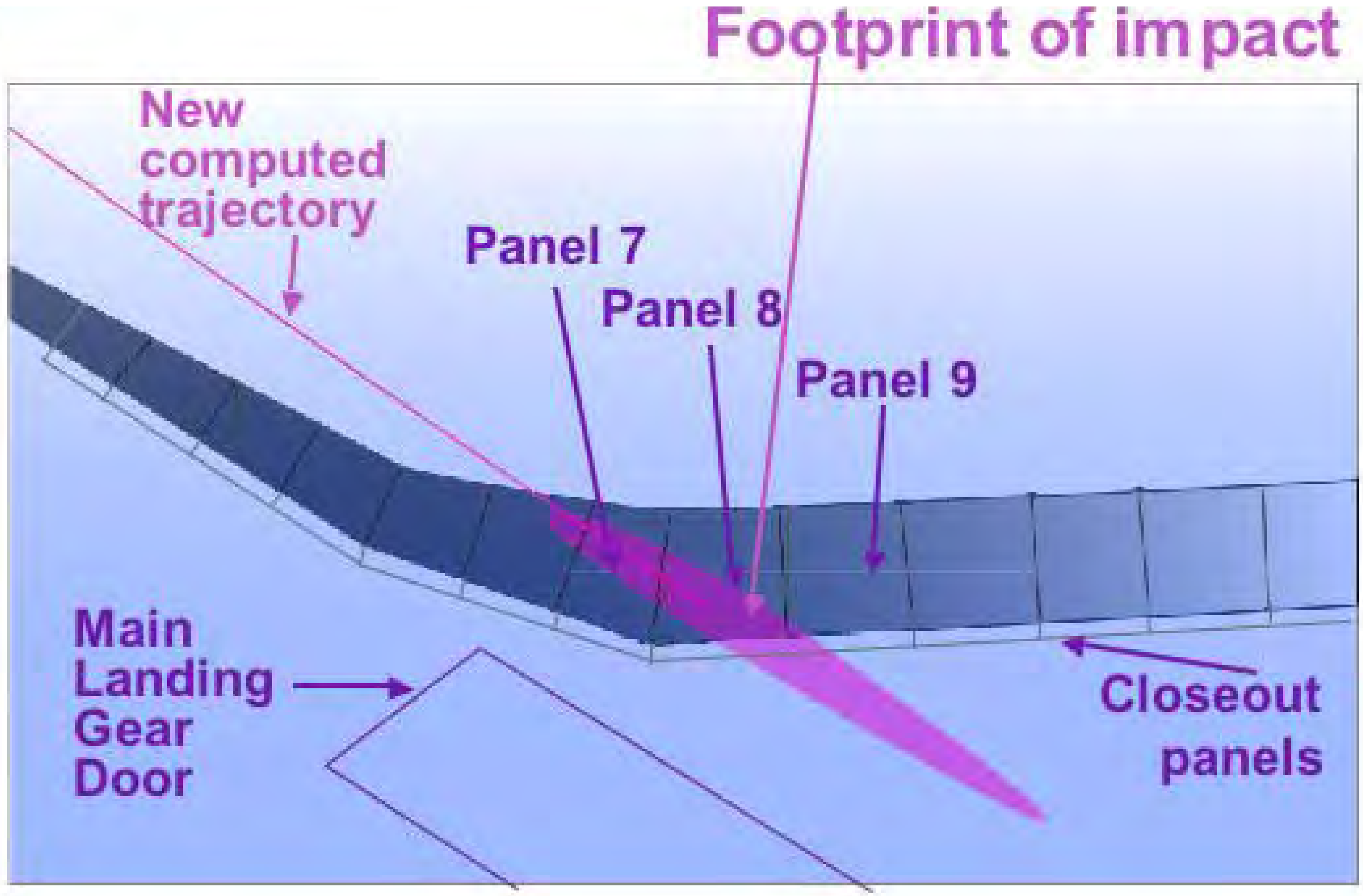

Leading Edge Test Article

Leading Edge Structural Subsystem

Test Article

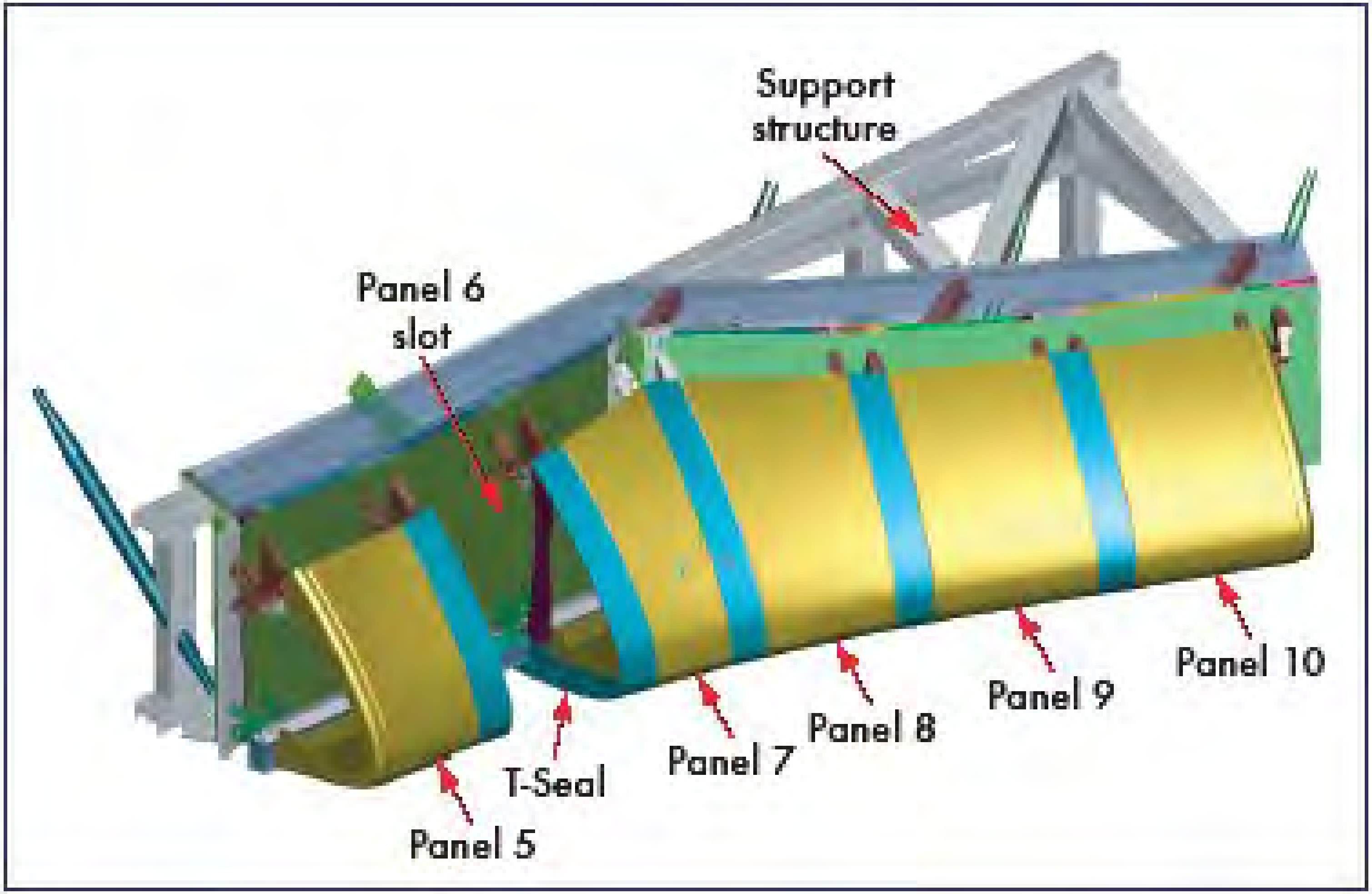

Interior Cameras and Gages

- Up to 16 high-speed video cameras were used per test (up to 8 outside of the target, up to 8 inside the target).
- Up to 250 channels of strain gage, accelerometer and load cell data were collected.

Exterior Cameras

RCC Panel 6 Test

- RCC Panel 6 had flown 30 flights on *Discovery*.
- The test resulted in a cracked rib.
- Damage thought insufficient to cause the loss of the vehicle.

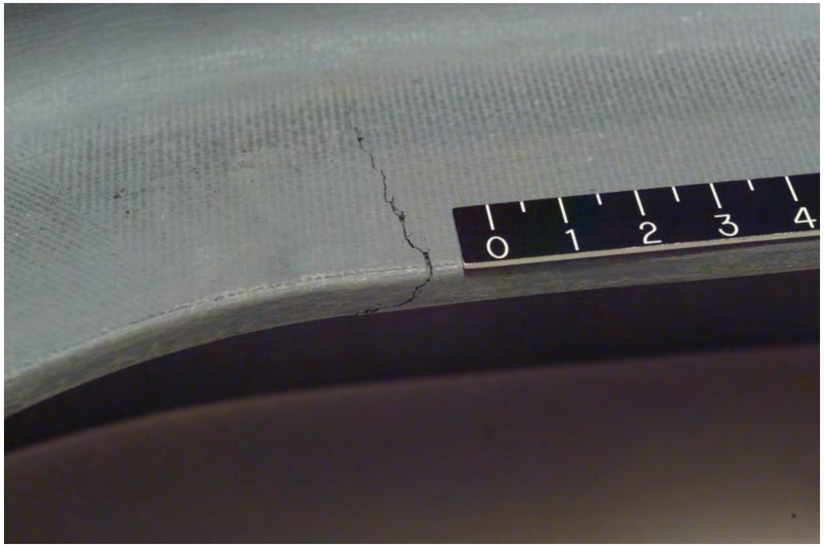

RCC Panel 8

RCC Panel 8

- RCC Panel 8 had flown 26 missions on *Atlantis*.

RCC Panel 8

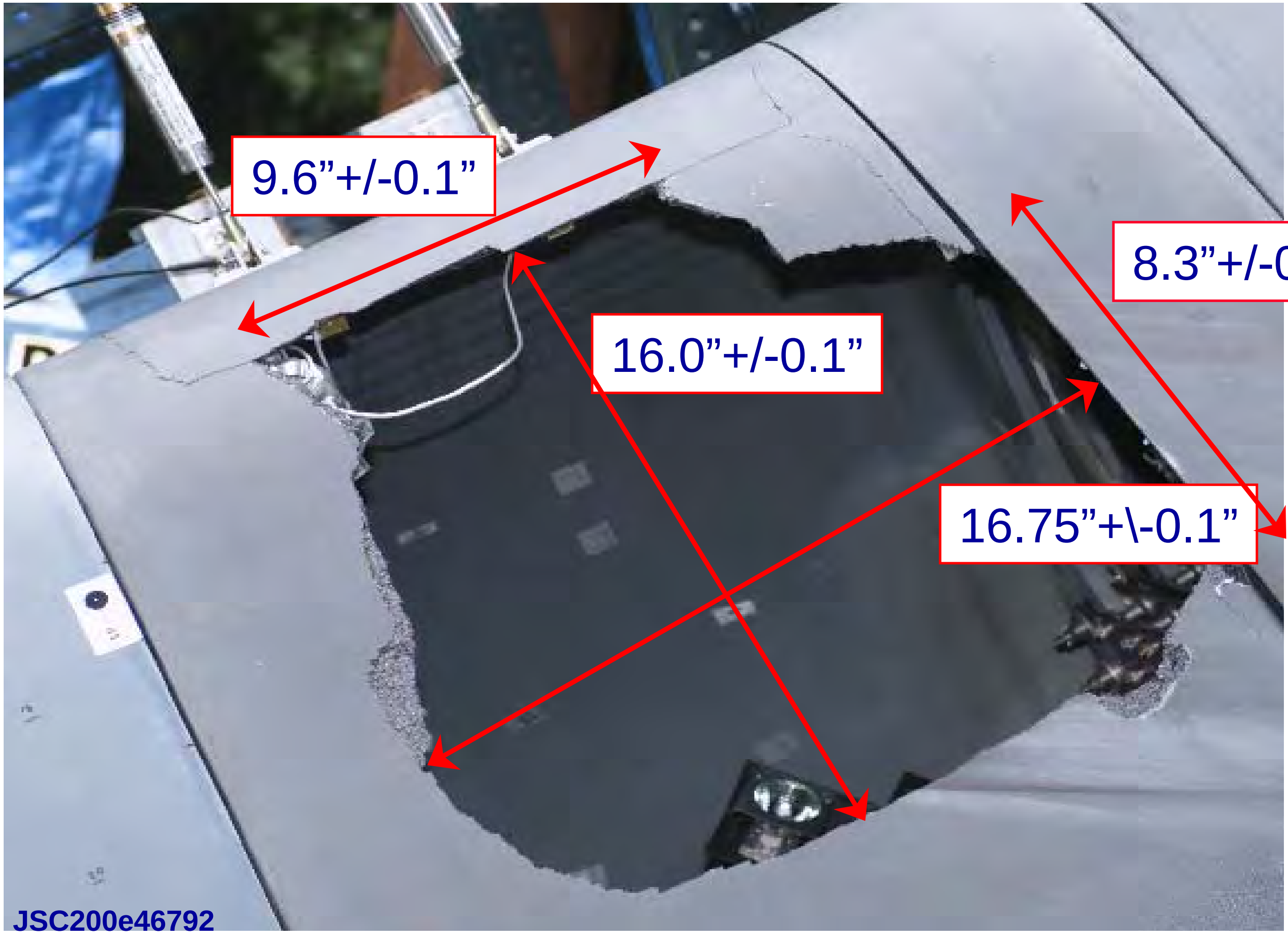

Modeling Foam Insulation Impact on RCC Panels 6 and 8

Experimental Results RCC Panel 6

Replicating RCC Panel 6 Test

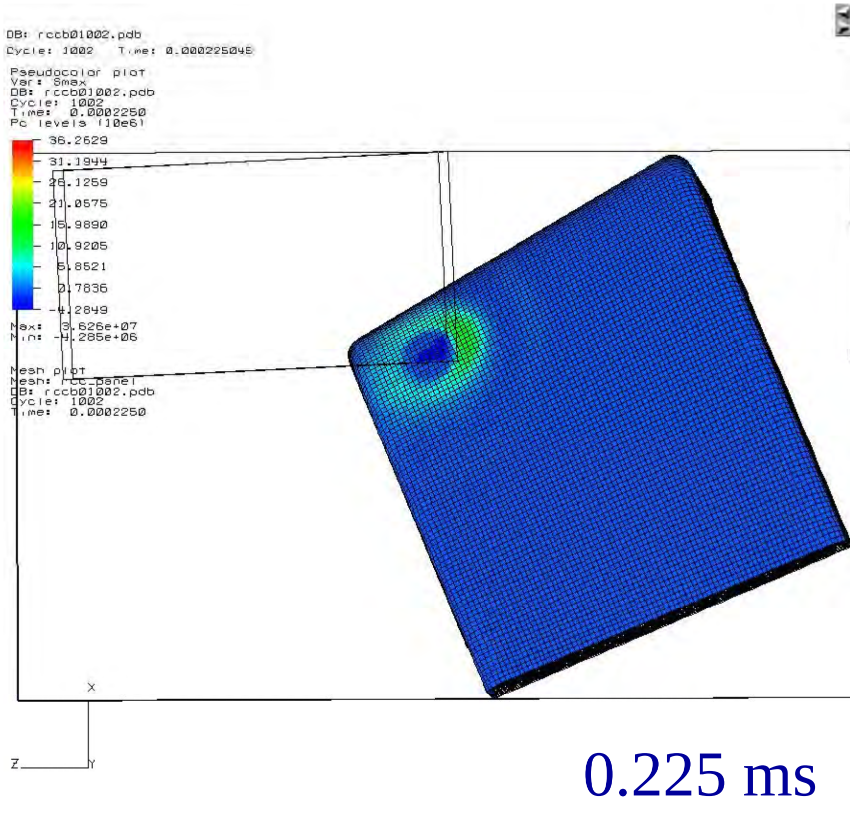

0.225 ms

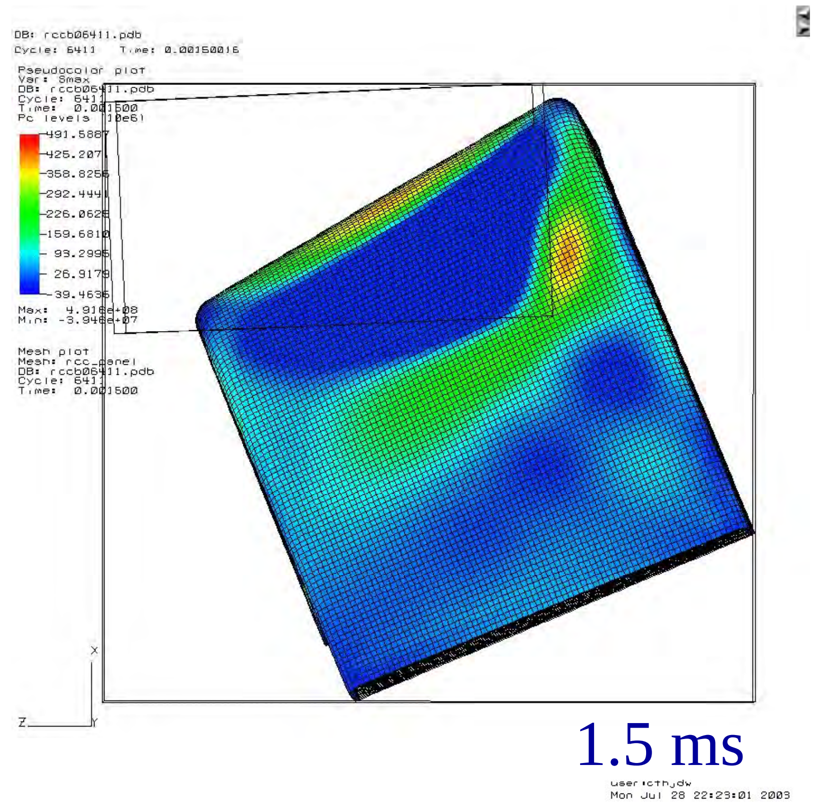

1.5 ms

- The impact point 0.83” left from the 5-6 T-seal, 18.7” up from the carrier panel.
- Flight direction: α=5.5° (bottom to top), β=2.5° (away from center).
- The impact velocity was 768 ft/s, computation carried out to 5 ms.

Replicating RCC Panel 6 Test

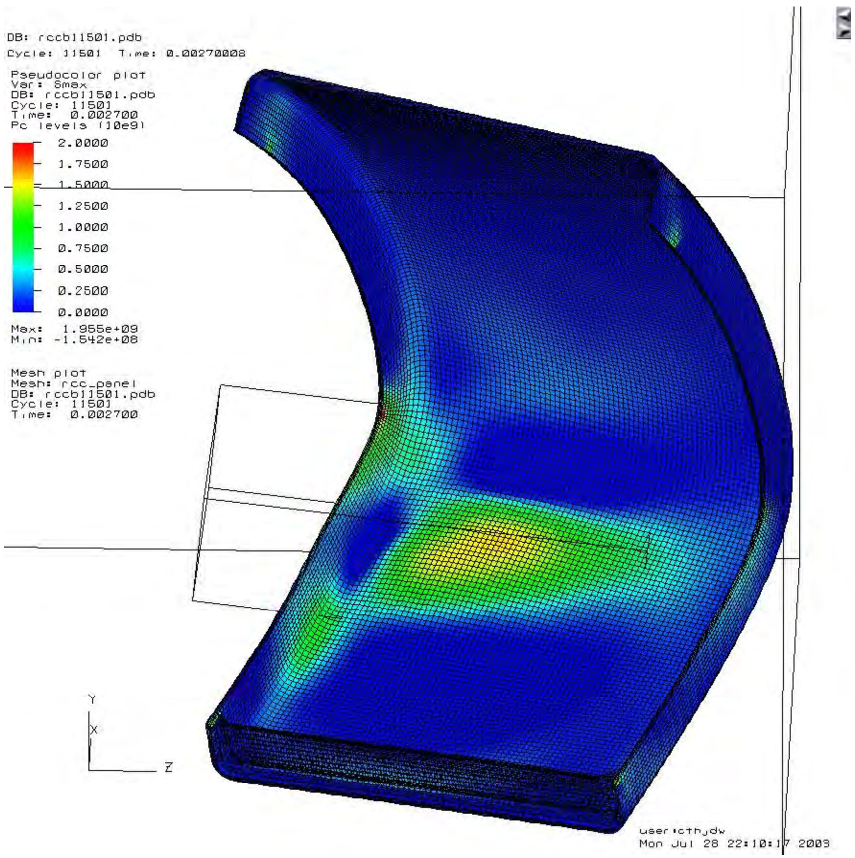

2.7 ms

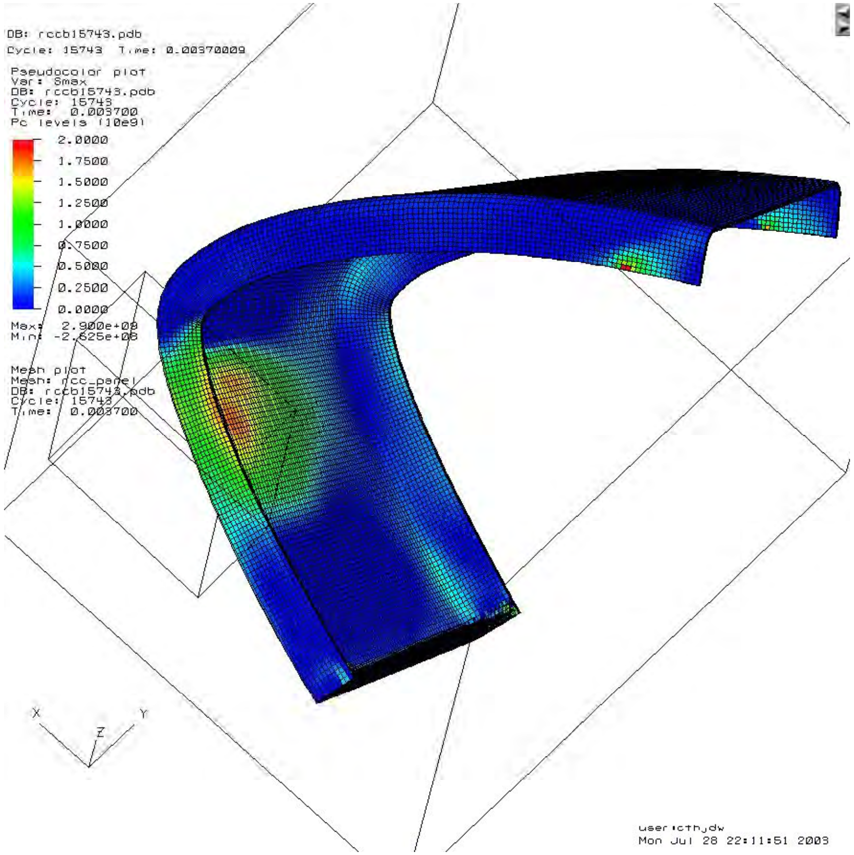

3.7 ms

Experimental Results RCC Panel 8

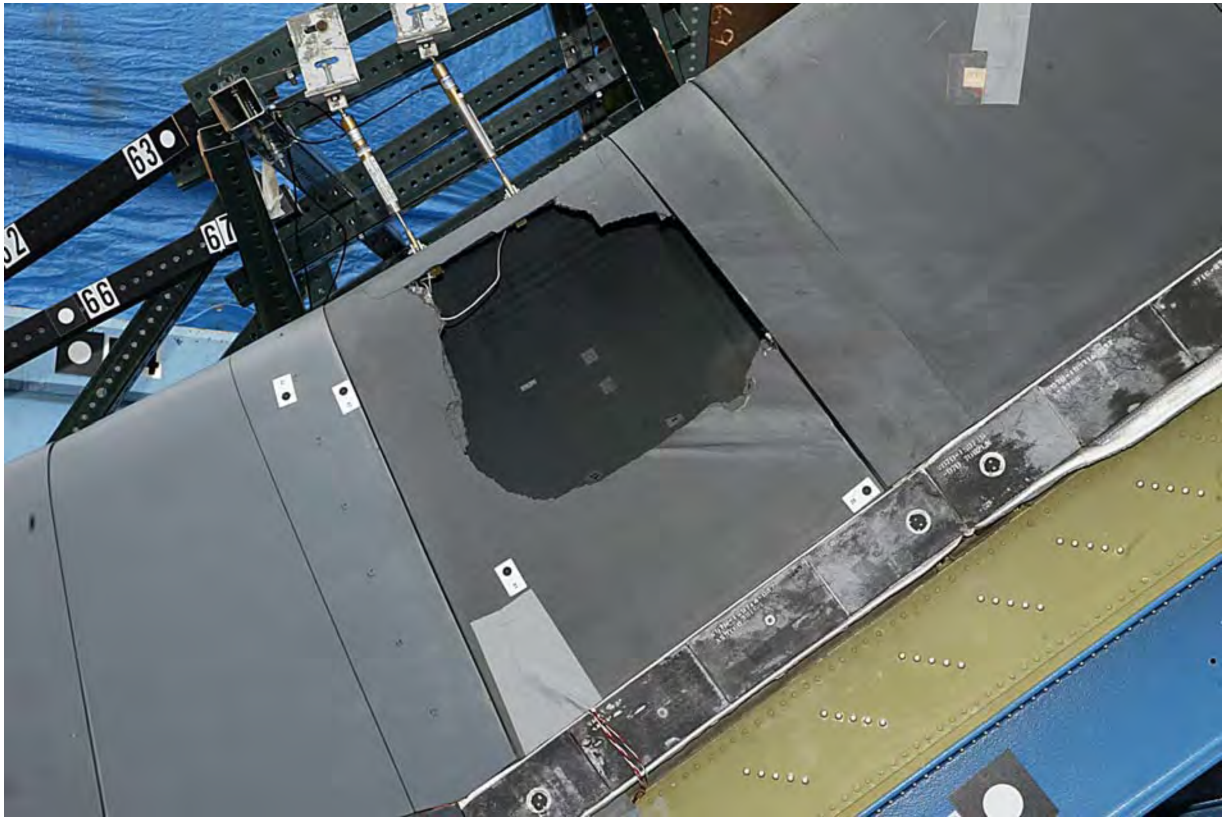

Replicating RCC Panel 8 Test

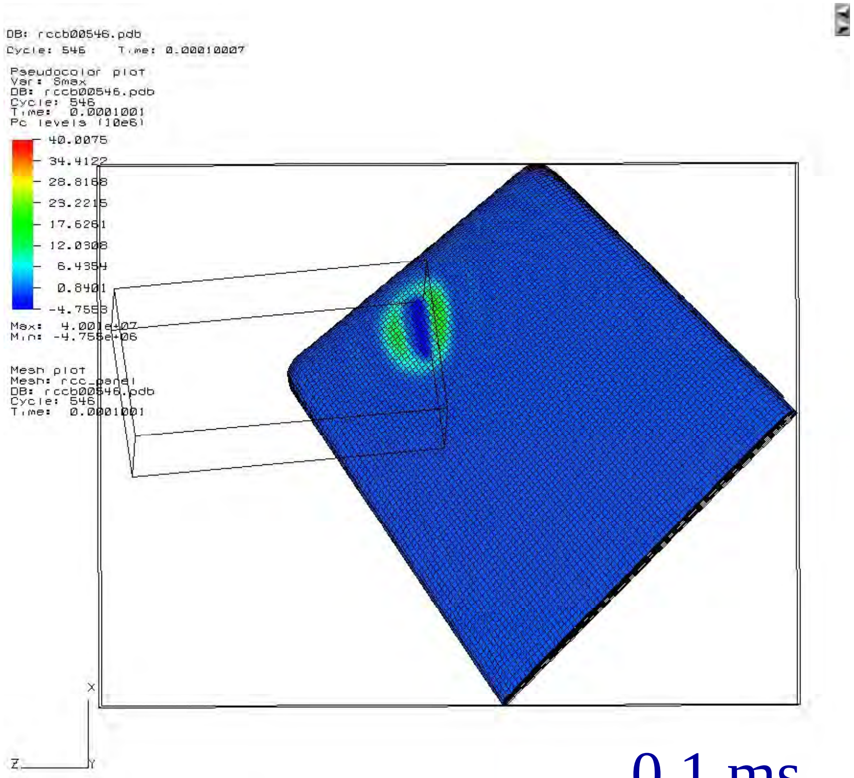

0.1 ms

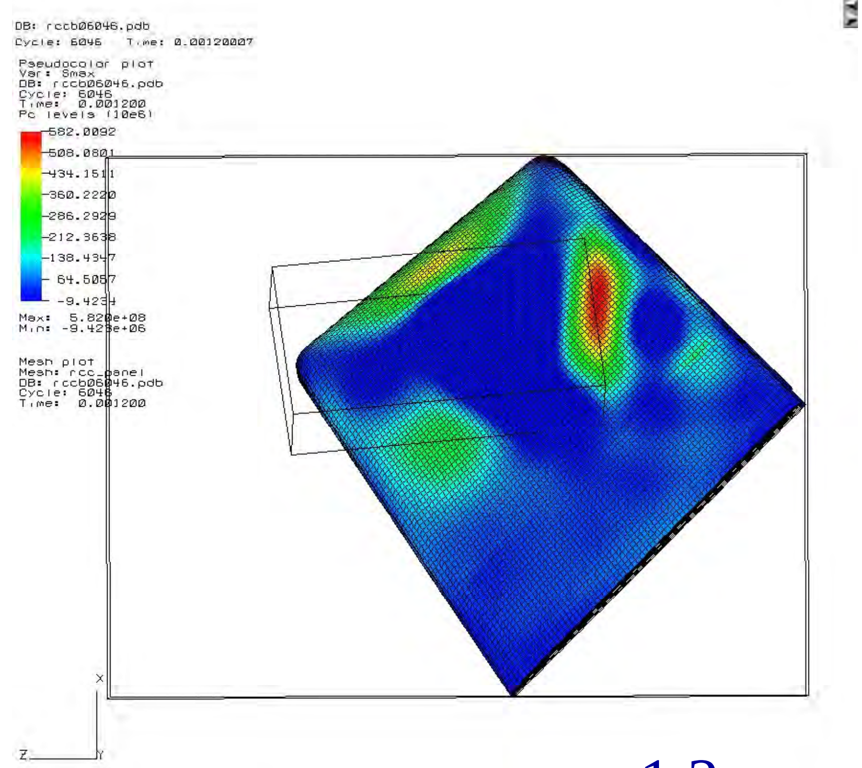

1.2 ms

- The impact point 7.3” left from the 7-8 T-seal, 25.5” up from the carrier panel.
- Flight direction: α=5.5° (bottom to top), β=5.0° (away from center), 30° clocking.
- The impact velocity was 777 ft/s, computation carried out to 5 ms.

Replicating RCC Panel 8 Test

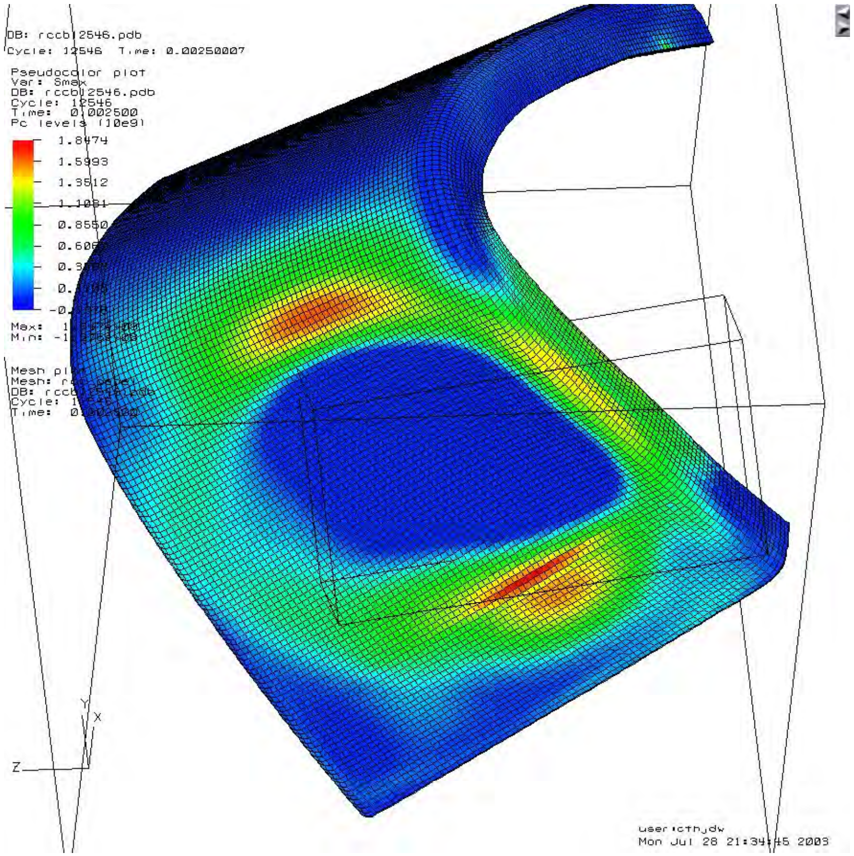

2.5 ms

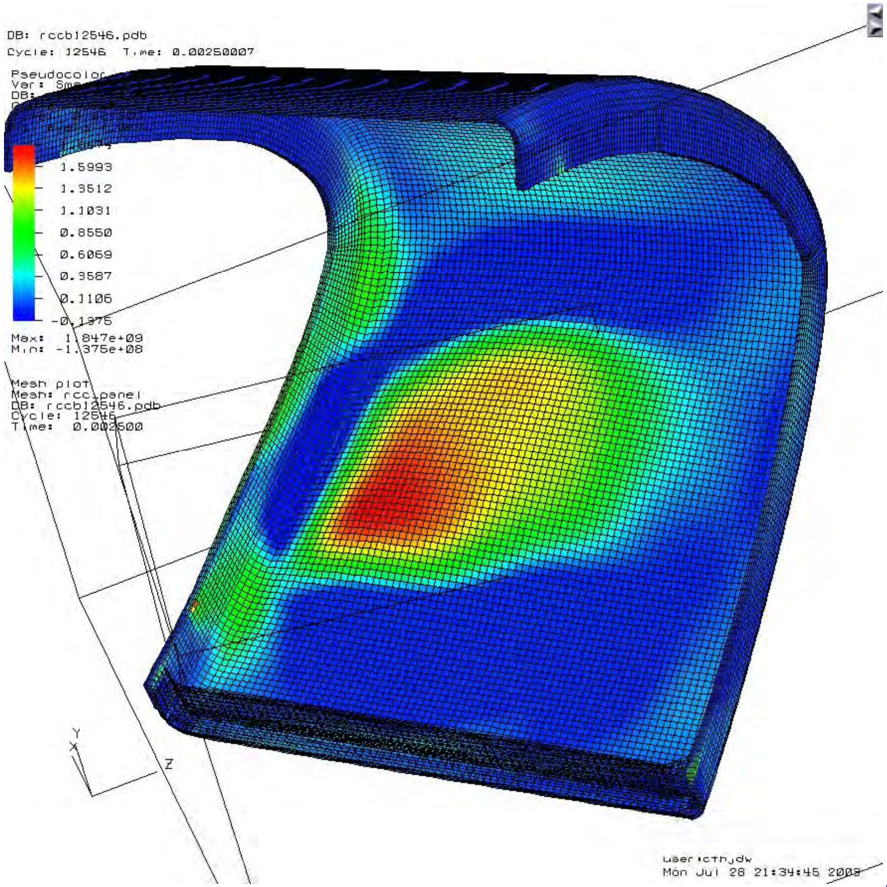

2.5 ms

Loading Footprint

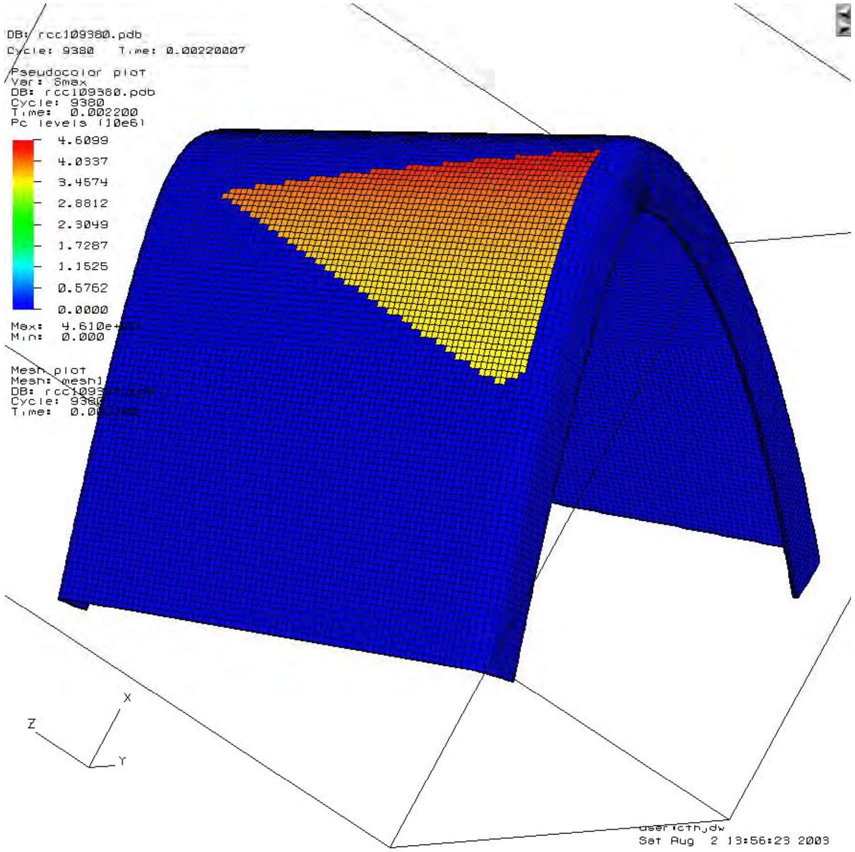

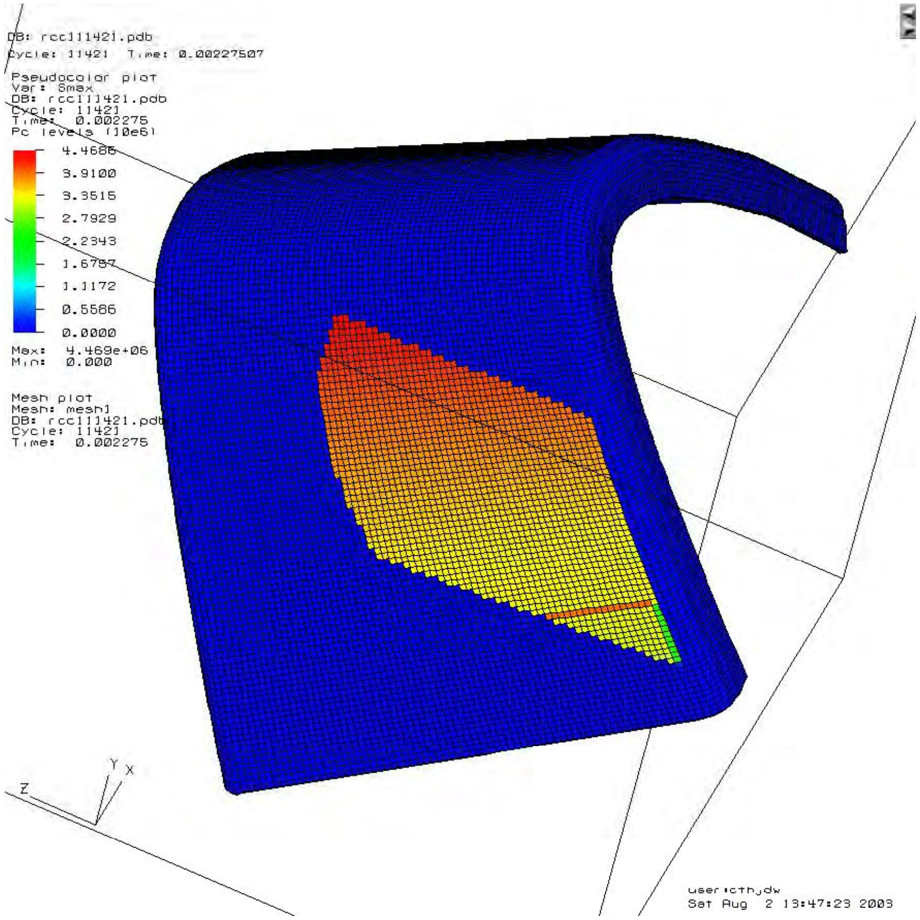

RCC panel 6 impact

RCC panel 8 impact

Stresses RCC Panels 6 and 8

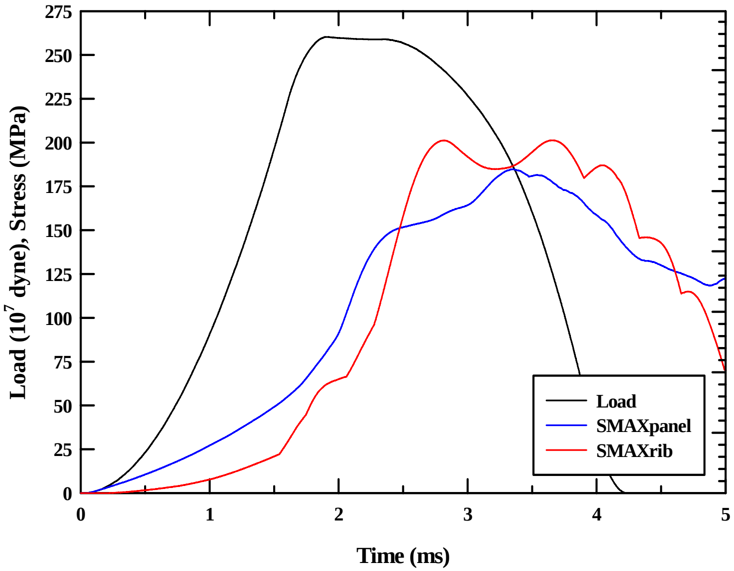

RCC Panel 6

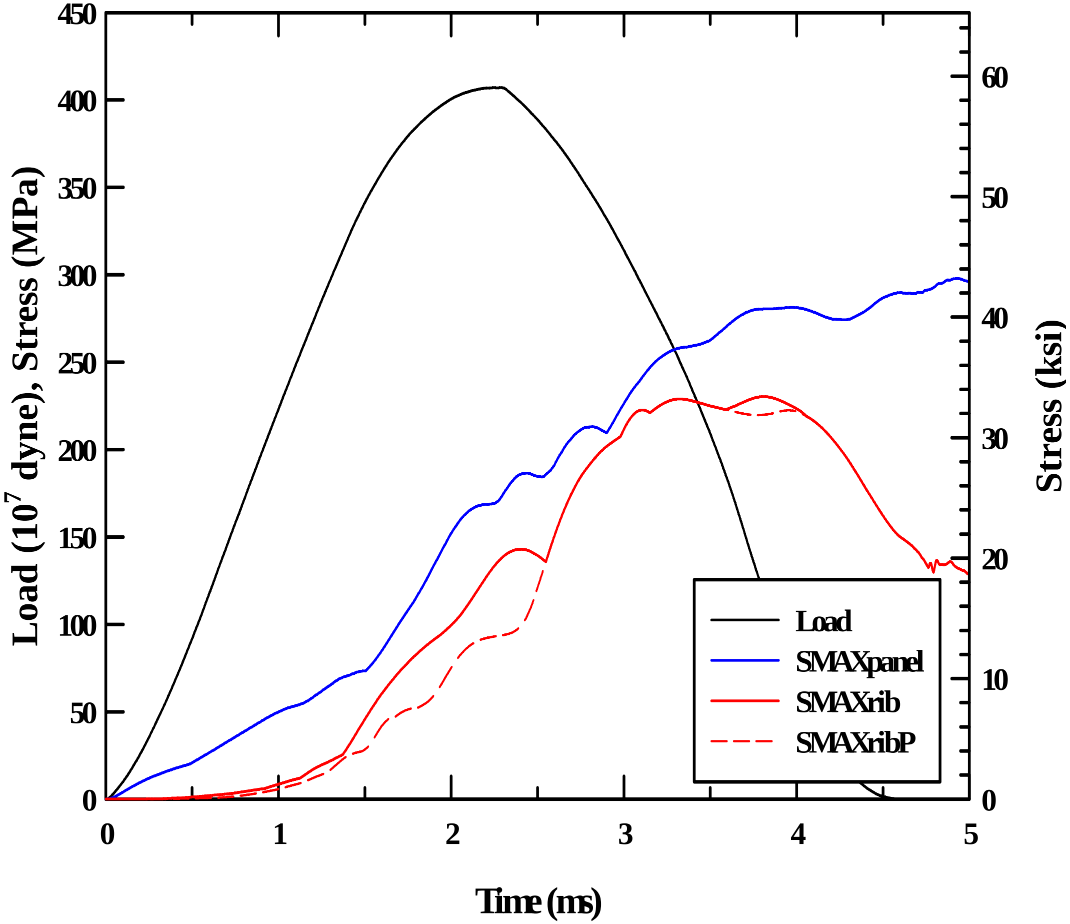

RCC Panel 8

Investigation Conclusions

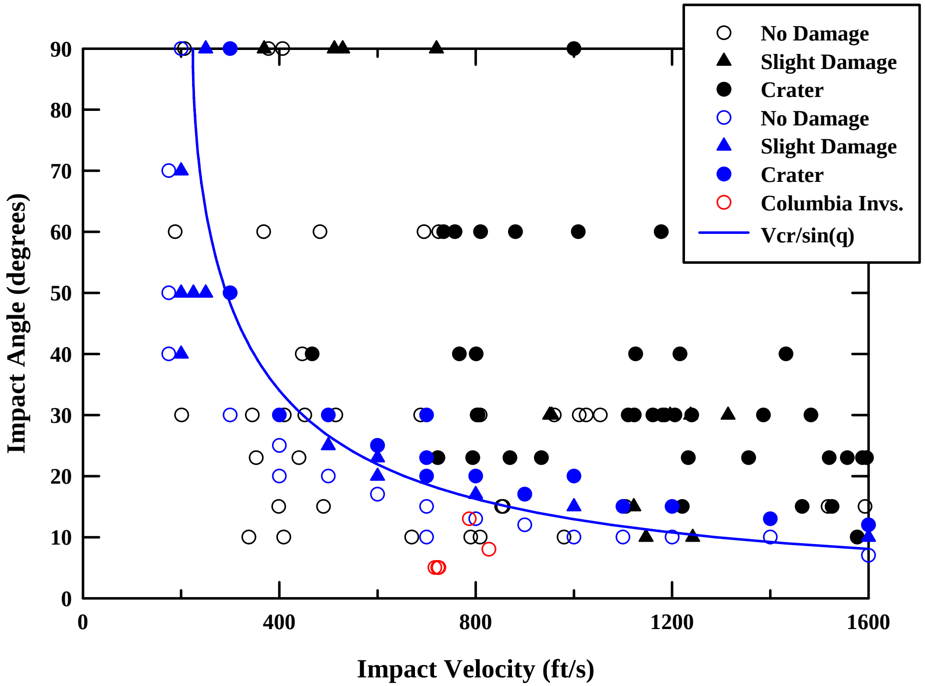

- The component of velocity normal to the impact surface determines the local loading pressure.
- Modeling and experiments showed that an impact on the underside of the wing was not the cause of the accident.
- Forensics, experiments and modeling showed that the loss of *Columbia* was due to a foam impact on RCC panel 8.

The Physical Cause

The physical cause of the loss of Columbia and its crew was a breach in the Thermal Protection System on the leading edge of the left wing. The breach was initiated by a piece of insulating foam that separated from the left bipod ramp of the External Tank and struck the wing in the vicinity of the lower half of Reinforced Carbon-Carbon panel 8 at 81.9 seconds after launch. During re-entry, this breach in the Thermal Protection System allowed superheated air to penetrate the leading-edge insulation and progressively melt the aluminum structure of the left wing, resulting in a weakening of the structure until increasing aerodynamic forces caused loss of control, failure of the wing, and breakup of the Orbiter.

SwRI Three-Pronged Approach

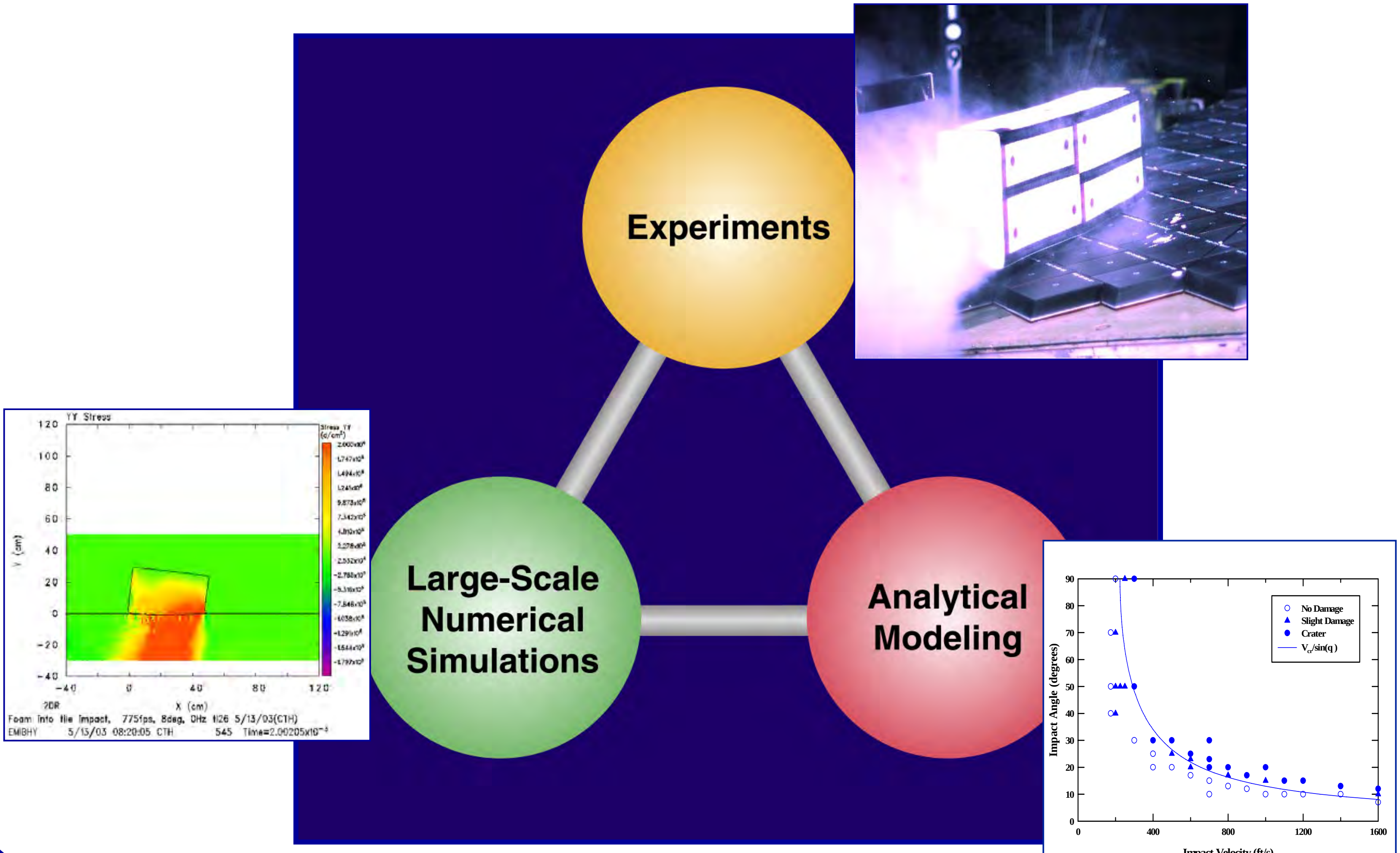

Return to Flight

CAIB Recommendations R3.2-2 Estimate Risk

- Initiate a program designed to increase the Orbiter's ability to sustain minor debris damage by measures such as improved impact-resistant Reinforced Carbon-Carbon and acreage tiles. This program should determine the actual impact resistance of current materials and the effect of likely debris strikes. [RTF]

CAIB Recommendation R3.8-2
Impact Damage Models

- Develop, validate, and maintain physics-based computer models to evaluate Thermal Protection System damage from debris impacts. These tools should provide realistic and timely estimates of any impact damage from possible debris from any source that may ultimately impact the Orbiter. Establish impact damage thresholds that trigger responsive corrective action, such as on-orbit inspection and repair, when indicated.

Foam and Ice on the External Tank

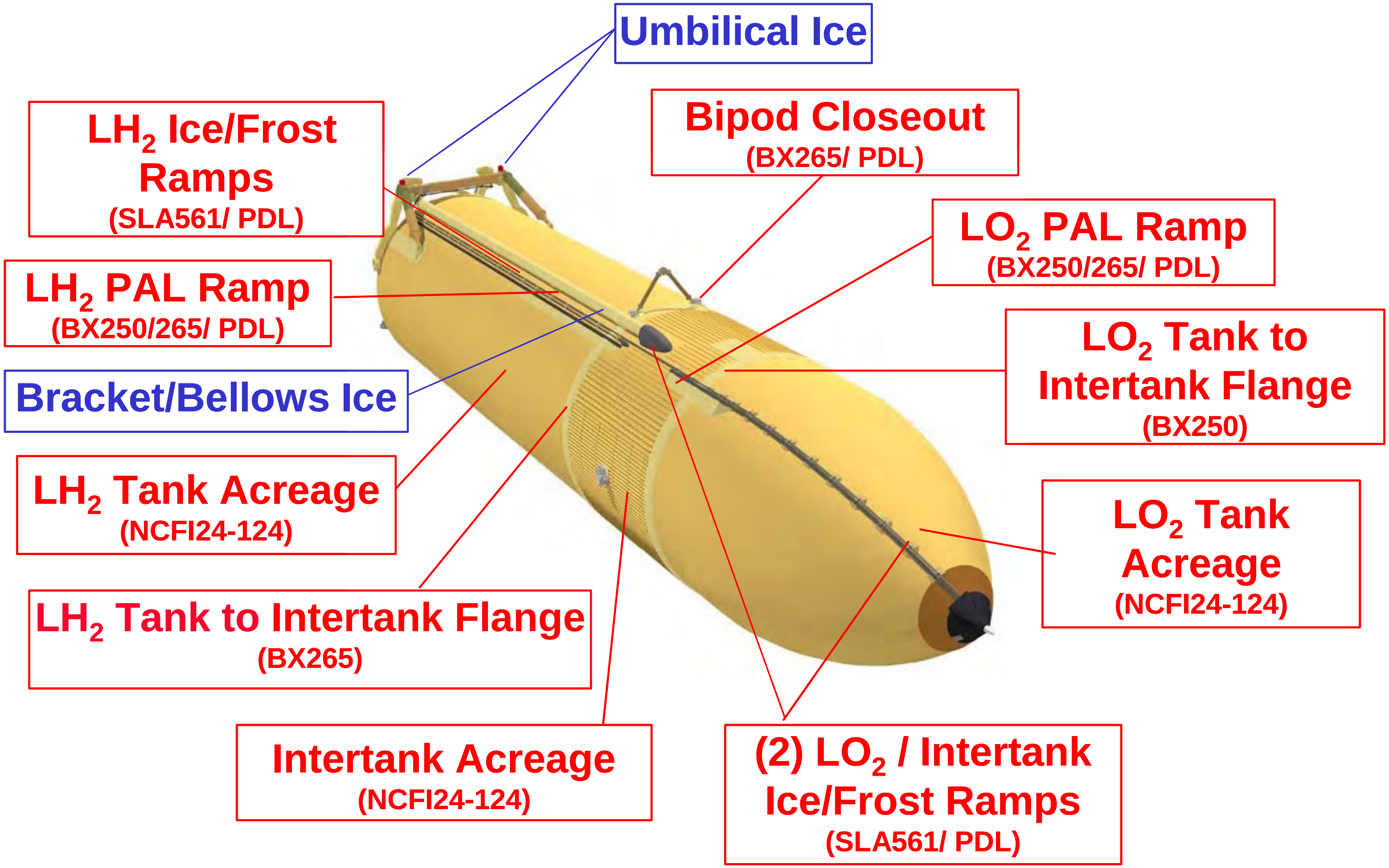

Impacts into Thermal Tiles

Physics-Based Impact Models: Inputs and Outputs

Specific Impact Event Input:

Impactor denstity: ρ_p

Impactor Dimensions:
Length L, Width W, Height H

Impact Velocity V and Angle θ

Large compression crush-up curve required (foam)

Projectile fracture (ice)

Foam, Ice and Ablator Impact Models

Tile Material Properties:

Large compression crush-up curve required (stress vs. strain in compression up to 90% compression)

Output: Computed Crater Dimensions

Depth, Length, Width

Our Validation Triangle

When experiments, large-scale numerical simulations and the analytical physics-based model agree, the physics-based model is assumed to be validated.

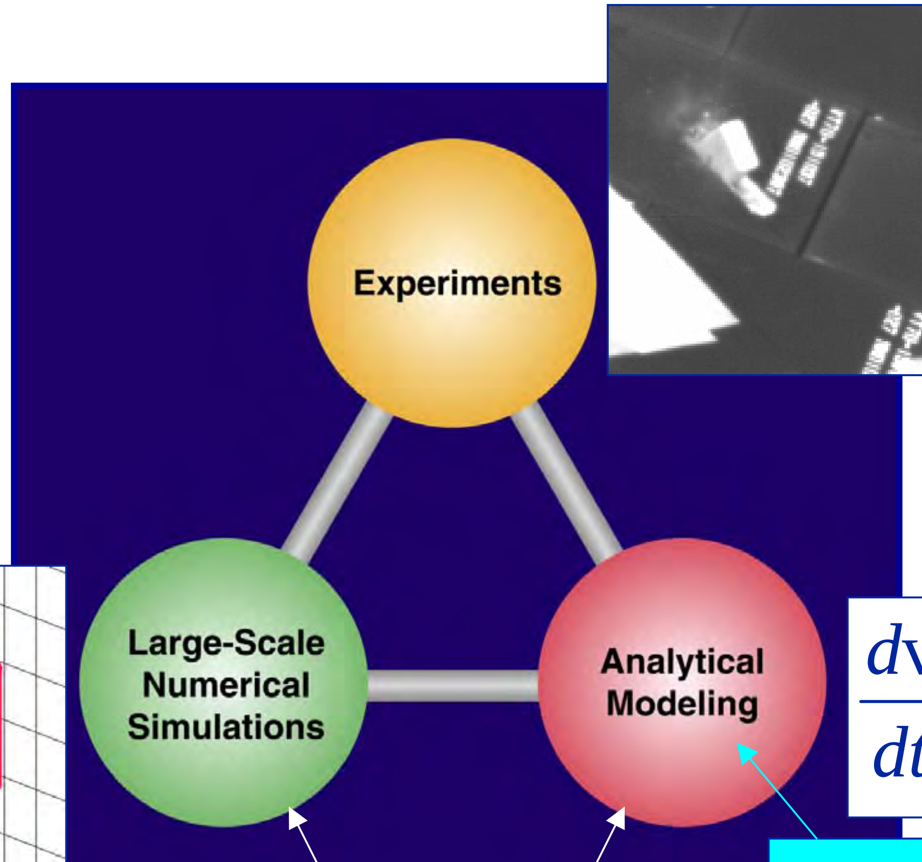

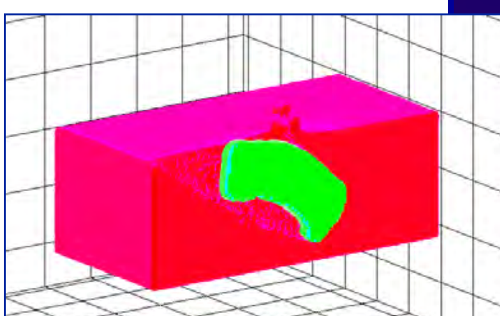

$$\frac{d\mathrm{v}}{dt} = -\frac{\sigma_{zz}(\mathrm{v})}{\rho_p L}$$

Both of these models are Physics Based

This is our fast-running, physics-based model for flight

Powerful Feature of the Models

- For both the fast-running physics-based model and CTH
  - *The model coding is exactly the same for all the different cases that will be shown – only the input material properties are changed.*
- Thus, it is not a different model for ice or low density ice, it is not a different model for LI-900 or FRCI-12; the impact model is exactly the same, only the input material properties change.
- As will be shown, excellent agreement between models and test data exists for all impact cases.

Material Properties for Tiles

Thermal Tiles (LI-900)

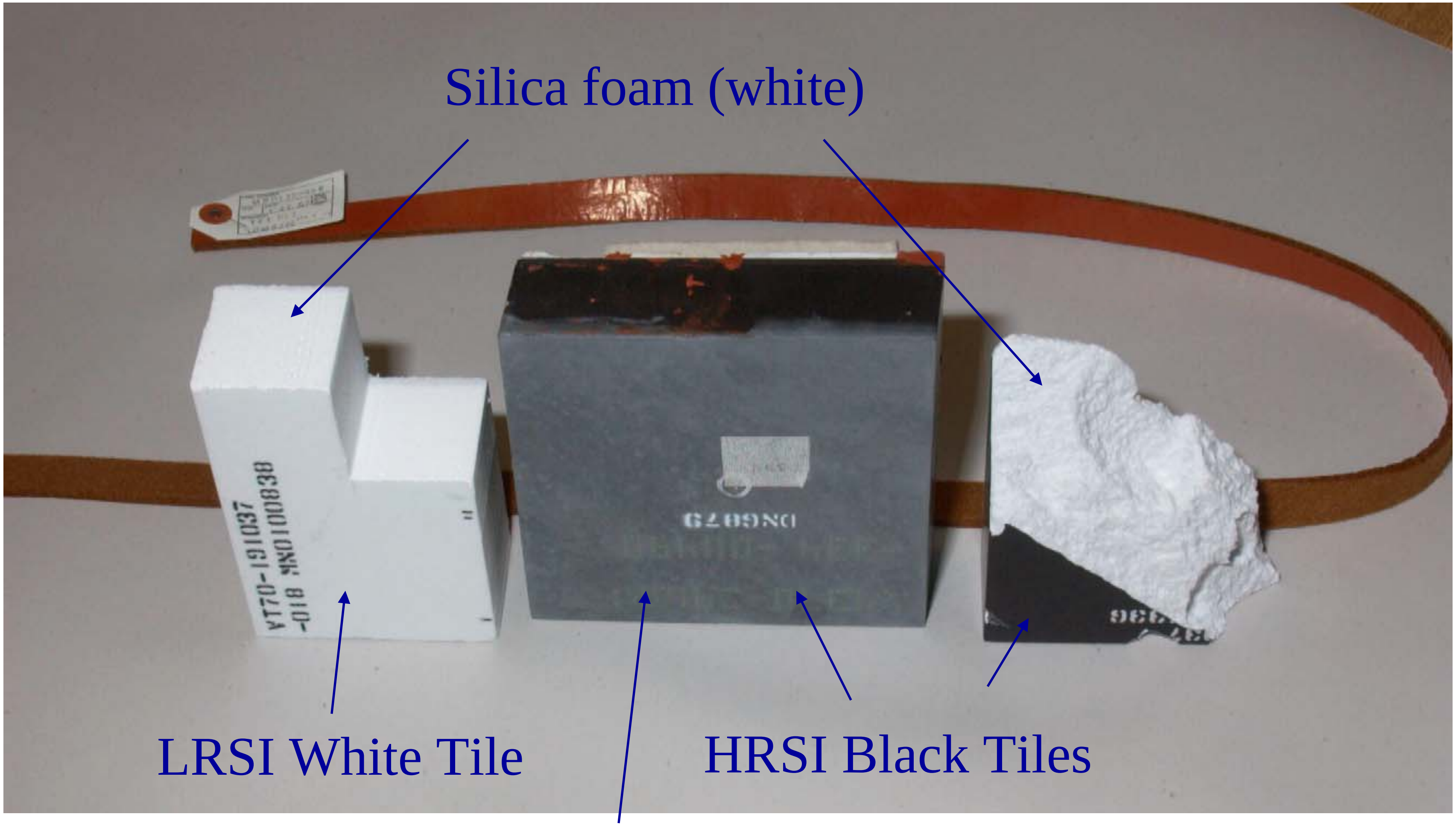

Thermal Tiles

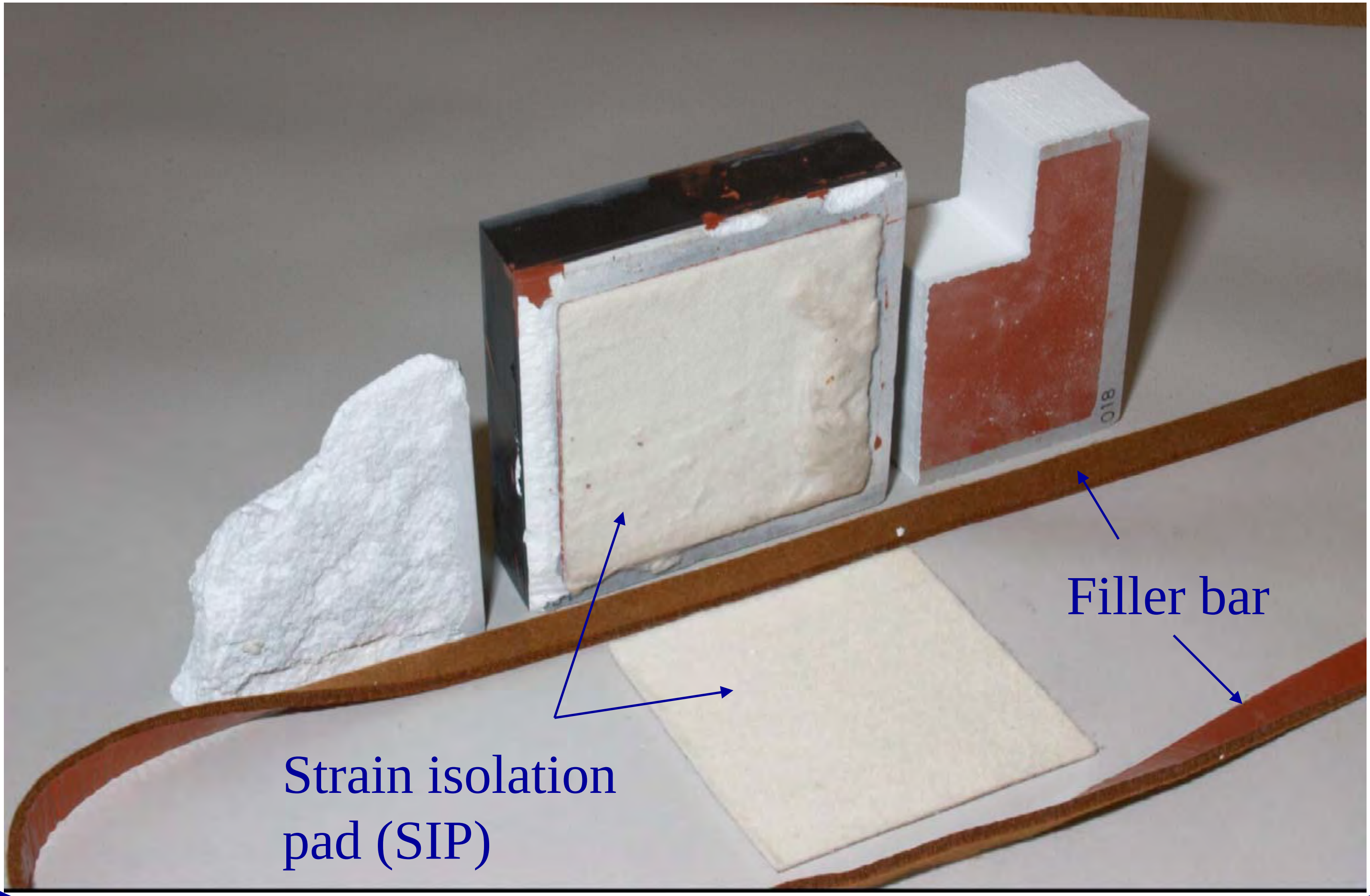

Larger strain behavior based on Crush-in-a-Box Uniaxial Strain Test Data

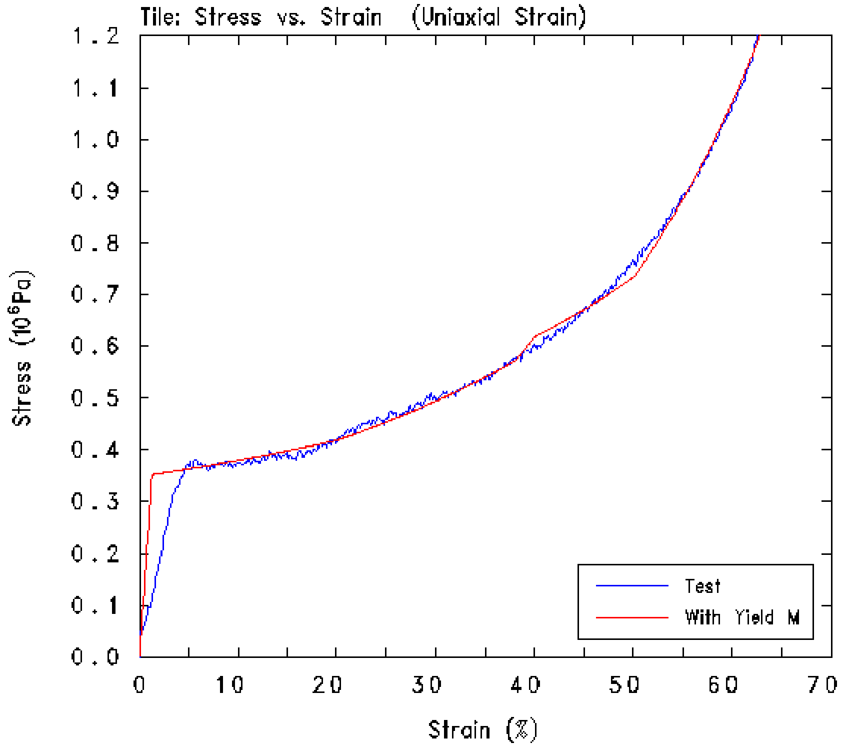

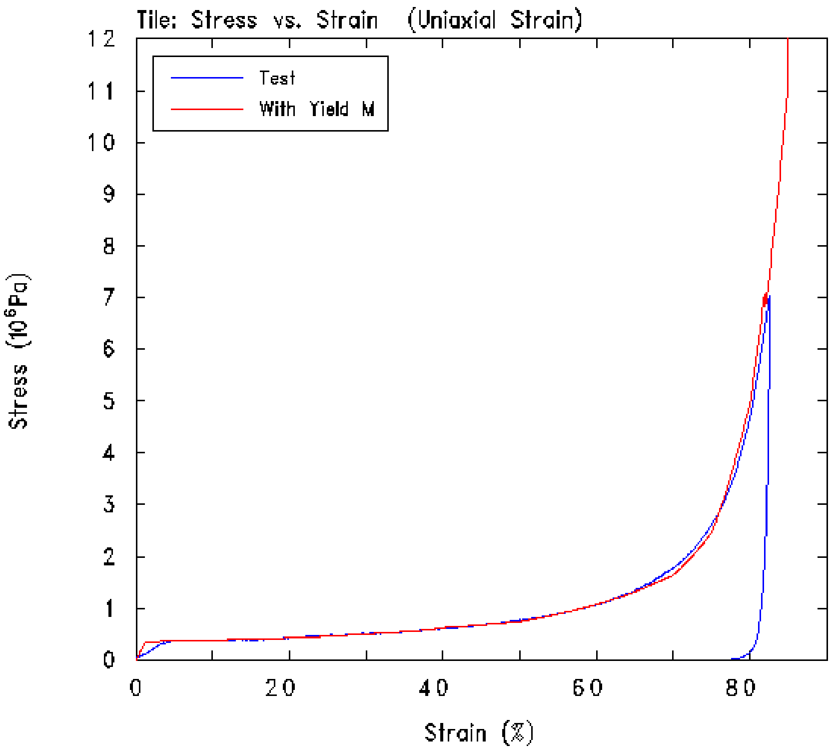

- Test performed with a cylinder from same tile specimen confined with a steel ring.
- Data placed into new tile model within CTH. Model includes a yield at 550 kPa.

Material Properties for Impactors

Ice Physical Properties

- The modeling assumed the following properties for ice (obtained from typical values found in the literature):

  - Modulus of Elasticity (E) = 8000 MPa
  - Shear Modulus (G) = 3000 MPa
  - Density = 0.914 g/cc (57 lb/ft^3)
  - Poisson's ratio = 0.33
  - Flow stress = 2.0 MPa
  - Tensile strength = 1.0 MPa
  - Sound speed (c_0) = 2954 m/s

RT-455 Ablator Model Developed for CTH

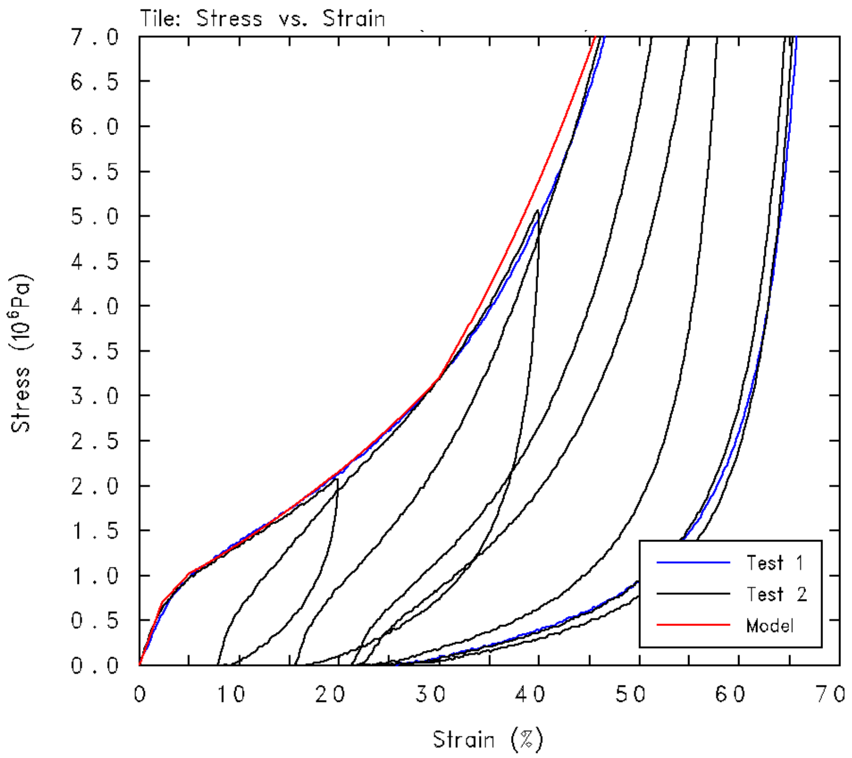

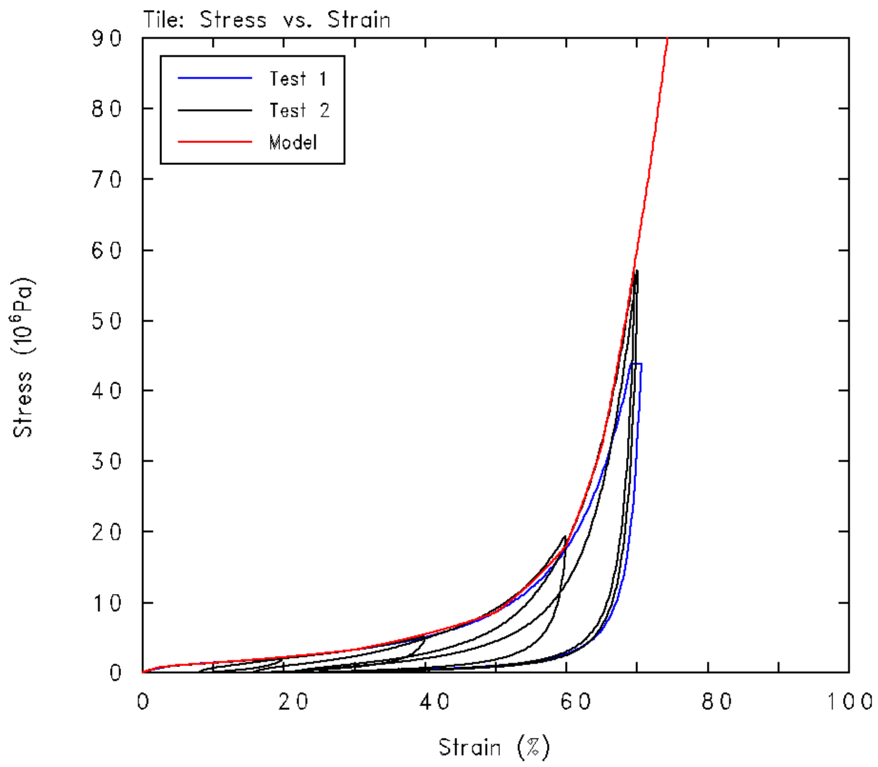

Initial density 0.66 g/cm^3

PDL Model for CTH

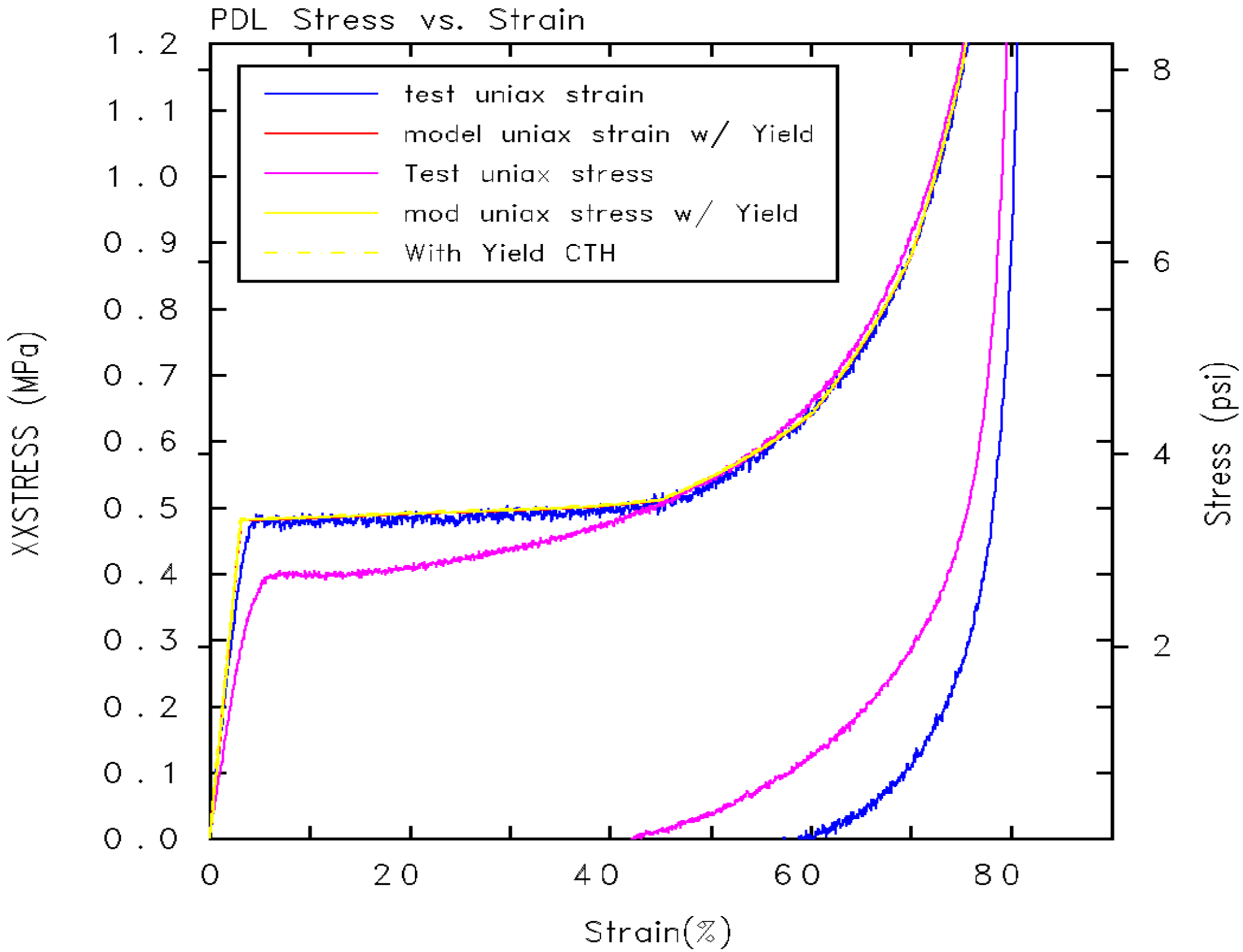

Ice into Tile

Physics-Based Ice into Tile Model

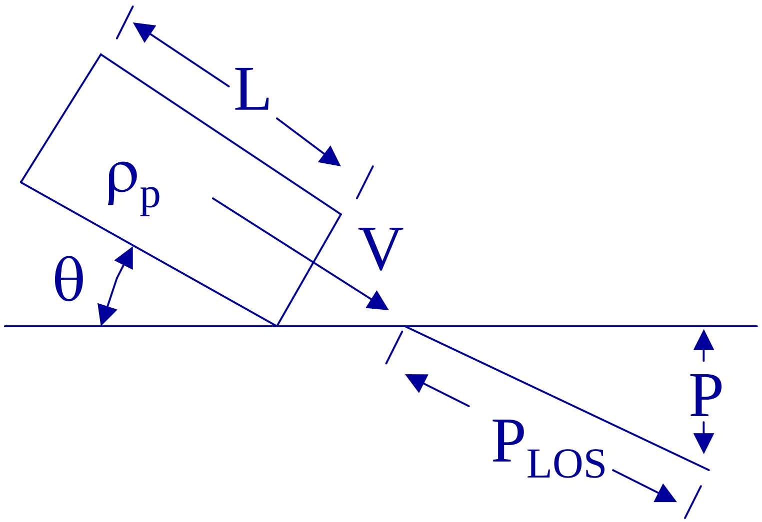

- Given the tile crush-up behavior, the model solves the Riemann problem to find the stress in the tile versus velocity, $\sigma_{zz}(v)$. A shear term is also included.
- Given this information, *F = ma* qualitatively translates into

$$\frac{dv}{dt} = -\frac{\sigma_{zz}(v)}{\rho_p L}$$

(see the rest of these charts for exactly how the full equations appear).

- The depth of penetration is calculated by integrating this equation with a numerical scheme to produce a line-of-sight depth of penetration P_{LOS}.

Tile Resistance to Penetration

- The model computes a penetration resistance stress of the form

$$\sigma_{zz}(v) = \sigma_{Hugoniot}(v) + \frac{7}{3}\sigma_{crush}\ln(\alpha)$$

- Here,
  - $\sigma_{Hugoniot}(v)$ is the stress as a function of particle velocity along the Hugoniot (the idealized one-dimensional planar impact). This function is computed based on the large-strain compression curves and the Hugoniot jump conditions. It is stored as a table for rapid look-up during the computation.
  - σ_{crush} is the crushing strength of the tile
  - $\alpha(v)$ is the extent of the deforming region within the tile, and is computed with a cavity expansion expression. It depends on the material properties of the tile and the penetration velocity.

The Hugoniot Contribution to the Resistance

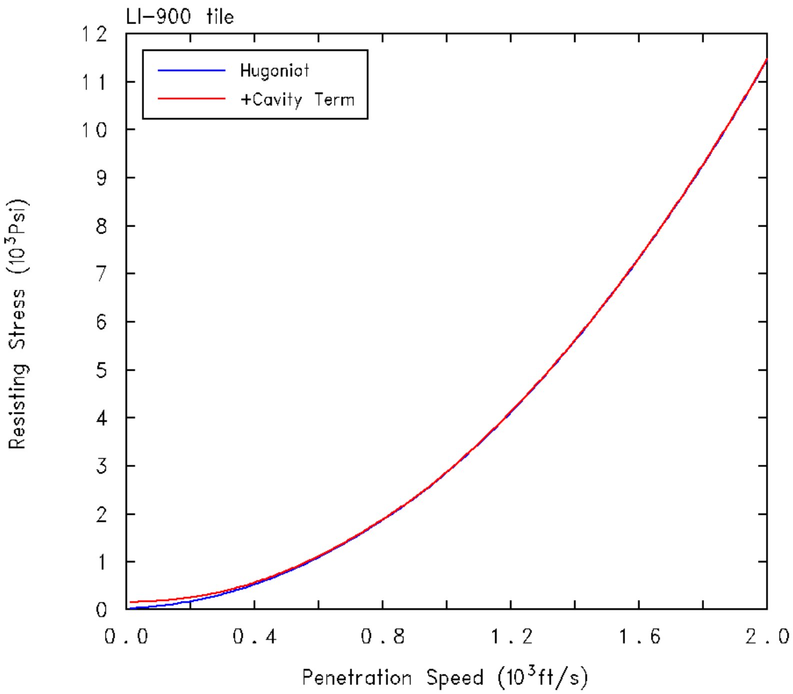

- The model solves the Riemann problem to find the stress in the tile versus velocity, $\sigma_{Hugoniot}(v)$.
- This term is found by simultaneously solving the Hugoniot jump conditions using the tabular data of tile properties

$$\frac{\rho_0}{\rho} = 1 - \frac{u}{U}$$

$$\sigma_{Hugoniot} = \rho_0 U u$$

where U is the shock speed and u is the penetration speed (U is solved for also).

- The plot shows the value of the $\sigma_{Hugoniot}(v)$ term (blue) as well as the total resisting stress including the shear resistance term (red) in terms of penetration velocity through the tile.

Embedment Phase

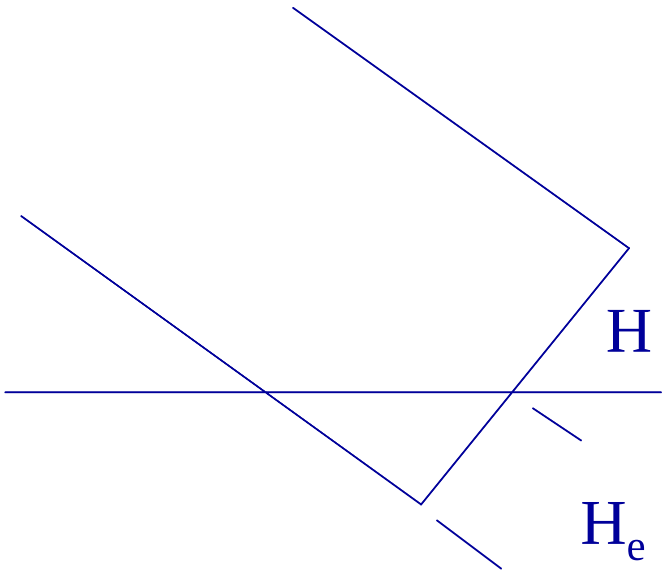

- When the projectile embeds itself into the target, only part of the face of the projectile is loaded by the target. Thus, the force on the face is reduced by the appropriate factor:

$$f = \frac{H_e}{H}$$

- where

$$\frac{d\mathrm{v}}{dt} = -f\,\frac{\sigma_{zz}(\mathrm{v})}{\rho_p L}$$

Equations of Motion

- For completeness, we write the full equations of motion, where *x* is the direction along the surface of the tile and *y* is the normal direction into the tile:

$$\frac{d\mathrm{v}_{\mathrm{x}}}{dt} = -f\,\frac{\sigma_{\mathrm{zz}}(\mathrm{v})}{\rho_p L}\cos(\theta) + \frac{F_n}{\rho_p LHW}\sin(\theta)$$

$$\frac{d\mathrm{v}_{\mathrm{y}}}{dt} = -f\,\frac{\sigma_{\mathrm{zz}}(\mathrm{v})}{\rho_p L}\sin(\theta) - \frac{F_n}{\rho_p LHW}\cos(\theta)$$

$$\mathrm{v} = \sqrt{\mathrm{v}_{\mathrm{x}}^2 + \mathrm{v}_{\mathrm{y}}^2}$$

- These equations are integrated forward in time until either the impactor speed v drops below the speed required to crush tile (i.e., it comes to rest) or the impactor is forced back to the tile surface (i.e., it ricochets).

Developing the 95% Bounding Model

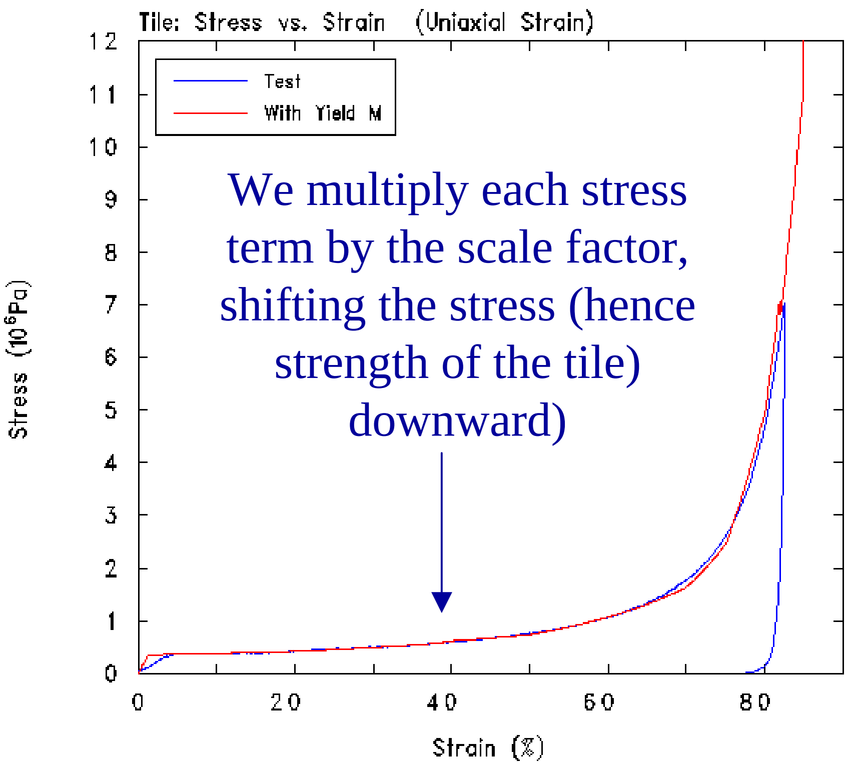

- Since the fast-running physics-based model is based on material properties, the only way to adjust the model is by adjusting those material properties.
- We provide a “bounding model” by adjusting the tile strength – that is, making the tile weaker.
- In particular, each point in the data curve is shifted down by the multiplicative scale factor, and then the Hugoniot and shear terms are recomputed.

Bounding Model: 95% Bounding

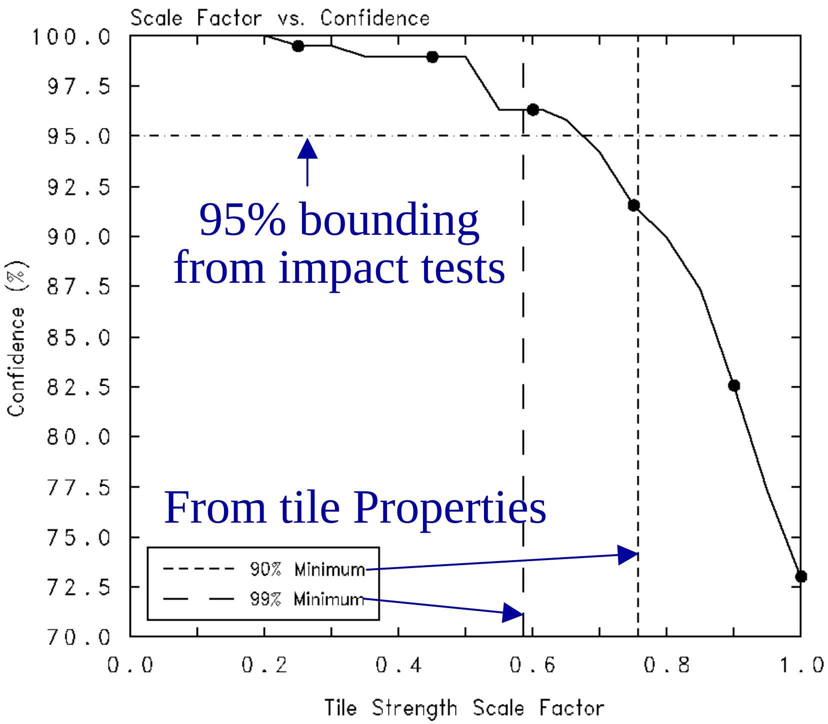

- Based on the experimental data, 95% bounding is achieved when only 9 data points lie above the curve.
- With the earlier version of the model, this level of bounding was achieved with a scale factor of 0.615. We have chosen to stick with this scale factor. For the updated model, at a scale factor of 0.615, 7 points lie above the curve.
- On page 13 of Material Properties Data, Volume 3, Thermal Protection System Materials Data, the in-plane compressive strength of the LI-900 tile material is listed:
  - average is 70 psi,
  - 90% minimum is 53 psi, corresponding to a scale factor of 0.76
  - 99% minimum is 41 psi, corresponding to a scale factor of 0.59.
- Thus, the scale factors from the material testing are in reasonable agreement with that found from the ice impact tests.

F: L=0.5”   W= 0.5” H =0. 5” 30º

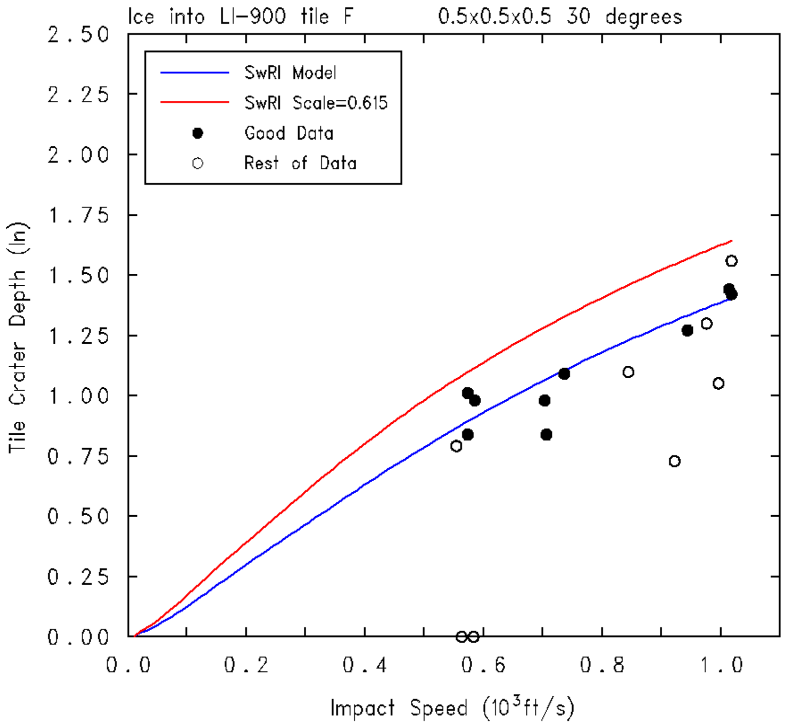

Depth

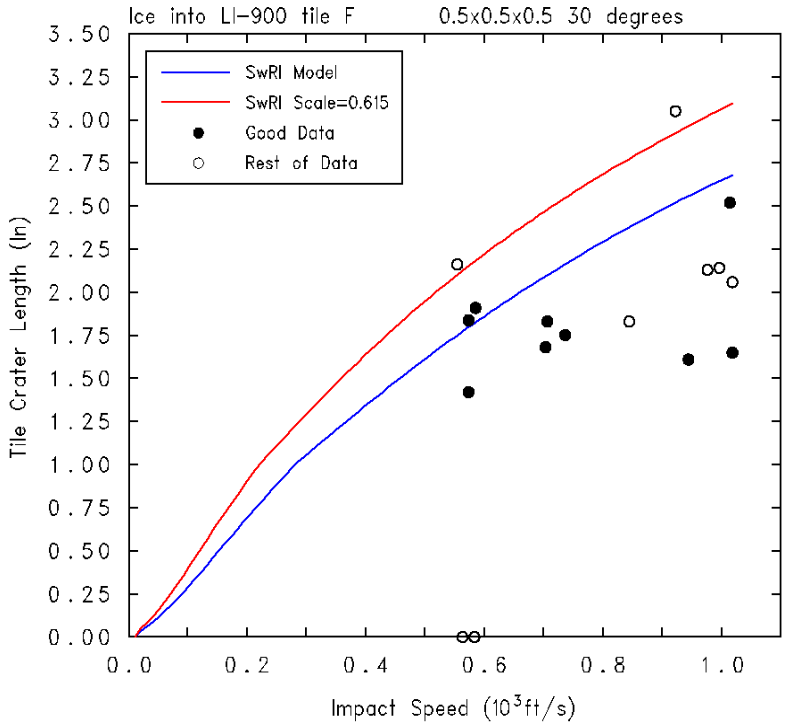

Length

CTH calculations of Ice impact into LI-900 Tile

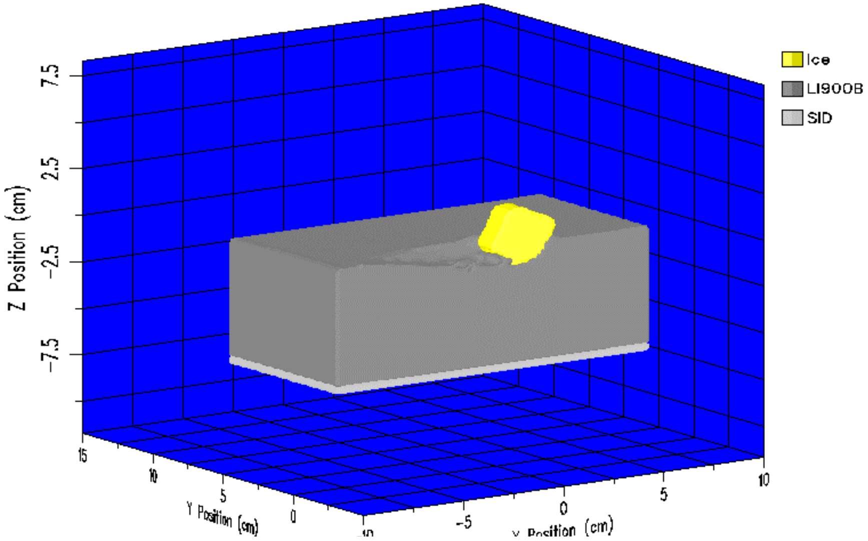

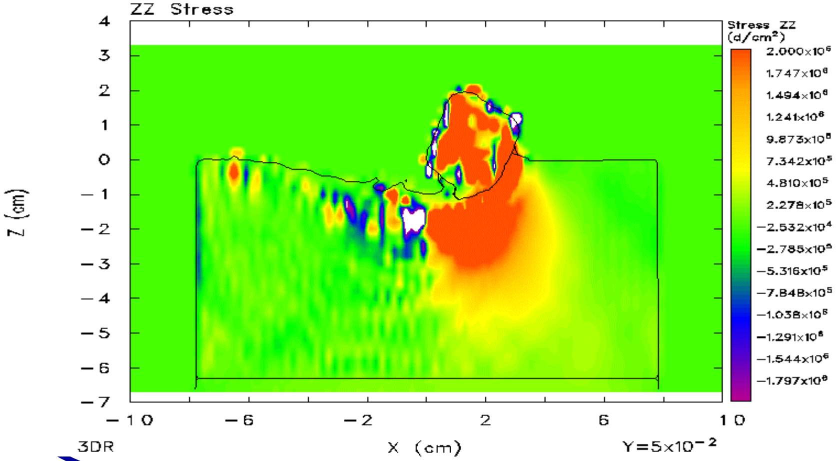

- Work has focused on 3-D computations of ice impact into LI-900 tile using new subroutines in CTH.
- Approximately 350 computations completed to date.
- Six different projectile geometries were examined
- Velocities ranged from 10 to 300 m/s, and impact angles varied from 10 to 30 degrees.

3-D CTH Ice Impact Computations

- 3-D Computations
- 2 upright individual LI900 tiles included in the computation
- 4 mm of SIP material included
- Bottom support is rigid
- Cell size 4 mm (0.016 in.)
- Y=0 is plane of symmetry

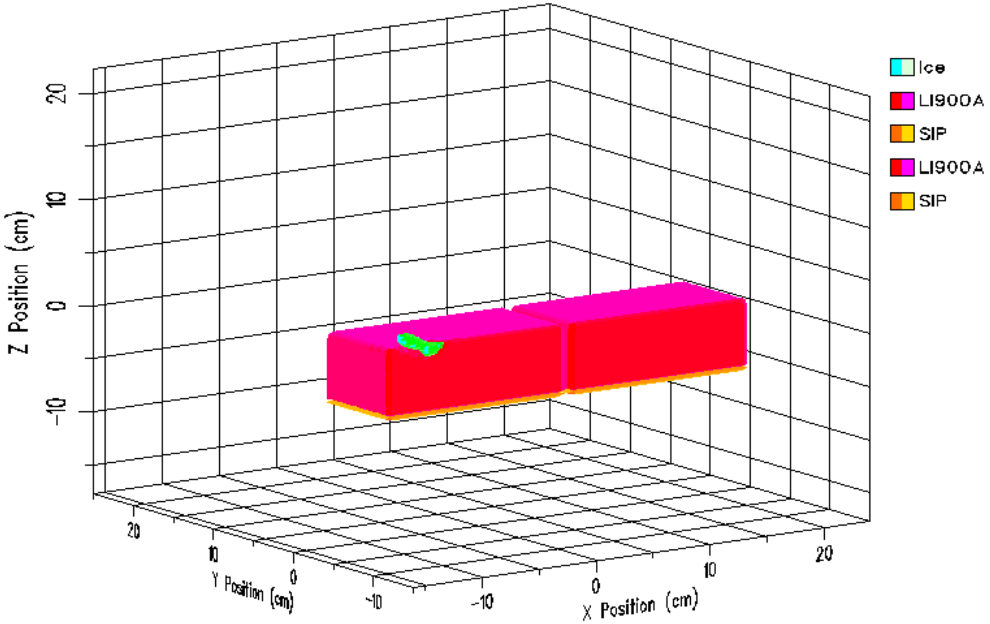

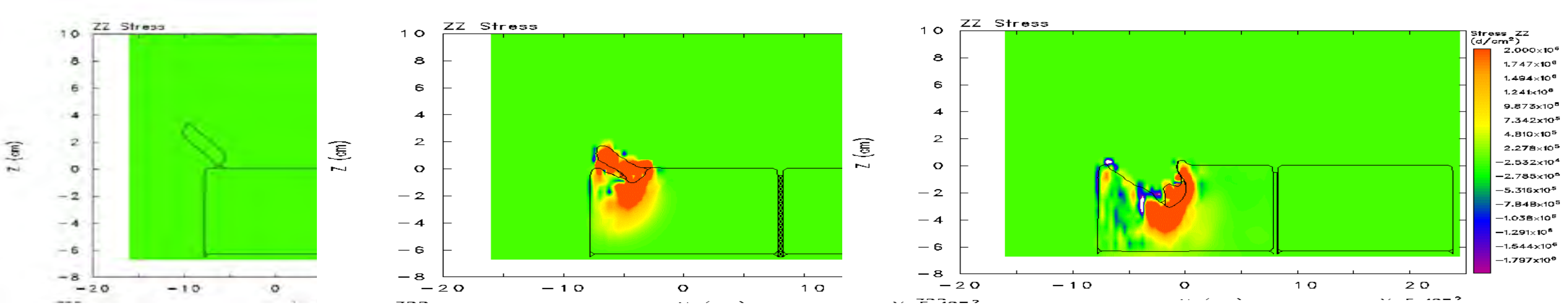

CTH Ablator Numerical Simulations

- Ablator 3’’ x 0.5’’ x 1’’
- Tile 6’’ x 6’’ x 2’’
- 3-D calculations
- Y=0 plane of symmetry
- Ablator and Tile EOS implemented by SwRI.
- No SIP
- 1.5 mm cell size (6 cells across ablator thickness)
- Ran a total of 26 cases
- Two examples follow

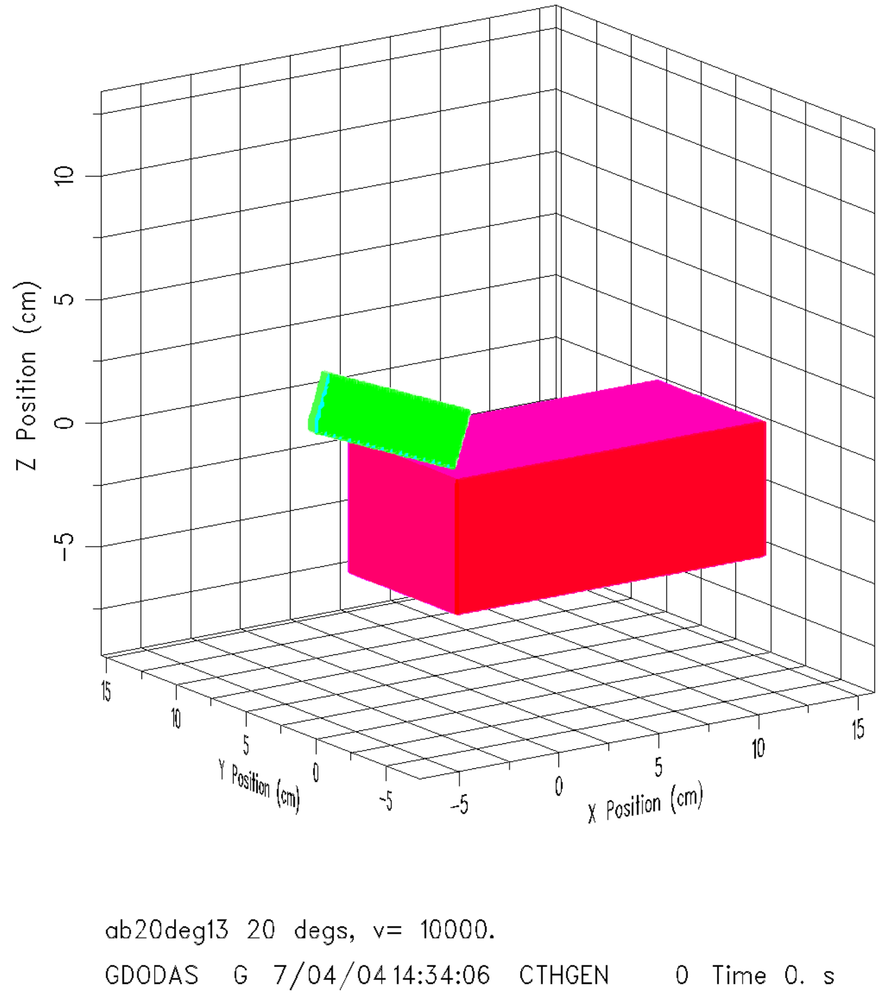

30° Impact at 350 ft/s (P2.11.7-1)

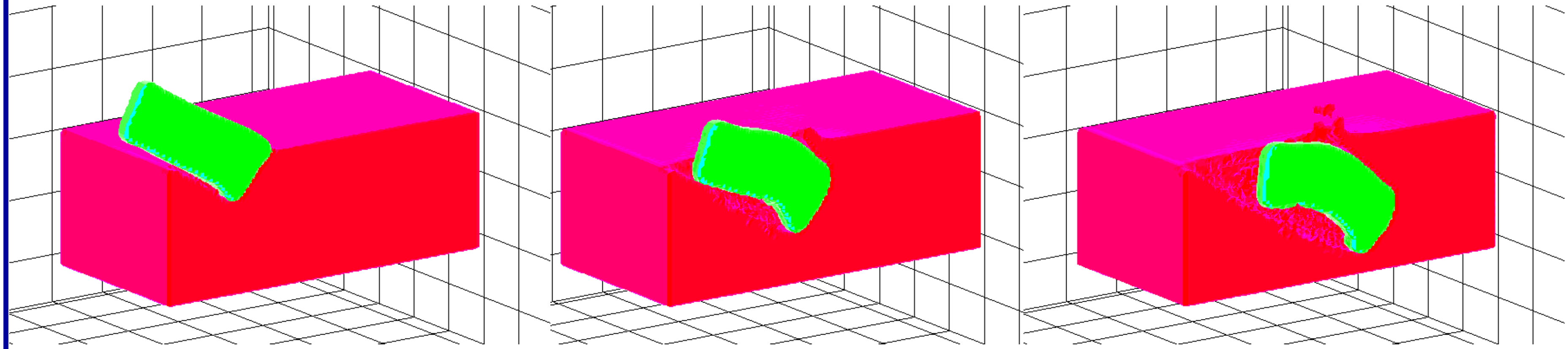

0.5 ms

1.0 ms

1.5 ms

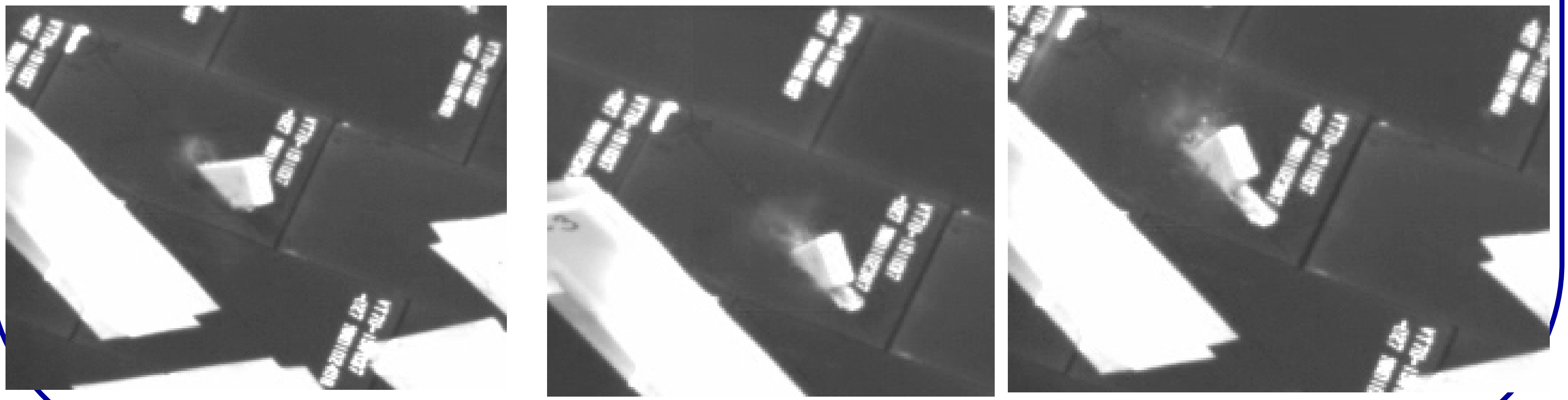

CTH crush-up profiles

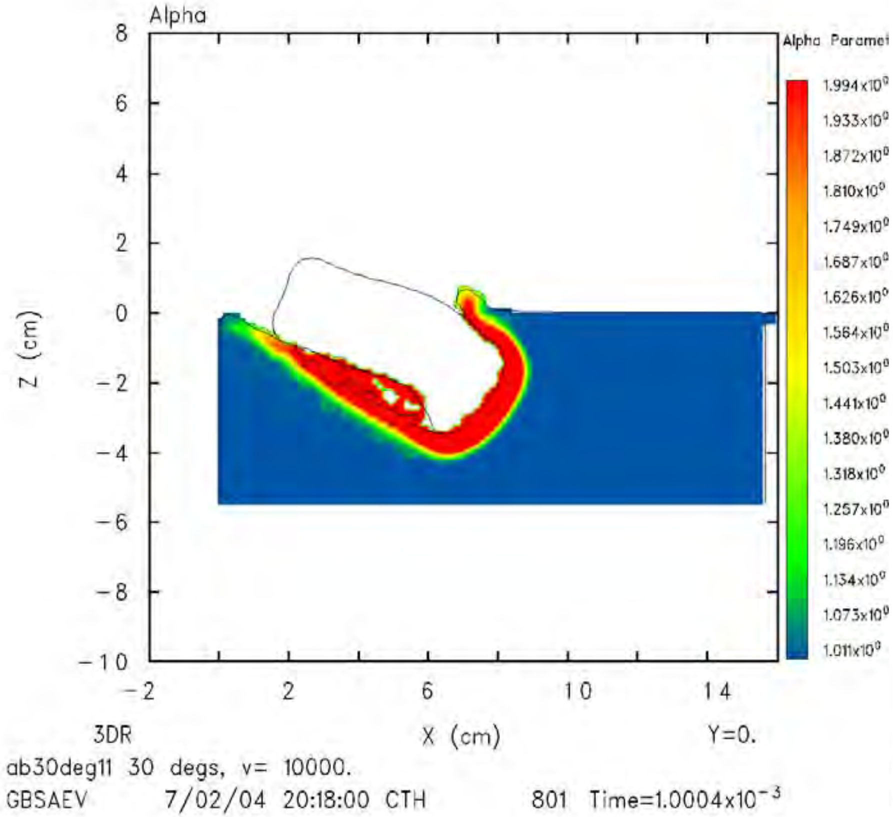

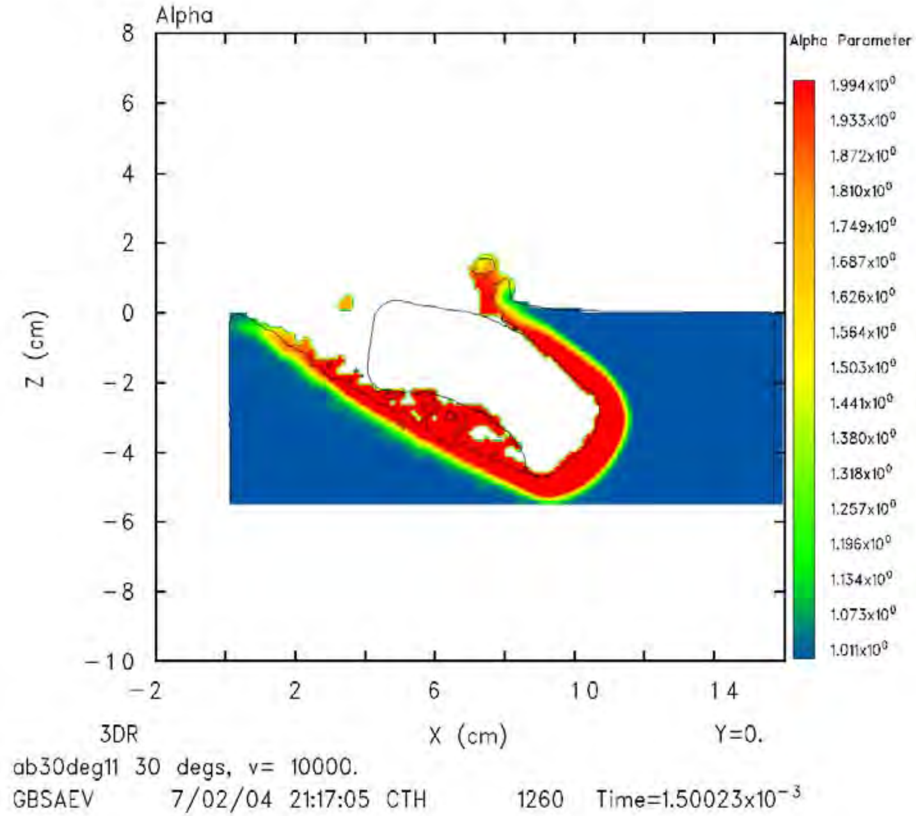

DOP given by the lowest point with alpha = 1.5

Alpha is the current density divided by initial density

Foam into Tile

BX-265 Foam Impactors

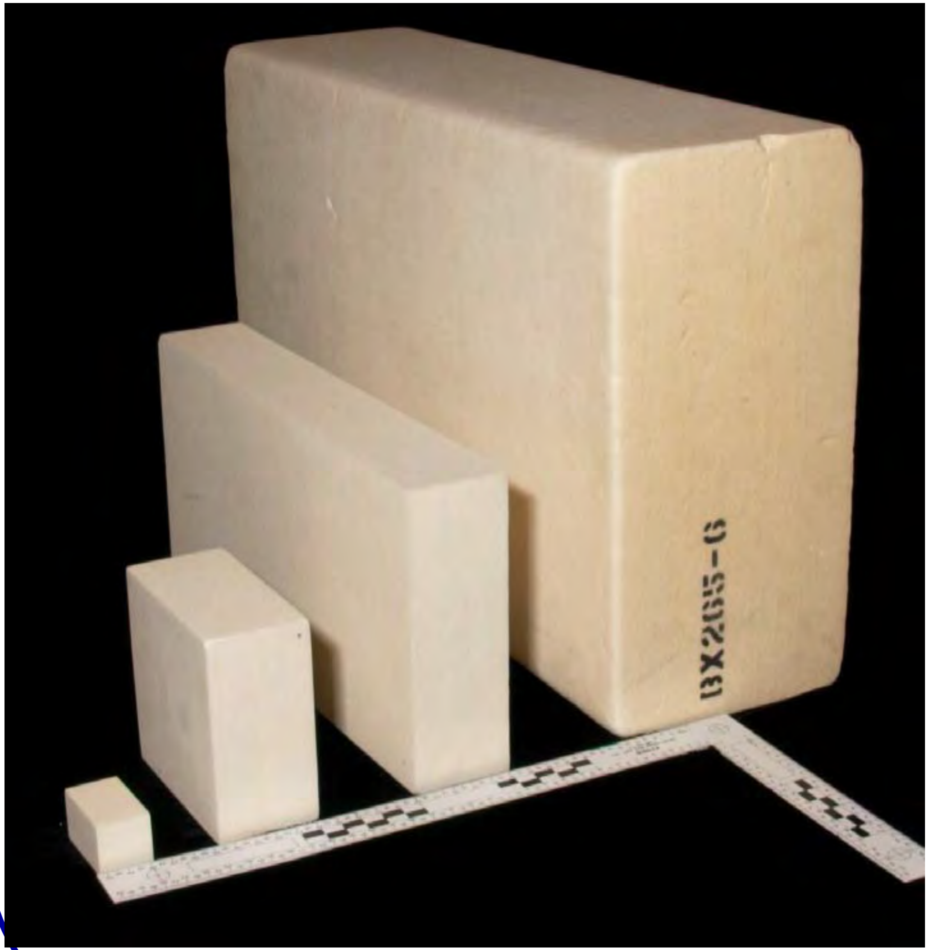

A wide range of projectiles were shot:

- Return to flight:
  - 1.6”×1”×1”; 1 gram (0.0022 lb)
  - 4”×4”×2”; 20 gram (0.044 lb)
  - 12”×6”×2”; 90 gram (0.2 lb)
- *Columbia* Investigation
  - 22”×12”×6”; 750 gram (1.67 lb)

Loading Surfaces

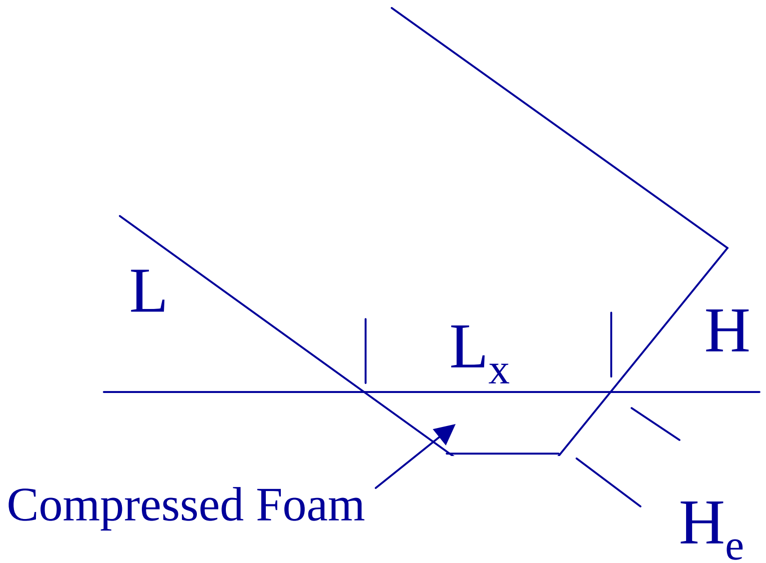

- As the foam projectile impacts the tile, only part of the face of the projectile is loaded by the target. Thus, the force on the face is reduced by the appropriate factor:

$$f = \frac{H_e}{H}$$

- The force on the length of the projectile acting upwards is

$$F_y = L_y W \min(\tilde{\sigma}_H(v_{y0})\cos(\theta) + \tilde{\sigma}_{crush-t}\sin(\theta), \tilde{\sigma}_{crush-t})$$

Equations of Motion

- The equations of motion, where *x* is the direction along the surface of the tile and *y* is the normal direction into the tile:

$$\frac{d\mathrm{v}_{\mathrm{x}}}{dt} = -f\,\frac{\sigma_{\mathrm{zz}}(\mathrm{v})}{\rho_p L}\cos(\theta)$$

$$\frac{d\mathrm{v}_{\mathrm{y}}}{dt} = -f\,\frac{\sigma_{\mathrm{zz}}(\mathrm{v})}{\rho_p L}\sin(\theta) - \frac{F_y}{\rho_p LHW}\cos(\theta)$$

$$\mathrm{v} = \sqrt{\mathrm{v}_{\mathrm{x}}^2 + \mathrm{v}_{\mathrm{y}}^2}$$

- These equations are integrated forward in time until either the impactor speed v drops below the speed required to crush tile (i.e., it comes to rest) or the impactor is forced back to the tile surface (i.e., it ricochets).
- (There is not a sine term in the first equation because the compliance of the foam leads to a nearly flat interface region between the tile and the foam.)

Tile Resistance to Penetration

- The resisting stress is of the form

$$\sigma_{\mathrm{zz}}(v) = \sigma_{Hugoniot}(v)$$

- $\sigma_{\mathrm{Hugoniot}}(v)$ is the stress as a function of particle velocity along the Hugoniot (the idealized one-dimensional planar impact). This function is computed based on the large-strain compression curves and the Hugoniot jump conditions. It is stored as a table for rapid look-up during the computation.

Riemann Solver

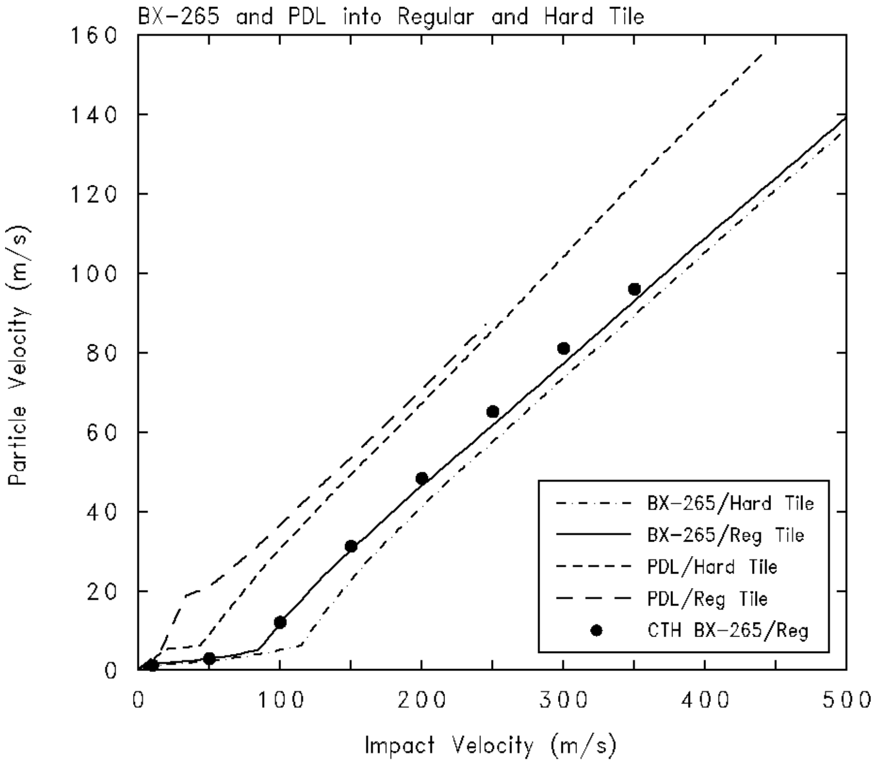

- A centerpiece of the penetration model is a Riemann solver that calculates the penetration speed for various impact speeds, as well as the wave speeds in the material.
- The solver solves the mass and momentum forms of the Hugoniot jump conditions to compute the stress and particle velocity at the interface between the two colliding materials
- The solver uses exactly the same equation-of-state tables used by CTH for modeling the tile and foam.
- The Riemann solver solves 2-, 3- and 4-wave problems, all of which can arise in foam vs. tile impacts.

Damage-No Damage Transition

- Explicit expression for the transition velocity for a 90° impact is

$$V_{crush} = u_{et} + u_{ef} + \left\{ \left(\frac{1}{\rho_{ef}} - \frac{1}{\rho_f(\tilde{\sigma}_{crush-t})} \right) (\tilde{\sigma}_{crush-t} - \tilde{\sigma}_{crush-f}) \right\}^{1/2}$$

- If there were no edge catching, then the transition would be given by

$$\mathrm{v} = \frac{V_{crush}}{\sin(\theta)}$$

Edge Catch

- The tile is pushed down by the foam, which has inertial resistance as well as a spring-like behavior of the SIP (represented by a spring constant *k*):

$$\ddot{y}_{tile} = \frac{L_y W \tilde{\sigma}_y - k A_{tile} y_{tile}}{m_{tile}}$$

- The current critical (transition) velocity is then computed according to

$$\mathrm{v} = \frac{V_{crush}}{\sqrt{\Delta y_{tile} / T_{SIP}}\,\sin(\pi/4) + (1 - \sqrt{\Delta y_{tile} / T_{SIP}})\sin\theta}$$

- If the current velocity is above this value, the edge catches and penetration into the tile begins.

Tile Fracture Algorithm

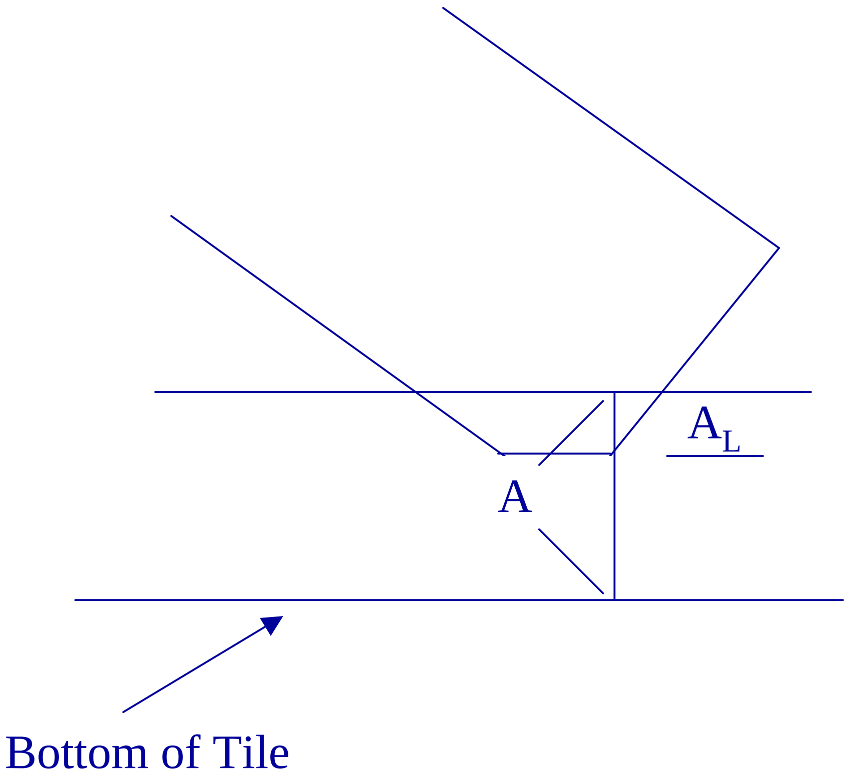

- There is a tile fracture algorithm, in an effort to determine when a tile breaks, as is seen in the shear-out tile failure mode, for example.
- The model is still under examination.
- A cross section is taken through the tile, with area *A*. If the area loaded by the impactor is given by A_L, then the tile breaks if the force exerted by the projectile is greater than the load the tile ligament can support (we assume that the tensile strength of the tile is equal to $\sigma_{crush\text{-}t}$):

$$A_L \sigma(v) > (A - A_L)\,\sigma_{crush-t}$$

Foam Model Examples

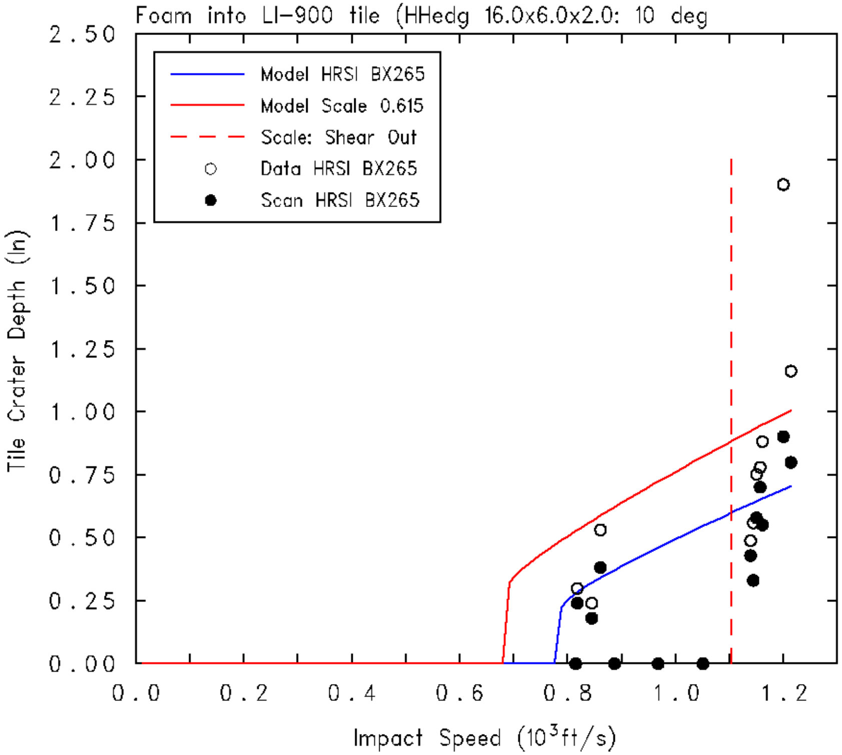

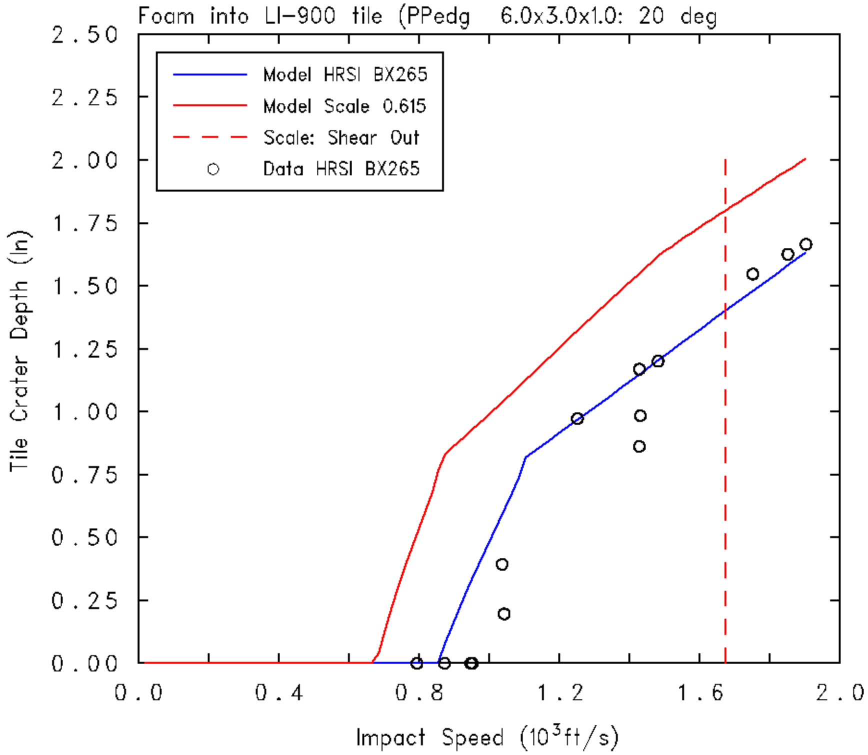

Test 1.1.9-2, 30 degs, 220 m/s (718 fps)

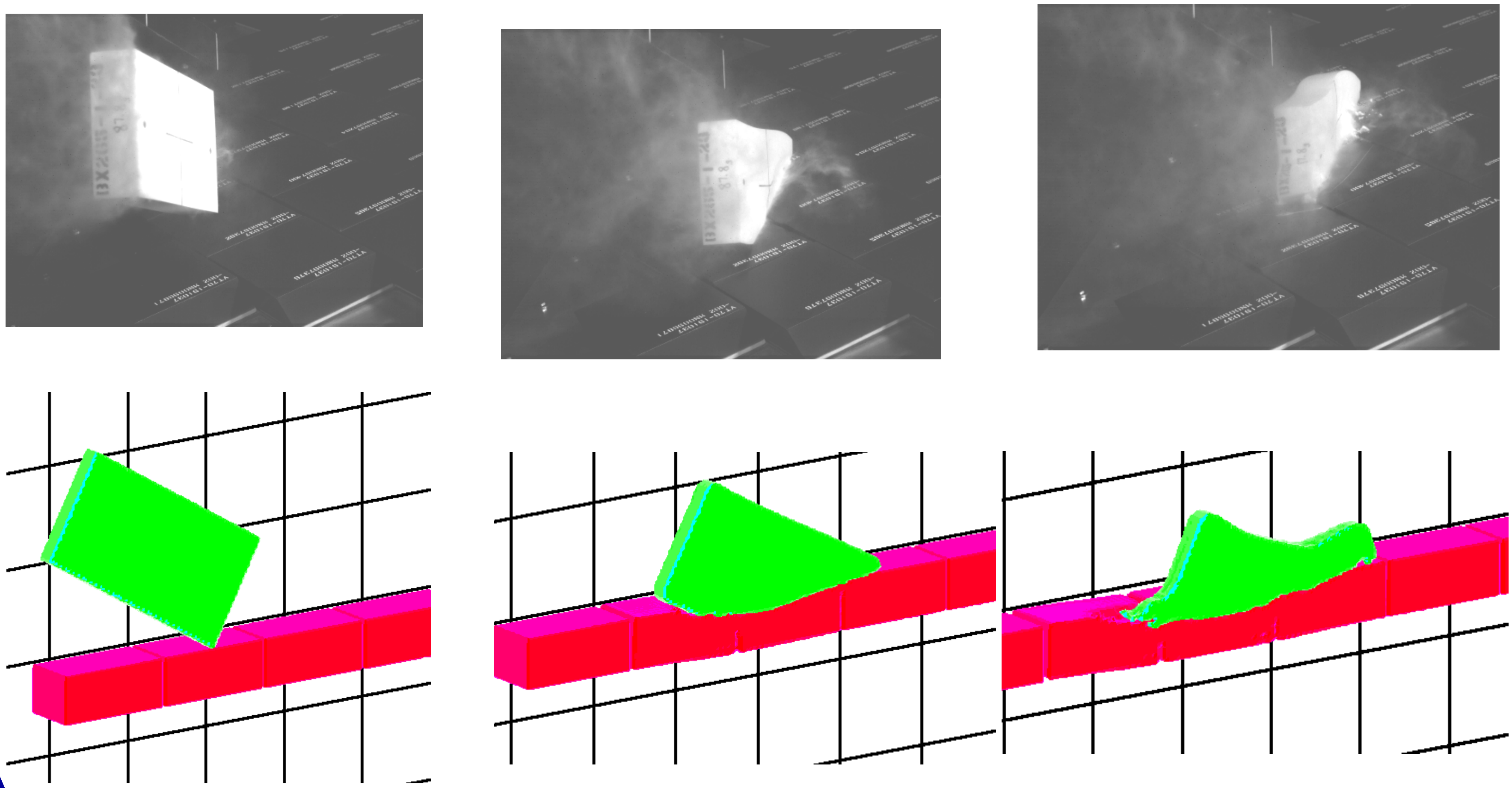

Tile-Out or Pop-Off

Tile Crush-Up at Bottom of Tile

- In 3d CTH computations, we do not quantitatively see as much crush-up at the bottom layer as we see in one-dimensional computations (to be shown later) (i.e., α is less): presumably this is due to the larger cell size in 3D.
- However, we do see crush-up all along the bottom of the tile.
- For example (next three charts)...

BX-265 vs. Tile CTH Computations

- 3-D Computations
- 9 upright individual LI-900 tiles included in the computation
- SIP simulated as a 4 mm (0.016 in.) gap
- Bottom support is rigid
- Cell size 4 mm (0.016 in.)
- Y=0 is plane of symmetry

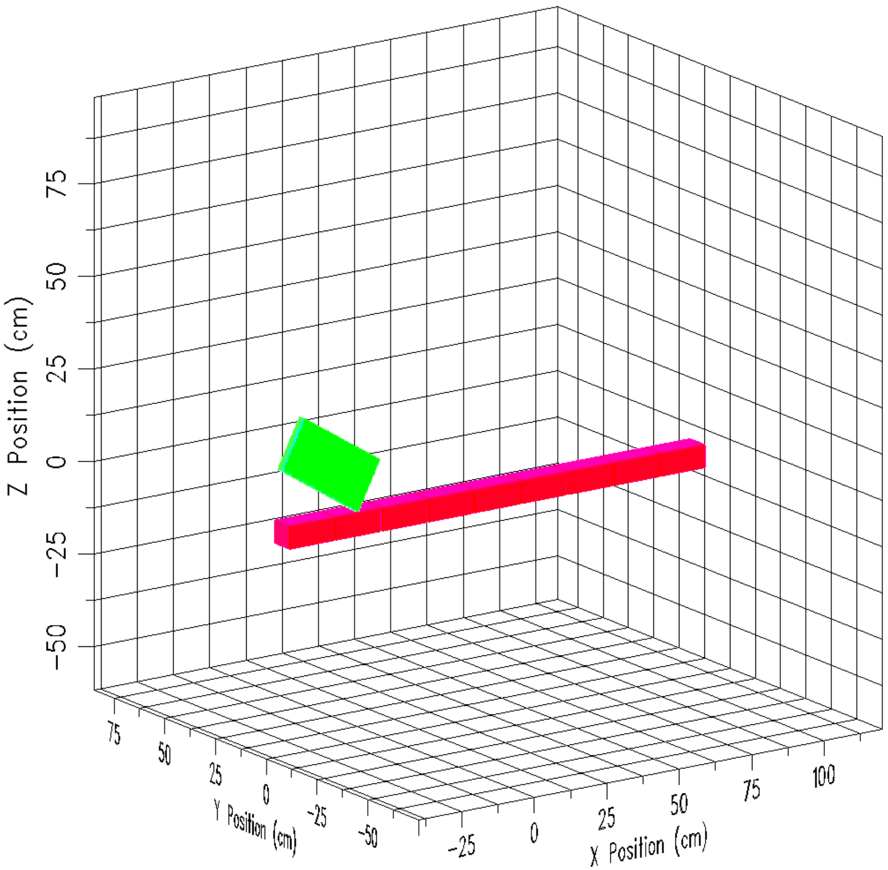

Simulation of P1.1.2-4: V=957 ft/s, θ = 20°
Crush-up plots in plane of symmetry

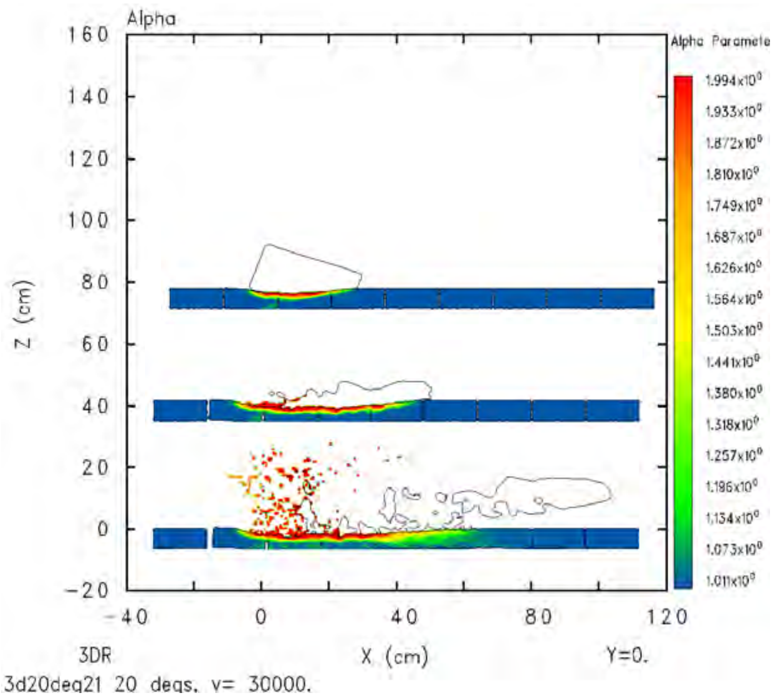

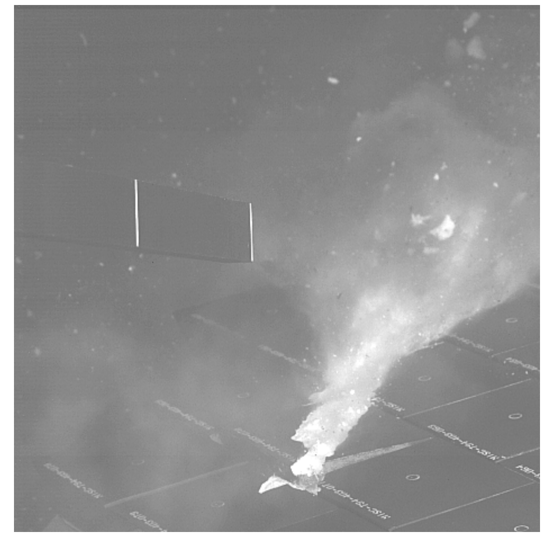

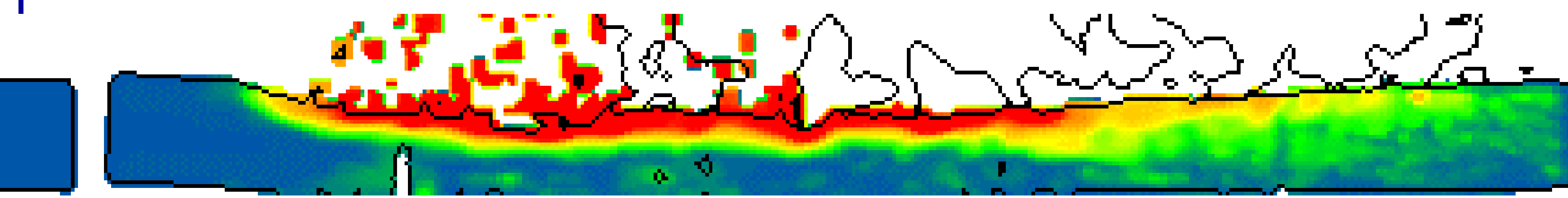

Simulation of P1.1.2-4: V=957 ft/s, θ = 20°
Crush-up plots in planes perpendicular to impact
(High resolution)

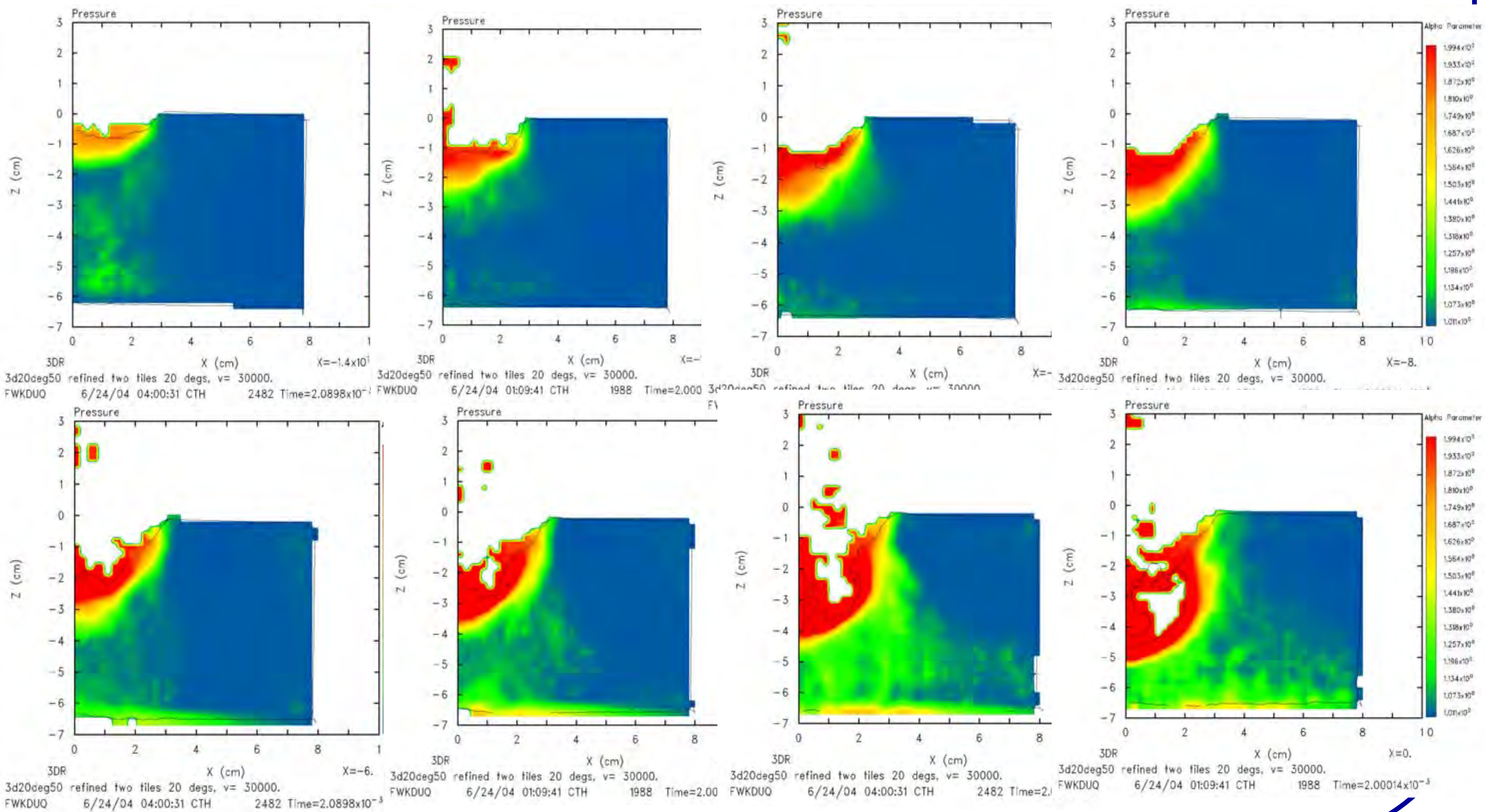

Simulation of P1.1.2-4: V=957 ft/s, θ = 20°
Crush-up plots in planes perpendicular to impact
(High resolution)

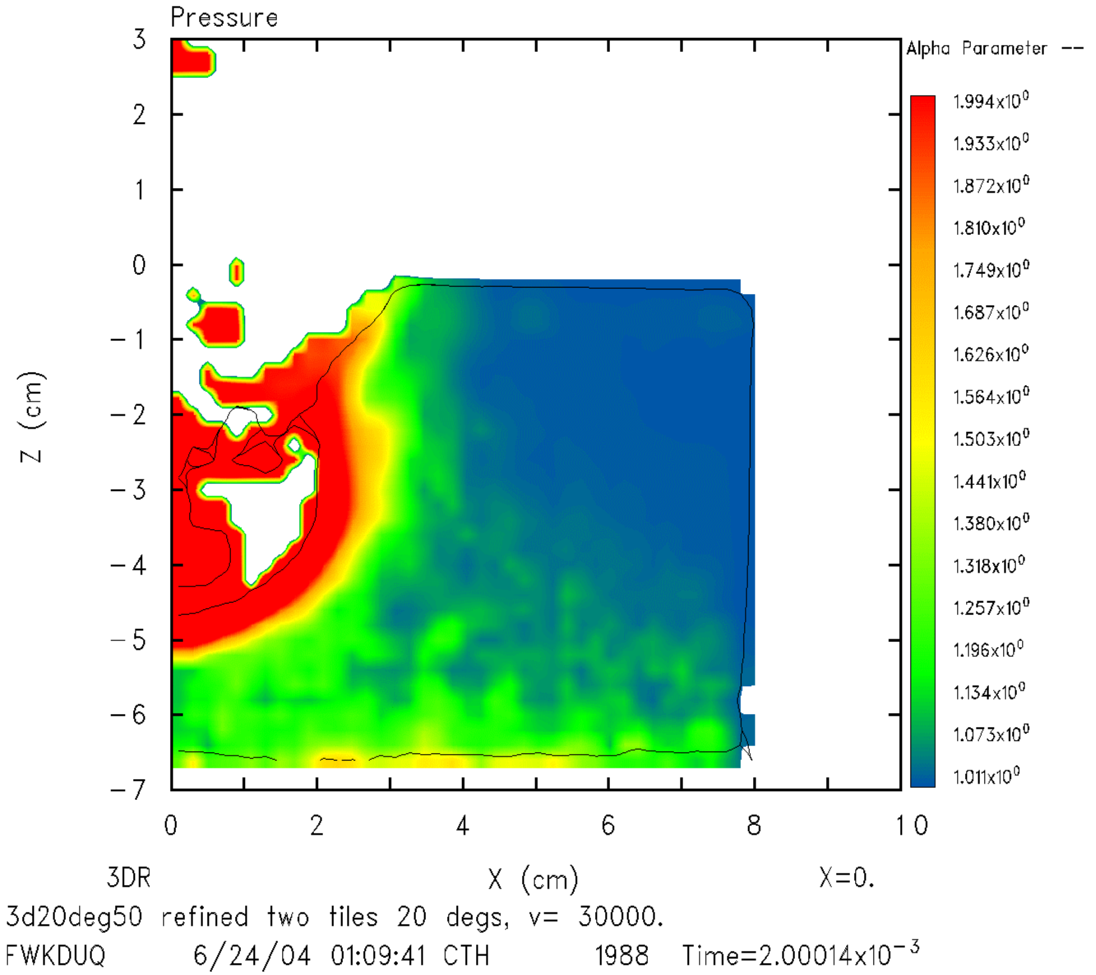

Yellow at bottom is crushed tile material

RCC Impact Testing

CAIB Recommendation R3.3-4
RCC Properties

- In order to understand the true material characteristics of Reinforced Carbon-Carbon components, develop a comprehensive database of flown Reinforced Carbon-Carbon material characteristics by destructive testing and evaluation.

Aramis System Allows Direct Measurement of Dynamic Displacements

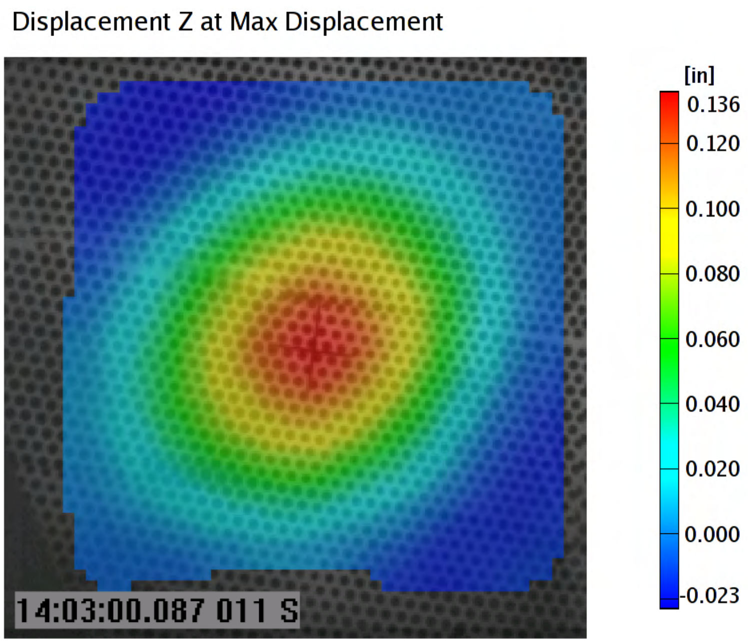

Strains can then be computed, and both displacements and strains can be compared to DYNA Team computations.

Return to Flight by *Discovery*

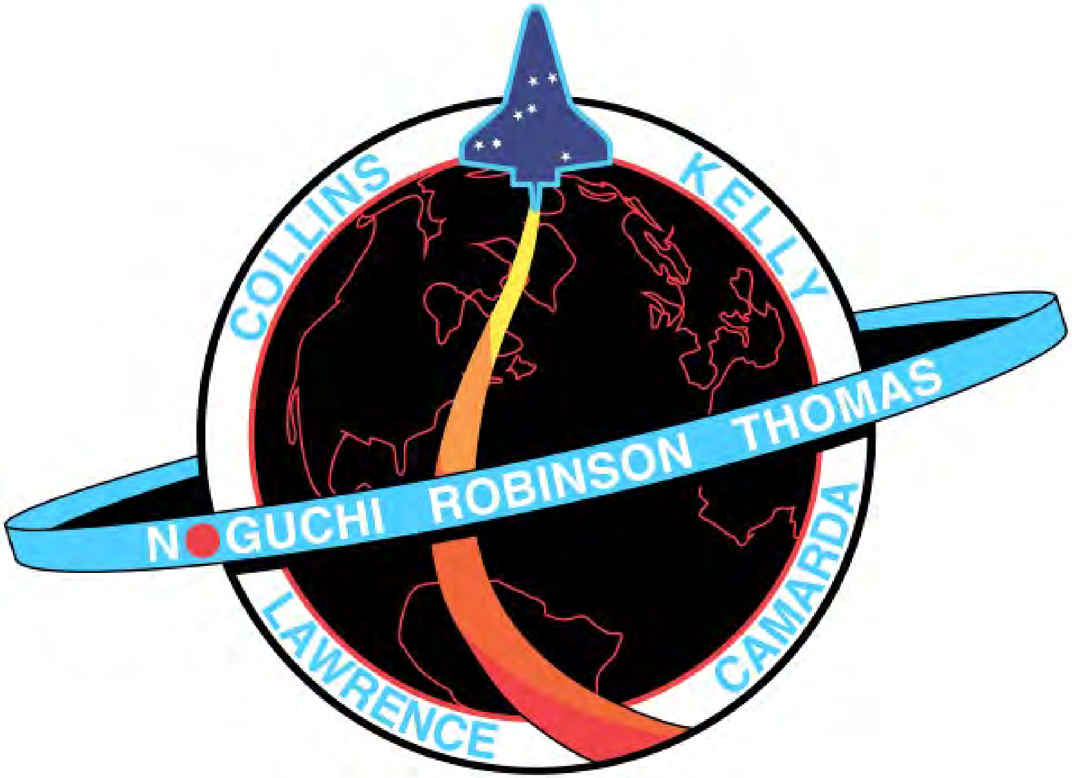

STS-114

- 114th flight of the Space Shuttle Program
- 31st flight of *Discovery*
- *Discovery* first flew in August, 1984 (it is now the oldest operational shuttle, as well as the most flown)
- Mission: Tuesday, July 26 – Tuesday, August 9, 2005
- Crewed by
  - Eileen Collins
  - Jim Kelly
  - Charlie Camarda
  - Wendy Lawrence
  - Steve Robinson
  - Andy Thomas
  - Soichi Noguchi

Prelaunch Ice Formation

The Plots

- The following plots from the ice model are for four masses:
  - Set Length (1.5” or 2”)
    - L=1.5”, H=W=0.767”, mass = 13.2 gram = 0.029 lb
    - L=2.0”, H=W=1.02”, mass = 31.2 gram = 0.069 lb
  - Length/Width ratio = 2.5
    - L=1.77”, H=W=0.707”, mass = 13.2 gram = 0.029 lb
    - L=2.35”, H=W=0.94”, mass = 31.1 gram = 0.069 lb
- Impact speed in plots goes from 0 to 200 ft/s. **Understand that the model has only been baselined for speeds of 80 ft/s** to 1500 ft/s. The concern is that ice may not fracture at the lower velocities, and so there may be larger depths of penetration than the model predicts (the model assumes the ice fractures).
- Impact angles range from 5° to 55° in 5° increments.
- Blue curves are the nominal model, red curves are the 95% bounding curves.
- (If you want, you can pull the picture out of the presentation and enlarge it.)

L=1.5”   W= 0.767”   H =0.767”   5° - 55°
Mass = 13.2 gram = 0.029 lb

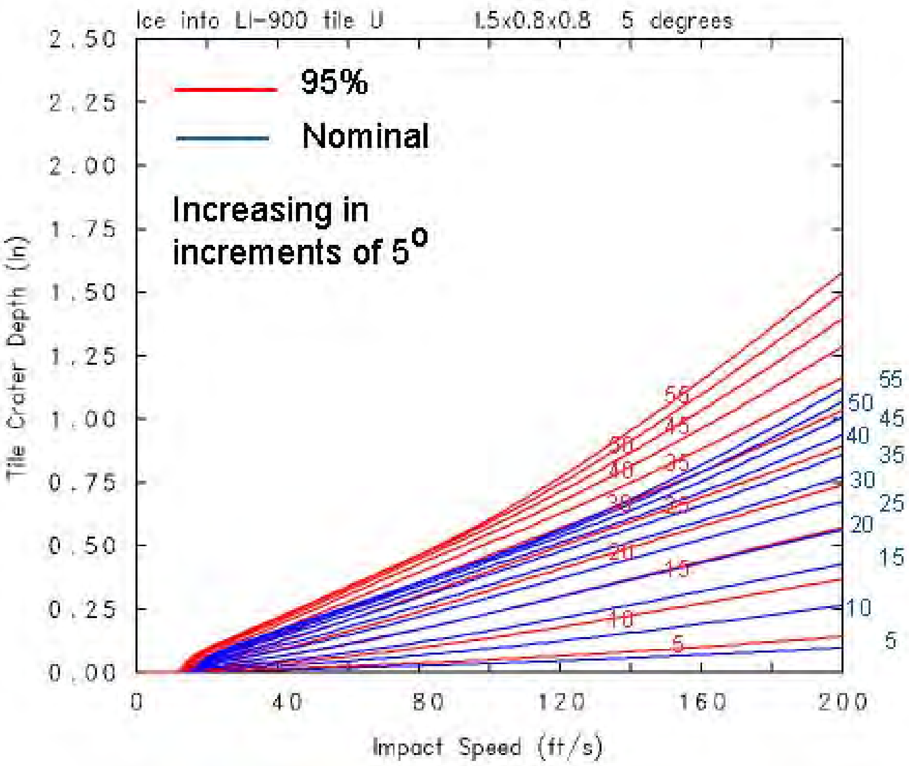

Depth

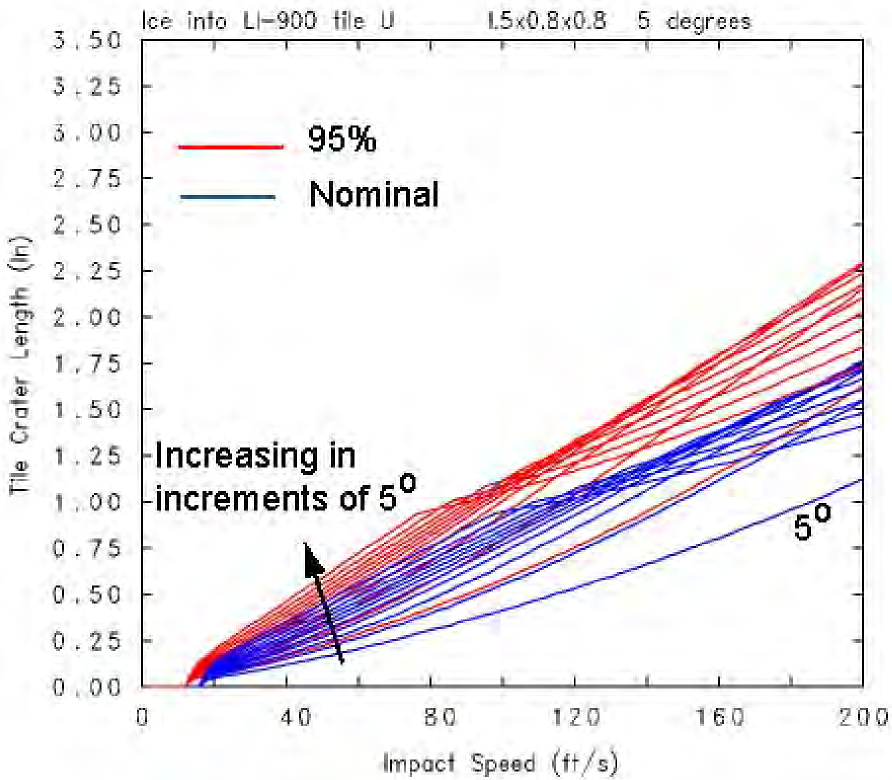

Length

L=2.0"   W= 1.02" H =1.02" 5° - 55°
Mass = 31.2 gram = 0.069 lb

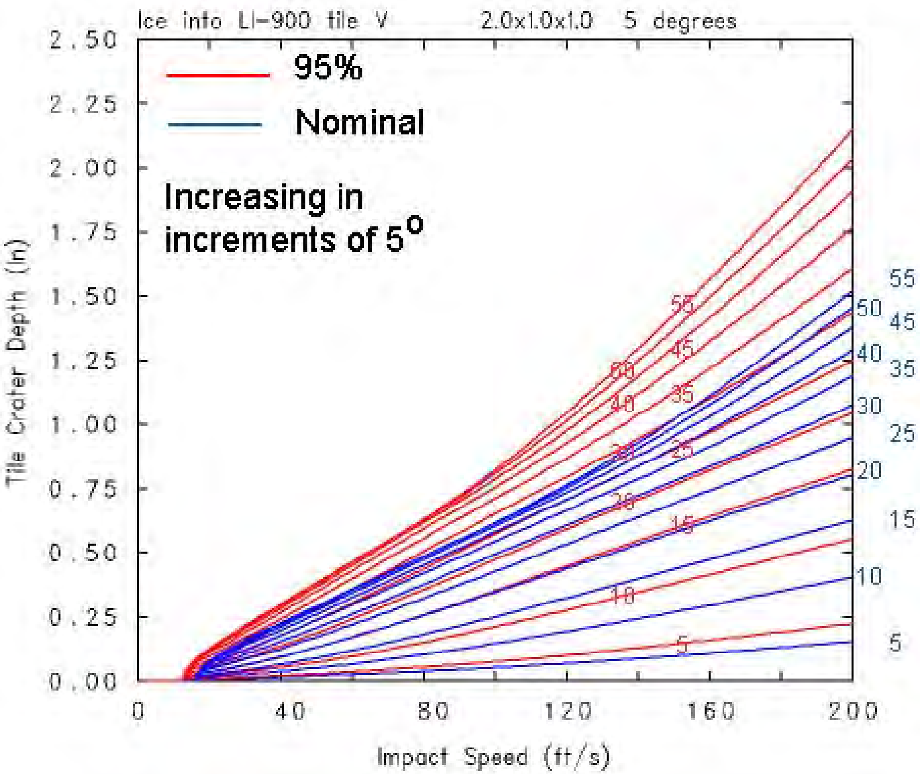

Depth

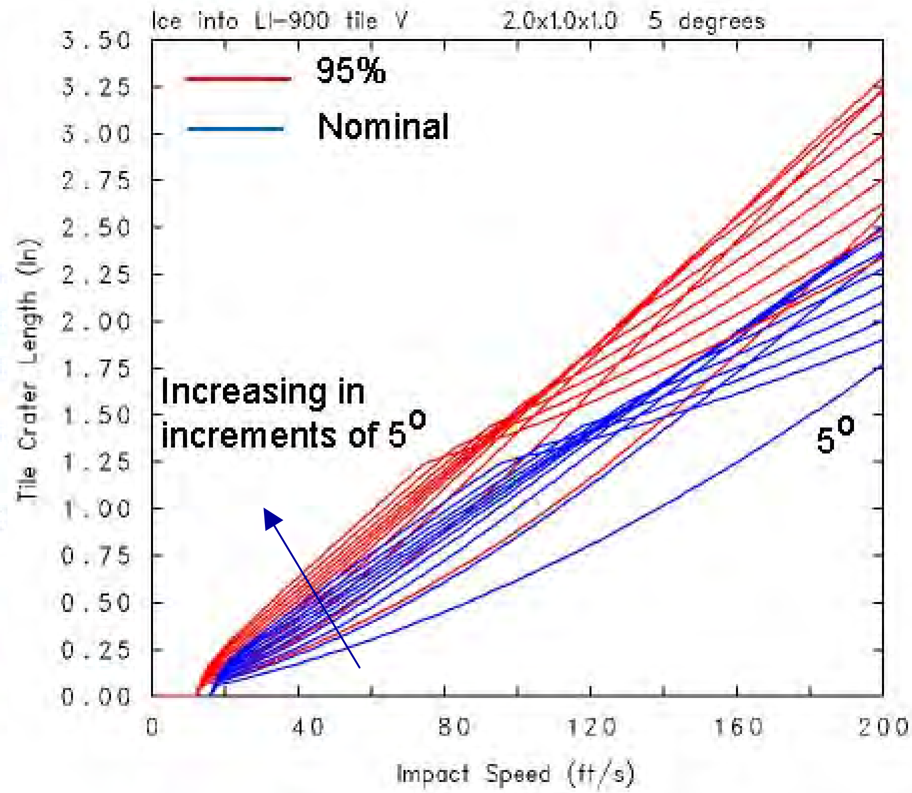

Length

Torn Thermal Blanket

Impact of Thermal Blanket on Speed Brake

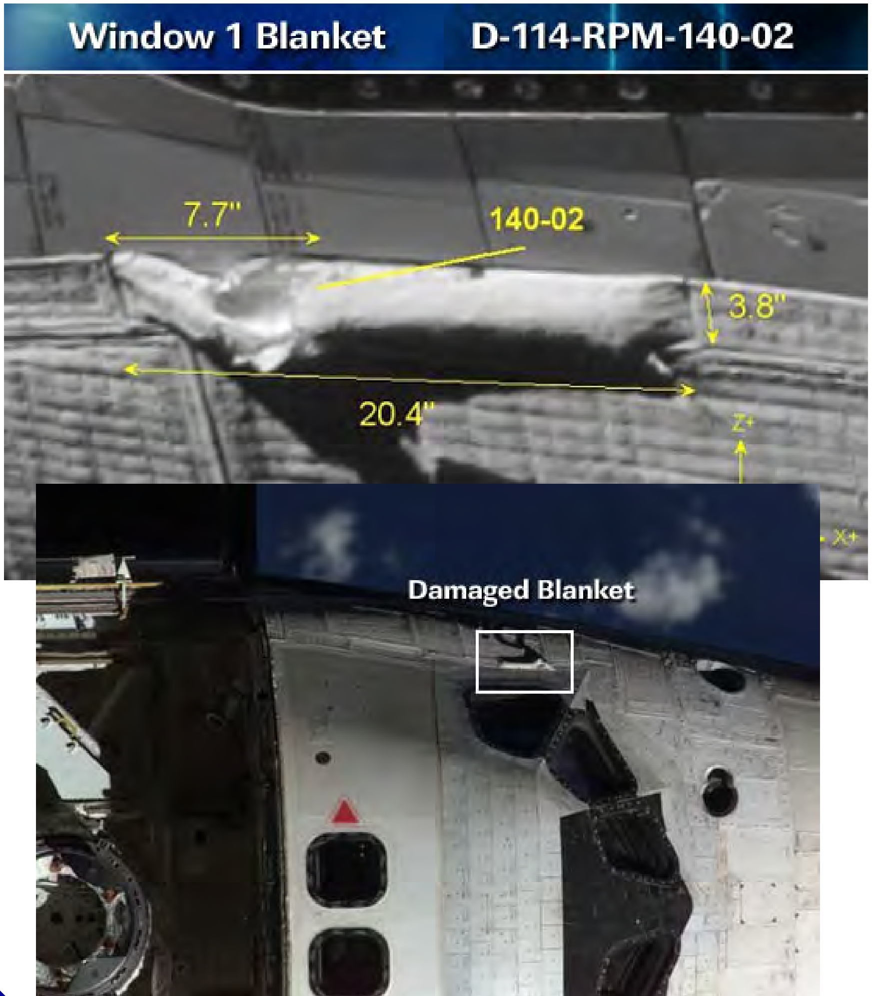

- We performed computations to examine the impact of the thermal blanket were it to tear free during re-entry for STS-114 and strike the speed brake.
- Computations were performed with the hydrocode CTH.
- The impact computations were performed for a velocity of 1600 ft/s.
- “Conservative” issues related to the modeling were explored with LS-DYNA.

Ribbon Fabric Projectile: 12.7” × 3.8” × 0.18” (.053lb) impacting thermal blanket and speed brake at 1600 ft/s

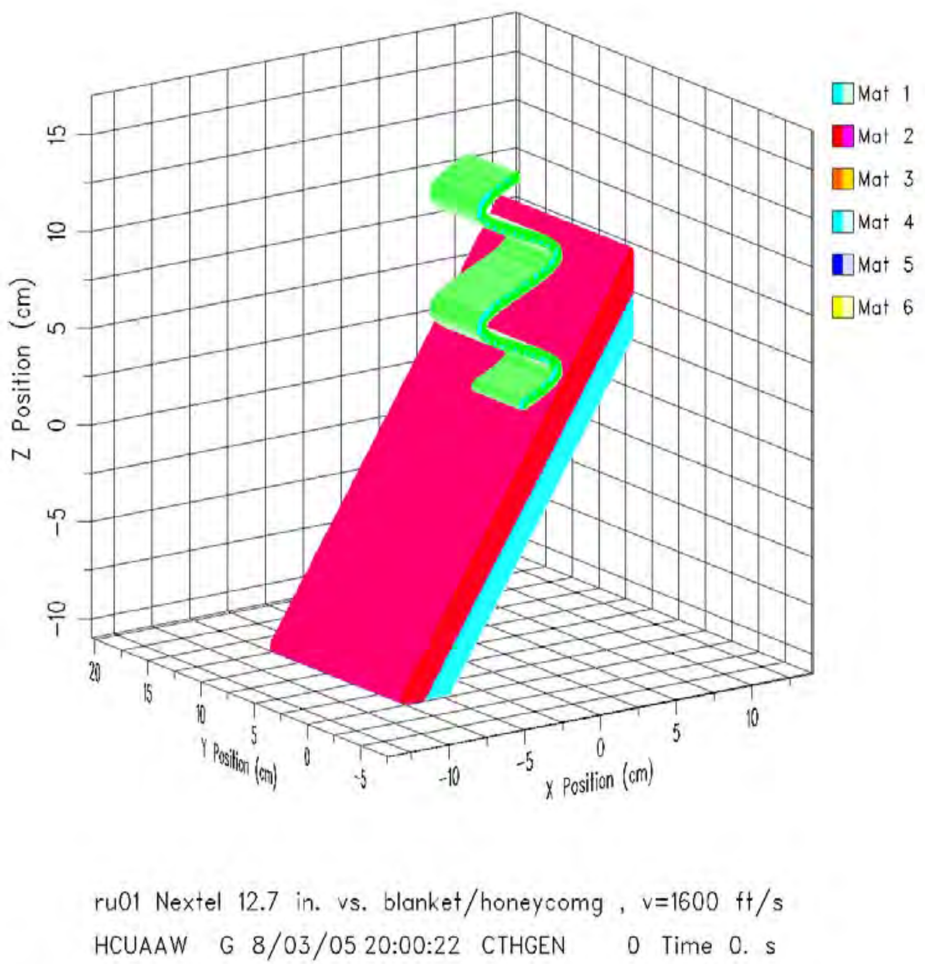

Ribbon Fabric Projectile: 12.7” × 3.8” × 0.18” (.053lb) impacting thermal blanket and speed brake at 1600 ft/s

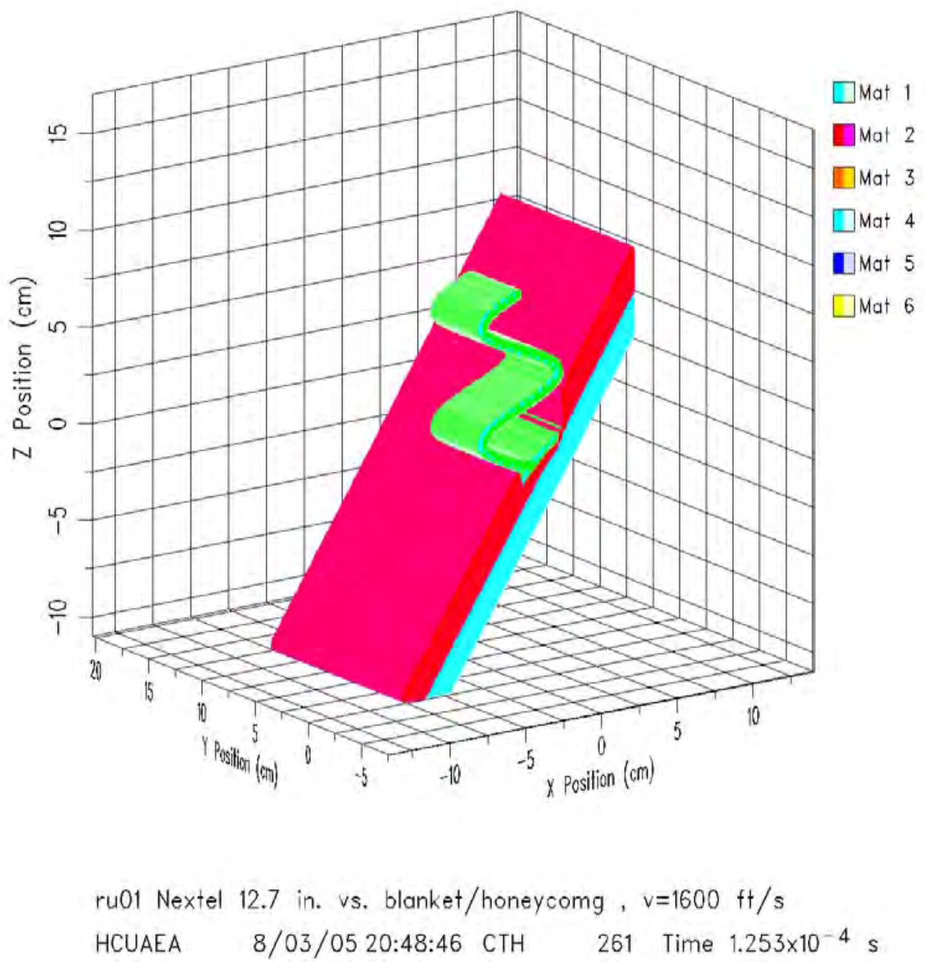

Ribbon Fabric Projectile: 12.7” × 3.8” × 0.18” (.053lb) impacting thermal blanket and speed brake at 1600 ft/s

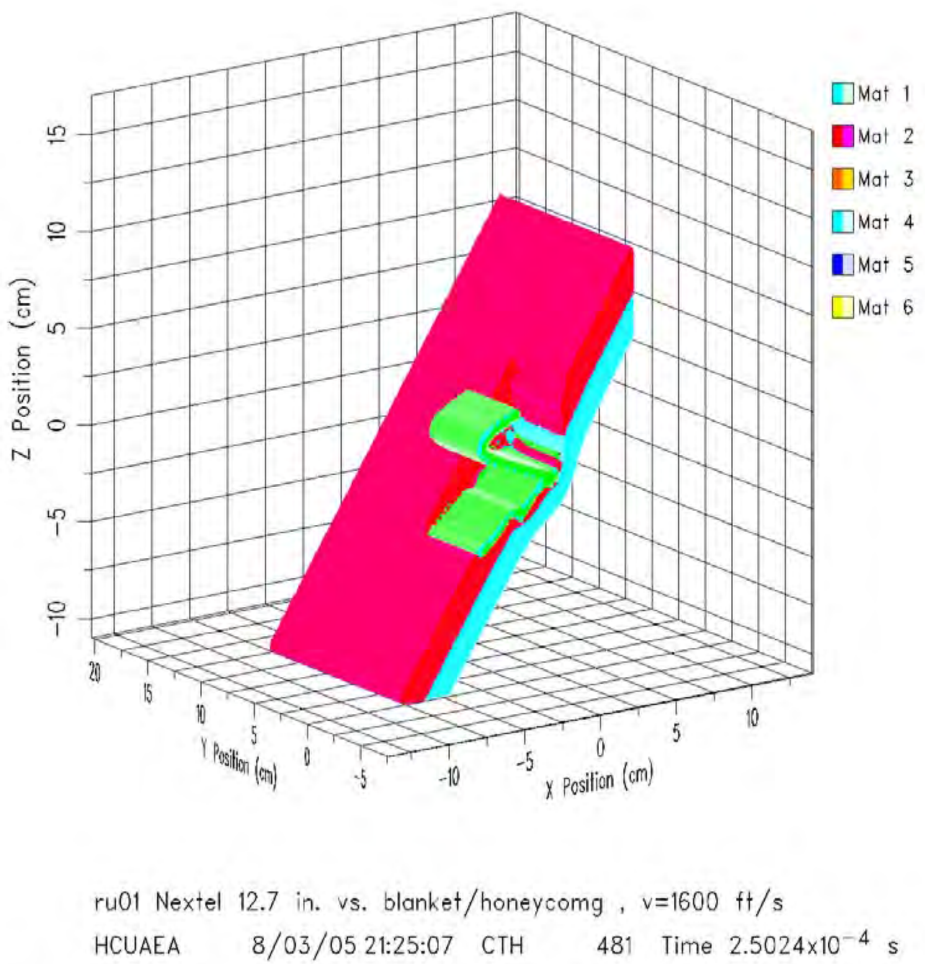

Ribbon Fabric Projectile: 12.7” × 3.8” × 0.18” (.053lb) impacting thermal blanket and speed brake at 1600 ft/s

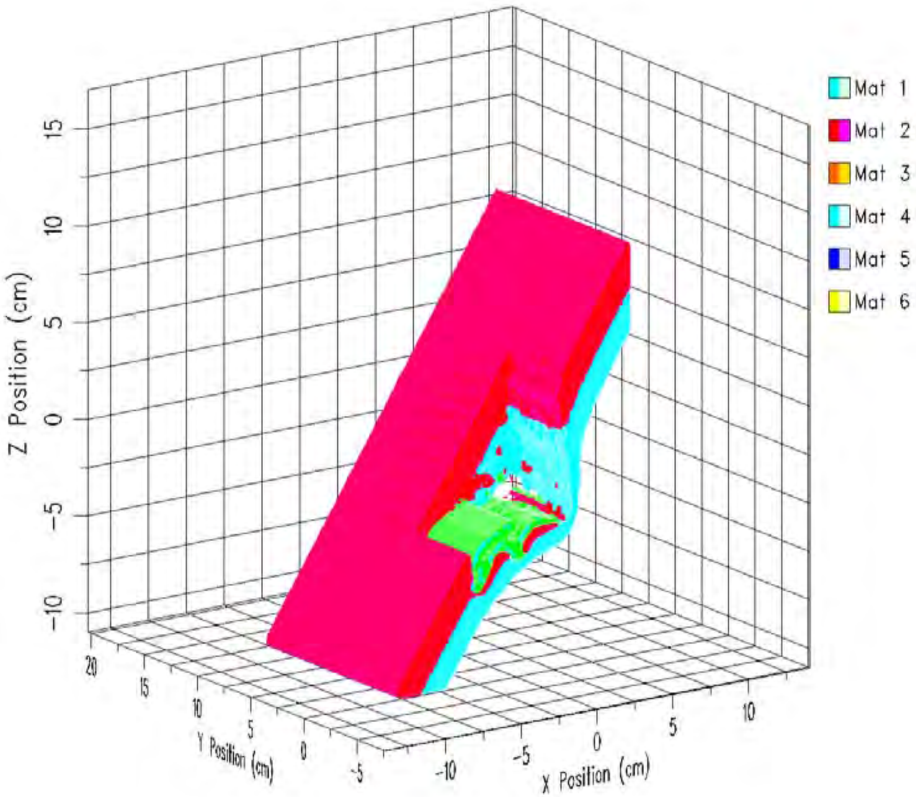

ru01 Nextel 12.7 in. vs. blanket/honeycomg , v=1600 ft/s

HCUAEA 8/03/05 21:59:46 CTH 692 Time 3.7543×10^{-4} s

Ribbon Fabric Projectile: 12.7” × 3.8” × 0.18” (.053lb) impacting thermal blanket and speed brake at 1600 ft/s

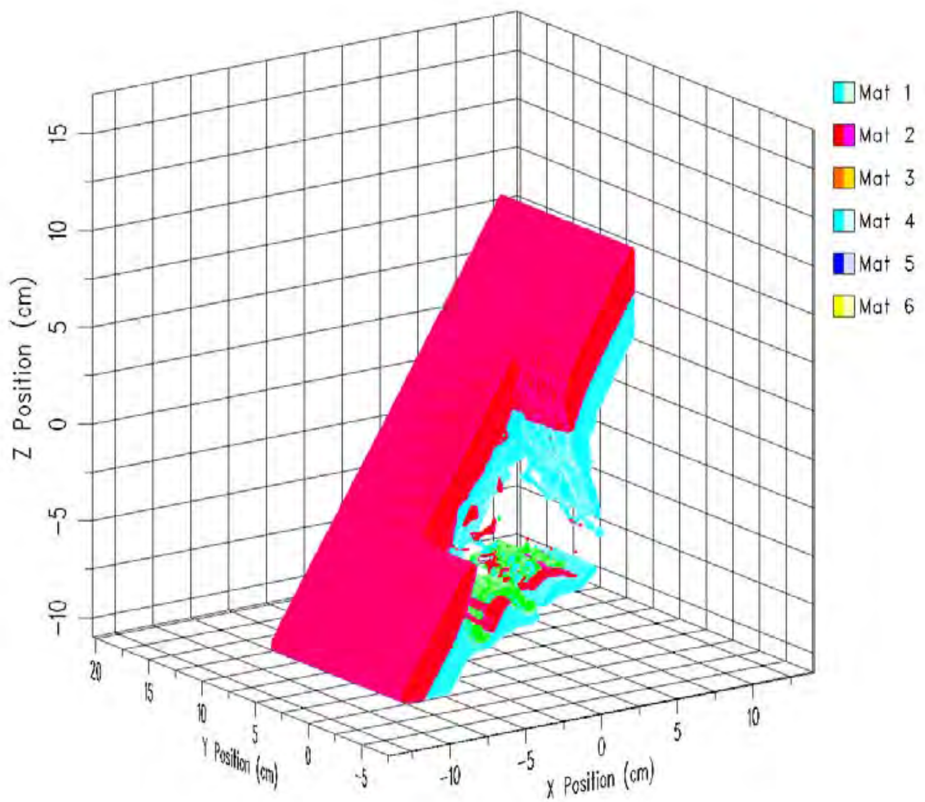

(Last)

ru01 Nextel 12.7 in. vs. blanket/honeycomg , v=1600 ft/s

HCUAEA 8/03/05 22:34:28 CTH 892 Time 5.0023×10^{-4} s

Initial Geometry
Impact speed: 1600 ft/s

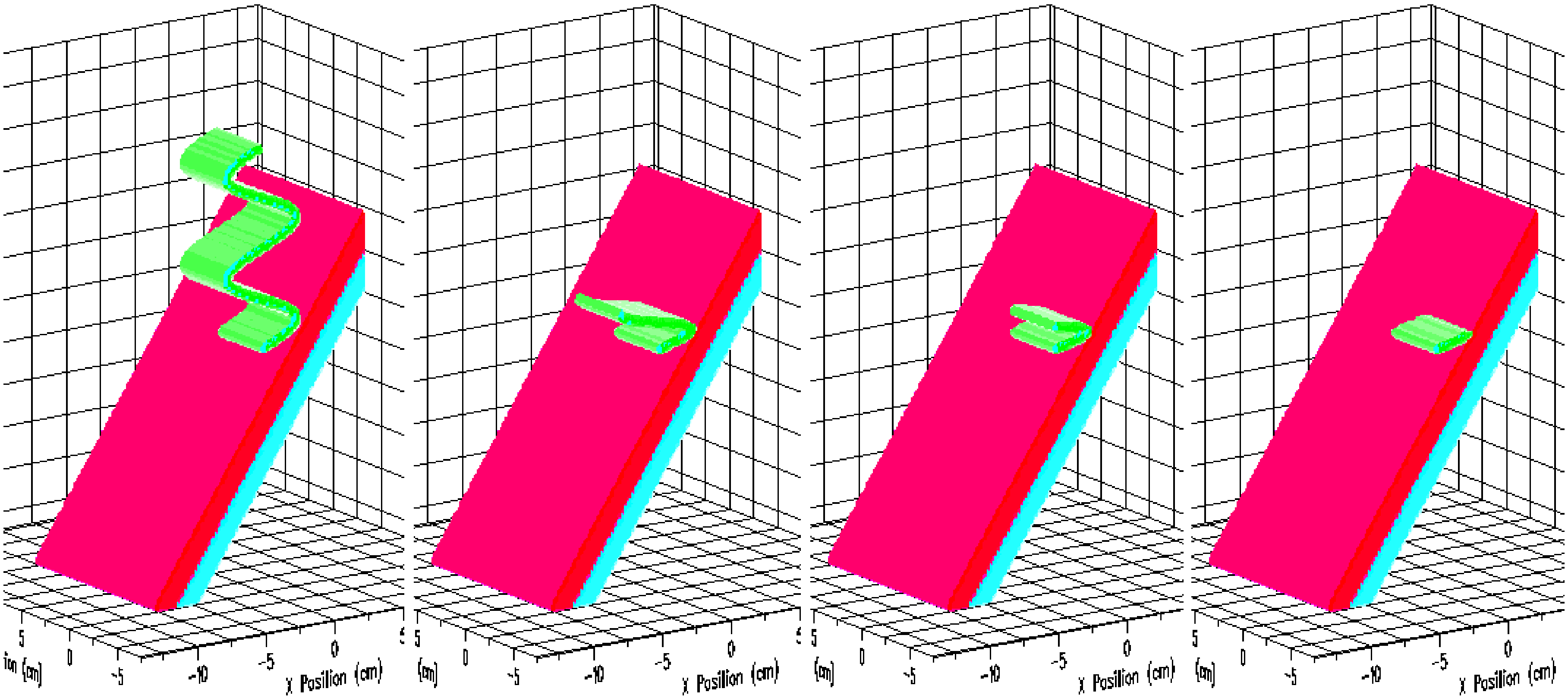

0.053 lb / 24 g	0.0177 lb / 8 g	0.0106 lb / 4.8 g	0.0053 lb / 2.4 g
12.7”×3.8”×0.18”	4.23”×3.8”×0.18”	2.54”×3.8”×0.18”	1.27”×3.8”×0.18”

Post Impact Geometry
Impact speed: 1600 ft/s

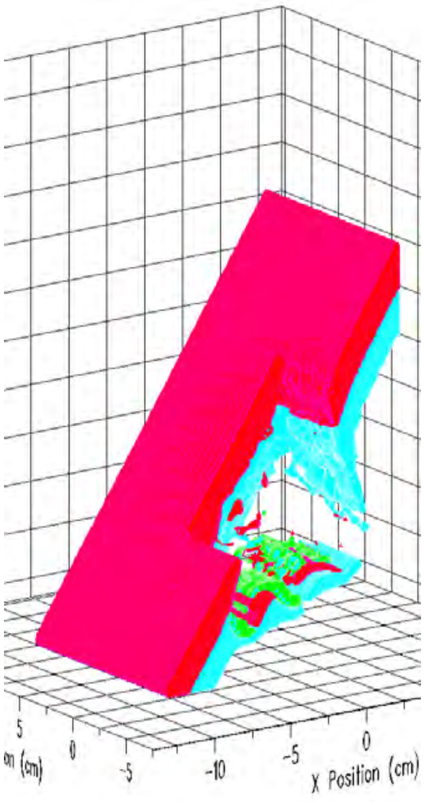

0.053 lb / 24 g
12.7”×3.8”×0.18”

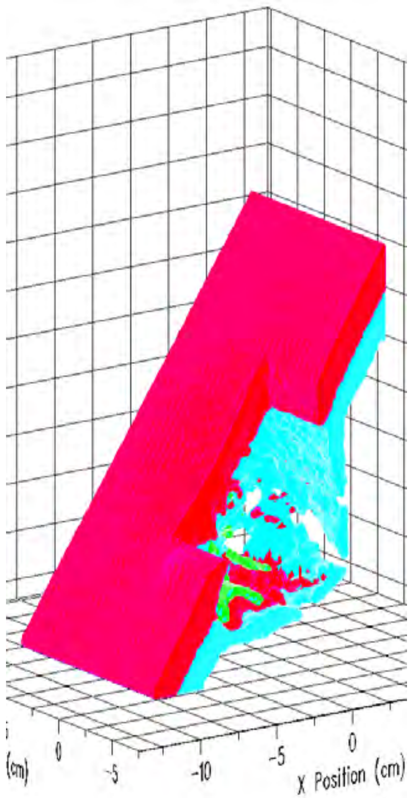

0.0177 lb / 8 g
4.23”×3.8”×0.18”

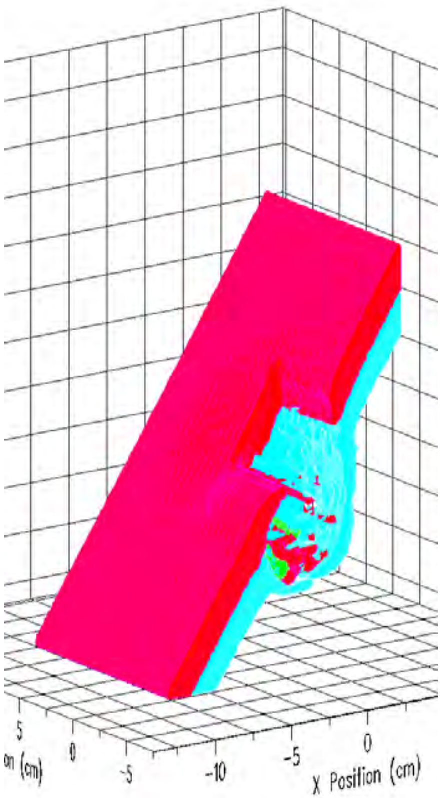

0.0106 lb / 4.8 g
2.54”×3.8”×0.18”

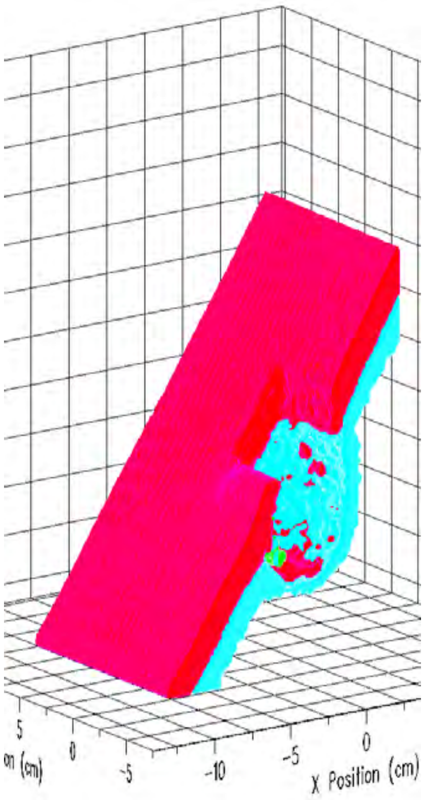

0.0053 lb / 2.4 g
1.27”×3.8”×0.18”

Examining an “Conservatism” in Our Honeycomb Modeling

- Modeling the aluminum honeycomb is difficult.
- In the Eulerian code CTH, we are unable to resolve the structure of the front and back sheets of the honeycomb, since our computational cell size is 2.5 mm and the thickness of the aluminum sheet is 0.11” (0.3 mm).
- To see if the honeycomb fails much more easily than it should, a series of computations were performed in DYNA to explore with a honeycomb we built out of shell elements.

Conclusions

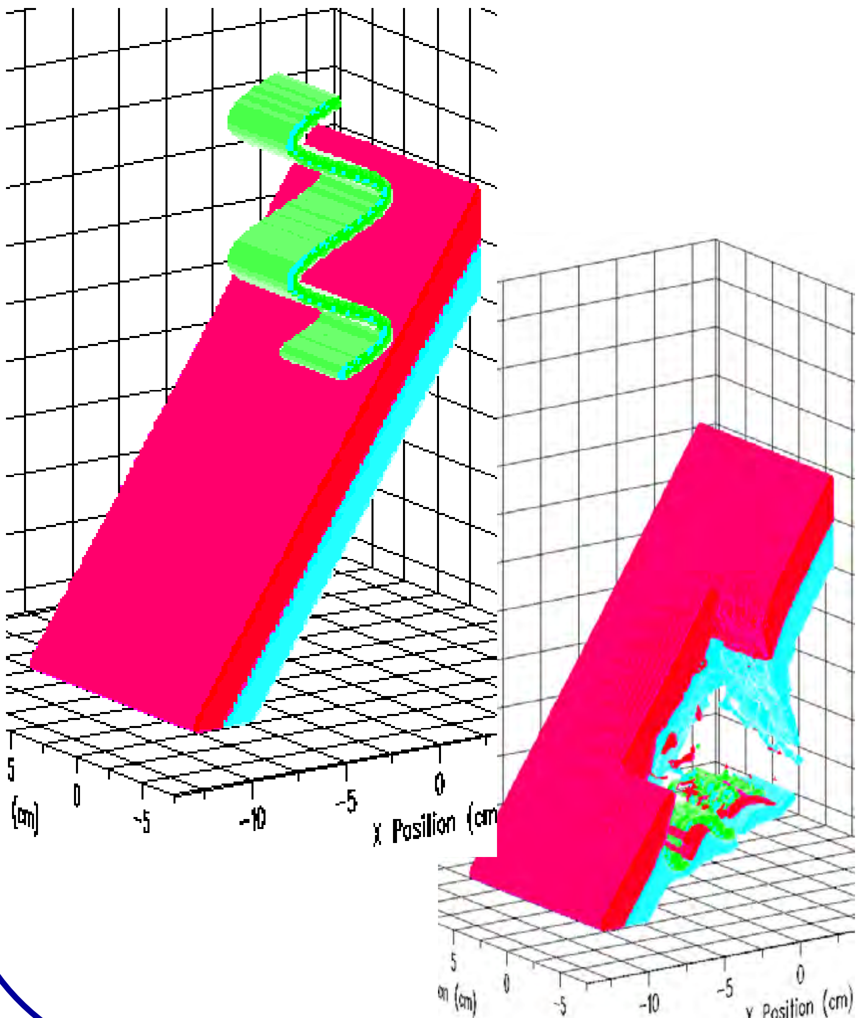

- Thermal blanket impact into the speed brake was modeled using current impact tools.
- It was assumed the fabric behaved similarly to LRSI LI-900 tiles (the density is similar).
- The blanket on the outside of the speed brake was modeled as an HRSI LI-900 tile.
- The honeycomb skin of the speed break was modeled with newly-created homogenized honeycomb material properties placed in the foam model.
- All impacts modeled in CTH (at 1600 ft/s) resulted in penetration of the tile and honeycomb.
- LS-DYNA honeycomb model contained a 0.0135 (6.1 g) impact (0.053/4).

Post Flight Inspection

Starboard Underside of Shuttle

Impact Damage to Tile

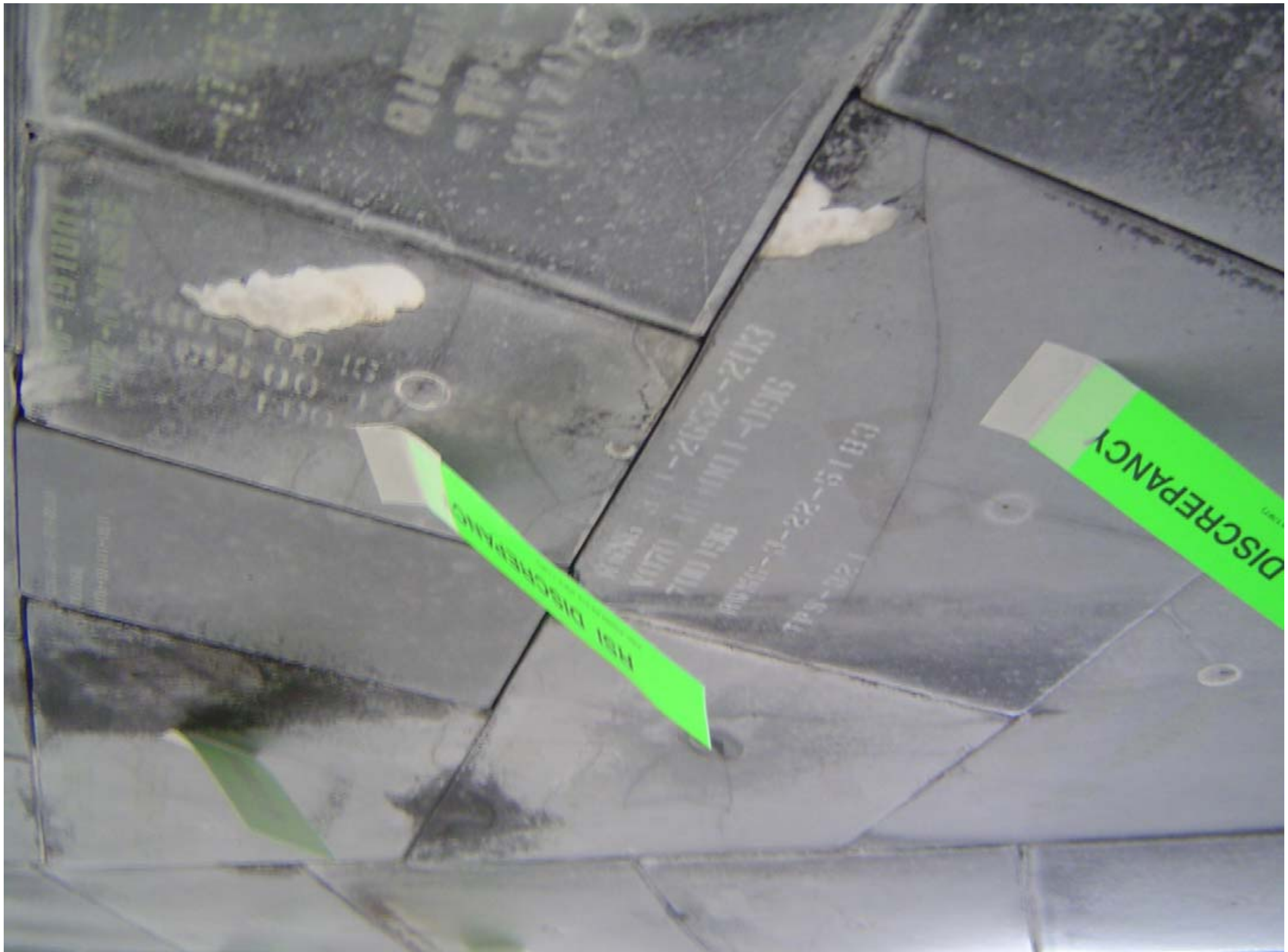

Charts to Estimate Debris Environment from Ice Damage

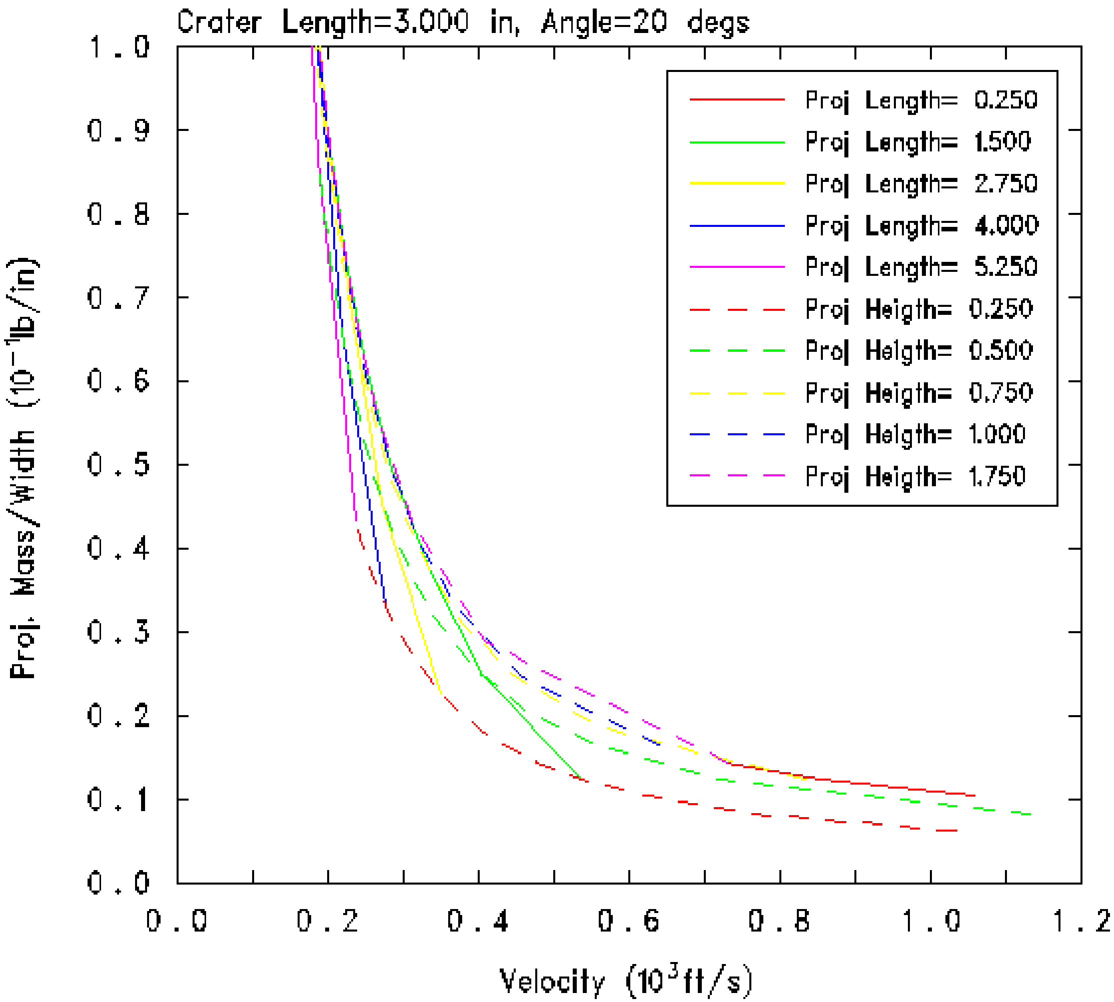

Charts to Estimate Debris Environment from Foam Damage

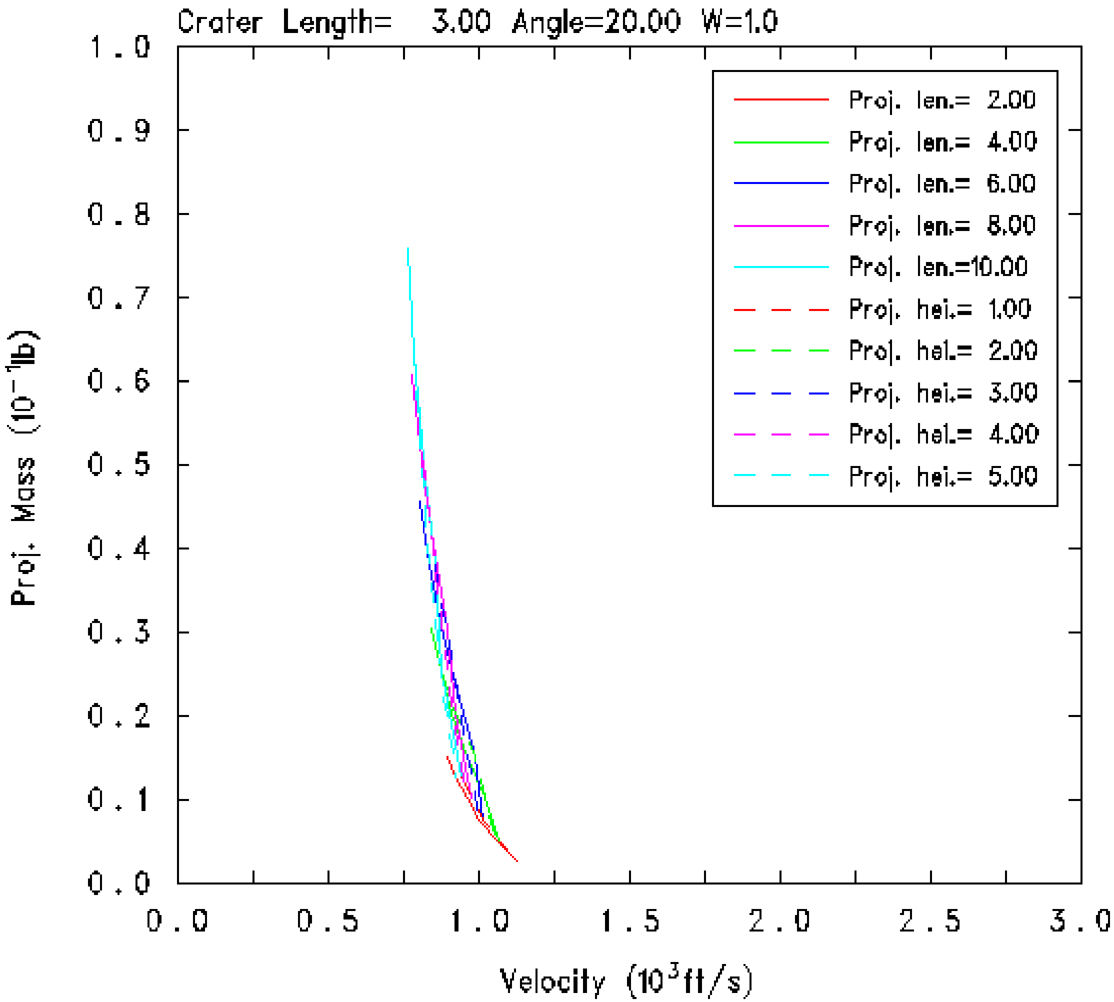

CAIB Recommendations R3.2-1,2
Reduce Damage and Risk

- Initiate an aggressive program to eliminate all External Tank Thermal Protection System debris-shedding at the source with particular emphasis on the region where the bipod struts attach to the External Tank. [RTF]
- Initiate a program designed to increase the Orbiter's ability to sustain minor debris damage by measures such as improved impact-resistant Reinforced Carbon-Carbon and acreage tiles. This program should determine the actual impact resistance of current materials and the effect of likely debris strikes. [RTF]

STS-121

- 115th flight of the Space Shuttle Program
- 32nd flight of *Discovery*
- *Discovery* first flew in 1984
- Projected Launch: May 2006
- Crewed by
  - Steve Lindsey
  - Mark Kelly
  - Michael Fossum
  - Lisa M. Nowak
  - Piers Sellers
  - Stephanie Wilson
  - Thomas Reiter

Our Approach to Understanding and Our Validation Triangle

When experiments, large-scale numerical simulations and the analytical physics-based model agree, the physics-based model is assumed to be validated.

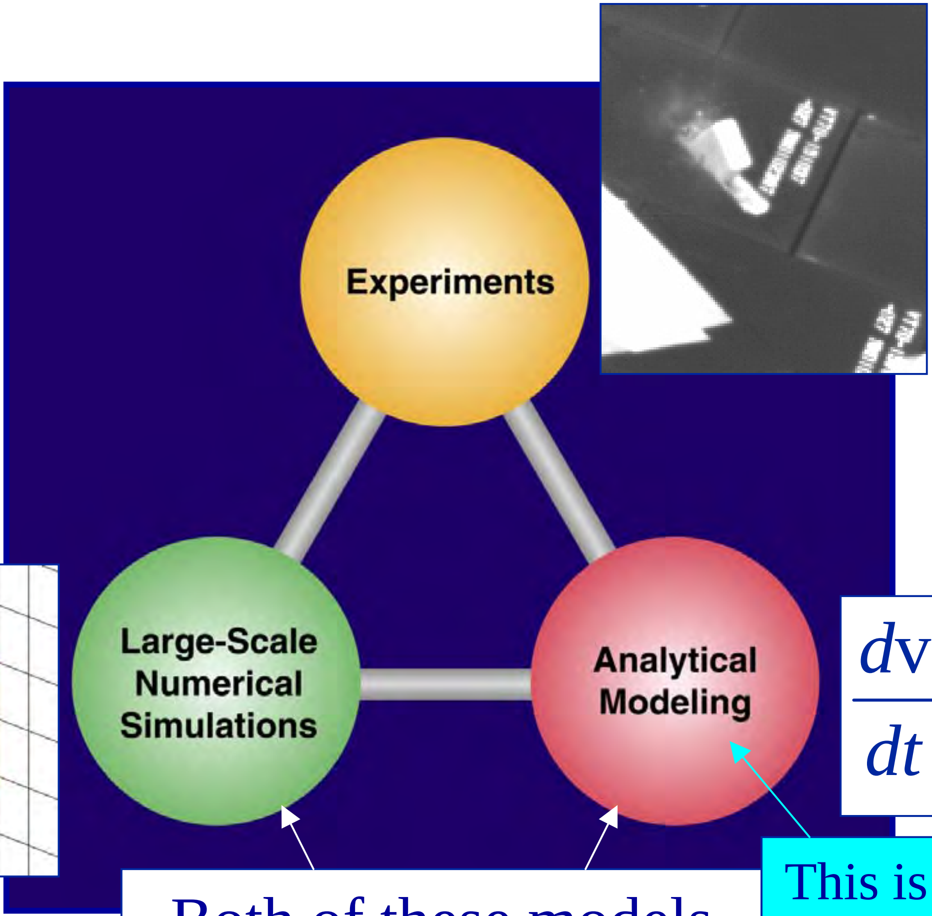

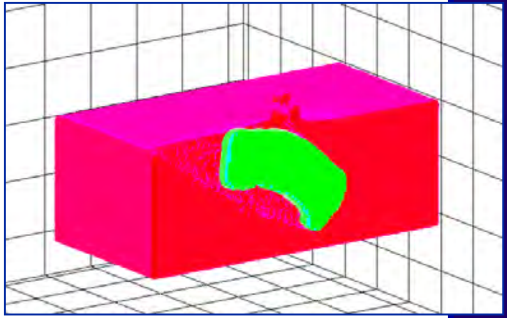

$$\frac{dv}{dt} = -\frac{\sigma_{zz}(v)}{\rho_p L}$$

Both of these models are Physics Based

This is our fast-running, physics-based model for flight

End of Charts

Progress on the NDE Characterization of Impact Damage in Armor Materials

Joseph M. Wells, Sc.D.

JMW ASSOCIATES

102 Pine Hills Blvd
Mashpee, MA 02649-2869
(508) 477-5764
jmwconsultant@comcast.net

XCT

Terminal Ballistics Oral Session #1 - Abstract #1854

Grateful Acknowledgements to:

W.H. Green, and N.L.Rupert, ***ARL Weapons & Materials Research Directorate, APG, MD, 21005***

2002 ARL Summer Students

Mr. Jeff Wheeler (UCSC),

Mr. Herb Miller, (UMBC)

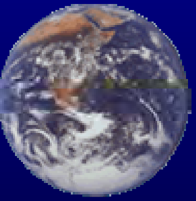

Dr. S.J. Cimpoeru, ***DSTO Aeronautical and Maritime Research Laboratory, PO Box 4331, Melbourne 30001, Australia***

Dr. Christof Reinhart, ***Volume Graphics Gmbh, Heidelberg, Germany***

Talk Outline

- Introduction – Challenge for Ceramic Armor
- Perspective on Damage Diagnostics & Cognitive Visualization
- Advanced 3D Voxel Analysis & Visualization
- 3D XCT Damage Characterization & Visualization
- Summary Comments

Challenge for Ceramic Armor

Ancient Chinese terra cotta armor vest

- History: Application of ceramic armor against high L/D penetrators is in its' third millennium.
- Still Searching for Best Ceramic Armor !
- Knowledge & Understanding - to design, make and apply notional ceramic armor materials.

Perspective – Damage Diagnostics & Performance

- **<u>Penetration Analysis:</u>**
  - **DOP, V50, Field Ballistic Tests**

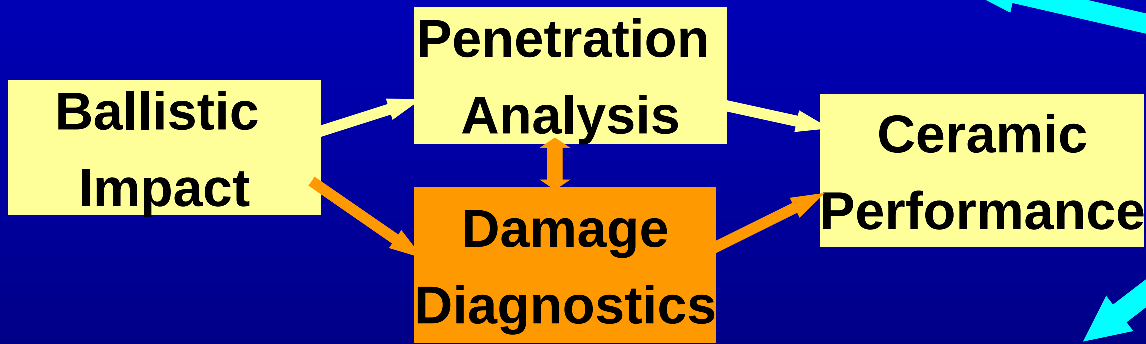

DESIGN BASIS:

- **Theoretical**
- **Empirical & Numerical Computational Focus**
- **Diagnostic/ Analytical & Mechanistic Focus**

- **<u>Damage Diagnostics & Assessment:</u>**
  - **Destructive Sectioning & 2D Examination**
  - **Traditional Nondestructive Examination**
  - **High Resolution X-ray Computed Tomography, XCT, for 3D Diagnosis**

- **Ideally we want a Engineering <u>Predictive Modeling Capability</u> addressing both penetration & damage considerations.**

Perspective on Problem Solving & Cognitive Visualization

"<u>Imagination</u> is more important than knowledge. Knowledge is limited. <u>Imagination</u> encircles the world." – Albert Einstein

Define Problem (Challenge)
- Create Engineering Approach (Plan)
  - Data (Acquire & Process)
    - Information (Analyze)
      - Knowledge (Understanding)
        - Visualization (Intellectual Conceptualization)
          - Creativity (New Ideas)
            - Innovation (Putting Ideas to Work)
              - Applications (Utilization of Technology)
                - Presentation & Reporting

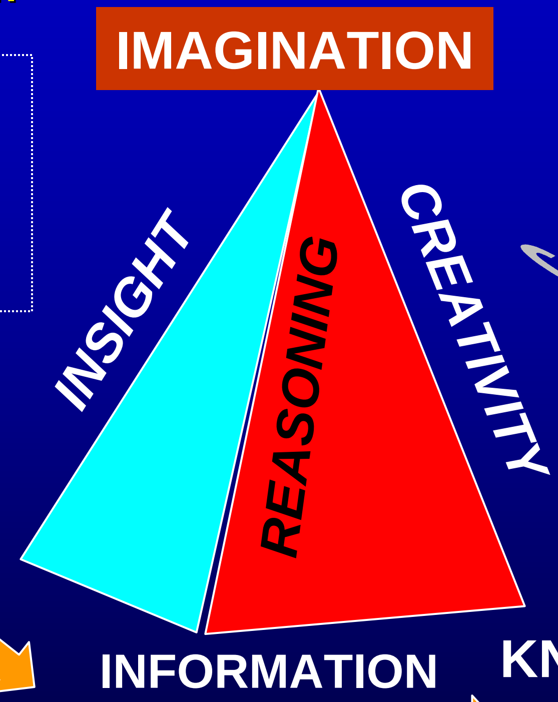

Cognitive

VISUALIZATION

XCT Digital Image Scans

Image Processing & Reconstruction

Understanding of feature relationships & significance

Primer on Modern XCT

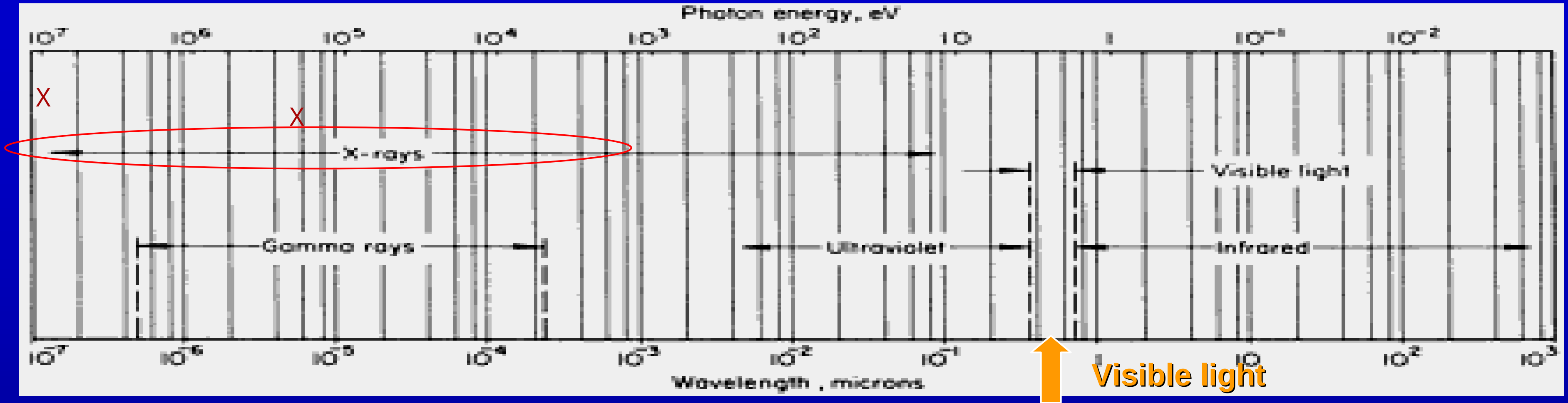

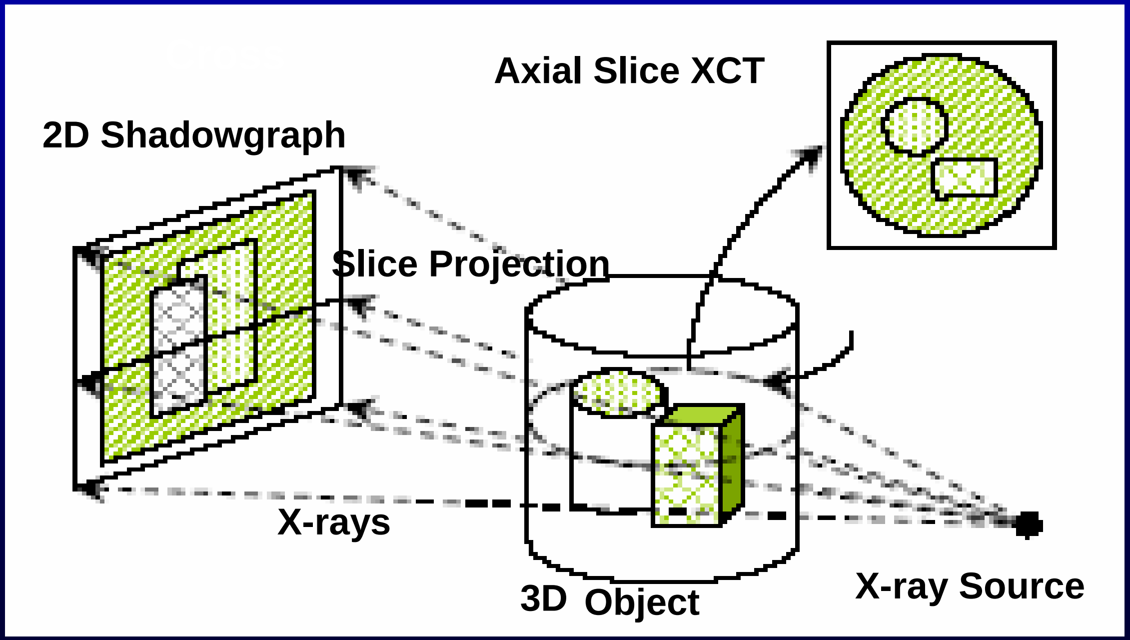

Advanced 3D Voxel Visualization & Analysis Software

StudioMax v1.2.1

www.volumegraphics.com

- Sophisticated image analysis and visualization capability to process, analyze and visualize voxel/volume data.
- Up to 3 GB of memory utilization with Windows XP Professional OS
- Multiple Import/Export File Formats
- Virtual Metrology Capabilities
- Variable Transparency & Virtual Sectioning
- Iso-Surface Extraction
- Segmentation & Grey-Value-Classification
- Porosity / Defect Analysis
- Wall Thickness Analysis
- Stereo Viewing Tool

Ballistic Impact Damage Diagnostics in Encapsulated TiB_2 Ceramic Targets

Encapsulated TiB_2 Experiment (N.L. Rupert, ARL ~1997)

- Single Shot (Full Penetration w/o compressive ring)
- Single Shot (Partial Penetration with compressive prestress ring)
- Double Shot (Full Penetration with compressive prestress ring)

Summary Damage Observations

Penetration Decrease with Prestress (17-4 PH Ring)

Surface Topography – Ring Steps, Radial Expansion & Cracking

W-alloy Residual Fragments

Complex Cracking Modes

Impact Induced Porosity

Impacted TiB2 Ceramics

Macro –Photos

Impact surface

Single Shot (Full Penetration w/o compressive ring)	Single Shot (Partial Penetration with compressive prestress ring)	Double Shot (Full Penetration with compressive prestress ring)

XCT Scans ~ mid-thickness

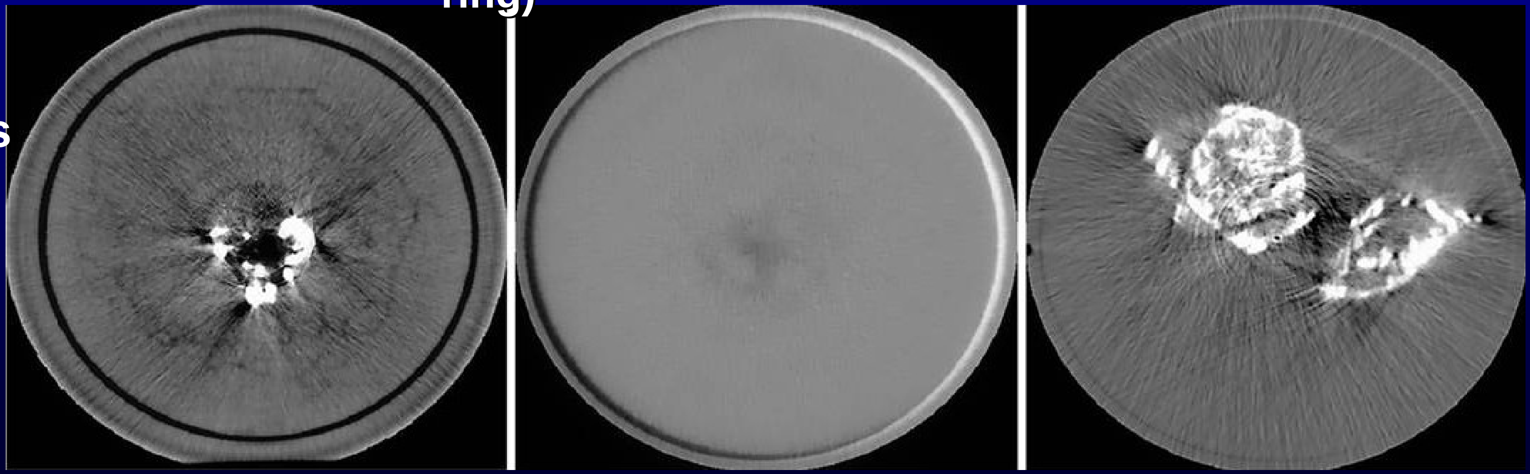

Penetration & Internal Damage

Back Face

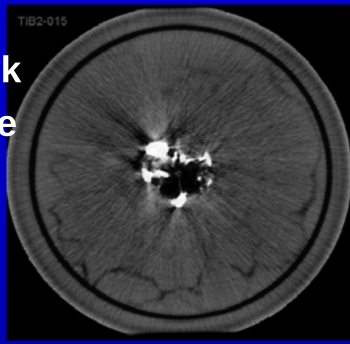

(z = 015)

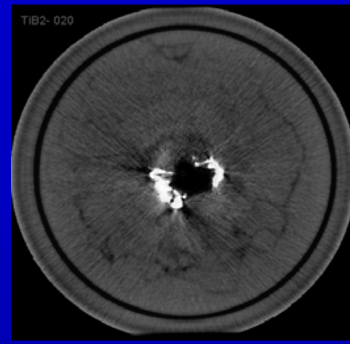

(z = 020)

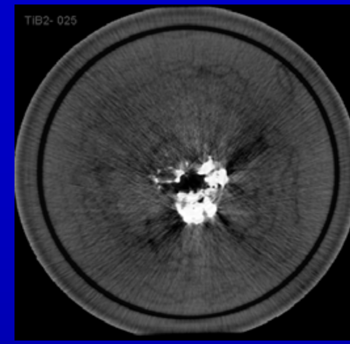

(z = 025)

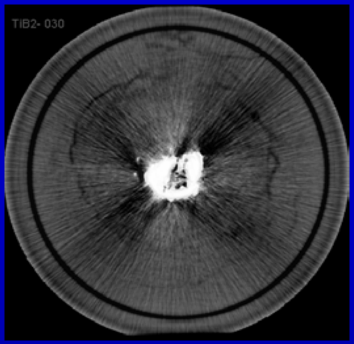

(z = 030)

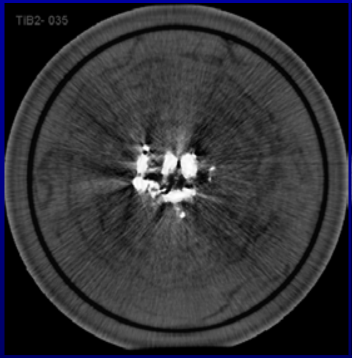

(z = 035)

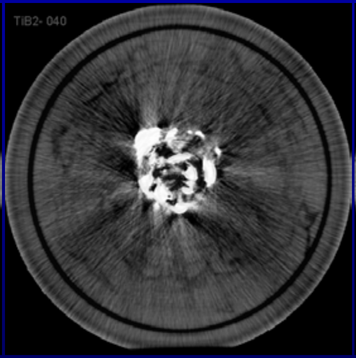

(z = 040)

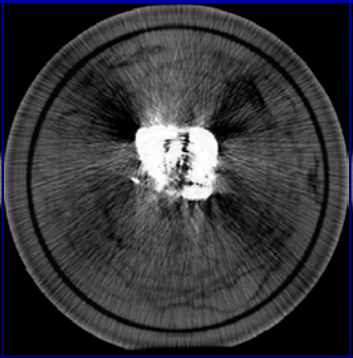

(z = 045)

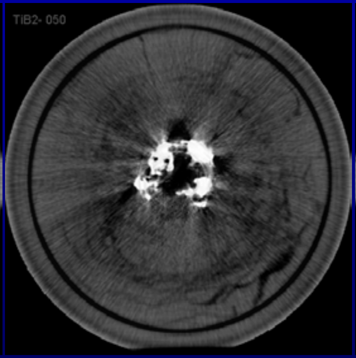

(z = 050)

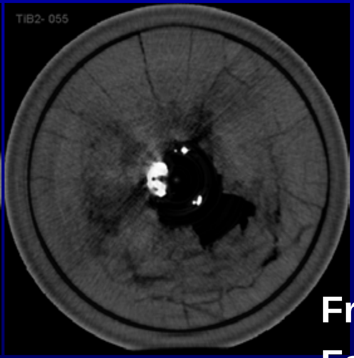

(z = 055)

Front Face

Sequential XCT Scans showing impact damage cracking features and residual penetrator (white) in TiB_2 S1wo Disk - near back (Z=015) to front face (Z=55).

Surface Topography -TiB_2 1S w/o prestress

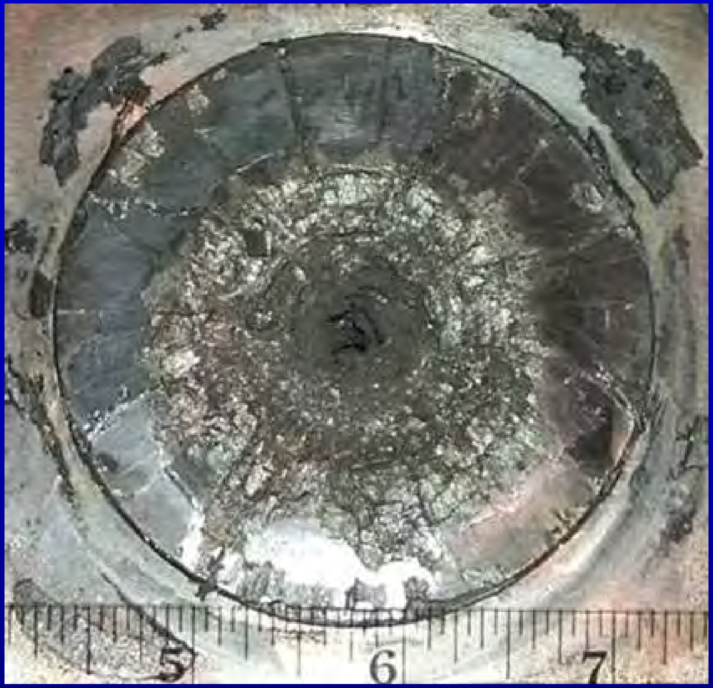

Macro-photograph - Normal View
*Surface Steps – **NOT** Visable*
Radial OD Cracks – ARE Visable

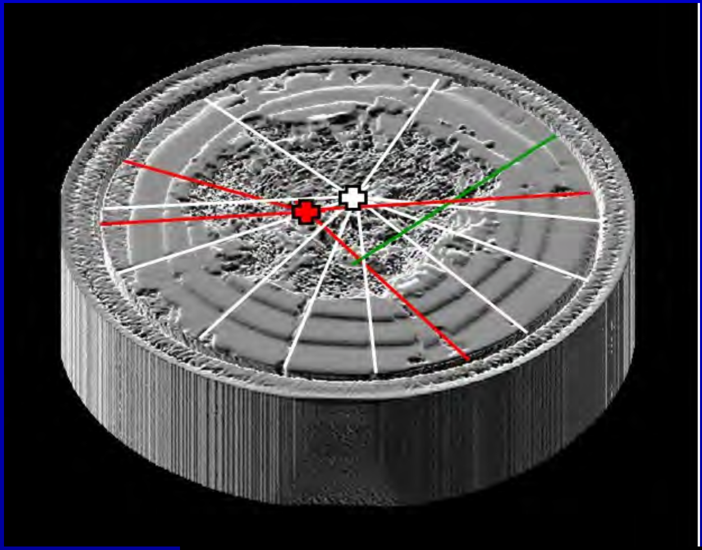

OD Radial cracks on Impact Surface **intersect at different loci**

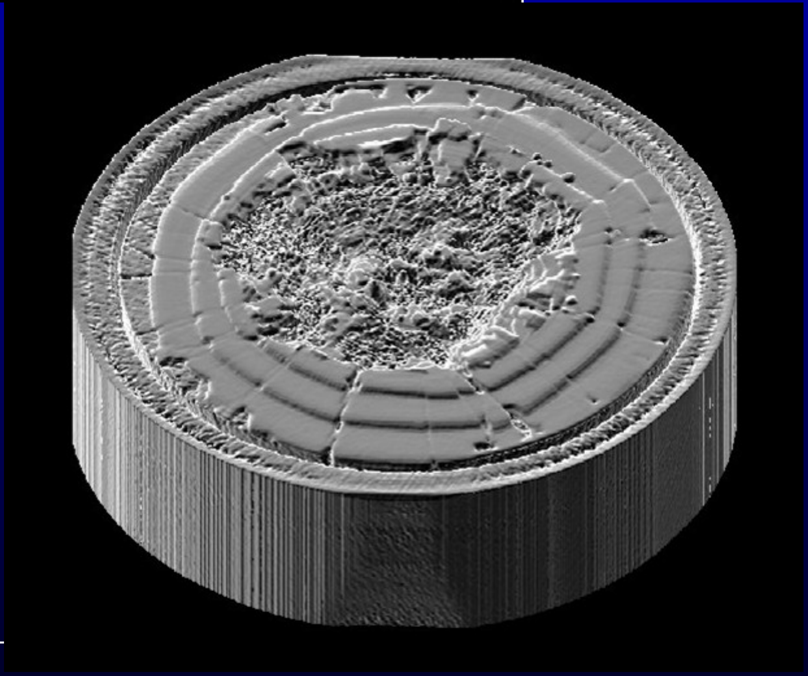

XCT 3D Solid Object - Oblique View
Surface Steps – ARE Visable
Radial OD Cracks – ARE Visable

Impact Surface- Flow of Mixed Penetrator & Ceramic Rubble

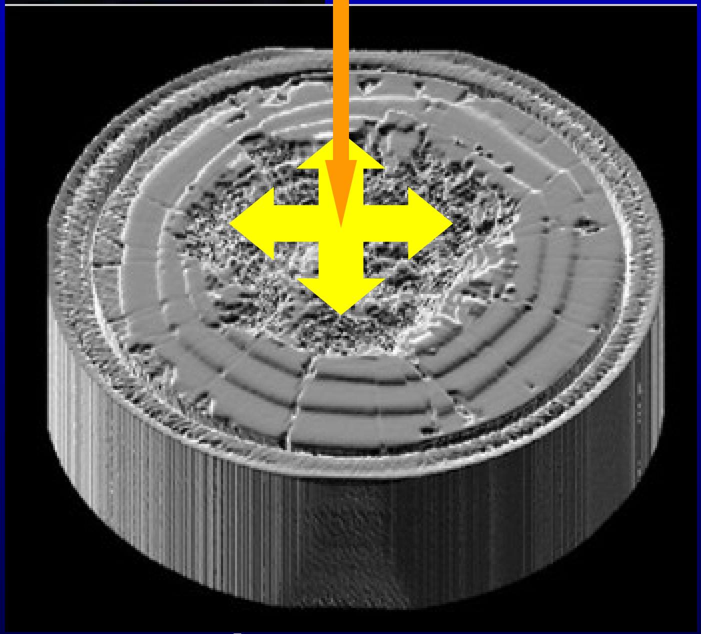

TiB_2 S1wo

Surface Steps –Sectioned

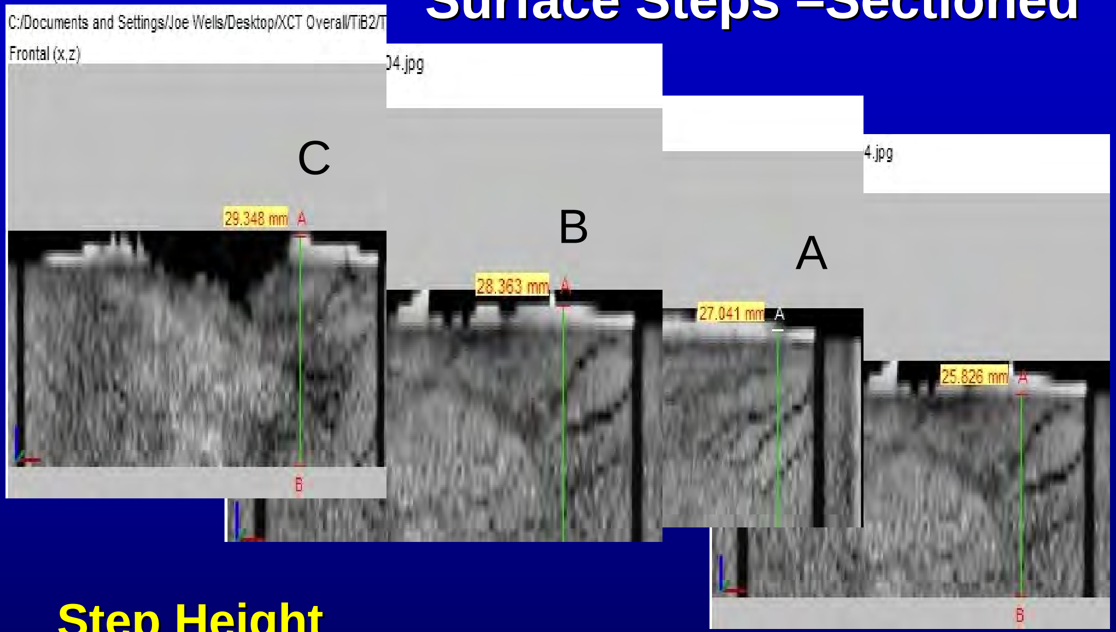

Step Height
C = ~3.5 mm
B = ~2.5 mm
A = ~1.2 mm

Step Heights Vary along the ring circumference

Note: Higher density (lighter color) of Steps vs Bulk TiB_2

Impact Surface Radial Expansion

Nonuniform – but localized radial expansion near impact surface

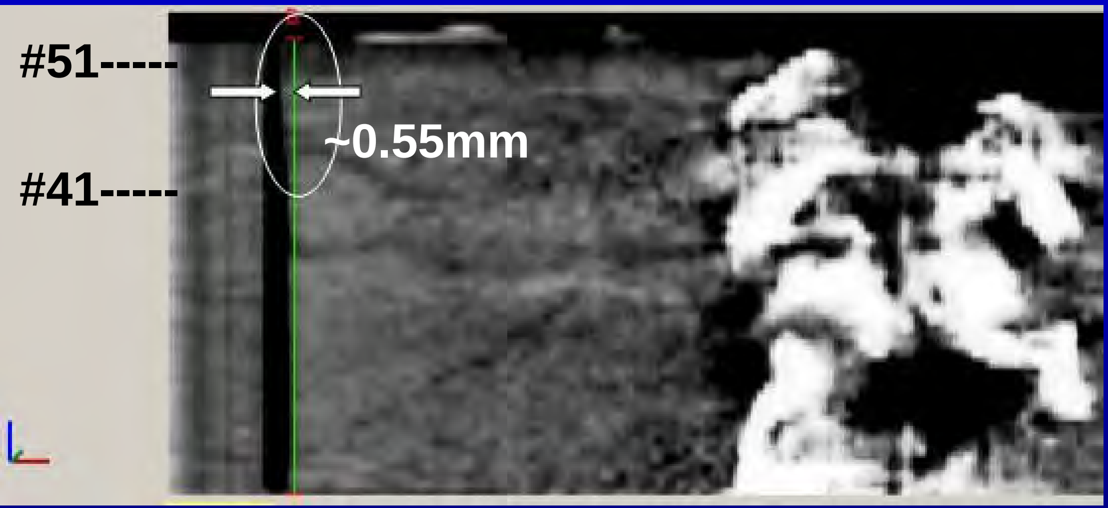

TiB$_2$ S1wo

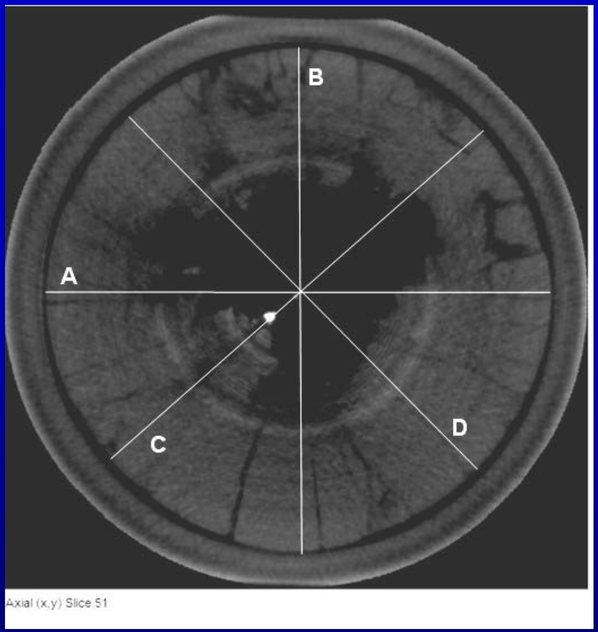

Axial Slice #51		Axial Slice #41
Dia. A = 73.8 mm	→	Dia. A = 72.7 mm
Dia. B = 73.4 mm		Dia. B = 72.9 mm
Dia. C = 72.3 mm		Dia. C = 72.1 mm
Dia. D = 72.4 mm		Dia. D = 72.0 mm

Fragments in TiB_2 - Segmented & Virtual Transparency

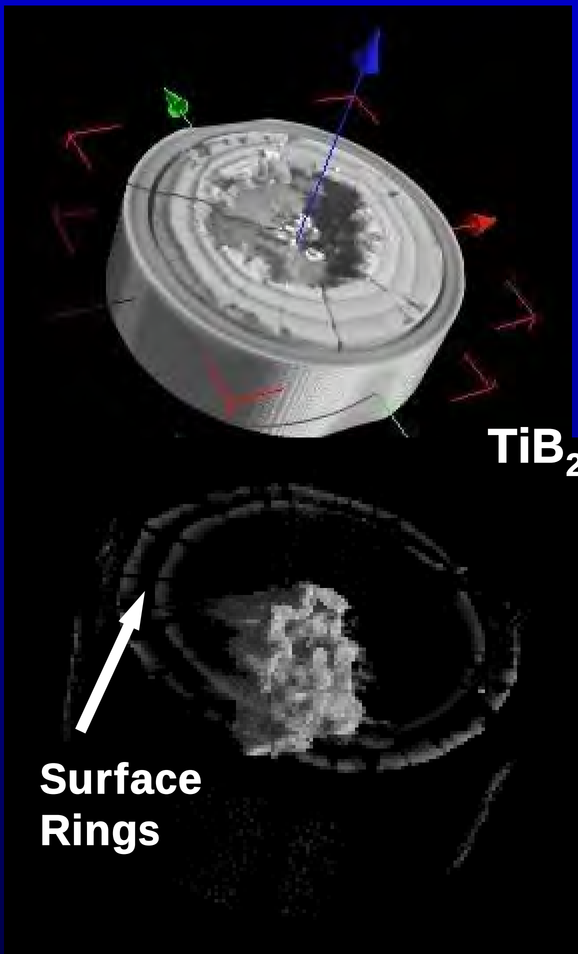

TiB_2 S1wo

Opaque 3D Solid Object Reconstructions

Segmented & Variable Transparency

Fragments are Porous

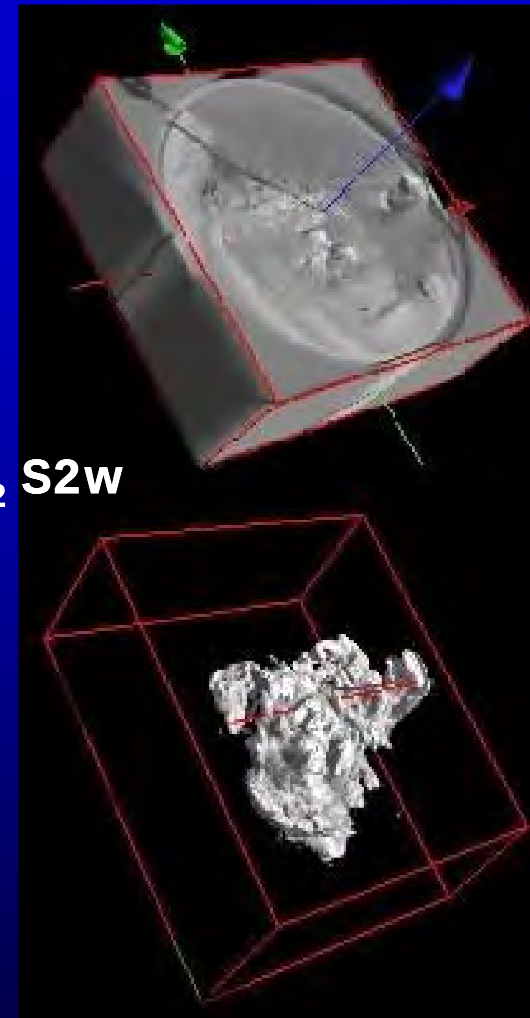

TiB_2 S2w

Virtual Metrology

W = ~22 mm   H = ~24.5 mm

A_s = 4794 mm^2 V = 2076 mm^3

W = ~60 mm   H = ~25.5 mm

A_s = 8911 mm^2 V = 2859 mm^3

Complexity of 3D Ring Cracking Damage

Early Point Cloud Images of 3D Cracking

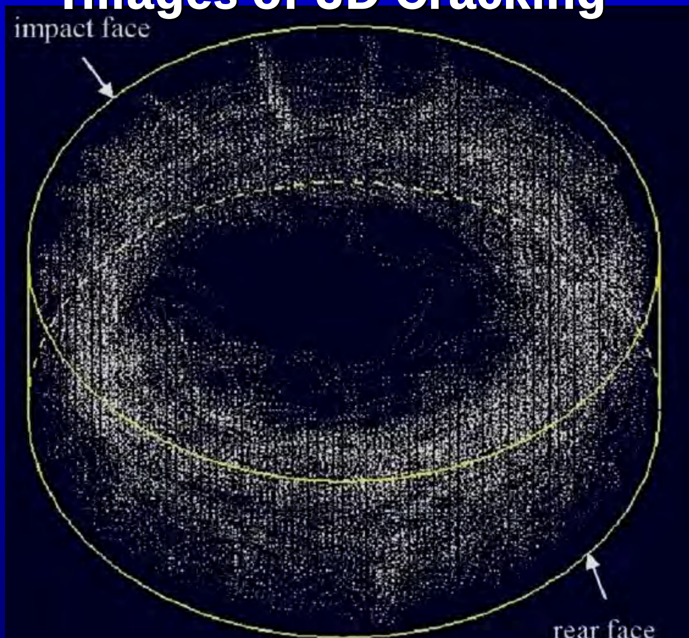

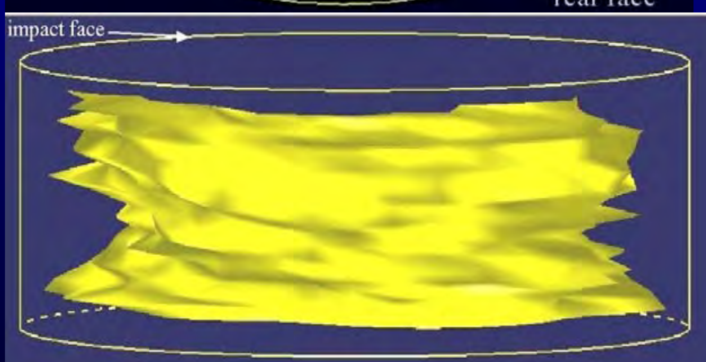

TiB2 1S w/o Prestress Ring

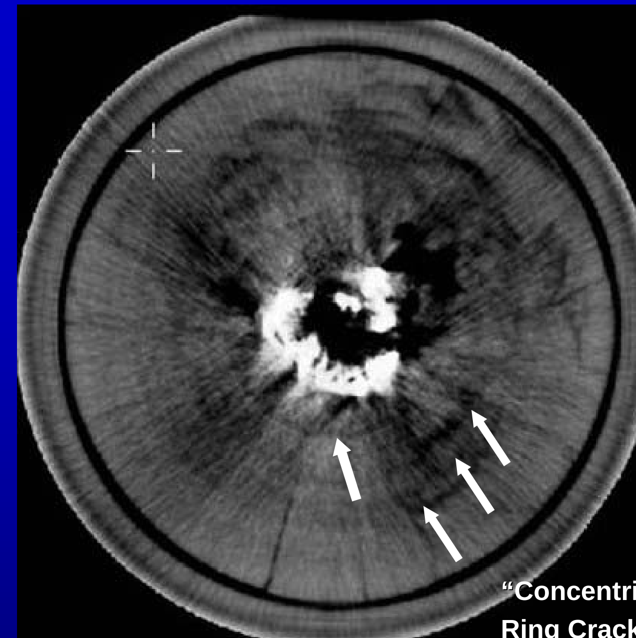

"Concentric" Ring Cracks

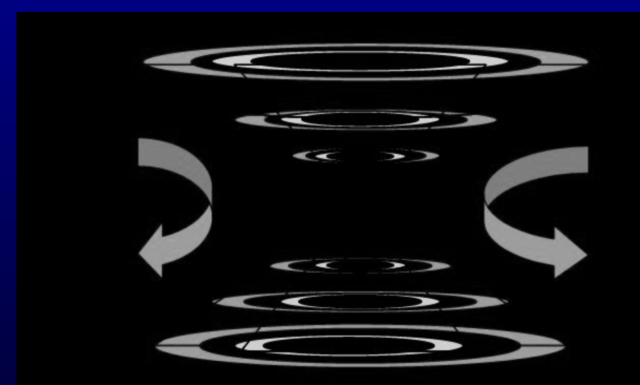

Schematic of Concentric Hourglass Ring Cracking

Visualization of 3D Cracking Damage in TiB_2

Orthogonal Sectioning
3D Oblique View

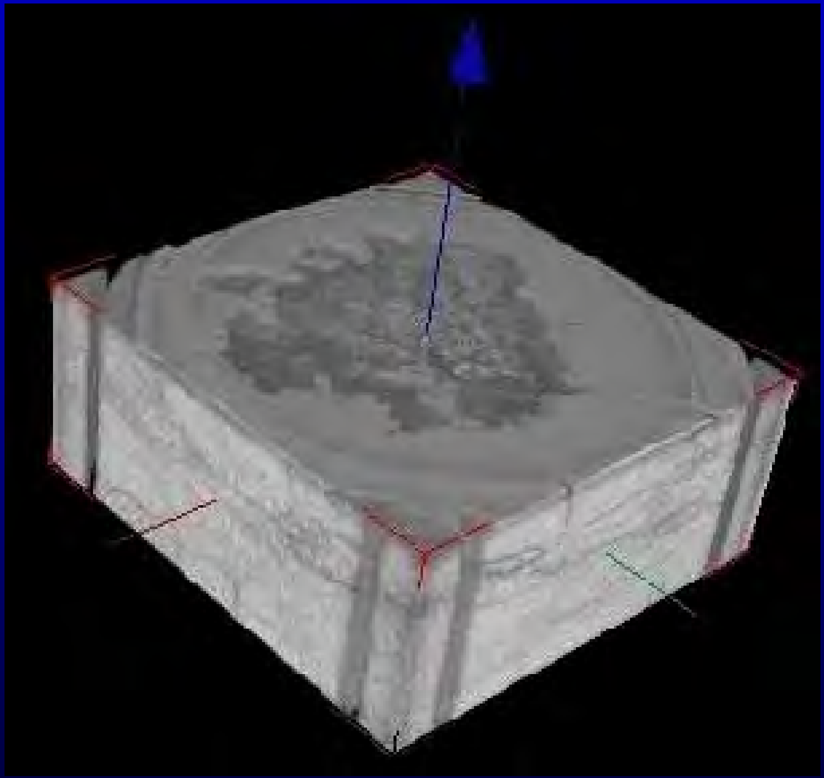

Recent (Preliminary) 3D Images of Segmented Impact Cracking

S1wo

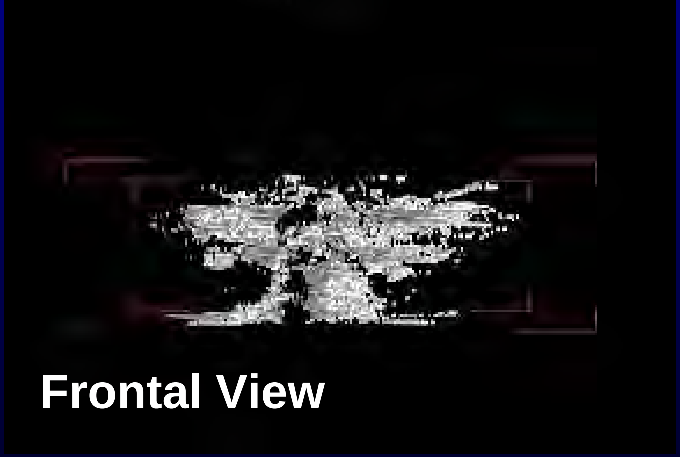

Impact Induced Porosity

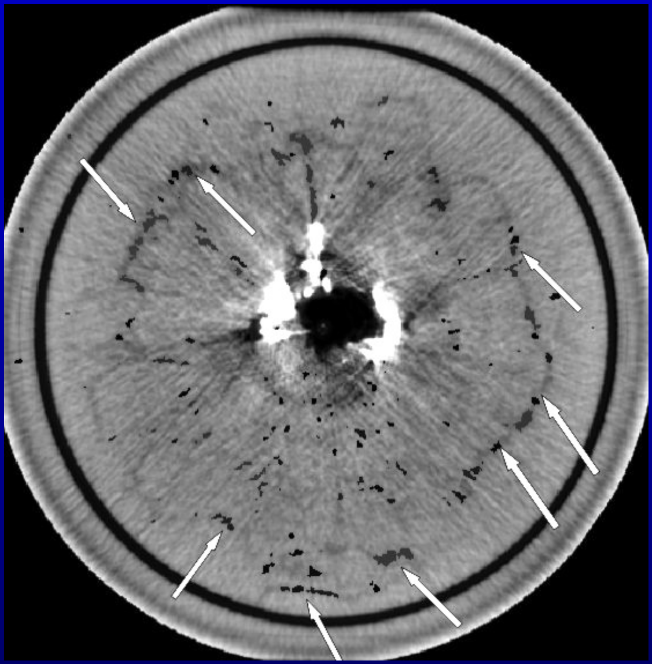

Porosity along Ring Cracks

TiB2 1S w/o Prestress Ring

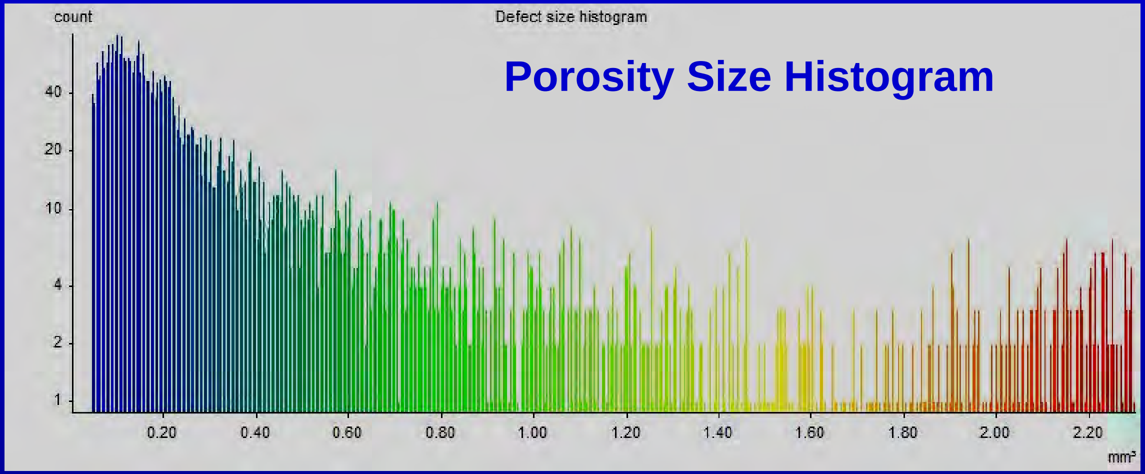

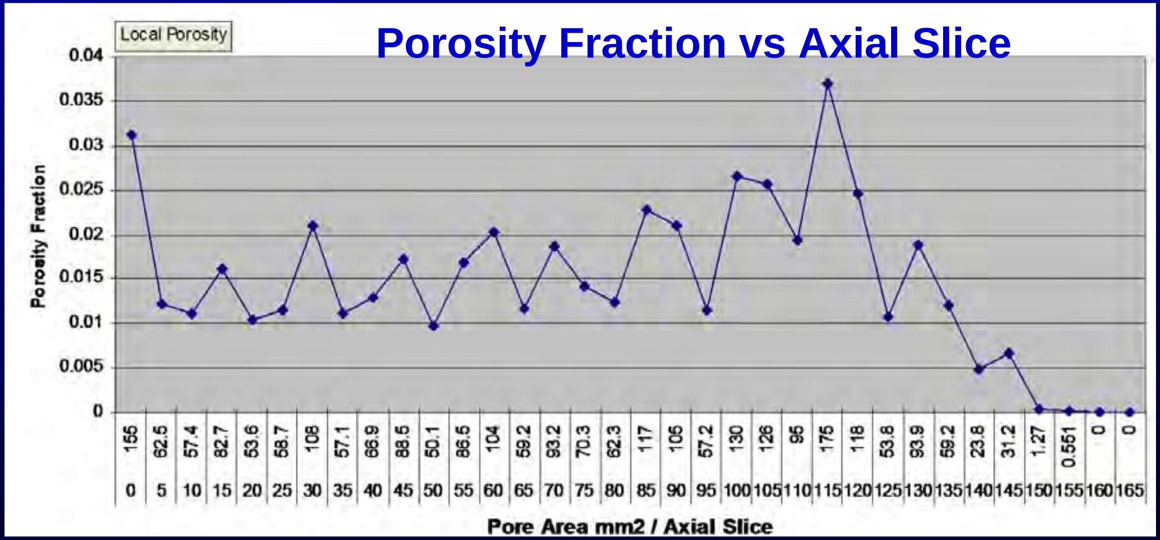

Point Cloud Visualizations of Spiral Cracking in Ballistic Impact Samples

Metallic

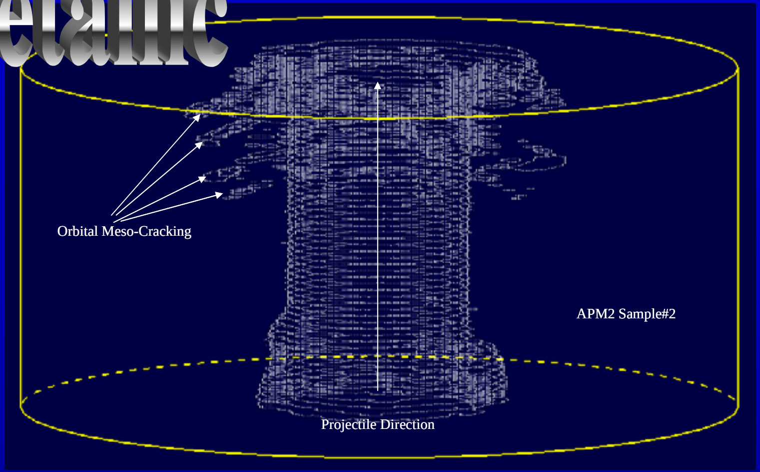

Ti-6Al-4V pc showing spiral cracking
(Full Penetration)

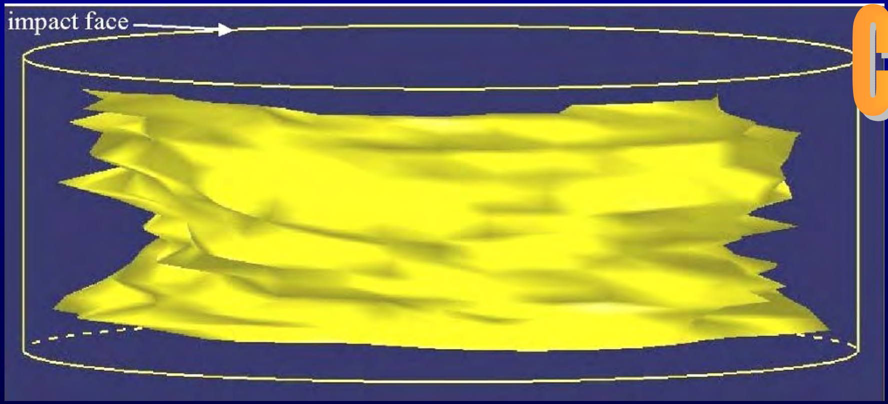

Ceramic

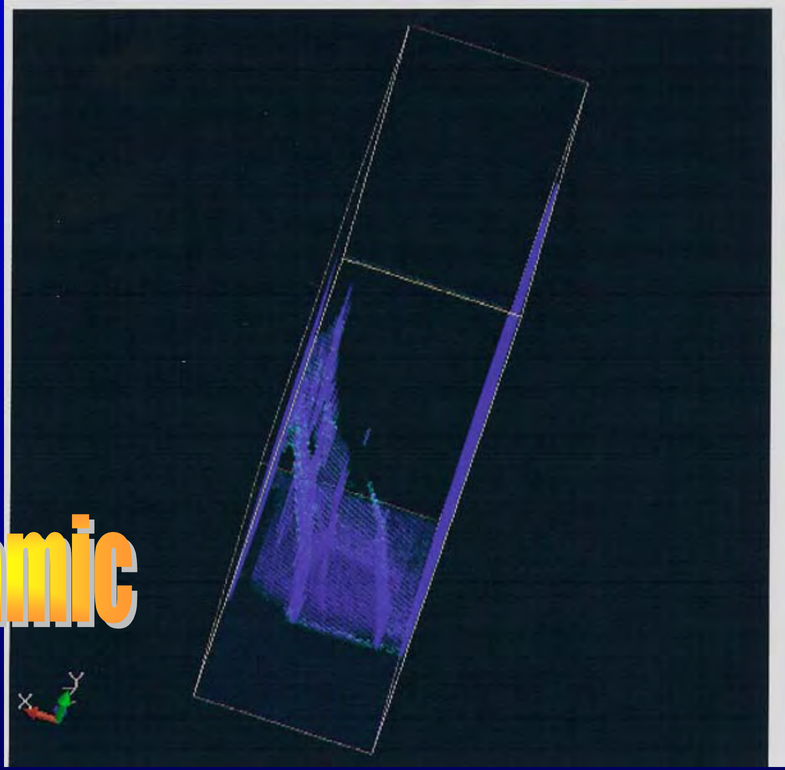

TiC pc showing spiral- blue
(No Penetration)

TiB_2 surfaced pc showing spiral
(Dual Impact – Full Penetration)

Summary Comments

- The NDE Diagnostic Interrogation of Impact Damage in Armor Ceramics is a Challenging Task.
- XCT Diagnostics, Voxel Analysis, and 3D Visualization have revealed new details & insights into:
  - Impact Surface - Topography & Damage
  - Internal Residual Fragment Distribution
  - Internal Mesoscale Cracking Modes
  - Impact-created Porosity/Void Distributions
  - Volumetric (3D) Damage Perspectives
- The XCT Diagnostic approach to armor ceramic Damage Analysis & Visualization is NOT yet widely practiced.
- Further Improvements in and Benefits from this technique are possible and realistically anticipated.

As far as the laws of mathematics refer to reality, they are not certain: and as far as they are certain, they do not refer to reality" – A. Einstein

Research of Flight Characteristics of Rod-Type Projectile with Triangular Cross-section

Dr. Wenjun Yi, Prof. Xiaobing Zhang, Prof. Jianping Qian

Ballistic Research Laboratory of China

Outline

- INTRODUCTION
- EXPERIMENT RESEARCH
- ANALYSIS OF FLIGHT PERFORMANCE
- CONCLUSIONS

INTRODUCTION

Recently, the projectile with non-circular cross-section has paid more and more attention. for example guidance projectile, the changing of the shell shape from common circular to non-circular cross-section makes it possible to improve projectiles storage, transport, discarding and aerodynamic characteristics. The experiments prove that the non-circular cross-section has better rigidity in the same area and lighter in the same length. This paper takes armor-piercing projectile for example, contrasting and researching the aerodynamic characteristics and trajectory characteristics of triangular cross-section projectile and circular cross-section projectile respectively.

EXPERIMENT RESEARCH

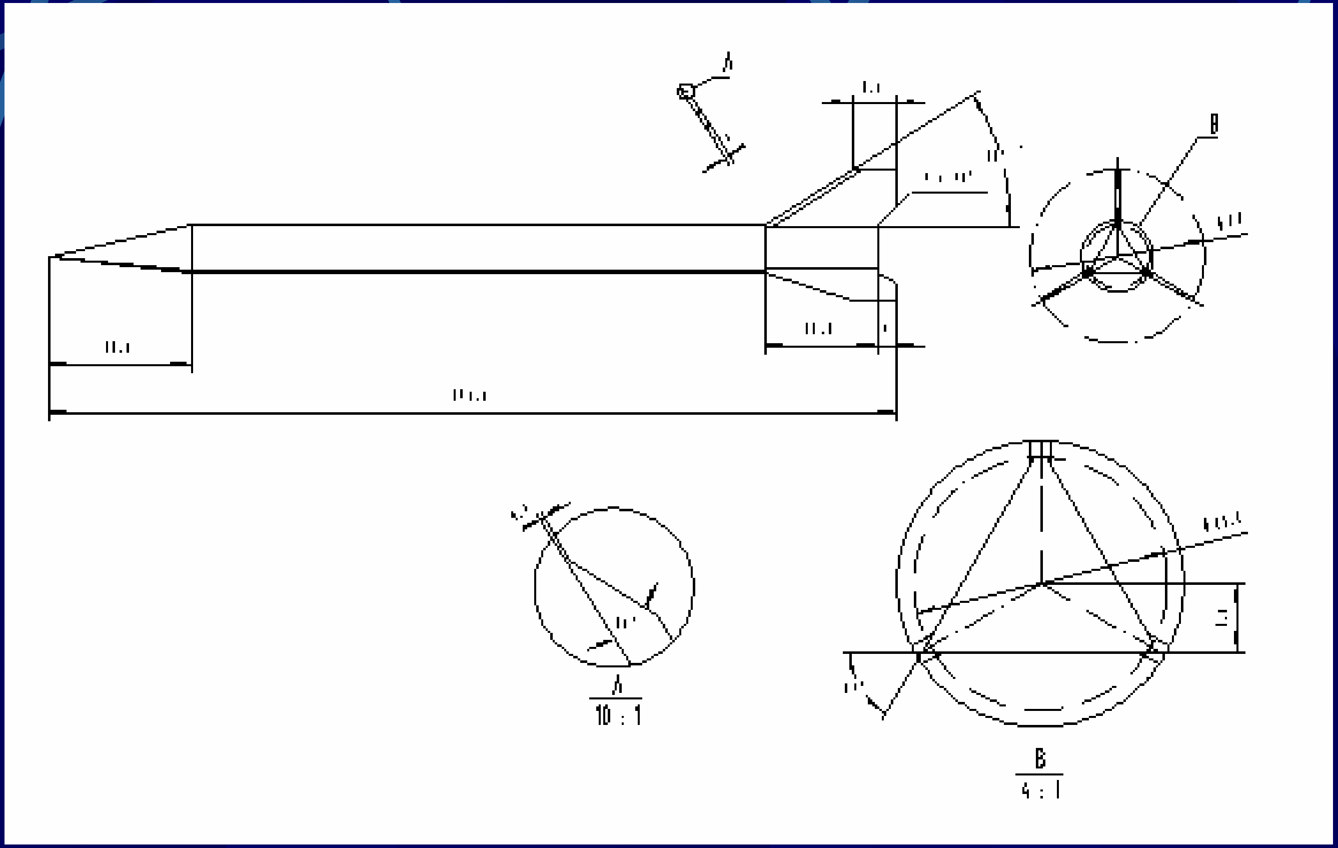

The structure of triangular cross-section projectile

EXPERIMENT RESEARCH

Triangular cross-section projectiles

EXPERIMENT RESEARCH

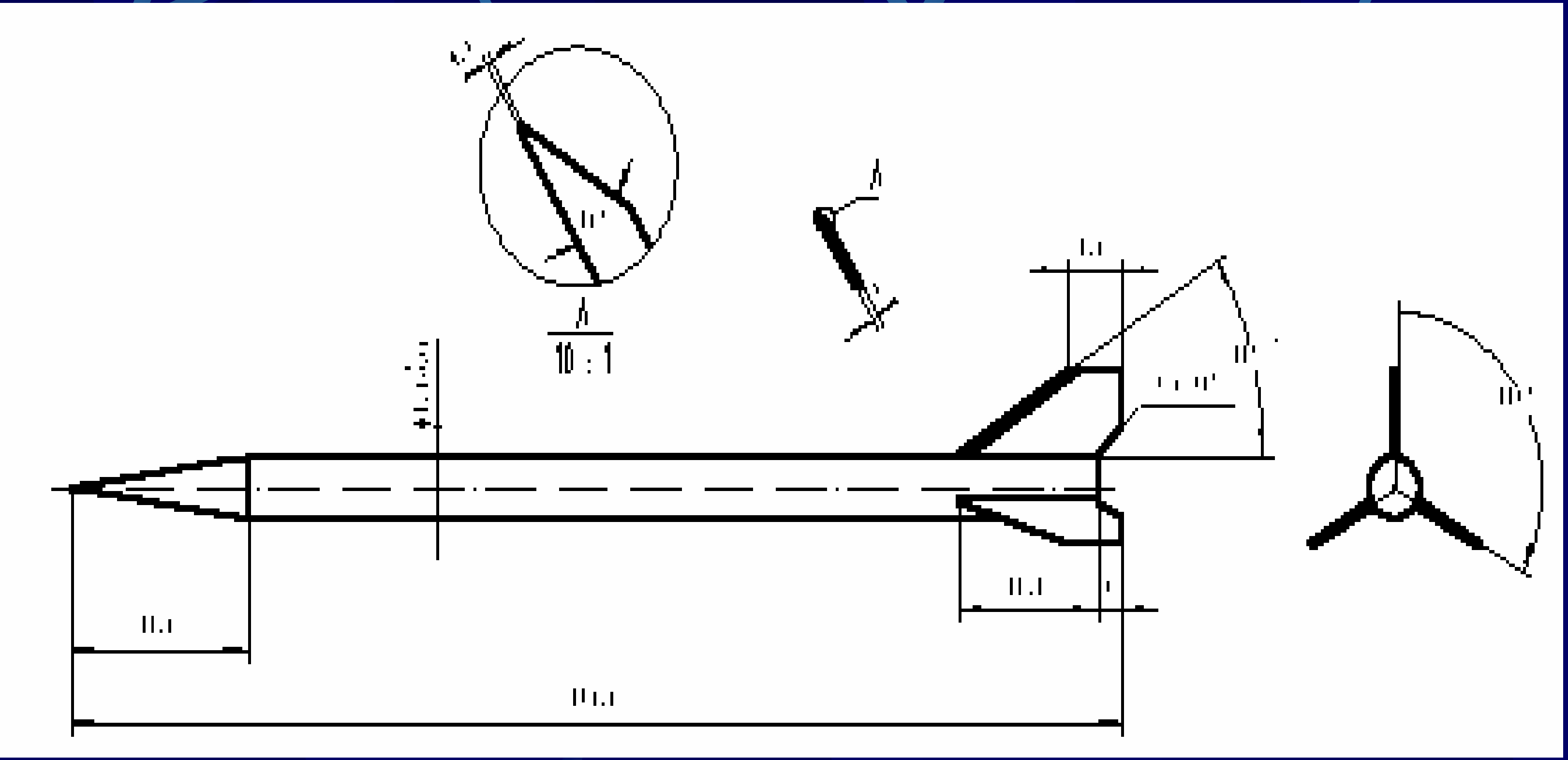

The structure of circular cross-section projectile

EXPERIMENT RESEARCH

Circular cross-section projectiles

EXPERIMENT RESEARCH

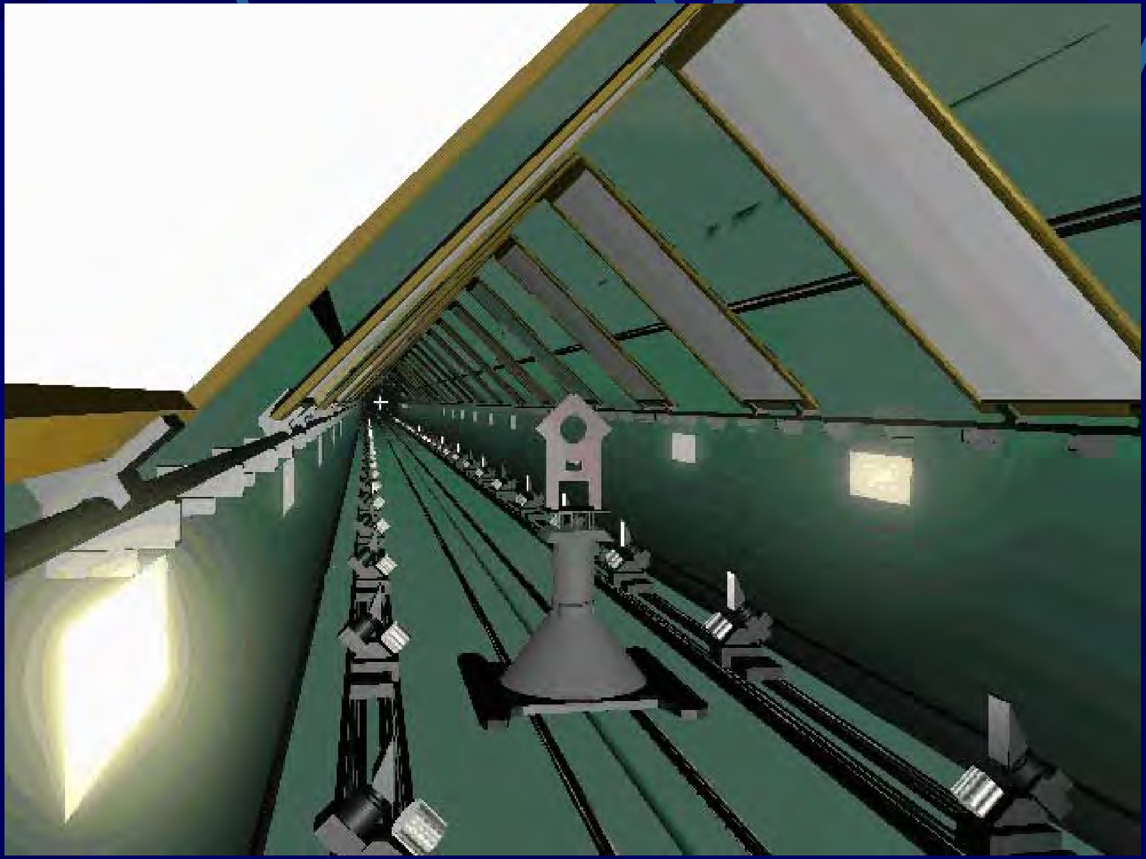

Range show

EXPERIMENT RESEARCH

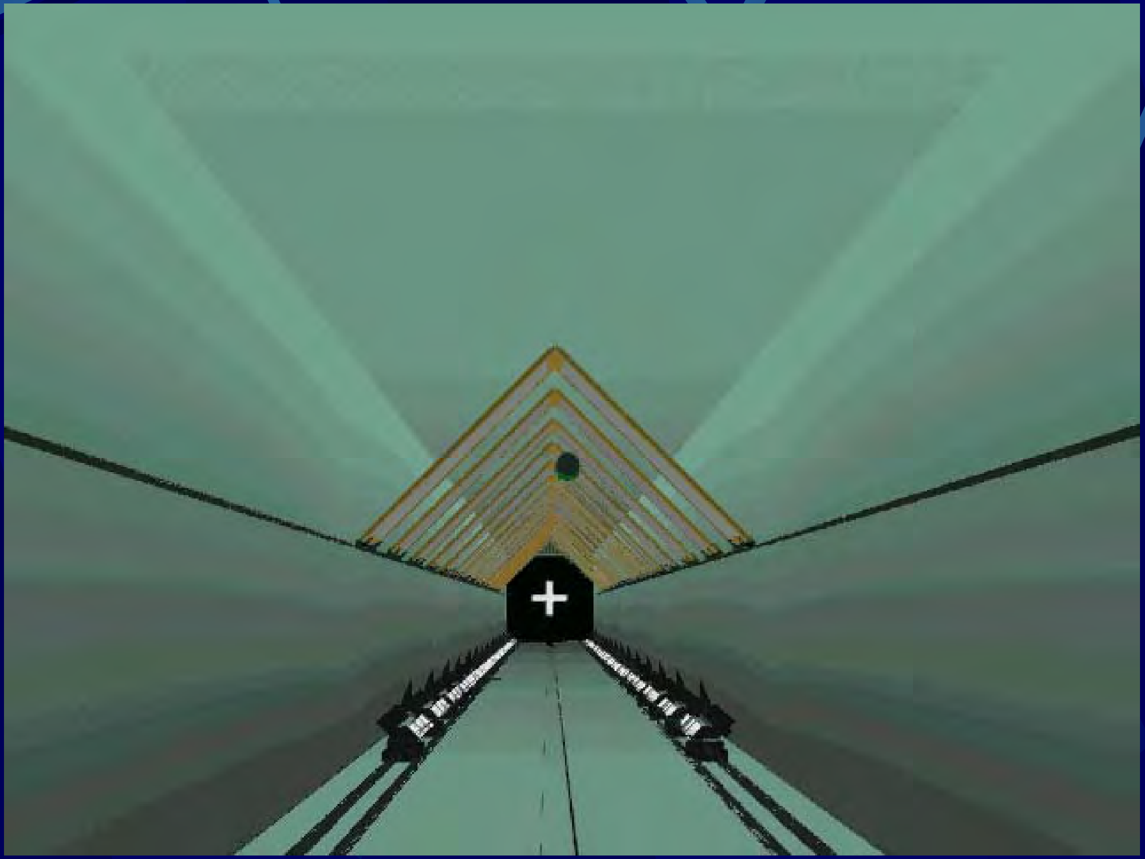

Experiment show

EXPERIMENT RESEARCH

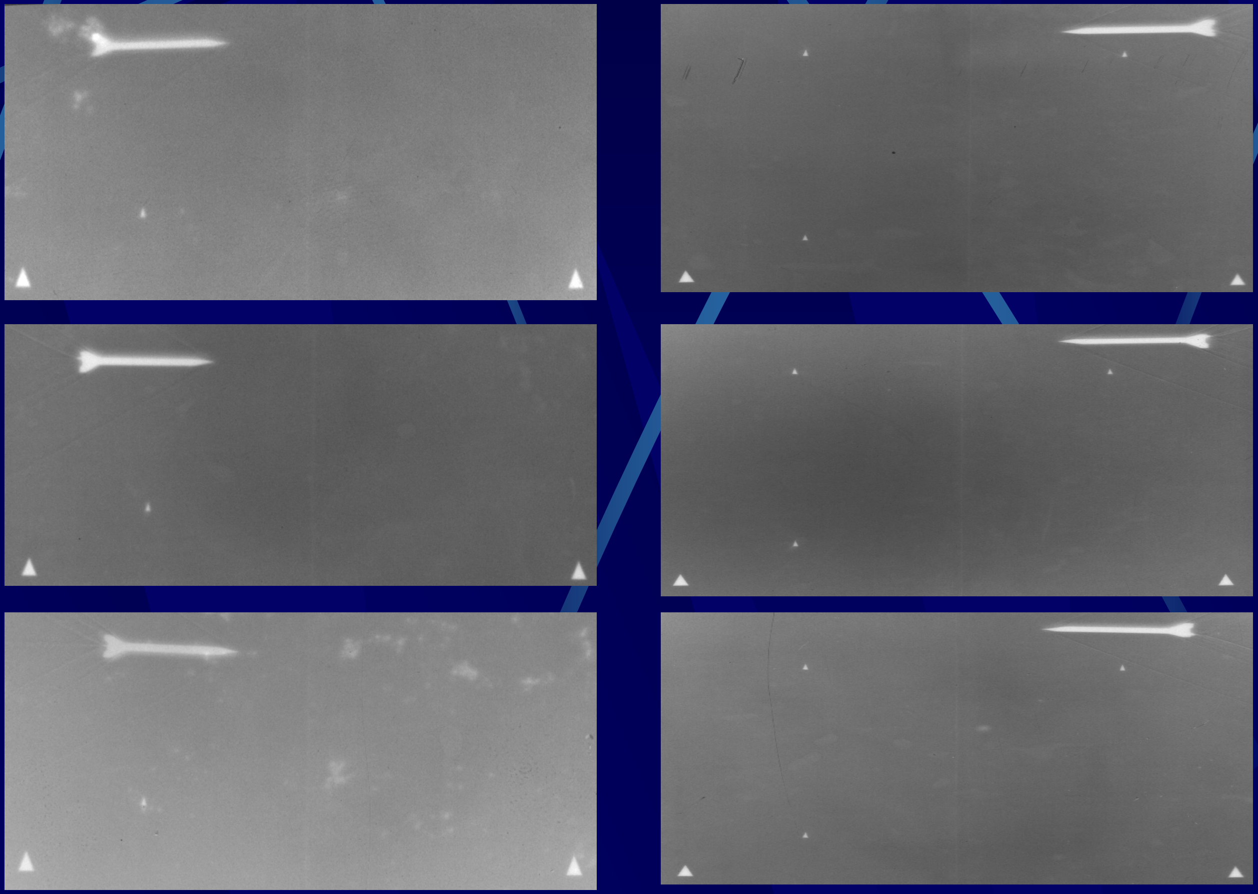

Shadowgraphic image of triangular cross-section projectile

EXPERIMENT RESEARCH

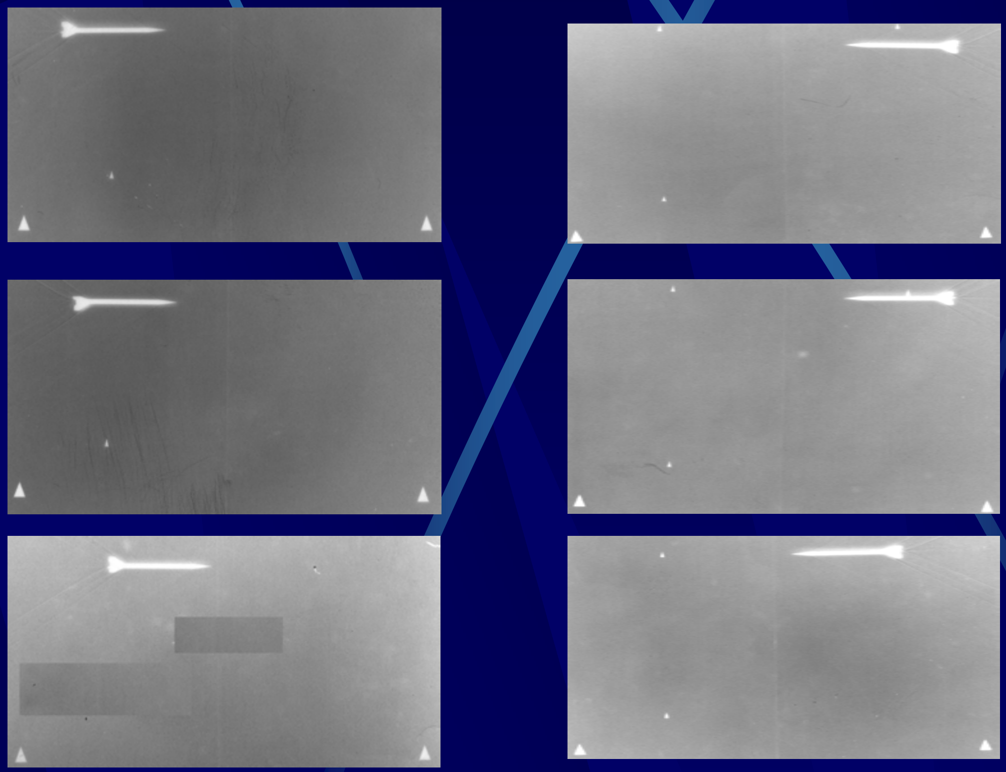

Shadowgraphic image of circular cross-section projectile

EXPERIMENT RESEARCH

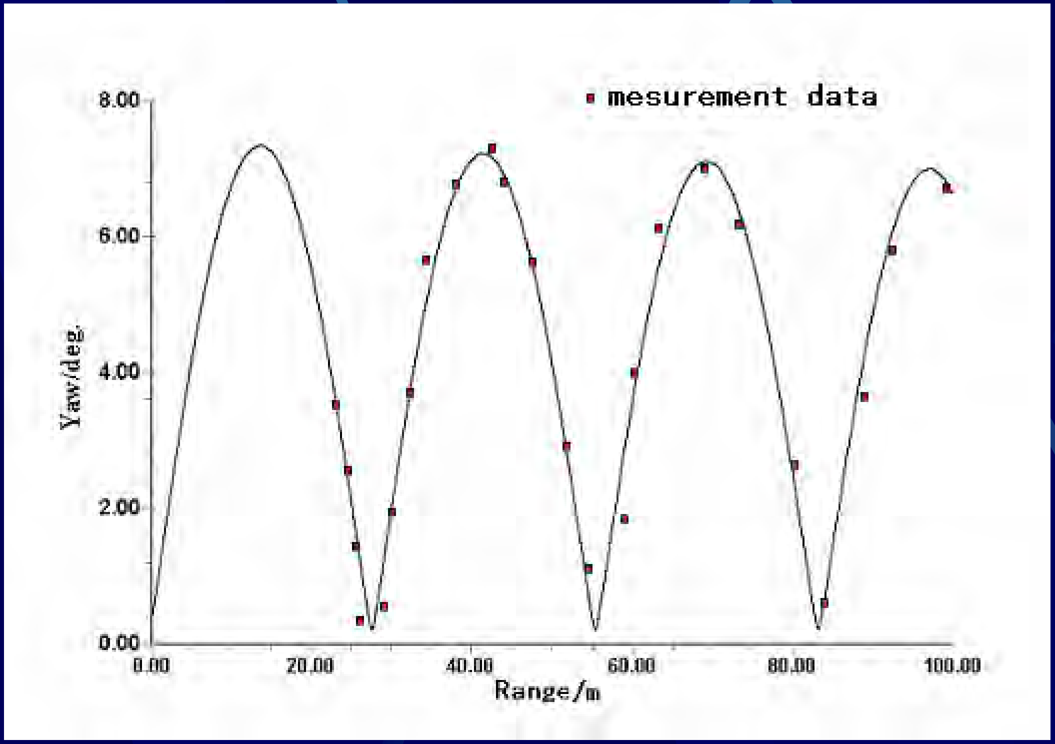

Yaw angle curve of triangular cross-section projectile

EXPERIMENT RESEARCH

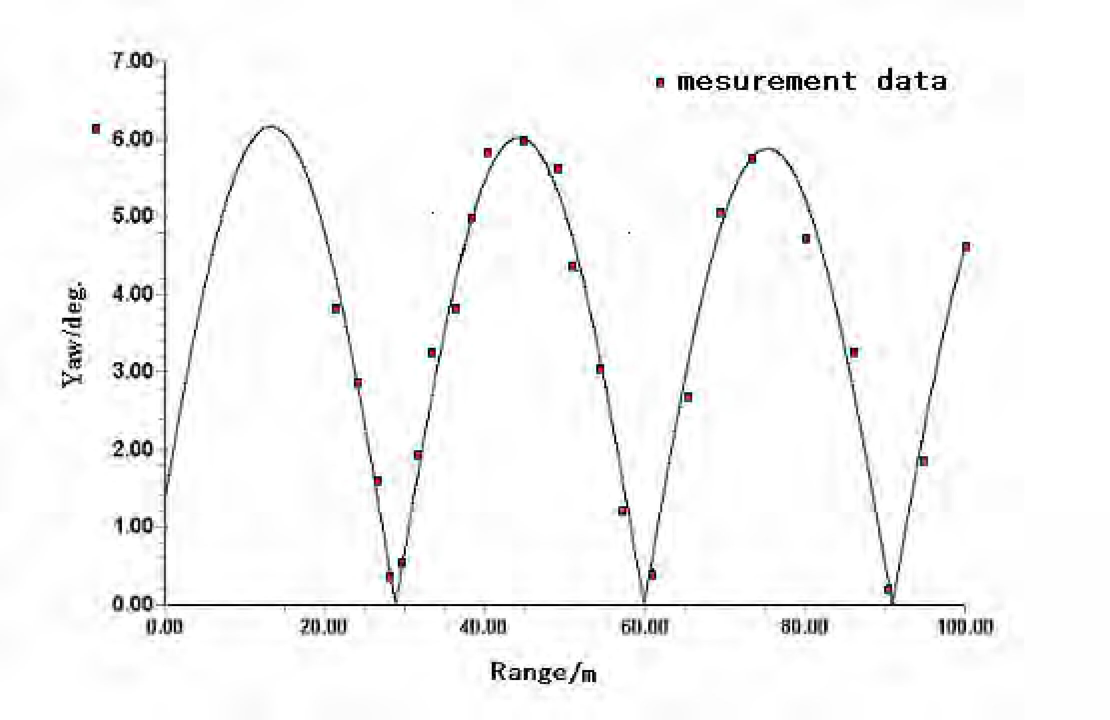

Yaw angle curve of circular cross-section projectile

EXPERIMENT RESEARCH

Table 1. The result of the experiment

item	No.1	No.2	No.3	No.4	No.5	No.6
Shape	Circular	Triangular	Circular	Triangular	Circular	Triangular
Mach	1.8514	1.9302	1.8996	1.9101	1.9034	1.8954
c_x	0.384	0.367	0.379	0.356	0.378	0.362
c_y'	2.387	2.764	2.475	2.661	2.296	2.736
m_z'	-2.683	-3.678	-2.676	-3.539	-2.737	-3.791
m_y''	-0.0036	-0.0038	-0.0031	-0.0038	-0.0041	-0.0052
m_{zz}'	2.472	2.463	2.397	2.517	2.413	2.529

EXPERIMENT RESEARCH

Table 1. The result of the experiment

item	No.1	No.2	No.3	No.4	No.5	No.6
Shape	Circular	Triangular	Circular	Triangular	Circular	Triangular
Mach	1.8514	1.9302	1.8996	1.9101	1.9034	1.8954
m'_{zz}	2.472	2.463	2.397	2.517	2.413	2.529
m'_{xz}	0.0025	0.0035	0.0024	0.0034	0.0024	0.0034
m'_{xw}	0.0024	0.0034	0.0024	0.0035	0.0025	0.0034
v_0	648.73	675.14	665.20	670.20	666.93	663.76
λ	62.08	55.71	61.79	54.94	61.44	54.17
δ_m	6.17	7.43	6.46	6.87	6.03	6.62

ANALYSIS OF FLIGHT PERFORMANCE

According to the aerodynamic coefficients of the projectile gained by experiments, contrasting and analyzing the triangular cross-section projectile and circular cross-section projectile in fight performance such as resistance characteristic, stability under low speed rotation, maneuverability and so on.

ANALYSIS OF FLIGHT PERFORMANCE

Table 2 shows the analysis result of triangular cross-section projectile and circular cross-section projectile in static stability.

Table 2. Static stability contrasts

Content	m_z^{δ}	c_y^{δ}	$m_z^{c_y}$	$f\,(hz)$	$T\,(ms)$	$\lambda\,(m)$
Triangular	-3.678	5.528	0.6653	75.49	83.23	55.71
Circular	-2.813	4.622	0.6086	69.37	90.57	60.13

(Notes: $\left|m_z^{c_y}\right| = \dfrac{\left|m_z^{\delta}\right|}{c_y^{\delta}} = \dfrac{l_{pc} - l_{mc}}{l} \times 100\%$, stand for static stability allowance)

ANALYSIS OF FLIGHT PERFORMANCE

The analysis and results shows that static stability allowance of triangular cross-section projectile is higher than circular cross-section projectile, its stabilizing moment and dumping moment is bigger than circular cross-section projectile, especial the stability moment.

To triangular cross-section projectile, the oscillatory frequency is higher and the oscillatory wavelength is short. These characteristics represent that the stability of triangular cross-section projectile is better.

ANALYSIS OF FLIGHT PERFORMANCE

Table 3 shows the analysis result of triangular cross-section projectile and circular cross-section projectile in stability characteristic under low speed rotation.

Table 3. Stability characteristic contrasts

Content	$I_x\,(kg.m^2)$	$m_x^{\delta_\omega}$	m_y^{α}
Triangular	0.0986×10^{-5}	0.00343	-0.0038
Circular	0.0979×10^{-5}	0.00245	-0.0032

ANALYSIS OF FLIGHT PERFORMANCE

The analysis and results shows: the Magnus moment of triangular cross-section projectile is higher than circular cross-section projectile. To the projectile in flight, the Magnus moment is disturbance moment. The bigger of Magnus moment, the bigger interaction of pitching and yaw by rolling, maybe it will lead to great distribution. So the effect of reduce offcenter and initial disturbance of triangular cross-section projectile by low speed rotation is not as well as circular cross-section projectile.

ANALYSIS OF FLIGHT PERFORMANCE

Table 4 shows the triangular cross-section projectile and circular cross-section projectile in maneuverability. The analysis and results shows: the drag coefficient of triangular cross-section projectile is lower than circular cross-section projectile's, the triangular cross-section projectile has higher lift-drag ratio, and could supply bigger normal overload, consequently it has better maneuverability.

Table 4. Maneuverability contrasts

Content	c_{x0}	c_N^{δ}	$(L/X)_{max}$
Triangular	0.366	0. 3093	2.197
Circular	0.378	0.2686	1.901

CONCLUSIONS

- The projectile with triangular cross-section has smaller flight resistance, less kinetic energy loss, higher ratio of kinetic energy to cross section area when impacting.

- The projectile with triangular cross-section has better static stability and it's static stability allowance is bigger than the circular cross-section projectile's.

CONCLUSIONS

❖ Under low speed rotation, the projectile with triangular cross-sections has great Magnus moment and more possible to increase the projectile dispersion.

❖ The projectile with triangular cross-section has higher lift-drag ratio, could supply bigger normal overload and better maneuverability. Therefore it's more suitably used for projectile missile shape.